

ABSTRACT

Development of a Ring Expansion Approach Toward (\pm)-Phyllantidine, Ring Expansion of Tetramic Acids to *N*-oxy-2,5-diketopiperazines, and Total Synthesis of (+)-Raistrickindole A

Amy Catherine Jackson, Ph.D.

Mentor: John L. Wood, Ph.D.

In 2020 we reported a concise total synthesis of (\pm)-phyllantidine, a member of the securinega alkaloid family of natural products, which contains a unique oxazabicyclo[3.3.1]nonane core. Our strategy features a ring expansion of a substituted cyclopentanone to a cyclic hydroxamic acid, which allows facile installation of the embedded nitrogen-oxygen (*N*-*O*) bond. Herein we discuss the optimization process of the ring expansion reaction on a series of modified substrates, along with the observed regiochemical outcomes, leading up to the eventual completion of the natural product. Additionally, computational analyses of the mechanistic underpinnings aided us in fine-tuning both the ring expansion system and the reaction conditions, in order to obtain a single regioisomer of the ring expansion product. (\pm)-Phyllantidine was completed in 12-steps from known materials (9% overall yield), or 14-steps from commercially-available 1,4-cyclohexadiene.

N-oxy-2,5-diketopiperazines (DKPs) are prevalent in many biologically-relevant natural products, and current methods of accessing this functionality are typically fraught

with difficulty. To overcome this, we describe a ring expansion of tetramic acids (pyrrolidine-2,4-diones) to *N*-oxy-2,5-DKPs, inspired by a similar 2-step ring expansion strategy used in our total synthesis of (\pm)-phyllantidine: oxidation of a hydroxamic acid moiety to a acyloxy nitroso, followed by nucleophilic cleavage of the appended acetate to effect carbon-carbon bond migration into the nitroso component giving the ring-expanded product. This method allows for the facile and late-stage construction of the *N*-*O* bond and can thereby serve as a general method for accessing *N*-oxy-2,5-DKP-containing natural products. Herein we develop several model substrates with varying functionality around the tetramic acid ring, and describe the different outcomes regarding regioselectivity and overall yield. We report the successful ring expansion of a Bn-substituted DMB-protected tetramic acid using optimized conditions in the 2-step sequence, with the expectation to apply this chemistry toward the synthesis of natural products.

(+)-Raistrickindole A was isolated in 2019 by Li and co-workers and shows modest activity against the hepatitis C virus. (+)-Raistrickindole A is embedded in a tryptophan/phenylalanine-derived 1,2-oxazine-containing tetraheterocycle, and features an *N*-oxy-2,5-DKP core, posing an attractive synthetic challenge. There are currently no reports to date of this natural product. Our synthetic efforts evolved through the attempted use of our developed ring expansion to synthesize the DKP core of the natural product, and eventually transformed into the successful utilization of a regio- and diastereoselective intermolecular nitroso Diels-Alder (NDA) reaction. We completed the first total synthesis of (+)-raistrickindole A in 9 steps from known materials, and we believe that this method can be used to synthesize other potentially pharmacologically-useful *N*-oxy-DKP/1,2-oxazine-containing natural products.

Development of a Ring Expansion Approach Toward (\pm)-Phyllantidine, Ring Expansion of Tetramic Acids to *N*-oxy-2,5-diketopiperazines, and Total Synthesis of (+)-Raistrickindole A

by

Amy Catherine Jackson, B.S.

A Dissertation

Approved by the Department of Chemistry and Biochemistry

John L. Wood, Ph.D., Chairperson

Submitted to the Graduate Faculty of
Baylor University in Partial Fulfillment of the
Requirements for the Degree
of
Doctor of Philosophy

Approved by the Dissertation Committee

John L. Wood, Ph.D., Chairperson

Daniel Romo, Ph.D.

Kevin G. Pinney, Ph.D.

Caleb D. Martin, Ph.D.

Rebecca J. Sheesley, Ph.D.

Accepted by the Graduate School

August 2022

J. Larry Lyon, Ph.D., Dean

Copyright © 2022 by Amy Catherine Jackson

All rights reserved

TABLE OF CONTENTS

LIST OF FIGURES	vii
LIST OF SCHEMES	xii
LIST OF TABLES	xiv
LIST OF ABBREVIATIONS	xvi
ACKNOWLEDGMENTS	xviii
CHAPTER ONE	1
Development of a Ring Expansion Approach Toward the Core of (\pm)-Phyllantidine ...	1
1.1 Background	1
1.2 Total Synthesis of (\pm)-Phyllantidine	4
1.3 Contribution to the Ring Expansion Optimization	7
1.4 Conclusion	16
1.5 References and Notes.....	17
CHAPTER TWO	19
Ring Expansion of Chiral Tetramic Acids to <i>N</i> -oxy-2,5-diketopiperazines.....	19
2.1 Background and Significance	19
2.2 Access to Functionalizable Chiral Tetramic Acids.....	27
2.3 Ring Expansion Sequence to Install the <i>N</i> - <i>O</i> Bond	37
2.4 Conclusion	48
2.5 Experimental	48
2.6 References.....	70
CHAPTER THREE	75
Total Synthesis of (+)-Raistrickindole A	75
3.1 Background and Significance	75
3.2 Applying the Ring Expansion Toward (+)-Raistrickindole A	76
3.3 Accessing (+)-Raistrickindole A <i>via</i> an Intramolecular Nitroso Diels-Alder	80
3.5 Completed Total Synthesis of (+)-Raistrickindole A	97
3.5 Proposed Access to (-)-Haenamindole from (+)-Raistrickindole A	105
3.6 Conclusion	107
3.7 Experimental	108
3.8 References.....	139
APPENDICES	142
APPENDIX A	143
Spectral Data for Chapter Two	143
APPENDIX B	217
Spectral Data for Chapter Three	217

APPENDIX C	309
X-ray Crystallographic Data	309
C.1. Crystal analysis of tetramic acid 2.51	310
C.2. Crystal analysis of DMB-tetramic acid 2.54	317
C.3. Crystal analysis of tetramic acid 2.56	324
C.4. Crystal analysis of oxime 2.57	344
C.5. Crystal analysis of oxime 2.63	352
C.6. Crystal analysis of NDA adduct 3.46	362
C.7. Crystal analysis of epoxide 3.52	371
C.8. Crystal analysis of alcohol 3.63	393
C.9. Crystal analysis of intermolecular NDA adduct 3.67	411
APPENDIX D	412
Compound Notebook Cross Reference.....	412
BIBLIOGRAPHY	415
ABOUT THE AUTHOR	424

LIST OF FIGURES

Figure 1.10. Parent skeletons and selected examples of securinega alkaloids	2
Figure 1.11. Selected <i>N</i> - <i>O</i> bond-containing securinega alkaloids	3
Figure 2.10. Selected tetramic acid-containing natural products.....	28
Figure 2.11. Diverse functionalization of tetramic acids.....	29
Figure 2.12. Calculated differences in carbon shifts of C2 and C11	42
Figure 2.13. Observed carbon shifts in the only isolated ring expansion product.....	42
Figure 3.10. Structure and isolation of (+)-raistrickindole A	76
Figure 3.11. Computed transition state energies showing favorability of the <i>endo</i> -pathway	98
Figure 3.12. General regioselectivity in NDA reactions.....	99
Figure A.01. ^1H NMR (400 MHz, CDCl_3) methyl ester 2.49	144
Figure A.02. Quantitative NMR (400 MHz, CDCl_3) methyl ester 2.49	145
Figure A.03. ^{13}H NMR (101 MHz, CDCl_3) methyl ester 2.49	146
Figure A.04. FTIR (neat) methyl ester 2.49	147
Figure A.05. ^1H NMR (400 MHz, CDCl_3) dioxopyrrolidine 2.50	148
Figure A.06. Quantitative NMR (400 MHz, CDCl_3) dioxopyrrolidine 2.50	149
Figure A.07. ^{13}H NMR (101 MHz, CDCl_3) dioxopyrrolidine 2.50	150
Figure A.08. FTIR (neat) dioxopyrrolidine 2.50	151
Figure A.09. ^1H NMR (400 MHz, CDCl_3) tetramic acid 2.51	152
Figure A.10. Quantitative NMR (400 MHz, CDCl_3) tetramic acid 2.51	153
Figure A.11. ^{13}C NMR (101 MHz, CDCl_3) tetramic acid 2.51	154
Figure A.12. FTIR (neat) tetramic acid 2.51	155
Figure A.13. ^1H NMR (600 MHz, CDCl_3) known methyl ester 2.52	156
Figure A.14. ^{13}C NMR (151 MHz, CDCl_3) known methyl ester 2.52	157
Figure A.15. ^1H NMR (400 MHz, CDCl_3) crude amide 2.53	158
Figure A.16. ^{13}C NMR (101 MHz, CDCl_3) crude amide 2.53	159
Figure A.17. FTIR Spectrum (neat) crude amide 2.53	160
Figure A.18. ^1H NMR (400 MHz, CDCl_3) DMB tetramic acid 2.54	161
Figure A.19. ^{13}C NMR (101 MHz, CDCl_3) DMB tetramic acid 2.54	162
Figure A.20. FTIR Spectrum (neat) DMB tetramic acid 2.54	163
Figure A.21. ^1H NMR (400 MHz, CDCl_3) alkene 2.55	164
Figure A.22. ^{13}C NMR (400 MHz, CDCl_3) alkene 2.55	165
Figure A.23. FTIR (neat) alkene 2.55	166
Figure A.24. ^1H NMR (400 MHz, CDCl_3) tetramic acid 2.56	167
Figure A.25. ^{13}C NMR (101 MHz, CDCl_3) tetramic acid 2.56	168
Figure A.26. FTIR (neat) tetramic acid 2.56	169
Figure A.27. ^1H NMR (600 MHz, CDCl_3) oxime 2.57	170
Figure A.28. ^{13}C NMR (151 MHz, CDCl_3) oxime 2.57	171

Figure A.29. FTIR (neat) oxime 2.57	172
Figure A.30. ^1H NMR (400 MHz, CDCl_3) acyloxy nitroso 2.58	173
Figure A.31. ^{13}C NMR (101 MHz, CDCl_3) acyloxy nitroso 2.58	174
Figure A.32. FTIR (neat) crude acyloxy nitroso 2.58	175
Figure A.33. ^1H NMR (600 MHz, CDCl_3) DKP 2.59	176
Figure A.34. ^{13}C NMR (151 MHz, CDCl_3) DKP 2.59	177
Figure A.35. COSY (600 MHz, CDCl_3) DKP 2.59	178
Figure A.36. HSQC (600, 151 MHz, CDCl_3) DKP 2.59	179
Figure A.37. FTIR (neat) DKP 2.59	180
Figure A.38. ^1H NMR (400 MHz, CDCl_3) alkene 2.61	181
Figure A.39. ^{13}C NMR (101 MHz, CDCl_3) alkene 2.61	182
Figure A.40. FTIR (neat) alkene 2.61	183
Figure A.41. ^1H NMR (600 MHz, CDCl_3) tetramic acid 2.62	184
Figure A.42. ^{13}C NMR (151 MHz, CDCl_3) tetramic acid 2.62	185
Figure A.43. FTIR (neat) tetramic acid 2.62	186
Figure A.44. ^1H NMR (600 MHz, CDCl_3) oxime 2.63	187
Figure A.45. ^{13}C NMR (151 MHz, CDCl_3) oxime 2.63	188
Figure A.46. FTIR (neat) oxime 2.63	189
Figure A.47. ^1H NMR (500 MHz, CDCl_3) crude acyloxy nitroso 2.64	190
Figure A.48. ^1H NMR (600 MHz, CDCl_3) DKP 2.65	191
Figure A.49. ^{13}C NMR (151 MHz, CDCl_3) DKP 2.65	192
Figure A.50. COSY (600 MHz, CDCl_3) DKP 2.65	193
Figure A.51. FTIR (neat) DKP 2.65	194
Figure A.52. ^1H NMR (400 MHz, CDCl_3) alkene 2.66	195
Figure A.53. ^{13}C NMR (101 MHz, CDCl_3) alkene 2.66	196
Figure A.54. ^{19}F NMR (400 MHz, CDCl_3) alkene 2.66	197
Figure A.55. FTIR (neat) alkene 2.66	198
Figure A.56. ^1H NMR (400 MHz, CDCl_3) tetramic acid 2.67	199
Figure A.57. ^{13}C NMR (151 MHz, CDCl_3) tetramic acid 2.67	200
Figure A.58. FTIR (neat) tetramic acid 2.67	201
Figure A.59. ^1H NMR (600 MHz, CDCl_3) oxime 2.68	202
Figure A.60. ^{13}C NMR (151 MHz, CDCl_3) oxime 2.68	203
Figure A.61. FTIR (neat) oxime 2.68	204
Figure A.62. ^1H NMR (500 MHz, CDCl_3) crude acyloxy nitroso 2.69	205
Figure A.63. ^1H NMR (600 MHz, DMSO) oxime 2.71	206
Figure A.64. ^{13}C NMR (600 MHz, DMSO) oxime 2.71	207
Figure A.65. FTIR (neat) oxime 2.71	208
Figure A.66. ^1H NMR (400 MHz, CDCl_3) crude acyloxy nitroso 2.72	209
Figure A.67. ^1H NMR (400 MHz, MeOD) known tetramic acid 2.73	210
Figure A.68. ^{13}C NMR (101 MHz, MeOD) known tetramic acid 2.73	211
Figure A.69. ^1H NMR (600 MHz, DMSO) known tetramic acid 2.73	212
Figure A.70. ^{13}C NMR (151 MHz, DMSO) known tetramic acid 2.73	213
Figure A.71. COSY (600 MHz, DMSO) known tetramic acid 2.73	214
Figure A.72. HSQC (600 MHz, 151 MHz, DMSO) known tetramic acid 2.73	215
Figure A.73. HMBC (600 MHz, 151 MHz, DMSO) known tetramic acid 2.73	216

Figure B.01. ^1H NMR (400 MHz, CDCl_3) known indole 3.08	218
Figure B.02. ^{13}C NMR (101 MHz, CDCl_3) known indole 3.08	219
Figure B.03. ^1H NMR (600 MHz, CDCl_3) alkene 3.07	220
Figure B.04. ^{13}C NMR (151 MHz, CDCl_3) alkene 3.07	221
Figure B.05. IR (neat) alkene 3.07	222
Figure B.06. ^1H NMR (400 MHz, CDCl_3) tetramic acid 3.06	223
Figure B.07. ^{13}C NMR (101 MHz, CDCl_3) tetramic acid 3.06	224
Figure B.08. FTIR (neat) tetramic acid 3.06	225
Figure B.09. ^1H NMR (600 MHz, CDCl_3) oxime 3.05	226
Figure B.10. ^{13}C NMR (151 MHz, CDCl_3) oxime 3.05	227
Figure B.11. FTIR (neat) oxime 3.05	228
Figure B.12. ^1H NMR (XXX MHz, CDCl_3) known cyclopentadiene adduct 3.24	229
Figure B.13. ^{13}C NMR (XXX, CDCl_3) known cyclopentadiene adduct 3.24	230
Figure B.14. FTIR (neat) known cyclopentadiene adduct 3.24	231
Figure B.15. ^1H NMR (400 MHz, CDCl_3) crude amino salt 3.25	232
Figure B.16. ^1H NMR (400 MHz, CDCl_3) known Ns-protected indole carbaldehyde 3.27	233
Figure B.17. ^1H NMR (400 MHz, DMSO) indoleacrylic acid 3.28	234
Figure B.18. ^{13}C NMR (101 MHz, DMSO) indoleacrylic acid 3.28	235
Figure B.19. FTIR (neat) indoleacrylic acid 3.28	236
Figure B.20. ^1H NMR (400 MHz, CDCl_3) known Bn-protected allyl ester 3.31	237
Figure B.21. ^1H NMR (400 MHz, CDCl_3) crude amide 3.32	238
Figure B.22. ^1H NMR (400 MHz, CDCl_3) crude carboxylic acid 3.33	239
Figure B.23. ^1H NMR (400 MHz, CDCl_3) crude hydroxamic acid 3.34	240
Figure B.24. ^1H NMR (400 MHz, CDCl_3) known hydroxamic acid 3.39	241
Figure B.25. ^1H NMR (400 MHz, DMSO) hydroxamic acid 3.37	242
Figure B.26. ^{13}C NMR (101 MHz, DMSO) hydroxamic acid 3.37	243
Figure B.27. FTIR (neat) hydroxamic acid 3.37	244
Figure B.28. ^1H NMR (400 MHz, CDCl_3) known hydroxamic acid 3.47	245
Figure B.29. ^{13}C NMR (151 MHz, CDCl_3) known hydroxamic acid 3.47	246
Figure B.30. FTIR (neat) known hydroxamic acid 3.47	247
Figure B.31. ^1H NMR (400 MHz, CDCl_3) NDA adduct 3.46	248
Figure B.32. ^{13}C NMR (101 MHz, CDCl_3) NDA adduct 3.46	249
Figure B.33. FTIR (neat) NDA adduct 3.46	250
Figure B.34. ^1H NMR (400 MHz, CDCl_3) epoxide 3.52	251
Figure B.35. ^{13}C NMR (101 MHz, CDCl_3) epoxide 3.52	252
Figure B.36. FTIR (neat) epoxide 3.52	253
Figure B.37. ^1H NMR (400 MHz, CDCl_3) hemiaminal 3.53	254
Figure B.38. ^{13}C NMR DEPT135 (101 MHz, CDCl_3) hemiaminal 3.53	255
Figure B.39. COSY (400 MHz, CDCl_3) hemiaminal 3.53	256
Figure B.40. HSQC (400 MHz, 101 MHz, CDCl_3) hemiaminal 3.53	257
Figure B.41. HMBC (400 MHz, 101 MHz, CDCl_3) hemiaminal 3.53	258
Figure B.42. ^1H NMR (400 MHz, CDCl_3) methyl carbamate 3.54	259
Figure B.43. ^{13}C NMR (101 MHz, CDCl_3) methyl carbamate 3.54	260
Figure B.44. HSQC (400 MHz, 101 MHz, CDCl_3) methyl carbamate 3.54	261
Figure B.45. COSY (400 MHz, CDCl_3) methyl carbamate 3.54	262

Figure B.46. HMBC (400 MHz, 101 MHz, CDCl ₃) methyl carbamate 3.54	263
Figure B.47. FTIR (neat) methyl carbamate 3.54	264
Figure B.48. ¹ H NMR (400 MHz, CDCl ₃) by-product methyl carbamate 3.56	265
Figure B.49. ¹³ C NMR (101 MHz, CDCl ₃) by-product methyl carbamate 3.56	266
Figure B.50. COSY (400 MHz, CDCl ₃) by-product methyl carbamate 3.56	267
Figure B.51. HSQC (400, 101 MHz, CDCl ₃) by-product methyl carbamate 3.56	268
Figure B.52. HMBC (400 MHz, 101 MHz, CDCl ₃) by-product methyl carbamate 3.56	269
Figure B.53. ¹ H NMR (300 MHz, CDCl ₃) proposed aldehyde 3.57	270
Figure B.54. ¹ H NMR (400 MHz, CDCl ₃) amino alcohol 3.55	271
Figure B.55. ¹³ C NMR (101 MHz, CDCl ₃) amino alcohol 3.55	272
Figure B.56. FTIR (neat) amino alcohol 3.55	273
Figure B.57. ¹ H NMR (400 MHz, solvent) known TBS alcohol 3.61	274
Figure B.58. ¹³ C NMR (101 MHz, solvent) known TBS alcohol 3.61	275
Figure B.59. ¹ H NMR (600 MHz, CDCl ₃) NDA adduct 3.60	276
Figure B.60. ¹³ C NMR (151 MHz, CDCl ₃) NDA adduct 3.60	277
Figure B.61. FTIR (neat) NDA adduct 3.60	278
Figure B.62. ¹ H NMR (400 MHz, solvent) deprotected NDA adduct 3.63	279
Figure B.63. ¹³ C NMR (101 MHz, solvent) deprotected NDA adduct 3.63	280
Figure B.64. FTIR (neat) deprotected NDA adduct 3.63	281
Figure B.65. ¹ H NMR (400 MHz, CDCl ₃) Ns-protected indole ethyl ester 3.64	282
Figure B.66. ¹³ C Spectra (101 MHz, CDCl ₃) Ns-protected indole ethyl ester 3.64	283
Figure B.67. FTIR Spectrum (neat) Ns-protected indole ethyl ester 3.64	284
Figure B.68. ¹ H Spectra (400 MHz, CDCl ₃) Ns-protected indole allylic alcohol 3.65	285
Figure B.69. ¹³ C Spectra (101 MHz, CDCl ₃) Ns-protected indole allylic alcohol 3.65	286
Figure B.70. FTIR Spectrum (neat) Ns-protected indole allylic alcohol 3.65	287
Figure B.71. ¹ H Spectra (400 MHz, CDCl ₃) Ns-protected indole allylic TBS alcohol 3.66	288
Figure B.72. ¹³ C Spectra (101 MHz, CDCl ₃) Ns-protected indole allylic TBS alcohol 3.66	289
Figure B.73. FTIR Spectrum (neat) Ns-protected indole allylic TBS alcohol 3.66	290
Figure B.74. ¹ H Spectra (400 MHz, CDCl ₃) Ns-protected indole NDA adduct 3.67	291
Figure B.75. ¹³ C Spectra (151 MHz, CDCl ₃) Ns-protected indole NDA adduct 3.67	292
Figure B.76. FTIR Spectrum (neat) Ns-protected indole NDA adduct 3.67	293
Figure B.77. ¹ H Spectra (600 MHz, CDCl ₃) Ns-protected indole Mukaiyama adduct 3.68	294
Figure B.78. ¹³ C Spectra (151 MHz, CDCl ₃) Ns-protected indole Mukaiyama adduct 3.68	295
Figure B.79. FTIR Spectrum (neat) Ns-protected indole Mukaiyama adduct 3.68	296
Figure B.80. ¹ H Spectra (300 MHz, CDCl ₃) crude carboxylic acid 3.69	297
Figure B.81. ¹ H Spectra (400 MHz, CDCl ₃) Ns-protected indole amino salt 3.70	298
Figure B.82. ¹³ C Spectra (101 MHz, CDCl ₃) Ns-protected indole amino salt 3.70	299
Figure B.83. FTIR Spectrum (neat) Ns-protected indole amino salt 3.70	300
Figure B.84. ¹ H Spectra (600 MHz, CDCl ₃) Ns-protected indole DKP 3.71	301
Figure B.85. ¹³ C Spectra (151 MHz, CDCl ₃) Ns-protected indole DKP 3.71	302
Figure B.86. FTIR Spectrum (neat) Ns-protected indole DKP 3.71	303
Figure B.87. ¹ H Spectra (400 MHz, MeOD) proposed spirocycle by-product 3.72	304

Figure B.88. ^1H Spectra (600 MHz, CDCl_3) (+)-raistrickindole A (3.01).....	305
Figure B.89. ^{13}C Spectra (151 MHz, CDCl_3) (+)-raistrickindole A (3.01).....	306
Figure B.90. FTIR Spectrum (neat) (+)-raistrickindole A (3.01)	307
Figure B.91. Comparison of ^1H NMR data for natural and synthetic (+)-raistrickindole A (3.01)	308
Figure C.01. ORTEP drawing of tetramic acid 2.51	310
Figure C.02. ORTEP drawing of DMB-tetramic acid 2.54	317
Figure C.03. ORTEP drawing of tetramic acid (enol tautomer) 2.56	324
Figure C.04. ORTEP drawing of oxime 2.57	344
Figure C.05. ORTEP drawing of oxime 2.63	352
Figure C.06. ORTEP drawing of NDA adduct 3.46	362
Figure C.07. ORTEP drawing of epoxide 3.52	371
Figure C.08. ORTEP drawing of alcohol 3.63	393
Figure C.09. ORTEP drawing of intermolecular NDA adduct 3.67	411

LIST OF SCHEMES

Scheme 1.10. Installation of the <i>N</i> - <i>O</i> bond in Kerr's synthesis of (\pm)-phyllantidine	4
Scheme 1.11. Ring expansion to hydroxamic acids by King and co-workers.....	5
Scheme 1.12. Original retrosynthetic analysis of (\pm)-phyllantidine	6
Scheme 1.13 Regioselectivity shown in the literature	6
Scheme 1.14. Ring expansion of a TBS-alcohol substrate	7
Scheme 1.15. Effects of a tertiary alcohol on regioselectivity	8
Scheme 1.16. Proposed mechanism for formation of spirocycle 1.37	9
Scheme 1.17. Unsubstituted control experiment	10
Scheme 1.18. Ring expansion of acetonide substrate	12
Scheme 1.19. Formation of acyloxy nitroso 1.49 as a single diastereomer.....	13
Scheme 1.20. Successful formation of the desired hydroxamic acid as a single regioisomer	16
Scheme 2.10. Common approaches toward 2,5-DKPs	20
Scheme 2.11. Brown's observed thermal fragmentation of an <i>N</i> -oxy-2,5-DKP	21
Scheme 2.12. Williams' synthesis of aspirochlorine	22
Scheme 2.13. Ottenheijm's observations of <i>N</i> - <i>O</i> bond lability	23
Scheme 2.14. <i>N</i> - <i>O</i> bond cleavage in Liu's attempts to functionalize arylidene-DKPs	24
Scheme 2.15. Baran's early attempts toward sarcodonin	25
Scheme 2.16. Extending the ring expansion to <i>N</i> -oxy-2,5-DKPs.....	27
Scheme 2.17. Keto-enol tautomerism in tetramic acids and metal complexation	29
Scheme 2.18. Two common approaches toward functionalized tetramic acids	31
Scheme 2.19. Efficient enantioselective preparation of chiral tetramic acids	34
Scheme 2.20. Preparation of <i>N</i> -protected, benzyl-substituted oxime for ring expansion..	38
Scheme 2.21. Regioselective ring expansion to <i>N</i> -oxy-2,5-DKP	40
Scheme 2.22. Mechanism of desired DKP and major by-product formation.....	41
Scheme 2.23. Preparation of a PMB-substituted DMB-protected oxime	43
Scheme 2.24. Ring expansion to PMB-substituted DMB-protected DKP	44
Scheme 2.25. Preparation of a CF ₃ -substituted DMB-protected oxime	45
Scheme 2.26. Ring expansion to CF ₃ -substituted DMB-protected DKP.....	46
Scheme 2.27. Oxidation of C5-substituted substrate	46
Scheme 2.28. Formation of C3- and C5-substituted oxime 2.74	47
Scheme 3.10. Retrosynthetic analysis for (+)-raistrickindole A utilizing the ring expansion	78
Scheme 3.11. Formation of a functionalized oxime, precursor to the ring expansion	79
Scheme 3.12. Intramolecular NDA reactions in the literature.....	82
Scheme 3.13. Plan to access (+)-raistrickindole A <i>via</i> an intramolecular NDA.....	83
Scheme 3.14. Synthesis of known cyclopentadiene adduct.....	84
Scheme 3.15. Synthesis of retro Diels-Alder/NDA sequence precursor	85
Scheme 3.16. Synthesis of Bn-protected allyl ester.....	86

Scheme 3.17. Attempt to synthesize alternative retro Diels-Alder/NDA precursor	87
Scheme 3.18. Retrosynthetic analysis featuring an intramolecular NDA	88
Scheme 3.19. Preparation of NDA precursor	89
Scheme 3.20. Possible side reactions in the unprotected system.....	91
Scheme 3.21. Revised retrosynthesis for intramolecular NDA at lower oxidation	92
Scheme 3.22. Synthesis of known Ts-protected hydroxamic acid	93
Scheme 3.23. Formation of tetracycle and epoxide intermediates	94
Scheme 3.24. Failure to advance the opened cyclic urethane.....	96
Scheme 3.25. Retrosynthesis for (+)-raistrickindole A featuring an intermolecular NDA	97
Scheme 3.26. Regio- and diastereoselective rationale for intermolecular NDA	98
Scheme 3.27. Selectivity in our system for the proximal NDA product	100
Scheme 3.28. Successful intermolecular NDA and confirmation of relative stereochemistry.....	101
Scheme 3.29. Completion of (+)-raistrickindole A	103
Scheme 3.30. Proposed formation of (-)-haenamindole from (+)-raistrickindole A	107

LIST OF TABLES

Table 1.10. The effect of different conditions on regiochemical outcome	15
Table 2.10. Optimization of base-mediated cyclization to 2.50	36
Table 2.11. Oxidation of oxime to acyloxy nitroso intermediate 2.58	39
Table 2.12. Ring expansion of acyloxy nitroso 2.58 to <i>N</i> -oxy-2,5-DKP 2.59	40
Table 3.10. Failed attempts to oxidize oxime 3.05 to acyloxy nitroso intermediate 3.04	80
Table 3.11. Attempts to effect the intramolecular NDA.....	90
Table 3.12. NDA reaction to tetracycle 3.46	93
Table 3.13. Attempts to open cyclic urethane 3.52	95
Table 3.14. Comparison of ^1H NMR shifts - natural and synthetic (+)-raistrickindole A	105
Table C.10. Crystal data and structure refinement for tetramic acid 2.49	311
Table C.11. Atomic coordinates and equivalent isotropic displacement parameters for tetramic acid 2.49	312
Table C.12. Bond lengths and angles for tetramic acid 2.49	313
Table C.13. Anisotropic displacement parameters for tetramic acid 2.49	315
Table C.14. Hydrogen bonds for tetramic acid 2.49	316
Table C.15. Crystal data and structure refinement for DMB-tetramic acid 2.52	318
Table C.16. Atomic coordinates and equivalent isotropic displacement parameters for DMB-tetramic acid 2.52	319
Table C.17. Bond lengths and angles for DMB-tetramic acid 2.52	320
Table C.18. Anisotropic displacement parameters for DMB-tetramic acid 2.52	323
Table C.19. Crystal data and structure refinement for benzyl tetramic acid 2.54	325
Table C.20. Atomic coordinates and equivalent isotropic displacement parameters for benzyl tetramic acid 2.54	326
Table C.21. Bond lengths and angles for benzyl tetramic acid 2.54	328
Table C.22. Anisotropic displacement parameters for benzyl tetramic acid 2.54	336
Table C.23. Hydrogen coordinates and isotropic displacement parameters for benzyl tetramic acid 2.54	338
Table C.24. Torsion angles for benzyl tetramic acid 2.54	340
Table C.25. Hydrogen bonds for benzyl tetramic acid 2.54	343
Table C.26. Crystal data and structure refinement for oxime 2.55	345
Table C.27. Atomic coordinates and equivalent isotropic displacement parameters for oxime 2.55	346
Table C.28. Bond lengths and angles for oxime 2.55	347
Table C.29. Anisotropic displacement parameters for oxime 2.55	351
Table C.30. Crystal data and structure refinement for oxime 2.60	353
Table C.31. Atomic coordinates and equivalent isotropic displacement parameters for oxime 2.60	354

Table C.32. Bond lengths and angles for oxime 2.60	355
Table C.33. Anisotropic displacement parameters for oxime 2.60	360
Table C.34. Hydrogen coordinates and isotropic displacement parameters for oxime 2.60	361
Table C.35. Crystal data and structure refinement for NDA adduct 3.46	363
Table C.36. Atomic coordinates and equivalent isotropic displacement parameters for NDA adduct 3.46	364
Table C.37. Bond lengths and angles for NDA adduct 3.46	365
Table C.38. Anisotropic displacement parameters for NDA adduct 3.46	369
Table C.39. Hydrogen coordinates and isotropic displacement parameters for NDA adduct 3.46	370
Table C.40. Crystal data and structure refinement for epoxide 3.52	372
Table C.41. Atomic coordinates and equivalent isotropic displacement parameters for epoxide 3.52	373
Table C.42. Bond lengths and angles for epoxide 3.52	375
Table C.43. Anisotropic displacement parameters for epoxide 3.52	383
Table C.44. Hydrogen coordinates and isotropic displacement parameters for epoxide 3.52	385
Table C.45. Torsion angles for epoxide 3.52	387
Table C.46. Hydrogen bonds for epoxide 3.52	392
Table C.47. Crystal data and structure refinement for alcohol 3.63	394
Table C.48. Atomic coordinates and equivalent isotropic displacement parameters for alcohol 3.63	395
Table C.49. Bond lengths and angles for alcohol 3.63	397
Table C.50. Anisotropic displacement parameters for alcohol 3.63	404
Table C.51. Hydrogen coordinates and isotropic displacement parameters for alcohol 3.63	406
Table C.52. Torsion angles for alcohol 3.63	408

LIST OF ABBREVIATIONS

AcOH	acetic acid
aq.	Aqueous
Boc	<i>tert</i> -Butoxycarbonyl
cat.	catalytic
Cbz	benzyloxycarbonyl
CDCl ₃	deuterated chloroform
CDI	1,1'-carbonyldiimidazole
COSY	correlated spectroscopy
DEPT	distortionless enhancement by polarization transfer
DBU	1,8-diazabicyclo[5.4.0]undec-7-ene
DCM	dichloromethane/methylene chloride
DIBAL-H	diisobutylaluminum hydride
DKP	2,5-diketopiperazine
DMB	3,4-dimethoxybenzyl
DMAP	4-(dimethylamino)pyridine
DMDO	dimethyldioxirane
DMSO	dimethyl sulfoxide
DMP	Dess-Martin periodinane
EC ₅₀	maximal effective concentration
EtOAc	ethyl acetate
Fmoc	fluorenylmethoxycarbonyl
FTIR	Fourier-transform infrared spectroscopy
hex	hexanes
HMBC	heteronuclear multiple bond correlation
HNO	nitroxyl/oxidanimine
HOMO	highest occupied molecular orbital
HRMS	high-resolution mass spectrometry
HSQC	heteronuclear single quantum correlation <i>hv</i> irradiation by light
HWE	Horner-Wadsworth-Emmons
IC ₅₀	half maximal inhibitory concentration
IPA	isopropyl alcohol/isopropanol
IPCF	isopropylchloroformate
LUMO	lowest unoccupied molecular orbital
MeCN	acetonitrile
MeOD	deuterated methanol (d ₄)
MeOH	methanol
MS	molecular sieves
NBS	<i>N</i> -bromosuccinimide
NDA	nitroso Diels-Alder
NMR	nuclear magnetic resonance
<i>N</i> -O	nitrogen-oxygen
Ns	4-nitrobenzenesulfonyl
PIDA	(diacetoxyiodo)benzene

ppm	parts per million
PPTS	pyridinium <i>p</i> -toluene sulfonate
py	pyridine
rt	room temperature (approx. 23 °C)
sat.	saturated solution
TBAF	<i>tetra</i> -Butylammonium fluoride
TBS	<i>tert</i> -Butyldimethylsilyl
TBTU	2-(1H-Benzotriazole-1-yl)-1,1,3,3-tetramethylaminium tetrafluoroborate
<i>t</i> -Bu	<i>tert</i> -Butyl
THF	tetrahydrofuran
TLC	thin-layer chromatography
Ts	4-toluenesulfonyl
UPLC	ultra-performance liquid chromatography
UV	ultraviolet
μw	microwave irradiation

ACKNOWLEDGMENTS

The words “By Him All Things Are Made” are carved into the Baylor Sciences Building, just above the beautiful Corinthian pillars on the D-wing. Every time I walk or drive by, those words inspire me. They serve as a constant reminder that through God all things are possible, and only through Him we are blessed with the ability to make natural products. I am grateful and forever humbled by God’s work, and I owe everything that I am to Him, “and let us not grow weary of doing good, for in due season we will reap, if we do not give up.” – Gal 6:9

I graciously thank Professor John L. Wood for his unwavering support, trust, and influence. I am so blessed to have spent four years under your tutelage, and I look forward to the future you helped prepare me for. Those who get to know you as an advisor and friend are truly blessed by your wisdom and loyalty, and I thank you for all of your great advice, for every time you pushed me to expand my limits, every time you told me to keep my chin up, and the countless times you helped me back up when I got knocked down, even when you didn’t know it. You have always rewarded my trust and dedication with honesty, guidance, and your unique sense of humor, and I am forever grateful. I hope that you will always be a part of my life.

I thank my committee members: Professor John L. Wood, Professor Daniel Romo, Professor Kevin G. Pinney, Professor Caleb D. Martin, and Professor Rebecca J. Sheesley for their generous support and patience throughout my graduate studies. I enjoyed getting to know you all, and I humbly thank you for trusting me as a viable candidate.

I thank my family for their love and support during this difficult journey. Every passing day through Christ we become better and stronger, together. Thank you, Mom, for being the bravest and strongest person I'll ever know. For your endless love and patience, and especially for your kindness and understanding during these difficult years. Thank you, Dan, for being a free spirit and for teaching me to have faith that everything will turn out fine. I continually find comfort in the fact that, no matter what happens, I will always have you by my side. Thank you, Dad, for teaching me everything I know and for inspiring me to be brave in hardship. It is both a blessing and a curse that I am just like you in every way. I love you all so much and I am "greatly beloved" because of you.

I thank Alex and the Aulds family for bringing me closer to God every day, and for being the ones that I look up to as an example of the bravest, most honest and resilient God-fearing people that everyone should aspire to be. The best part of living in Texas was when God brought you into my life, Alex, and my life is so much better because you're in it.
11:11...

I thank Evan Woods for his unrelenting support and for being my center for joy and laughter during the most difficult years of my life. It's been a blessing to learn and grow beside you and Tiberius, and the many fond memories of our adventures together is what keeps me going every day. For your love and kindness, you and your family will always hold a special place in my heart.

I thank Dr. Jeff Gustafson for mentoring me in his lab during my most formative years, and for persuading me to go to graduate school. My life has become everything I've ever wanted and more, and I couldn't have realized that without your support. You have always believed in me, even in times when I struggled to believe in myself.

I thank Dr. Andrew Dinh and Dr. Mariel Cardenas for taking me under their wing and teaching me everything I know in the lab. You're both the most patient, kind-hearted, and ambitious people I have ever met, and you continue to inspire me every day.

I thank Claire and Ricky Jackson for sponsoring me in my journey toward Confirmation in the Catholic Church, a step in my faith which has meant the world to me.

I thank the members of the W6, past and present. I love everything this group stands for, everything it's been through, and the great chemists who have come out of it. Thank you for your friendship, support, and guidance, as well as the many laughs we've shared while going through the ringer together. I know that you will all go on to be incredibly successful and find much pride and reward in your work, and God will bless you because of your perseverance.

I thank Bean for being such a loyal and affectionate companion. You are always there to comfort me, and you have always been the best listener. Your bright, loyal, patient, and mischievous personality brings unremitting joy to my life. I've never known an animal who could love so big.

I'd like to thank every woman in chemistry who came before me, as well as those who helped pave the way for women to be able to thrive in science. I am wholeheartedly dedicated to this mission, and it is only because of their strength, bravery, and perseverance that I am able to make my way in this world.

Lastly, I'd like to thank Wilhelm Conrad Röntgen who discovered X-ray exactly 100 years before I was born. On the evening of November 8th, 1895, he created the first "röntgenogram" produced by the impact of cathode rays on a material object (and later on his wife's wedding ring-adorned hand). He was known to be amiable and empathetic, and

was a great mountaineer who often got himself into dangerous situations, attributes that I can closely identify with. Because of his noble pursuits, I have had the pleasure of immersing myself in the art of X-ray crystallography, and I continue to be inspired by his words, true to form, “I didn’t think, I investigated.”

To my family

CHAPTER ONE

Development of a Ring Expansion Approach Toward the Core of (\pm)-Phyllantidine

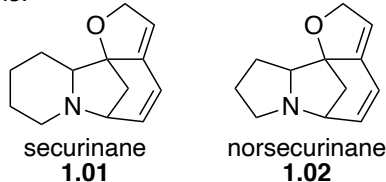
1.1 Background

1.1.1 The Securinega Alkaloids

The securinega alkaloids are isolated from Euphorbiaceae plants (of the *Flueggea*, *Margaritaria*, *Phyllanthus*, and *Securinega* genera), which have been used in traditional medicine in the Americas, Africa, and Asia to treat ailments such as indigestion, rheumatism, liver and kidney problems, malaria, and diabetes. They have captivated chemists for decades, and for good reason: it is a rich family of natural products with over 70 isolated compounds containing unique bridged tetracyclic or pentacyclic cores.^{1,2} Their diverse and complex molecular architecture, in conjunction with their potent biological activities, has made them very attractive targets for drug development.

The names of the securinega alkaloids are derived from the two prevalent parent skeletons: securinane (**1.01**) and norsecurinane (**1.02**, Figure 1.10). A few natural products that possess these patterns are (-)-securinine (**1.03**), (-)-allosecurinine (**1.04**), and (-)-norsecurinine (**1.05**).

Parent Skeletons:



Selected Representative Alkaloids:

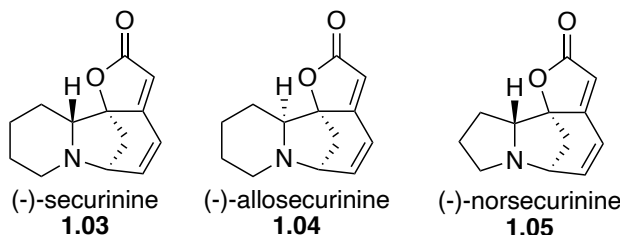


Figure 1.10. Parent skeletons and selected examples of securinega alkaloids.

The subtle structural complexity of the securinega alkaloids has inspired more than twenty publications aimed at their preparation, with the first successful total synthesis of parent compound securinine (**1.03**) reported in 1967.³ Since then, an abundance of methods and strategies have derived from efforts focused on preparing this family of natural products.¹

A unique subset of the securinega alkaloids is comprised of congeners containing an embedded nitrogen-oxygen (*N*-*O*) bond (Figure 1.11). The lack of syntheses reported on *N*-*O* bond-containing securinega alkaloids, versus the relative abundance of syntheses reported for related alkaloids, supports the notion that there is relatively limited knowledge on how to install *N*-*O* bonds within complex polycyclic systems. This additional synthetic challenge renders this subset a more daunting target.

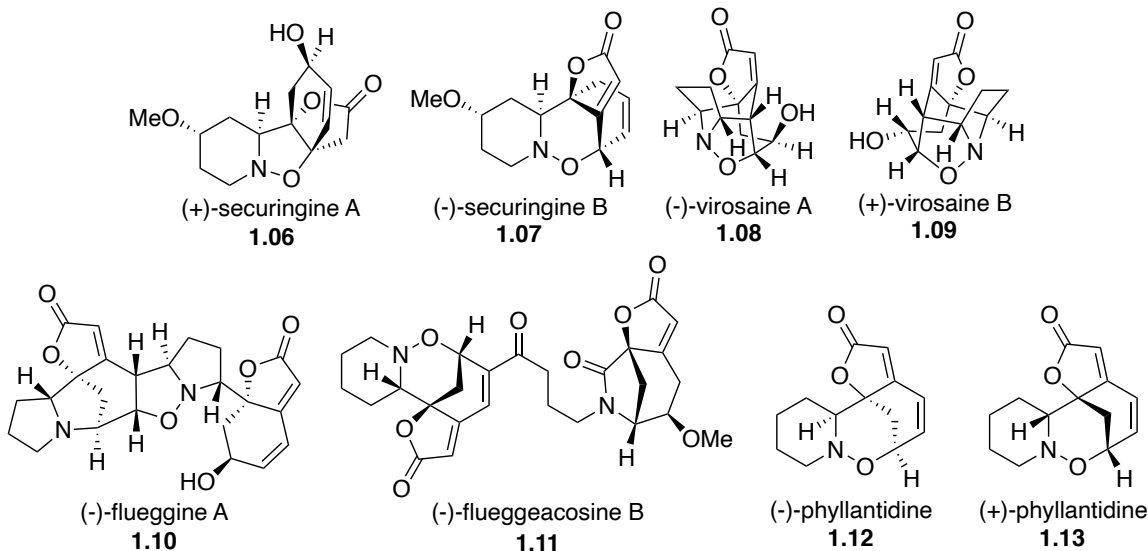


Figure 1.11. Selected *N*-*O* bond-containing securinega alkaloids.

1.1.2 Isolation of (\pm)-Phyllantidine

Phyllantidine (or “phyllanthidine”) was isolated in 1965 by Parelo and Munavalli from the root bark of *Phyllanthus discoides*.⁴ The discrepancy in its name arises from the interchangeable use of the plant genus it was derived from: *phyllanthus/phyllantus*. During these initial studies, with rudimentary characterization data, it was described only as an “oxidation product” of allosecurinine (1.04, Figure 1.10). The structure was finally assigned to that of (-)-phyllantidine (1.12) in 1972⁵ via ^1H NMR, UV-Vis, and chemical degradation studies. The enantiomer, (+)-phyllantidine (1.13), was isolated twenty years later from the leaves of *Breynia coronata*.⁶

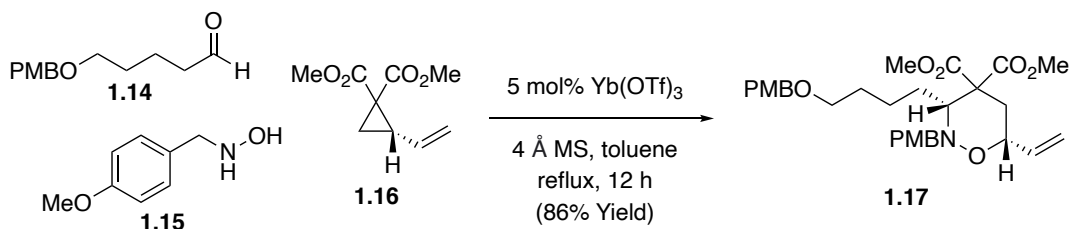
The structure of phyllantidine is comprised of a unique oxazabicyclo[3.3.1]nonane core and a tetrahydro-1,2-oxazine ring, and is thought to be derived from the amino acids tyrosine and lysine.⁷ Phyllantidine is biologically active in its own right, exhibiting selective leishmanicidal toxicity by hindering the growth rate of promastigotes and amastigotes by 67.68% (IC_{50} 353 μM) and 83.96% (IC_{50} 210 μM), respectively. It also

exhibits anti-inflammatory properties, supported by evidence of activity in lipopolysaccharide-stimulated murine microglial BV-2 cells (IC_{50} 12.1 μ M).⁸

1.2 Total Synthesis of (\pm)-Phyllantidine

1.2.1 Previous Syntheses of (+)-Phyllantidine

Although phyllantidine was isolated nearly 60 years ago, there has only been one reported synthesis.⁹ Notably, this synthesis by Kerr and co-workers employs a [3+3] cycloaddition of an intermediate iminium ion, generated upon condensation of **1.14** and **1.15** with cyclopropane **1.16** (Scheme 1.10). As illustrated, this rather unique strategy of installing the *N*-*O* bond was found to deliver **1.17** in excellent yield.



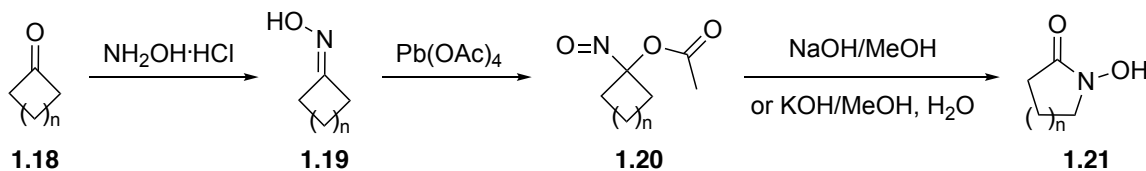
Scheme 1.10. Installation of the *N*-*O* bond in Kerr's synthesis of (+)-phyllantidine.

Given the limited accessibility of the 1,2-oxazine ring system and our general interest in the *securinega* alkaloid family of natural products,¹⁰ we sought to develop an innovative and general approach that would allow for the installation of *N*-*O* bonds embedded in densely functionalized scaffolds, such as those found in **1.13**.

1.2.2 A Ring Expansion from King and Co-workers

In our efforts to design a synthetic approach to the tetrahydro-1,2-oxazine core of phyllantidine, we considered the inherent lability of the *N*-*O* bond and thus surveyed the

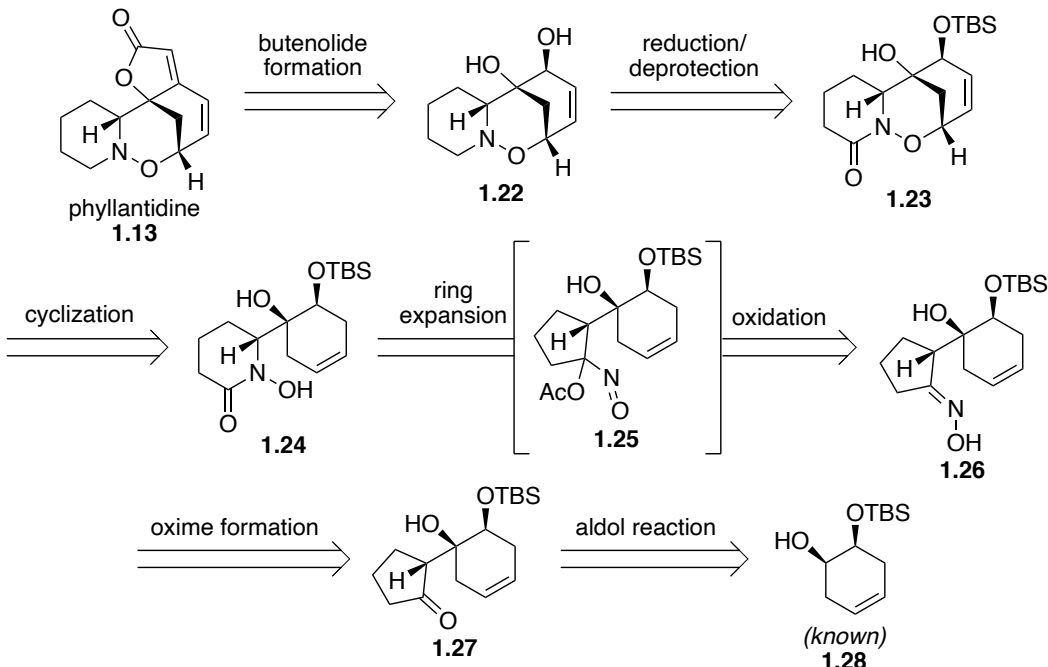
literature for mild methods which could be used to install this functionality.¹¹ During this effort, we became intrigued by an interesting and concise procedure for preparing cyclic hydroxamic acids, reported by King and co-workers in 2015 (Scheme 1.11).¹² They demonstrate that treatment of cyclopentanone and cyclobutanone oxime derivatives with Pb(OAc)₄ produces blue acyloxy nitroso intermediates, which, upon basic hydrolysis, undergo regioselective insertion of the -NOH group into the more substituted position of the ring to give cyclic hydroxamic acids in 12-81% yield. This work highlights the versatility of acyl nitroso intermediates as well as demonstrating that relatively complex molecules can be accessed through simple transformations. Given the potential of providing a mild and facile method for installing the *N*-O bond, we proposed to incorporate this strategy in our synthesis of (+)-phyllantidine.



Scheme 1.11. Ring expansion to hydroxamic acids by King and co-workers.

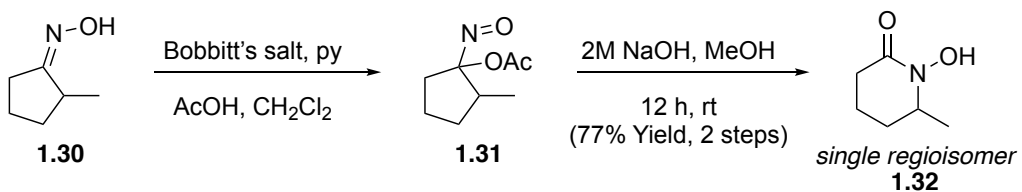
1.2.2 Retrosynthetic Analysis

We envisioned that phyllantidine could be prepared employing a strategy wherein the butanolide would be installed at a late stage from diol **1.22** (Scheme 1.12), which results from TBS-deprotection and reduction of hydroxamate **1.23**. The oxazine found in **1.23** could be derived from cyclization of hydroxamic acid **1.24** which, in turn, would result from ring expansion reaction of oxime **1.26** (through acyloxy nitroso intermediate **1.25**). Oxime **1.26** is derived from ketone **1.27**, which can be prepared from known TBS-alcohol **1.28**.¹³



Scheme 1.12. Original retrosynthetic analysis of (\pm)-phyllantidine.

The main consideration when employing the ring expansion reaction was the uncertainty of the regiochemical outcome. As consolation, we noted that King reported a non-symmetrical methyl-substituted system (Scheme 1.13)¹², and observed regioselectivity in the migration of the more substituted carbon onto the nitrogen during the ring expansion. We hoped to observe the same selectivity, as migration of the more hindered carbon would give us the desired hydroxamic acid **1.24** (correct configuration of the *N*-O bond present in the natural product).



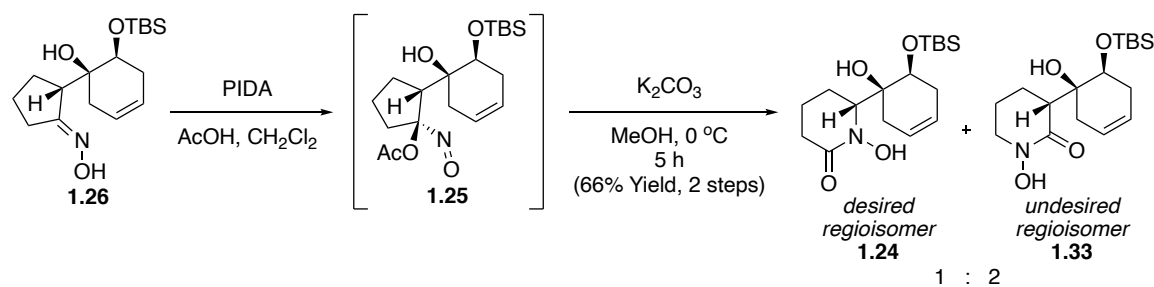
Scheme 1.13. Regioselectivity shown in the literature.

1.3 Contribution to the Ring Expansion Optimization

Given that the total synthesis of (\pm)-phyllantidine was the focus of a dissertation written by Josh Cox, this section details primarily on my efforts in the development of the ring expansion sequence (the formation of **1.24** from **1.26**) as the key step in the total synthesis of (\pm)-phyllantidine.^{14,15}

1.3.1 The TBS-alcohol Substrate

From crystalline intermediate **1.26** (Scheme 1.14), the stereochemistry of which was confirmed by X-ray analysis, we briefly screened oxidation conditions and found that treatment with (diacetoxyiodo)benzene (PIDA) in AcOH/CH₂Cl₂ co-solvent gave the best conversion to acyloxy nitroso intermediate **1.25**. The blue acyloxy nitroso compound was found to be unstable at ambient temperature, thus the crude mixture was passed through a short pad of silica gel and used immediately in the next step of the ring expansion sequence. Subsequent cleavage of the acetate group by exposure to K₂CO₃ in MeOH at 0 °C induced ring expansion to the desired hydroxamic acid **1.24**, albeit as a mixture with the undesired regioisomer **1.33** (1:2, respectively).



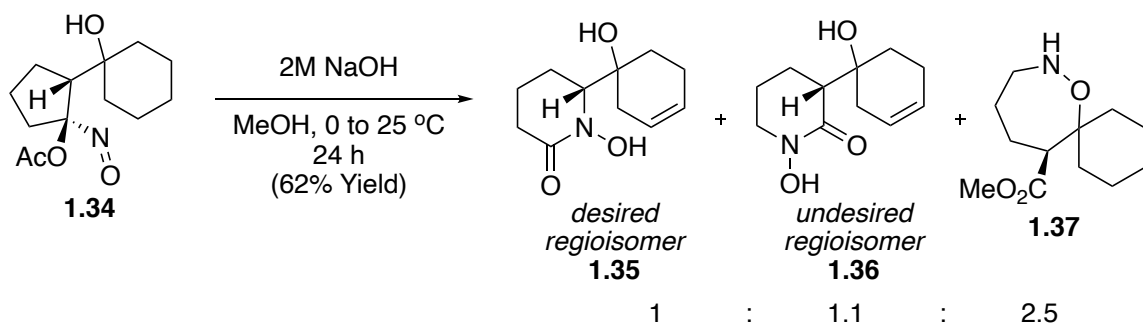
Scheme 1.14. Ring expansion of a TBS-alcohol substrate.

This result was disappointing, considering our regiochemical prediction based on King's work (Scheme 1.13) and expectation of a migratory aptitude reminiscent to that of a

Baeyer-Villiger oxidation, which also proceeds *via* selective migration of the more heavily-substituted carbon. Notably, the latter regioselectivity has been demonstrated to be influenced by stabilization of the developing carbocation, whether it be through inductive or resonance effects from adjacent functional groups.^{16,17}

1.3.2 The Tertiary Alcohol Substrate

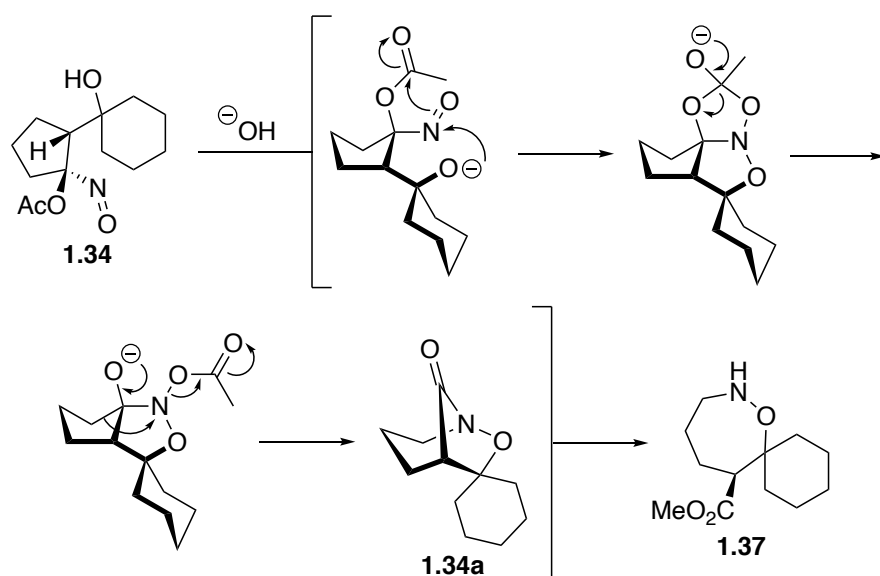
The lack of regioselectivity in our system (**1.26**) encouraged us to explore the possible negative impact of the tertiary alcohol on the ring expansion due to the inductively withdrawing nature of the oxygen. To this end, we prepared substrate **1.34**, which only contains a tertiary alcohol, and subjected it to similar conditions (2M NaOH in MeOH with warming from 0 to 25 °C) only to find that any and all modifications to the conditions yielded either an unfavorable mixture of regioisomers or regeneration of the starting ketone *via* loss of HNO, as well as the formation of an unexpected spirocycle product (**1.37**, Scheme 1.15).



Scheme 1.15. Effects of a tertiary alcohol on regioselectivity.

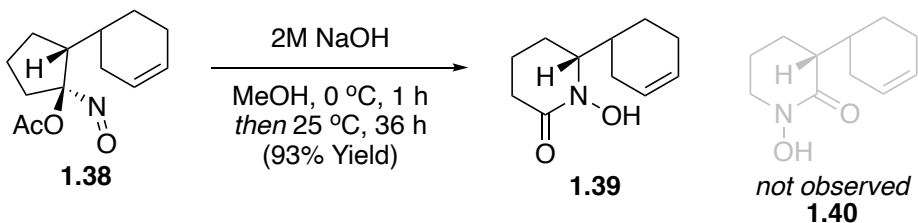
In contrast to the ring expansion of **1.25**, the tertiary alcohol-substituted system **1.34** is less sterically encumbered and thus amenable to the formation of the spirocycle (**1.37**) which, as illustrated in Scheme 1.16, likely arises from initial attack of the less sterically

encumbered tertiary alcohol onto the nitroso group, which then induces an acyl shift. This sets the stage for carbon bond migration to the proposed bicyclic **1.34a**, which undergoes methanolysis to give spirocycle **1.37**. We believe that this occurs due to the twisted conformation of the bridgehead hydroxamic ester.¹⁹ In order to prevent formation of this spirocycle by-product, we sought to increase the rate of intermolecular acetolysis of the acyloxy nitroso intermediate.



Scheme 1.16. Proposed mechanism for formation of spirocycle **1.37**.

As a control experiment, we also prepared a substrate lacking hydroxyl substitution on the cyclohexane ring (**1.38**, Scheme 1.17). As expected, in the absence of inductive effects from the oxygen, we observed only formation of the desired regioisomer wherein migration of the more hindered carbon predominates to the exclusion of the regiomeric.



Scheme 1.17. Control experiment with no substitution on the cyclohexane ring.

From the results obtained in the two model systems, it became clear that the regiochemical outcome of this reaction was heavily influenced by inductive effects. Additionally, we suspected that hydrogen bonding between the nitroso and hydroxyl moieties, as well as solvent interactions, could play a role. In any event, it was clear that overcoming the undesired regioselectivity would be a prerequisite to completing the natural product (**1.13**) *via* this strategy. To help guide these efforts, we initially elected to investigate the transformation computationally.¹⁵ Using RB3LYP/6-311 + G* calculations, we determined that in the tertiary alcohol system (**1.34**) the two transition states leading to the two different regioisomers only differ by 0.5 kcal mol⁻¹, thus a mixture of regioisomers is expected. It is also important to note that calculations regarding the formation of **1.35** and **1.36** suggested that hydrogen bonding between the tertiary alcohol and nitroso moieties were likely contributing factors in the transition states leading to both products. In contrast, the transition state energies calculated for the unsubstituted system **1.38** were found to differ by 1.9 kcal mol⁻¹ in favor of the desired regioisomer. Thus, the computations for **1.38** support the observed predominance of the regioisomer derived from migration of the more substituted carbon; however, based on the calculated energy difference one might still have expected to observe a minor amount of the regiomer. On light of the latter, we sought to investigate effects of solvent on the regiochemical outcome of the ring expansion.

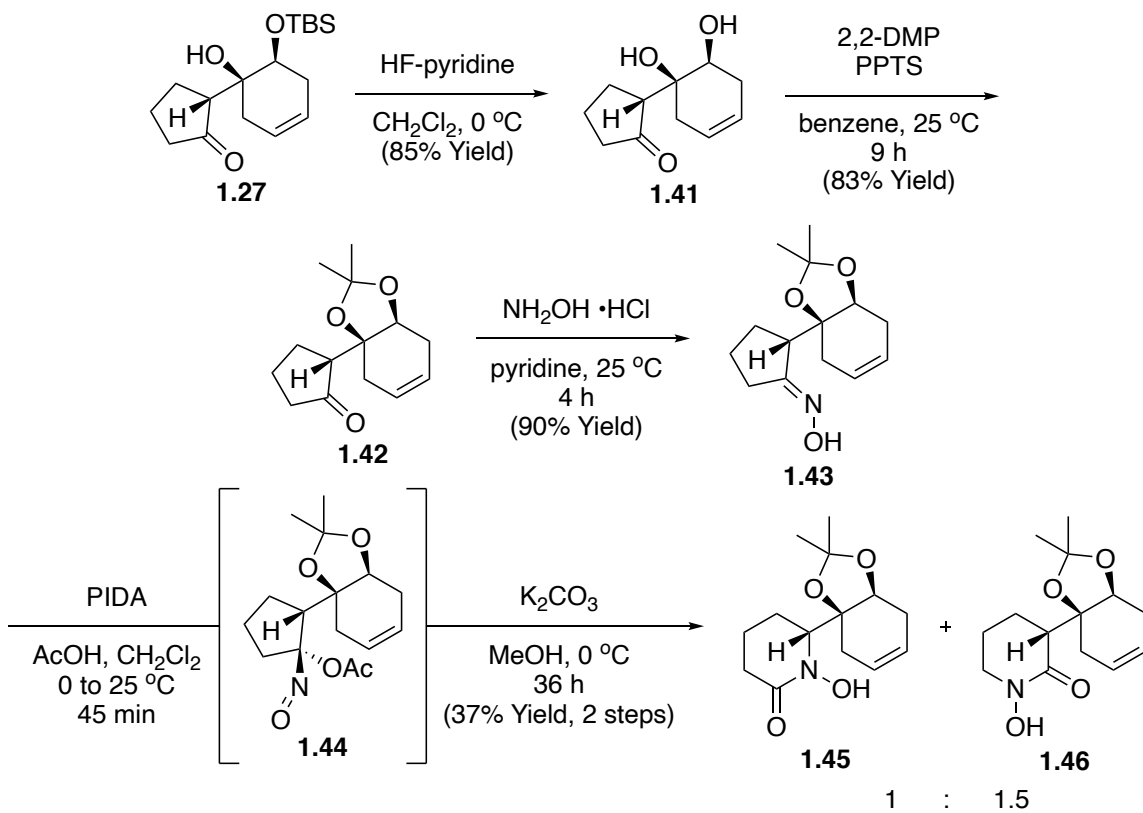
Starting materials, products, and transition states of the **1.34** and **1.38** systems were modeled using the integral equation formalism polarizable continuum model (IEFPCM) in *Gaussian 16* to model both a THF and MeOH continuum. The calculations suggest that THF has the potential of inducing greater differences in transition state energy than MeOH, and thus may lead to improved regioselectivity. Additionally, THF also has the ability to disrupt intramolecular hydrogen bonds and can thereby substantially change the hydrogen bonding patterns in the calculated transition states leading to the formation of **1.35** and **1.36**.

Based on our computational studies, exploration of solvents, and other factors that could disrupt the formation of intramolecular hydrogen bonding, could potentially influence the regiochemical outcome. We proceeded to explore different protection patterns of the β -tertiary alcohol in an attempt to investigate this hypothesis, as well as screening different solvents which could potentially result in regioselectivity in the ring expansion.

1.3.3 The Acetonide Substrate

As part of our efforts to disrupt intramolecular hydrogen bonding in the ring expansion, we sought to protect the tertiary alcohol and immediately encountered difficulty which we attributed to steric congestion. To overcome this, we turned to protecting the diol as the corresponding acetonide (**1.42**, Scheme 1.18). In order to access **1.42**, we started from TBS-alcohol **1.27**, which was readily accessible in scalable quantities from the previous sequence (Scheme 1.12). Rapid exposure of **1.27** to excess HF-pyridine gave 1,2-*syn* diol **1.41** in 85% yield, which, upon exposure to 2,2-dimethoxypropane (2,2-DMP) and pyridinium *p*-toluene sulfonate (PPTS) underwent smooth conversion to acetonide **1.42** in

83% yield (Scheme 1.18). Transformation of **1.42** to oxime **1.43** with hydroxylamine hydrochloride under standard conditions proceeded in 90% yield.



Scheme 1.18. Ring expansion of acetonide substrate.

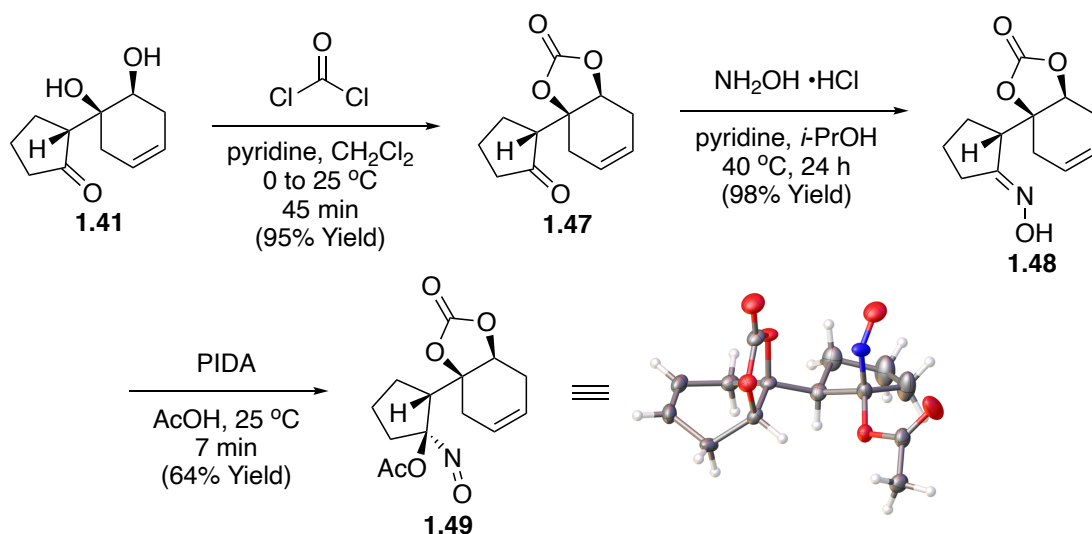
With **1.43** in hand, exposure to the established ring expansion conditions yielded the hydroxamic acid product as a mixture of regioisomers. From this result, despite having the aforementioned “problematic” tertiary alcohol protected, we deduced that intramolecular hydrogen bonding interaction of the hydroxy and nitroso moieties had only a modest effect on the regiochemical outcome.

1.3.4 The Carbonate Substrate – Successful Regiochemical Outcome

Given that our efforts were signifying that inductive effects were the likely culprit in guiding the ring expansion to the undesired regiomer, we sought to explore this notion

by preparing the corresponding carbonate (Scheme 1.19). Although the carbonyl carbon in the carbonate would be more electronegative, and perhaps further enhance the undesired inductive effect on the β -oxygen, our computational studies¹⁵ suggest that THF is able to disrupt metal-substrate coordination in carbonate systems, as opposed to the corresponding acetonides and alcohols, which is a phenomenon consistent with the known differences in Lewis basicity of acetonide and carbonate oxygens.¹⁸ Thus, although the introduction of the cyclic carbonate appears counterintuitive when one considers disrupting metal coordination, this change could potentially mitigate the inductively withdrawing nature of the oxygen.

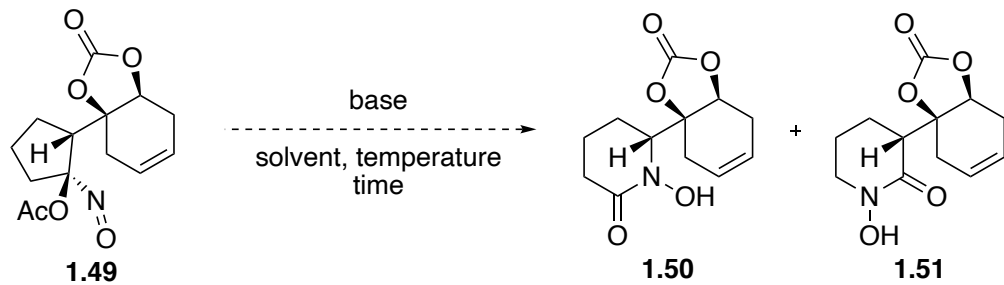
In the event, treatment of diol **1.41** with phosgene and pyridine gave the desired cyclic carbonate **1.47** in 95% yield, and subsequent treatment with hydroxylamine hydrochloride yielded oxime **1.48** in 98% yield. Oxidation with PIDA produced acyloxy nitroso **1.49** in 64% yield as a single diastereomer (confirmed by X-ray analysis, Scheme 1.19).



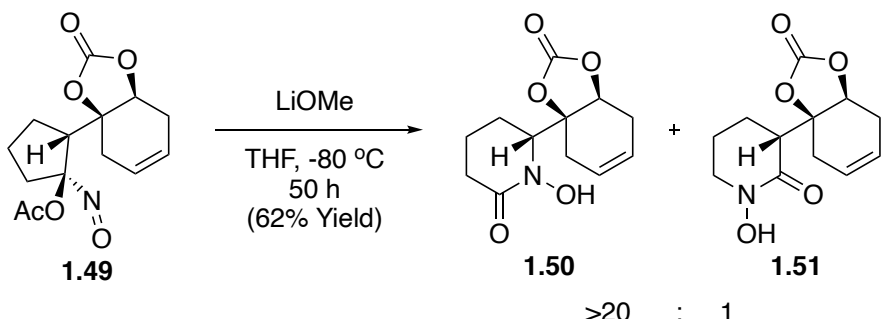
Scheme 1.19. Formation of acyloxy nitroso **1.49** as a single diastereomer.

Upon treatment of **1.49** with K₂CO₃ in MeOH, we were delighted to find that the desired regioisomer **1.50** was the major product. Guided by this outcome, as well as our computational observations,¹⁵ we conducted a brief screen of different conditions to identify whether or not there were significant effects on the regiochemical outcome of the ring expansion. Reactions were conducted on 10 mg scale in 2 mL of the given solvent, and ratios were determined by integration of signals in ¹H NMR spectra of the crude mixtures. We found that 2 equivalents of LiOMe in THF -15 °C for 45 minutes gave us the highest yield and >20:1 selectivity of the desired hydroxamic acid **1.50** over **1.51** (Scheme 1.19).

Table 1.10. The effect of different conditions on regiochemical outcome.



Entry	Base (equiv)	Solvent	Time, Temperature	Ratio 1.50:1.51
1	Na ₂ CO ₃ (1.6)	MeOH	2 h, 0 °C	1.3:1
2	K ₂ CO ₃ (1.2)	MeOH	2 h, 0 °C	2.4:1
3	K ₂ CO ₃ (1.6)	MeOH	2 h, -15 °C	5.3:1
4	CsCO ₃ (1.6)	MeOH	30 min, 0 °C	3.3:1
5	KOH (1.6)	MeOH	5 min, 0 °C	2.5:1
6	NaOH (1.6)	MeOH	5 min, 0 °C	4:1
7	LiOH (1.6)	MeOH	5 min, 0 °C	3:1
8	LiOMe (1.1)	MeOH	5 min, 0 °C	3:1
9	LiOMe (1.6)	MeOH	1 h, -15 °C	2.2:1
10	LiOMe (1.6)	THF	5 min, 0 °C	4:1
11	LiOMe (1.0)	THF	20 min, -10 °C	5.5:1
12	LiOMe (2.0)	THF	45 min, -15 °C	>20:1
13	LiOMe (5.0)	THF	2 days, -80 °C	1:0
14	LiOMe (1.6)	Et ₂ O	2 h, -15 °C	5:1
15	LiOMe (1.6)	MeCN	2 h, -15 °C	1.6:1
16	LiOMe (1.6)	CH ₂ Cl ₂	15 min, -15 °C	1:1
17	LiOMe (1.6)	toluene	1 h, -15 °C	1:1
18	LiOMe (1.6)	benzene	5 min, 10 °C	1:1
19	KOMe (1.6)	THF	5 min, -15 °C	13:1
20	NaOMe (1.6)	THF	25 min, -15 °C	6:1
21	LiOMe (1.6)	THF	45 min, -15 °C	15:1



Scheme 1.20. Successful formation of the desired hydroxamic acid as a single regioisomer.

1.4 Conclusion

Our total synthesis of (\pm)-phyllantidine features the first implementation of a ring expansion approach to install an *N*-*O* bond into the functionally-dense architecture typical of the securinega family. The sequence we reported involves the stereo-retentive conversion of a substituted cyclopentanone to a cyclic hydroxamic acid intermediate, *via* ring expansion of an acyloxy nitroso precursor. It is necessary to comment on the regiochemical outcome of this reaction: migration of the more substituted carbon onto the nitrogen during the ring expansion in our optimized system matches the observed reactivity reported by King and co-workers in their methyl-substituted ketone system. However, as we witnessed in other substrates leading up to the successful ring expansion, the presence of an inductively withdrawing oxygen substituent adjacent to the center of migration can override this effect, as well as participate in possible hydrogen bonding with the nitroso moiety, causing either opposite or a mixture of regiochemical outcomes. Evaluation of these effects *via* computational studies revealed that we could control the regiochemical outcome of the ring expansion by careful selection of solvent and substitution on the substrate, thus allowing us to obtain the desired ring expansion product as a single regioisomer and ultimately advancing it to the natural product.

1.5 References and Notes

- ¹ For comprehensive reviews on the isolation, identification, and syntheses of the securinega alkaloids see:
- (a) Wehlauch, R.; Gademann, K. *Asian J. Org. Chem.* **2017**, *6*, 1146-1159.
 - (b) Chirkin, E.; Atkatlian, W.; Poreé, F. -H. *The Alkaloids. Chemistry and Biology* (Ed.: H.-J. Knölker), Academic Press, London, **2015**, 1-120, and references therein.
 - (c) Weinreb, S. M. *Nat. Prod. Rep.* **2009**, *26*, 758-775, and references therein.
 - (d) Raj, D.; Luczkiewicz, M. *Fitoterapia* **2008**, *79*, 419, and references therein.
 - (e) Pau, B.; Felix, B; Marta, F. *Targets in Heterocyclic Systems* **2005**, *9*, 281, and references therein.
- ² For examples of dimeric, trimeric, tetrameric, and pentameric securinega alkaloids see:
- (a) Park, J.; Jeon, S.; Kang, G.; Lee, J.; Baik, M. -H.; Han, S. *J. Org. Chem.* **2019**, *84*, 1398-1406, and references therein.
 - (b) Jeon, S.; Han, S. *J. Am. Chem. Soc.* **2017**, *139*, 6302-6305, and references therein.
- ³ Horii, Z.; Hanaoka, M.; Yamawaki, Y.; Tamura, Y.; Saito, S.; Shigematsu, N.; Kotera, K.; Yoshikawa, H.; Sato, Y.; Nakai, H.; Sugimoto. N. *Tetrahedron* **1967**, *23*, 1165-1174.
- ⁴ Parello, J.; Munavalli, S.; Hebd. C. R. *Seances Acad. Sci.* **1965**, *260*, 337-340.
- ⁵ Horii, Z.; Imanishi, T.; Yamauchi, M.; Hanaoka, M.; Parello, J.; Munavalli, S. *Tetrahedron Lett.* **1972**, *13*, 1877-1880.
- ⁶ Lajis, N. H.; Guan, O. B.; Sargent, M. V.; Skelton, B. W.; White, A. H. *Aust. J. Chem.* **1992**, *45*, 1893-1897.
- ⁷ (a) Parry, R. J. *Tetrahedron Lett.* **1974**, *15*, 307.
(b) R. J. Parry, *J. Chem. Soc. Chem. Commun.* **1975**, 144-145.
(c) Parry, R. J. *Bioorg. Chem.* **1978**, *7*, 277.
- ⁸ Moraes, L. S.; Donza, M. R.; Rodrigues, A. P.; Silva, B. J.; Brasil, D. S.; Zoghbi, M.; Andrade, E. H.; Guilhon, G. M.; Silva, E. O. *Molecules* **2015**, *20*, 22157.
- ⁹ Previous total synthesis of phyllantidine: Carson, C. A.; Kerr, M. A. *Angew. Chem. Int. Ed.* **2006**, *45*(39), 6560-6563.
- ¹⁰ (a) Chen, J-H.; Levine, S. R.; Buergler, J. F.; McMahon, T. C.; Medeiros, M. R.; Wood, J. L. *Org. Lett.* **2012**, *14*, 4531-4533.
(b) Medeiros, M. R.; Wood, J. L. *Tetrahedron* **2010**, *66*, 4701-4709.

¹¹ (a) Trapencieris, P.; Strazdina, J.; Bertrand, P. *Chem. Heterocycl. Compd.* **2012**, *48*, 833-835.

(b) Bapat, J. B.; Black, D. C.; Brown, R. F. C. *Adv. Heterocycl. Chem.* **1969**, *10*, 199-240.

(c) *The chemistry of hydroxylamines, oximes and hydroxamic acids* (Eds.: Z. Rappoport, J. F. Lieberman), Wiley, Chichester, 2009.

¹² For the original reports of this interesting transformation, see:

(a) Hadimani, M. B.; Mukherjee, R.; Banerjee, R.; Shoman, M. E.; Aly, O. M.; King, S. B. *Tetrahedron Lett.* **2015**, *56*(43), 5870-5873.

(b) Banerjee, R.; King, S. B. *Org. Lett.* **2009**, *11*(20), 4580-4583.

¹³ Preparation of TBS-alcohol: O'Brien, P.; Poumellec, P. *J. Chem. Soc. Perkin. Trans. I.* **1998**, *15*, 2435-2441.

¹⁴ Cox, J. B. (**2019**) “Total Synthesis of (-)-Herquiline B and (+)-Herquiline C, Total Synthesis of (\pm)-Phyllantidine, and Synthetic Studies Toward Longercemine” [Doctoral dissertation, Baylor University], and references therein.

¹⁵ Lambert, K. M.; Cox, J. B.; Liu, L.; Jackson, A. C.; Yruegas, S.; Wiberg, K. B.; Wood, J. L. *Angew. Chem. Int. Ed.* **2020**, *59*, 9757-9766, and references therein.

Footnote: Computational analysis was done in collaboration with post-doctoral fellow Dr. Kyle Lambert, and Professor Kenneth Wiberg at Yale University.

¹⁶ (a) Renz, M.; Meunier, B. *Eur. J. Org. Chem.* **1999**, 737-750, and references therein.
(b) Moulay, S. *Chem. Educ. Res. Pract. Eur.* **2002**, *3*, 33-64, and references therein.

¹⁷ Coffen, D. L.; Katonak, D. A. *Helv. Chim. Acta* **1981**, *64*, 1645.

¹⁸ (a) Laurence, C.; Gal, J.-F. in *Lewis Basicity and Affinity Scales: Data and Measurement*, Wiley, Chichester, **2010**, 1-447, and references therein.
(b) Gruver, J. M.; Liou, L. R.; McNeil, A. J.; Ramirez, A.; Collum, D. B. *J. Org. Chem.* **2008**, *73*, 7743-7747.
(c) Brown, C. A. *J. Chem. Soc. Chem. Commun.* **1974**, 680-681.
(d) Reich, H. J. *J. Org. Chem.* **2012**, *77*, 5471-5491, and references therein.
(e) Reich, H. J.; Sikorski, W. H. *J. Org. Chem.* **1999**, *64*, 14-15.

¹⁹ Tani, K.; Stoltz, B. M. *Nature*, **2006**, *441*, 731.

CHAPTER TWO

Ring Expansion of Chiral Tetramic Acids to *N*-oxy-2,5-diketopiperazines

2.1 Background and Significance

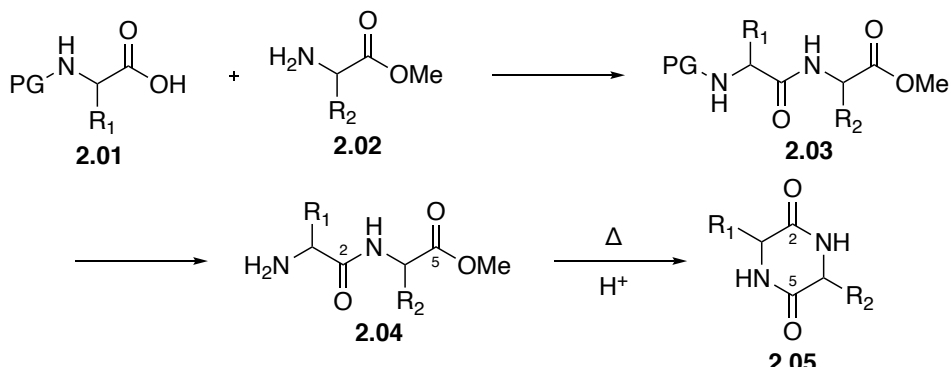
2.1.1 The 2,5-diketopiperazine Scaffold

2,5-diketopiperazines (DKPs) are found in many biologically active natural products that exhibit a broad range of activities, rendering them attractive targets in the context of drug discovery. Perhaps lending to their biological proclivities, is the tendency, as evidence from crystal structure data, of DKPs to adopt relatively rigid “clamshell” conformations in the solid state, particularly with the presence of aromatic groups on either side of the ring which lends to favorable π -stacking interactions.¹ Despite their relative abundance in nature and potential for biological activity, a search of the literature for synthetic methods providing access to DKP-containing molecules gives only limited results.

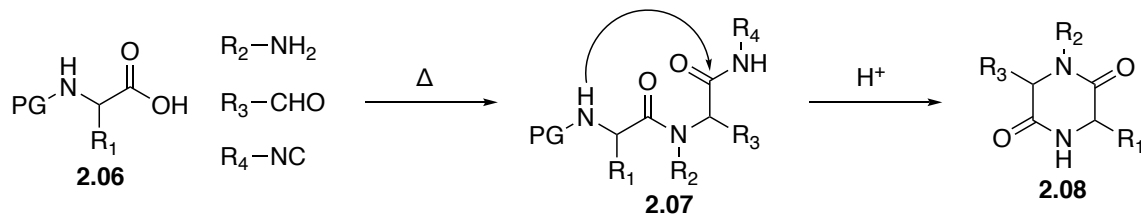
The most common approach for producing these cyclic dipeptides involves the cyclization of *N*-protected dipeptide precursors (which can either be constructed by amide coupling or fully-functionalized *via* a Ugi 4-component cyclization, Scheme 2.10) and, upon deprotection, are poised to undergo cyclization. The advantage of this approach is that it can utilize a large chiral pool of commercially-available enantiopure amino acids (Scheme 2.10),^{1,2} but in order to induce this transformation profuse heating under acidic/basic conditions is often required. The rate of reaction is also limited by sterics and the tendency of the amides to exist in extended conformations (as opposed to the necessary

s-cis conformation) which are not amenable to cyclization. Additionally, with enantioenriched substrates, these conditions also pose the risk of epimerization.

Amino Acid Condensation:



Ugi-4CR Cyclization:

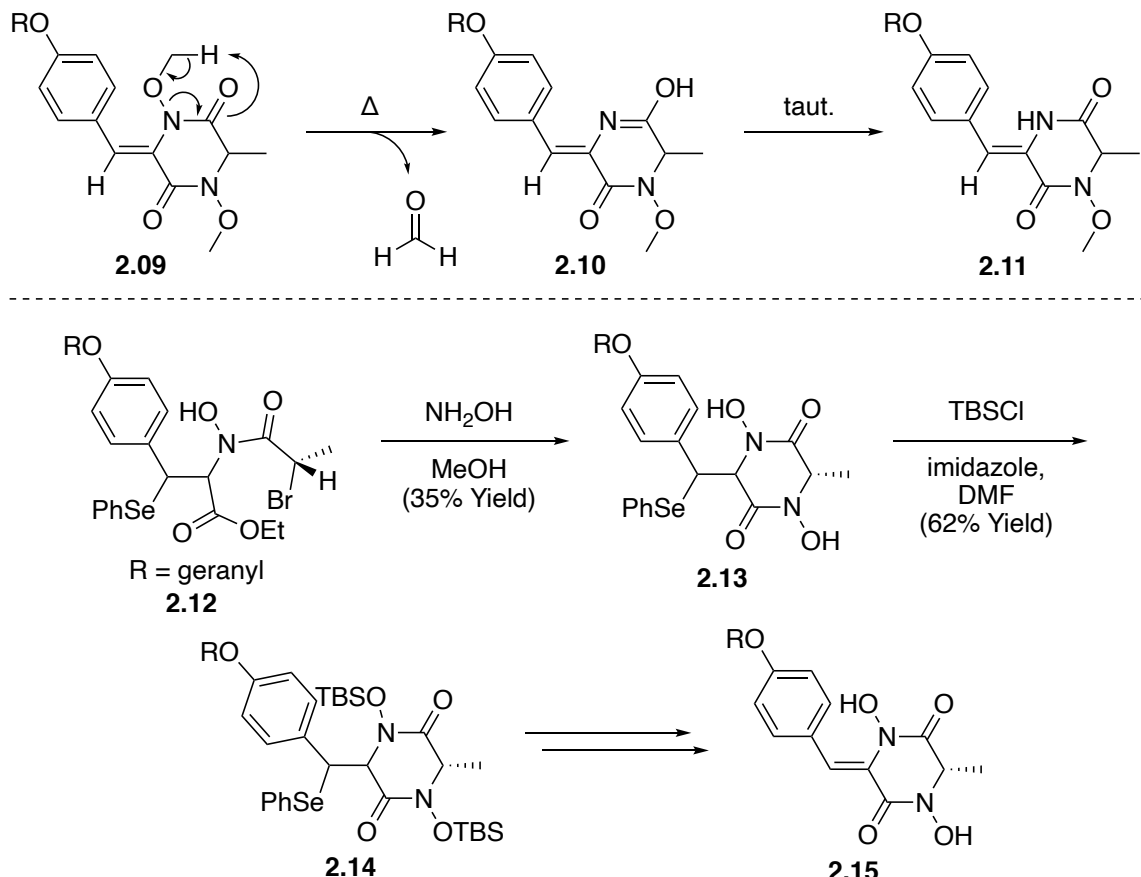


Scheme 2.10. Common approaches toward 2,5-DKPs.

2.1.2 An Interesting Subclass: *N*-oxy-2,5-diketopiperazines

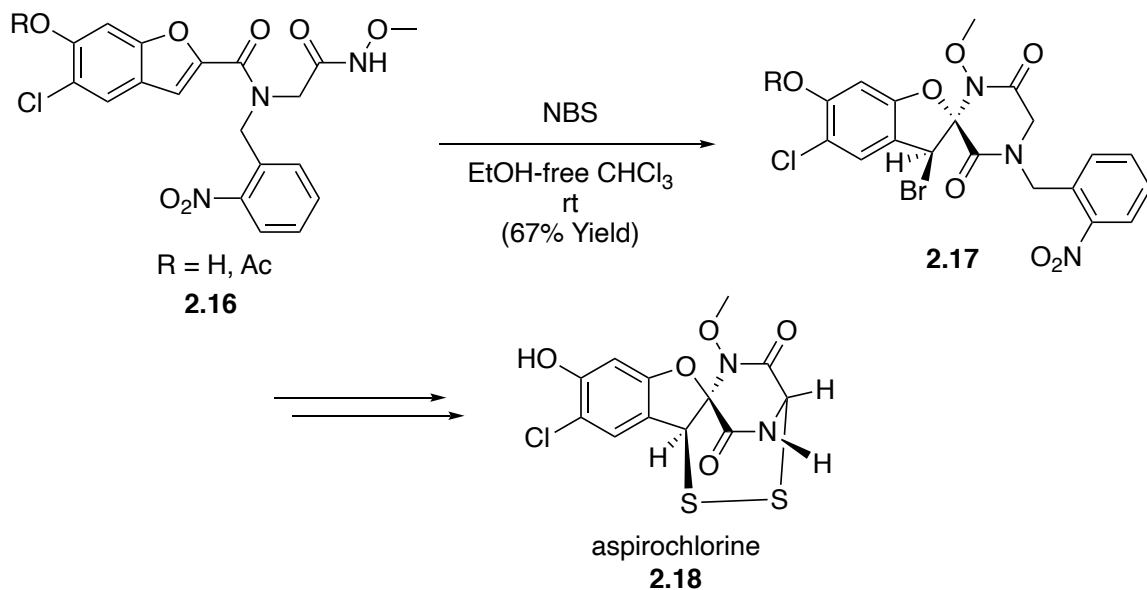
Under the category of 2,5-DKPs is an interesting subclass, *N*-oxy-2,5-DKPs, which present a unique synthetic challenge due to the presence of an *N*-O bond. There have been very few successful examples of installing this functionality and completed syntheses of molecules in this family are typically tailored around this sensitive functional group.

Brown and co-workers describe, in their efforts toward the synthesis of mycelianamide,³ the facile thermal fragmentation of an *N*-oxy-2,5-DKP intermediate into a 2,5-DKP by expulsion of formaldehyde (Scheme 2.11). Years later, they completed their target and overcame *N*-O bond cleavage by protecting this sensitive functionality, as well as avoiding the use of elevated temperature.



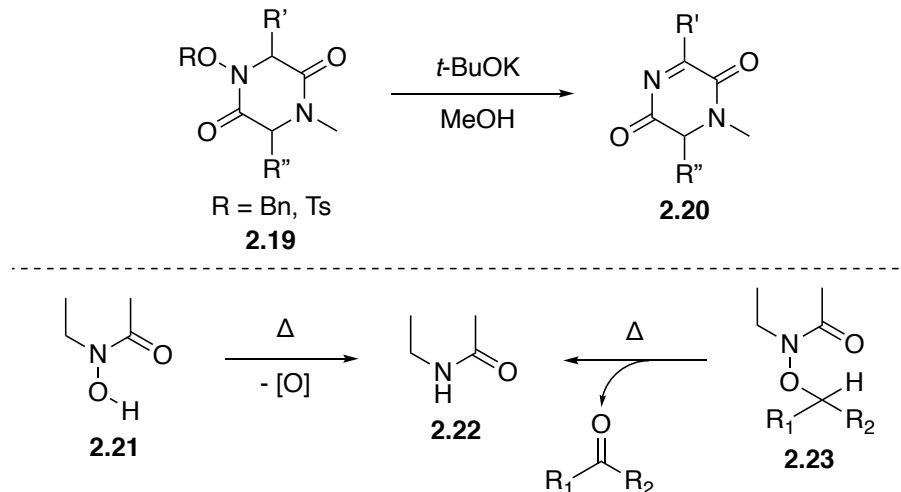
Scheme 2.11. Brown's observed thermal fragmentation of an *N*-oxy-2,5-DKP.

Aspirochlorine (Scheme 2.12), was completed by the late Robert Williams in 1993.⁴ The concise total synthesis features early cyclization to the DKP with the *N*-*O* bond already present as a methyl hydroxamate, and it is interesting to note the apparent stability of the methyl-substituted *N*-*O* bond once encapsulated in the spirocycle of the natural product.



Scheme 2.12. Williams' synthesis of aspirochlorine.

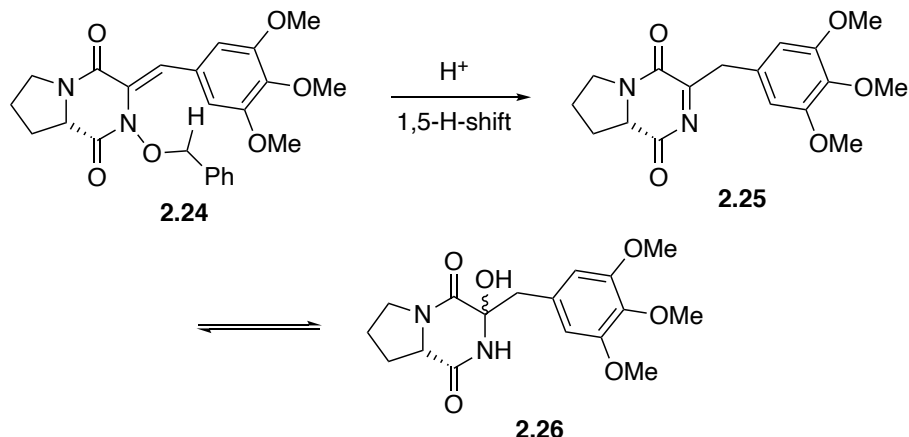
In most cases, however, it is noted that the *N*-*O* bond is prone to fragmentation and/or migration. In several reports, Ottenheijm and co-workers⁵ demonstrate the lability of *N*-*O* bonds (Scheme 2.13) under basic conditions, or thermal *N*-*O* bond cleavage (such as observed by Brown). He confirms the challenges mentioned above by saying that “...conventionally, dioxopiperazines are prepared by ring closure of the corresponding dipeptide alkyl esters [but this] approach...resisted all attempts to produce [the title compound] by ring closure. This failure can be rationalized by assuming...increased steric hindrance and decreased nucleophilicity...” He also states that “a characteristic reaction of hydroxamic acids, in particular cyclic ones, is thermal reduction to the corresponding amides.”



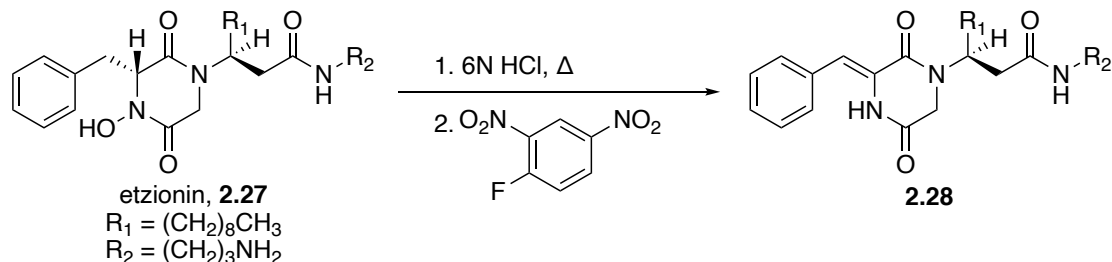
Scheme 2.13. Ottenheijm's observations of *N*-*O* bond lability.

In a similar vein, Liu and co-workers^{6a,b} report, in their attempts to functionalize a series of arylidene-DKP compounds, an interesting *N*-*O* bond fragmentation which they propose goes by way of a 1,5-hydrogen shift (Scheme 2.14) under acidic conditions. Due to this persistent occurrence, they were unable to obtain their desired targets and their paper is something of a tribute to the difficulty in synthesizing this type of functionality. Kashman and co-workers report a similar fragmentation in their isolation of the natural product etzionin, an antifungal metabolite containing an *N*-oxy-2,5-DKP scaffold. In the presence of acid at elevated temperatures, they observe cleavage of the *N*-*O* bond to give an enamine (**2.28**).^{6c}

Liu and co-workers:

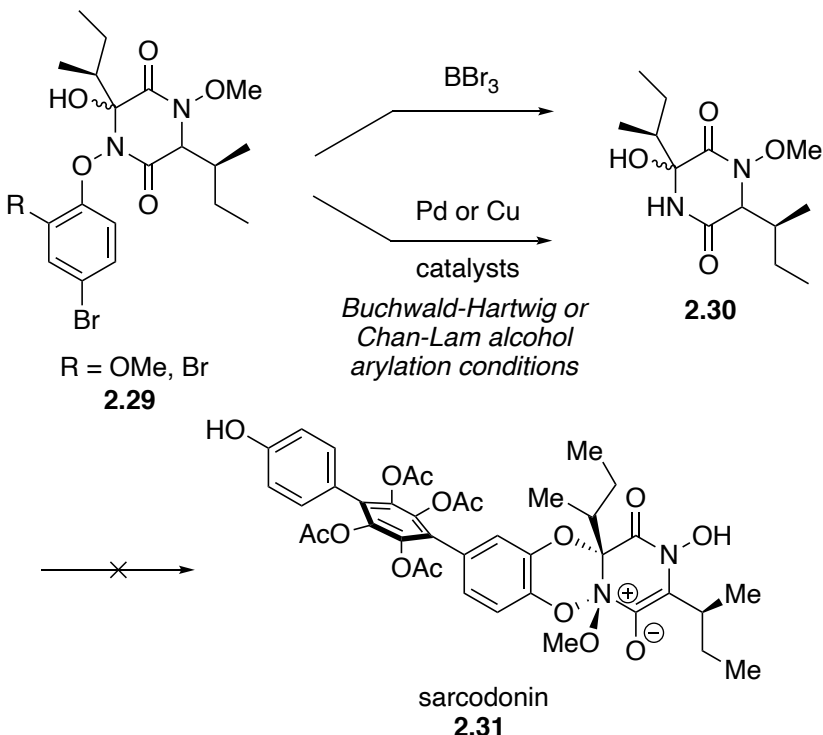


Kashman and co-workers:



Scheme 2.14. *N-O* bond cleavage under acidic conditions.

Two targets recently completed by Baran and co-worker's, sarcodonin ε and phellodonin, feature a charged variation of an *N*-oxy-2,5-DKP moiety, and their two reports⁷ on these molecules discusses the difficulty with advancing *N*-*O* bond-containing intermediates. Baran states that "...cleavage of the *N*-*O* bond was particularly facile," affirming that the synthesis of *N*-oxy-2,5-DKPs is no trivial matter. Persistent bond cleavage while trying to advance *N*-*O* bond-containing intermediates through the synthesis, such as exposure to Buchwald-Hartwig or Chan-Lam arylation conditions (Scheme 2.15), required them to amend their route and delayed the eventual completion of their targets.



Scheme 2.15. Baran’s early attempts toward sarcodonin.

Other pertinent natural products containing this functionality include the penicisulfuranol class, which contain disulfide bonds (similar to aspirochlorine) and have yet to succumb to total synthesis. Our group recently reported synthetic efforts toward this class of compounds, and therein further highlighted the challenges imposed by the *N-O* bond.⁸

Based on synthetic difficulties reported in the literature and experienced in our own laboratory, it is clear that *N*-oxy-2,5-DKPs can pose a substantial synthetic challenge. Considering, in hindsight, ways to remediate the problems faced by Brown, Ottenheijm, Liu, Kashman, and Baran, we proposed a solution which would involve late-stage incorporation of the *N-O* bond in a complex system. In the aforementioned examples, it appeared that the challenge was not in installing the *N-O* functionality, but in advancing

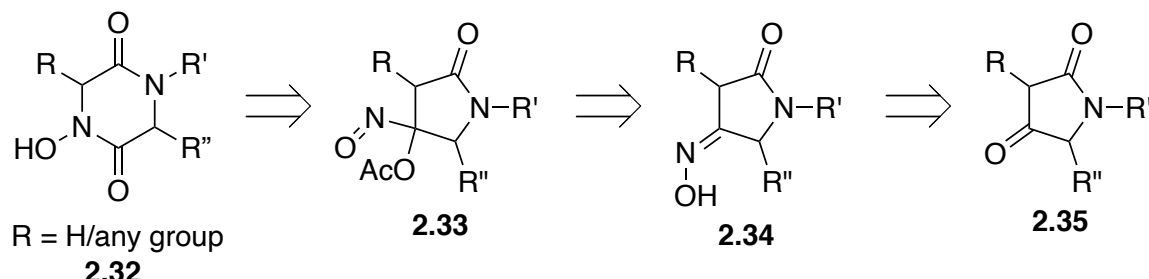
N-*O* bond-containing intermediates in the synthesis. We envisioned that a method of fully functionalizing intermediates prior to facile incorporation of the *N*-*O* bond could circumvent difficulties associated with *N*-*O* bond cleavage.

2.1.3 Extending the Ring Expansion to *N*-oxy-2,5-DKPs

Taking inspiration from our recent effort in the total synthesis of (\pm)-phyllantidine,^{9,10} which features a ring expansion sequence to install the *N*-*O* bond in a hydroxamic acid intermediate, we sought to implement a similar strategy toward the synthesis of *N*-oxy-2,5-DKPs. To this end, we envisioned a sequence that would originate from functionalized tetramic acid precursors (Scheme 2.16) and, given that tetramic acids can be prepared possessing a wide range of functionality, this unique extension of the ring expansion held the potential of providing a general synthetic solution for accessing a wide-range of structurally-complex *N*-oxy-2,5-DKPs. Of significance in this approach is the potential for installing a majority of the DKP functionality prior to revealing the *N*-*O* bond, thereby avoiding exposure of this sensitive functional group to harsh reaction conditions often employed in subsequent synthetic steps. This work would also provide general access to these types of natural products in a truly divergent manner: *N*-oxy-2,5-DKPs being derived from tetramic acid precursors that are fully-functionalizable at three different positions around the ring (e.g., R, R', and R'' in Scheme 2.16).

As described in our synthesis of (\pm)-phyllantidine, we envisioned using the same ring expansion sequence in the context of accessing *N*-oxy-2,5-DKPs. The process would begin with a fully-functionalized tetramic acid (i.e., **2.35**, Scheme 2.16), which can be accessed in a variety of ways, and progress through the formation of an oxime (**2.34**), then

oxidation to an acyloxy nitroso intermediate (**2.33**), and finally ring expansion to the cyclic six-membered *N*-oxy-2,5-DKP (**2.32**).



Scheme 2.16. Extending the ring expansion to *N*-oxy-2,5-DKPs.

2.2 Access to Functionalizable Chiral Tetramic Acids

In order to prepare *N*-oxy-2,5-DKPs using the described method (*vide supra*), we sought to develop an efficient and scalable synthesis of tetramic acids. This section includes a brief discussion of the overall bioactivity and structural diversity of tetramic acids, notable total syntheses of tetramic acid-containing compounds, and our recent development of a concise procedure that, as outlined in our *Organic Syntheses* article, provides a means for preparing scalable quantities of enantiopure tetramic acids from commercially-available amino acid esters without the need for chromatographic separation.

2.2.1 Tetramic Acids in the Context of Natural Products

The tetramic acid (pyrrolidine-2,4-dione) scaffold can be found in numerous terrestrial and marine metabolites, giving rise to many structurally-diverse natural products (selected examples in Figure 2.10) exhibiting a wide range of biological activity, and their significant characteristics have been a topic of thorough review.¹¹ The level of structural complexity of these scaffolds can vary dramatically. Predicated on their diversity and

biomedical potential, tetramic acid-containing natural products have gained more attention from the synthetic community in the last two decades.

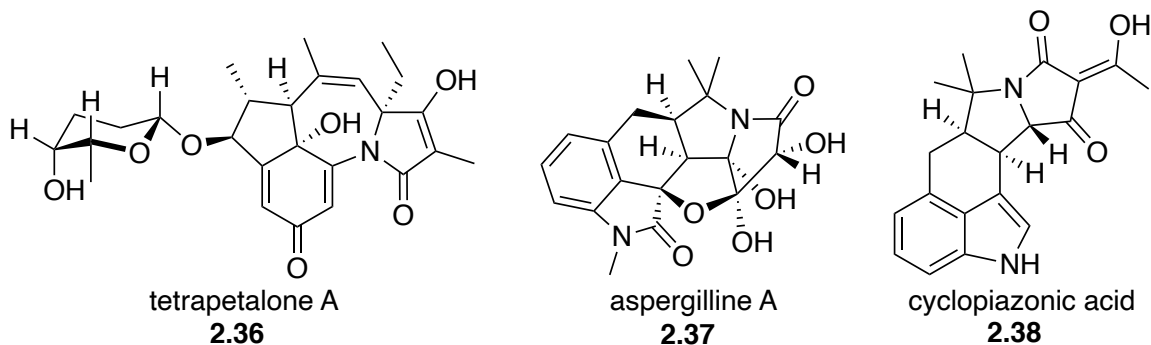
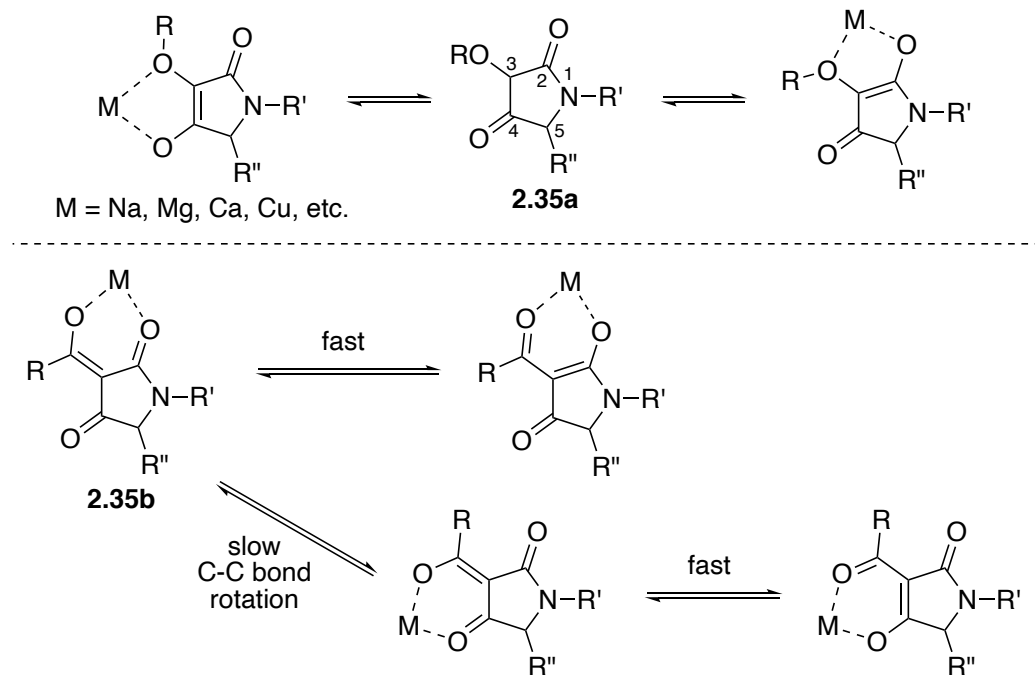


Figure 2.10. Selected tetramic acid-containing natural products.

2.2.2 Tetramic Acids as Versatile Building Blocks

The simplest tetramic acid (pyrrolidine-2,4-dione) is known colloquially as “tetramic acid,” coined in 1909 by Anschutz¹² while describing the nitrogen counterpart of tetroanic acid. Although named much earlier, tetramic acid wasn’t actually prepared synthetically until 1972, by Mulholland and co-workers.¹³ Tetramic acids can exist in either the keto form (pyrrolidine-2,4-dione) or the corresponding enolic form (4-hydroxy-3-pyrrolin-2-one), with the former being the more predominant species (Scheme 2.17, top). This propensity for tautomerism lends to the ability of certain tetramic acids to form metal-chelate complexes (Scheme 2.17, bottom), which is an important factor for transport across biological membranes. Complexes with Na, Mg, Ca, Cu, Ni, and Fe have been isolated and characterized.^{11f,14}



Scheme 2.17. Keto-enol tautomerism in substituted tetramic acids and metal complexation.

The typical reactivity around the tetramic acid ring is shown in Figure 2.11 which serves to illustrate their ability to be versatile synthetic building blocks. The cyclic lactam in general is remarkably stable, surviving exposure to strongly basic and acidic conditions without opening. It also has the unique ability to maintain a chiral center at C5 and possesses fairly acidic protons at C3.¹⁵

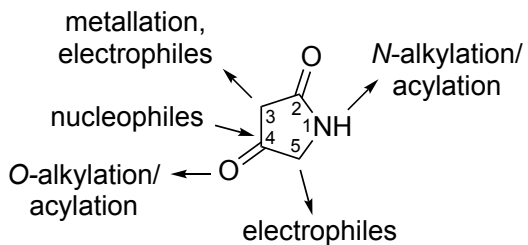
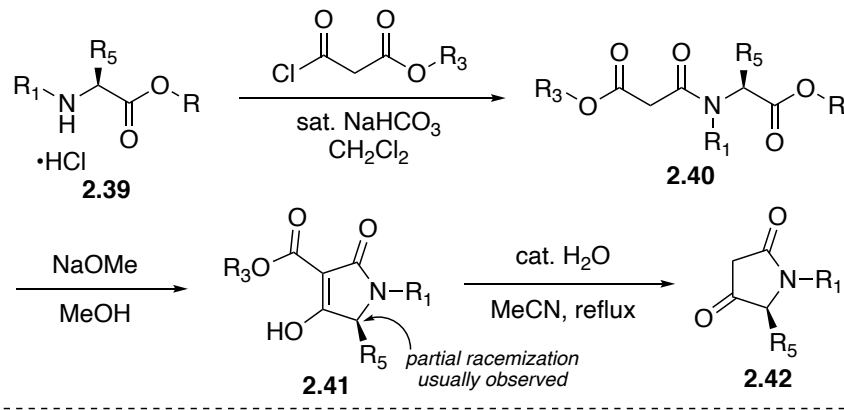


Figure 2.11. Diverse functionalization of tetramic acids.

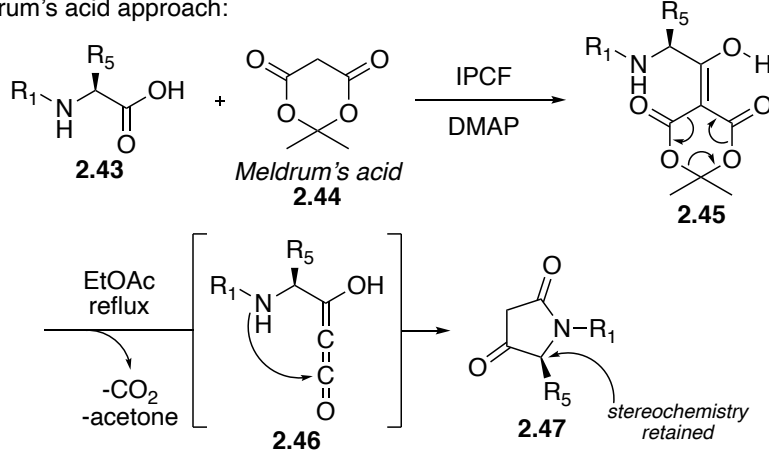
2.2.3 Functionalized Tetramic Acids in the Literature

The most traditional way to prepare tetramic acids, as often shown in the literature, is by way of a Lacey-Dieckmann cyclization (Scheme 2.18).¹⁶ Aside from being one of the first methods developed for accessing substituted tetramic acids, it is still one of the most operationally simple methods available. Acyclic precursors such as **2.40** can be prepared from commercially-available amino acid ester derivatives in high yields under Schotten-Baumann conditions,¹⁷ and subsequent cyclization upon treatment with base, such as NaOMe in methanol, and decarboalkoxylation *via* reflux in wet acetonitrile leads to the formation of tetramic acid (**2.42**). The main drawback of this method, however, is the susceptibility to racemization at C5 during the cyclization step. This is generally due to the strongly basic conditions used and has also been found to be dependent on overall reaction time,¹⁸ the identity of the substrate,¹⁹ and the type of base employed in the reaction.²⁰

Lacey-Dieckmann approach:



Meldrum's acid approach:



Scheme 2.18. Two common approaches toward functionalized tetramic acids.

To address this synthetic disadvantage, Nisato and co-workers developed a method which involves acylating Meldrum's acid (**2.44**, Scheme 2.18) with a protected chiral amino acid (**2.43**). They accomplish this by employing isopropylchloroformate (IPCF) to generate a mixed anhydride of the amino acid which then acylates Meldrum's acid in the presence of DMAP, giving a substituted derivative of the starting amino acid (**2.45**). Upon reflux in EtOAc, carbon dioxide and acetone are expelled resulting in the formation of an intermediate ketene (**2.46**). Intramolecular attack of the ketene by the amino acid nitrogen gives a nitrogen-protected tetramic acid (**2.47**). The conditions employed preclude the epimerization of C5, as no base is necessary, but the experimental procedure must be

followed stringently as slight variations in the stoichiometry or reversal of reagent addition can result in lower yields of the product.²¹ Another limitation of this approach is that the nitrogen of the amino acid must be protected, and yields can vary greatly based on the nature of the chosen protecting group (Boc, Cbz, and Fmoc most commonly used).

Direct C3 functionalization of tetramic acids is of particular interest, as this type of functionality is often present in natural products. Unfortunately, this transformation is made difficult due to the latent acidity and ambident nucleophilicity of tetramic acids. Current reports of syntheses of natural products containing tetramic acids have exhibited several creative solutions to these problems. The total syntheses of tirandamycin, by Schlessinger,²² Deshong,²³ Boeckman,²⁴ and Bartlett and co-workers,²⁵ utilize an activated phosphonate ester intermediate (chemistry developed by Ley and co-workers²⁶) in order to build the functionalized tetramic acid without epimerization. This Ley modification to the Lacey-Dieckmann cyclization was also employed in the final sequence of Miyashita's progress toward tirandalydigin.²⁷ Another unique method of functionalizing the tetramic acid core, as described in the total synthesis of indolocarbazole natural products such as K252a and staurosporine,²⁸ is the installation of a diazo moiety at the 3-position which can allow for the formation of a metal carbenoid species, effectively reversing the C3 position's latent nucleophilicity to one that is strongly electrophilic.

The use of classic Lacey-Dieckmann conditions (sodium alkoxide base in alcohol solvent) in total synthesis is not limited to the preparation of simplified tetramic acid building blocks, but rather has been used in a number of syntheses late-stage to append the tetramic acid moiety directly, such as in Laschat's and Philips' enantioselective syntheses of (+)-cyclindramide A,²⁹ Philips' synthesis of aburatubolactam A,³⁰ and more recently in

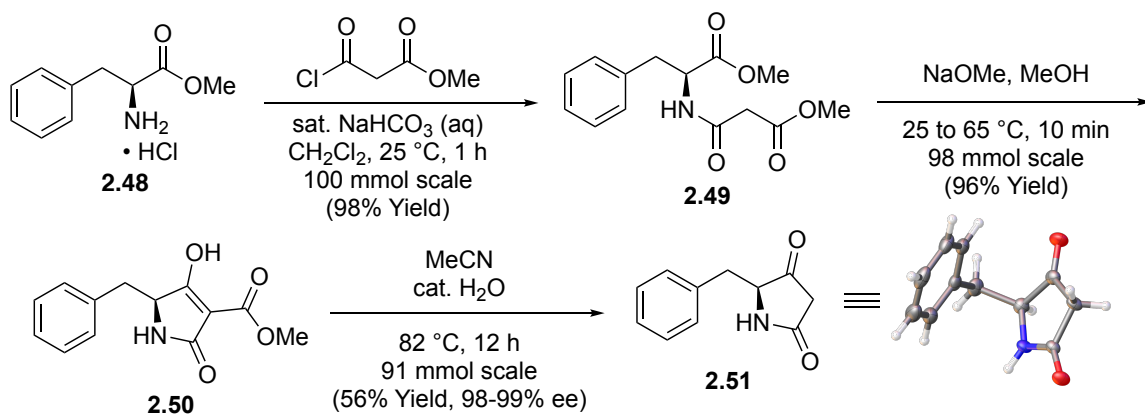
Suzuki's synthesis of macrocidin A.³¹ Likewise, the reactive C3-methylated tetramic acid moiety found in the tetrapetalones, a rare substitution pattern for tetramic acid natural products, required late installation as well as masking its acidity and reactivity as a C3 quaternary ethoxycarbonyl moiety.³² Due to the unique synthetic challenge they pose, the tetrapetalones have inspired a number of synthetic strategies to access and functionalize tetramic acids from pyrroles,³³ aldol reactions,^{34,35} a samarium diiodide-initiated cyclization,³⁶ and modified Lacey-Dieckmann cyclization conditions.³⁷ In more recent developments, Wood and co-worker's synthesis of (\pm)-aspergilline A features a unique construction of a tetramic acid moiety from a formal [3+2] cycloaddition with cyclopropanone.³⁸

2.2.4 Development of an Organic Syntheses Procedure

Given the versatility of tetramic acids as synthetic building blocks, as well as the structural diversity and biomedical potential of tetramic acid-containing natural products, investing efforts to further advance the preparation of tetramic acids appeared reasonable. With that in mind, we developed a general method of building tetramic acids in an efficient and enantioselective manner from commercially-available amino acid esters using an improved Lacey-Dieckmann cyclization, without the need for purification. We anticipate that this protocol can be used in the enantioselective preparation of natural products and other advanced systems.

The overall approach shown in Scheme 2.19 begins with commercially-available (L)-phenylalanine methyl ester hydrochloride (**2.48**), and dropwise addition of methyl malonyl chloride in saturated sodium bicarbonate/CH₂Cl₂ solution effectively delivers the desired amide **2.49** in 98% yield. This reaction was done on 100 mmol scale and does not

require purification. Thus, any variation in substitution pattern can allow for facile preparation of synthetically-useful quantities.

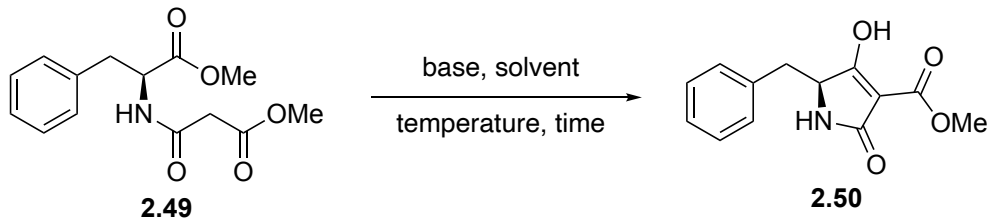


Scheme 2.19. Efficient enantioselective preparation of chiral tetramic acids.

The second step, akin to typical Lacey-Dieckmann conditions, is where our concern for loss of enantiopurity guided our optimization. In order to cyclize **2.49** into **2.50** without significant racemization, we conducted extensive screening of reaction conditions on 1 mmol scale using various bases, solvents, and temperatures (Table 2.10). Aliquots of the test reactions were taken at various time points and evaluated by UPLC analysis to determine the conversion to and enantiomeric excess of **2.50**. The use of NaOMe was beneficial for larger-scale reactions, as it avoids the necessity to sublime commercial potassium *tert*-butoxide to remove trace amounts of potassium hydroxide, and only causes minor epimerization of the C5 asymmetric center. We found that subjection to NaOMe and careful warming from 25 to 65 °C for exactly 10 minutes gave us the highest yields of the cyclized product (96% yield, **2.50**). This gave the reaction mixture just enough time to reach reflux; longer reaction times led to lower yields and degradation of the enantioenriched material. This reaction was done on 98 mmol scale and also did not require

any purification. Lastly, decarboalkoxylation of the methyl ester in wet acetonitrile at elevated temperature gave the desired C5-substituted tetramic acid in 56% yield. Upon recrystallization of the crude from hot EtOAc, we were able to obtain enantiopure tetramic acid (98-99% ee).

Table 2.10. Optimization of base-mediated cyclization to **2.50**.



Base	Solvent	Temperature (°C)	Time	Yield, ee
NaOMe	MeOH	-78	2 h	no reaction
NaOMe (2 equiv)	MeOH	0	10 min	34%, 38% ee
NaOMe	THF	-40	2 h	no reaction
<i>t</i> -BuOK	THF/ <i>t</i> -BuOH	-40	1 h	6%, <95% ee
<i>t</i> -BuOK	THF/ <i>t</i> -BuOH	0	20 min	61% 64% ee
<i>t</i> -BuOK	THF/ <i>t</i> -BuOH	0	105h	85%, 60% ee
<i>t</i> -BuOK	<i>t</i> -BuOH	23	1 h	70%, 94% ee
<i>t</i> -BuOK	<i>t</i> -BuOH	40	30 min	89%, 74% ee
<i>t</i> -BuOK (sublimed)	<i>t</i> -BuOH	40	4 h	91%, 82% ee
<i>t</i> -BuOK	<i>t</i> -BuOH	50	10 min	100%, 74% ee
<i>t</i> -BuOK	<i>t</i> -BuOH	23	20 min	12%, 90% ee
<i>t</i> -BuOK	<i>t</i> -BuOH	23	45 min	97%, 80% ee
<i>t</i> -BuOK	<i>t</i> -BuOH	40	4 h	78%, 92% ee
<i>t</i> -BuOK	MTBE	23	20 min	74%, 85% ee
<i>t</i> -BuOK	MTBE/ <i>t</i> -BuOH	23	20 min	100%, 74% ee
<i>t</i> -BuOK	<i>t</i> -BuOH	pre-heated 60	5 min	100%, 78% ee
DBU	THF	70	30 min	31%, 58% ee
1M NaOH	water/CH ₂ Cl ₂	23	30 min	no reaction
sat. K ₂ CO ₃	water/CH ₂ Cl ₂	23	30 min	no reaction
NaHMDS	THF	-78	2 h	no reaction
NaHMDS	THF	0	20 min	61%, 86% ee
NaHMDS (0.5 equiv)	THF	70	20 min	28%, 86% ee
TBAF (2 equiv)	THF	23	1 h	25%, >99% ee
TBAF (2 equiv)	THF	23	2 h	44%, >99% ee
TBAF (2 equiv)	THF	23	8 h	64%, >99% ee
TBAF (2 equiv)	THF	23	11 h	67%, >99% ee

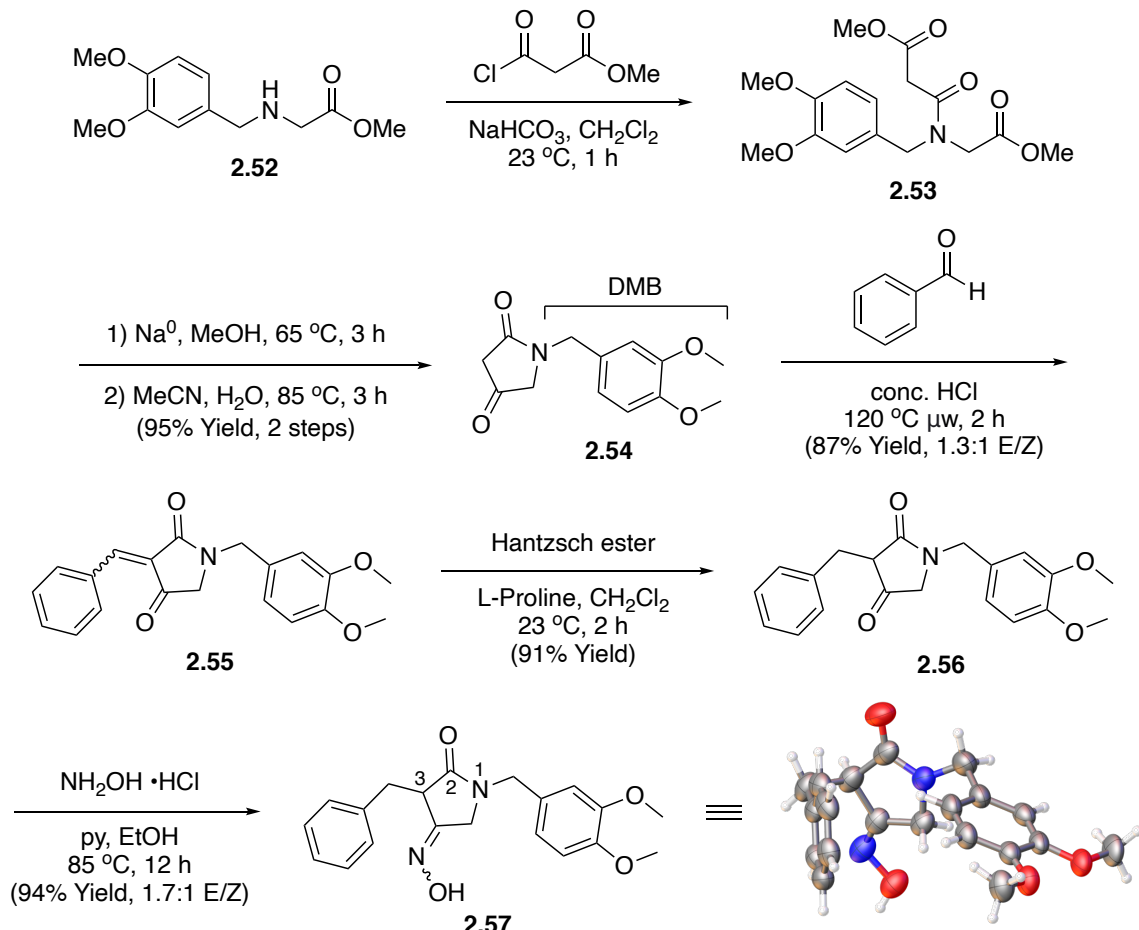
2.3 Ring Expansion Sequence to Install the N-O Bond

2.3.1 Proof of Concept

With facile access to fully-functionalizable enantioenriched tetramic acids in hand, we then sought to develop valid proof of concept for our proposed ring expansion. The first system we opted to prepare was *N*-substituted with a dimethoxybenzyl (DMB) group, and benzyl substituted at the 3-position of the tetramic acid. Our rationale for this was benzyl could serve as a neutral example of substitution at C3. The DMB-protected amide would add complexity, improve solubility, and could eventually be removed under relatively mild conditions. We would later attempt to functionalize the 5-position using our method of preparing chiral tetramic acids in order to expand the scope of the reaction.

In a forward sense, we sought to prepare the requisite oxime with the above-described substitution pattern. Our point of departure was known 3,4-dimethoxybenzene *N*-protected (DMB) glycine methyl ester (**2.52**, Scheme 2.20),³⁹ which was converted to amide **2.53** upon exposure to methyl malonyl chloride under Schotten-Baumann conditions.¹⁷ Subsequent Dieckmann cyclization of the crude gave an intermediate tetramic acid ester (not shown), which, upon solvent exchange to wet acetonitrile and reflux at 85 °C, underwent decarboalkoxylation to produce DMB-protected tetramic acid **2.54** in 95% yield. The 3-position was substituted *via* acid-promoted Claisen-Schmidt condensation with benzaldehyde to produce benzylidene **2.55** as an inconsequential ~1.3:1 mixture of E/Z isomers. Subsequent L-proline-mediated Hantzsch ester reduction⁴⁰ of the alkene produced desired tetramic acid **2.56** in 80% yield, over the two steps. Exposure of ketone **2.53** to hydroxylamine hydrochloride provided the corresponding oxime **2.57** (structurally

confirmed by X-ray analysis) in 94% yield as a ~1.7:1 inconsequential mixture of E/Z isomers, and set the stage for oxidation and subsequent ring expansion.

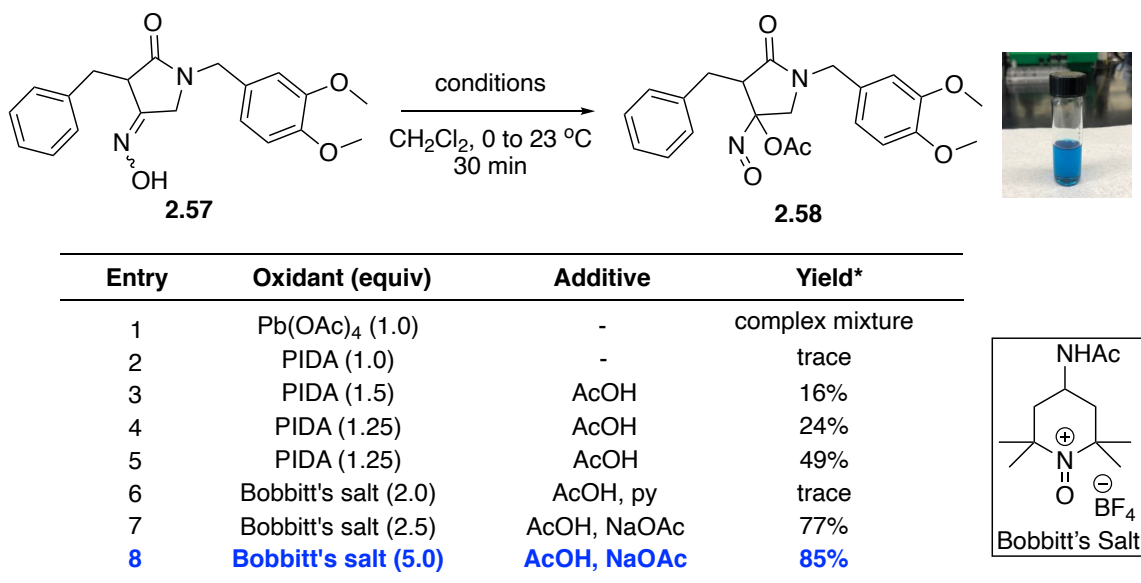


Scheme 2.20. Preparation of *N*-protected, benzyl-substituted oxime for ring expansion.

Early attempts to oxidize oxime **2.57** to the requisite acyloxy nitroso intermediate (**2.58**, Table 2.10) involved exploring the conditions reported by King,⁹ as well as those that we screened in the synthesis of (\pm)-phyllantidine.⁹ To our dismay, we were unable to isolate oxidized compound **2.58**. Based on literature reports and our own experience, our efforts were guided by the bright blue color of the derived nitroso intermediates which served as a convenient indicator of the reaction's progress. Upon screening different

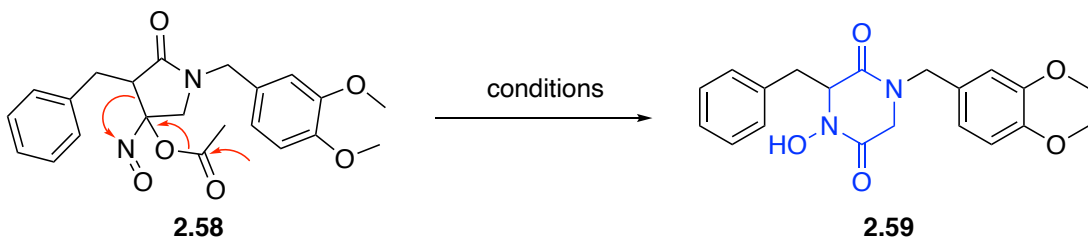
oxidants and conditions, we found that Bobbitt's Salt⁴¹ (Table 2.11, entry 8) gave the highest conversion to the bright blue acyloxy nitroso intermediate (**2.58**); found to be quite unstable and best advanced directly to the ring expansion step, following rapid filtration through a short pad of silica gel. There is likely a mixture of diastereomers produced in **2.58**, however the mixture is inconsequential and we decided not to speculate on the diastereomeric ratio based on the quality of the crude NMR data.

Table 2.11. Oxidation of the oxime to acyloxy nitroso intermediate **2.58**.

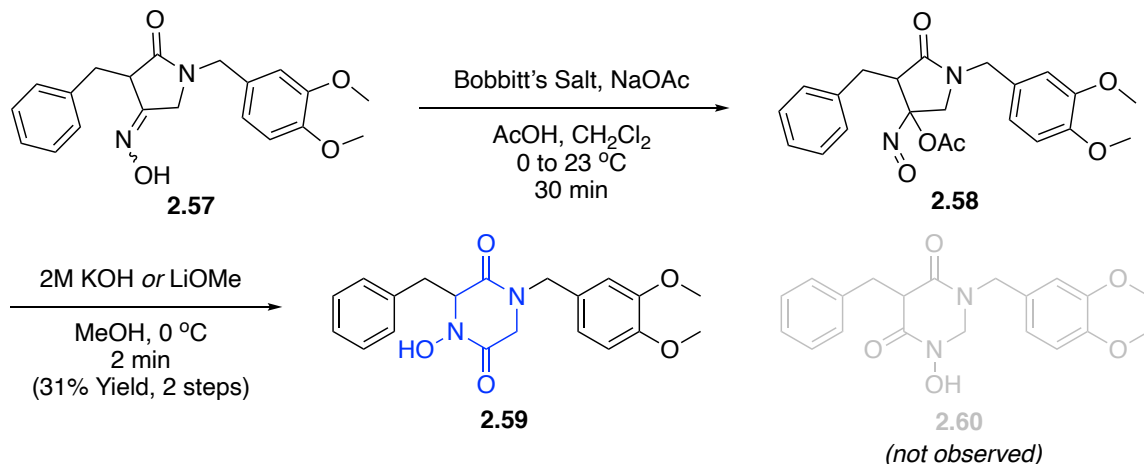


Once the optimal oxidant was found, we focused our efforts toward defining viable conditions for ring expansion to the desired *N*-oxy-2,5-DKP **2.59** (*via* nucleophilic cleavage of the acetate group). To this end, we performed a brief screen of conditions and found that both those employed by King (KOH) and by our group in our synthesis of phyllantidine (LiOMe) were equally effective in promoting the desired transformation to **2.59** (31% yield from **2.57**, Table 2.12, entries 2 and 6),^{9,10} with no observation of the undesired regioisomer (**2.60**).

Table 2.12. Ring expansion of acyloxy nitroso **2.58** to *N*-oxy-2,5-DKP **2.59**.



Entry	Base	Solvent	Yield (over 2 steps)
1	LiOMe	THF	complex mixture
2	LiOMe	MeOH	31%
3	NaOMe	MeOH	complex mixture
4	NaOH	MeOH	19%
5	LiOH	MeOH	18%
6	KOH	MeOH	31%
7	(<i>n</i> Bu) ₄ NOH	MeOH	complex mixture
8	Ca(OH) ₂	MeOH	trace
9	K ₂ CO ₃	MeOH	29%

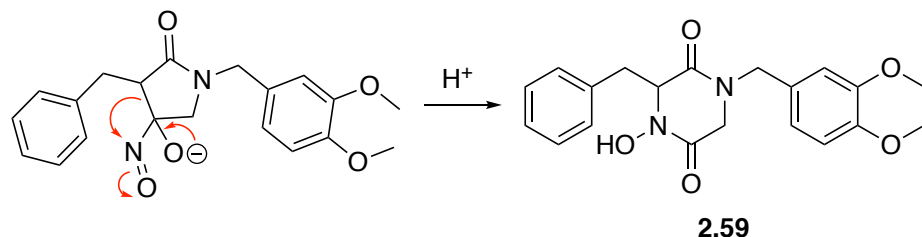


Scheme 2.21. Regioselective ring expansion to *N*-oxy-2,5-DKP.

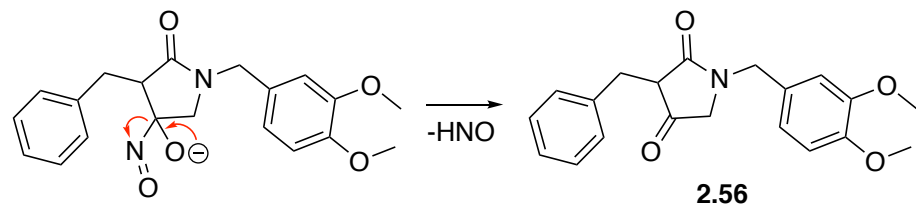
The modest yield of **2.59** results from the formation of ketone **2.56**, a major by-product derived *via* loss of HNO from acyloxy nitroso intermediate **2.58**. The mass balance is accounted for by the observed 1:3 ratio of **2.59** and **2.56** in the crude NMR. Similar

results were observed in the original reports by King.¹⁰ The mechanisms of both the by-product and DKP formation are discussed in Scheme 2.22.

a) Formation of desired DKP **2.59**



b) Formation of major by-product ketone **2.56**



Scheme 2.22. Mechanistic rationale for formation of desired DKP and major ketone by product.

The desired ring expansion product **2.59** was structurally assigned *via* 1H , 13C , COSY, and HSQC NMR data. The illustrated regiochemical outcome is based on several observations: as shown in Figure 2.12, the calculated ^{13}C ppm shifts of C2 (71.6 ppm) and C11 (48.2 ppm) in the desired regioisomer differ greatly, with C2 expected to be more downfield. Conversely, the carbon shifts in the undesired regioisomer should have the opposite pattern, with C11 (68.6 ppm) being more downfield than C2. The actual carbon shifts are depicted in Figure 2.13, and C2 was indeed shown to have the more downfield peak compared to C11, as well as corresponding to an sp^3 CH carbon (HSQC) and the protons of which coupling with C3 (COSY), thus supporting our assignment of the desired DKP regioisomer.

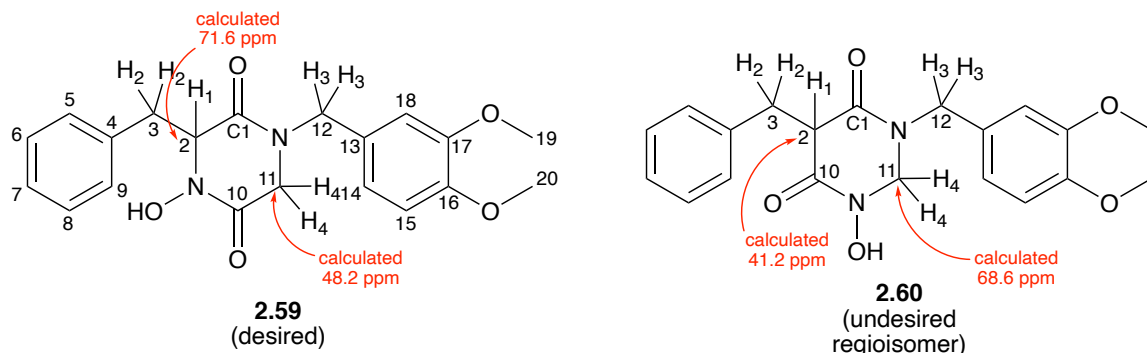


Figure 2.12. Calculated differences in carbon shifts of C2 and C11.

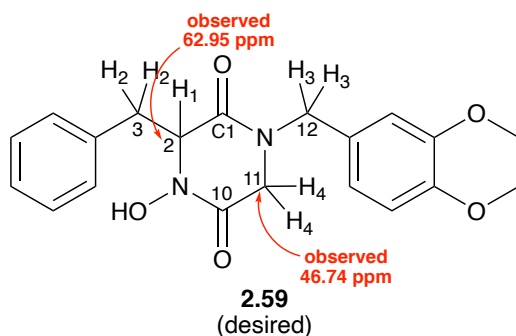


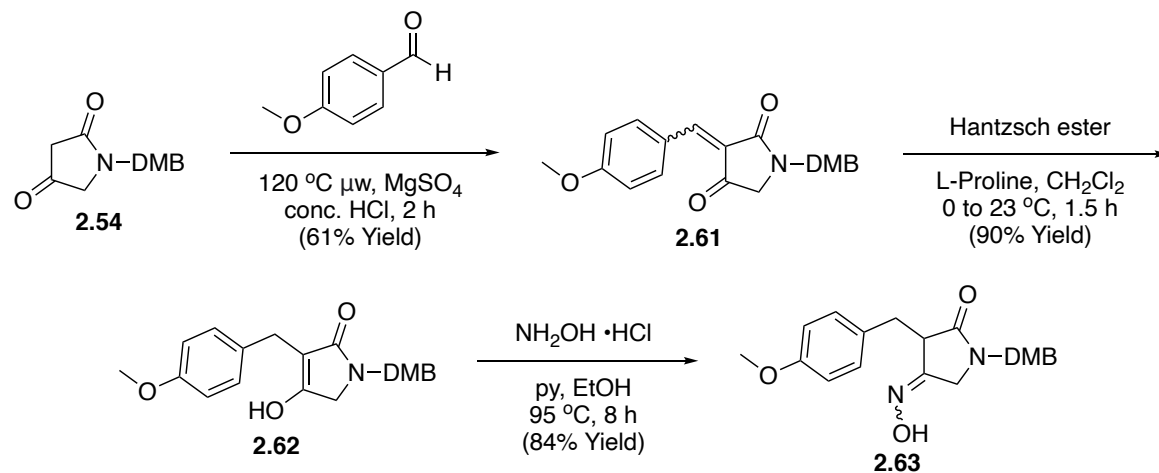
Figure 2.13. Observed carbon shifts in the only isolated ring expansion product.

In conclusion, we developed a ring expansion approach which allows for the conversion of tetramic acids to *N*-oxy-2,5-DKPs (summarized in Scheme 2.21), and this work was recently published in *Tetrahedron Letters*.⁴² This strategy allows for late-stage installation of the labile *N*-*O* bond and offers potential for use in the preparation of *N*-oxy-2,5-DKP-containing natural products. Guided by this successful system, we began to explore other patterns of functionality on requisite tetramic acids in hopes of observing the same regioselectivity in the ring expansion reaction.

2.3.2 Substrate Scope and Limitations

In an effort to broaden the scope of the ring expansion reaction, we prepared a number of substrates with variable substitution patterns around the tetramic acid ring. We developed nitrogen-substituted substrates as well as tetramic acids with C3 and C5 functionalization.

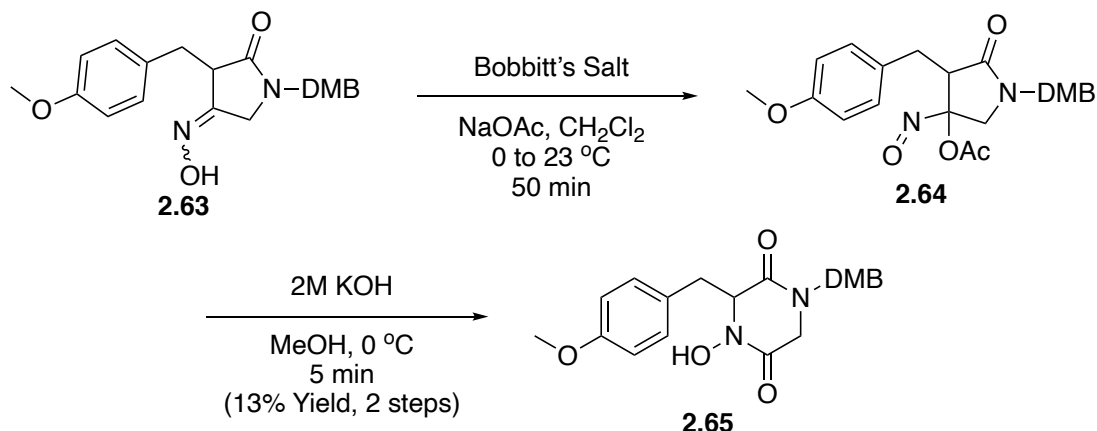
Similar to ring expansion substrate **2.57**, we synthesized system with a more electron-rich *p*-methoxybenzyl group (**2.63**, Scheme 2.23). Tetramic acid **2.54** underwent an acid-catalyzed Claisen-Schmidt condensation with *p*-anisaldehyde to yield alkene **2.61** in 61% yield, which was then reduced upon subjection to Hantzsch ester and L-Proline,⁴⁰ giving substituted tetramic acid **2.62** in 90% yield. Treatment of the ketone with hydroxylamine hydrochloride and pyridine delivered oxime **2.63** in 84% yield.



Scheme 2.23. Preparation of a PMB-substituted DMB-protected oxime.

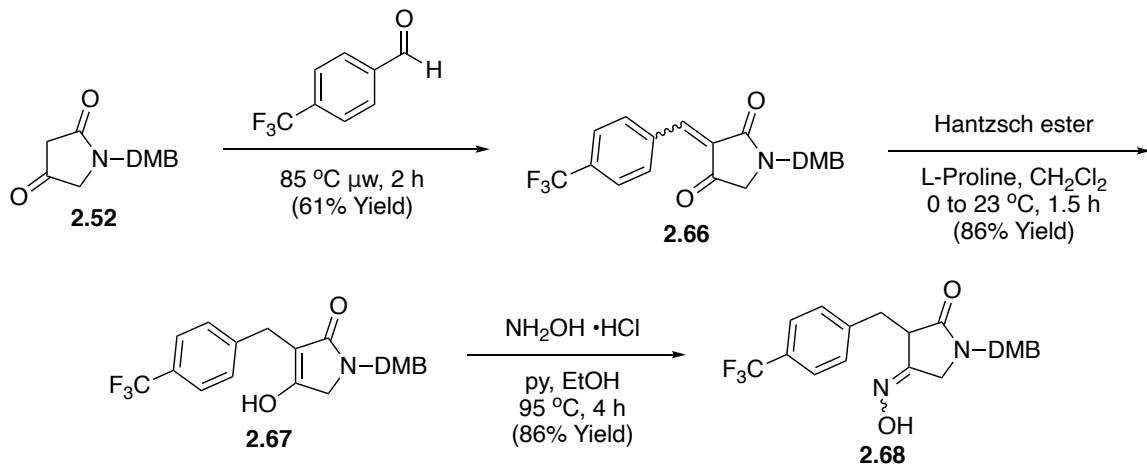
Using our optimized conditions described above, we advanced oxime **2.63** to the ring expansion sequence. Oxidation with Bobbitt's Salt gave **2.64** as a light blue oil, which was quickly filtered through a short pad of silica and advanced to the KOH-mediated ring

expansion. To our delight, we obtained the desired *N*-oxy-2,5-DK, the regiochemistry of which was confirmed by NMR experiments (**2.64**, Scheme 2.24).



Scheme 2.24. Ring expansion to PMB-substituted DMB-protected DKP.

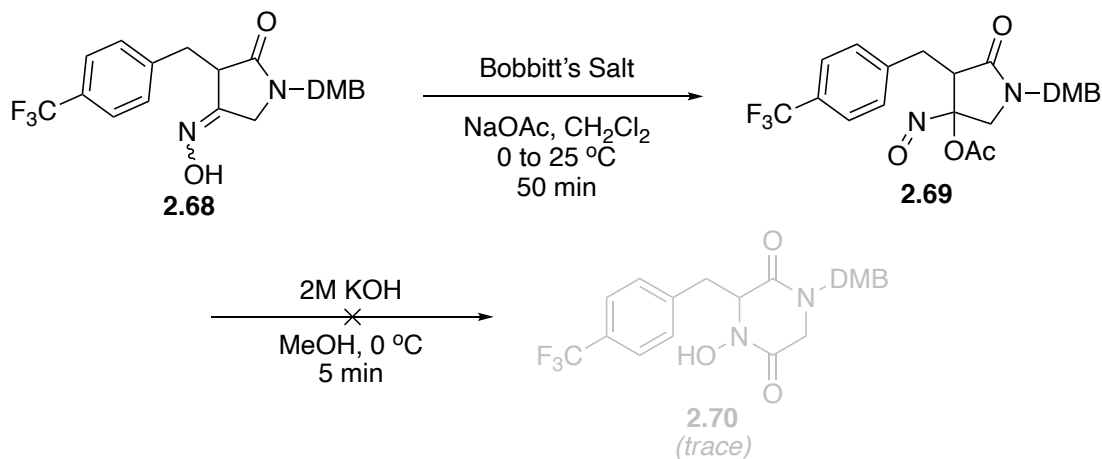
A third substrate we prepared contrasts that of **2.65** in that it contains an electron-withdrawing trifluoromethyl group on the C3 benzyl (Scheme 2.25). Oxime **2.68** was prepared in a similar manner to the methoxy-substituted system: Claisen-Schmidt condensation with commercially-available 4-(Trifluoromethyl)benzaldehyde afforded alkene **2.66** in 61% yield, and subsequent L-Proline-mediated Hantzsch ester reduction⁴⁰ gave tetramic acid **2.67** in 86% yield. Treatment with hydroxylamine hydrochloride and pyridine produced the desired oxime **2.68** as an inconsequential mixture of E/Z isomers.



Scheme 2.25. Preparation of a CF_3 -substituted DMB-protected oxime.

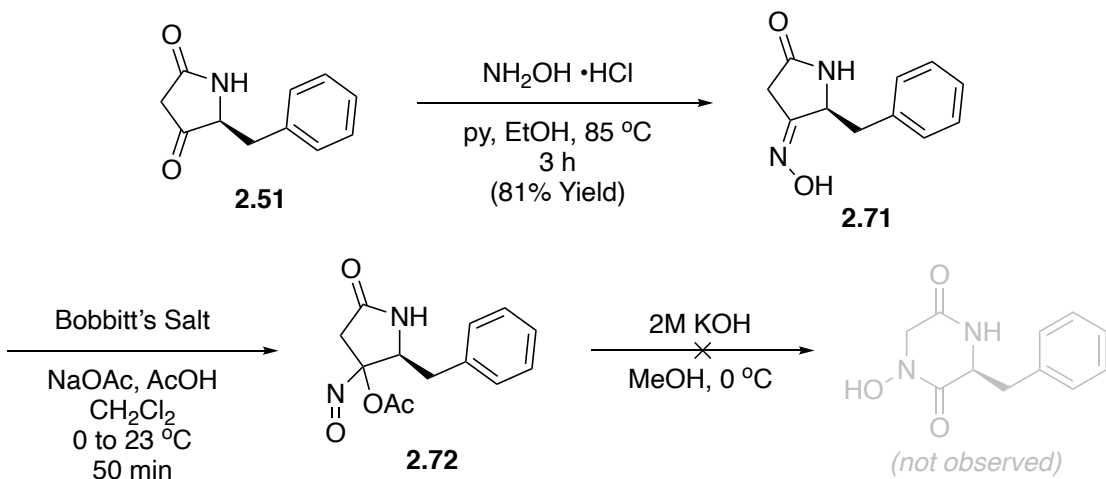
Oxidation to the acyl nitroso intermediate (**2.69**, Scheme 2.26) using our most optimized conditions produced a blue oil, which, after filtration through silica, was treated with 2M KOH to effect the ring expansion. Unfortunately, multiple attempts at the ring expansion provided only trace amounts of anything resembling an *N*-oxy-2,5-DKP (i.e., **2.70**), and insufficient amounts to confidently confirm by NMR.

The ring expansion between these three systems (Bn, OMe-Bn, and CF_3 -Bn) exhibited no distinct trend in reactivity, and it appeared that the presence of either an electron donating or withdrawing group on the C3 benzyl had no effect on regiochemical outcome.



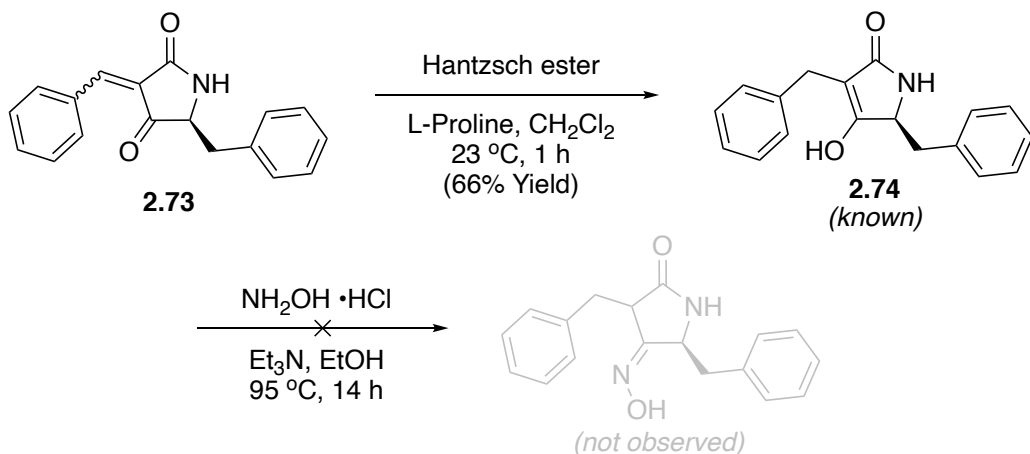
Scheme 2.26. Ring expansion to CF₃-substituted DMB-protected DKP.

Another substrate was developed with formation of oxime **2.71** (Scheme 2.27) under standard conditions from C5 benzyl-substituted tetramic acid **2.51**, of which we had access to large quantities from the development of our *Organic Syntheses* article.⁴³ Oxidation with Bobbitt's Salt⁴¹ gave acyloxy nitroso intermediate **2.72** as a bright blue oil, which was then filtered through a short pad of silica and treated with 2M KOH. Unfortunately, no desired product was ever observed from the ring expansion.



Scheme 2.27. Attempted ring expansion of a C5-substituted substrate.

Although we were unable to advance **2.72** to a ring-expanded product we continued exploring other functionalized tetramic acids, preparing a similar substrate with an additional benzyl group at C3 (i.e., **2.74**, Scheme 2.28).



Scheme 2.28. Attempted synthesis of a C3- and C5-substituted substrate.

Known tetramic acid **2.74**⁴⁴ was prepared by typical transfer hydrogenation conditions⁴⁰ on **2.73** and then subjected to oximation. Strangely, every attempt to react the substrate with hydroxylamine hydrochloride only gave recovered starting material. It was difficult to rationalize this lack of reactivity, since the aforementioned systems which had successfully formed the requisite oximes were not so different electronically, thus we are left to speculate that sterics were preventing us from moving this substrate further.

Oxidations by trapping the acyl nitroso species with different oxanion nucleophiles other than acetate were attempted (e.g., benzoate, formate), but attempts to isolate nitroso intermediates seemed to cause observable accelerated decomposition. Postulating that the nitroso intermediates might be sensitive to silica during filtration, we attempted the ring expansion sequences in one-pot, but this only led to complex mixtures of products that did not resemble the desired *N*-oxy-2,5-DKPs.

2.4 Conclusion

In conclusion, the proposed ring expansion of functionalized tetramic acids to *N*-oxy-2,5-DKPs proved successful but the efficiency of the ring expansion was found to be low and highly substrate-dependent. This is supported by the indiscriminate array of results we obtained while exploring substrates with different substitution patterns.

2.5 Experimental

2.4.1 General

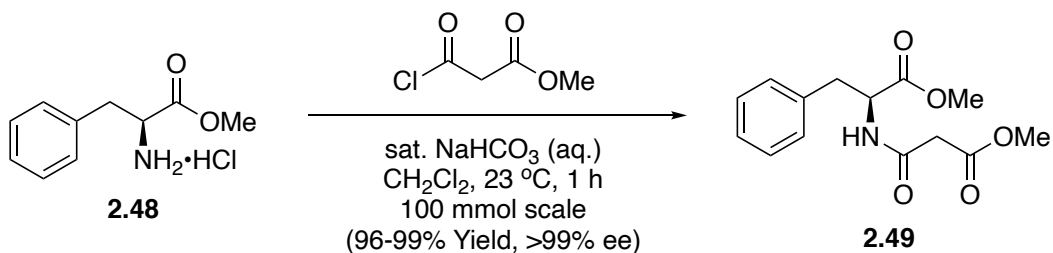
Unless otherwise stated, all reactions were performed in flame-dried glassware under a nitrogen (N_2) atmosphere, and reagents were used as received from the manufacturers. The reactions were monitored and analytical samples purified by normal phase thin-layer chromatography (TLC) using Millipore Sigma glass-backed 60 Å plates (indicator F-254, 250 μM). Tetrahydrofuran, diethyl ether, dichloromethane, acetonitrile, dimethylformamide, and toluene were dried using a solvent purification system manufactured by SG Water, USA LLC. Triethylamine and pyridine were dried over CaH_2 and freshly distilled prior to use. Reactions involving organometallic reagents were conducted in flame-dried glassware under an argon (Ar) atmosphere using standard techniques for handling air-sensitive reagents, and solvents were deoxygenated by bubbling dry Ar gas through the neat liquid for 10 min before use. Manual flash chromatography was performed using the indicated solvent systems with Silicycle SiliaFlash® P60 (230–400 mesh) silica gel as the stationary phase. Automated flash chromatography was performed on a Teledyne RF+UV-Vis MS Comp MPLC using the indicated solvent systems, and Teledyne RediSep® R_f normal phase disposable silica gel

columns of the indicated size at the indicated flow rate. ^1H and ^{13}C NMR spectra were recorded on a Bruker AvanceTM III 300 MHz, Bruker AscendTM 400 MHz, or Bruker AscendTM 600 MHz spectrometer, fitted with autosamplers. Chemical shifts (δ) are reported in parts per million (ppm) relative to the residual solvent resonance, and coupling constants (J) are reported in hertz (Hz). NMR peak pattern abbreviations are as follows: s = singlet, bs = broad singlet, d = doublet, dd = doublet of doublets, ddd = doublet of doublet of doublets, dt = doublet of triplets, dtd = doublet of triplet of doublets, dq = doublet of quartets, t = triplet, td = triplet of doublets, q = quartet, m = multiplet. Proton spectra recorded in chloroform-d are referenced to the residual ^1H signal of CHCl_3 at $\delta = 7.26$ and are reported relative to TMS at $\delta = 0.00$; carbon spectra are referenced to the residual central ^{13}C signal for CDCl_3 at $\delta = 77.16$ and are reported relative to TMS at $\delta = 0.00$. Proton spectra recorded in methanol-d₄ are referenced to the residual methyl ^1H signal of CH_3OH at $\delta = 3.31$ and are reported relative to TMS at $\delta = 0.00$; carbon spectra are referenced for the residual methyl ^{13}C signal for CH_3OH at $\delta = 49.00$ and are reported relative to TMS at $\delta = 0.00$. Proton spectra recorded in dimethylsulfoxide-d₆ are referenced to the residual ^1H signal of $(\text{CH}_3)_2\text{SO}$ at $\delta = 2.50$ and are reported relative to TMS at $\delta = 0.00$; carbon spectra are referenced to the residual methyl ^{13}C signal for $(\text{CH}_3)_2\text{SO}$ at $\delta = 39.52$. Fourier-transform infrared (FTIR) spectra were recorded on a Bruker Platinum-ATR IR spectrometer with diamond window. High Resolution mass spectra (HRMS) were obtained in the Baylor University Mass Spectrometry Center on a Thermo Scientific LTQ Orbitrap Discovery mass spectrometer or Thermo Fisher Q-Exactive Plus Hybrid Quadrupole-Orbitrap mass spectrometer, using +ESI or -ESI and reported for the molecular ion ($[\text{M}+\text{H}]^+$ and $[\text{M}+\text{Na}]^+$ or $[\text{M}-\text{H}]^-$, respectively). Single crystal X-ray

diffraction data were collected on a Bruker Apex IV-CCD detector using Mo-K_a radiation ($\lambda = 0.71073 \text{ \AA}$). Crystals were selected under Paratone® oil, placed on MiTeGen MicroMounts™, then immediately positioned under an N₂ cold stream at 150 K. Structures were solved and refined using APEX IV and SHELXTL software. Crystal graphics were generated using either SHELXTL and OLEX 2 software.

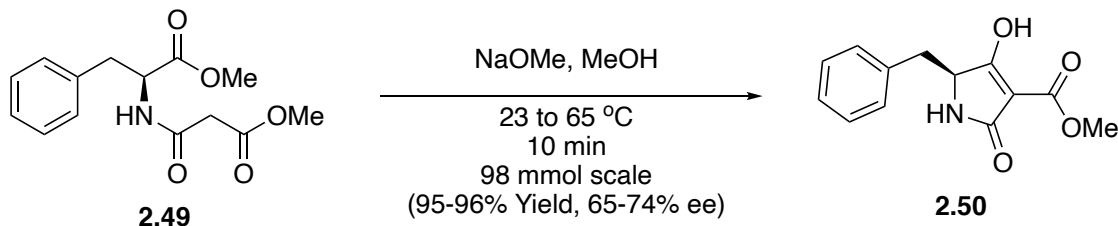
(Data for compounds **2.49-2.51** extracted from published *Organic Syntheses* prep.⁴³)

2.4.2 Data for Known **2.49**



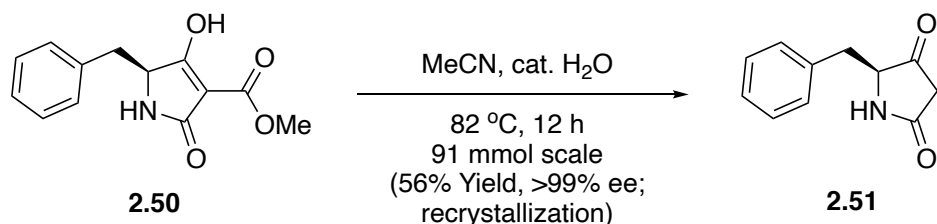
¹H NMR (400 MHz, CDCl₃) δ 7.38 (d, $J = 7.7$ Hz, 1H), 7.26 - 7.32 (m, 2H), 7.20 - 7.26 (m, 1H), 7.12 (d, $J = 6.4$ Hz, 1H), 4.86 (dt, $J = 7.6, 6.1$ Hz, 1H), 3.71 (s, 6H), 3.23 - 3.36 (m, 2H), 3.17 (dd, $J = 13.9, 5.7$ Hz, 1H), 3.08 (dd, $J = 13.9, 6.4$ Hz, 1H). **¹³C NMR** (101 MHz, CDCl₃) δ 171.7, 169.3, 164.6, 135.9, 129.3, 128.7, 127.2, 53.6, 52.6, 52.5, 41.2, 37.9. **FTIR** (neat) 3318, 3029, 2953, 1737, 1652, 1531, 1497, 1435, 1346, 1274, 1169, 1118, 1079, 1016, 744 cm⁻¹. **HRMS** (ESI) calc'd for [M+H]⁺ C₁₄H₁₇NO₅ 280.1179, found 280.1176 m/z. **R_f** = 0.68 (75% EtOAc/hexanes). $[\alpha]_D^{23} = +24.1^\circ$ (c = 1.01, MeOH).

2.4.3 Data for Known 2.50



¹H NMR (400 MHz, CDCl₃) δ 11.20 (br s, 1H), 7.20 - 7.34 (m, 3H), 7.16 - 7.23 (m, 2H), 6.11 (s, 1H), 4.36 (dd, *J* = 9.0, 4.0 Hz, 1H), 3.89 (s, 3H), 3.27 (dd, *J* = 14.1, 4.1 Hz, 1H), 2.77 (dd, *J* = 13.8, 8.7 Hz, 1H). **¹³C NMR** (101 MHz, CDCl₃) δ 187.8, 168.2, 168.0, 135.6, 129.5, 129.1, 127.7, 99.2, 57.5, 52.6, 38.2. **FTIR** (neat) 3377, 2865, 2534, 1643, 1589, 1496, 1441, 1423, 1394, 1224, 1296, 1116, 1093, 1061, 983, 908, 846, 795, 759, 743 cm⁻¹. **HRMS** (ESI) calc'd for C₁₃H₁₃NO₄ [M+H]⁺ 248.0917, found 248.0917 m/z; calc'd for C₁₃H₁₃NO₄ [M+Na]⁺ 270.0737, found 270.0741 m/z. **R_f** = 0.16 (10% MeOH/CH₂Cl₂). $[\alpha]_D^{23.5} = -72.43^\circ$ (c = 1.00, MeOH).

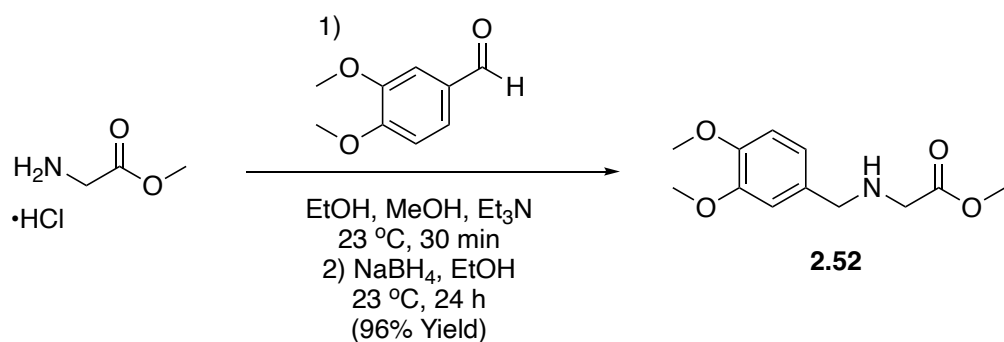
2.4.4 Data for Known 2.51



¹H NMR (400 MHz, CDCl₃) δ 7.28 - 7.34 (m, 2H), 7.23 - 7.28 (m, 1H), 7.10 - 7.18 (m, 2H), 6.76 (s, 1H), 4.23 (ddd, *J* = 8.1, 4.1, 1.5 Hz, 1H), 3.14 (dd, *J* = 13.9, 4.0 Hz, 1H),

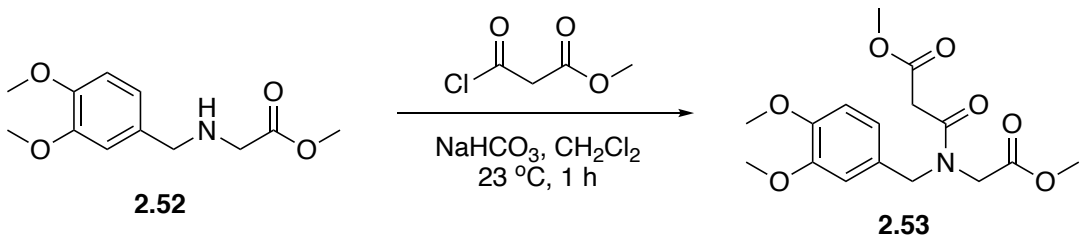
2.91 (d, $J = 22.2$ Hz, 1H), 2.85 (dd, $J = 13.9, 8.0$ Hz, 1H), 2.69 (dd, $J = 22.2, 1.6$ Hz, 1H). **^{13}C NMR** (101 MHz, CDCl_3) δ 206.6, 171.0, 135.2, 129.4, 129.0, 127.5, 65.2, 41.0, 38.5. **FTIR** (neat) 3209, 3029, 2919, 1765, 1666, 1625, 1278, 766, 703, 632, 571 cm^{-1} . **HRMS** (ESI): calc'd for $\text{C}_{11}\text{H}_{11}\text{NO}_2$ [$\text{M}+\text{H}]^+$ 190.0863, found 190.0860 m/z. **m.p.** = 161 – 163 °C. **R_f** = 0.16 (10% MeOH/CH₂Cl₂). $[\alpha]_D^{24.1} = -44.77^\circ$ (c = 1.02, MeOH). The structure was confirmed by X-ray crystallography.

2.4.5 Data for Known 2.52



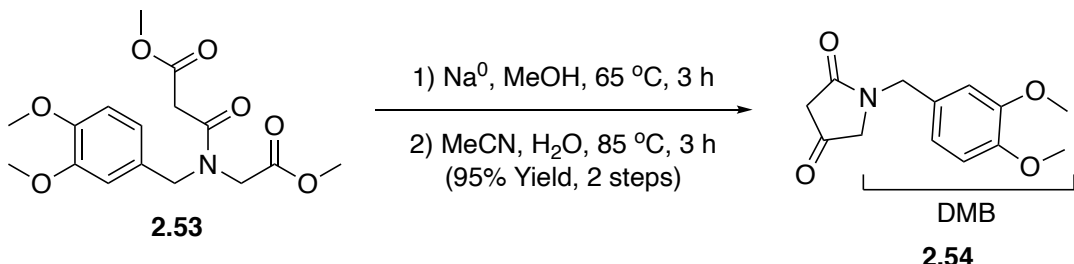
^1H NMR (600 MHz, CDCl_3) δ 6.89 (s, 1H), 6.80 - 6.85 (m, 2H), 3.88 (s, 3H), 3.86 (s, 3H), 3.74 (s, 2H), 3.72 (s, 3H), 3.41 (s, 2H). **^{13}C NMR** (151 MHz, CDCl_3) δ 173.08, 149.21, 148.38, 132.18, 120.62, 111.57, 111.16, 56.10, 56.03, 53.25, 51.97, 49.95. **m.p.** = 34 – 35.8 °C. Data is consistent with the literature.³⁹

2.4.6 Preparation of Amide **2.53**



To a 1L round-bottom flask, methyl ester **2.52** (50.5 g, 211.1 mmol, 1.0 equiv) was added to sat. aq. NaHCO_3 (1.17 L). CH_2Cl_2 (706 mL) was added with vigorous stirring at 23°C . After 20 minutes methyl malonyl chloride (27.2 mL, 232.2 mmol, 1.1 equiv) was added dropwise over 5 minutes. After 20 minutes, the mixture was transferred to a separatory funnel and the organic layer was collected. The aqueous layer was extracted (3 x 100 mL) with CH_2Cl_2 , dried (Na_2SO_4), and concentrated *in vacuo* to give amide **2.53** as a thick yellow oil, which was advanced to the next step without purification. $\text{R}_f = 0.69$ (EtOAc).

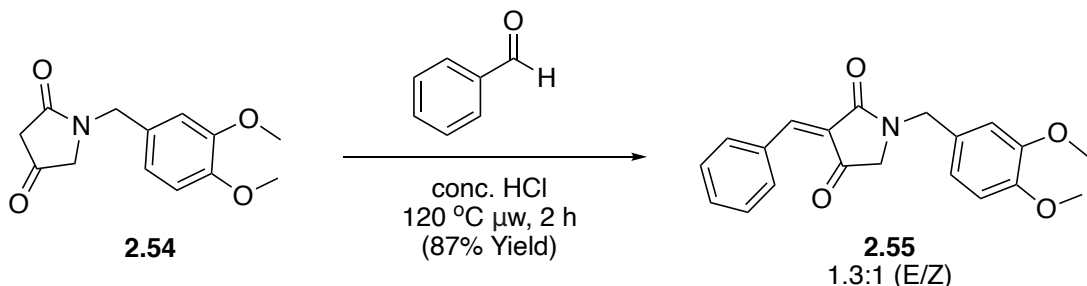
2.4.7 Preparation of DMB Tetramic Acid 2.54



To a flame-dried 500 mL round-bottom flask, portions of Na^0 metal (100 mg, 3.0 mmol, 1.0 equiv) were added to freshly distilled MeOH (15 mL). Once effervescence stopped, a solution of amide **2.53** (1.12 g, 3.0 mmol, 1.0 equiv) in dry MeOH was added dropwise over 45 minutes. The reaction stirred at $65\text{ }^\circ\text{C}$ for 1.5 hours. The reaction was cooled to rt and concentrated *in vacuo*. The residue was redissolved in water and extracted with EtOAc (3×10 mL). The aqueous layer was acidified to pH 2 with 1M HCl and extracted with CH_2Cl_2 (3×10 mL), dried (Na_2SO_4), and concentrated *in vacuo*. The residue was redissolved in MeCN (127 mL) and H_2O (0.04 mL) and heated at $85\text{ }^\circ\text{C}$ for 3 hours. The reaction was cooled to rt and the solvent was removed *in vacuo* to provide DMB tetramic acid **2.54** as a yellow wax (700 mg, 95% yield over 2 steps). The structure was confirmed by X-ray crystallography. **$^1\text{H NMR}$** (400 MHz, CDCl_3) δ 6.80 – 6.82 (m, 3H), 4.56 (s, 2H), 3.87 (s, 6H), 3.74 (s, 2H), 3.10 (s, 2H). **$^{13}\text{C NMR}$** (101 MHz, CDCl_3) δ 203.41, 168.81, 149.59, 149.14, 127.68, 121.13, 111.72, 111.35, 56.83, 56.13, 56.08, 46.04, 41.89. **FTIR** (neat) 3432, 2935, 2836, 1772, 1744, 1665, 1607, 1513, 1441, 1417, 1360, 1307, 1257, 1234, 1153, 1137, 1022, 854, 809, 765, 674, 550 cm^{-1} . **HRMS** (ESI) calc'd for $\text{C}_{13}\text{H}_{15}\text{NO}_4$

$[M+H]^+$ 250.1074, found 250.1074 m/z; calc'd for $[M+Na]^+$ 272.0893, found 272.0894 m/z. R_f = 0.14 (60% EtOAc/hexanes). **m.p.** = 92 – 94 °C.

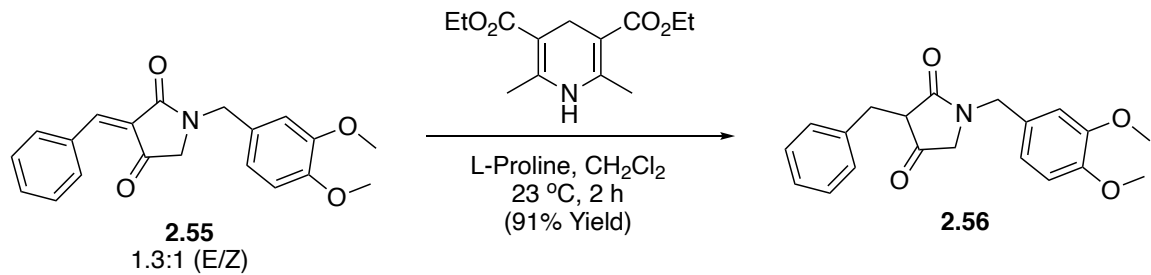
2.4.8 Preparation of Alkene **2.55**



In a 35 mL CEM® microwave tube, DMB tetramic acid **2.54** (25 mg, 0.1 mmol, 1.0 equiv), benzaldehyde (16 mL, 0.15 mmol, 1.5 equiv), and MeOH (17 mL) were added. 6 drops of concentrated HCl were added and the mixture was irradiated at 120 °C for 2 hours. Once cooled to rt, solvent was removed *in vacuo* and the crude was purified *via* flash column chromatography to yield alkene **2.55** as a yellow foam (176 mg, 87% yield, ~1.3:1 E/Z). E-isomer: **1H NMR** (400 MHz, CDCl₃) δ 8.31 (d, *J* = 7.27 Hz, 1H), 7.77 (s, 1H), 7.42 – 7.52 (m, 3H), 6.81 (s, 3H), 4.64 (s, 2H), 3.83 (s, 6H), 3.67 (s, 1H). **13C NMR** (101 MHz, CDCl₃) δ 193.43, 167.05, 148.95, 147.19, 134.85, 133.48, 133.00, 128.77, 127.87, 123.91, 120.99, 111.57, 111.24, 55.97, 55.93, 53.64, 46.01. Z-isomer: **1H NMR** (400 MHz, CDCl₃) δ 8.46 (d, *J* = 7.27 Hz, 1H), 7.70 (s, 1H), 7.42 – 7.52 (m, 3H), 6.81 (s, 3H), 4.64 (s, 2H), 3.83 (s, 6H), 3.76 (s, 1H). **13C NMR** (101 MHz, CDCl₃) δ 165.24, 149.44, 148.95, 134.85, 133.45, 133.06, 132.46, 128.77, 127.90, 124.43, 120.99, 111.59, 111.28, 56.01, 55.93, 53.88, 46.32. **FTIR** (neat) 3068, 2933, 2835, 2251, 1731, 1671, 1609, 1593, 1570, 1513, 1452, 1406, 1375, 1301, 1257, 1236, 1215, 1190, 1156, 1138, 1205, 912, 858,

809, 767, 729, 687, 664, 552, 435 cm^{-1} . **HRMS** (ESI) calc'd for $\text{C}_{20}\text{H}_{19}\text{NO}_4$ [$\text{M}+\text{Na}$] $^+$ 360.1206, found 360.1208 m/z. $\text{R}_f = 0.4, 0.53$ (E/Z) (50% EtOAc/hexanes).

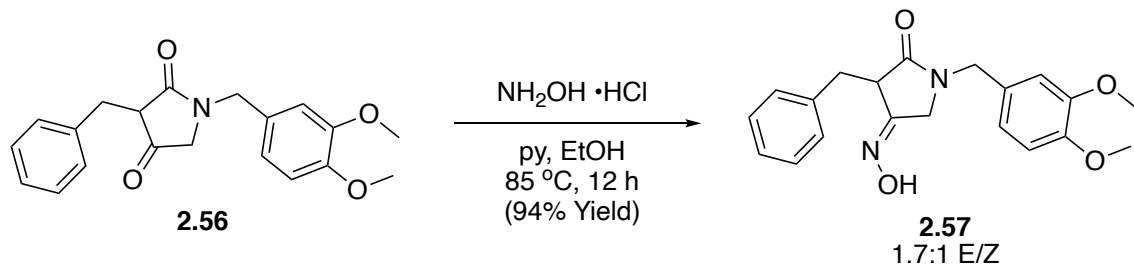
2.4.9 Preparation of Tetramic Acid **2.56**



In a flame-dried 250 mL round-bottom flask, L-Proline (50.3 mg, 0.4 mmol, 0.05 equiv) and Hantzsch ester (2.21 g, 8.7 mmol, 1.0 equiv) were suspended in CH_2Cl_2 (98 mL) and stirred at 23°C for 10 minutes. Alkene **2.55** (2.95 g, 8.7 mmol, 1.0 equiv) was added dropwise *via* syringe pump (5 mL/hr) in minimal CH_2Cl_2 , and stirred for 2 hours. Solvent was removed *in vacuo* and the crude product was purified *via* flash column chromatography to yield benzyl tetramic acid **2.56** as an off-white solid (2.7 g, 91% yield). The structure was confirmed by X-ray crystallography. **$^1\text{H NMR}$** (400 MHz, CDCl_3) δ 7.17 – 7.23 (m, 5H), 6.70 (d, $J = 8.16$ Hz, 1H), 6.63 (d, $J = 2.00$ Hz, 1H), 6.44 (dd, $J = 8.16, 2.12$ Hz, 1H), 4.54 (d, $J = 14.48$ Hz, 1H), 4.32 (d, $J = 14.48$ Hz, 1H), 3.85 (s, 3H), 3.80 (s, 3H), 3.55 (d, $J = 17.26$ Hz, 1H), 3.25 – 3.27 (m, 2H), 3.17 – 3.19 (m, 1H), 3.11 (dd, $J = 17.73, 1.87$ Hz, 1H). **$^{13}\text{C NMR}$** (101 MHz, CDCl_3) δ 207.00, 171.02, 149.50, 149.01, 136.67, 136.08, 129.80, 128.67, 127.48, 127.19, 120.81, 111.73, 111.42, 56.21, 56.14, 55.95, 52.37, 45.95, 33.04. **FTIR** (neat) 2927, 2594, 1686, 1583, 1513, 1443, 1381, 1310, 1261, 1234, 1211, 1150, 1136, 1039, 1023, 989, 937, 863, 817, 757, 737, 698, 672, 650,

546, 459 cm⁻¹. **HRMS** (ESI) calc'd for C₂₀H₂₁NO₄ [M+Na]⁺ 362.1363, found 362.1366 m/z. **R_f** = 0.57 (EtOAc).

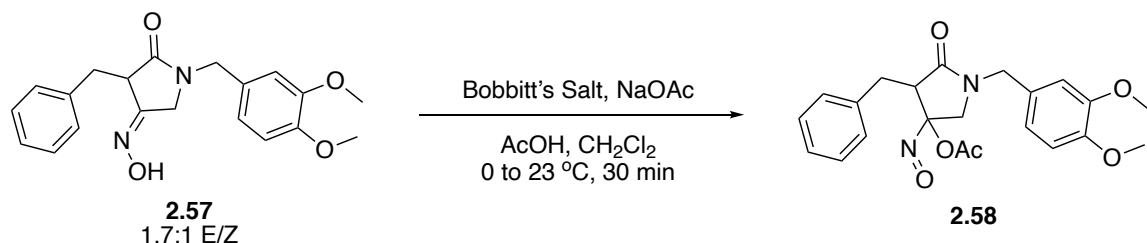
2.4.10 Preparation of Oxime 2.57



In a flame-dried 2 L round-bottom flask, benzyl tetramic acid **2.56** (3.13 g, 9.2 mmol, 1.0 equiv), hydroxylamine hydrochloride (609.2 mg, 18.4 mmol, 2.0 equiv), and pyridine (1.5 mL, 18.4 mmol, 2.0 equiv) were dissolved in EtOH (922 mL) and heated at 85 °C for 12 hours. The reaction was cooled to rt and the solvent was removed *in vacuo*. The residue was redissolved in H₂O and acidified to pH 6 with 1M HCl, then extracted with CH₂Cl₂ (3 x 50 mL), dried (Na₂SO₄), and concentrated *in vacuo*. The crude product was purified *via* flash column chromatography to yield oxime **2.57** as a white foam (3.09 g, 94% yield, ~1.7:1 E/Z). The structure was confirmed by X-ray crystallography. **¹H NMR** (600 MHz, CDCl₃) δ 7.16 – 7.19 (m, 5H), 6.70 (d, *J* = 8.30 Hz, 1H), 6.63 (d, *J* = 2.30 Hz, 1H), 6.43 (dd, *J* = 8.30, 2.30 Hz, 1H), 4.33 (dd, *J* = 49.81, 14.66 Hz, 2H), 3.85 (s, 3H), 3.81 (s, 3H), 3.54 – 3.58 (m, 1H), 3.42 (dd, *J* = 16.60, 1.77 Hz, 1H), 3.29 (dd, *J* = 13.60, 5.30 Hz, 1H), 3.19 (dd, *J* = 13.60, 5.30 Hz, 1H). **¹³C NMR** (151 MHz, CDCl₃) δ 172.13, 155.50, 149.28, 148.78, 136.94, 130.55, 129.95, 129.49, 128.36, 127.67, 126.97, 126.85, 120.85, 120.78, 111.81, 111.70, 111.29, 111.24, 56.13, 56.07, 48.80, 47.26, 46.61, 46.32,

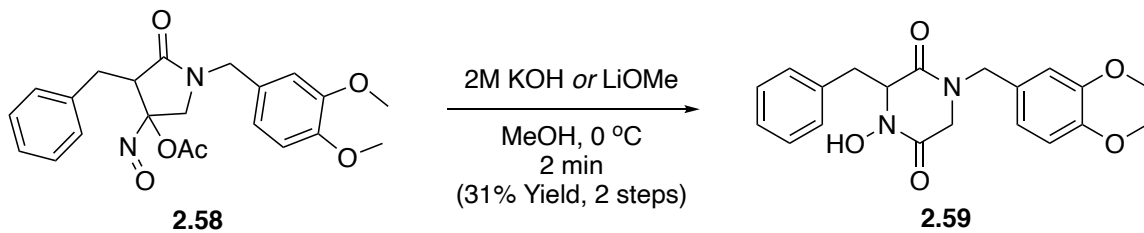
46.25, 46.19, 36.29, 32.94, 14.33. **FTIR** (neat) 3242, 2931, 1697, 1659, 1513, 1453, 1417, 1258, 1235, 1154, 1139, 1025, 968, 932, 809, 762, 729, 700, 593 cm⁻¹. **HRMS** (ESI) calc'd for C₂₀H₂₂N₂O₄ [M+Na]⁺ 377.1472, found 377.1472 m/z. **R_f** = 0.63 (EtOAc). **m.p.** = 55 – 58 °C.

2.4.11 Preparation of Acyloxy Nitroso **2.58**



In a flame-dried 25 mL round-bottom flask, oxime **2.57** (50.7 mg, 0.1 mmol, 1.0 equiv) was dissolved in dry CH₂Cl₂ (13 mL, 0.01 M) and cooled to 0 °C. Sodium acetate (34.7 mg, 0.4 mmol, 3.0 equiv) was added, followed by 40 µL glacial acetic acid. The reaction stirred at 0 °C for 5 minutes, then was warmed to rt for an additional 30 minutes (reaction times longer than 30 minutes led to decreases in yield). The crude mixture was loaded directly onto a short pad of silica and eluted with 5% EtOAc/CH₂Cl₂, then the solvent was removed *in vacuo*. The crude acyloxy nitroso **2.58** was taken on to the next step without further purification, as a bright blue oil. **HRMS** (ESI) calc'd for C₂₂H₂₄N₂O₆ [M+Na]⁺ 435.1527, found 435.1526 m/z.

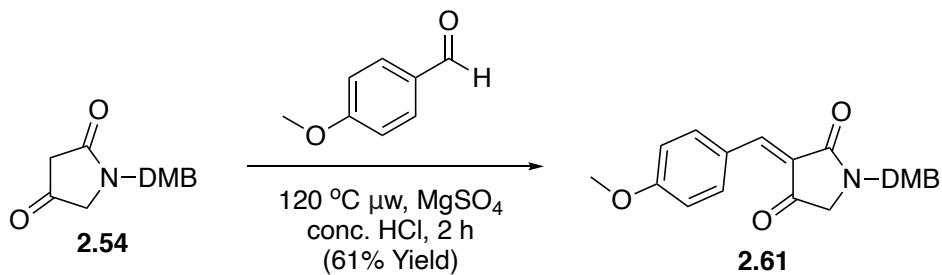
2.4.12 Preparation of DKP 2.59



2M KOH (1.44 mL, 2.9 mmol, 21.0 equiv) was dissolved in HPLC-grade MeOH (1.44 mL) and cooled to 0 °C. Crude acyloxy nitroso **2.58** was then added dropwise in a solution of minimal MeOH at 0 °C. The reaction stirred for 2 minutes then quenched with 1M HCl and extracted with CH₂Cl₂ (3 x 1 mL). The crude was dried (MgSO₄), solvent was removed *in vacuo*, and then purified *via* flash column chromatography to yield DKP **2.59** as a white solid (15.9 mg, 31% yield, 2 steps). Alternate procedure: Crude acyloxy nitroso **2.58** was dissolved in MeOH and cooled to 0 °C. 2M LiOMe in MeOH (0.2 mL, 0.4 mmol, 3.0 equiv) was added and the reaction stirred for 4 hours. The reaction was acidified to pH 2 with 1M HCl and extracted with CH₂Cl₂ and dried. The crude was purified *via* flash column chromatography to yield DKP **2.59**. **¹H NMR** (600 MHz, CDCl₃) δ 7.19 (t, *J* = 7.19 Hz, 1H), 7.10 (t, *J* = 7.46 Hz, 2H), 7.04 (d, *J* = 7.19 Hz, 2H), 6.76 (d, *J* = 7.99 Hz, 1H), 6.72 (d, *J* = 1.86 Hz, 1H), 6.63 (dd, *J* = 7.99, 2.66 Hz, 1H), 4.70 (m, 1H), 4.44 (d, *J* = 14.12 Hz, 1H), 4.13 (d, *J* = 14.65 Hz, 1H), 3.87 (s, 3H), 3.86 (s, 3H), 3.43 – 3.46 (m, 1H), 3.42 (d, *J* = 16.52 Hz, 1H), 3.29 (dd, *J* = 13.32, 3.20 Hz, 1H), 2.42 (d, *J* = 17.32 Hz, 1H). **¹³C NMR** (151 MHz, CDCl₃) δ 164.09, 149.45, 149.29, 134.09, 130.20, 128.67, 127.93, 127.04, 121.75, 112.39, 111.25, 62.95, 56.22, 56.20, 49.51, 46.74, 35.89. **FTIR** (neat) 3402, 2926, 2853, 1761, 1694, 1667, 1594, 1514, 1463, 1454, 1420, 1259, 1236, 1155,

1139, 1113, 1079, 1024, 990, 940, 811, 767, 738, 701, 551 cm^{-1} . **HRMS** (ESI) calc'd for $\text{C}_{20}\text{H}_{22}\text{N}_2\text{O}_5$ $[\text{M}+\text{H}]^+$ 371.1601, found 371.1623 m/z. **R_f** = 0.67 (EtOAc).

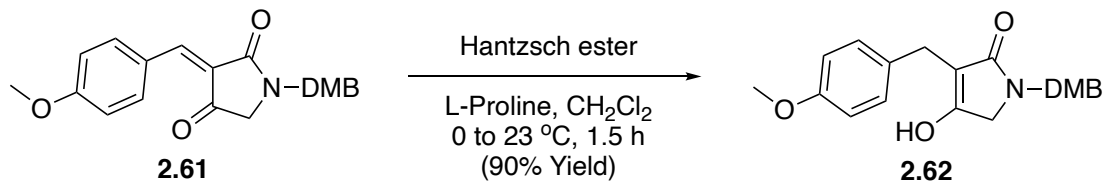
2.4.13 Preparation of Alkene **2.61**



In a 35 mL CEM® microwave tube was added tetramic acid **2.54** (1.5 g, 6.02 mmol, 1.0 equiv), *p*-anisaldehyde (2.46 g, 18.05 mmol, 3.0 equiv), 160 mg of MgSO_4 , 4 drops of concentrated HCl, and 17 mL MeOH. The solution was irradiated at 120 °C for 2 hours. Once cooled to rt, the crude was purified *via* flash column chromatography to yield alkene **2.61** as an inconsequential mixture of E/Z isomers. (1.24g, 61% yield, orange foam). **¹H NMR** (400 MHz, CDCl_3) δ 8.58 (d, J = 9.0 Hz, 2H), 8.44 (d, J = 9.0 Hz, 2H), 6.98 (dd, J = 9.0, 2.0 Hz, 2H), 6.83 (m, 3H), 4.67 (d, J = 2.1 Hz, 2H), 3.90 (s, 3H), 3.87 (s, 3H), 3.87 (s, 3H), 3.73 (d, J = 34.3 Hz, 2H). **¹³C NMR** (101 MHz, CDCl_3) δ 195.29, 193.67, 167.94, 166.18, 164.25, 163.91, 149.47, 148.92, 148.90, 148.83, 147.04, 137.95, 136.57, 128.22, 126.63, 125.76, 121.81, 121.11, 120.97, 114.40, 114.36, 111.60, 111.58, 111.32, 111.27, 56.07, 56.03, 56.00, 55.92, 55.64, 55.62, 54.01, 53.68, 46.30, 46.00. **FTIR** (neat) 2934, 2836, 1726, 1668, 1578, 1557, 1509, 1455, 1429, 1405, 1310, 1254, 1218, 1155, 1137, 1116, 1201, 931, 835, 810, 755, 725, 662, 551, 523, 421 cm^{-1} . **HRMS** (ESI) calc'd for

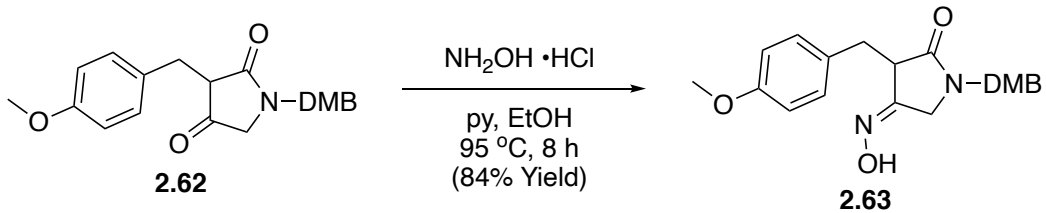
$C_{21}H_{21}NO_5 [M+Na]^+$ 390.1312, found 390.1314 m/z. $R_f = 0.64, 0.70$ (E/Z) (EtOAc). **m.p.** = 129.8 – 130.4 °C.

2.4.14 Preparation of Tetramic Acid **2.62**



To a 250 mL round-bottom flask was added Hantzsch ester (452.6 mg, 1.23 mmol, 1.0 equiv), L-Proline (311.5 mg, 1.23 mmol, 1.0 equiv), and CH_2Cl_2 (77 mL). The solution was cooled to 0 °C under N_2 and alkene **2.61** was added dropwise over 1 hour. The reaction was stirred for an additional 1.5 hours, warming to rt, and concentrated *in vacuo*. The crude was purified *via* flash column chromatography to yield PMB-DMB tetramic acid **2.62** as an off-white solid (407.2 mg, 90% yield). **1H NMR** (600 MHz, DMSO) δ 10.80 (s, 1H, OH), 7.13 (d, $J = 8.6$ Hz, 2H), 6.89 (d, $J = 8.2$ Hz, 1H), 6.79 – 6.81 (m, 2H), 6.75 (d, $J = 2.0$ Hz, 1H), 6.69 (dd, $J = 8.1, 2.0$ Hz, 1H), 4.38 (s, 2H), 3.72 (s, 3H), 3.70 (s, 3H), 3.68 (s, 3H), 3.66 (s, 2H), 3.35 (s, 2H). **13C NMR** (151 MHz, DMSO) δ 172.56, 165.28, 157.32, 148.76, 147.88, 132.53, 130.61, 129.04, 119.59, 113.49, 111.82, 111.25, 104.66, 55.49, 55.31, 54.97, 48.79, 44.39, 25.98. **FTIR** 2934, 2839, 2655, 1584, 1509, 1446, 1421, 1403, 1374, 1353, 1300, 1283, 1256, 1239, 1211, 1176, 1153, 1134, 1109, 1025, 980, 950, 914, 862, 840, 811, 785, 766, 745, 713, 671, 655, 596, 554, 510, 414 (neat) cm^{-1} . **HRMS** (ESI) calc'd for $C_{21}H_{23}NO_5 [M+Na]^+$ 392.1468, found 392.1469 m/z. $R_f = 0.73$ (EtOAc). **m.p.** = 151 – 152 °C.

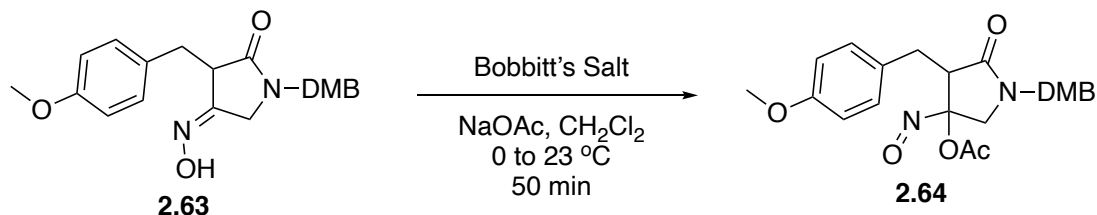
2.4.15 Preparation of Oxime 2.63



To a 500 mL round-bottom flask, tetramic acid **2.62** (489.3 mg, 1.32 mmol, 1.0 equiv) was dissolved in EtOH (207 mL). Hydroxylamine hydrochloride (87.5 mg, 2.65 mmol, 2.0 equiv) and pyridine (0.21 mL, 2.65 mmol, 2.0 equiv) were added, and the solution was refluxed for 8 hours. The reaction was cooled to rt and the solvent removed *in vacuo*. The residue was redissolved in CH₂Cl₂ and washed with 1M HCl (2 x 50 mL). The organic layers were combined, dried (MgSO₄) and purified *via* flash column chromatography to give oxime **2.63** as a yellow foam (427.8 mg, 84% yield) and an inconsequential mixture of E/Z isomers. The structure was confirmed by X-ray crystallography. **¹H NMR** (600 MHz, CDCl₃) δ 7.88 (br s, 1H), 7.06 – 7.13 (m, 2H), 6.68 – 6.73 (m, 3H), 6.63 – 6.65 (m, 1H), 6.33 – 6.38 (m, 1H), 4.46 (d, *J* = 14.7 Hz, 0.8H), 4.29 (dd, *J* = 14.52, 36.01 Hz, 0.6H), 4.19 (d, *J* = 14.7 Hz, 0.8H), 3.85 (s, 3H), 3.81 – 3.83 (m, 3H), 3.75 – 3.76 (m, 3H), 3.50 – 3.53 (m, 1H), 3.42 (d, *J* = 17.2 Hz, 0.8H), 3.19 – 3.26 (m, 1H), 3.13 (dd, *J* = 13.3, 4.5 Hz, 1H). **¹³C NMR** (151 MHz, CDCl₃) δ 172.32, 172.16, 158.63, 158.55, 155.78, 149.21, 149.19, 148.72, 131.02, 130.84, 130.56, 129.08, 128.92, 127.67, 120.79, 120.67, 120.62, 113.94, 113.74, 113.71, 111.81, 111.65, 111.20, 111.15, 56.11, 55.97, 55.21, 52.51, 48.81, 47.24, 46.49, 46.32, 46.22, 46.15, 45.80, 35.48, 32.29, 32.07. **FTIR** (neat) 3442, 3236, 3117, 2916, 1695, 1673, 1611, 1592, 1511, 1464, 1422, 1333, 1302, 1253, 1178, 1158, 1139, 1109, 1025, 976, 950, 925, 862, 828, 810, 763, 744,

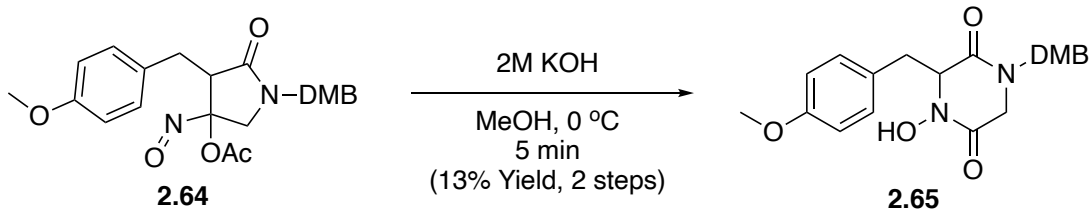
708, 667, 582, 558, 518, 461, 424 cm⁻¹. **HRMS** (ESI) calc'd for C₂₁H₂₄N₂O₅ [M+Na]⁺ 407.1577, found 407.1578 m/z. **R_f** = 0.63, 0.78 (E/Z) (EtOAc).

2.4.16 Preparation of Acyloxy Nitroso **2.64**



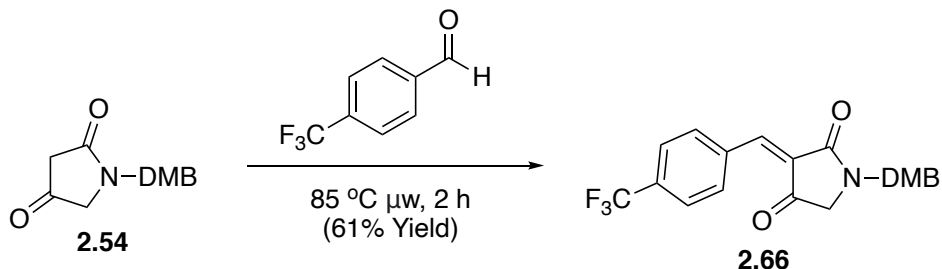
To a flame-dried 50 mL round-bottom flask, oxime **2.63** (50 mg, 0.130 mmol, 1.0 equiv) was dissolved in CH₂Cl₂ (13 mL). The solution was cooled to 0 °C, then NaOAc (32 mg, 0.390 mmol, 3.0 equiv) was added, followed by acetic acid (40 µL, 4.0 equiv). Bobbitt's Salt (97.5 mg, 0.325 mmol, 2.5 equiv), was added last and the reaction stirred at 0 °C for 5 minutes then was warmed to rt. The reaction was quenched with 0.1 mL sat. aq. NaHCO₃, solvent was reduced *in vacuo* and the crude solution was passed through a short pad of silica with 5% EtOAc/CH₂Cl₂. The crude bright blue acyloxy nitroso **2.64** was advanced to the next step without purification. **R_f** = 0.61 (60% EtOAc/hexanes)

2.4.17 Preparation of DKP 2.65



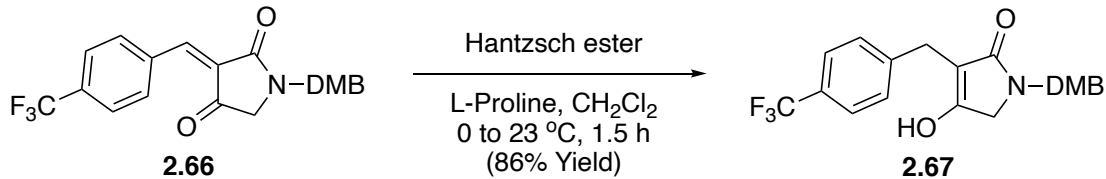
To a 2-Dram vial containing crude **2.64** was added MeOH (1.95 mL). The solution was cooled to 0 °C and 2M KOH (1.95 mL) was added in one portion. The reaction stirred for 5 minutes then was quenched with 1M HCl (1 mL). The crude was concentrated *in vacuo* and purified *via* flash column chromatography to yield DKP **2.65** as an off-white solid (1.4 mg, 13% over 2 steps). The desired product can be visualized with FeCl₃ TLC stain. **¹H NMR** (600 MHz, CDCl₃) δ 8.00 (br s, 1H), 6.91 – 6.94 (m, 2H), 6.79 (d, *J* = 8.2 Hz, 1H), 6.75 (d, *J* = 2.0 Hz, 1H), 6.64 (dd, *J* = 8.1, 2.0 Hz, 1H), 6.61 – 6.63 (m, 2H), 4.68 (t, *J* = 3.9 Hz, 1H), 4.39 (d, *J* = 14.2 Hz, 1H), 4.24 (d, *J* = 14.2 Hz, 1H), 3.87 (d, *J* = 2.0 Hz, 6H), 3.72 (s, 3H), 3.46 – 3.49 (m, 1H), 3.37 (dd, *J* = 14.0, 4.3 Hz, 1H), 3.23 (dd, *J* = 14.0, 2.7 Hz, 1H), 2.53 (d, *J* = 17.0 Hz, 1H). **¹³C NMR** (151 MHz, CDCl₃) δ 163.91, 159.23, 159.08, 149.23, 149.07, 131.03, 126.88, 125.55, 121.58, 113.81, 112.27, 111.02, 62.59, 56.02, 55.95, 55.10, 49.33, 46.53, 34.80, 29.71, 14.13. **FTIR** (neat) 3180, 3001, 2929, 2837, 1668, 1635, 1610, 1595, 1511, 1464, 1438, 1420, 1357, 1327, 1300, 1238, 1180, 1166, 1142, 1112, 1095, 1025, 984, 948, 918, 864, 804, 752, 731, 653, 608, 576, 553, 514, 459 cm⁻¹. **HRMS** (ESI) calc'd for C₂₁H₂₄N₂O₆ [M+Na]⁺ 423.1527, found 423.1526 m/z. **R_f** = 0.36 (EtOAc).

2.4.18 Preparation of Alkene **2.66**



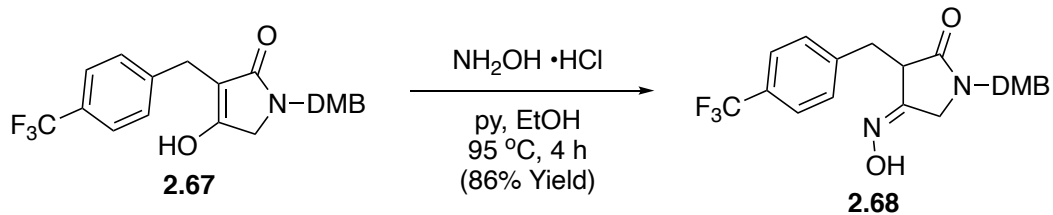
In a 35 mL CEM® microwave tube was added tetramic acid **2.54** (792.2 mg, 3.18 mmol, 1.0 equiv), 4-(Trifluoromethyl)benzaldehyde (830 mg, 4.77 mmol, 1.5 equiv), and MeOH (17 mL). The solution was irradiated at 85 °C for 2 hours then cooled to rt. The crude was purified *via* flash column chromatography to yield alkene **2.66** as a light orange foam (789.2 mg, 61% yield, inconsequential mixture of E/Z isomers). **¹H NMR** (400 MHz, CDCl₃) δ 8.47 (d, *J* = 8.2 Hz, 2H), 7.77 (d, *J* = 32.8 Hz, 2H), 7.71 (s, 1H), 6.82 – 6.86 (m, 3H), 4.68 (s, 2H), 3.87 (s, 6H). **¹³C NMR** (101 MHz, CDCl₃) δ 194.65, 193.49, 166.43, 164.76, 149.71, 149.26, 146.62, 144.91, 135.99, 135.59, 134.69, 134.30, 133.97, 133.39, 127.72, 126.62, 126.24, 125.83, 125.79, 125.69, 125.65, 121.27, 111.82, 111.50, 111.46, 56.24, 56.20, 56.16, 54.08, 53.85, 46.68, 46.38. **FTIR** (neat) 2937, 2837, 1736, 1677, 1319, 1593, 1514, 1459, 1419, 1320, 1258, 1237, 1158, 1122, 1066, 1018, 912, 844, 809, 730, 666, 552, 448 cm⁻¹. **HRMS** (ESI) calc'd for C₂₁H₁₈F₃NO₄ [M+Na]⁺ 428.1080, found 428.1079 m/z. **R_f** = 0.65, 0.83 (E/Z) (50% EtOAc/hexanes).

2.4.19 Preparation of Tetramic Acid **2.67**



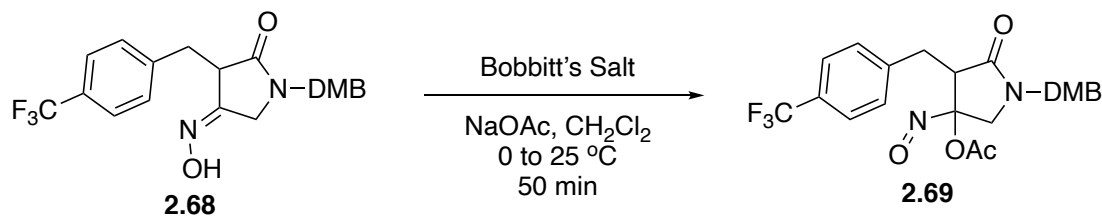
To a 100 mL round-bottom flask was added Hantzsch ester (202.6 mg, 0.80 mmol, 1.0 equiv), L-Proline (4.6 mg, 0.04 mmol, 0.05 equiv), and CH_2Cl_2 (55 mL). Alkene **2.66** was added dropwise *via* syringe pump over 30 minutes. The reaction stirred for 1.5 hours, warming to rt, then concentrated *in vacuo*. The crude was purified *via* flash column chromatography to yield tetramic acid **2.67** as a white solid (279.3 mg, 86% yield). **$^1\text{H NMR}$** (400 MHz, CDCl_3) δ 7.48 (d, $J = 8.22$ Hz, 2H), 7.32 (d, $J = 8.22$ Hz, 2H), 6.68 (d, $J = 8.22$ Hz, 1H), 6.66 (d, $J = 1.96$ Hz, 1H), 6.32 (dd, $J = 1.96, 8.22$ Hz, 1H), 4.68, (d, $J = 14.45$ Hz, 1H), 4.25 (d, $J = 14.45$ Hz, 1H), 3.84 (s, 3H), 3.82 (s, 3H), 3.62 (d, $J = 17.70$ Hz, 1H), 3.23 – 3.32 (m, 2H), 3.19 (d, $J = 17.70$ Hz, 1H). **$^{13}\text{C NMR}$** (151 MHz, CDCl_3) δ 206.33, 170.40, 149.40, 149.06, 130.36, 127.13, 125.61, 125.58, 120.40, 111.74, 111.35, 56.16, 56.02, 55.86, 52.00, 45.95, 32.26. **FTIR** (neat) 2964, 2922, 2841, 2445, 1686, 1582, 1515, 1468, 1451, 1420, 1410, 1375, 1356, 1325, 1258, 1216, 1195, 1160, 1136, 1112, 1064, 1020, 1039, 1020, 984, 952, 912, 854, 814, 788, 765, 750, 731, 660, 632, 591, 563, 552, 498, 432 cm^{-1} . **HRMS** (ESI) calc'd for $\text{C}_{21}\text{H}_{20}\text{F}_3\text{NO}_4$ $[\text{M}+\text{H}]^+$ 408.1417, found 408.1419 m/z; for $[\text{M}+\text{Na}]^+$ 430.1237, found 430.1238 m/z. $\text{R}_f = 0.36$ (EtOAc).

2.4.20 Preparation of Oxime **2.68**



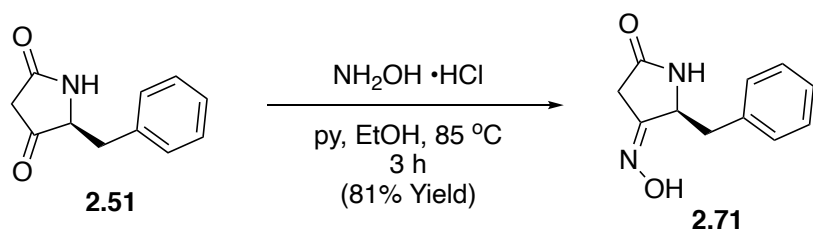
To a 100 mL round-bottom flask was added tetramic acid **2.67** (112.5 mg, 0.28 mmol, 1.0 equiv) and EtOH (50 mL). Hydroxylamine hydrochloride (18.24 mg, 0.55 mmol, 2.0 equiv) and pyridine (44 μ L, 0.55 mmol, 2.0 equiv) were added and the mixture was refluxed for 4 hours. The reaction was cooled to rt and quenched with 1M HCl (20 mL). The crude was purified *via* flash column chromatography to yield oxime **2.68** as a white foam (101.8 mg, 86% yield) and an inconsequential ~1:1 mixture of E/Z isomers. For simplicity in the NMR, one isomer was separated and tabulated. ¹H NMR (400 MHz, CDCl₃) δ 8.73 (br s, 1H), 7.43 (d, *J* = 7.9 Hz, 2H), 7.30 (d, *J* = 7.9 Hz, 2H), 6.66 – 6.69 (m, 2H), 6.29 (dd, *J* = 8.2, 2.1 Hz, 1H), 4.54 (d, *J* = 14.5 Hz, 1H), 4.14 (d, *J* = 14.6 Hz, 1H), 3.87 (dd, *J* = 16.9, 1.6 Hz, 1H), 3.57 – 3.60 (m, 1H), 3.49 (dd, *J* = 16.8, 1.9 Hz, 1H), 3.32 (dd, *J* = 13.5, 5.3 Hz, 1H), 3.23 (dd, *J* = 13.5, 4.8 Hz, 1H). ¹³C NMR (101 MHz, CDCl₃) δ 171.77, 154.54, 149.17, 148.85, 141.22, 130.36, 127.28, 125.27, 125.23, 120.39, 111.76, 111.22, 56.05, 55.89, 47.25, 46.26, 45.92, 35.65. FTIR (neat) 3432, 3260, 2933, 2909, 2839, 1697, 1662, 1617, 1593, 1515, 1465, 1441, 1418, 1322, 1259, 1237, 1157, 1109, 1065, 1020, 972, 933, 880, 833, 808, 764, 748, 723, 666, 622, 605, 552, 414 cm⁻¹. HRMS (ESI) calc'd for C₂₁H₂₁F₃N₂O₄ [M+Na]⁺ 445.1346, found 445.1342 m/z. R_f = 0.64, 0.76 (E/Z) (EtOAc).

2.4.21 Preparation of Acyloxy Nitroso **2.69**



To a 50 mL round-bottom flask was added oxime **2.68** (50 mg, 0.118 mmol, 1.0 equiv) and CH_2Cl_2 (13 mL). The solution was cooled to 0 °C, and NaOAc (29.04 mg, 0.354 mmol, 3.0 equiv) and acetic acid (40 μ L, 4.0 equiv) were added. Bobbitt's Salt (88.8 mg, 0.296 mmol, 2.5 equiv) was added last, and the solution was stirred at 0 °C for 5 minutes then warmed to rt for an additional 50 minutes. The reaction was quenched with 0.1 mL sat. aq. NaHCO_3 and the solvent was reduced *in vacuo*. The crude was passed through a short pad of silica with 5% EtOAc/ CH_2Cl_2 and the crude bright blue acyloxy nitroso **2.69** was advanced to the next step without purification. $\text{R}_f = 0.63$ (50% EtOAc/hexanes).

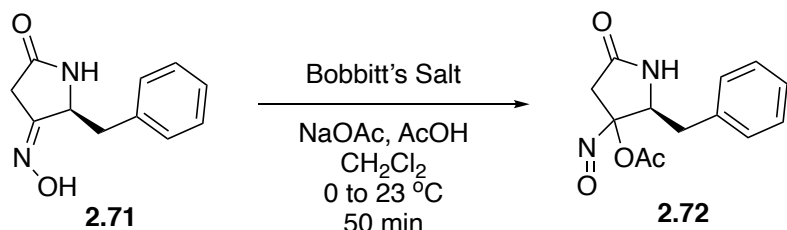
2.4.22 Preparation of Oxime **2.71**



To a 100 mL round-bottom flask was added known tetramic acid **2.51** (500 mg, 2.6 mmol, 1.0 equiv), hydroxylamine hydrochloride (550 mg, 7.92 mmol, 3.0 equiv), and

pyridine (0.61 mL, 7.66 mmol, 2.9 equiv) in EtOH (25 mL). The solution was heated at 85 °C for 3 hours then cooled to rt, concentrated *in vacuo*, and neutralized with 1M HCl (10 mL). The aqueous phase was extracted with CH₂Cl₂ (3 x 20 mL), dried (MgSO₄), and purified *via* flash column chromatography to yield oxime **2.71** as a yellow foam (530 mg, 81% yield) and an inconsequential ~3:1 mixture of E/Z isomers. **¹H NMR** (400 MHz, DMSO) δ 11.03 (d, *J* = 38.1 Hz, 1H), 8.11 (d, *J* = 31.0 Hz, 1H), 7.20 – 7.29 (m, 3H), 7.11 – 7.17 (m, 2H), 4.59 (dt, *J* = 78.6, 4.6 Hz, 1H), 2.81 – 3.24 (m, 2H), 2.64 (dd, *J* = 21.7, 1.6 Hz, 1H), 2.19 (dd, *J* = 21.7, 1.6 Hz, 1H). **¹³C NMR** (101 MHz, DMSO) δ 171.56, 154.88, 154.18, 136.39, 136.36, 129.97, 129.81, 127.98, 126.47, 126.33, 56.81, 55.90, 36.27, 33.65, 31.93. **FTIR** (neat) 3221, 3027, 2922, 1694, 1666, 1494, 1456, 1432, 1391, 1367, 1301, 1082, 961, 942, 724, 700, 635, 467 cm⁻¹. **HRMS** (ESI) calc'd for C₁₁H₁₂N₂O₂ [M+H]⁺ 205.0972, found 205.1008 m/z; for [M+Na]⁺ 227.0791, found 227.0832 m/z. **R_f** = 0.55, 0.66 (E/Z) (EtOAc). [α]_D²²: (c = 0.10, MeOH), -104°.

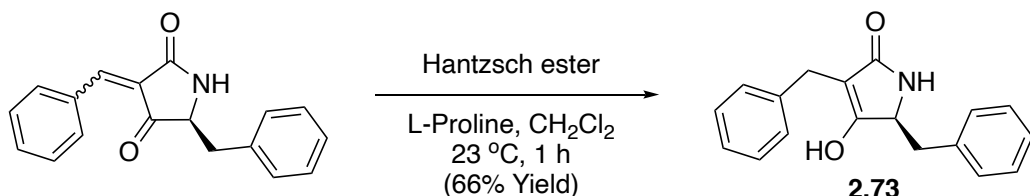
2.4.23 Preparation of Acyl Nitroso **2.72**



To a 5 mL round-bottom flask was added oxime **2.71** (18.5 mg, 0.09 mmol, 1.0 equiv) and CH₂Cl₂ (1.3 mL). The solution was cooled to 0 °C and NaOAc (22.4 mg, 0.27 mmol, 3.0 equiv) and AcOH (20.8 μL, 0.36 mmol, 4.0 equiv) were added, sequentially.

Bobbitt's Salt (67.8 mg, 0.23 mmol, 2.5 equiv) was added last and the reaction stirred for 5 minutes at 0 °C, then warmed to rt for 50 minutes. The crude was filtered directly through a short pad of silica, concentrated *in vacuo*, and the light blue oil acyl nitroso **2.72** was advanced to the next step without purification.

2.4.24 Data for Known Tetramic Acid **2.73**



$^1\text{H NMR}$ (400 MHz, MeOD) δ 7.21 (s, 5H), 7.03 – 7.11 (m, 3H), 6.82 (d, J = 6.8 Hz, 2H), 4.28 (t, J = 4.8 Hz, 1H), 3.38 (dd, J = 38.37, 15.18 Hz, 2H), 3.15 (dd, J = 13.8, 4.1 Hz, 1H), 2.94 (dd, J = 13.8, 5.5 Hz, 1H). **$^{13}\text{C NMR}$** (101 MHz, MeOD) δ 177.82, 171.66, 140.85, 136.97, 130.96, 129.15, 129.04, 128.98, 127.73, 126.49, 106.52, 58.40, 37.91, 27.23.

2.6 References

¹ (a) Borthwick, A. D. “2,5-Diketopiperazines: Synthesis, Reactions, Medicinal Chemistry, and Bioactive Natural Products” *Chem. Rev.* **2012**, *112*, 3641-3716. (b) “Diketopiperazines from Marine Organisms:” Huang, R.; Zhou, X.; Xu, T.; Yang, X.; Liu, Y. *Chem. Biodivers.* **2010**, *7*, 2809-2829.

² Jida, M.; Ballet, S. *Chemistry Select*, **2018**, *3*, 1027-1031.

³ (a) Brown, R.; Meehan, G. *Aust. J. Chem.* **1968**, *21*(6), 1581-1599.
 (b) Shinmon, N.; Cava, M. P. *J. C. S. Chem. Comm.* **1980**, *21*, 1020-1021.

⁴ (a) Isolation and analysis of aspirochlorine: Berg, D. H.; Massing, R. P.; Hoehn, M. M.; Boeck, L. D.; Hamill, R. L. *J. Antibiot.*, **1976**, *29*, 394-397.

(b) Sakata, K.; Masago, H.; Sakurai, A.; Takahashi, N. *Tetrahedron Lett.* **1982**, *28*, 5607-5610.

(c) Sakata, K.; Kuwatsuka, T.; Sakurai, A.; Takahashi, N.; Tamura, G. *Agric. Biol. Chem.* **1983**, *47*(11), 2673-2674.

(d) Sakata, K.; Maruyama, M.; Uzawa, J.; Sakurai, A.; Lu, H. S. M.; Clardy, J. *Tetrahedron Lett.* **1987**, *28*(46), 5607-5610.

(e) Completion of aspirochlorine: Miknis, G. F.; Williams, R. M. *J. Am. Chem. Soc.* **1993**, *115*, 536-547.

⁵ (a) Ottenheijm, H.; Herscheid, J. D. M.; Nivard, R. *J. Org. Chem.* **1977**, *42*(5), 925-926.

(b) Herscheid, J. D. M.; Nivard, R.; Tijhuis, M.; Ottenheijm, H. *J. Org. Chem.* **1980**, *45*, 1885-1888.

(c) Herscheid, J. D. M.; Nivard, R.; Tijhuis, M.; Scholten, H.; Ottenheijm, H. *J. Org. Chem.* **1980**, *45*, 1880-1885.

(d) Herscheid, J. D. M.; Colstee, J.; Ottenheijm, H.; *J. Org. Chem.* **1981**, *46*, 3346-3348. Ottenheijm, H.; Herscheid, J. D. M. *J. Chem. Rev.* **1986**, *86*, 697-707.

⁶ (a) Liu, S.; Mu, Y.; Han, J.; Zhen, X.; Yang, Y.; Tian, X.; Whiting, A. *Org. Biomol. Chem.* **2011**, *9*, 7476-7481.

(b) Tian, X.; Feng, J.; Fan, S.; Zhen, X.; Han, J.; Liu, S. *Bioorg. Med. Chem.* **2016**, *24*(21), 5197-5205.

Isolation of etzionin: (c) Hirsch, S.; Miroz, A.; McCarthy, J.P.; Kashman, Y. *Tetrahedron Lett.* **1989**, *30*(32), 4291-4294.

(d) Kouchaksaraee, R. M.; Li, F.; Nazemi, M.; Farimani, M. M.; Tasdemir, D. *Mar. Drugs* **2021**, *19*, 439.

⁷ (a) Lin, D. W.; Masuda, T.; Biskup, M. B.; Nelson, J. D.; Baran, P. S. *J. Org. Chem.* **2011**, *76*(4), 1013-1030.

(b) Usui, I.; Lin, D. W.; Masuda, T.; Baran, P. S. *Org. Lett.* **2013**, *15*(9), 2080-2083.

⁸ (a) Gayler, K. M.; Lambert, K. M.; Wood, J. L. *Tetrahedron*, **2019**, *75*(24), 3154-3159.

(b) Gayler, K. M. (2020) "Synthetic Studies towards Penicisulfuranol B; C-H Activation Borylation of Staurosporine; Design, Synthesis, and Biological Evaluation of Rapamycin and Tak-242 Bioconjugates; Design, Synthesis, and Evaluation of Gemfibrozil Analogs." [Doctoral dissertation, Baylor University].

(c) Isolation of penicisulfurans: Zhu, M.; Zhang, X.; Feng, H.; Dai, J.; Li, J.; Che, Q.; Gu, Q.; Zhu, T.; Li, D. *J. Nat. Prod.* **2017**, *80*(1), 71-75.

⁹ Lambert, K. M.; Cox, J. B.; Liu, L.; Jackson, A. C.; Yruegas, S.; Wiberg, K. B.; Wood, J. L. *Angew. Chem. Int. Ed.* **2020**, *59*, 9757-9766.

¹⁰ For the original reports of this interesting transformation, see: (a) Hadimani, M. B.; Mukherjee, R.; Banerjee, R.; Shoman, M. E.; Aly, O. M.; King, S. B. *Tetrahedron Lett.* **2015**, *56*(43), 5870-5873.
(b) Banerjee, R.; King, S. B. *Org. Lett.* **2009**, *11*(20), 4580-4583.

¹¹ (a) Royles, B. J. *Chem. Rev.* **1995**, *95*, 1981-2001.
(b) Ghisalberti, E. L. *Studies in natural products chemistry*, **2003**, *28*, 109-163.
(c) Gossauer, A. *Fortschritte der Chemie organischer Naturstoffe/Progress in the Chemistry of Organic Natural Products*, Springer, **2003**, 1-188.
(d) Schobert R.; Schlenk, A. *Bioorg. Med. Chem.* **2008**, *16*, 4203-4221.
(e) Mo, X.; Li, Q.; Ju, J. *RSC Adv.* **2014**, *4*, 50566-50593.
(f) Athanasellis, G.; Igglesti-Markopoulou, O.; Markopoulos, J. *Bioinorg. Chem. Appl.* **2010**, 1-11.

¹² Henning, H-G.; Gelbin, A. *Adv. Heterocycl. Chem.* **1993**, *57*, 139-185.

¹³ Mulholland, T. P. C.; Foster, R.; Haydock, D. B. *J. Chem. Soc., Perkin Trans. I.* **1972**, 2121-2128.

¹⁴ (a) Steyn, P. S.; Rabie, C. J. *Phytochemistry* **1976**, *15*, 1977-1979.
(b) Lebrun, M. H.; Duvert, P.; Gaudemer, F.; Gaudemer, A.; Deballon, C.; Boucly, P. *Inorg. Biochem.* **1985**, *24*, 167-181.
(c) Lebrun, M. H.; Nicolas, L.; Boutar, M.; Gaudemer, F.; Ranomenjanahary, S.; Gaudemer, A. *Phytochemistry* **1988**, *27*, 77-84.
(d) Kaufmann, G. F.; Sartorio, R.; Lee, S. H.; Rogers, C. J.; Meijler, M. M.; Moss, J. A.; Clapham, B.; Brogan, A. P.; Dickerson, T. J.; Janda, K. D. *Proc. Natl. Acad. Sci. U.S.A.* **2005**, *102*, 309-314.
(e) Fujita, M.; Nakao, Y.; Matsunaga, S.; Seiki, M.; Itoh, Y.; van Soest, R. W. M.; Fusetani, N. *Tetrahedron* **2001**, *57*, 1229-1234.

¹⁵ (a) Henning, H-G; Gelbin, A. *Adv. Heterocycl. Chem.* **1993**, *57*, 139-185.
(b) Royles, B. J. L. *Chem. Rev.* **1995**, *95*, 1981-2001.
(c) Schobert, R.; Schlenk, A. *Bioorg. Med. Chem.* **2008**, *16*, 4203-4221.
(d) Mo, X.; Li, Q.; Ju. J. *RSC Adv.* **2014**, *4*, 50566-50593, and references within.

¹⁶ Lacey, R. N. *J. Chem. Soc.* **1954**, 850-854.

¹⁷ (a) Schotten, C. *Ber. Dtsch. Chem. Ger.* **1884**, *17*, 2544-2547. Baumann, E. *Ber. Dtsch. Chem. Ger.* **1886**, *19*, 2982-2992.

¹⁸ For an extensive evaluation of the racemization of C5 under Lacey- Dieckmann conditions see: Poncet, J.; Jouin, P.; Castro, B.; Louisette, N.; Boutar, M.; Gaudemer, A. *J. Chem. Soc. Perkin, Trans. I* **1990**, 611-616.

¹⁹ For an example of substrate dependence see the following dissertation: Petsch, D. T. (1999) "The Design and Synthesis of Selective Kinase Inhibitors Based on the Indolocarbazole Natural Product K252a." [Doctoral Dissertation, Yale University].

²⁰ For a discussion of the effect of the use of sodium methoxide versus potassium tert-butoxide on the rate of racemization and a mild preparation of enantiopure tetramic acids and their precursors see: Ley, S.; Smith, S. C.; Woodward, P. R. *Tetrahedron* **1992**, *48*, 1145-1174.

²¹ Jouin, P.; Castro, B.; Nisato, D. *J. Chem. Soc. Perkin Trans. I* **1987**, 1177-1182.

²² Schlessinger, R. H.; Bebernitz, G. R.; Lin, P. *J. Am. Chem. Soc.* **1985**, *107*, 1777- 1778.

²³ Deshong, P.; Ramesh, S.; Elango, V.; Perez, J. J. *J. Am. Chem. Soc.* **1985**, *107*, 5219-5224.

²⁴ Boeckman, R. K.; Starrett, J. E.; Nickell, D.G.; Sum, P.-E. *J. Am. Chem. Soc.* **1986**, *108*, 5549-5559.

²⁵ Neukom, C.; Richardson, D. P.; Myerson, J. H.; Bartlett, P. A. *J. Am. Chem. Soc.* **1986**, *108*, 5559-5568.

²⁶ For a discussion of the effect of the use of sodium methoxide versus potassium tert-butoxide on the rate of racemization and a mild preparation of enantiopure tetramic acids and their precursors see: Ley, S.; Smith, S. C.; Woodward, P. R. *Tetrahedron* **1992**, *48*, 1145-1174.

²⁷ Iwata, Y.; Maekawara, N.; Tanino, K.; Miyashita, M. *Angew. Chem. Int. Ed.* **2005**, *44*, 1532-1536.

²⁸ (a) Wood, J. L.; Stoltz, B. M.; Dietrich, H. J. *J. Am. Chem. Soc.* **1995**, *117*, 10413- 10414.
(b) Wood, J. L.; Stoltz, B. M.; Dietrich, H. J.; Pflum, D. A.; Petsch, D. T. *J. Am. Chem. Soc.* **1997**, *119*, 9641-9651.
(c) Wood, J. L.; Stoltz, B. M.; Goodman, S. N. *J. Am. Chem. Soc.* **1996**, *118*, 10656-10657.
(d) Wood, J. L.; Stoltz, B. M.; Goodman, S. N.; Onwueme, K. *J. Am. Chem. Soc.* **1997**, *119*, 9652-9661.

²⁹ (a) Cramer, N.; Laschat, S.; Baro, A.; Schwalbe, H.; Richter, C. *Angew. Chem. Int. Ed.* **2005**, *44*, 820-822.
(b) Hart, A. C.; Philips, A. J. *J. Am. Chem. Soc.* **2006**, *128*, 1094-1095.

³⁰ Henderson, J. A.; Philips, A. J. *Angew. Chem. Int. Ed.* **2008**, *47*, 8499-8501.

³¹ Yoshinari, T.; Ohmori, K.; Schrems, M. G.; Pfaltz, A.; Suzuki, K. *Angew. Chem. Int. Ed.* **2010**, *49*, 881-885.

- ³² (a) Dhanjee, H. H.; Kobayashi, Y.; Buerger, J. F.; McMahon, T. C.; Haley, M. W.; Howell, J. M.; Fujiwara, K.; Wood, J. L. *J. Am. Chem. Soc.* **2017**, *139*, 14901-14904.
(b) Wang, X.; Porco, J. A. *Angew. Chem. Int. Ed.* **2005**, *44*, 3067-3071.
(c) Marcus, A. P.; Sarpong, R. *Org. Lett.* **2010**, *12*, 4560-4563. (For a correction see: Marcus, A. P.; Sarpong, R. *Org. Lett.* **2014**, *16*, 3420.)
(d) Carlsen, P. N.; Mann, T. J.; Hoveyda, A. H.; Frontier, A. J. *Angew. Chem. Int. Ed.* **2014**, *53*, 9334-9338.
(e) Bai, W. -J.; Pettus, T. R. R. *Org. Lett.* **2018**, *20*, 901-904.
- ³³ (a) Marcus, A. P.; Sarpong, R. *Org. Lett.* **2010**, *12*, 4560-4563. (b) For a correction see: Marcus, A. P.; Sarpong, R. *Org. Lett.* **2014**, *16*, 3420.
- ³⁴ Carlsen, P. N.; Mann, T. J.; Hoveyda, A. H.; Frontier, A. J. *Angew. Chem. Int. Ed.* **2014**, *53*, 9334-9338.
- ³⁵ David, J. G.; Bai, W. -J.; Weaver, M. G.; Pettus, T. R. R. *Org. Lett.* **2014**, *16*, 4384-4387.
- ³⁶ Bai, W. -J.; Jackson, S. K.; Pettus, T. R. R. *Org. Lett.* **2012**, *14*, 3862-3865.
- ³⁷ Dhanjee, H. H.; Kobayashi, Y.; Buerger, J. F.; McMahon, T. C.; Haley, M. W.; Howell, J. M.; Fujiwara, K.; Wood, J. L. *J. Am. Chem. Soc.* **2017**, *139*, 14901-14904.
- ³⁸ Nakhla, M. C.; Wood, J. L. *J. Am. Chem. Soc.* **2017**, *139*, 18504-18507.
- ³⁹ Gil, C.; Bräse, S. *Chem. Eur. J.* **2005**, *11*(9), 2680-2688.
- ⁴⁰ (b) Hantzsch ester reduction: Zheng, C.; You, S-L. *Chem. Soc. Rev.* **2012**, *41*, 2498-2518.
- ⁴¹ (a) Merbouh, N.; Bobbitt, J. M.; Brückner, C. *The New Journal for Organic Synthesis*, **2004**, *36*(1), 1-31.
(b) *Organic Syntheses* prep of Bobbitt's Salt: Bobbitt, J. M.; Eddy, N. A.; Richardson, J. J.; Murray, S. A.; Tilley, L. J. *Org. Synth.* **2013**, *90*, 215-228.
- ⁴² Jackson, A. C.; Olsen, J. T.; Sundstrom, S. S.; Lambert, K. M. *Tetrahedron Lett.* **2022**, *99*(153851), 1-5.
- ⁴³ Lambert, K. M.; Medley, A. W.; Jackson, A. C.; Markham, L. E.; Wood, J. L. *Org. Synth.* **2019**, *96*, 528-585.
- ⁴⁴ Karaiskos, C. S. *Molecules*, **2011**, *16*, 6116-6128. Xie, Z. China, CN107056672 A 2017-08-18.

CHAPTER THREE

Total Synthesis of (+)-Raistrickindole A

3.1 Background and Significance

3.1.1 Isolation

(+)-Raistrickindole A (Figure 3.10) was isolated in 2019 by Li and co-workers from *Penicillium raistrickii* IMB17-034 collected from marine sediments in a mangrove swamp.¹ Biological evaluation revealed modest cytotoxicity in an *in vitro* inhibitory assay against the hepatitis C virus, with an EC₅₀ value of 5.7 μM. (+)-Raistrickindole A contains an oxygenated 1,2-oxazine core, which is considered a rare and, despite its potential in drug discovery, underexplored heterocycle due to a very limited number of natural products known to contain it, and is embedded in a tryptophan/phenylalanine-derived tetraheterocycle which has no known matching counterpart in nature.¹ Most importantly, we were interested in (+)-raistrickindole A for its *N*-oxy-2,5-DKP core, which poses an attractive synthetic challenge and a valuable opportunity to develop methods for accessing novel targets containing this functionality.

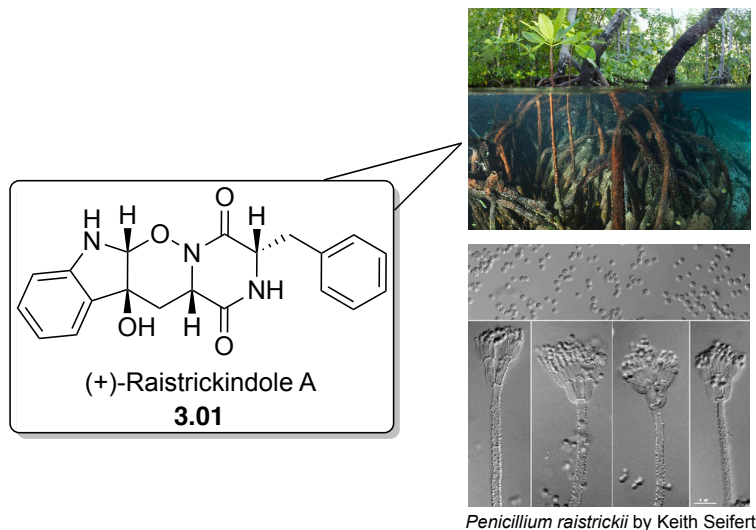


Figure 3.10. Structure and isolation of (+)-raistrickindole A.

3.1.2 The Ring Expansion in the Context of Total Synthesis

The original motivation for the development of the ring expansion discussed *vide supra* was its potential utility in the total synthesis of *N*-oxy-2,5-DKP-containing natural products. Therefore, it was our expectation to incorporate our optimized sequence in the total synthesis of (+)-raistrickindole A.

3.2 Applying the Ring Expansion Toward (+)-Raistrickindole A

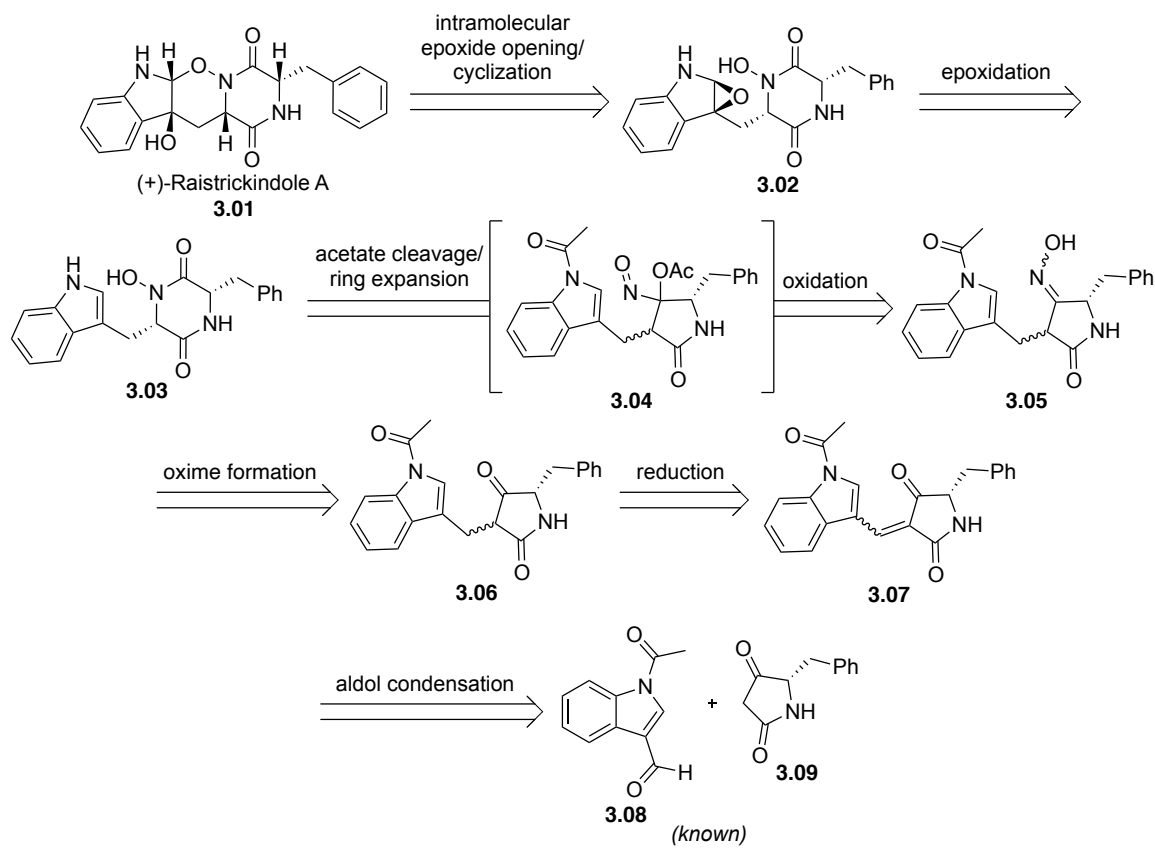
In the development of a substrate scope for the ring expansion of tetramic acids, we found the reaction to be highly substrate-dependent. Nevertheless, we believed that the total synthesis of (+)-raistrickindole A might be amenable to its incorporation. Using this strategy, we could potentially access the natural product in a concise fashion while demonstrating the potential utility of this method for installing an *N*-*O* bond in a complex natural product.

As described in our ring expansion of various substituted tetramic acid substrates (Chapter Two), we sought to first prepare a functionalized chiral tetramic acid derivative

containing the indole moiety necessary for a synthesis of (+)-raistrickindole A, and then subject this substrate to a ring expansion (c.f., **3.03** and **3.05**, Scheme 3.10). By design, the late-stage incorporation of the *N*-*O* bond was expected to maintain its integrity.

3.2.1 Retrosynthetic Analysis

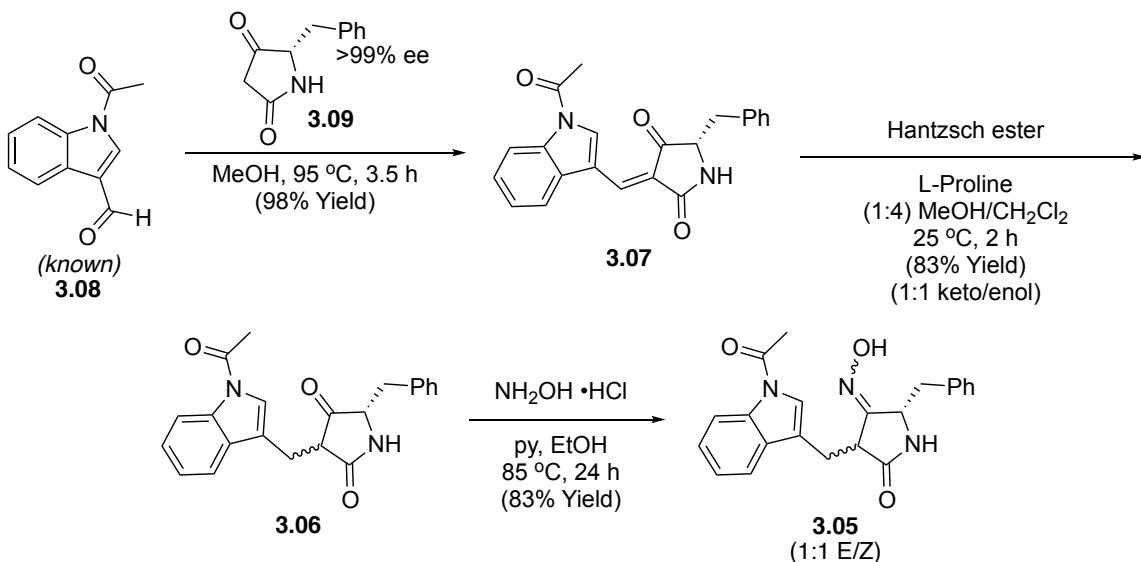
We envisioned that both the tertiary alcohol and 1,2-oxazine core in (+)-raistrickindole A (**3.01**) could arise from a late-stage intramolecular epoxide opening/cyclization of **3.02** (Scheme 3.10). This late-stage maneuver was inspired by biosynthetic speculations made in the isolation paper.¹ In these early planning stages, the stereochemical outcome in the epoxidation of **3.03** was difficult to predict; however, the tendency for DKPs to adopt rather rigid “clamshell”-like conformations led us to speculate that some level of 1,3-induction would be observed.² DKP **3.03** would be the result of the ring expansion sequence, proceeding through acyloxy nitroso intermediate **3.04**, which derives from oxidation of oxime **3.05**. The oxime can be formed from ketone **3.06**, which bears the necessary pre-functionalization: indole moiety at the 3-position and (5*S*)-benzyl group. Tetramic acid **3.06** is obtained from reduction of benzylidene **3.07** which is assembled from an aldol condensation of known acyl-protected indole carbaldehyde **3.08**³ and known enantiopure (>99% ee) (5*S*)-benzyl substituted tetramic acid **3.09**.⁴



Scheme 3.10. Retrosynthetic analysis for (+)-raistrickindole A utilizing the ring expansion.

3.2.2 Attempting the Ring Expansion

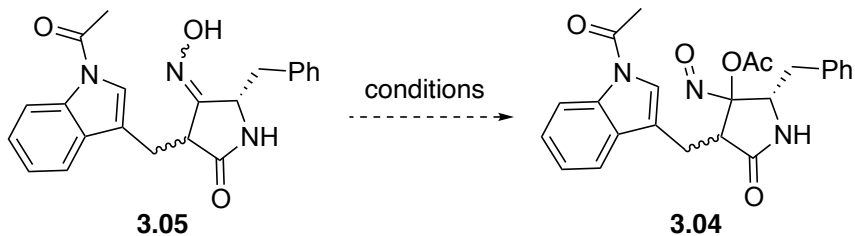
Our synthesis commenced with a microwave-assisted Claisen-Schmidt condensation of two known compounds: acyl-protected indole carbaldehyde **3.08** and (5*S*)-benzyl tetramic acid **3.09**⁴ (Scheme 3.11). We obtained the desired condensation product **3.07** in 98% yield as a single diastereomer, upon which an L-Proline-mediated 1,4-reduction with Hantzsch ester⁵ led to the formation of substituted tetramic acid **3.06** in 83% yield.



Scheme 3.11. Formation of a functionalized oxime, precursor to the ring expansion.

Unlike our di-benzyl-substituted tetramic acid in Chapter Two, the treatment of **3.06** with hydroxylamine hydrochloride and pyridine produced the desired oxime **3.05** in 83% yield (as an inconsequential ~1:1 mixture of E/Z isomers). To our dismay, every attempt to oxidize the oxime to acyloxy nitroso intermediate **3.04** (Table 3.10) led to either complex mixtures of unidentifiable products or presumed collapse of the tetrahedral intermediate (**3.04**) to give earlier ketone precursor **3.06** (a common by-product observed in the ring expansion of various tetramic acids). In some experiments, trace evidence of desired product formation was visible *via* UPLC but isolable quantities were never obtained.

Table 3.10. Attempts to oxidize oxime **3.05** to acyloxy nitroso intermediate **3.04**.



Entry	Oxidant	Additive	Solvent	Result
1	Bobbitt's Salt	AcOH	CH ₂ Cl ₂	complex mixture
2	Bobbitt's Salt	AcOH, py	CH ₂ Cl ₂	SM & ketone 3.06
3	PIDA	-	CH ₂ Cl ₂	trace
4	PIDA	AcOH	CH ₂ Cl ₂	trace
5	PIDA	AcOH	MeOH	trace
6	PIDA	AcOH	MeCN	trace
7	PIDA	AcOH	DMF	trace
8	PIFA	-	CH ₂ Cl ₂	trace
9	DMP	-	CH ₂ Cl ₂	ketone
10	Pb(OAc) ₄	-	CH ₂ Cl ₂	ketone

These results, in concurrence with the troubles we faced in the development of the ring expansion method, led us to seek alternatives for accessing (+)-raistrickindole A (**3.01**). To this end, we opted to revise our synthetic plan so as to incorporate a nitroso Diels-Alder strategy, an alternative yet still convergent method for installing the *N*-*O* bond in **3.01**.

3.3 Accessing (+)-Raistrickindole A via an Intramolecular Nitroso Diels-Alder

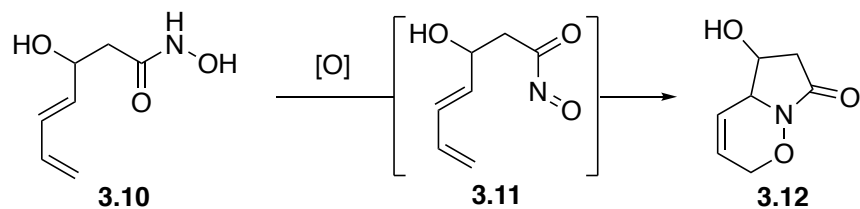
3.3.1 Background on the Nitroso Diels-Alder (NDA) Reaction

There are a number of reports in the literature describing the use of both aryl and acyl nitroso intermediates as dienophiles in nitroso Diels-Alder (NDA) cycloadditions to access 1,2-oxazine-containing compounds. The NDA reaction was first reported by Wichterle and Arbuzov,⁶ and there have since been several reviews on the subject⁷

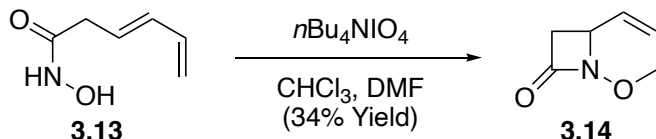
discussing the regio- and diastereoselective tendencies of the reaction, as well as the broad range of oxidants that can be used to generate the requisite acyl nitroso dienophiles. In considering ways to access (+)-raistrickindole using this method, we turned toward the literature for inspiration.

The NDA reaction, used to access 1,2-oxazine rings, has been reported various times in the literature. *Intramolecular* NDA reactions are less common than their *intermolecular* counterparts^{7c} with the first example reported by Keck in 1978,^{8a} and later extensively described by Miller^{8b} (Scheme 3.12). Perhaps more relevant to our natural product is a report by Sheradsky and co-workers in 1998,^{7a} which utilizes an intramolecular NDA reaction to form a fused DKP/1,2-oxazine system (**3.18**, Scheme 3.12) which closely resembles the core of (+)-raistrickindole A (**3.01**).

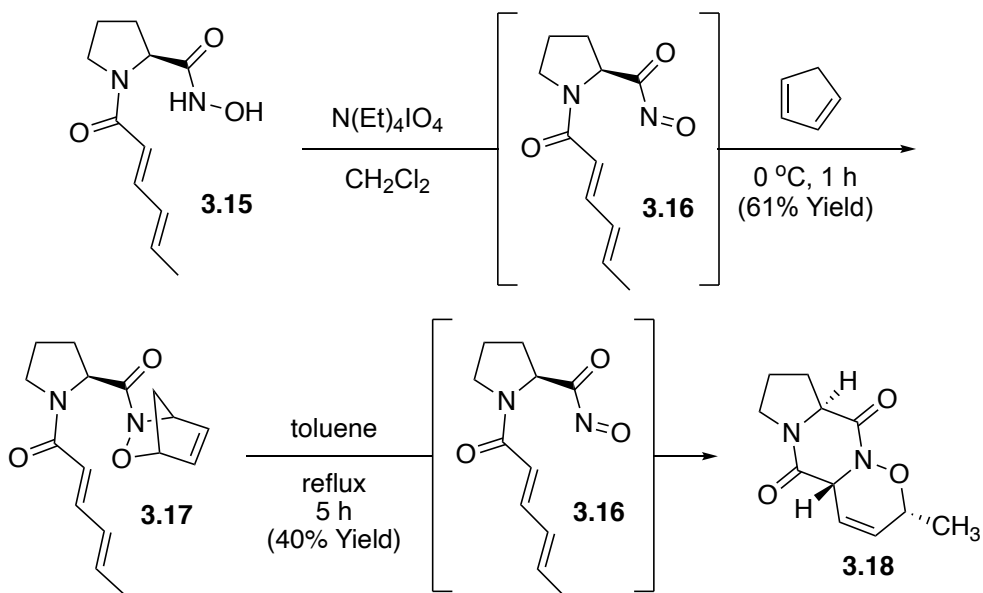
Keck and co-workers:



Miller and co-workers:



Sheradsky and co-workers:



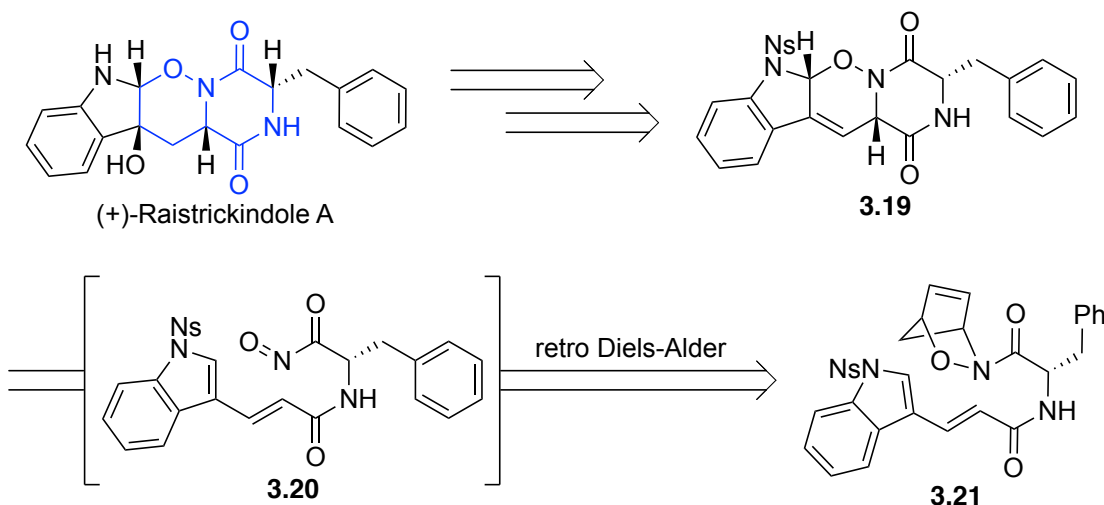
Scheme 3.12. Intramolecular NDA reactions in the literature.

Sheradsky and co-workers utilize an “auxiliary” approach to obtain **3.18**. Oxidation of hydroxamic acid **3.15** with tetraethylammonium (meta)periodate produces acyl nitroso dienophile **3.16**, which is then captured with cyclopentadiene to form a [2.2.1] bicyclic (**3.17**). The acyl nitroso is then regenerated *via* a retro Diels-Alder reaction and immediately followed by intramolecular NDA to give **3.18**. This type of strategy can be

beneficial on the occasion that the NDA reaction is the rate limiting step in the cyclization (i.e., due to a sluggish diene, or spacial configuration). Trapping the reactive nitroso with cyclopentadiene (a known facile reaction) can also allow for isolation of the [2.2.1] bicycle with the removal of harsh oxidizing reagents/by-products prior to exposing the substrate to the thermal conditions required for cyclopentadiene expulsion and intramolecular NDA reaction. Since the core of (+)-raistrickindole A is so similar to the system reported by Sheradsky, we believed that we could benefit from this same “auxiliary” approach in our synthesis.

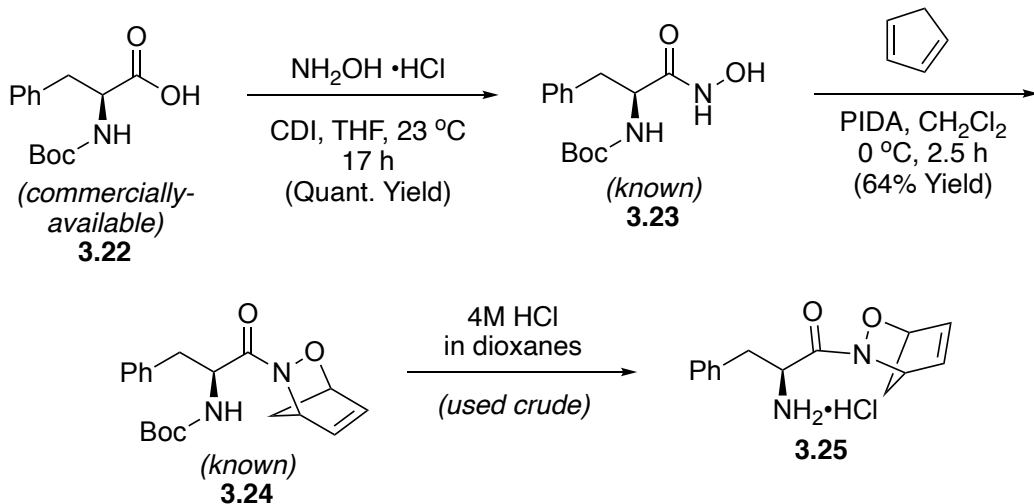
3.3.2 A “Protective” Intramolecular NDA Approach

Shown retrosynthetically, we believed that (+)-raistrickindole A could be traced back to a 1,2-oxazine-containing intermediate such as **3.19** (Scheme 3.13). Following precedence by Sheradsky, this oxazine intermediate could be generated *via* a retro Diels-Alder reaction from cyclopentadiene adduct **3.21**.



Scheme 3.13. Plan to access (+)-raistrickindole A *via* an intramolecular NDA.

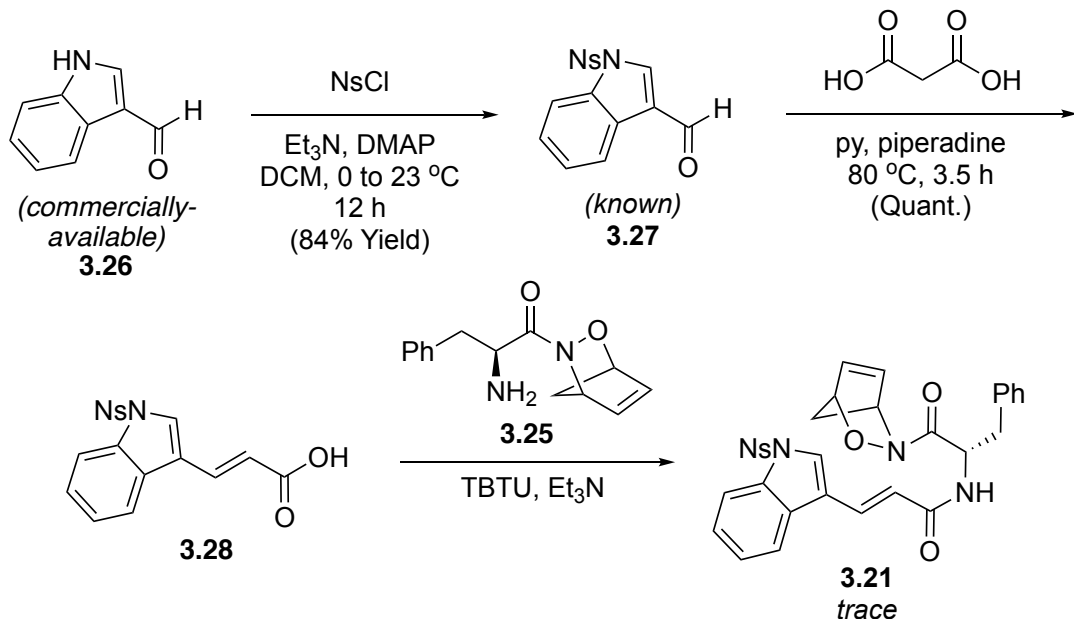
We first sought to design an efficient approach to cyclopentadiene adduct **3.21**, considering that formation of the cyclopentadiene adduct with the requisite L-phenylalanine derivative and then coupling it to the indole component would be nicely convergent. To this end, the known hydroxamic acid **3.23**⁹ fragment was prepared from commercially-available Boc-protected L-phenylalanine amino acid **3.22** in quantitative yield by treatment with carbonyldiimidazole (CDI) and hydroxylamine hydrochloride (Scheme 3.14). Hydroxamic acid **3.23** was then oxidized to the nitroso intermediate with PIDA and treated with freshly-distilled cyclopentadiene to afford known NDA adduct **3.24**.¹⁰ The NDA adduct **3.24** was then deprotected with 4M HCl in dioxanes to reveal the amine as an HCl salt (**3.25**), and poised for amide coupling with indoleacrylic acid.



Scheme 3.14. Synthesis of known cyclopentadiene adduct.

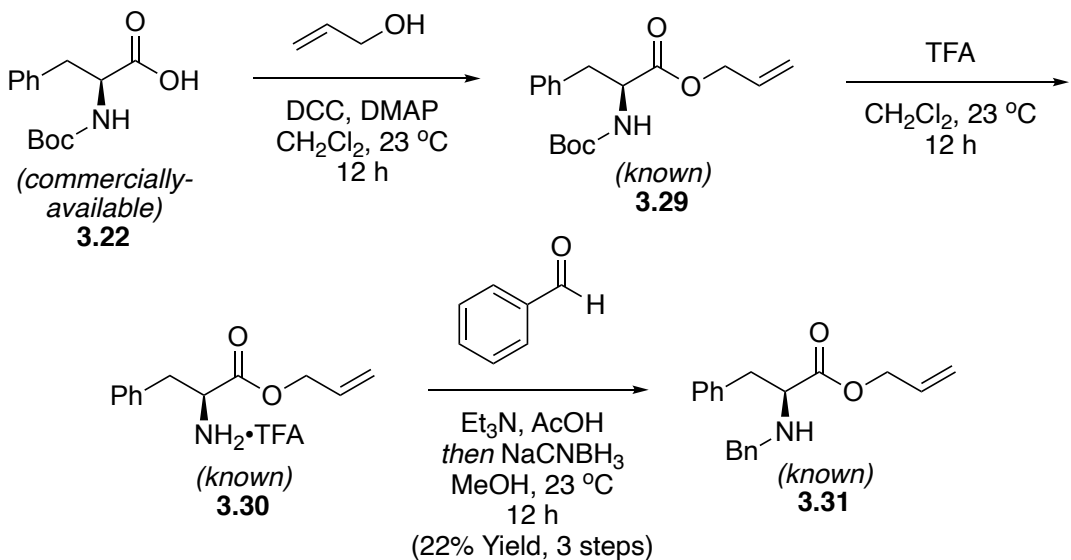
In order to access the indoleacrylic acid moiety (**3.28**, Scheme 3.15) to couple with **3.25**, we first prepared known Ns-protected indole carbaldehyde **3.27**³ by treatment of commercially-available **3.26** with NsCl (84% yield). Indole **3.27** was then subjected to

Doebner-modified Knoevenagel condensation with malonic acid to afford Ns-protected indoleacrylic acid **3.28** in quantitative yield.



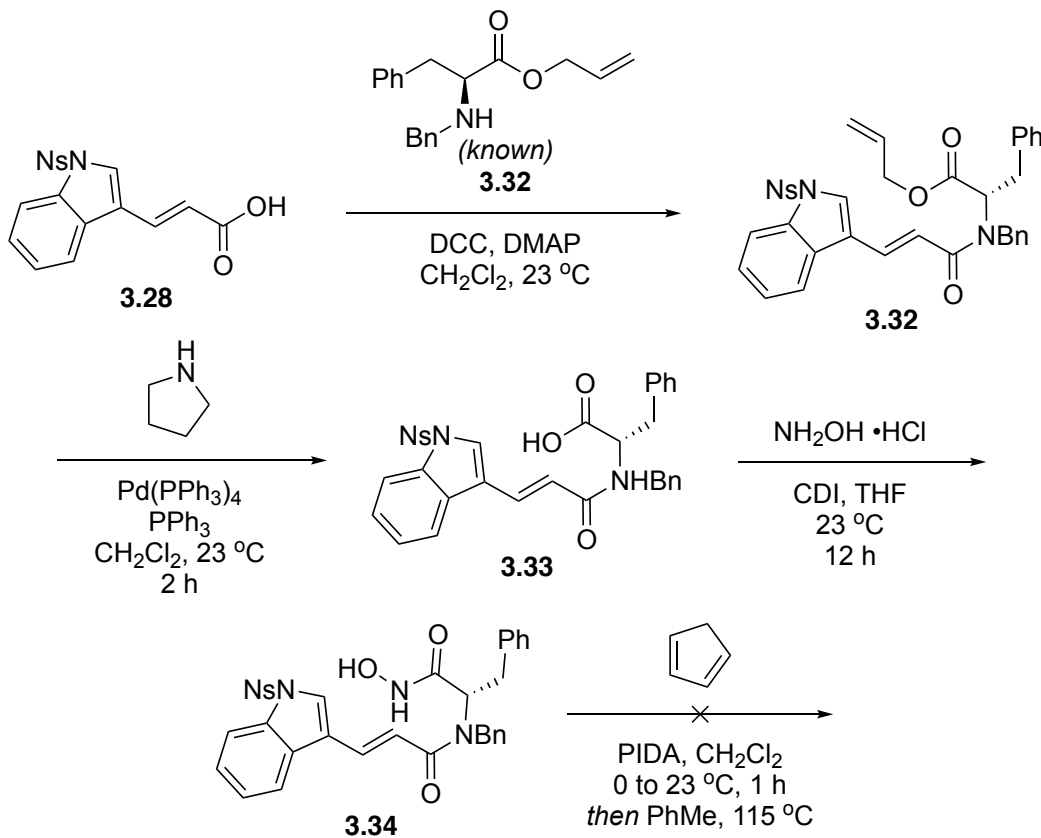
Scheme 3.15. Synthesis of retro Diels-Alder/NDA sequence precursor.

Unfortunately, coupling of indoleacrylic acid **3.28** and cyclopentadiene adduct **3.25** with TBTU and Et₃N gave only trace amounts of the desired amide **3.21**. Additional attempts to prepare **3.21** under a number of amide coupling procedures proved unsuccessful and we never obtained quantities of **3.21** sufficient to enable exploration of the retro Diels-Alder/NDA sequence. Thus, we turned toward the alternative approach of performing the amide coupling prior to forming the cyclopentadiene adduct (Scheme 3.16).



Scheme 3.16. Synthesis of Bn-protected allyl ester.

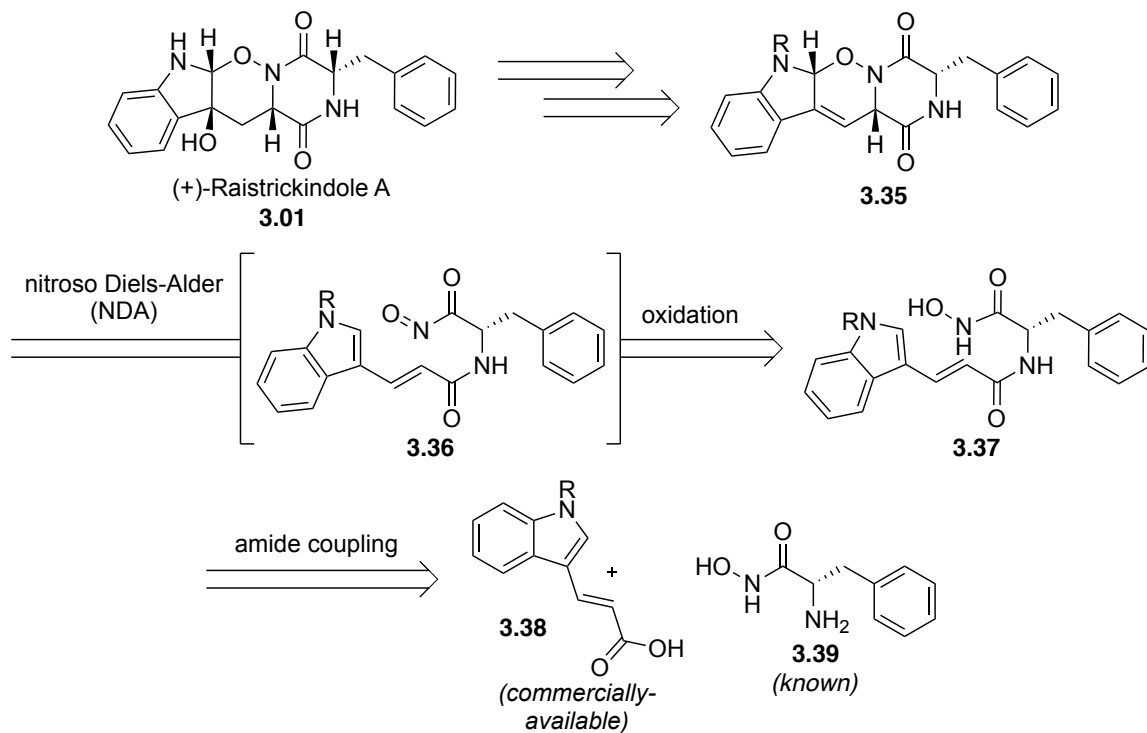
In the event, commercially-available **3.22** was treated with allyl alcohol and DCC, catalyzed with DMAP, to afford Boc-protected allyl ester **3.29**. Deprotection with TFA gave primary amine **3.30**, and subsequent reductive amination with benzaldehyde gave Bn-protected allyl ester **3.31**. As illustrated in Scheme 3.17, the derived ester **3.31** was coupled with Ns-protected indoleacrylic acid **3.28** to furnish amide **3.32**. Given difficulties with purification, we attempted to telescope the sequence to the retro Diels-Alder precursor. Thus, direct subjection of **3.32** to de-allylation in the presence of catalytic Pd(PPh₃)₄ and PPh₃ gave **3.33**, which was then treated with hydroxylamine hydrochloride to furnish hydroxamic acid **3.34**. Unfortunately, all efforts to effect the NDA reaction by oxidation of **3.34** in the presence of cyclopentadiene were unsuccessful. Due to our inability to access the retro Diels-Alder precursor, we turned our attention toward accessing the desired 1,2-oxazine/DKP bicycle *via* direct NDA reaction of an intermediate acyl nitroso compound.



Scheme 3.17. Attempt to synthesize an alternative retro Diels-Alder/NDA precursor.

3.3.3 An Intramolecular 3-Step Approach

As illustrated in Scheme 3.18, our alternative strategy called for an NDA cycloaddition of an intermediate hydroxamic acid (**3.37**) to furnish the 1,2-oxazine ring *via* the intermediacy of the corresponding acyl nitroso compound **3.36**. This change in strategy was an exciting prospect as it potentially allows for a very short route to **3.01**. As illustrated, we believed that the stereochemical outcome in the formation of **3.35** could be governed by the resident stereogenic center and potentially by the aforementioned “clamshell”-type conformations of the DKPs,² which induce a kinetic preference *via* differing transition state energies or perhaps a thermodynamic preference in the case of a reversible NDA.



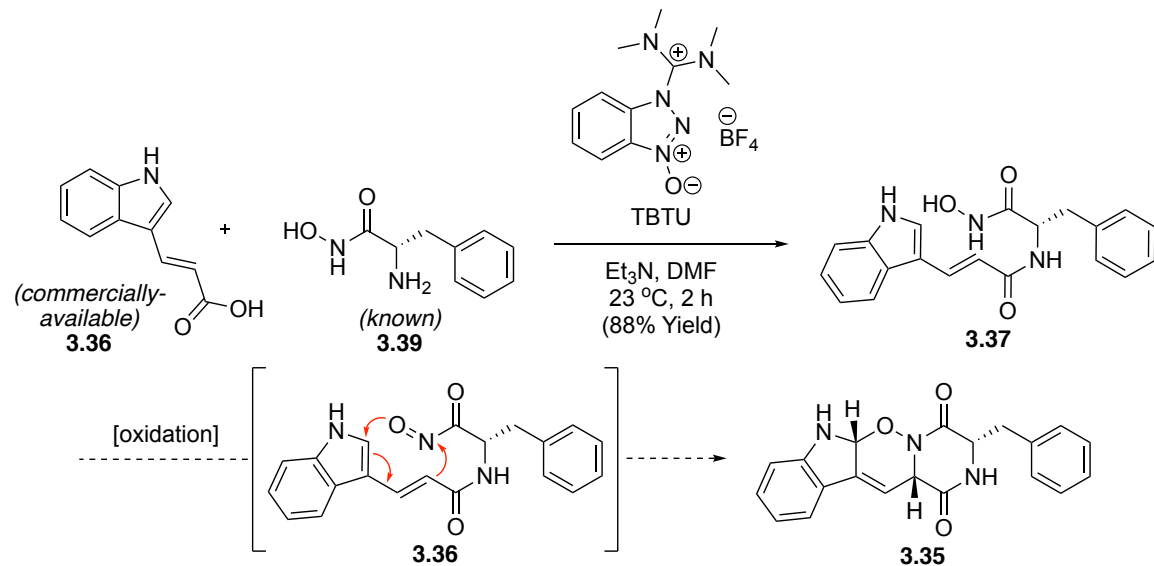
Scheme 3.18. Retrosynthetic analysis featuring an intramolecular NDA.

In the event, the unsaturated 1,2-oxazine **3.35**, was envisioned as being delivered *via* an intramolecular NDA reaction of acyl nitroso intermediate **3.36** which, in turn, was expected to arise *via in situ* oxidation of hydroxamic acid **3.37**. The intramolecular NDA precursor **3.37** could be assembled by an amide coupling reaction between an indoleacrylic acid **3.38** and readily-accessible phenylalanine hydroxamic acid **3.39**.²⁶

Given the ability of **3.36** to adopt a conformation which places the nitroso moiety and diene sufficiently proximal, our expectation was that this could prove to be a good substrate for transformation *via* an intramolecular NDA.

Guided by the proposed route, we set out to prepare the requisite NDA precursor **3.37**. The synthesis commenced with an amide coupling between known hydroxamic acid **3.39** and commercially-available indoleacrylic acid **3.38** which, when promoted by

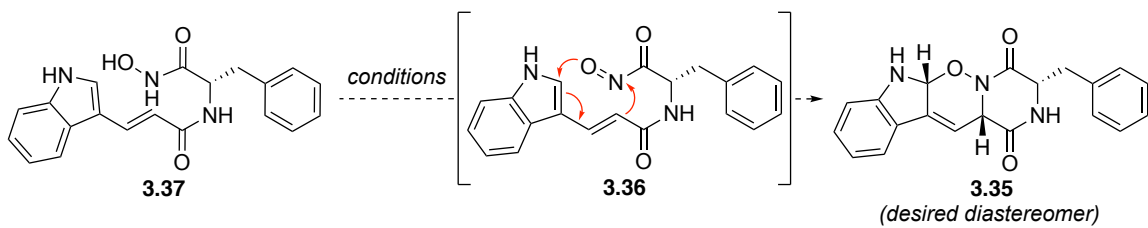
coupling agent 2-(1H-Benzotriazole-1-yl)-1,1,3,3-tetramethylaminium tetrafluoroborate (TBTU), proceeded without difficulty, yielding the desired NDA precursor in 88% yield (**3.37**, Scheme 3.19).



Scheme 3.19. Preparation of intramolecular NDA precursor.

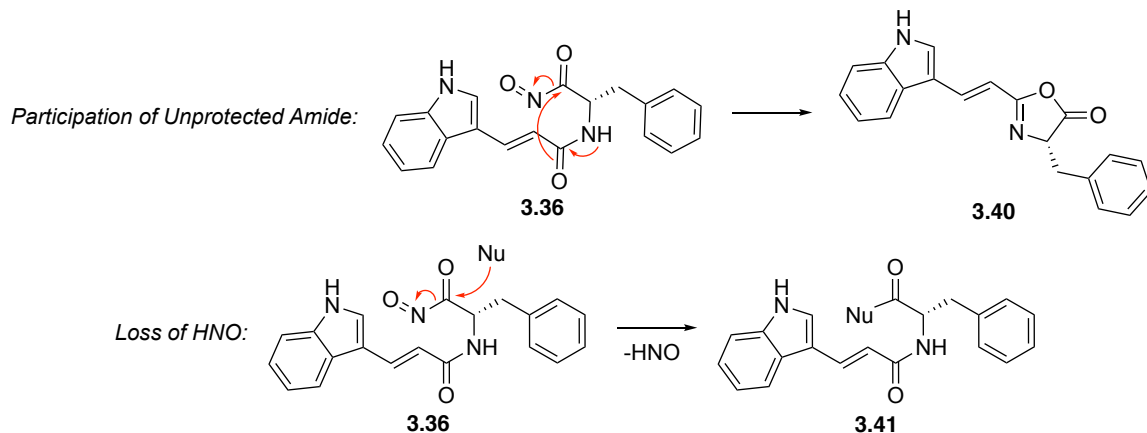
Unfortunately, every attempt to oxidize the hydroxamic acid to the acyl nitroso species **3.36** proved unsuccessful, yielding only complex mixtures (Table 3.11) and no observation of the desired intramolecular Diels-Alder product **3.35**. Although this result was discouraging, we suspected that unfavorable electronics of the indole moiety may have been a contributing factor.

Table 3.11. Attempts to effect the intramolecular NDA.



Entry	Oxidant	Solvent	Temperature	Result
1	DMP	CH ₂ Cl ₂ /DMF	23 °C	
2	DMP	CHCl ₂ /DMF	0 °C	
3	Bobbitt's Salt	MeCN	0 °C	
4	Bobbitt's Salt	CH ₂ Cl ₂ /DMF	-78 °C	
5	Bobbitt's Salt	MeOH	-78 °C	complex mixture
6	Bu ₄ NIO ₄	MeCN	0 °C	
7	Bu ₄ NIO ₄	MeOH/H ₂ O	0 °C	
8	NaIO ₄	MeOH/H ₂ O	0 °C	
9	Pb(OAc) ₄	MeOH/H ₂ O	0 °C	
10	PIDA	MeOH	0 °C	

More specifically, examples in the literature, such as the Erlenmeyer-Plöchl azlactone synthesis,¹¹ show possible side reactions that can occur with systems akin to **3.36**, forming azlactone by-products such as **3.40** which results from nucleophilic insertion of the amide into the acyl nitroso with loss of HNO gas (Scheme 3.15, under the presumption that our system was indeed oxidized to the acyl nitroso intermediate). Additionally, nucleophilic solvents such as methanol or water can add into the acyl nitroso intermediate expelling HNO, an excellent leaving group, giving products such as **3.41**. Although we theorized the formation of these by-products could occur, we were unable to confirm this due to a lack of clean isolation from the complex mixtures that resulted (Table 3.11).

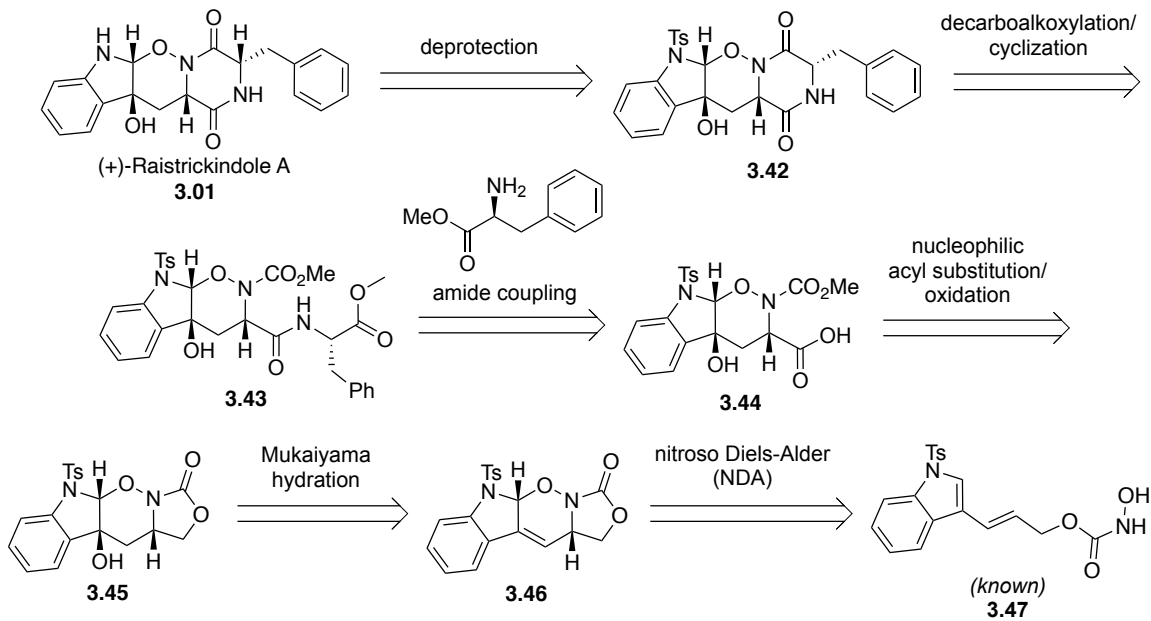


Scheme 3.20. Possible side reactions in the unprotected system.

From the results observed, and having screened many oxidants designated in the literature (e.g., PIDA, DMP, NaIO₄, CuCl₂), we speculated that the rate limiting step was associated with the derived intermediates at both the acyl nitroso and diene moieties. Acyl nitroso compounds are known to be extremely reactive and the lack of a reactive diene to trap it could mean eventual decomposition of the short-lived nitroso intermediate. In an attempt to circumvent this problem, we decided to remove the carbonyl adjacent to the diene (i.e., reducing the ester precursor before attaching a hydroxamic acid moiety) thus making it more electron-rich to promote the desired intramolecular NDA cycloaddition.

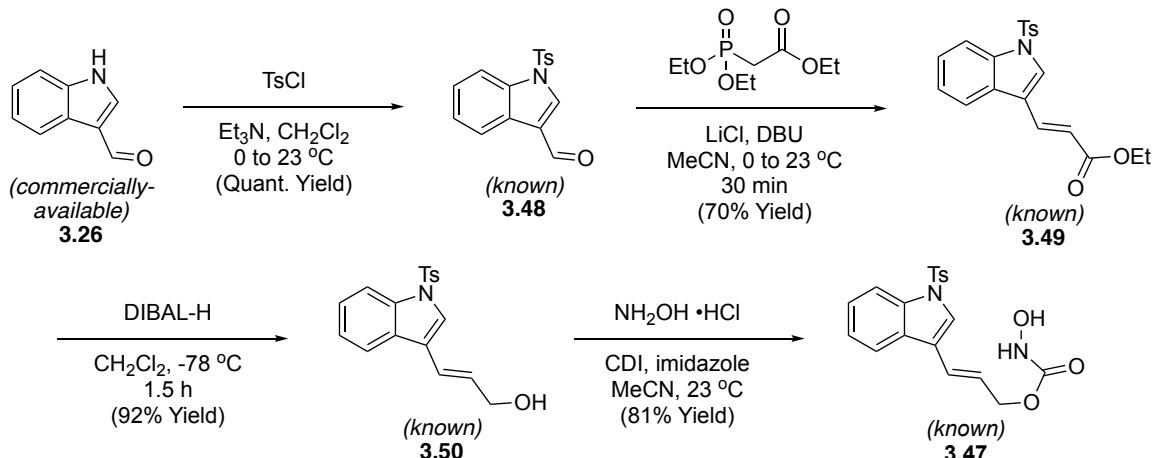
3.3.4 Intramolecular NDA at a Lower Oxidation State

The revised rendition of our retrosynthetic analysis begins with known hydroxamic acid **3.47**,¹² which differs from our original intramolecular NDA precursor **3.37** in that there is an electron-rich methylene adjacent to the diene instead of a deactivating amide. We postulated that we could later increase the oxidation level of this carbon following the intramolecular NDA reaction and cleavage of the cyclic urethane in **3.45**.



Scheme 3.21. Revised retrosynthesis for intramolecular NDA at lower oxidation.

Implementation of this revised approach began with synthesis of known hydroxamic acid **3.47** (Scheme 3.22).¹² Commercially-available indole carbaldehyde **3.26** was treated with TsCl to give Ts-protected indole carbaldehyde **3.48** in quantitative yield, and then subjected to Masamune-Roush olefination conditions to give ethyl ester **3.49**. The ester was reduced with neat DIBAL-H at -78 °C to give allylic alcohol **3.50** in 92% yield. The alcohol was converted to the hydroxamic acid **3.47** in the presence of hydroxylamine hydrochloride and CDI (81% yield).



Scheme 3.22. Synthesis of known Ts-protected hydroxamic acid.

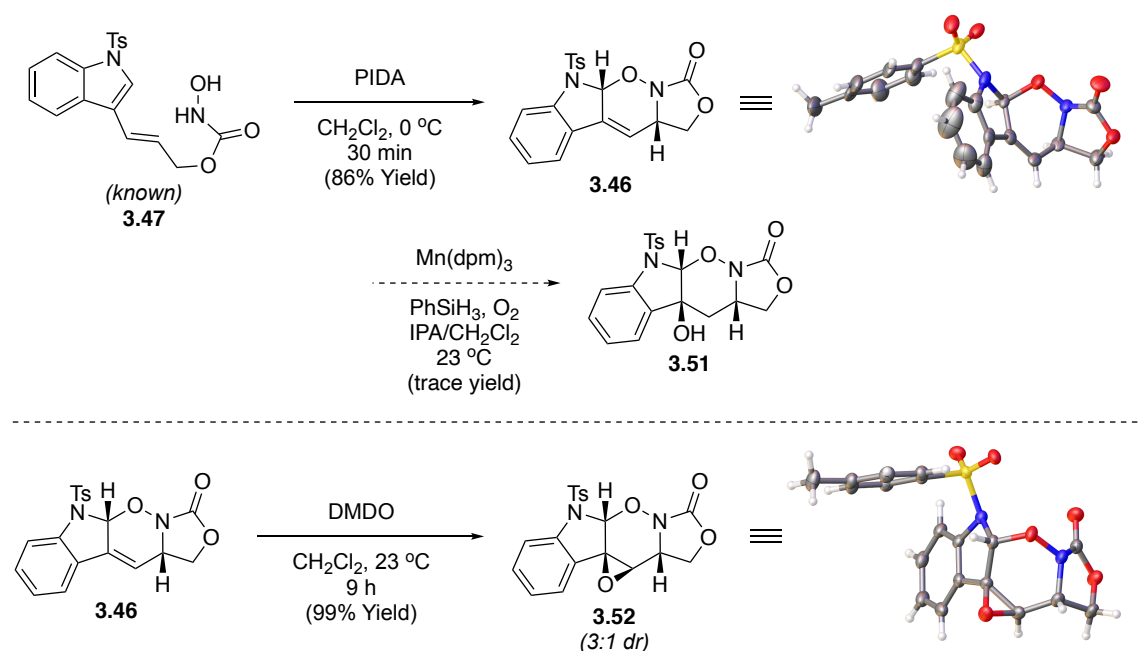
Hydroxamic acid **3.47** was exposed to various oxidants reported to be effective for the preparation of acyl nitroso intermediates (Table 3.12), and to our delight we found that (diacetoxyiodo)benzene (PIDA)¹³ gave **3.46** in excellent yield (86%) after brief optimization.

Table 3.12. NDA reaction to tetracycle **3.47**.

Entry	Oxidant*	Solvent	Temperature	Time	Result
1	NaIO_4	CH_2Cl_2	0 to 23 °C	2 h	returned SM
2	DMP	CH_2Cl_2	0 to 23 °C	2.5 h	8% Yield
3	DMP	CH_2Cl_2	0 °C	50 min	64% Yield
4	PIDA	CH_2Cl_2	0 °C	4 h	50% Yield
5	PIDA	CH_2Cl_2	0 °C	30 min	86% Yield

*1 equiv

The relative stereochemistry of **3.46** was confirmed by X-ray crystallography (Scheme 3.23, top). In accordance with the original retrosynthesis, we attempted to form the tertiary alcohol **3.51** *via* Mukaiyama hydration, but only observed traces of the desired product. As an alternative, we turned to epoxidation of alkene **3.46** and found that freshly-prepared dimethyldioxirane (DMDO)²⁵ readily delivered epoxide **3.52**, the structure of which was confirmed by X-ray analysis (Scheme 3.23, bottom).



Scheme 3.23. Formation of tetracycle and epoxide intermediates.

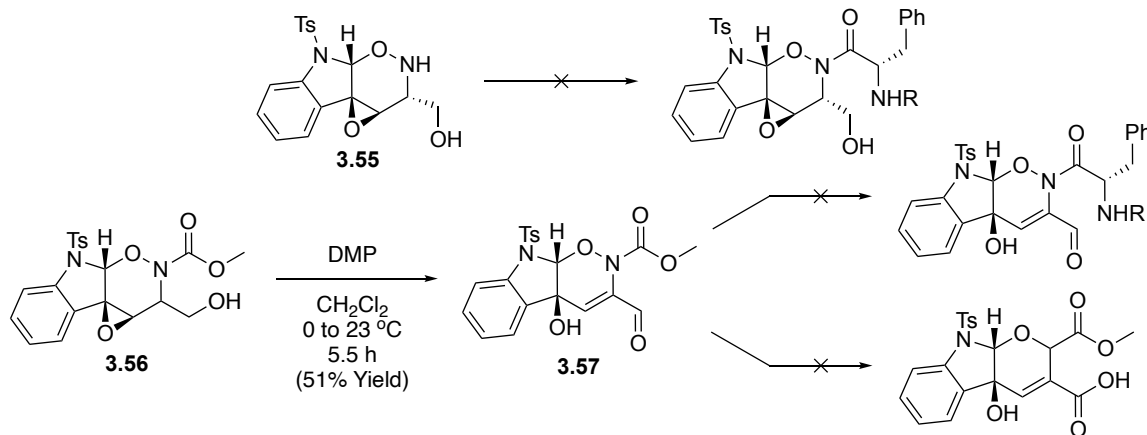
In efforts to advance epoxide **3.52**, we next focused on removing the cyclic urethane so as to enable oxidation of the primary alcohol to the acid and introduction of the DKP moiety. Unfortunately, many conditions we tried were met with failure (Table 3.13), giving us products such as reduction of the urethane to the corresponding *N*-*O* acetal (**3.53**), and, although not fully delineated, a compound consistent with nucleophilic addition of diamine into the epoxide. We finally observed desired cleavage in the presence of methoxide and

hydroxide bases, yielding either a methyl carbamate (**3.54**, loss of Ts) or an amino alcohol (**3.55**), respectively.

Table 3.13. Attempts to open cyclic urethane **3.52**.

Entry	Reagent	Solvent	Result
1	LAH	CH ₂ Cl ₂	3.53
2	LAH	THF	3.53
3	LiBH ₄	CH ₂ Cl ₂	3.53
4	NaBH ₄	THF	3.53
5	Et ₃ SiH, BF ₃ •OEt ₂	CH ₂ Cl ₂	complex mixture
6	MeLi	THF	complex mixture
7	ethylenediamine, DOWEX	THF	amine insertion into epoxide
8	ethylenediamine	THF	amine insertion into epoxide
9	30% w/w NaOMe	MeOH	Quant. Yield (3.54)
10	2M NaOH	-	99% Yield (3.55)

Notably, the concomitant cleavage of the Ts when using NaOMe was found to be dependent upon the conditions. Slight variations in temperature or reaction time either led to Ts-cleaved methyl carbamate **3.55** or the Ts-protected methyl carbamate **3.56** (Scheme 3.24). In efforts to advance **3.56** to the requisite acid, we subjected it to DMP and observed the intermediate aldehyde to readily undergo epoxide opening and furnish enal **3.57**. This unexpected result was still considered a productive step toward building the DKP ring, however, all attempts to further functionalize these intermediates were met with failure (Scheme 3.24).



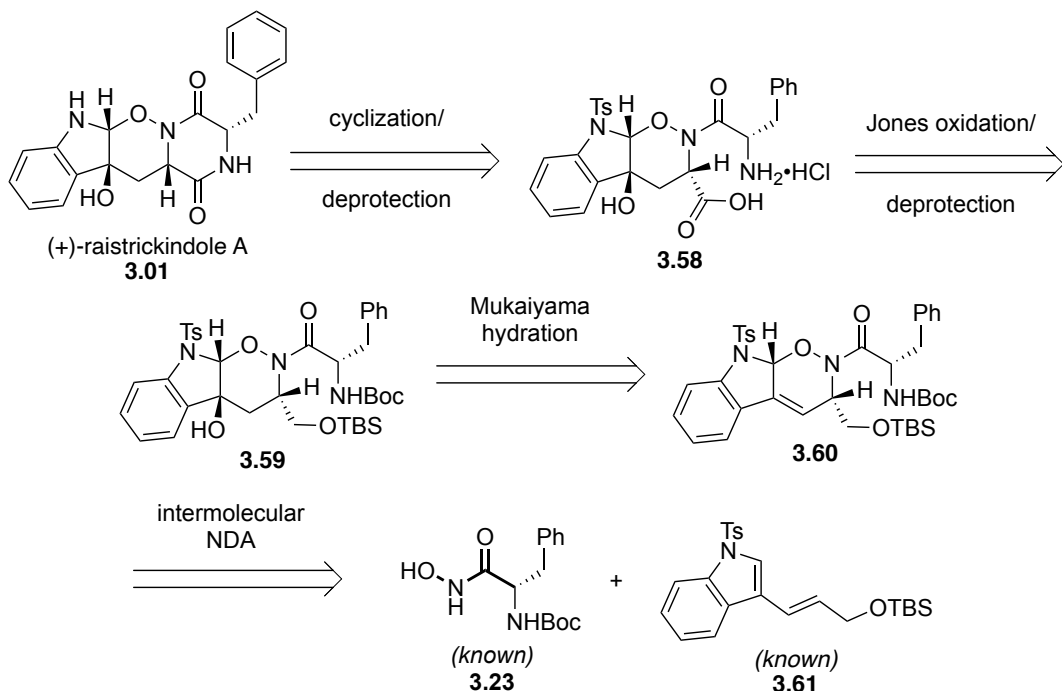
Scheme 3.24. Failure to advance the opened cyclic urethane.

Although the intramolecular reactions leading to tetracyclic intermediates ultimately proved to be unsuccessful, these efforts clearly established that the indole-containing diene (at a lower oxidation state) was a viable intermediate for NDA reactions and could lead to excellent yields upon cycloaddition with an acyl nitroso dienophile. With these positive developments in mind, we turned toward an alternative strategy wherein the stage for *N*-oxy-2,5-DKP formation would be set by constructing the 1,2-oxazine core *via* an intermolecular NDA (instead of the intramolecular variant), discussed hereafter. Moreover, based on literature precedent (*vide infra*), there was the expectation that this approach could also potentially deliver the 1,2-oxazine ring diastereoselectively.

3.5 Completed Total Synthesis of (+)-Raistrickindole A

3.4.1 Implementing an Intermolecular NDA and Regio- and Stereochemical Predictions

In a revised strategy, shown retrosynthetically in Scheme 3.25, we approach the natural product with late-stage cyclization of **3.58** to the DKP and deprotection of the indole serves as the final step. Jones oxidation with *in situ* deprotection of the TBS alcohol gives the acid in **3.58**. Mukaiyama hydration of the alkene in **3.60** would give the desired tertiary alcohol **3.59**. Intermediate **3.60** is a direct result of the intermolecular NDA reaction, shown with the desired and expected stereochemistry (*vide infra*). The NDA reaction would proceed between two known counterparts: hydroxamic acid¹⁵ and allylic TBS alcohol **3.61**.¹⁵



Scheme 3.25. Retrosynthesis for (+)-raistrickindole A featuring an intermolecular NDA.

In most cases, the NDA reaction proceeds *via* an asynchronous concerted mechanism with complete stereoselectivity, and exhibits preference for the *endo*- pathway which arises from a combination of electrostatic repulsion between the diene and the dienophile, as well as repulsive interactions between the HOMO of the nitroso dienophile and the HOMO of the electron-rich diene (Figure 3.11).^{7b,7g}

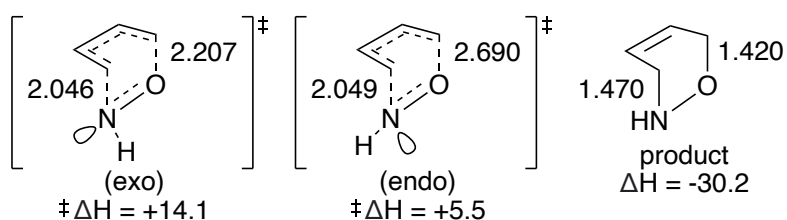
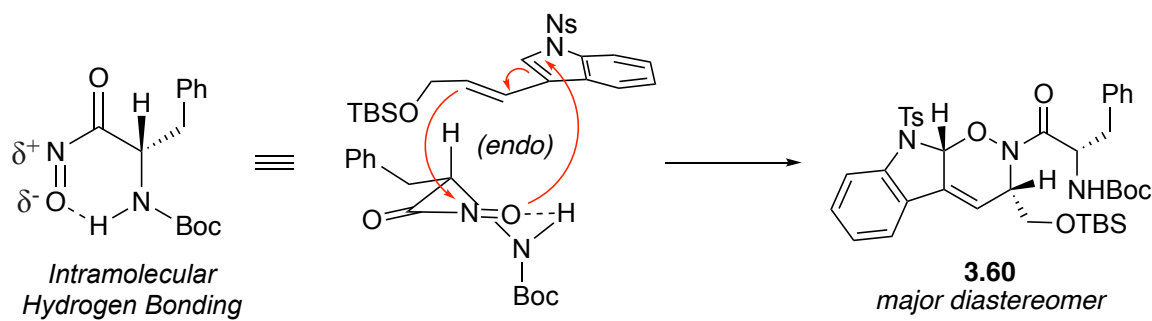


Figure 3.11. Computed transition state energies showing favorability of the *endo* pathway.

In considering the NDA reactions of acyl nitroso compounds derived from chiral α -amino acids, Miller (Notre Dame) hypothesized that the diastereoselectivity could be guided by the propensity of α -amino acyl nitroso derivatives to form six-membered hydrogen-bonded transition states (Scheme 3.26). It is also suggested that the outcome is highly influenced by steric and electronic effects on the substituents attached to the acyl nitroso species.^{7f,17} Thus, the reaction could proceed with complete stereoselectivity (Scheme 3.26).



Scheme 3.26. Regio- and diastereoselective rationale for intermolecular NDA.

NDA cycloadditions also have the ability to form two regioisomers, referred to as *proximal* and *distal* (Figure 3.12). This classification was first introduced by Boger¹⁶ and the results shown are derived from computational studies involving the HOMO of the diene and the LUMO of the dienophile. Although NDA reactions generally follow this reactivity pattern, varying substitution on both reactive components can technically influence the regiochemical outcome.

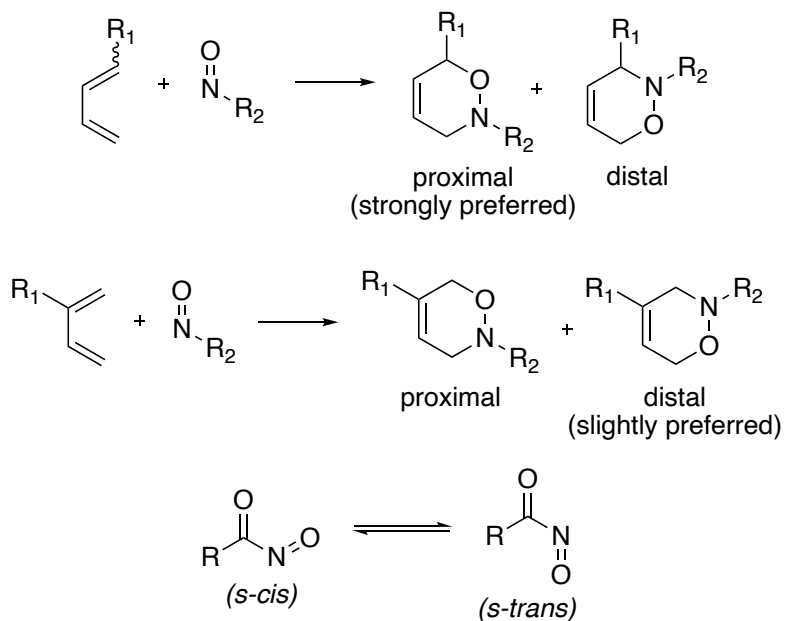
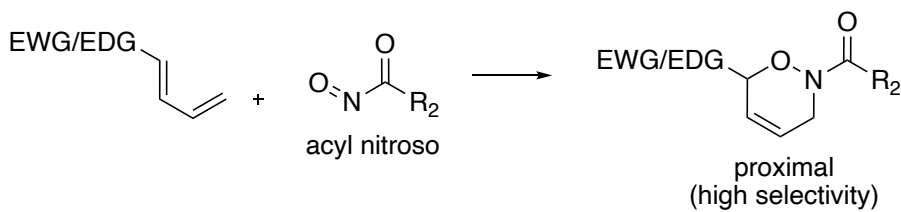


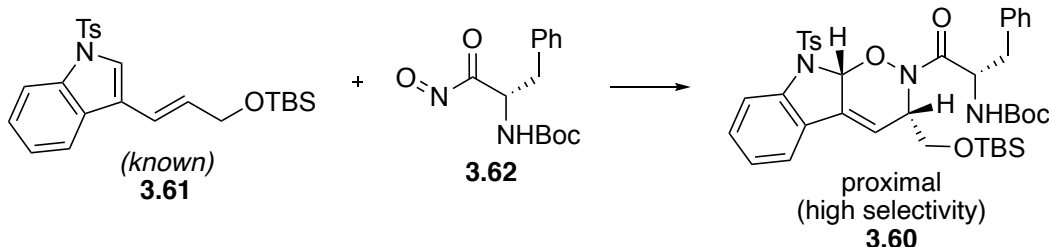
Figure 3.12. General regioselectivity in NDA reactions.

Miller⁷ also specifies the proclivity of proximal vs. distal based on the substitution pattern of the diene in addition to the use of either an acyl or aryl nitroso (Scheme 3.27). The general pattern is described in Scheme 3.27, and illustrates how our system follows the same pattern where one regio- and diastereomer should predominate.

From the Literature:



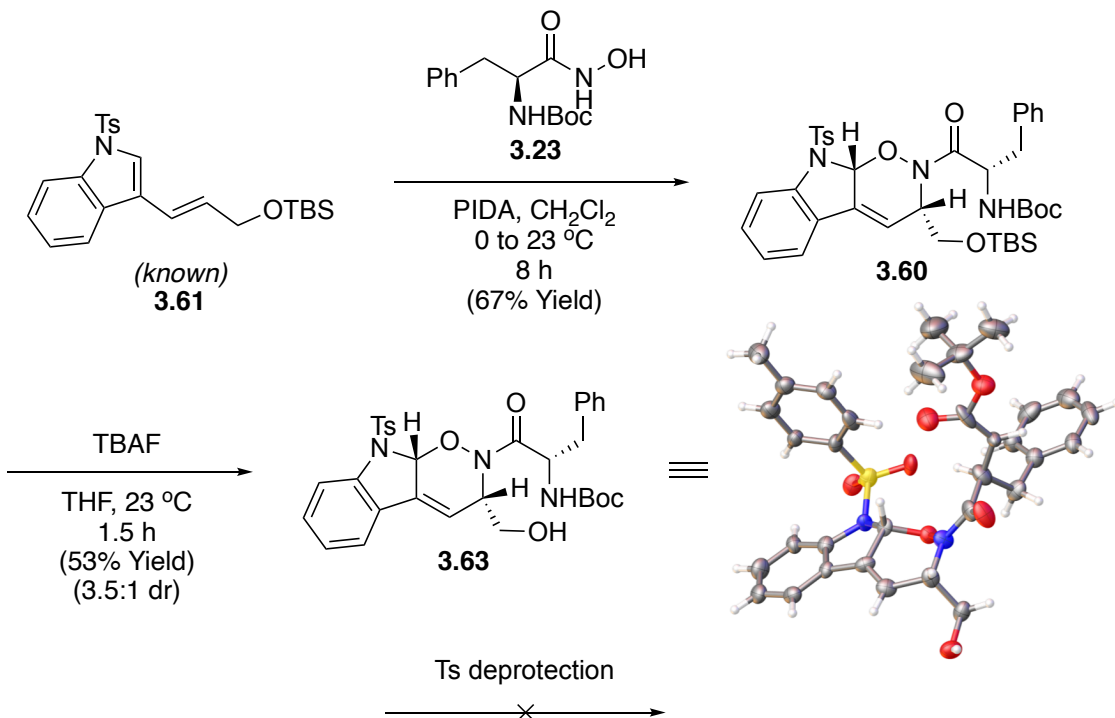
Our System:



Scheme 3.27. Selectivity in our system for the proximal NDA product.

3.4.2 Successful Intermolecular NDA

Our synthesis commenced with the synthesis of known Ts-protected TBS alcohol **3.61** (Scheme 3.28) which was prepared from known allylic alcohol **3.50** (*vide supra*),¹⁸ in quantitative yield. Under our previous oxidation conditions, we were able to successfully generate the phenylalanine-derived acyl nitroso intermediate from the corresponding hydroxamic acid (**3.23**) and effect the intermolecular NDA with **3.61**, giving the desired 1,2-oxazine adduct **3.60** in 67% yield (Scheme 3.28). Removal of the TBS-group under standard conditions gave primary alcohol **3.63** in 53% yield, and allowed us to clearly discern a 3.5:1 dr as well as obtain a crystal structure which helped us confirmed the relative stereochemistry and regiochemistry (matching our predictions). The crystals were determined to be representative of the major isomer by NMR studies.



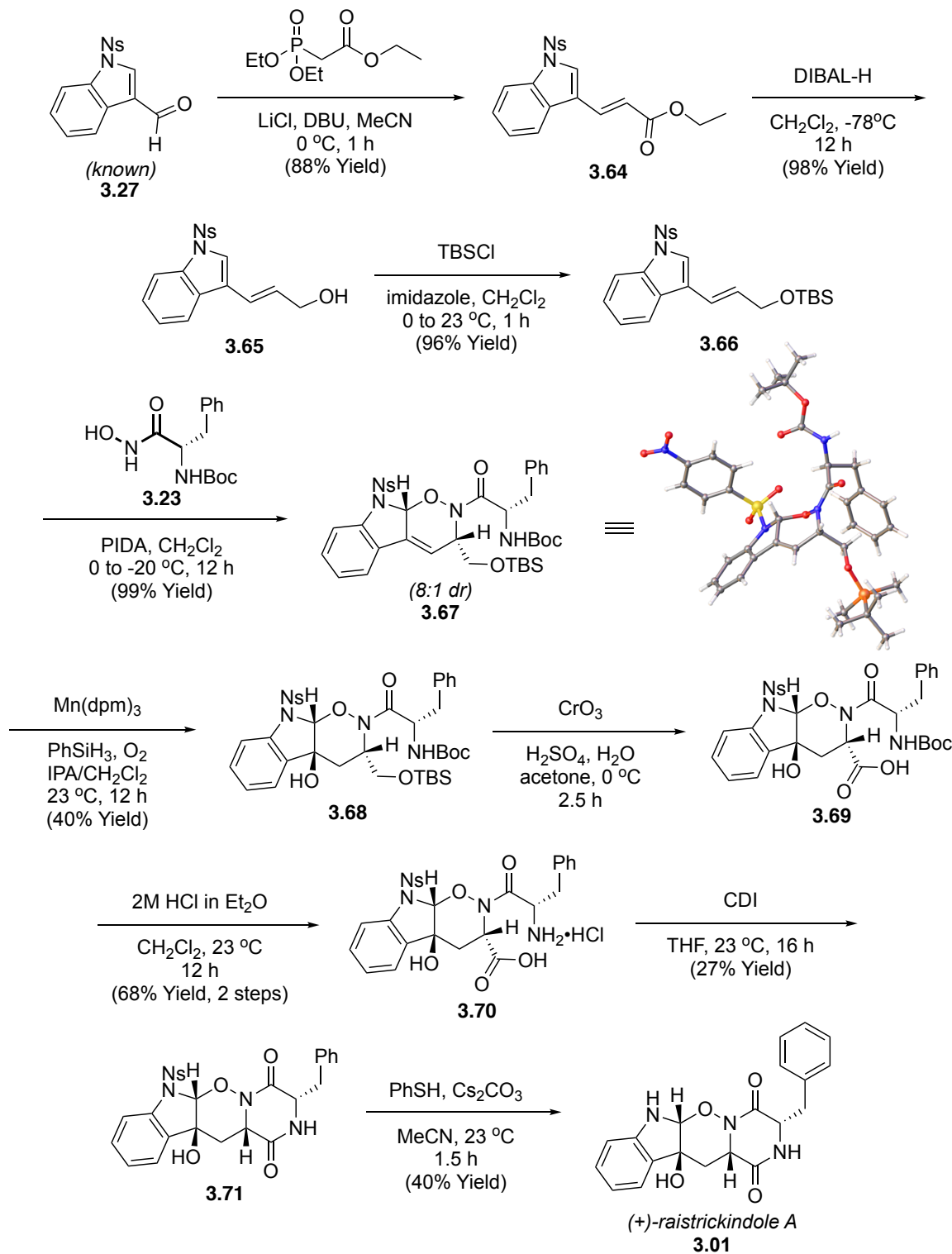
Scheme 3.28. Successful intermolecular NDA and confirmation of relative stereochemistry.

Preliminary attempts to remove the Ts protecting group proved to be problematic, therefore at this juncture we chose to replace the Ts with a *p*-nitrotoluene (Ns) group, a protecting group that is well known to be amenable to milder nucleophilic cleavage, while still offering the stability of a sulfone-type protecting group which proved to be a successful protection pattern for the intermolecular NDA.

3.4.3 Completed Total Synthesis of (+)-Raistrickindole A

In accord with the change outlined above and illustrated in Scheme 3.29, the Ns-protected indole ethyl ester **3.64** was prepared by exposure of **3.27** to triethyl phosphonoacetate under Masamune-Roush HWE conditions¹⁷ to afford **3.64** in 88% yield (Scheme 3.29). Reduction with DIBAL-H gave primary alcohol **3.65** in 98% yield which was then protected to give TBS-alcohol **3.66** in 96% yield, thus setting the stage for an

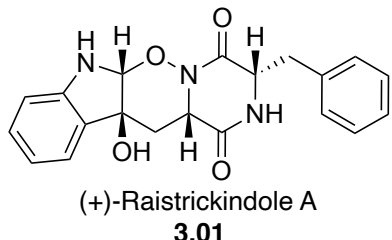
intermolecular NDA. Our well-established conditions of oxidizing the hydroxamic acid **3.23** to the acyl nitroso intermediate using PIDA, and consequent NDA reaction with the TBS-alcohol diene, smoothly afforded the NDA adduct (**3.67**). As in the Ts-protected series, the major diastereomer of the NDA reaction was separated by prep HPLC and the relative stereo- and regiochemistry was confirmed by X-ray crystallography (~1Å resolution), illustrated as the desired product **3.67**.



Scheme 3.29. Completion of (+)-raistrickindole A.

To install the tertiary alcohol, we subjected NDA adduct **3.67** to Mukaiyama hydration conditions using Mn(dpm)₃ and PhSiH₃ to afford alcohol **3.68** in 40% yield. Subsequent Jones oxidation with *in situ* TBS deprotection gave carboxylic acid **3.69** which was advanced crude to the next reaction. Treatment of the acid with 2M ethereal HCl in CH₂Cl₂ resulted in precipitation of the corresponding ammonium salt **3.70** in 68% over the 2-steps. Activation of the carboxylic acid and *in situ* free-basing of the ammonium salt with carbonyldiimidazole (CDI) in THF, over the course of 16 hours, afforded the desired DKP **3.71** which contained the embedded *N-O* bond in 27% yield. Finally, Ns-deprotection of the indole with thiophenol and cesium carbonate yielded the natural product (+)-raistrickindole A (**3.01**) in 40% yield as a white solid. The spectral data of synthetic (+)-raistrickindole A including the NMR and optical rotation matched that of the natural sample.¹ For the purpose of comparison, the ¹H NMR shifts of synthetic and natural material are tabulated in Table 3.14.

Table 3.14. Comparison of ^1H NMR shifts - natural and synthetic (+)-raistrickindole A.



	Natural Raistrickindole A	Synthetic Raistrickindole A	Δ ppm
1			
2			
3			
4	5.27, s	5.28, s	0.01
5			
6			
7	6.71, d	6.72, d	0.01
8	7.15,ddd	7.16,ddd	0.01
9	6.75,ddd	6.74,ddd	0.01
10	7.05,dd	7.05,dd	-
11			
12			
13	2.13, dd and 1.22, dd 4.38,ddd	2.13, dd and 1.21, dd 4.38,ddd	0.01 -
14			
15			
16			
17	4.32,ddd	4.33,ddd	0.01
18	2.97, dd and 2.84, dd	2.97, dd and 2.85, dd	0.01
19			
20,24	7.07, dd	7.06, dd	0.01
21,23	7.00, t	6.99, t	0.01
22	6.84, tt	6.84, tt	-
OH-12			

3.5 Proposed Access to (-)-Haenamindole from (+)-Raistrickindole A

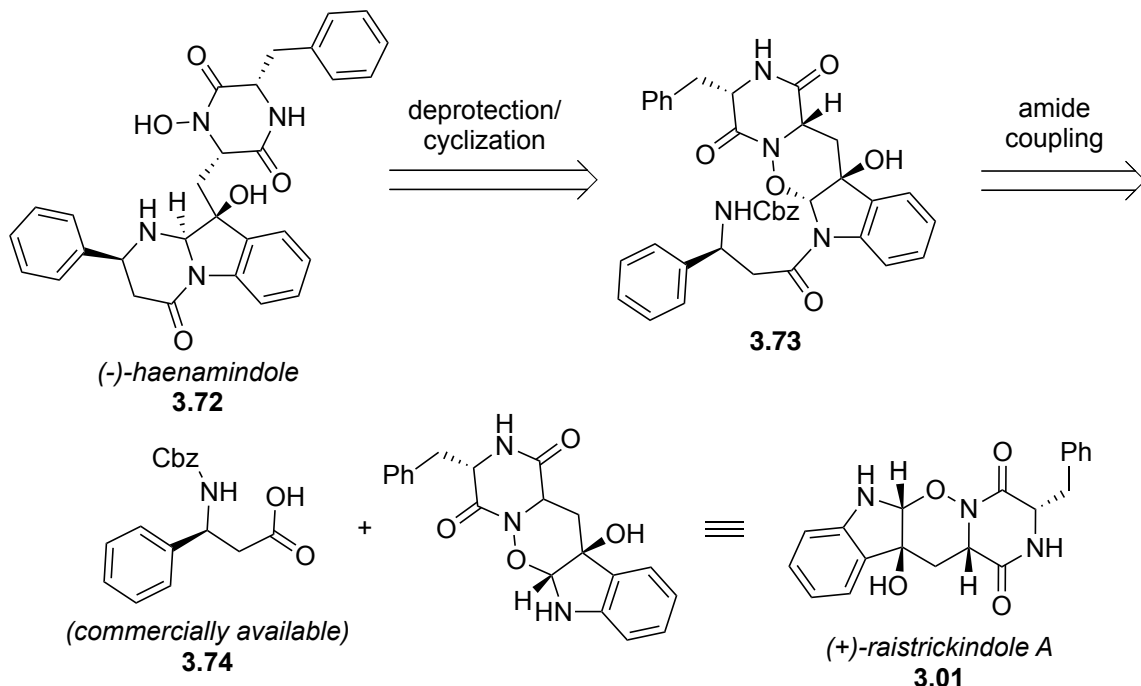
3.5.1 Isolation and Similarity

(-) -Haenamindole (**3.72**, Scheme 3.30) was isolated in 2015 by Kim and co-workers¹⁸ off the coast of Haenam, Korea from fungal strain *Penicillium* sp. KCB12F0055 and isolated again in 2016 by Hwang and co-workers¹⁹ from a fungicolous isolate of *Penicillium lanosum*. The latter effort was accompanied by an unambiguous assignment by X-ray crystallography. Notably, (-)-haenamindole features an N-hydroxy-2,5-DKP core

and an additional amino acid β -phenylalanine, appended to the indoline moiety. After biological screening, **3.72** was found to exhibit potent insecticidal activity against the invasive fall armyworm, which currently has extremely harmful effects on the crops in Africa, Asia, and North and Central America.²⁰ Although not directly related to the same bacterial source, both (-)-haenamindole and (+)-raistrickindole A are reported to be in the same *Penicillium* clade (*Brevicompacta* and *Ramosa*),²¹ and are both derived from the same two amino acids: phenylalanine and tryptophan. (-)-Haenamindole complements (+)-raistrickindole A due to its structural and biological similarity, and in the (+)-raistrickindole A isolation paper (-)-haenamindole is proposed to be biosynthetically-derived from a common intermediate.¹

3.5.2 Retrosynthetic Analysis

Inspired by the biosynthetic hypothesis, we postulated that (-)-haenamindole (**3.72**) can be derived *via* an amide coupling of (+)-raistrickindole A (**3.01**) with commercially-available Cbz-protected β -phenylalanine (**3.74**) and late-stage deprotection and cyclization of the hemiaminal **3.73** to assemble the tricycle in the natural product (Scheme 3.30). Efforts to implement this divergent approach are currently underway.



Scheme 3.30. Proposed access to (*-*)-haenamindole from (*+*)-raistrickindole A.

3.6 Conclusion

In conclusion, we report the first total synthesis of (*+*)-raistrickindole A in 9 steps from known materials featuring a diastereoselective nitroso Diels-Alder cycloaddition. The approach evolved from the use of a ring expansion strategy to construct the DKP core, to the use of an intramolecular NDA reaction. Although the latter approach proved effective, efforts to implement it led to the discovery that manipulation of the electronic nature of the indole-containing diene could have a dramatic effect on the NDA reaction. In addition, these efforts expand the scope of diastereoselective NDA chemistry of α -amino acids, and firmly establishes the utility of NDA chemistry in the synthesis of *N*-oxy-DKP-containing natural products which, in turn, has the potential to be further leveraged in drug discovery efforts.

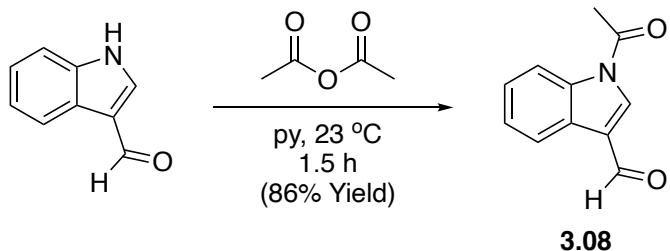
3.7 Experimental

3.5.1 General

Unless otherwise stated, all reactions were performed in flame-dried glassware under a nitrogen (N_2) atmosphere, and reagents were used as received from the manufacturers. The reactions were monitored and analytical samples purified by normal phase thin-layer chromatography (TLC) using Millipore Sigma glass-backed 60 Å plates (indicator F-254, 250 μM). Tetrahydrofuran, diethyl ether, dichloromethane, acetonitrile, dimethylformamide, and toluene were dried using a solvent purification system manufactured by SG Water, USA LLC. Triethylamine and pyridine were dried over CaH_2 and freshly distilled prior to use. Reactions involving organometallic reagents were conducted in flame-dried glassware under an argon (Ar) atmosphere using standard techniques for handling air-sensitive reagents, and solvents were deoxygenated by bubbling dry Ar gas through the neat liquid for 10 min before use. Manual flash chromatography was performed using the indicated solvent systems with Silicycle SiliaFlash® P60 (230–400 mesh) silica gel as the stationary phase. Automated flash chromatography was performed on a Teledyne RF+UV-Vis MS Comp MPLC using the indicated solvent systems, and Teledyne RediSep® R_f normal phase disposable silica gel columns of the indicated size at the indicated flow rate. 1H and ^{13}C NMR spectra were recorded on a Bruker AvanceTM III 300 MHz, Bruker AscendTM 400 MHz, or Bruker AscendTM 600 MHz spectrometer, fitted with autosamplers. Chemical shifts (δ) are reported in parts per million (ppm) relative to the residual solvent resonance, and coupling constants (J) are reported in hertz (Hz). NMR peak pattern abbreviations are as follows: s = singlet, bs = broad singlet, d = doublet, dd = doublet of doublets, ddd = doublet of doublet

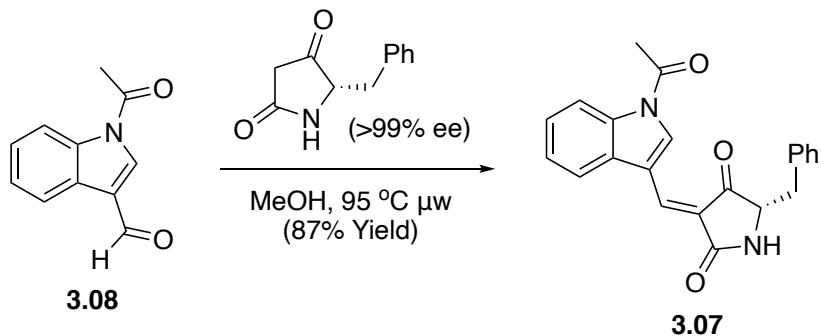
of doublets, dt = doublet of triplets, dtd = doublet of triplet of doublets, dq = doublet of quartets, t = triplet, td = triplet of doublets, q = quartet, m = multiplet. Proton spectra recorded in chloroform-d are referenced to the residual ^1H signal of CHCl_3 at $\delta = 7.26$ and are reported relative to TMS at $\delta = 0.00$; carbon spectra are referenced to the residual central ^{13}C signal for CDCl_3 at $\delta = 77.16$ and are reported relative to TMS at $\delta = 0.00$. Proton spectra recorded in methanol-d₄ are referenced to the residual methyl ^1H signal of CH_3OH at $\delta = 3.31$ and are reported relative to TMS at $\delta = 0.00$; carbon spectra are referenced for the residual methyl ^{13}C signal for CH_3OH at $\delta = 49.00$ and are reported relative to TMS at $\delta = 0.00$. Proton spectra recorded in dimethylsulfoxide-d₆ are referenced to the residual ^1H signal of $(\text{CH}_3)_2\text{SO}$ at $\delta = 2.50$ and are reported relative to TMS at $\delta = 0.00$; carbon spectra are referenced to the residual methyl ^{13}C signal for $(\text{CH}_3)_2\text{SO}$ at $\delta = 39.52$. Fourier-transform infrared (FTIR) spectra were recorded on a Bruker Platinum-ATR IR spectrometer with diamond window. High Resolution mass spectra (HRMS) were obtained in the Baylor University Mass Spectrometry Center on a Thermo Scientific LTQ Orbitrap Discovery mass spectrometer or Thermo Fisher Q-Exactive Plus Hybrid Quadrupole-Orbitrap mass spectrometer, using +ESI or -ESI and reported for the molecular ion ($[\text{M}+\text{H}]^+$ and $[\text{M}+\text{Na}]^+$ or $[\text{M}-\text{H}]^-$, respectively). Single crystal X-ray diffraction data were collected on a Bruker Apex IV-CCD detector using Mo-K α radiation ($\lambda = 0.71073 \text{ \AA}$). Crystals were selected under Paratone® oil, placed on MiTeGen MicroMountsTM, then immediately positioned under an N₂ cold stream at 150 K. Structures were solved and refined using APEX IV and SHELXTL software. Crystal graphics were generated using either SHELXTL and OLEX 2 software.

3.5.2 Data for Known Indole **3.08**



¹H NMR (400 MHz, CDCl₃) δ 10.12 (s, 1H), 8.40 (d, *J* = 7.5 Hz, 1H), 8.27 (dd, *J* = 7.7, 1.3 Hz, 1H), 8.06 (s, 1H), 7.49 – 7.37 (m, 2H), 2.74 (s, 3H). **¹³C NMR** (101 MHz, CDCl₃) δ 185.60, 168.55, 136.40, 135.11, 126.90, 126.07, 125.44, 122.72, 121.95, 116.42, 23.93. Data is consistent with the literature.²²

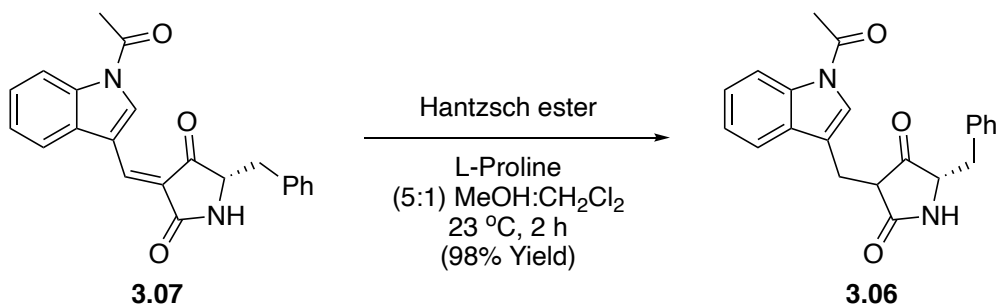
3.5.3 Preparation of Alkene **3.07**



In a 35 mL CEM® microwave tube was added known indole **3.08** (1 g, 5.34 mmol, 1.0 equiv) and known tetramic acid **2.51**⁴ (1.01 g, 5.34 mmol, 1.0 equiv) in dry MeOH (20 mL). The microwave vessel was irradiated at 95 °C for 3.5 hours, and the resulting precipitate was filtered to give alkene **3.07** as a bright yellow solid (1.67 g, 87% Yield)

without purification. **¹H NMR** (600 MHz, CDCl₃) δ 9.95 (s, 1H), 8.52 (d, *J* = 7.7 Hz, 1H), 8.14 (s, 1H), 7.91 (d, *J* = 6.7 Hz, 1H), 7.44 – 7.49 (m, 3H), 7.35 (t, *J* = 7.4 Hz, 3H), 7.29 – 7.30 (m, 2H), 7.23 – 7.25 (m, 2H), 5.99 (s, 1H), 4.20 (dd, *J* = 10.3, 3.6 Hz, 1H), 3.39 (dd, *J* = 13.8, 3.6 Hz, 1H), 2.87 (s, 3H), 2.78 – 2.69 (m, 1H). **¹³C NMR** (151 MHz, CDCl₃) δ 197.13, 169.41, 168.51, 137.69, 136.43, 136.02, 135.40, 129.65, 129.33, 129.31, 127.60, 126.73, 125.42, 121.24, 118.58, 117.28, 117.03, 62.04, 39.18, 24.16. **IR** (neat): 3181, 3152, 2852, 1716, 1675, 1599, 1579, 1509, 1449, 1390, 1369, 1353, 1314, 1250, 1206, 1122, 1000, 938, 771, 760, 749, 699, 677, 649, 588, 525, 501 cm⁻¹. **HRMS** (ESI) calc'd for C₂₂H₁₈N₂O₃ [M+H]⁺ 359.1390, found 359.1392 m/z; calc'd for [M+Na]⁺ 381.1210, found 381.1210 m/z. **R_f** = 0.47 (60% EtOAc/hexanes). [α]_D²²: (c = 0.04, MeOH), -510°.

3.5.4 Preparation of Tetramic Acid **3.06**

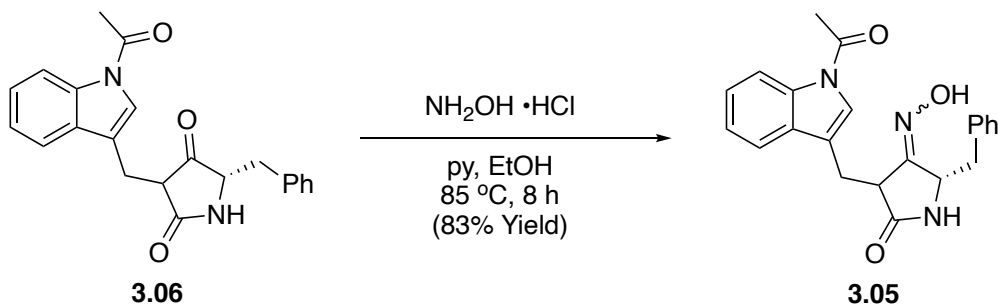


To a 100 mL round-bottom flask was added Hantzsch ester (65.6 mg, 0.259 mmol, 1.0 equiv) and L-Proline (1.5 mg, 0.013 mmol, 0.05 equiv) in 20 mL of a 5:1 mixture of MeOH/CH₂Cl₂. Alkene **3.07** (93 mg, 0.259 mmol, 1.0 equiv) was added dropwise over 10 minutes in 16 mL of MeOH. The reaction stirred for 2 hours at 23 °C, was concentrated *in vacuo*, and purified *via* flash column chromatography to give tetramic acid **3.06** as a yellow

foam (91.2 mg, 98% yield) and an inconsequential ~1:1 mixture of keto/enol tautomers.

¹H NMR (400 MHz, CDCl₃) δ 8.41 (d, *J* = 8.2 Hz, 1H), 8.36 (d, *J* = 8.2 Hz, 1H), 7.62 (d, *J* = Hz, 7.54 1H), 7.57 (d, *J* = 7.54 Hz, 1H), 7.27 – 7.38 (m, 6H), 7.23 – 7.25 (m, 1H), 7.18 – 7.20 (m, 3H), 7.07 – 7.10 (m, 2H), 6.79 (d, *J* = 2.9 Hz, 1H), 6.77 (d, *J* = 2.9 Hz, 1H), 6.29 (s, 1H), 6.20 (s, 1H), 4.10 (dd, *J* = 9.4, 3.9 Hz, 1H), 3.75 (ddd, *J* = 8.4, 4.0, 1.5 Hz, 1H), 3.17 – 3.30 (m, 2.5H), 3.11 – 3.16 (m, 2.5H), 3.04 – 3.09 (m, 1H), 2.76 – 2.87 (m, 3H), 2.59 (s, 3H), 2.56 (s, 3H), 1.82 (dd, *J* = 13.9, 9.5 Hz, 1H). **¹³C NMR** (101 MHz, CDCl₃) δ 209.59, 208.80, 172.92, 172.88, 168.66, 168.63, 135.70, 135.37, 135.23, 129.90, 129.43, 129.25, 129.16, 129.12, 129.03, 128.80, 127.60, 127.44, 125.66, 125.55, 124.70, 124.55, 123.89, 123.79, 119.60, 119.41, 118.14, 117.71, 116.70, 116.56, 64.24, 63.76, 50.62, 50.09, 38.54, 37.33, 24.15, 21.49, 21.39. **FTIR** (neat) 3029, 2922, 2677, 1687, 1603, 1496, 1451, 1386, 1368, 1349, 1329, 1244, 1212, 1145, 1117, 1082, 1010, 934, 908, 745, 699, 649, 608, 571, 422 cm⁻¹. **HRMS** (ESI) calc'd for C₂₂H₂₀N₂O₃ [M+H]⁺ 361.1547, found 361.1547 m/z; calc'd for [M+Na]⁺ 383.1366, found 383.1366 m/z. **R_f** = 0.39 (EtOAc). [α]_D²³: (c = 1.15, MeOH), -34.78°.

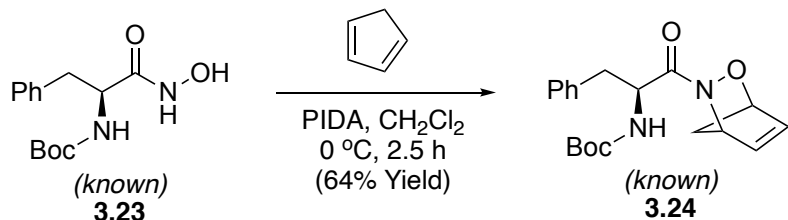
3.5.5 Preparation of Oxime **3.05**



To a 50 mL round-bottom flask was dissolved tetramic acid **3.06** (80.9 mg, 0.224 mmol, 1.0 equiv) in EtOH (34 mL). Hydroxylamine hydrochloride (14.8 mg, 0.449 mmol, 2.0 equiv) and pyridine (36 μ L, 0.449 mmol, 2.0 equiv) were added, and the solution was heated at 85 °C for 8 hours with an affixed Vigreux condenser. The reaction was cooled to rt and the solvent removed *in vacuo*. The residue was dissolved in CH₂Cl₂ and purified *via* flash column chromatography to give oxime **3.05** as a yellow foam (69.4 mg, 83% yield) as an inconsequential ~1:1 mixture of E/Z isomers. **¹H NMR** (600 MHz, CDCl₃) δ 8.42 (d, *J* = 8.3 Hz, 1H), 8.37 (d, *J* = 8.1 Hz, 1H), 7.64 (d, *J* = 7.8 Hz, 1H), 7.58 (d, *J* = 7.8 Hz, 1H), 7.27 – 7.38 (m, 8H), 7.22 – 7.25 (m, 3H), 7.19 – 7.20 (m, 3H), 7.09 (d, *J* = 7.4 Hz, 2H), 6.76 – 6.78 (m, 2H), 6.00 (s, 1H), 5.93 (s, 1H), 4.10 – 4.12 (m, 1H), 3.72 – 3.74 (m, 1H), 3.30 (dd, *J* = 14.8, 5.0 Hz, 1H), 3.22 (dd, *J* = 21.6, 6.2 Hz, 2H), 3.17 (d, *J* = 6.2 Hz, 2H), 3.08 (dd, *J* = 14.0, 3.9 Hz, 1H), 2.83 – 2.85 (m, 2H), 2.77 (dd, *J* = 14.0, 8.6 Hz, 1H), 2.61 (s, 3H), 2.58 (s, 3H), 1.74 (dd, *J* = 13.85, 9.67 Hz, 1H). **¹³C NMR** (151 MHz, CDCl₃) δ 209.54, 208.76, 172.73, 172.68, 168.66, 168.63, 135.75, 135.38, 135.26, 129.89, 129.38, 129.18, 129.10, 127.64, 127.49, 125.69, 125.57, 124.77, 124.61, 123.92, 123.83, 119.66, 119.43, 118.11, 117.67, 116.71, 64.40, 64.25, 63.74, 50.73, 50.11, 38.60, 37.36, 24.18,

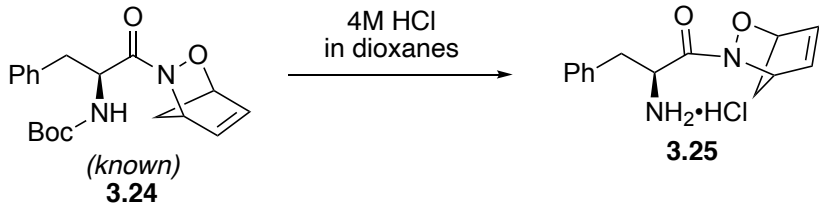
21.56, 21.46. **FTIR** (neat) 3247, 3027, 2925, 1695, 1651, 1604, 1496, 1451, 1386, 1370, 1350, 1329, 1244, 1222, 1145, 1118, 1082, 1033, 1011, 935, 746, 699, 632, 607, 561, 488, 421 cm⁻¹. **HRMS** (ESI) calc'd for C₂₂H₂₁N₃O₃ [M+Na]⁺ 398.1475, found 398.1475 m/z. R_f = 0.71 (EtOAc). [α]_D²⁴: (c = 0.37, MeOH), -24.86°.

3.5.6 Data for Known Cyclopentadiene Adduct 3.24



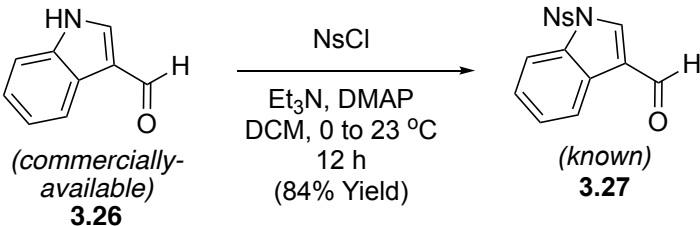
¹H NMR (400 MHz, CDCl₃) δ 7.14 – 7.24 (m, 5H), 6.49 (s, 1H), 6.37 – 6.22 (m, 1H), 5.30 (s, 1H), 5.13 (s, 1H), 4.75 (s, 1H), 2.95 (dd, J = 13.0, 6.2 Hz, 1H), 2.68 (s, 1H), 1.81 (s, 1H), 1.37 (s, 9H). **¹³C NMR** (101 MHz, CDCl₃) δ 171.60, 155.20, 136.54, 136.08, 133.34, 129.64, 128.32, 126.68, 84.85, 79.54, 61.68, 53.00, 48.58, 36.22, 28.37. **FTIR** (neat) 3429, 3327, 2977, 2244, 1708, 1654, 1495, 1454, 1442, 1391, 1365, 1327, 1246, 1164, 1080, 1048, 1018, 916, 845, 824, 801, 729, 699, 646, 539, 510, 465, 431 cm⁻¹. **HRMS** calc'd for C₁₉H₂₄N₂O₄ [M+Na]⁺ 367.1628, found 367.1628 m/z. [α]_D²²: (c = 1.50, MeOH), -13.34°.

3.5.7 Preparation of Amino Salt 3.25



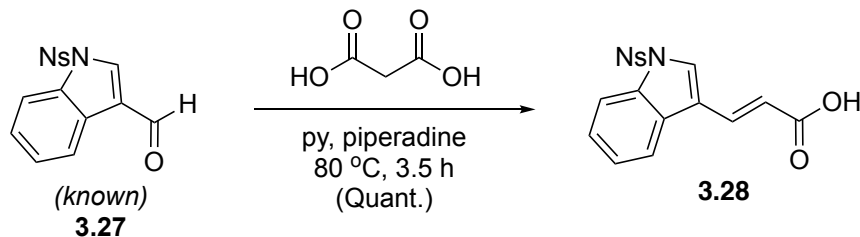
To a 5 mL round-bottom flask was added known Boc-protected cyclopentadiene adduct **3.24**¹⁰ (172.4 mg, 0.501 mmol, 1.0 equiv), CH₂Cl₂ (2.5 mL), and TFA (0.84 mL, 11.012 mmol, 22.0 equiv) at 23 °C. The reaction stirred for 1 h and then concentrated *in vacuo*. The crude amino salt **3.25** was advanced to the next step without purification.

3.5.8 Data for Known Ns-protected Indole Carbaldehyde 3.27



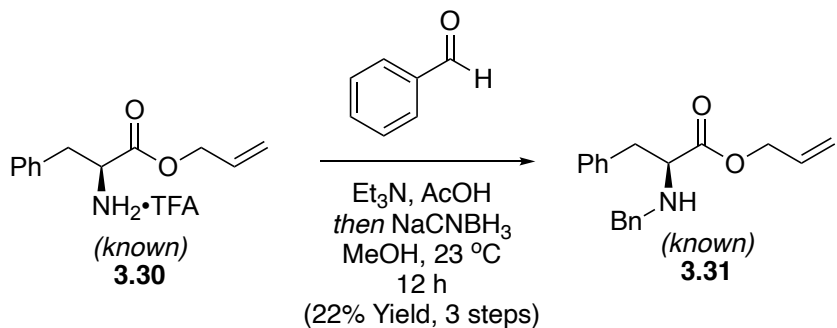
1H NMR (400 MHz, CDCl₃) δ 10.12 (s, 1H), 8.41 – 8.32 (m, 2H), 8.28 (dd, *J* = 7.3, 1.5 Hz, 1H), 8.21 (s, 1H), 8.18 – 8.12 (m, 2H), 7.96 (d, *J* = 8.2 Hz, 1H), 7.44 (dtd, *J* = 19.2, 7.3, 1.3 Hz, 2H). Data is consistent with the literature.³

3.5.9 Preparation of Indoleacrylic Acid 3.28



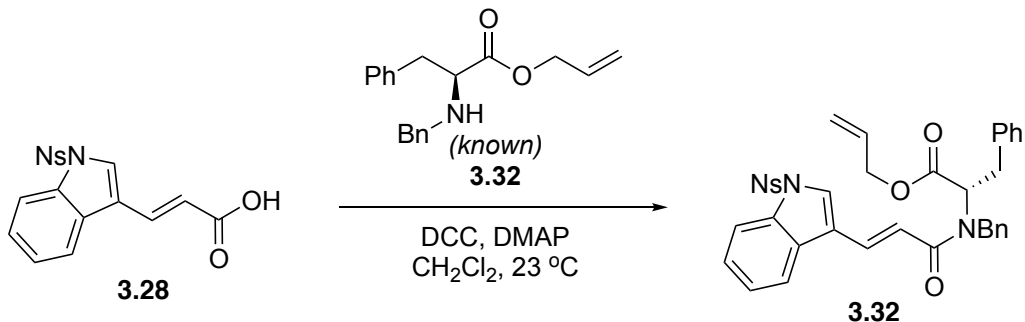
To a 50 mL round-bottom flask was added known Ns-protected indole carbaldehyde **3.27**³ (8.33 g, 25.219 mmol, 1.0 equiv) and malonic acid (8.40 g, 80.700 mmol, 3.2 equiv).²⁷ Pyridine (32 mL) and piperidine (3 mL) were added and the reaction was heated neat at 80 °C for 3.5 h. The reaction was quenched with water (195 mL) and acidified with 6N HCl. The flask was stored in the freezer overnight and the precipitate was filtered and washed with cold water. No further purification was needed to give indoleacrylic acid **3.28** as a bright-yellow solid (9.4 g, quantitative yield). **1H NMR** (400 MHz, DMSO) δ 12.43 (s, 1H), 8.49 (s, 1H), 8.41 – 8.33 (m, 2H), 8.33 – 8.26 (m, 2H), 8.00 (d, J = 8.3 Hz, 1H), 7.94 (d, J = 7.9 Hz, 1H), 7.75 (d, J = 16.2 Hz, 1H), 7.45 (t, J = 7.2 Hz, 1H), 7.38 (t, J = 7.6 Hz, 1H), 6.61 (d, J = 16.2 Hz, 1H). **13C NMR** (101 MHz, DMSO) δ 167.60, 151.00, 149.45, 141.34, 134.72, 134.69, 129.37, 128.61, 127.87, 126.00, 125.27, 124.85, 124.01, 121.12, 119.85, 118.73, 113.40. **FTIR** (neat) cm⁻¹. **HRMS** (ESI) calc'd for C₁₇H₁₂N₂O₆S [M+Na]⁺ 395.0308, found 395.0310 m/z. **R_f** = 0.43 (70% EtOAc/hexanes).

3.5.10 Data for Known Bn-protected Allyl Ester 3.31



¹H NMR (400 MHz, CDCl₃) δ 7.34 – 7.21 (m, 9H), 7.20 – 7.14 (m, 2H), 5.82 (ddt, *J* = 17.3, 10.3, 5.8 Hz, 1H), 5.32 – 5.18 (m, 2H), 4.55 (dq, *J* = 6.0, 1.2 Hz, 2H), 3.83 (d, *J* = 13.2 Hz, 1H), 3.65 (d, *J* = 13.2 Hz, 1H), 3.57 (t, *J* = 6.9 Hz, 1H), 2.98 (d, *J* = 6.9 Hz, 2H).²⁴

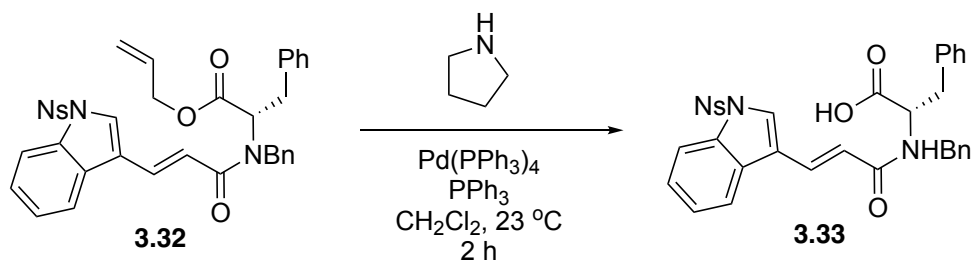
3.5.11 Preparation of Amide 3.32



To a 10 mL round-bottom flask was added known allyl ester **3.32**²⁴ (211 mg, 0.714 mmol, 1.0 equiv), indoleacrylic acid **3.28** (293 mg, 0.786 mmol, 1.1 equiv), and CH₂Cl₂ (3.6 mL). DCC (162 mg, 0.786 mmol, 1.1 equiv) and DMAP (8.7 mg, 0.071 mmol, 10

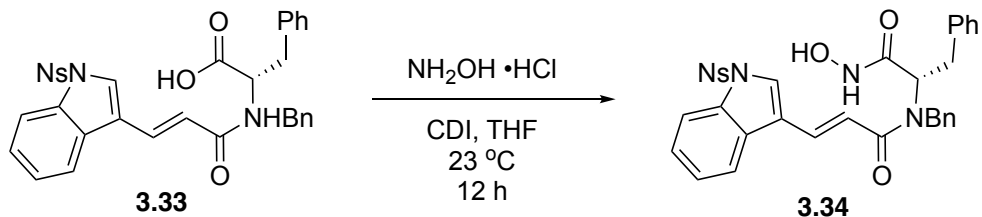
mol%) were added, and the reaction stirred for 12 h. The crude amide **3.32** was concentrated *in vacuo*, passed through a silica plug with 50% EtOAc/hexanes, and advanced to the next step without further purification.

3.5.12 Preparation of Acid **3.33**



To a 2-Dr vial was added crude amide **3.32** (43.1 mg, 0.066 mmol, 1.0 equiv), pyrrolidine (0.011 mL, 0.132 mmol, 2.0 equiv), $\text{Pd}(\text{PPh}_3)_4$ (2.3 mg, 0.002 mmol, 3 mol%), PPh_3 (1.0 mg, 0.004 mmol, 6 mol%), and dry CH_2Cl_2 (0.2 mL). The reaction was stirred at 23°C for 2 h, then washed with 1M HCl, dried (MgSO_4), and concentrated *in vacuo*. The crude acid **3.33** was advanced to the next step without purification.

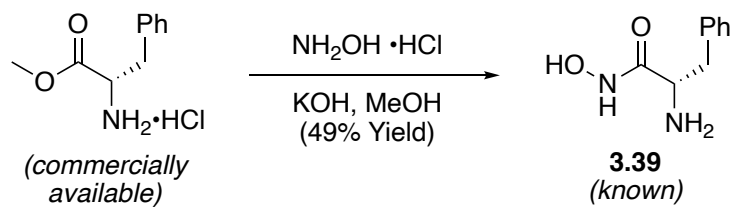
3.5.13 Preparation of Hydroxamic Acid **3.34**



To a 2-Dr vial was added crude acid **3.33** (40 mg, 0.066 mmol, 1.0 equiv), hydroxylamine hydrochloride (9.1 mg, 0.131 mmol, 2.0 equiv), and CDI (16.1 mg, 0.099

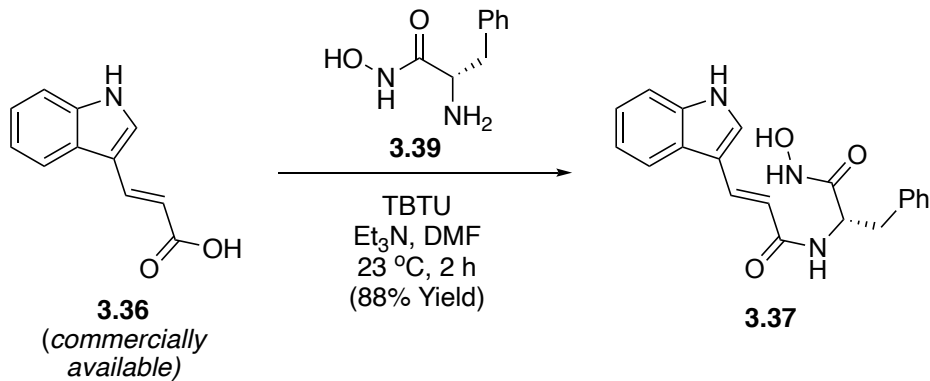
mmol, 1.5 equiv) in dry THF (0.1 mL). The reaction stirred for 12 h at 23 °C and then was diluted with 1M HCl. The organic phase was partitioned, dried (MgSO_4), and used crude in the next reaction following some difficulties in purification.

3.5.14 Data for Known Hydroxamic Acid 3.39



$^1\text{H NMR}$ (400 MHz, DMSO) δ 7.25 – 7.29 (m, 2H), 7.17 – 7.20 (m, 3H), 3.25 (dd, $J = 7.7, 6.1$ Hz, 1H), 2.84 (dd, $J = 13.2, 6.1$ Hz, 1H), 2.61 (dd, $J = 13.3, 7.7$ Hz, 1H). Data is consistent with the literature.²⁶

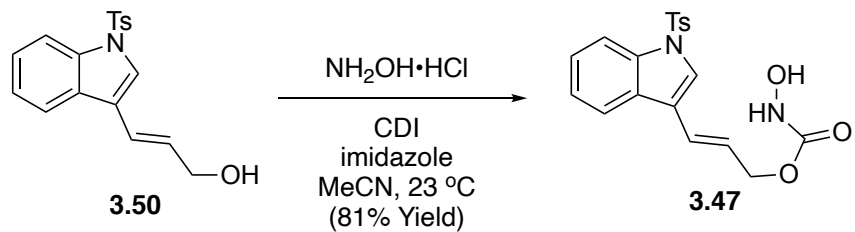
3.5.15 Preparation of Hydroxamic Acid 3.37



To a flame-dried 100 mL round-bottom flask, indoleacrylic acid **3.36** (1 g, 5.342 mmol, 1.0 equiv) was dissolved in dry DMF (53 mL). TBTU (2.06 g, 6.411 mmol, 1.2 equiv) and Et_3N (0.89 mL, 6.411 mmol, 1.2 equiv) were added at 23°C . A color change to bright yellow was observed, and known phenylalanine hydroxamic acid **3.39**²⁶ (1.16 g, 6.411 mmol, 1.2 equiv) was added in one portion. The reaction was stirred for 2 hours and washed with water and sat. aq. LiCl (10 x 15 mL). The aqueous was extracted with EtOAc (3 x 50 mL), dried (Na_2SO_4), and concentrated *in vacuo*. The crude was purified *via* flash column chromatography to give hydroxamic acid **3.37** as a bright yellow solid (1.64 g, 88% yield). **1H NMR** (400 MHz, DMSO) δ 11.54 (s, 1H), 10.76 (s, 1H), 8.90 (s, 1H), 8.26 (d, $J = 8.6$ Hz, 1H), 7.94 (d, $J = 5.2$ Hz, 2H), 7.73 (d, $J = 2.8$ Hz, 1H), 7.55 (d, $J = 15.8$ Hz, 1H), 7.47 – 7.42 (m, 1H), 7.27 (d, $J = 4.4$ Hz, 4H), 7.23 – 7.13 (m, 3H), 6.72 (d, $J = 15.8$ Hz, 1H), 4.57 (td, $J = 8.8, 5.8$ Hz, 1H), 2.98 (dd, $J = 13.7, 5.7$ Hz, 1H), 2.87 – 2.81 (m, 1H). **13C NMR** (101 MHz, DMSO) δ 168.06, 166.05, 137.88, 137.43, 133.34, 130.48, 129.16, 128.15, 126.32, 124.85, 122.24, 120.34, 120.13, 116.02, 112.28, 112.20, 51.70, 38.31. **FTIR** (neat) 3427, 3276, 3057, 2542, 2445, 2321, 1639, 1616, 1595, 1538, 1518, 1455,

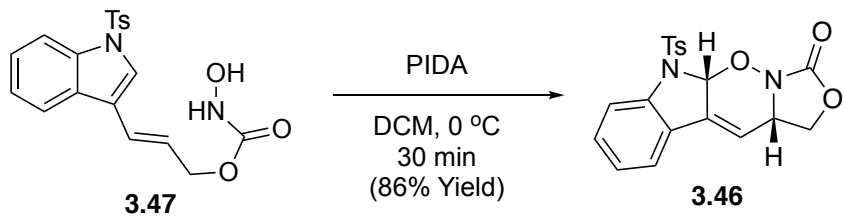
1405, 1375, 1329, 1269, 1249, 1226, 1111, 1019, 982, 969, 913, 856, 825, 736, 699, 657, 521, 509, 484, 418 cm⁻¹. **HRMS** (ESI) calc'd for C₂₀H₁₉N₃O₃ [M+Na]⁺ 372.1319, found 372.1327 m/z. **R_f** = 0.26 (EtOAc). [α]_D²¹: (c = 0.68, MeOH), +69.41°.

3.5.16 Data for Known Hydroxamic Acid 3.47



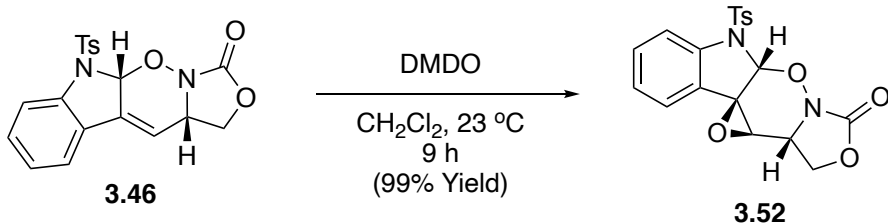
¹H NMR (400 MHz, CDCl₃) δ 7.99 (d, *J* = 7.7 Hz, 1H), 7.76 (d, *J* = 8.3 Hz, 2H), 7.71 (d, *J* = 7.8 Hz, 1H), 7.62 (s, 1H), 7.37 – 7.15 (m, 5H), 6.74 (d, *J* = 16.0 Hz, 1H), 6.35 (dt, *J* = 16.1, 6.5 Hz, 1H), 5.85 (br s, 1H), 4.83 (d, *J* = 6.6 Hz, 2H), 2.33 (s, 3H). **¹³C NMR** (101 MHz, CDCl₃) δ 159.12, 145.31, 135.58, 135.10, 130.09, 128.81, 126.99, 125.87, 125.23, 124.96, 123.80, 123.77, 120.47, 119.43, 113.90, 67.12, 21.69. **FTIR** (neat) 3338, 3127, 2922, 1718, 1595, 1492, 1445, 1362, 1259, 1215, 1169, 1119, 1093, 1019, 962, 811, 742, 670, 567, 534 cm⁻¹. Data is consistent with the literature.²³

3.5.17 Preparation of NDA Adduct **3.46**



To a flame-dried 2-Dram vial was added known hydroxamic acid **3.47** (45.2 mg, 0.117 mmol, 1.0 equiv) and dry CH_2Cl_2 (0.6 mL). The solution was cooled to 0 °C and PIDA (37.7 mg, 0.117 mmol, 1.0 equiv) was added in one portion. The reaction stirred for 30 minutes and quenched with sat. aq. NaHCO_3 (2 mL), $\text{Na}_2\text{S}_2\text{O}_3$ (2 mL), and brine (1 mL). The aqueous phase was extracted with CH_2Cl_2 and dried (MgSO_4). The crude was purified *via* flash column chromatography to yield NDA adduct **3.46** as a yellow foam (38.7 mg, 86% yield). The structure was confirmed by X-ray crystallography. **1H NMR** (400 MHz, CDCl_3) δ 8.06 – 7.99 (m, 2H), 7.38 (t, J = 7.5 Hz, 2H), 7.28 – 7.32 (m, 3H), 7.04 (td, J = 7.5, 1.1 Hz, 1H), 6.39 (t, J = 2.8 Hz, 1H), 6.27 (dd, J = 2.8, 1.5 Hz, 1H), 4.61 – 4.65 (m, 1H), 4.56 – 4.59 (m, 1H), 4.37 (d, J = 8.5 Hz, 1H), 2.38 (s, 3H). **13C NMR** (101 MHz, CDCl_3) δ 157.11, 145.05, 142.72, 137.32, 135.37, 131.52, 130.03, 128.18, 124.25, 124.10, 121.72, 118.54, 114.90, 88.09, 66.21, 54.04, 21.76. **FTIR** (neat) 1782, 1597, 1460, 1356, 1295, 1169, 1111, 1084, 1046, 1014, 985, 955, 945, 908, 880, 815, 780, 746, 704, 663, 643, 592, 570, 553, 539, 488 cm^{-1} . **HRMS** (ESI) calc'd for $\text{C}_{19}\text{H}_{16}\text{N}_2\text{O}_5\text{S}$ [M+Na]⁺ 407.0672, found 407.0680 m/z. **R_f** = 0.25 (50% EtOAc/hexanes). **m.p.** = 179 – 181 °C.

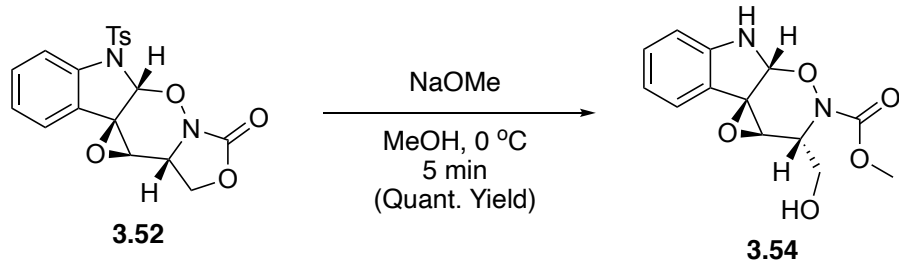
3.5.18 Preparation of Epoxide **3.52**



To a 100 mL round-bottom flask was added NDA adduct **3.46** (0.55 g, 1.444 mmol, 1.0 equiv) and CH_2Cl_2 (7.2 mL). Freshly-prepared DMDO was added in excess over the course of 9 hours until completion of the reaction by TLC. The solvent was removed *in vacuo* and the crude was purified *via* flash column chromatography to give epoxide **3.52** as a pale-yellow foam (573.6 mg, 99% yield). The structure was confirmed by X-ray crystallography. **$^1\text{H NMR}$** (400 MHz, CDCl_3) δ 8.11 – 7.95 (m, 2H), 7.44 (d, J = 8.3 Hz, 1H), 7.31 – 7.35 (m, 3H), 7.06 (t, J = 7.5 Hz, 1H), 6.97 (d, J = 6.9 Hz, 1H), 6.12 – 6.13 (m, 1H), 4.61 (t, J = 8.5 Hz, 1H), 4.25 (dd, J = 9.1, 6.5 Hz, 1H), 4.08 (ddd, J = 8.1, 6.4, 1.9 Hz, 1H), 3.64 (t, J = 2.2 Hz, 1H), 2.41 (s, 3H). **$^{13}\text{C NMR}$** (101 MHz, CDCl_3) δ 153.61, 145.26, 142.57, 134.88, 131.28, 130.11, 128.46, 124.43, 122.71, 121.48, 115.09, 92.02, 64.39, 61.88, 59.08, 54.76, 53.58, 21.79. **FTIR** (neat) 2924, 2853, 1788, 1731, 1597, 1465, 1364, 1245, 1170, 1088, 1041, 944, 814, 753, 705, 660, 575, 539, 475 cm^{-1} . **HRMS** (ESI) calc'd for $\text{C}_{19}\text{H}_{16}\text{N}_2\text{O}_6\text{S} [\text{M}+\text{H}]^+$ 401.0802, found 401.0807 m/z. R_f = 0.56 (60% EtOAc/hexanes).

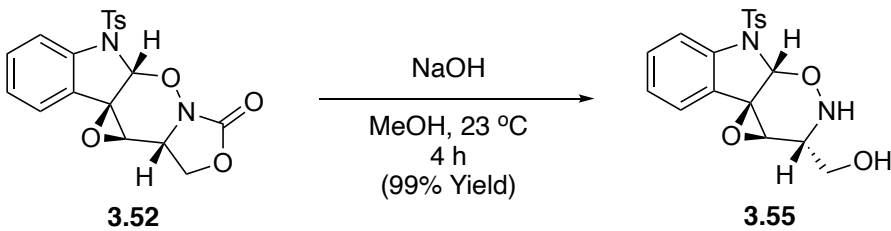
m.p. = 103 – 106 °C.

3.5.19 Preparation of Methyl Carbamate 3.54



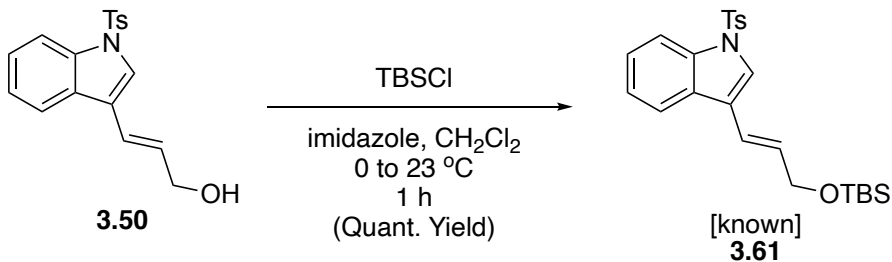
In a 2-Dram vial was added epoxide **3.52** (36.2 mg, 0.09 mmol, 1.0 equiv) and MeOH (0.5 mL). The solution was cooled to 0 °C and NaOMe (18.48 μ L, 0.099 mmol, 1.1 equiv, 30% w/w in MeOH) was added in one portion. The reaction stirred for 5 minutes at 0 °C and quenched with sat. aq. NH₄Cl (5 mL). The aqueous phase was extracted with EtOAc (3 x 5 mL), dried (MgSO_4) and concentrated *in vacuo*. The crude was purified *via* flash column chromatography to give methyl carbamate **3.54** as a white foam (39 mg, quantitative yield). **¹H NMR** (400 MHz, CDCl₃) δ 7.78 (d, *J* = 7.9 Hz, 2H), 7.69 (d, *J* = 8.3 Hz, 1H), 7.35 – 7.39 (m, 1H), 7.28 (s, 1H), 7.08 (t, *J* = 7.5 Hz, 1H), 6.98 (d, *J* = 6.2 Hz, 1H), 5.65 (s, 1H), 4.72 (s, 1H), 3.85 – 3.94 (m, 4H), 3.53 (s, 1H), 2.38 (s, 3H). **¹³C NMR** (101 MHz, CDCl₃) δ 145.42, 143.13, 131.54, 130.17, 127.90, 124.96, 123.97, 122.71, 115.16, 63.78, 61.53, 54.02, 21.75. **FTIR** (neat) 3501, 2956, 1712, 1598, 1446, 1364, 1287, 1171, 1090, 1036, 946, 914, 812, 754, 723, 662, 575, 538, 492 cm⁻¹. **HRMS** (ESI) calc'd for C₂₀H₂₀N₂O₇S [M+Na]⁺ 301.0795, found 301.0796 m/z. **R_f** = 0.20 (50% EtOAc/hexanes).

3.5.20 Preparation of Amino Alcohol 3.55



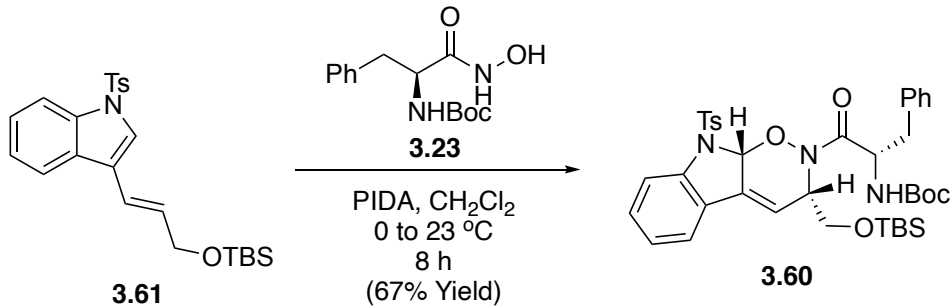
In a 10 mL round-bottom flask was added epoxide **3.52** (107.4 mg, 0.268 mmol, 1.0 equiv) and MeOH (2.7 mL). 2M NaOH (aq.) was added in one portion at 23 °C, and the solution stirred for 4 hours. The reaction was quenched with sat. aq. NH₄Cl (5 mL), and the aqueous extracted with EtOAc (10 mL), dried (MgSO₄), and concentrated *in vacuo*. The crude was purified *via* flash column chromatography to give amino alcohol **3.55** as an off-white foam (100 mg, 99% yield). **¹H NMR** (400 MHz, CDCl₃) δ 7.83 – 7.73 (m, 2H), 7.65 (d, *J* = 8.3 Hz, 1H), 7.35 (td, *J* = 7.8, 1.4 Hz, 1H), 7.26 (d, *J* = 8.3 Hz, 2H), 7.07 (t, *J* = 7.5 Hz, 1H), 6.97 (d, *J* = 8.9 Hz, 1H), 5.57 (s, 1H), 3.90 (dd, *J* = 10.9, 9.0 Hz, 1H), 3.79 (dd, *J* = 10.9, 4.6 Hz, 1H), 3.49 (dd, *J* = 9.1, 4.5 Hz, 1H), 3.27 (s, 1H), 2.38 (s, 3H). **¹³C NMR** (101 MHz, CDCl₃) δ 145.27, 142.98, 133.90, 131.27, 130.13, 127.87, 124.80, 124.60, 122.57, 115.06, 91.75, 63.41, 60.94, 57.39, 55.89, 21.74. **FTIR** (neat) 3541, 3282, 2919, 1730, 1607, 1597, 1486, 1464, 1359, 1292, 1186, 1169, 1113, 1083, 1041, 981, 943, 914, 813, 755, 733, 708, 661, 629, 574, 538, 490 cm⁻¹. **HRMS** (ESI) calc'd for C₁₈H₁₈N₂O₅S [M+Na]⁺ 397.0829, found 397.0827 m/z. **R_f** = 0.38 (60% EtOAc/hexanes).

3.5.21 Data for Known TBS Alcohol **3.61**



$^1\text{H NMR}$ (400 MHz, CDCl_3) δ 7.98 (d, $J = 8.2$ Hz, 1H), 7.75 (d, $J = 8.4$ Hz, 2H), 7.70 (d, $J = 7.8$ Hz, 1H), 7.57 (s, 1H), 7.24 – 7.34 (m, 2H), 7.21 (d, $J = 8.2$ Hz, 2H), 6.64 – 6.69 (m, 1H), 6.35 (dt, $J = 16.0, 4.9$ Hz, 1H), 4.37 (dd, $J = 4.9, 1.8$ Hz, 2H), 2.33 (s, 3H), 0.96 (s, 9H), 0.13 (s, 6H). **$^{13}\text{C NMR}$** (101 MHz, CDCl_3) δ 145.09, 135.65, 135.28, 130.60, 130.02, 129.37, 126.97, 124.98, 123.69, 123.57, 120.53, 120.45, 119.95, 113.89, 64.05, 26.13, 21.70, 18.61, -5.01. $\text{R}_f = 0.66$ (50% EtOAc/hexanes). Data is consistent with the literature.¹⁵

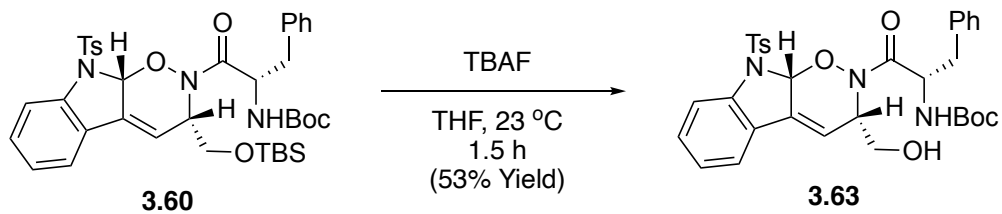
3.5.22 Preparation of NDA Adduct **3.60**



To a 50 mL round-bottom flask was added known TBS alcohol **3.61**¹⁵ (1.05 g, 2.377 mmol, 1.0 equiv), known hydroxamic acid **3.23**⁹ (1.0 g, 3.566 mmol, 1.5 equiv), and dry CH_2Cl_2 (24 mL). The solution was cooled to 0 °C and stirred for 8 hours while warming to rt. The reaction was quenched with sat. aq. NaHCO_3 (10 mL), $\text{Na}_2\text{S}_2\text{O}_3$ (10 mL), and brine (5 mL). The aqueous phase was extracted with CH_2Cl_2 (3 x 20 mL), dried (MgSO_4), and concentrated *in vacuo*. The crude residue was purified *via* flash column chromatography to yield NDA adduct **3.60** as a light-yellow foam (1.14 g, 67% yield). **1H NMR** (600 MHz, CDCl_3) δ 8.01 (d, J = 8.1 Hz, 2H), 7.73 – 7.76 (m, 1H), 7.37 (d, J = 7.5 Hz, 2H), 7.27 – 7.33 (m, 5H), 7.19 – 7.21 (m, 2H), 7.03 – 7.07 (m, 1H), 6.14 (d, J = 2.7 Hz, 2H), 5.50 – 5.54 (m, 1H), 5.00 – 5.02 (m, 2H), 3.78 (dd, J = 9.4, 5.6 Hz, 1H), 3.45 (t, J = 9.2 Hz, 1H), 3.23 (dd, J = 13.9, 5.5 Hz, 1H), 2.99 (dd, J = 13.9, 8.7 Hz, 1H), 2.34 (s, 3H), 1.45 (s, 9H), 0.88 (s, 10H), 0.06 (s, 3H), 0.05 (s, 3H). **13C NMR** (151 MHz, CDCl_3) δ 172.16, 155.87, 145.17, 142.40, 136.23, 134.10, 132.63, 130.39, 130.01, 129.92, 129.70, 128.84, 128.61, 128.52, 126.99, 126.32, 124.96, 121.10, 117.66, 115.31, 92.45, 63.25, 53.12, 52.42, 38.17, 28.54, 26.06, 25.94, 21.76, 18.35, -5.22, -5.32. **FTIR** (neat) 2951, 2926, 2856, 1701, 1663, 1600, 1495, 1455, 1391, 1366, 1248, 1171, 1111, 1088, 1069, 1016, 953, 938, 835, 813,

776, 749, 699, 660, 576, 541, 495, 460, 444 cm^{-1} . **HRMS** (ESI) calc'd for $\text{C}_{38}\text{H}_{49}\text{N}_3\text{O}_7\text{SSI}$ $[\text{M}+\text{Na}]^+$ 742.2953, found 742.2953 m/z. $\text{R}_f = 0.17$ (10% EtOAc/hexanes). $[\alpha]_D^{23}$: (c = 0.40, MeOH), -105°.

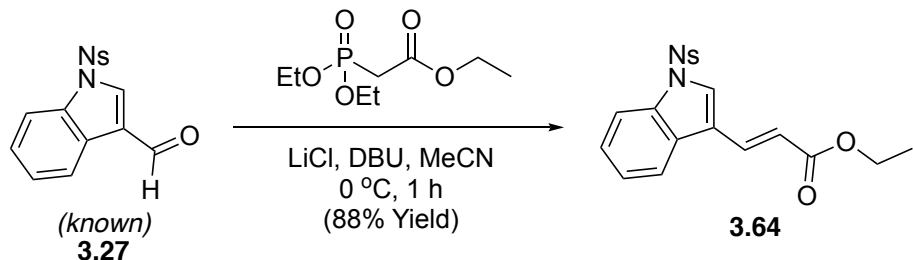
3.5.23 Preparation of Alcohol **3.63**



To a 2-Dram vial was added NDA adduct **3.60** (50 mg, 0.069 mmol, 1.0 equiv) and dry THF (0.3 mL). A solution of TBAF (0.08 mL, 0.076 mmol, 1.1 equiv, 1M in THF) was added in one portion at 23 °C. The reaction stirred for 2.5 hours and was quenched with sat. aq. NH₄Cl (2 mL). The aqueous phase was extracted with EtOAc (3 x 5 mL), dried (MgSO_4), and concentrated *in vacuo*. The crude was purified *via* flash column chromatography to yield alcohol **3.63** as a beige-colored foam (26.5 mg, 63% yield). The structure was confirmed by X-ray crystallography. **¹H NMR** (400 MHz, CDCl_3) δ 8.01 (d, $J = 8.0$ Hz, 2H), 7.79 (br s, 1H), 7.73 (d, $J = 8.2$ Hz, 1H), 7.28 – 7.41 (m, 6H), 7.19 – 7.23 (m, 3H), 7.04 (t, $J = 7.5$ Hz, 1H), 6.19 (t, $J = 2.7$ Hz, 1H), 5.94 (t, $J = 2.6$ Hz, 1H), 5.56 (q, $J = 7.5$ Hz, 1H), 5.07 – 5.11 (m, 2H), 3.65 – 3.70 (m, 2H), 3.19 (dd, $J = 13.8, 6.5$ Hz, 1H), 3.09 (dd, $J = 13.7, 8.0$ Hz, 1H), 2.34 (s, 3H), 1.46 (s, 9H). **¹³C NMR** (101 MHz, CDCl_3) δ 173.30, 155.90, 145.24, 142.43, 135.93, 135.29, 132.57, 130.63, 130.14, 130.00, 129.98, 128.82, 128.57, 127.13, 125.95, 124.99, 121.31, 116.11, 115.31, 92.24, 64.58, 54.36,

52.33, 38.19, 28.53, 21.75. **FTIR** (neat) 3483, 3462, 2974, 2929, 2881, 1703, 1677, 1650, 1598, 1494, 1457, 1438, 1393, 1364, 1295, 1249, 1172, 1114, 1090, 1073, 1055, 1019, 985, 954, 913, 871, 848, 815, 767, 741, 729, 697, 677, 660, 580, 547, 530, 493, 446 cm⁻¹. **HRMS** (ESI) calc'd for C₃₂H₃₅N₃O₇S [M+H]⁺ 606.2268, found 606.2271 m/z; for [M+Na]⁺ 628.2088, found 628.2087 m/z. **R_f** = 0.21 (50% EtOAc/hexanes). **m.p.** = 209 – 211 °C. $[\alpha]_D^{22}$: (c = 0.85, MeOH), -78.59°.

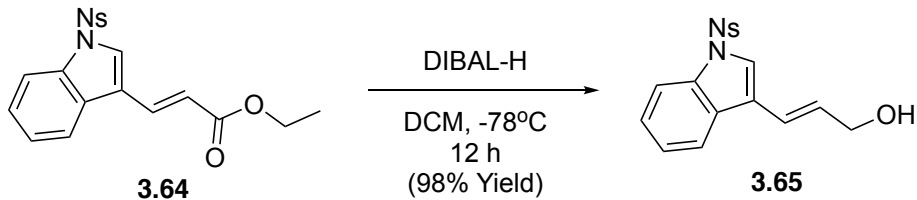
3.5.24 Preparation of Ethyl Ester **3.64**



In a flame-dried 1L round-bottom flask, LiCl (1.93 g, 45.41 mmol, 1.5 equiv) and DBU (6.8 mL, 45.41 mmol, 1.5 equiv) were dissolved in dry acetonitrile (303 mL, 0.1 M). The mixture was cooled to 0 °C and triethyl phosphonate ester (7.2 mL, 36.33 mmol, 1.2 equiv) was added in one portion. The reaction stirred at 0 °C for 30 minutes then known Ns-protected indole **3.27**³ (10 g, 30.28 mmol, 1.0 equiv) was added in one portion. The reaction stirred for 12 hours under an atmosphere of N₂, then washed with sat. aq. NH₄Cl (25 mL) and brine (25 mL). The aqueous phase was extracted with EtOAc then dried (MgSO₄) and concentrated *in vacuo*. Et₂O was added and the precipitate was filtered and washed with cold Et₂O to yield ethyl ester **3.64** as a bright yellow solid (10.61 g, 88% yield). **¹**H NMR (400 MHz, CDCl₃) δ 8.32 – 8.28 (m, 2H), 8.10 – 8.06 (m, 2H), 8.01 (d, *J*

δ = 8.2 Hz, 1H), 7.82 (d, J = 8.1 Hz, 1H), c7.80 (s, 1H), 7.76 (d, J = 16.1 Hz, 1H), 7.40 (m, 2H), 6.54 (d, J = 16.1 Hz, 1H), 4.28 (q, J = 7.1 Hz, 2H), 1.35 (t, J = 7.2 Hz, 3H). **¹³C NMR** (101 MHz, CDCl₃) δ 166.94, 143.04, 135.63, 134.93, 128.54, 128.37, 127.60, 126.30, 125.00, 124.89, 121.23, 119.89, 119.75, 113.82, 60.83, 14.48. **IR** (neat) 3121, 2989, 1704, 1638, 1528, 1444, 1385, 1346, 1311, 1169, 1119, 1083, 979, 833, 747, 678, 638, 598, 559, 463 cm⁻¹. **HRMS** (ESI) calc'd for C₁₉H₁₆N₂O₆S [M+H]⁺ 401.0802, found 401.0807 m/z. **R_f** = 0.48 (20% EtOAc/hexanes).

3.5.25 Preparation of Allylic Alcohol **3.65**

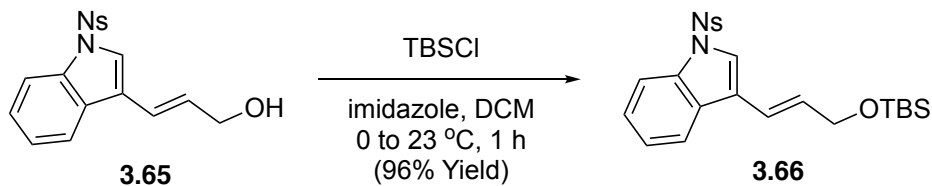


In a flame-dried 500 mL round-bottom flask, ethyl ester **3.64** (12.29 g, 30.69 mmol, 1.0 equiv) was dissolved in dry CH₂Cl₂ (153 mL, 0.2 M). The solution was cooled to -78 °C and neat DIBAL-H (12 mL, 2.2 equiv, 67.53 mmol) was added dropwise over 5 minutes. The reaction was allowed to warm to 23 °C over 12 hours under an atmosphere of N₂, then quenched with 150 mL aq. 1M NaOH and stirred for 1 hour. The aqueous phase was extracted with CH₂Cl₂, dried (MgSO₄), concentrated *in vacuo*, and purified by flash column chromatography to yield allylic alcohol **3.65** as a waxy orange solid (10.8 g, 98% yield).

¹H NMR (400 MHz, CDCl₃) δ 8.30 – 8.18 (m, 2H), 8.08 – 8.01 (m, 2H), 7.99 (d, J = 8.2 Hz, 1H), 7.73 (d, J = 7.8 Hz, 1H), 7.55 (s, 1H), 7.41 – 7.27 (m, 2H), 6.73 – 6.62 (d, J = 16.11 Hz, 1H), 6.46 (dt, J = 16.1, 5.5 Hz, 1H), 4.42 – 4.28 (d, J = 5.23 Hz, 2H). **¹³C NMR**

(101 MHz, CDCl₃) δ 150.77, 143.21, 135.53, 131.09, 129.44, 128.19, 125.78, 124.68, 124.49, 123.35, 121.80, 121.03, 120.85, 113.81, 63.85. **IR** (neat) 3559, 3098, 3062, 2866, 1605, 1532, 1445, 1399, 1377, 1347, 1302, 1176, 1126, 1089, 1010, 979, 964, 854, 791, 736, 681, 619, 564, 458 cm⁻¹. **HRMS** (ESI) calc'd for C₁₇H₁₄N₂O₅S [M+H]⁺ 359.0696, found 359.0700 m/z. **R_f** = 0.13 (50% EtOAc/hexanes).

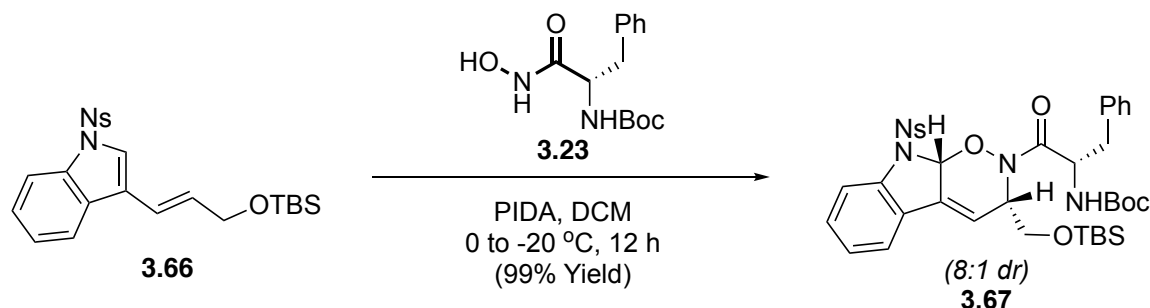
3.5.26 Preparation of Allylic TBS Alcohol **3.66**



In a flame-dried flask allylic alcohol **3.65** (22 g, 61.39 mmol, 1.0 equiv) and imidazole (12.5 g, 184.17 mmol, 3.0 equiv) were dissolved in dry CH₂Cl₂ (307 mL, 0.2 M). The solution was cooled to 0 °C and TBSCl (27.8 g, 184.17 mmol, 3.0 equiv) was added in one portion. The reaction was warmed to 23 °C and stirred for 12 hours under an atmosphere of N₂, then quenched with sat. aq. NH₄Cl (50 mL). The aqueous phase was extracted with CH₂Cl₂, dried (MgSO₄), concentrated *in vacuo*, then purified by flash column chromatography to yield allylic TBS alcohol **3.66** as a waxy yellow solid (27.7 g, 96% yield). **1H NMR** (400 MHz, CDCl₃) δ 8.32 – 8.20 (m, 2H), 8.07 – 8.01 (m, 2H), 7.99 (dt, *J* = 8.3, 1.0 Hz, 1H), 7.76 – 7.68 (m, 1H), 7.53 (s, 1H), 7.42 – 7.28 (m, 2H), 6.66 (dtd, *J* = 16.0, 1.9, 0.7 Hz, 1H), 6.38 (dt, *J* = 16.0, 4.7 Hz, 1H), 4.37 (dd, *J* = 4.7, 1.9 Hz, 2H), 0.96 (s, 9H), 0.13 (s, 6H). **13C NMR** (101 MHz, CDCl₃) δ 150.76, 143.30, 135.55, 131.82, 129.69, 128.19, 125.67, 124.67, 124.41, 122.91, 122.24, 120.86, 119.17, 113.79, 63.81,

26.11, 18.61. **IR** (neat) 2929, 2855, 1606, 1532, 1445, 1381, 1347, 1251, 1180, 1120, 985, 962, 835, 776, 738, 681, 615, 567, 460 cm^{-1} . **HRMS** (ESI) calc'd for $\text{C}_{23}\text{H}_{28}\text{N}_2\text{O}_5\text{SSI}$ [$\text{M}+\text{H}]^+$ 473.1561, found 473.1565 m/z. $\text{R}_f = 0.36$ (10% EtOAc/hexanes).

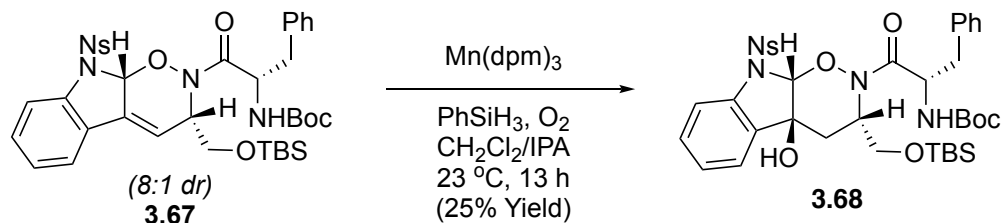
3.5.27 Preparation of Nitroso Diels-Alder Adduct **3.67**



In a flame-dried 500 mL round-bottom flask, allylic TBS alcohol **3.40** (8.6 g, 18.20 mmol, 1.0 equiv) and known Boc-protected hydroxamic acid **3.66**⁹ (7.65 g, 27.29 mmol, 1.5 equiv) were dissolved in dry CH_2Cl_2 (182 mL, 0.1 M) then the mixture was cooled to 0 °C. PIDA (8.79 g, 27.29 mmol, 1.5 equiv) was added in one portion at 0 °C and the reaction stirred for 30 minutes under an atmosphere of N_2 . The flask was placed in a freezer (-20 °C) for 17 hours, then quenched with sat. aq. NaHCO_3 (30 mL), sat. aq. $\text{Na}_2\text{S}_2\text{O}_3$ (30 mL), and brine (30 mL). The aqueous phase was extracted with CH_2Cl_2 (3 x 50 mL), dried (MgSO_4), and concentrated *in vacuo*. The crude mixture was purified *via* flash column chromatography to yield unsaturated oxazine **3.67** as a pale-yellow foam (13.6 g, 99% yield, ~8:1 dr). The structure was confirmed by X-ray crystallography. **¹H NMR** (400 MHz, CDCl_3) δ 8.39 (d, $J = 8.9$ Hz, 2H), 8.25 (d, $J = 8.9$ Hz, 2H), 7.75 (d, $J = 8.8$ Hz, 1H), 7.34 (m, 7H), 7.24 (d, $J = 7.1$ Hz, 1H), 7.11 (t, $J = 7.5$ Hz, 1H), 6.17 (p, $J = 2.5$ Hz, 2H),

5.50 (m, 1H), 5.06 – 5.01 (m, 2H), 3.77 (dd, J = 9.3, 5.7 Hz, 1H), 3.42 (t, J = 9.1 Hz, 1H), 3.20 (dd, J = 13.9, 5.7 Hz, 1H), 2.98 (dd, J = 13.8, 8.7 Hz, 1H), 1.46 (d, J = 12.3 Hz, 10H), 0.88 (s, 10H), 0.06 (d, J = 4.8 Hz, 6H). **^{13}C NMR** (101 MHz, CDCl_3) δ 172.20, 156.17, 151.05, 141.43, 141.08, 141.00, 136.93, 136.02, 133.40, 130.71, 130.63, 130.31, 130.03, 129.85, 129.69, 128.74, 128.57, 127.10, 126.99, 126.43, 125.75, 125.27, 124.75, 124.50, 124.16, 121.52, 121.12, 118.54, 115.01, 92.07, 63.22, 54.24, 53.11, 52.28, 38.28, 37.90, 31.08, 28.56, 26.00, 25.93, 25.84, 18.51, 18.34. **IR** (neat) 2951, 2929, 1703, 1666, 1604, 1532, 1496, 1459, 1402, 1377, 1366, 1348, 1250, 1175, 1110, 1089, 1068, 1011, 958, 836, 778, 737, 699, 684, 610, 568, 462 cm^{-1} . **HRMS** (ESI) calc'd for $\text{C}_{37}\text{H}_{46}\text{N}_4\text{O}_9\text{SSi}$ [$\text{M}+\text{H}$] $^+$ 751.2828, found 751.2828 m/z; calc'd for [$\text{M}+\text{Na}$] $^+$ 773.2647, found 773.2650 m/z. **R_f** = 0.14 (10% EtOAc/hexanes). **m.p.** = 88 – 92 °C. $[\alpha]_D^{22}$: (c = 0.08, CH_2Cl_2), -145°.

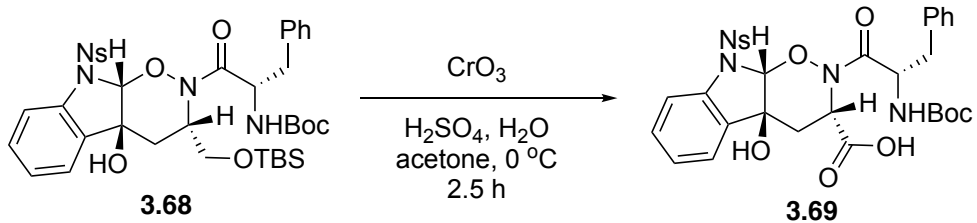
3.5.28 Preparation of Mukaiyama Hydration Adduct **3.68**



In a flame-dried 10 mL round-bottom flask, unsaturated oxazine **3.67** (94.5 mg, 0.126 mmol, 1.0 equiv) was dissolved in a ~2:1 mixture of CH_2Cl_2 /IPA at 23 °C. Mn(dpm)_3 (22.8 mg, 0.038 mmol, 30 mol %) was added under an atmosphere of O_2 , then O_2 was bubbled *via* balloon for 30 minutes. PhSiH_3 (0.05 mL, 0.378 mmol, 3.0 equiv) was added dropwise *via* syringe pump over the course of 1 hour, and the reaction stirred at 23 °C for

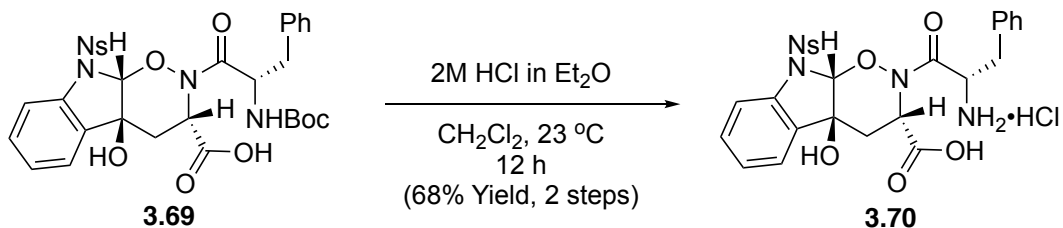
12 hours after addition, under an atmosphere of O₂. The reaction was quenched with sat. aq. NaHCO₃ (1.5 mL) and sat. aq. Na₂S₂O₃ (1.5 mL), then the aqueous phase was extracted with EtOAc, dried (MgSO₄), and concentrated *in vacuo*. The crude was purified by flash column chromatography to give tertiary alcohol **3.68** as a pale-yellow foam (24 mg, 25% yield). **¹H NMR** (600 MHz, CDCl₃) δ 8.20 (d, *J* = 8.7 Hz, 2H), 8.12 (d, *J* = 8.6 Hz, 2H), 7.67 (d, *J* = 8.2 Hz, 1H), 7.41 (td, *J* = 7.9, 1.3 Hz, 1H), 7.31 – 7.35 (m, 5H), 7.25 (m, 1H), 7.16 – 7.19 (m, 1H), 6.16 (s, 1H), 5.38 (td, *J* = 8.5, 5.5 Hz, 1H), 5.01 (d, *J* = 7.7 Hz, 1H), 4.54 (d, *J* = 6.8 Hz, 1H), 3.59 (dd, *J* = 10.0, 4.2 Hz, 1H), 3.49 (dd, *J* = 10.0, 7.1 Hz, 1H), 3.20 (dd, *J* = 14.1, 5.3 Hz, 1H), 2.98 (br s, 1H), 2.90 (dd, *J* = 14.1, 9.3 Hz, 1H), 2.41 (dd, *J* = 14.2, 5.8 Hz, 1H), 2.23 (dd, *J* = 14.2, 9.6 Hz, 1H), 1.44 (s, 9H), 0.84 (s, 9H), 0.00 (s, 3H), -0.01 (s, 3H). **¹³C NMR** (151 MHz, CDCl₃) δ 172.87, 156.59, 150.76, 142.53, 139.52, 136.02, 133.94, 131.02, 129.68, 129.43, 128.68, 127.14, 125.97, 124.38, 124.22, 115.05, 99.01, 80.39, 62.39, 52.29, 52.23, 38.20, 33.53, 29.85, 28.55, 25.96, 18.36, -5.30, -5.32. **FTIR** (neat) 3419, 2954, 2929, 2857, 1668, 1605, 1531, 1497, 1475, 1463, 1366, 1348, 1251, 1171, 1090, 1047, 1028, 958, 910, 835, 777, 737, 699, 683, 613, 565, 494, 461 cm⁻¹. **HRMS** (ESI) calc'd for C₃₇H₄₈N₄O₁₀SSi [M+H]⁺ 769.2933, found 769.2933 m/z; calc'd for [M+Na]⁺ 791.2753, found 791.2753 m/z. **R_f** = 0.59 (40% EtOAc/hexanes). **[α]_D²⁰**: (*c* = 0.16, MeOH), 20.00°.

3.5.29 Preparation of Carboxylic Acid 3.69



A solution of tertiary alcohol **3.68** (115.1 mg, 0.15 mmol, 1.0 equiv) in acetone (1.5 mL, 0.1 M) was cooled to 0 °C, and Jones reagent (0.2 mL, 0.45 mmol, 3.0 equiv) was added dropwise. The reaction was allowed to warm to 23 °C over 2.5 h under an atmosphere of N₂, then quenched with *i*PrOH (1 mL) and H₂O (5 mL). The aqueous layer was extracted with EtOAc (3 x 5 mL), dried (MgSO₄), and concentrated *in vacuo*. The crude carboxylic acid **3.69** was advanced to the next step without purification.

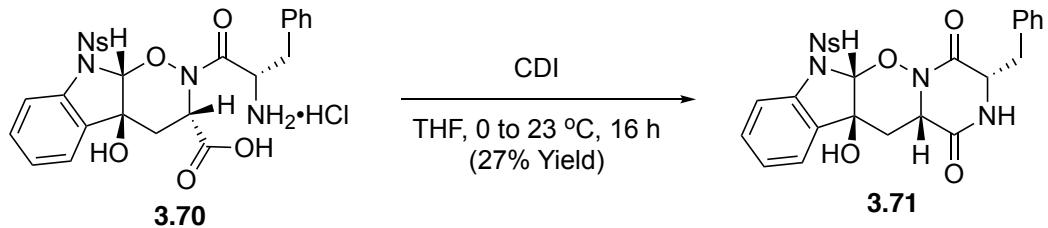
3.5.30 Preparation of Amino Salt 3.70



In a 2-Dram vial, crude carboxylic acid **3.69** (0.15 mmol, 1.0 equiv) was dissolved in dry CH₂Cl₂ (1.5 mL, 0.1 M) at 23 °C. 2M HCl in Et₂O (0.4 mL, 0.75 mmol, 5.0 equiv) was added in one portion. The reaction stirred at 23 °C for 12 hours under an atmosphere of N₂, ether was added, and the resulting precipitate was filtered and washed with cold

Et_2O . The mother liquor was concentrated *in vacuo*, resuspended in Et_2O , and filtered again. The precipitate was combined to yield amino salt **3.70** as a tan-colored solid (61.7 mg, 68% yield over 2 steps). **1H NMR** (400 MHz, MeOD) δ 8.38 (d, J = 8.6 Hz, 2H), 8.25 (d, J = 8.4 Hz, 2H), 7.53 – 7.56 (m, 1H), 7.42 – 7.48 (m, 3H), 7.32 – 7.40 (m, 5H), 7.20 (t, J = 7.5 Hz, 1H), 5.86 (s, 1H), 5.00 (dd, J = 10.0, 5.8 Hz, 1H), 4.94 (dd, J = 9.8, 3.6 Hz, 2H), 3.56 (dd, J = 14.7, 3.9 Hz, 1H), 3.00 (dd, J = 14.9, 9.7 Hz, 1H), 2.81 (dd, J = 14.1, 5.8 Hz, 1H), 2.45 (dd, J = 14.1, 9.9 Hz, 1H). **13C NMR** (151 MHz, MeOD) δ 199.49, 197.61, 180.67, 171.80, 168.76, 163.48, 162.72, 160.10, 159.05, 158.51, 158.31, 157.08, 154.99, 154.14, 153.89, 143.66, 130.01, 104.79, 83.03, 82.68, 65.23, 62.83. **IR** (neat) 2935, 2107, 1729, 1702, 1672, 1604, 1530, 1498, 1476, 1462, 1401, 1370, 1348, 1313, 1291, 1244, 1172, 1109, 1087, 1043, 964, 854, 814, 737, 700, 683, 613, 586, 565, 461, 419 cm^{-1} . **HRMS** (ESI) calc'd for $\text{C}_{26}\text{H}_{24}\text{N}_4\text{O}_9\text{S} [\text{M}+\text{Na}]^+$ 591.1156, found 591.1157 m/z. $[\alpha]_D^{22}$: (c = 0.19, MeOH), -6.32°.

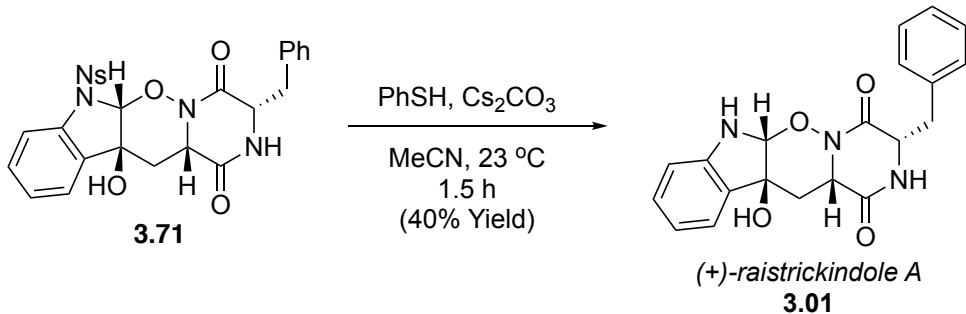
3.5.31 Preparation of DKP **3.71**



In a 2-Dram vial, amino salt **3.70** (163.3 mg, 0.270 mmol, 1.0 equiv) was dissolved in dry THF (1.8 mL) then cooled to 0 °C. CDI (52.5 mg, 0.324 mmol, 1.2 equiv) was added in one portion at 0 °C. The reaction was allowed to warm to 23 °C for 16 h under an

atmosphere of N₂, then washed with sat. aq. NH₄Cl (2 mL) and brine (2 mL). The aqueous phase was extracted with EtOAc, dried (MgSO₄), and concentrated *in vacuo*. The crude mixture was purified by flash column chromatography to yield DKP **3.71** as an orange foam (39.9 mg, 27% yield). **¹H NMR** (600 MHz, MeOD) δ 8.35 – 8.29 (m, 2H), 8.27 – 8.21 (m, 2H), 7.32 – 7.22 (m, 2H), 7.20 (d, *J* = 1.3 Hz, 1H), 7.16 – 7.10 (m, 3H), 7.03 (td, *J* = 7.5, 1.2 Hz, 1H), 6.90 (dd, *J* = 7.3, 2.2 Hz, 2H), 5.87 (s, 1H), 4.63 (dt, *J* = 9.5, 1.8 Hz, 1H), 4.59 (br s, 1H), 4.14 (ddd, *J* = 6.6, 4.6, 1.8 Hz, 1H), 3.10 (dd, *J* = 13.9, 1.9 Hz, 1H), 2.89 (dd, *J* = 14.4, 4.6 Hz, 1H), 2.49 (dd, *J* = 13.9, 9.5 Hz, 1H), 2.44 (dd, *J* = 14.4, 6.8 Hz, 1H). **¹³C NMR** (151 MHz, MeOD) δ 168.17, 166.04, 152.14, 145.06, 143.05, 136.89, 132.67, 131.60, 130.47, 130.43, 129.59, 127.83, 126.52, 125.43, 125.38, 115.09, 100.71, 76.33, 56.11, 55.74, 38.05, 33.08, 30.05, 23.74, 14.43. **IR** (neat) 2919, 2872, 2851, 1756, 1733, 1681, 1594, 1530, 1463, 1432, 1409, 1348, 1328, 1307, 1294, 1280, 1204, 1171, 1129, 1109, 1080, 1049, 1021, 983, 962, 941, 851, 805, 743, 735, 701, 683, 656, 610, 566, 548, 461, 437 cm⁻¹. **HRMS** (ESI) calc'd for C₂₆H₂₂N₄O₈S [M+Na]⁺ 573.1051, found 573.1050 m/z. **R_f** = 0.48 (100% EtOAc). [α]_D²²: (c = 0.04, MeOH), 70°.

3.5.32 Preparation of (+)-Raistrickindole A **3.01**



To a 2-Dram vial, DKP **3.71** (39.9 mg, 0.072, 1.0 equiv), PhSH (15 μ L, 0.145 mmol, 2.0 equiv), Cs_2CO_3 (59 mg, 0.181 mmol, 2.5 equiv), and MeCN (2.4 mL) were added. The reaction stirred for 1.5 hours at 23 °C and was quenched with sat. aq. NaHCO_3 (2 mL). The aqueous layer was extracted with EtOAc (3 x 2 mL), dried (MgSO_4), and purified *via* flash column chromatography to give (+)-raistrickindole A (**3.01**) as a white solid (10.5 mg, 40% yield). **1H NMR** (600 MHz, MeOD) δ 7.16 (ddd, J = 1.28, 7.70, 7.70 Hz, 1H), 7.06 (dd, J = 1.22, 7.88 Hz, 2H), 7.05 (dd, J = 1.23, 7.79 Hz, 1H), 6.99 (t, J = 7.88 Hz, 2H), 6.84 (tt, J = 1.24, 7.82 Hz, 1H), 6.74 (ddd, J = 1.16, 7.78, 7.78 Hz, 1H), 6.72 (d, J = 7.82 Hz, 1H), 5.28 (s, 1H), 4.38 (ddd, J = 1.25, 5.34, 8.82 Hz, 1H), 4.33 (ddd, J = 1.22, 4.84, 4.84 Hz, 1H), 2.97 (dd, J = 4.82, 13.87 Hz, 1H), 2.85 (dd, J = 4.82, 13.87 Hz, 1H), 2.13 (dd, J = 5.47, 13.87 Hz, 1H), 1.21 (dd, J = 8.95, 13.87 Hz, 1H). **13C NMR** (151 MHz, MeOD) δ 168.02, 163.39, 148.76, 136.03, 131.82, 131.28, 130.52, 129.47, 127.84, 124.01, 120.13, 110.91, 101.31, 75.96, 56.46, 55.83, 39.60, 36.51. **IR** (neat) 3323, 2921, 2851, 2039, 1985, 1668, 1615, 1559, 1484, 1469, 1454, 1377, 1337, 1318, 1303, 1208, 1174, 1065, 1040, 1010, 951, 905, 820, 801, 743, 699, 673, 654, 605, 592, 473, 453, 424 cm^{-1} . **HRMS** (ESI) calc'd for $\text{C}_{20}\text{H}_{19}\text{N}_3\text{O}_4$ [$\text{M}+\text{Na}$]⁺ 388.1268, found 388.1268 m/z; calc'd

for $[M+H]^+$ 366.1448, found 366.1456 m/z. $R_f = 0.17$ (100% EtOAc). $[\alpha]_D^{21}$: ($c = 0.07$, MeOH), $+11.43^\circ$. Spectral data is consistent with the literature.¹

3.8 References

¹ Li, J.; Hu, Y.; Hao, X.; Tan, J.; Li, F.; Qiao, X.; Chen, S.; Xiao, C.; Chen, M.; Peng, Z.; Gan, M. *J. Nat. Prod.* **2019**, *82*, 1391-1395.

² Borthwick, A. D. “2,5-Diketopiperazines: Synthesis, Reactions, Medicinal Chemistry, and Bioactive Natural Products” *Chem. Rev.* **2012**, *112*, 3641-3716.

³ Pettersson, B.; Hasimbegovic, V.; Bergman, J. *J. Org. Chem.* **2011**, *76*(6), 1554-1561.

⁴ Lambert, K. M.; Medley, A. W.; Jackson, A. C.; Markham, L. E.; Wood, J. L. *Org. Synth.* **2019**, *96*, 528-585.

⁵ Hantzsch ester reduction: Zheng, C.; You, S-L. *Chem. Soc. Rev.* **2012**, *41*, 2498-2518.

⁶ Wichterle, O. *Collect. Czech. Chem. Commun.* **1947**, *12*, 292-304.

⁷ The NDA reaction:

- (a) Sheradsky, T.; Silcoff, E. R. *Molecules* **1998**, *3*, 80-87.
- (b) Brulíková, L.; Harrison, A.; Miller, M. J.; Hlaváč, J. *Beilstein J. Org. Chem.* **2016**, *12*, 1949-1980, and references therein.
- (c) Xu, X-B.; Liu, Y-N.; Rao, G-W. *Russ. J. Org. Chem.* **2019**, *55*(4), 559-568, and references therein.
- (d) Bollans, L., Bacsa, J.; Iggo, J. A.; Morris, G. A.; Stachulski, A. V. *Org. Biomol. Chem.* **2009**, *7*, 4531-4538.
- (e) Sparks, S. M.; Chow, C. P.; Zhu, L.; Shea, K. J. *J. Org. Chem.* **2004**, *69*, 3025-3035.
- (f) Yamamoto, H.; Kawasaki, M. *Bull. Chem. Soc. Jpn.* **2007**, *80*(4), 595-607.
- (g) Anand, A.; Bhargava, G.; Singh, P.; Mehra, S.; Kumar, V.; Mahajan, M. P.; Singh, P.; Bisetty, K. *Lett. Org. Chem.* **2012**, *9*, 411-421.
- (h) Jenkins, N. E.; Ware, R. W.; Atkinson, R. N.; King, S. B. *Synth. Comm.* **2000**, *30*(5), 947-953.
- (i) Levandowski, B. J.; Houk, K. N. *J. Org. Chem.* **2015**, *80*, 3530-3537.
- (j) Houk, K. N.; Leach, A. J. *J. Org. Chem.* **2001**, *66*, 5192. Leach, A. G.; Houk, K. N. *Chem. Commun.* **2002**, 1243-1255.
- (k) Miller, M. J.; Carosso, S. *Org. Biomol. Chem.* **2014**, *12*(38), 7445-7468, and references therein.

⁸ (a) Keck, G. E. *Tetrahedron Lett.* **1978**, *19*, 4767.

(b) Watson, K. D.; Carosso, S.; Miller, M. J. *Org. Lett.* **2013**, *15*(2), 358.

⁹ Usachova, N.; Leitis, G.; Jirgensons, A.; Kalvinsh, I. *Synth. Commun.* **2010**, *40*(6), 927-935.

¹⁰ Cyclopentadiene adduct: Zhangtao, Z.; Weiping, Y.; Anjie, F.; Yang, W.; Zhongwen, Q.; Xingbao, Z. CN109651178, 2019, A.

¹¹ Early examples of azlactone formation in similar systems:

(a) Plöchl, J. "Über einige Derivate der Benzoylimidozimtsäure" [On some derivatives of benzoyl-imido-cinnamic acid] *Berichte der deutschen chemischen Gesellschaft* **1884**, *17*(2), 1616-1624.

(b) Erlenmeyer, F. "Ueber die Condensation der Hippursäure mit Phtalsäureanhydrid und mit Benzaldehyd" [On the condensation of hippuric acid with phthalic acid anhydride and with benzaldehyde] *Annalen der Chemie* **1893**, 275, 1-8. doi:10.1002/jlac.18932750102; see especially pp. 3-8.

(c) Chen, F. M. F.; Sleboda, M.; Benoiton, N. L. *Int. J. Pept. Protein Res.* **1988**, *31*(3), 339-344.

(d) Wipf, P.; Li, W. Sekhar, V. *Bioorg. Med. Chem. Lett.* **1991**, *1*(12), 745-750.

(e) Avenoza, A.; Bustos, J. H.; Cativiela, C.; Peregrina, J. M.; Rodriguez, F. *Tetrahedron Lett.* **2002**, *43*(8), 1429-1432.

(f) Andersch, J.; Hennig, L.; Wilde, H. *Carbohydr. Res.* **2000**, *329*(3), 693-697.

¹² Known extended hydroxamic acid: Tan, Y.; Han, F.; Hemming, M.; Wang, J.; Harms, K.; Xie, X.; Meggers, E. *Org. Lett.* **2020**, *22*(16), 6653-6656.

¹³ Shimizu, H.; Yoshimura, A.; Noguchi, K.; Nemykin, V. N.; Zhdankin, V. V.; Saito, A. *Beilstein J. Org. Chem.* **2018**, *14*, 531-536.

¹⁴ Jankolovits, J.; Lim, C-S.; Mezei, G.; Kampf, J. W.; Pecoraro, V. L. *Inorg. Chem.* **2012**, *51*, 4527-4538.

¹⁵ Gritsch, P. J.; Stempel, E.; Gaich, J. *Org. Lett.* **2013**, *15*(21), 5472-5475.

¹⁶ Boger, D. L.; Patel, M.; Takusagawa, F. *J. Org. Chem.* **1985**, *50*, 1911-1916.

¹⁷ Vogt, P. F.; Miller, M. J. *Tetrahedron*, **1998**, *54*, 1317-1348.

¹⁸ Kim, J. W.; Ko, S.; Son, S.; Shin, K.; Ryoo, I.; Hong, Y.; Oh, H.; Hwang, B. Y.; Hirota, H.; Takahashi, S.; Kim, B. Y.; Osada, H.; Jang, J.; Ahn, J. *Bioorg. Med. Chem. Lett.* **2015**, *25*, 5398-5401.

¹⁹ Hwang, I. H.; Che, Y.; Swenson, D. C.; Gloer, J. B.; Wicklow, D. T.; Peterson, S. W.; Dowd, P. F. *J. Antibiot.* **2016**, *69*, 631-636.

²⁰ Damage by the fall armyworm: (a) Hruska, A. J. *CAB Reviews*, **2019**, *14*, 043. (b) UN News, <https://news.un.org/en/story/2019/03/1035071>, “‘Growing alarm’ over Fall Armyworm advance, with cash crops ‘under attack’ across Asia” (see Food and Agriculture Organization of the United Nations).

²¹ Visagie, C. M., Hirooka, Y., Tanney, J. B., Whitfield, E., Mwange, K., Meijer, M., Amend, A. S., Seifert, K. A., Samson, R. A. *Studies in Mycology*, **2014**, *78*, 63-139.

²² Pedras, M.; Soledade, C.; Okinyo-Owiti, D. P.; Thoms, K.; Adio, A. M. *Phytochemistry* **2009**, *70*(9), 1129-1138.

²³ Tan, Y.; Han, F.; Hemming, M.; Wang, J.; Harms, K.; Xie, X.; Meggers, E. *Org. Lett.* **2020**, *22*(16), 6653-6656.

²⁴ Katoh, T.; Watanabe, T.; Nishitani, M.; Ozeki, M.; Kajimoto, T.; Node, M. *Tetrahedron Lett.* **2008**, *49*(4), 598-600.

²⁵ Taber, D. F.; DeMatteo, P. W.; Hassan, R. A. *Org. Synth.* **2013**, *90*, 350-357 (*checked by Wood, J. L.; Enquist, J. A., Jr.*).

²⁶ Pirrung, M. C.; Chau, J. H-L. *J. Org. Chem.* **1995**, *60*(24), 8084-8085.

APPENDICES

APPENDIX A
Spectral Data for Chapter Two

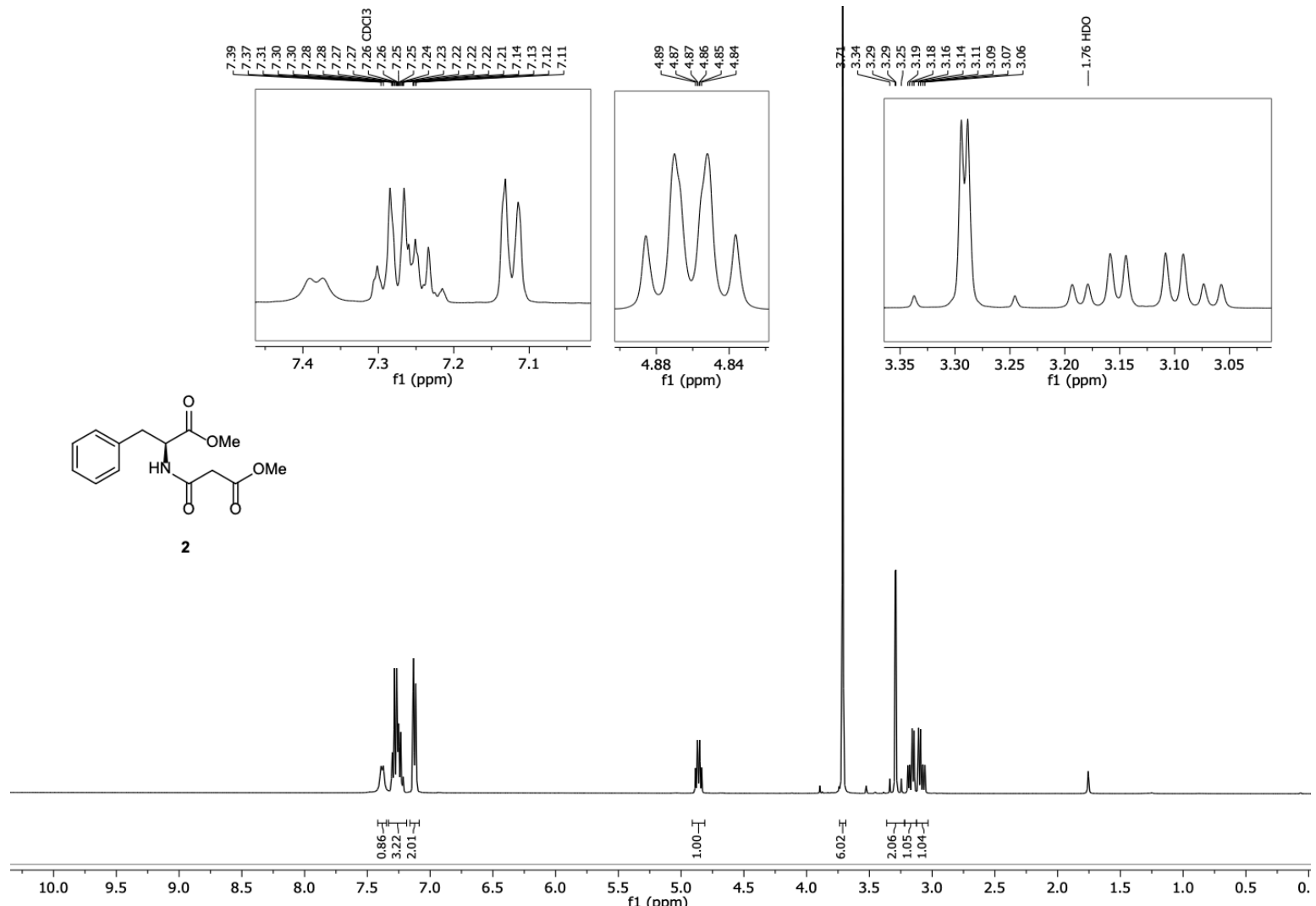


Figure A.01. ^1H NMR (400 MHz, CDCl_3) methyl ester **2.49**

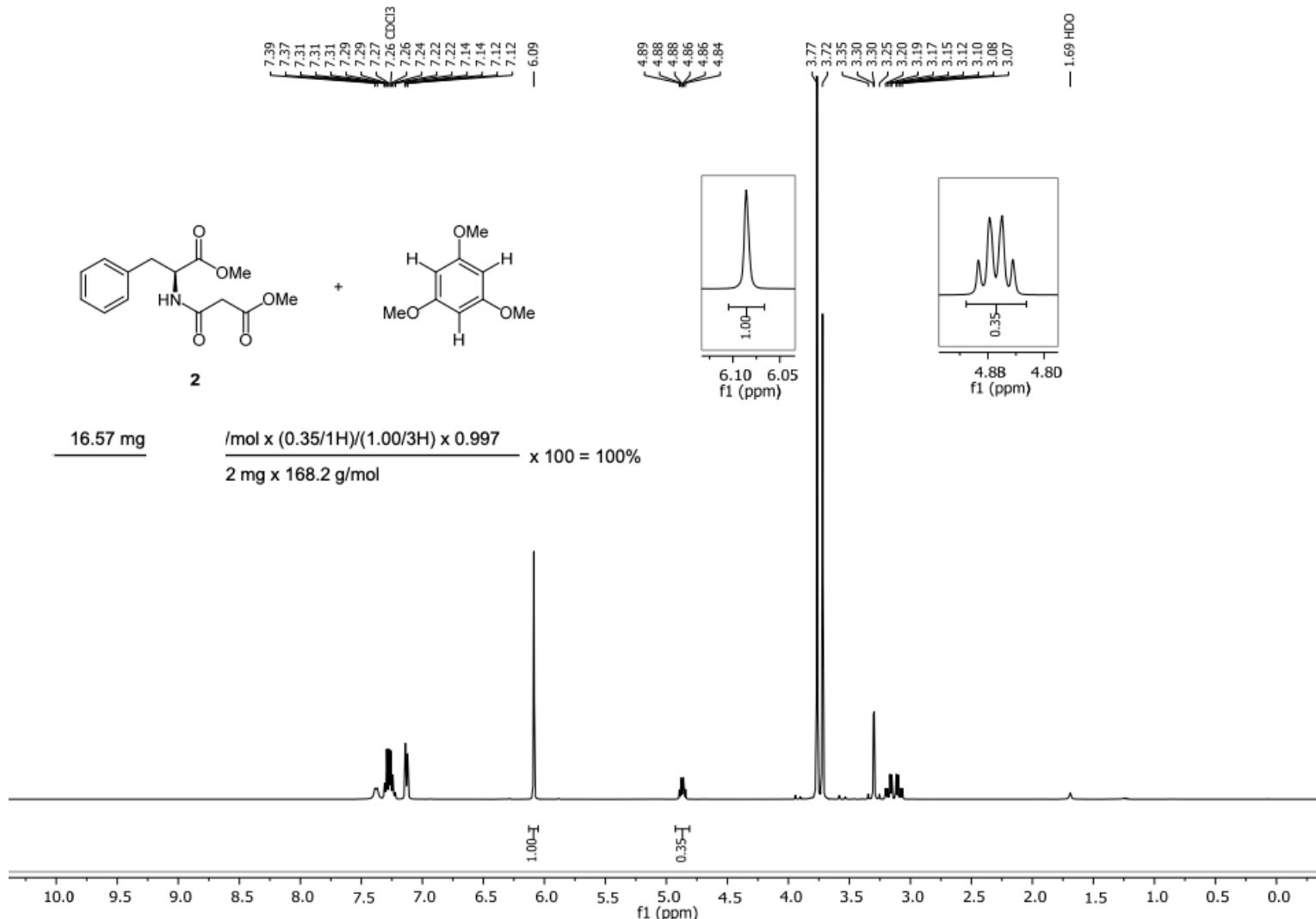


Figure A.02. Quantitative NMR (400 MHz, CDCl_3) methyl ester **2.49**

(Relaxation delay: 30 sec) shows >99% purity (28.72 mg of analyte with 16.57 mg of 99.7% purity 1,3,5-trimethoxybenzene standard

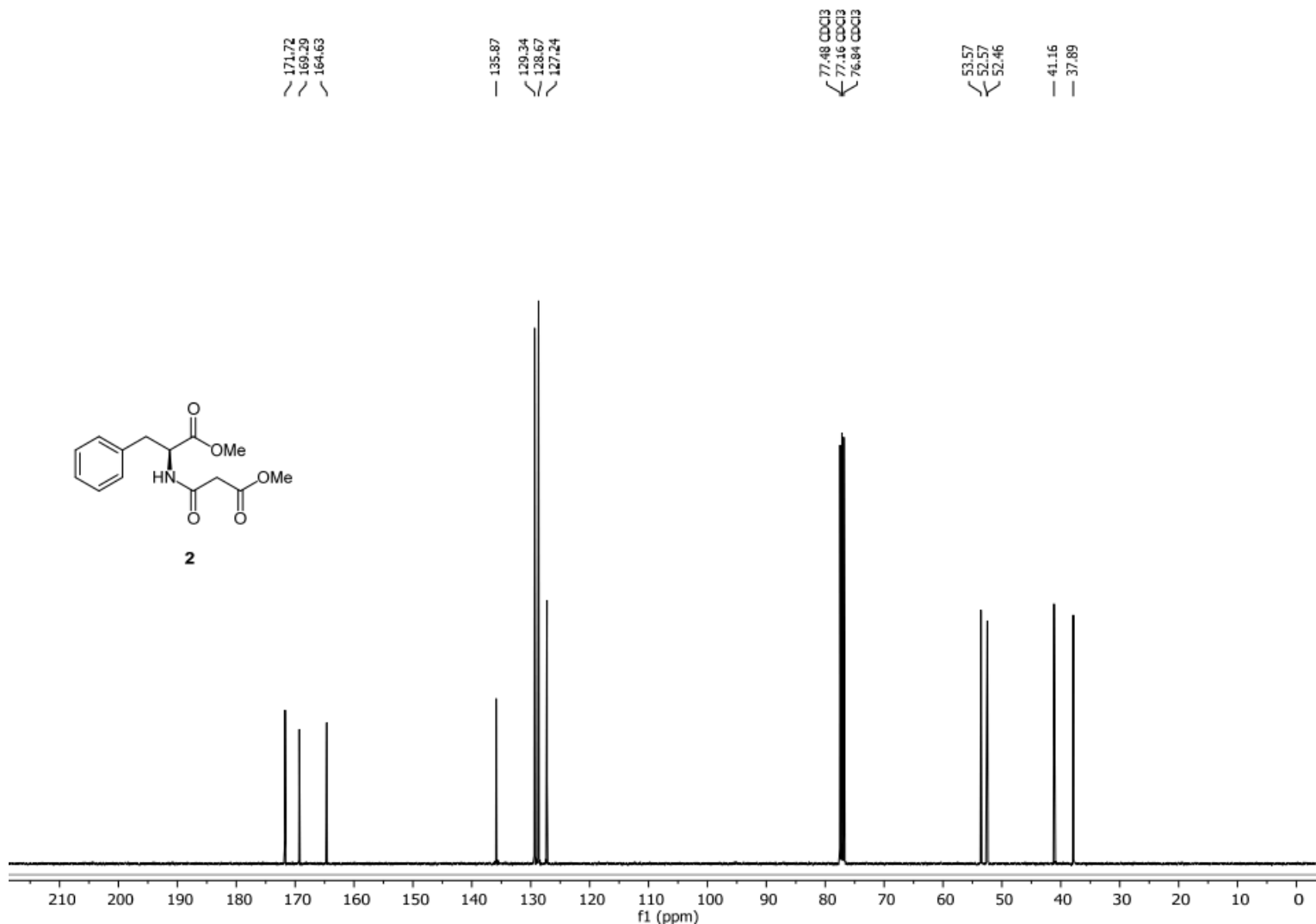


Figure A.03. ^{13}H NMR (101 MHz, CDCl_3) methyl ester 2.49

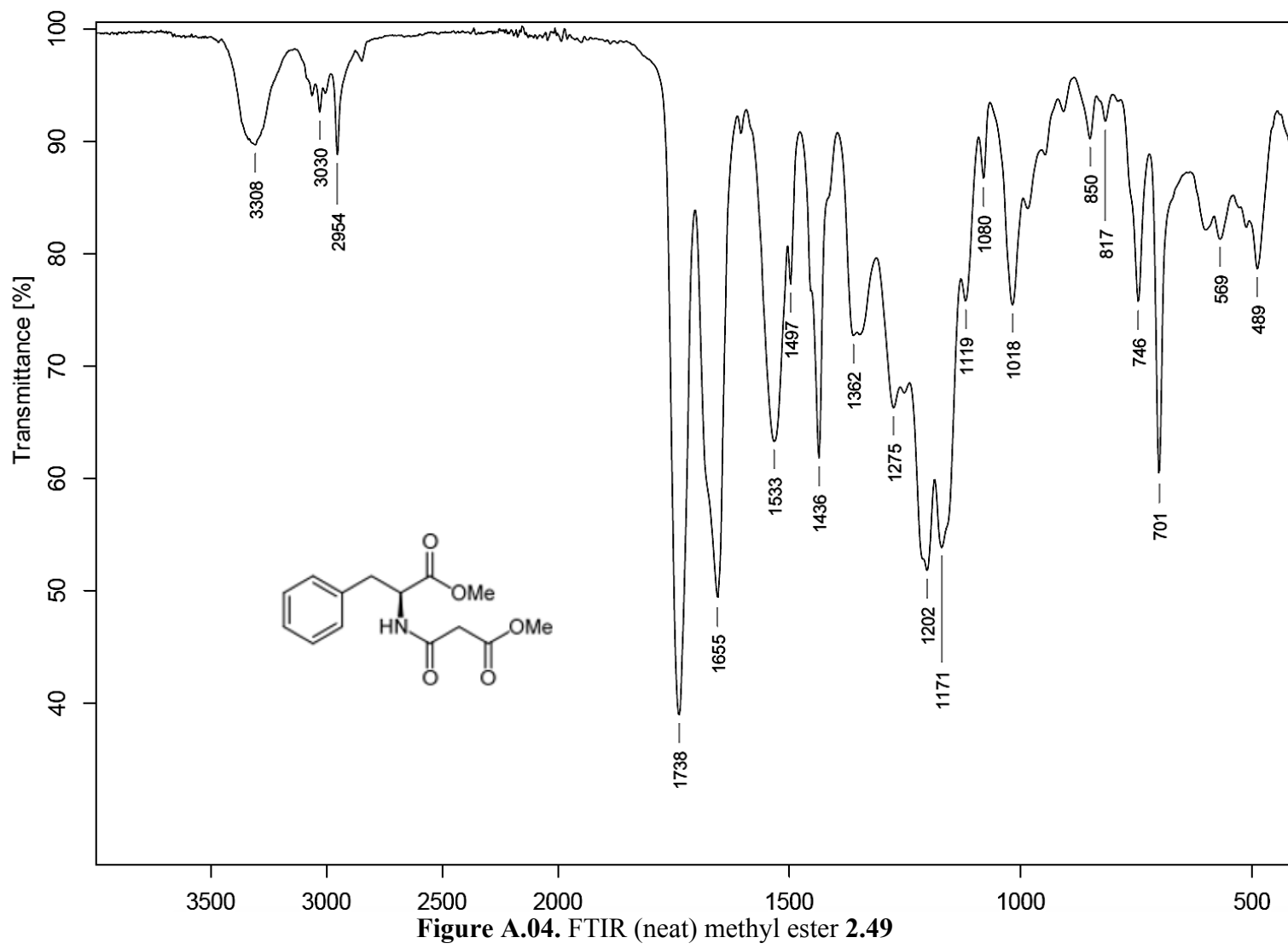


Figure A.04. FTIR (neat) methyl ester **2.49**

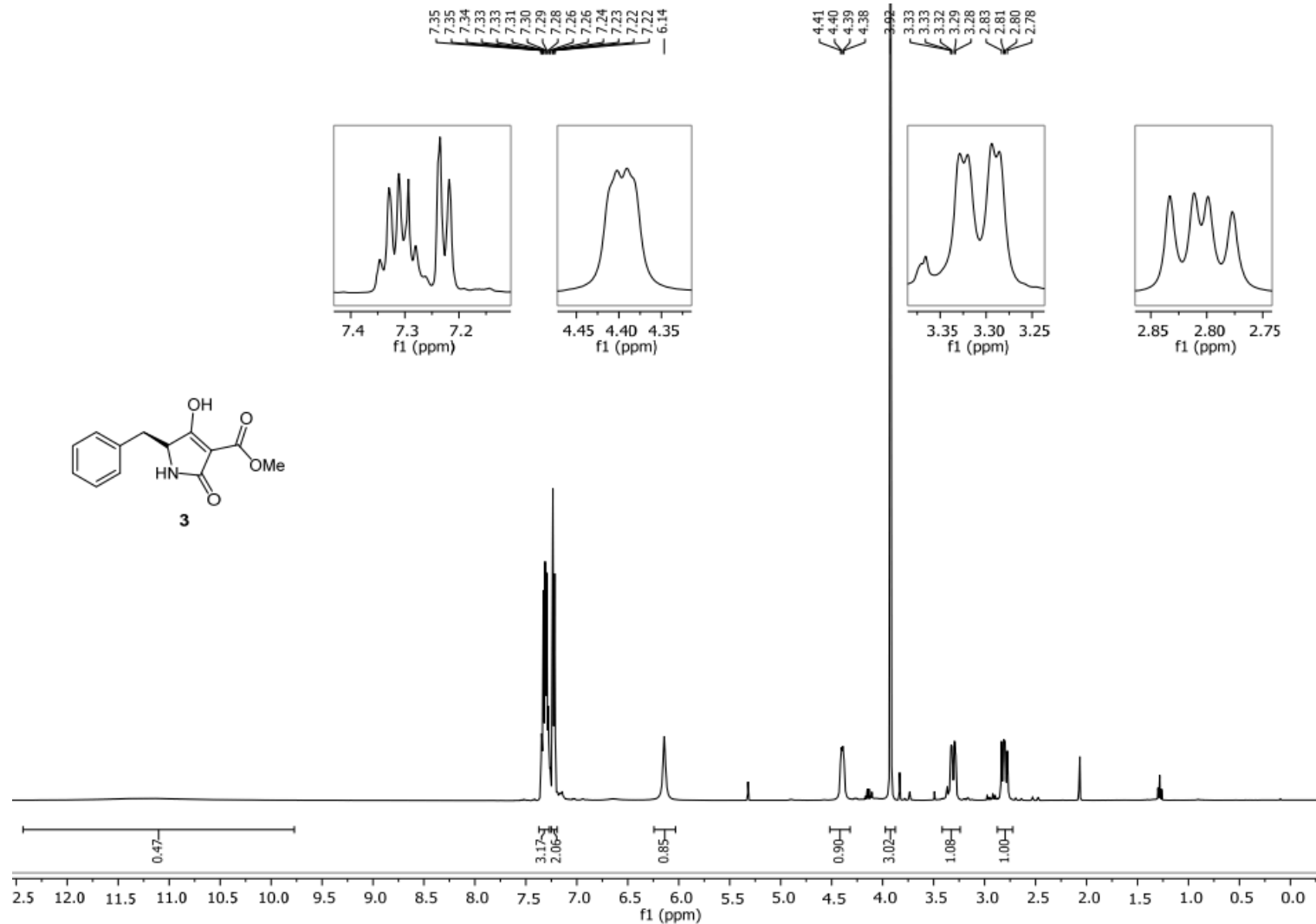


Figure A.05. ¹H NMR (400 MHz, CDCl₃) dioxopyrrolidine **2.50**

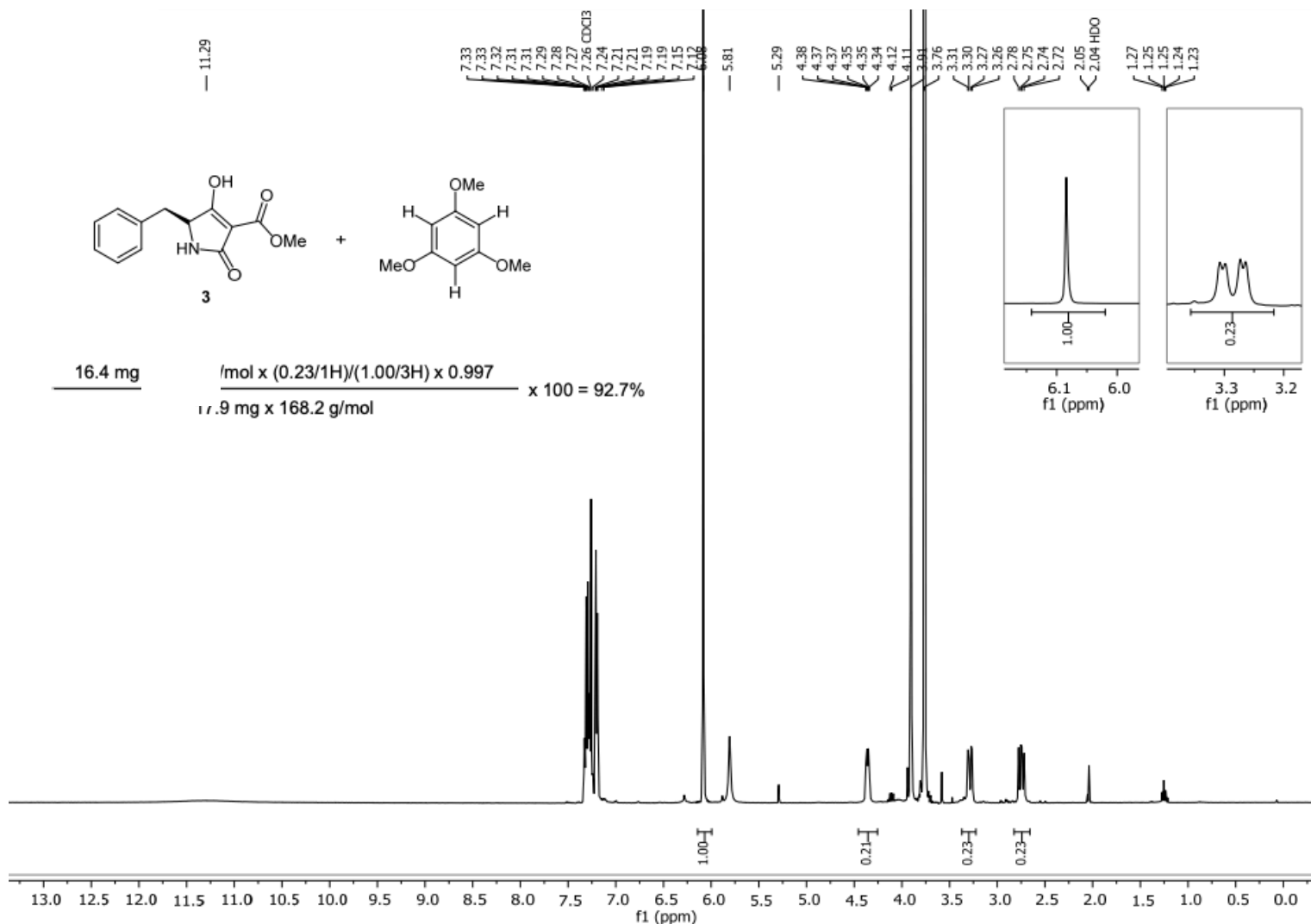


Figure A.06. Quantitative NMR (400 MHz, CDCl₃) dioxopyrrolidine **2.50** (Relaxation delay: 30 sec) shows 93% purity (28.4 mg of analyte with 15.0 mg of 99.7% purity 1,3,5-trimethoxybenzene standard

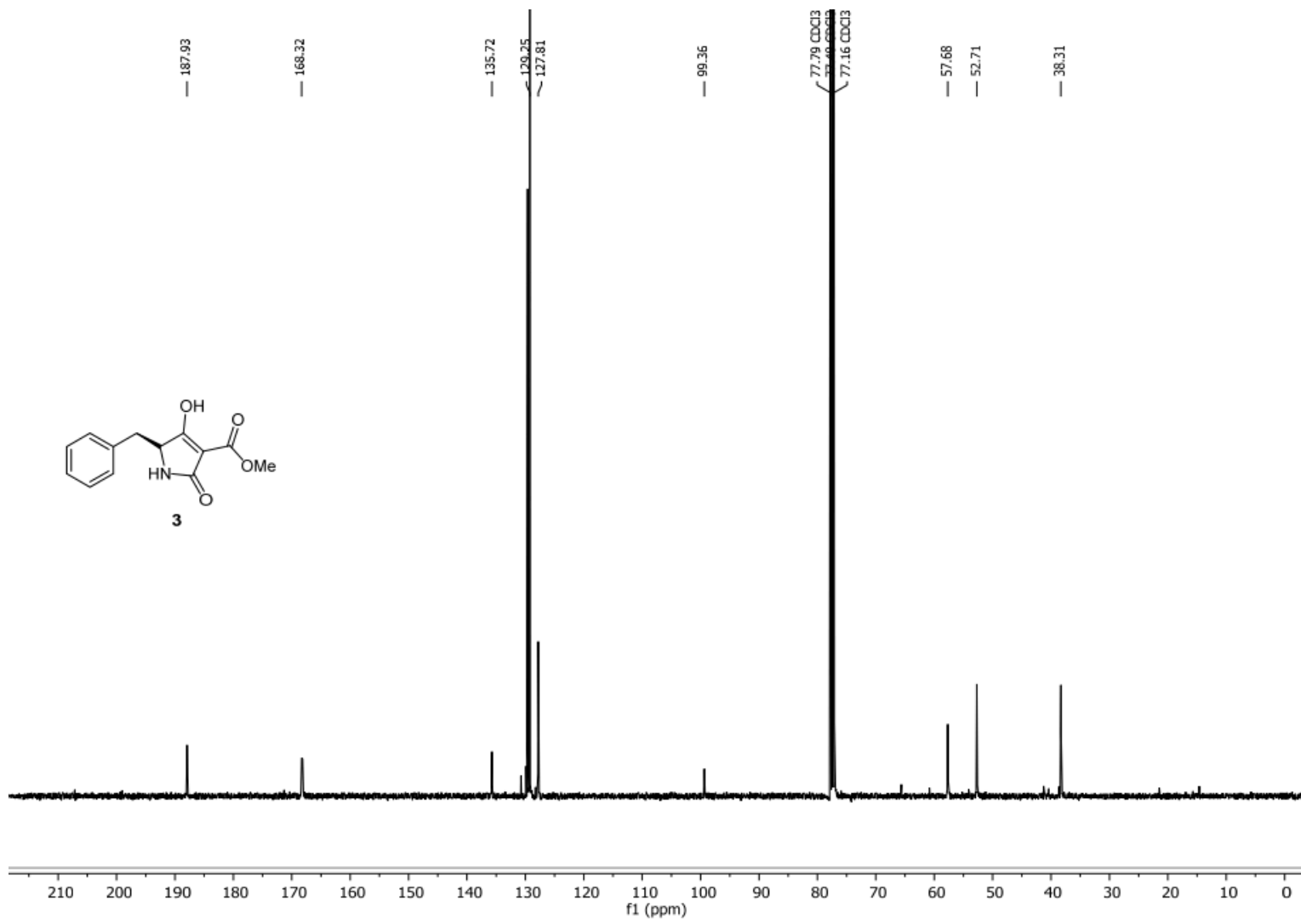


Figure A.07. ^{13}H NMR (101 MHz, CDCl_3) dioxopyrrolidine **2.50**

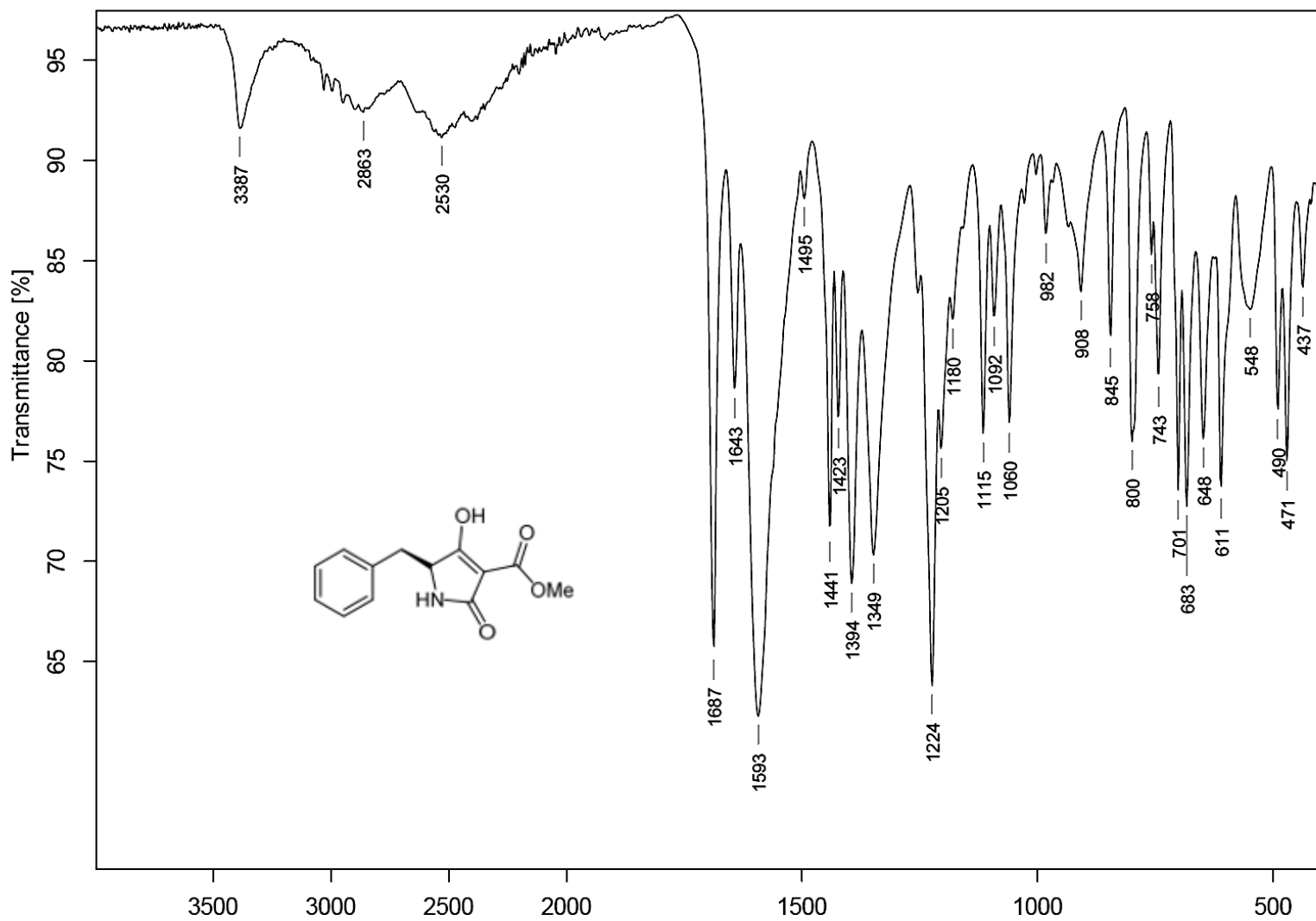


Figure A.08. FTIR (neat) dioxopyrrolidine 2.50

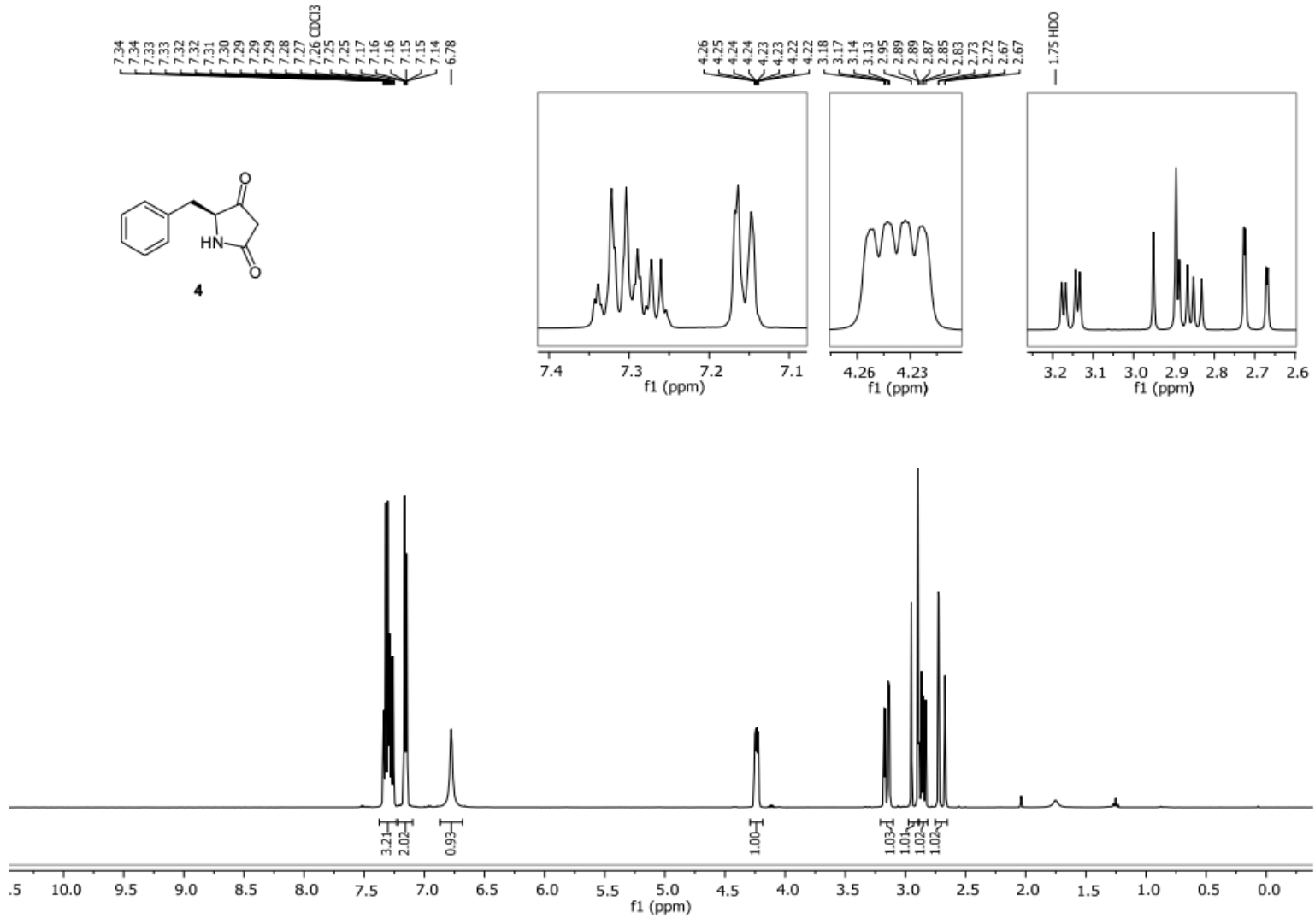


Figure A.09. ^1H NMR (400 MHz, CDCl_3) tetramic acid **2.51**

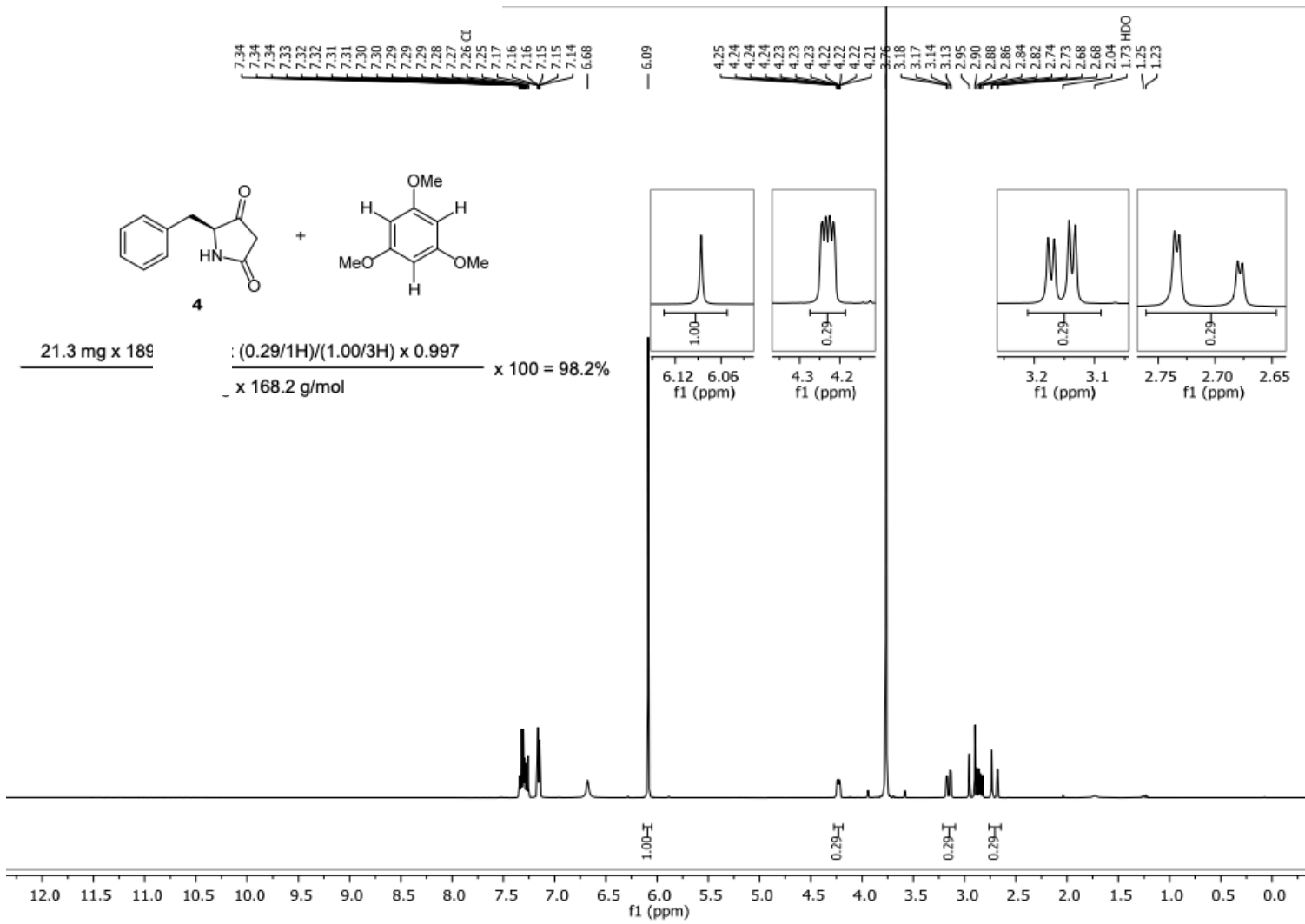


Figure A.10. Quantitative NMR (400 MHz, CDCl₃) tetrameric acid **2.51**(Relaxation delay: 30 sec) shows 98% purity (21.17 mg of analyte with 21.30 mg of 99.7% purity 1,3,5-trimethoxybenzene standard

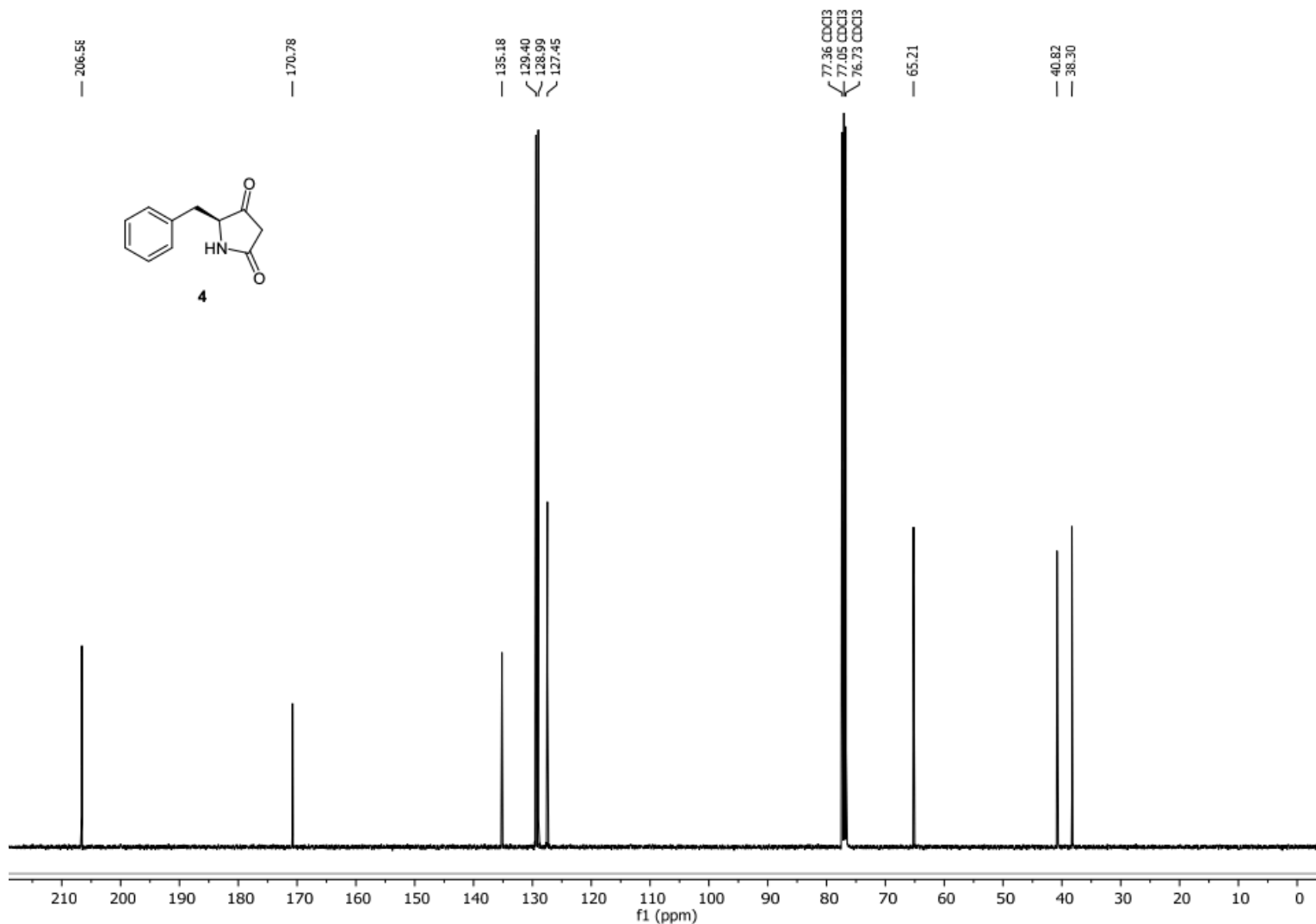


Figure A.11. ^{13}C NMR (101 MHz, CDCl_3) tetramic acid **2.51**

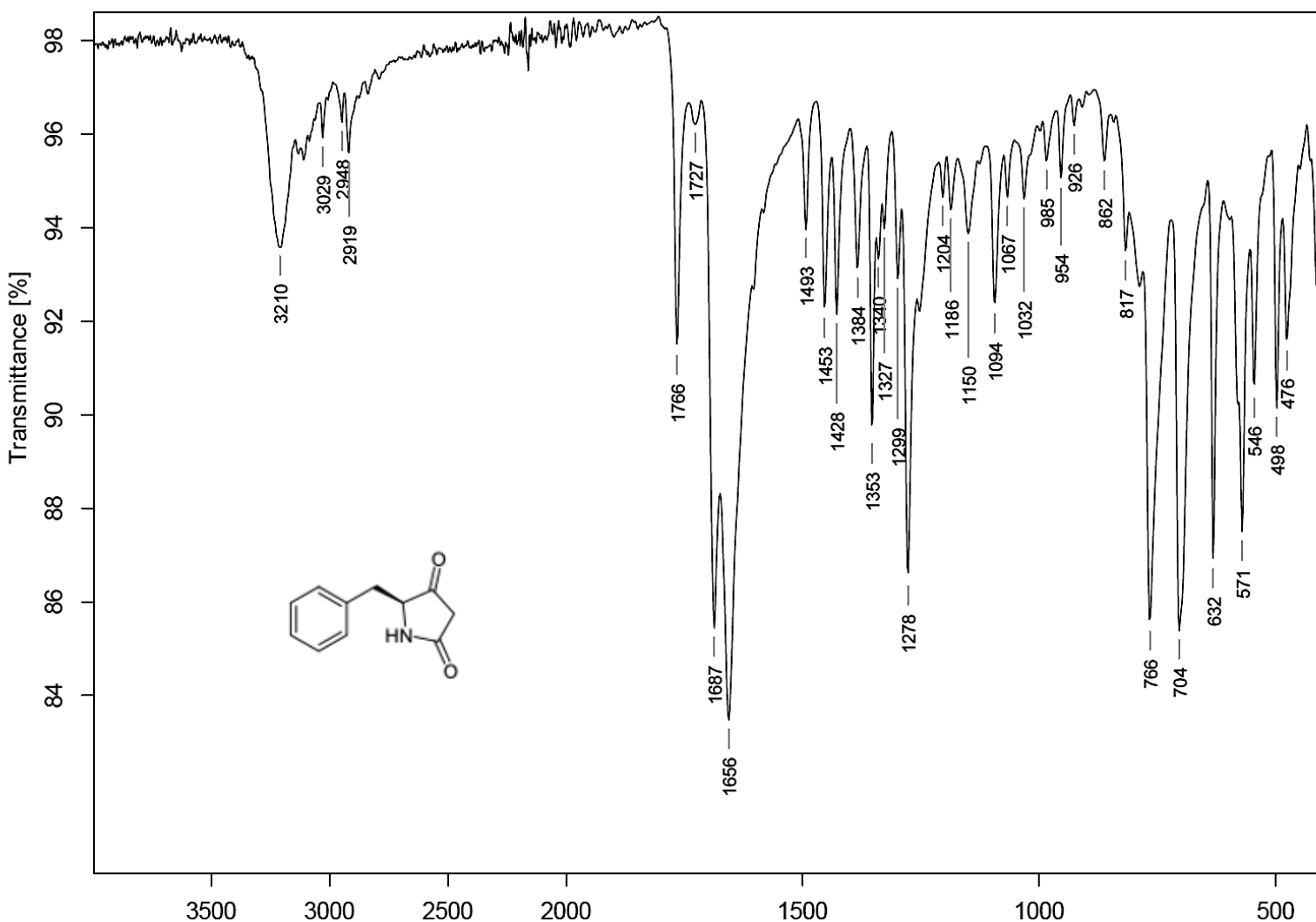


Figure A.12. FTIR (neat) tetramic acid 2.51

J-01-081 1H.10.fid



Figure A.13. ¹H NMR (600 MHz, CDCl₃) known methyl ester **2.52**

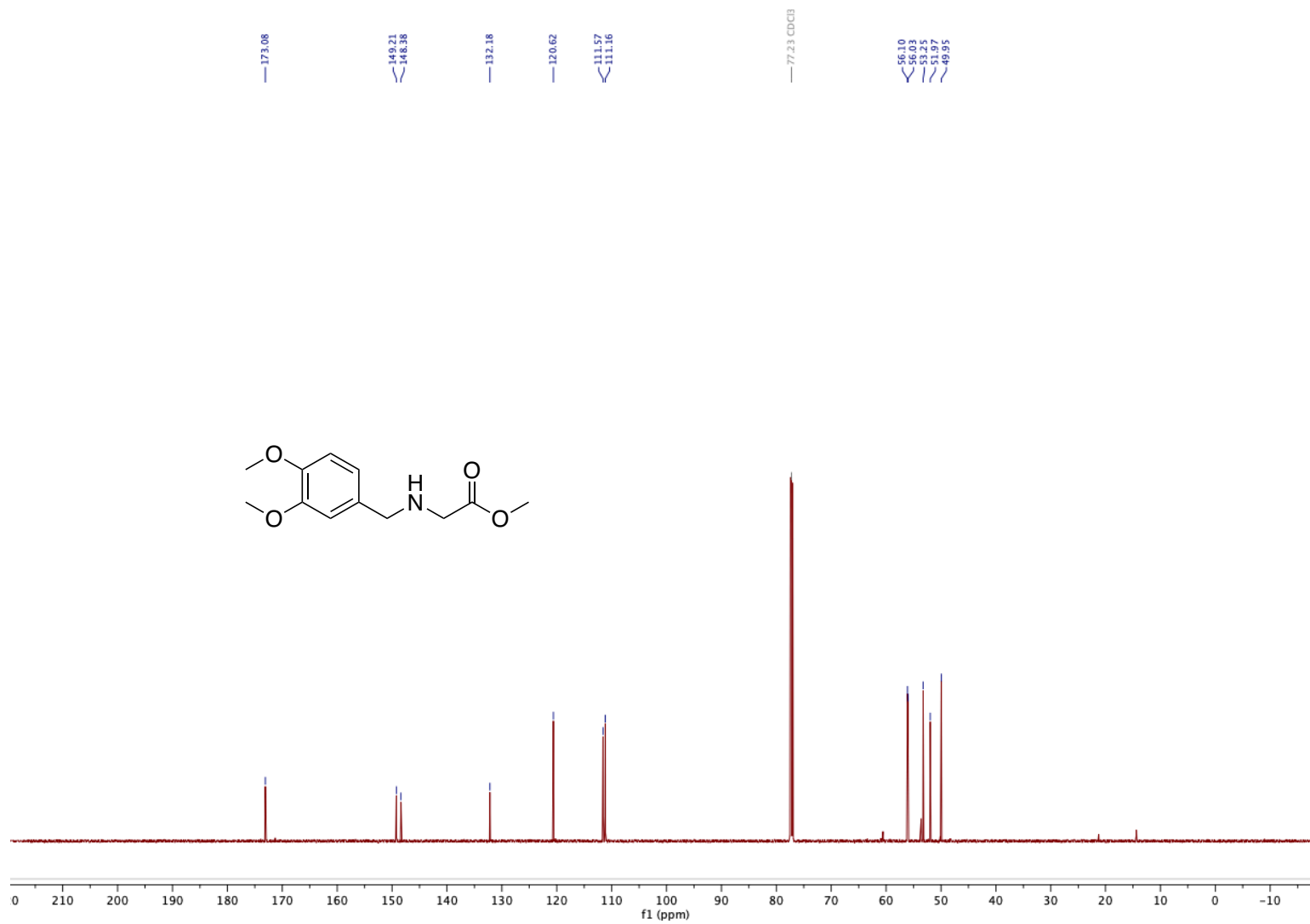


Figure A.14. ^{13}C NMR (151 MHz, CDCl_3) known methyl ester **2.52**

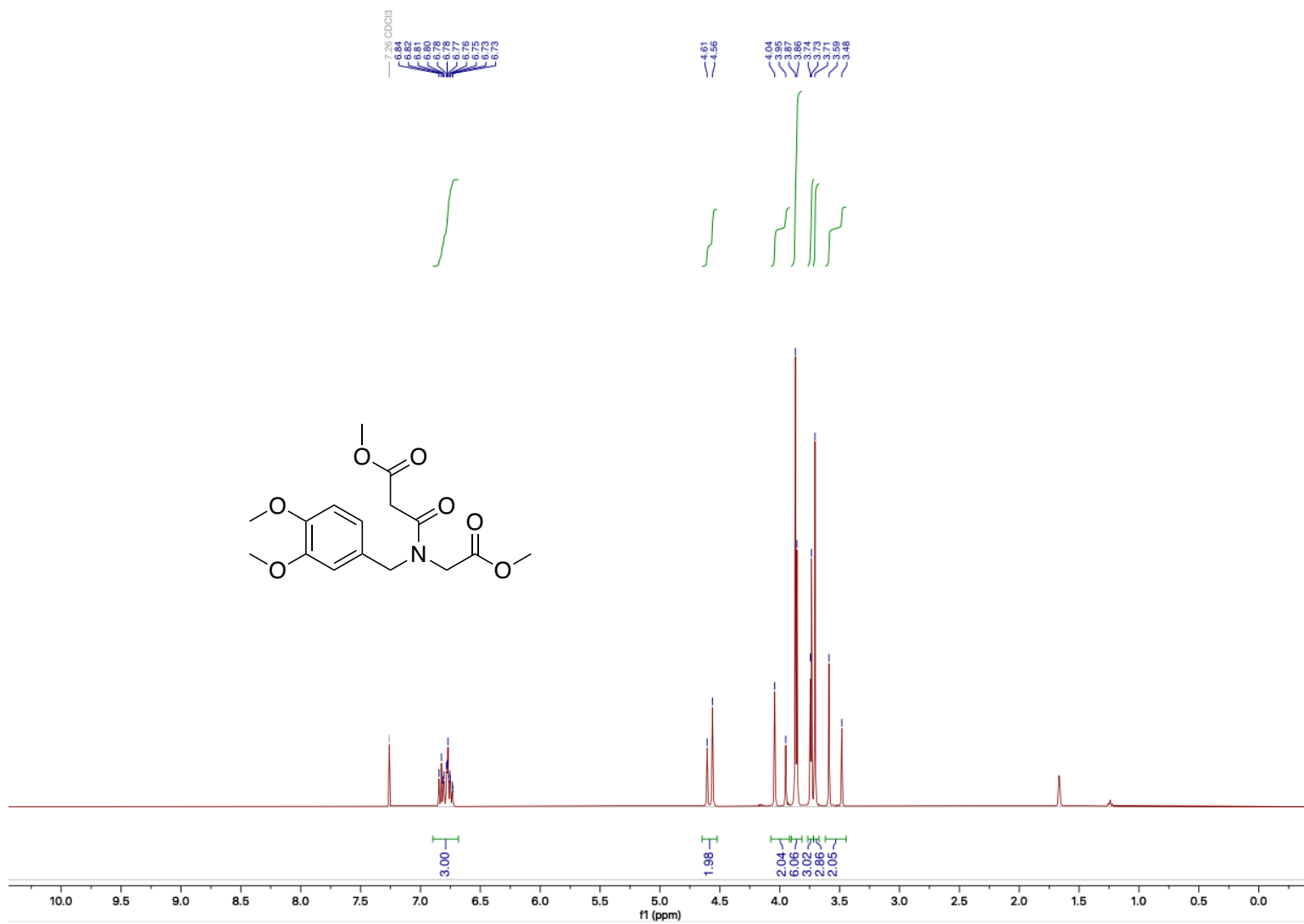


Figure A.15. ¹H NMR (400 MHz, CDCl₃) crude amide **2.53**

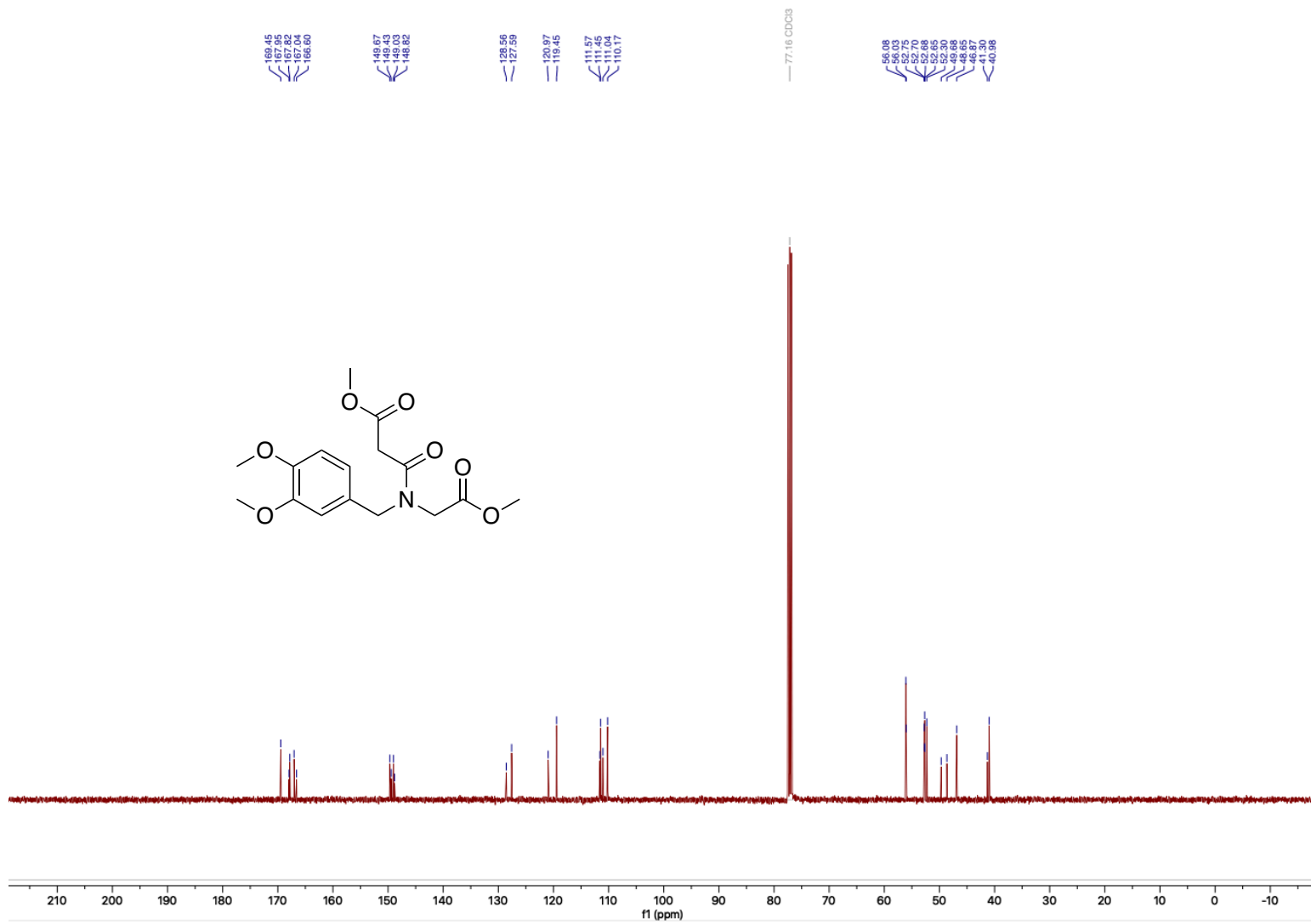


Figure A.16. ^{13}C NMR (101 MHz, CDCl_3) crude amide **2.53**

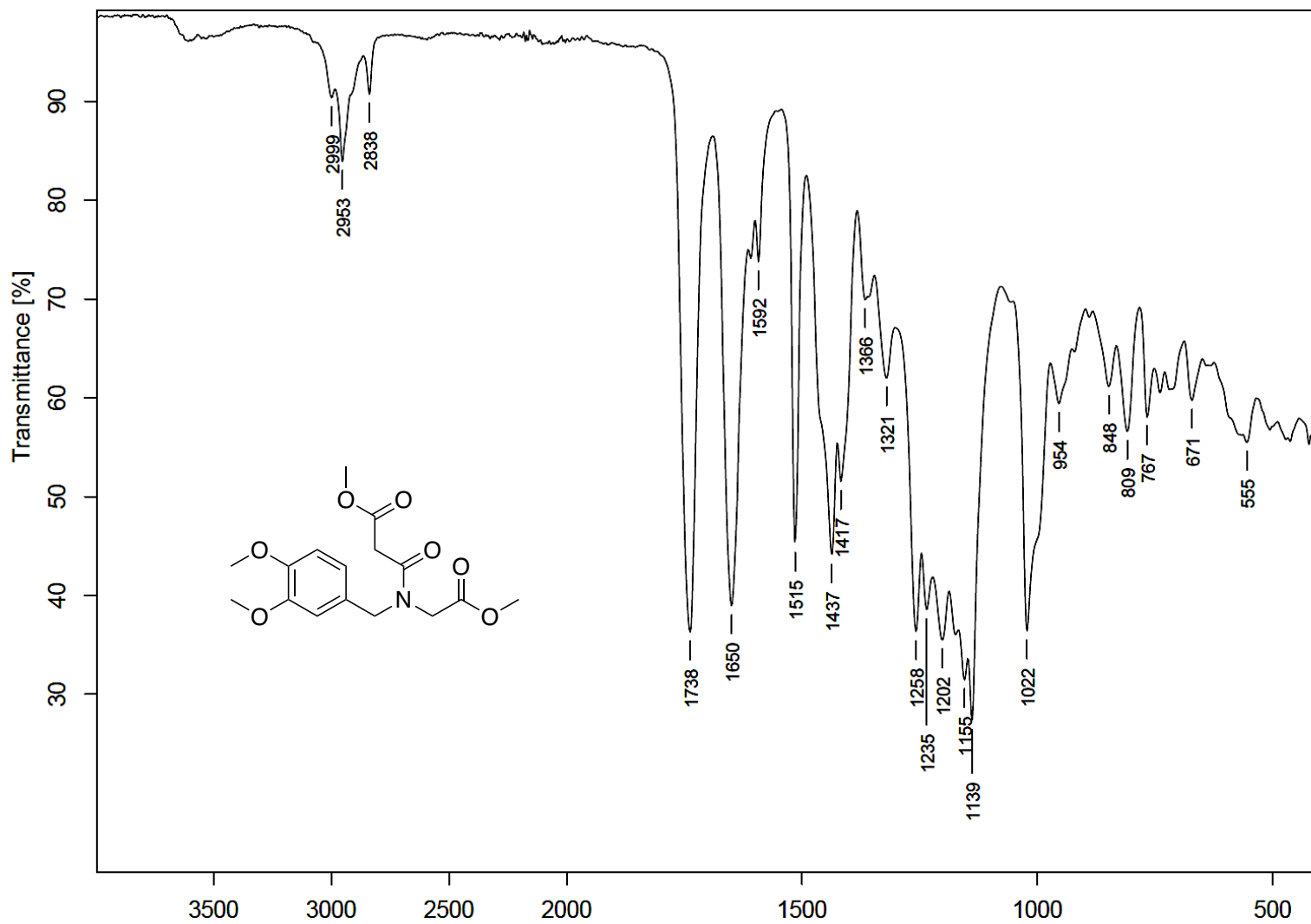


Figure A.17. FTIR Spectrum (neat) crude amide 2.53

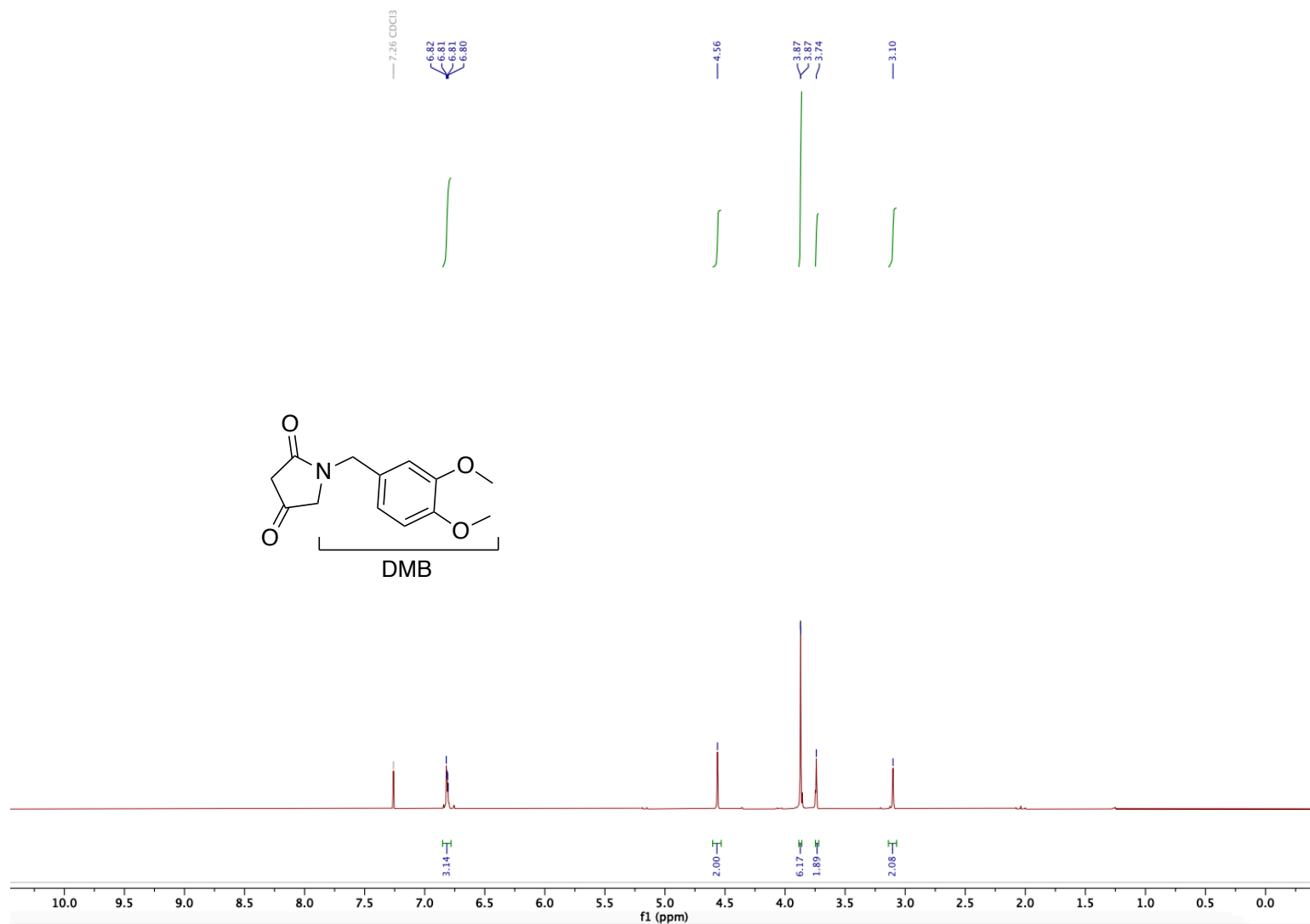


Figure A.18. ^1H NMR (400 MHz, CDCl_3) DMB tetrameric acid **2.54**

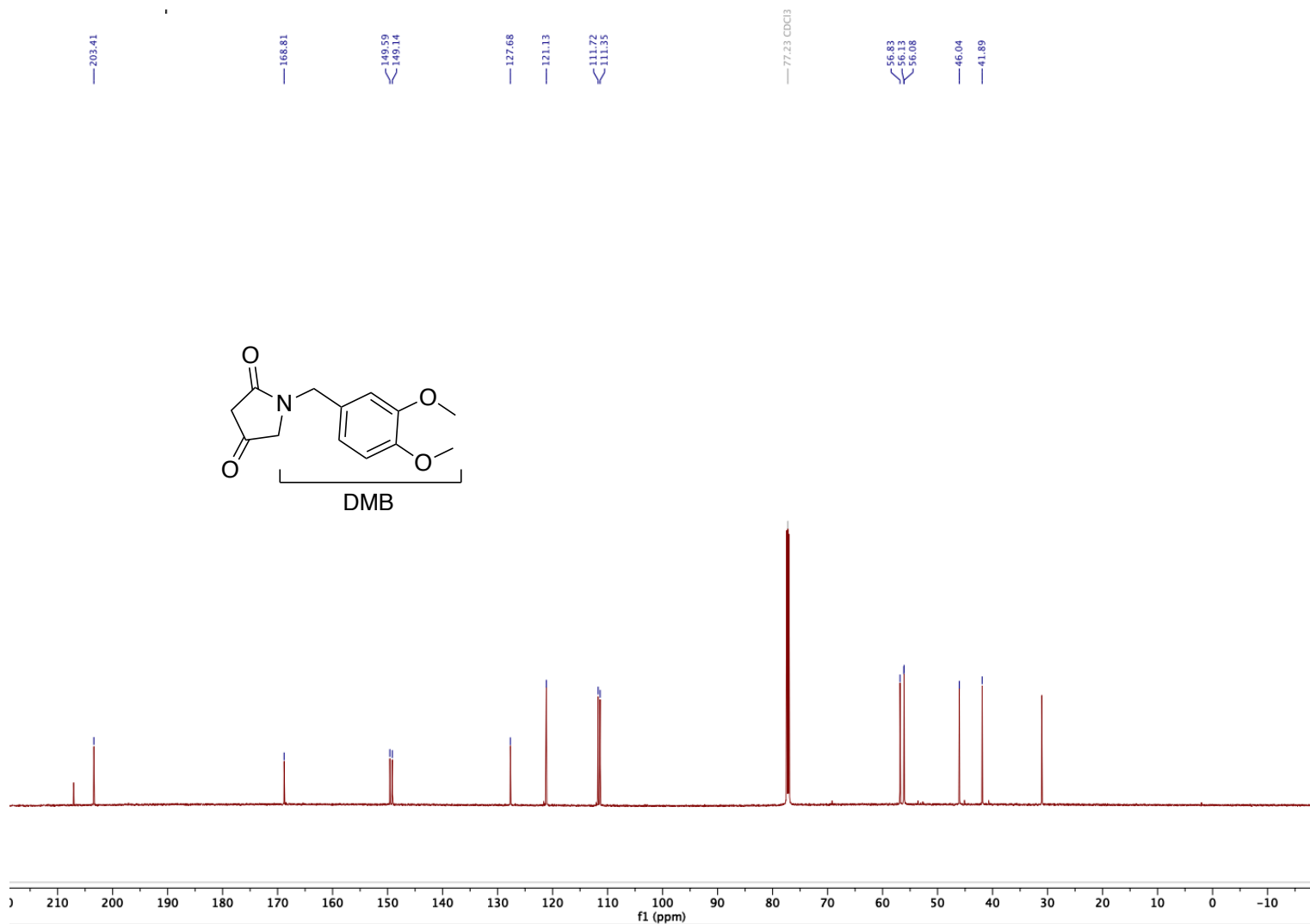


Figure A.19. ^{13}C NMR (101 MHz, CDCl₃) DMB tetrameric acid **2.54**

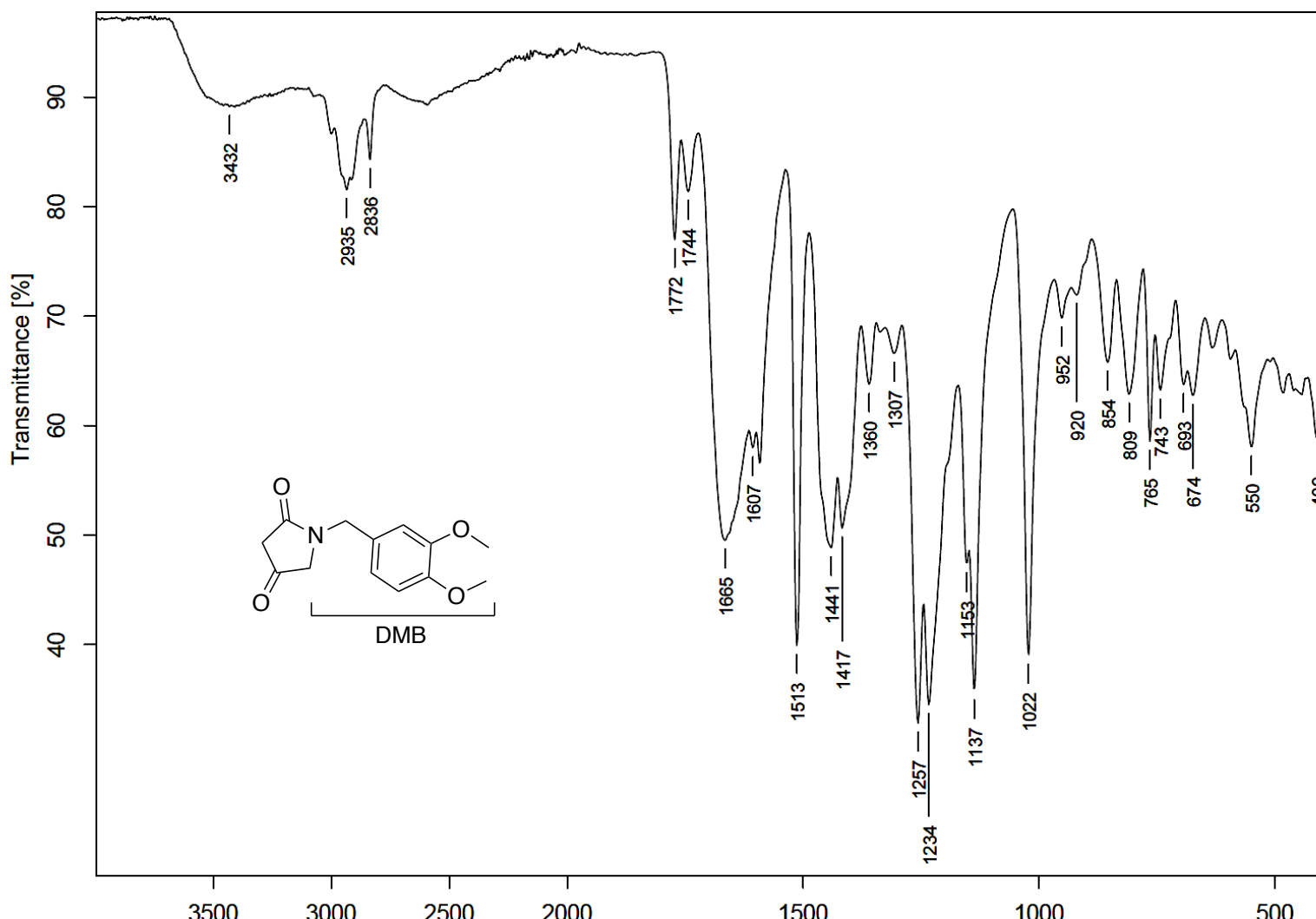


Figure A.20. FTIR Spectrum (neat) DMB tetrameric acid **2.54**

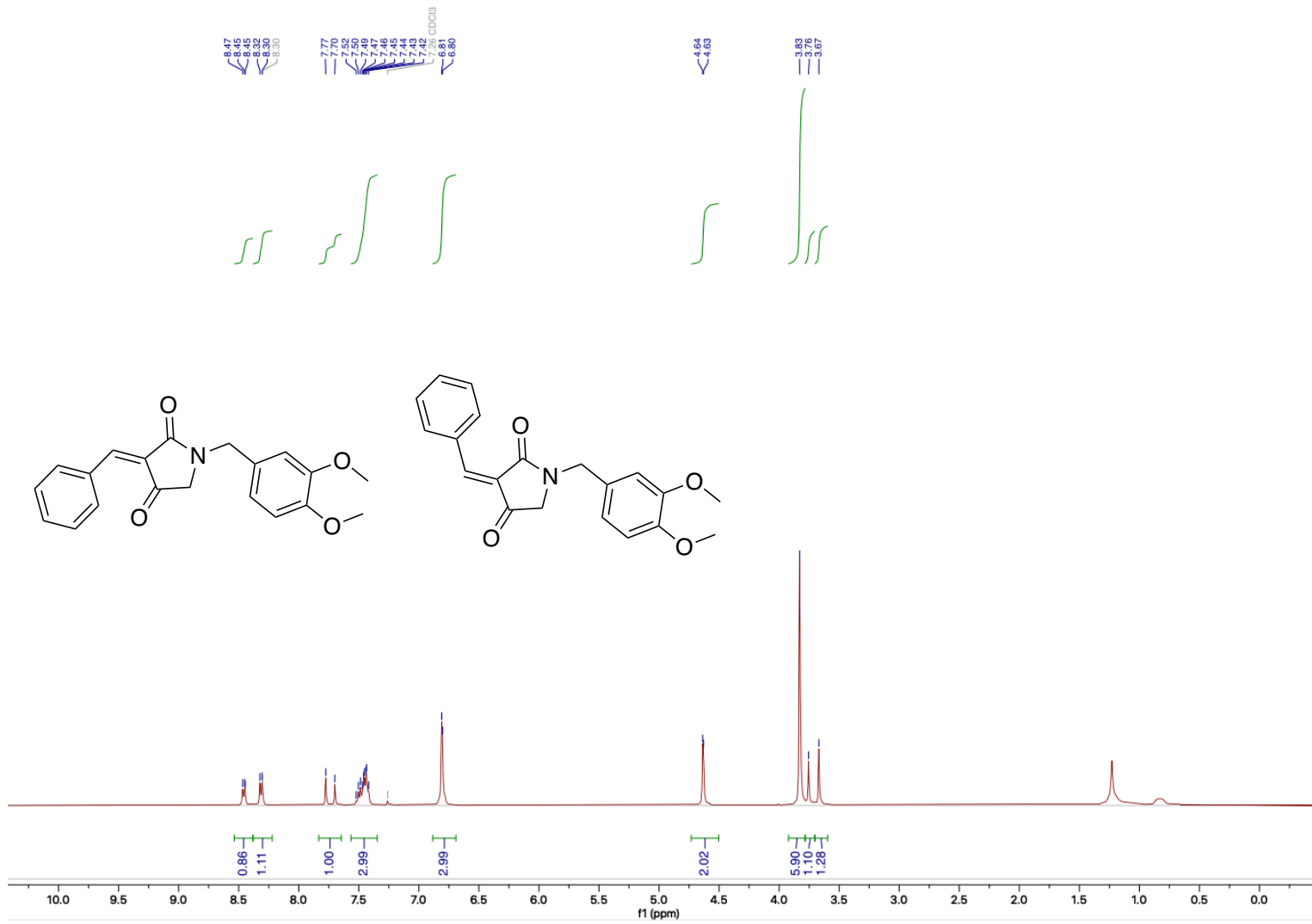


Figure A.21. ^1H NMR (400 MHz, CDCl_3) alkene **2.55**

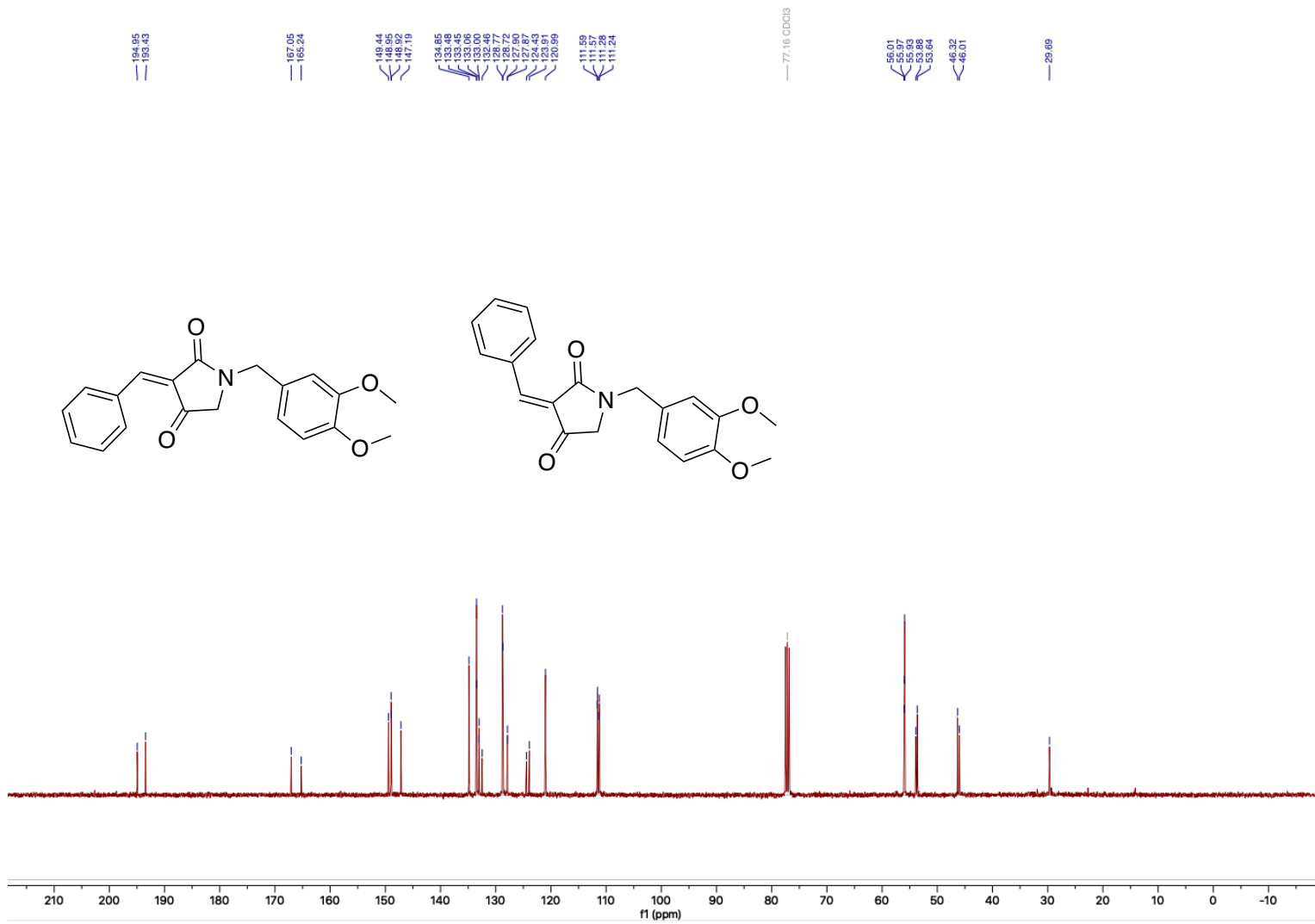


Figure A.22. ^{13}C NMR (400 MHz, CDCl_3) alkene 2.55

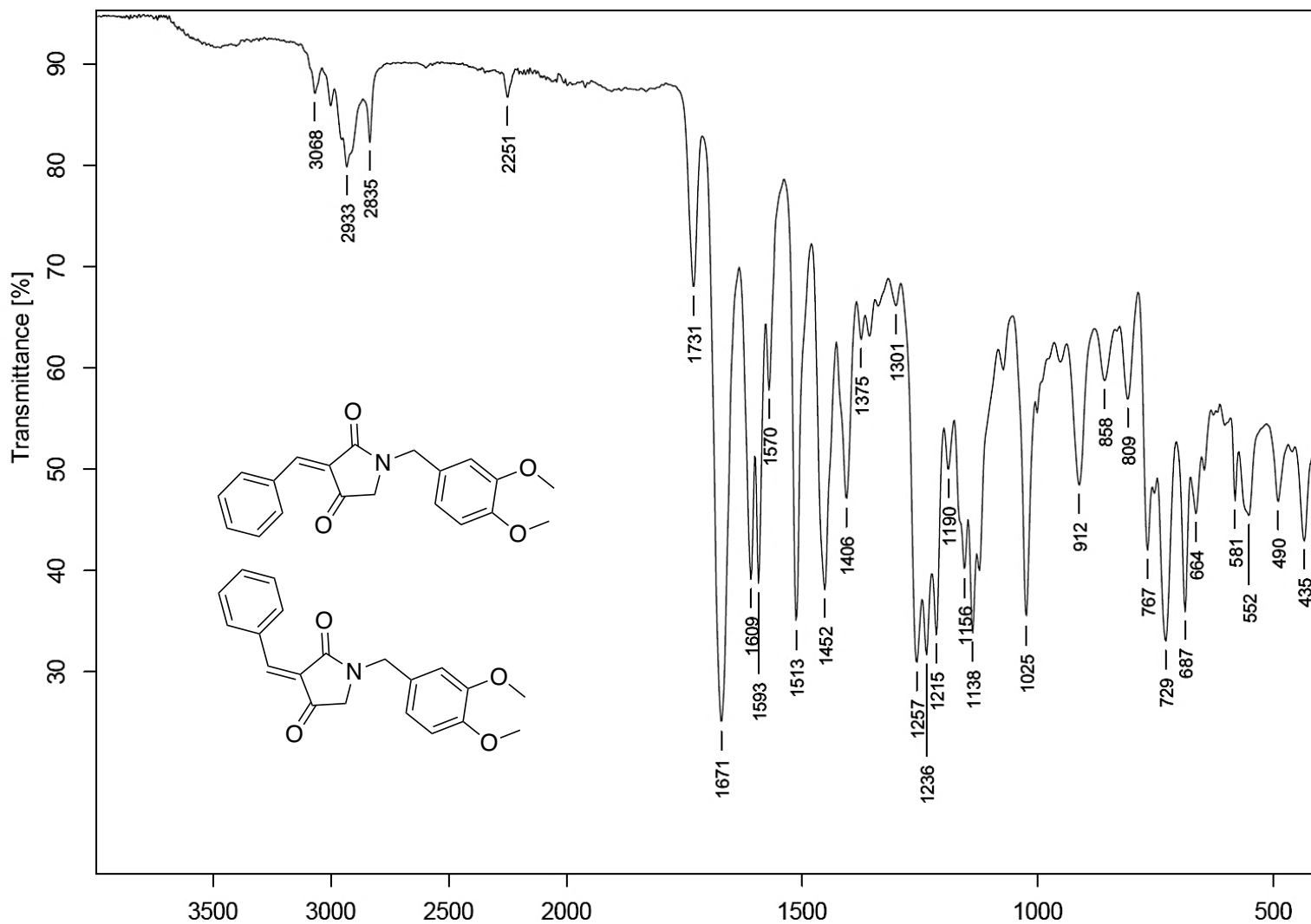


Figure A.23. FTIR (neat) alkene 2.55

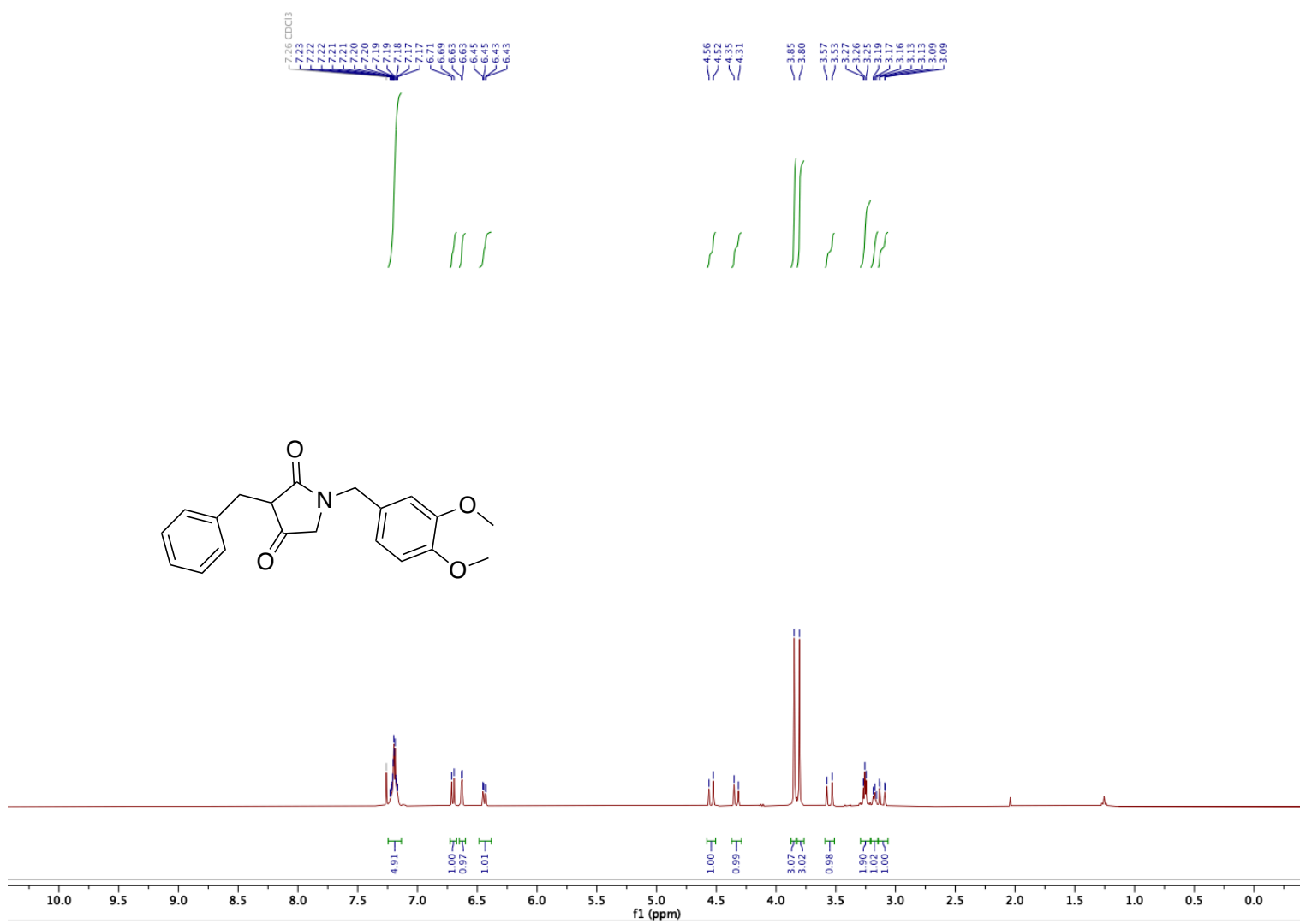


Figure A.24. ¹H NMR (400 MHz, CDCl₃) tetrameric acid **2.56**

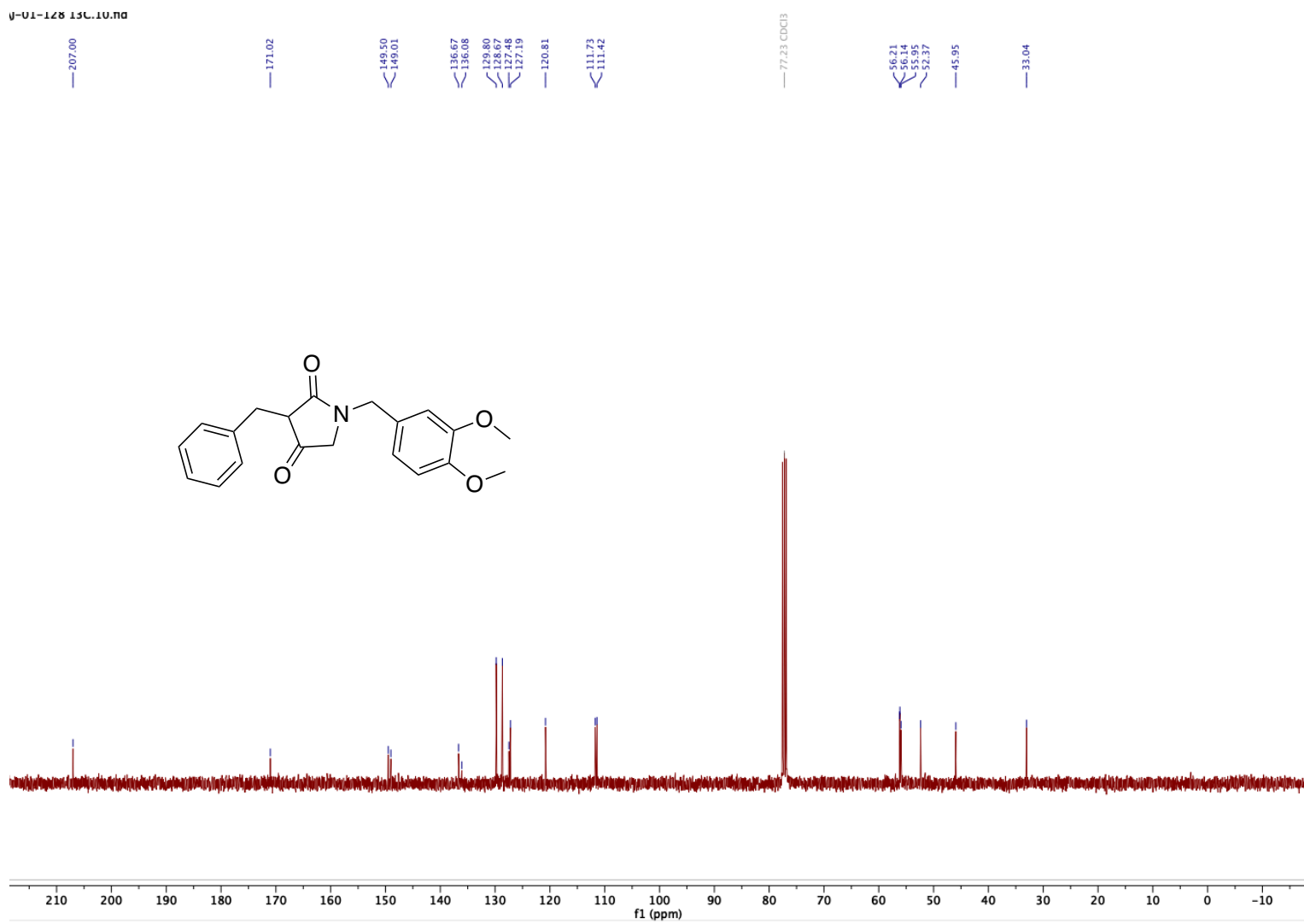


Figure A.25. ¹³C NMR (101 MHz, CDCl₃) tetramic acid **2.56**

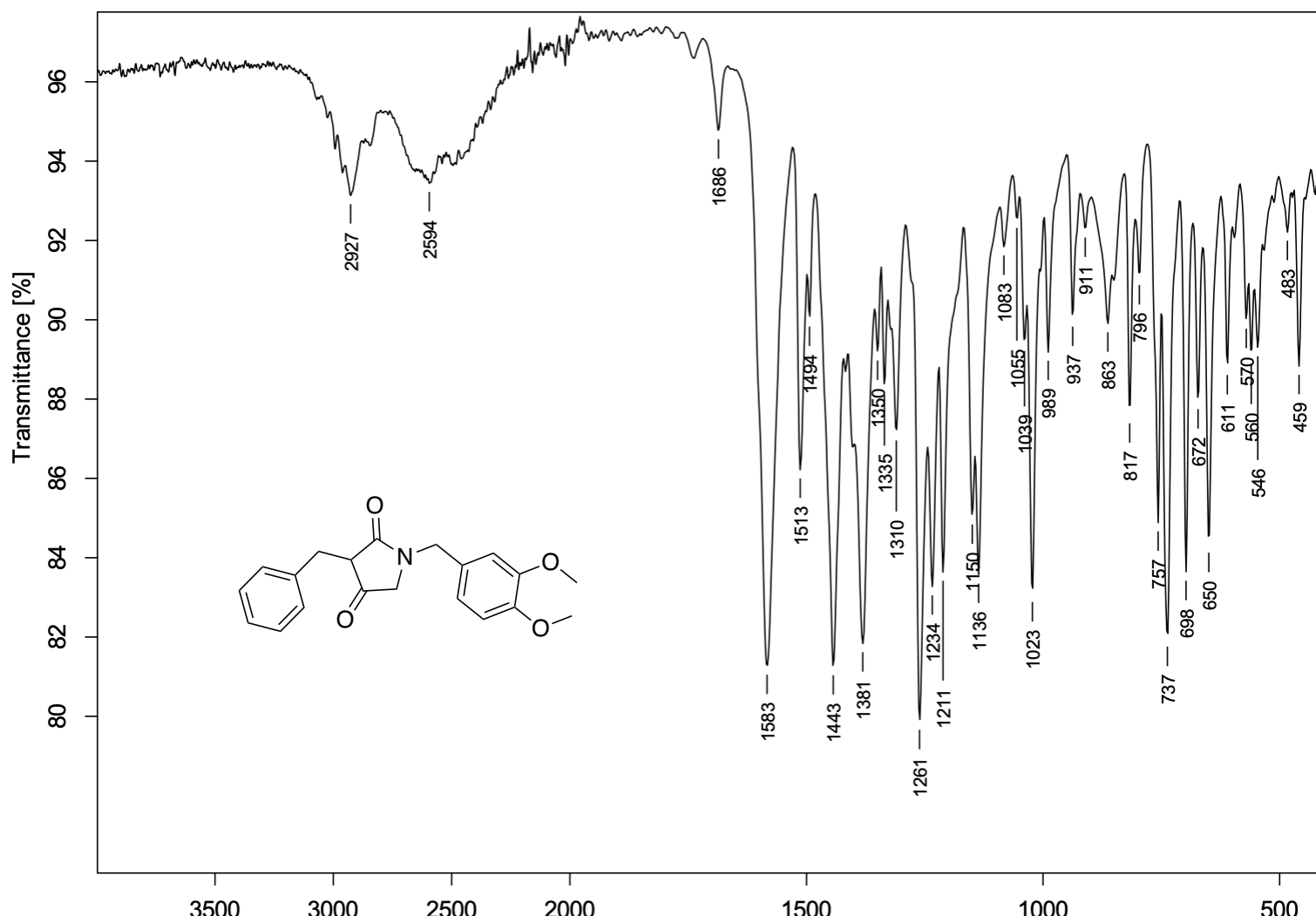


Figure A.26. FTIR (neat) tetramic acid **2.56**

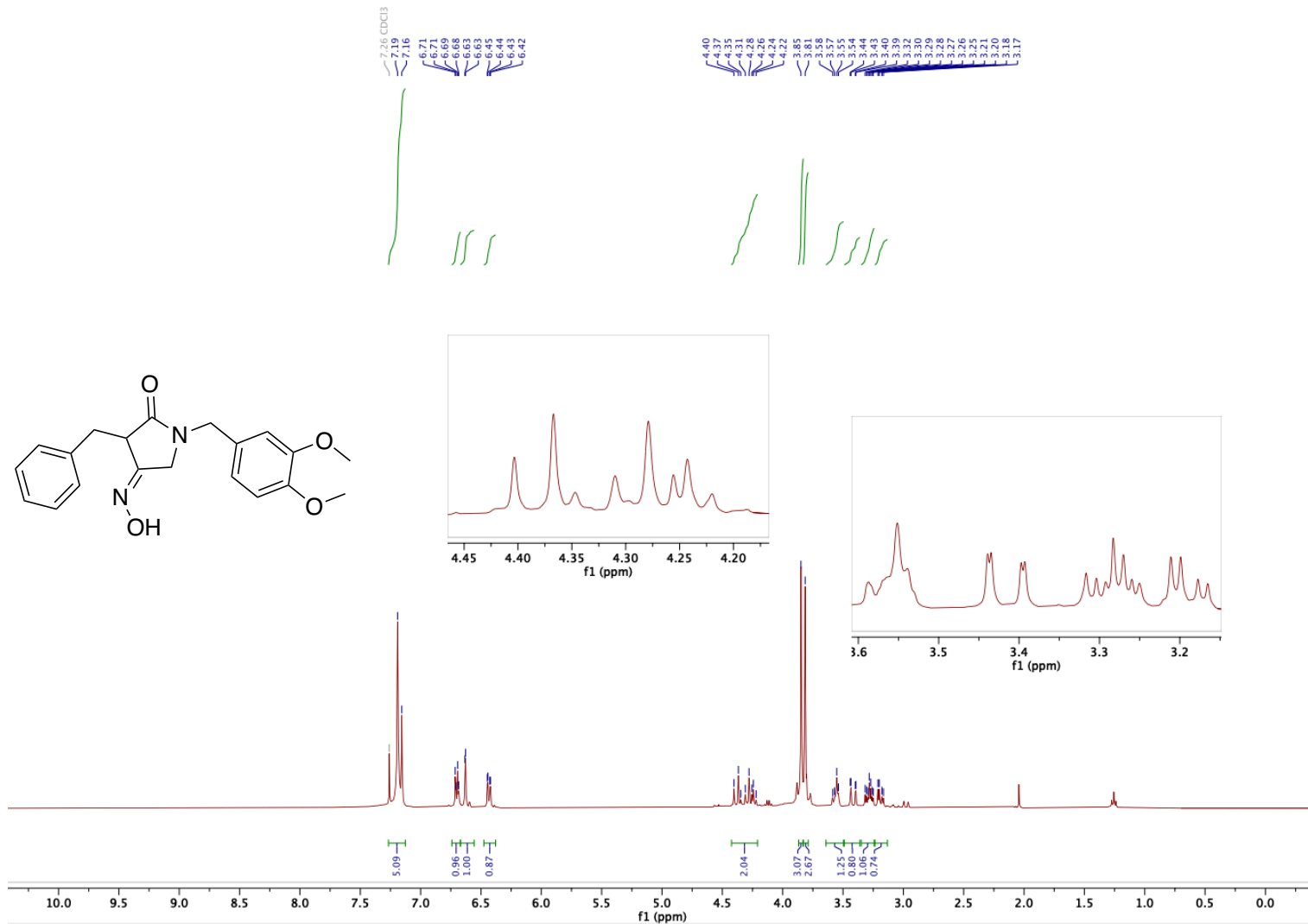


Figure A.27. ¹H NMR (600 MHz, CDCl₃) oxime 2.57

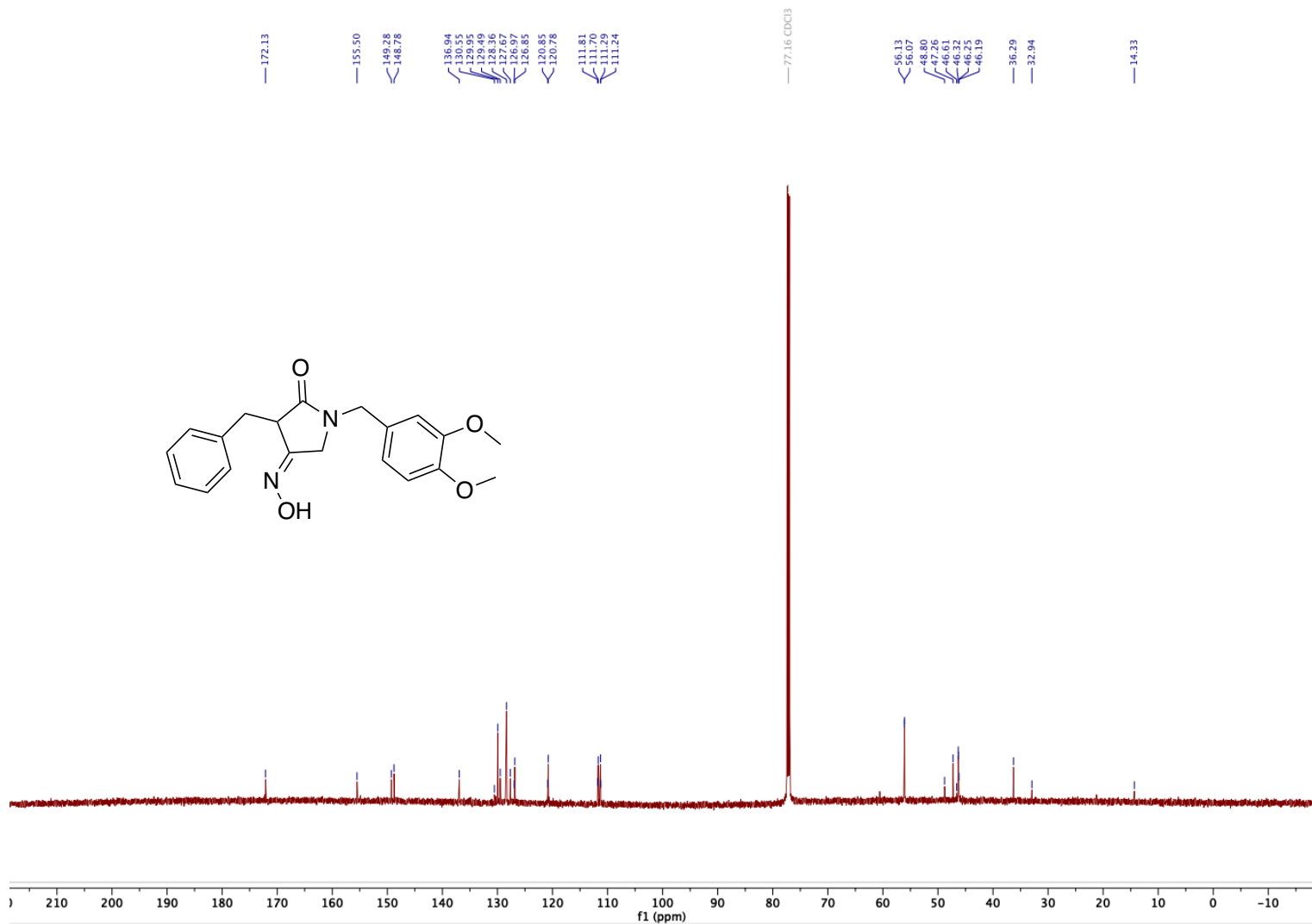


Figure A.28. ^{13}C NMR (151 MHz, CDCl_3) oxime 2.57

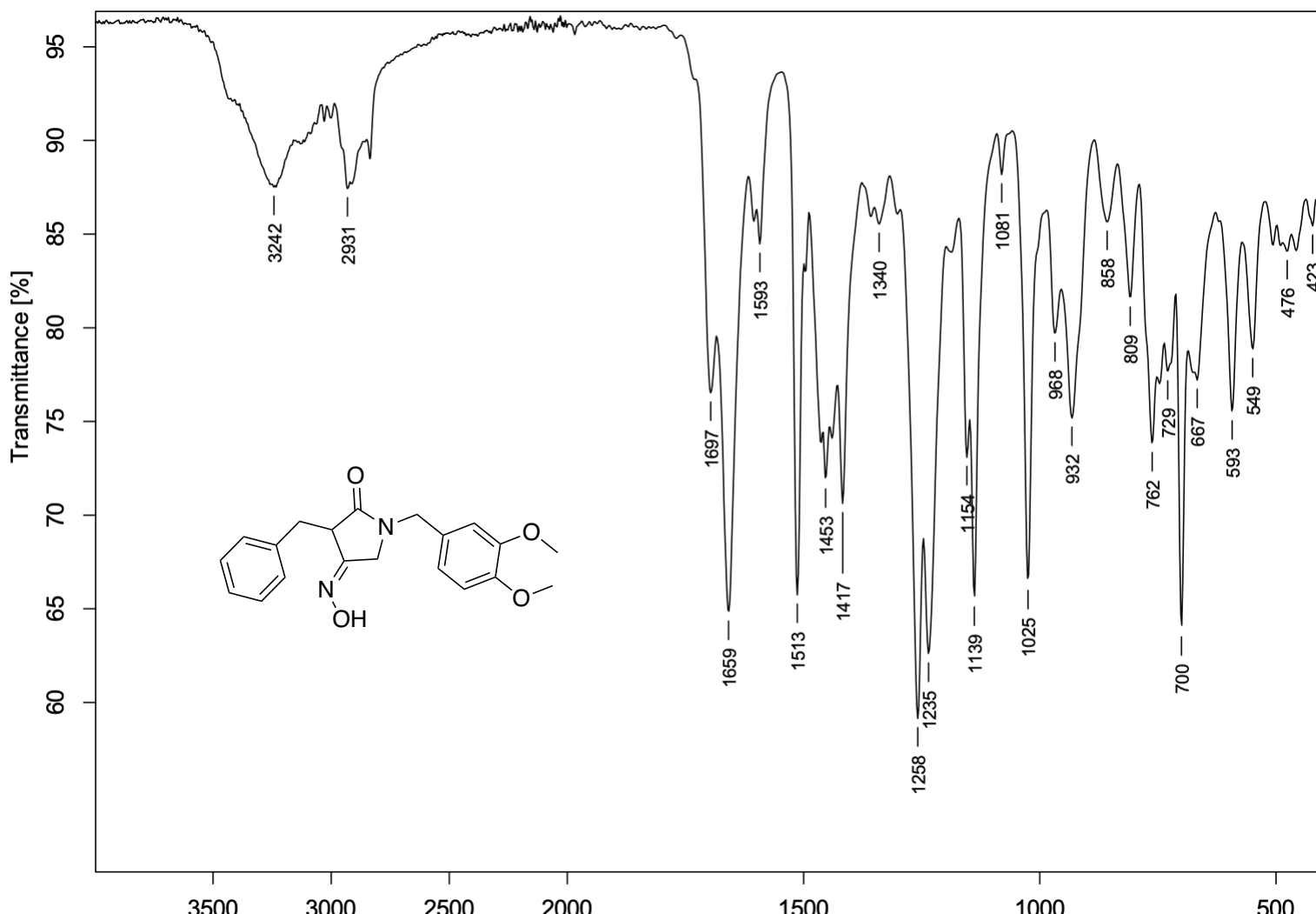


Figure A.29. FTIR (neat) oxime 2.57

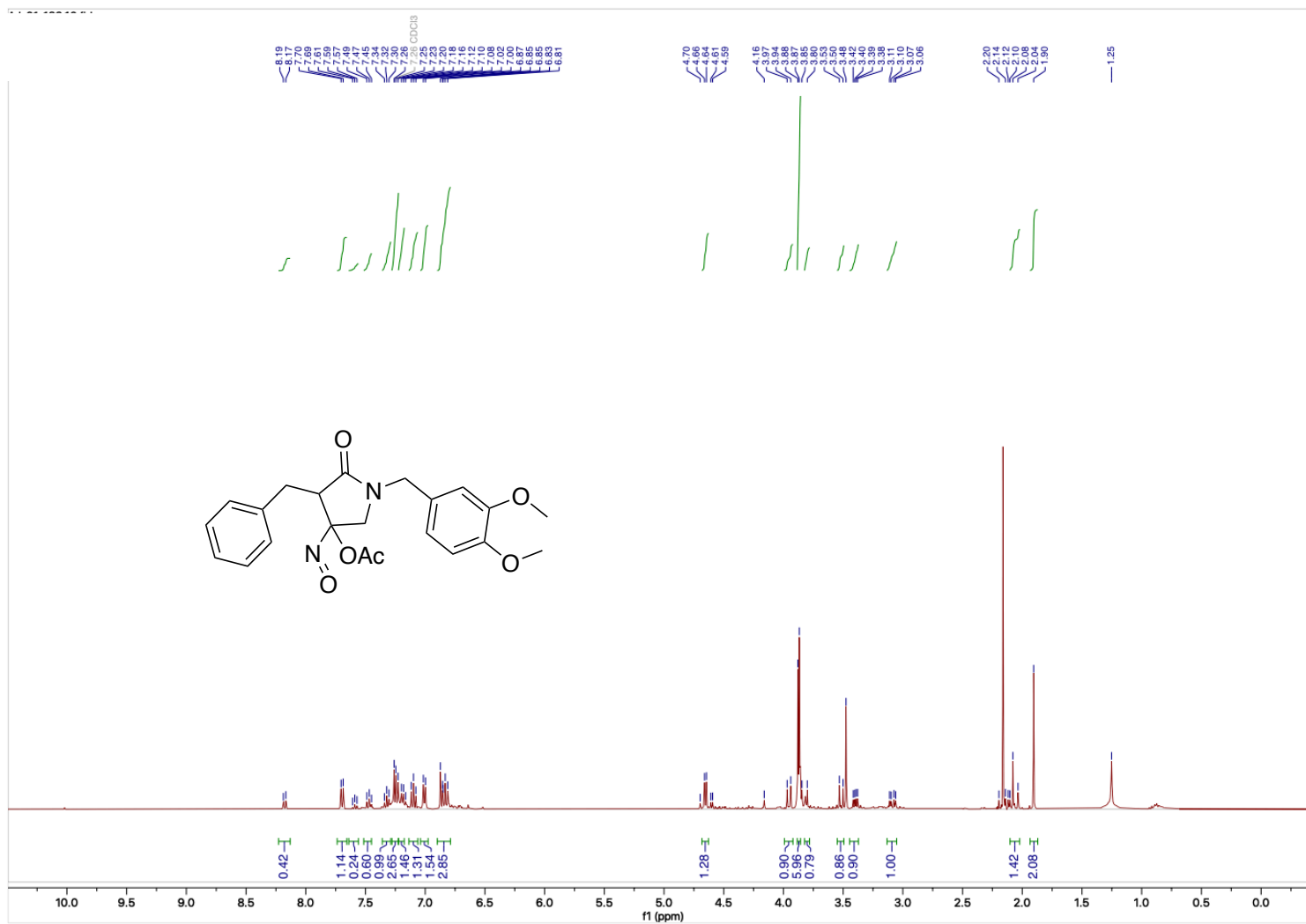


Figure A.30. ^1H NMR (400 MHz, CDCl_3) acyloxy nitroso **2.58**

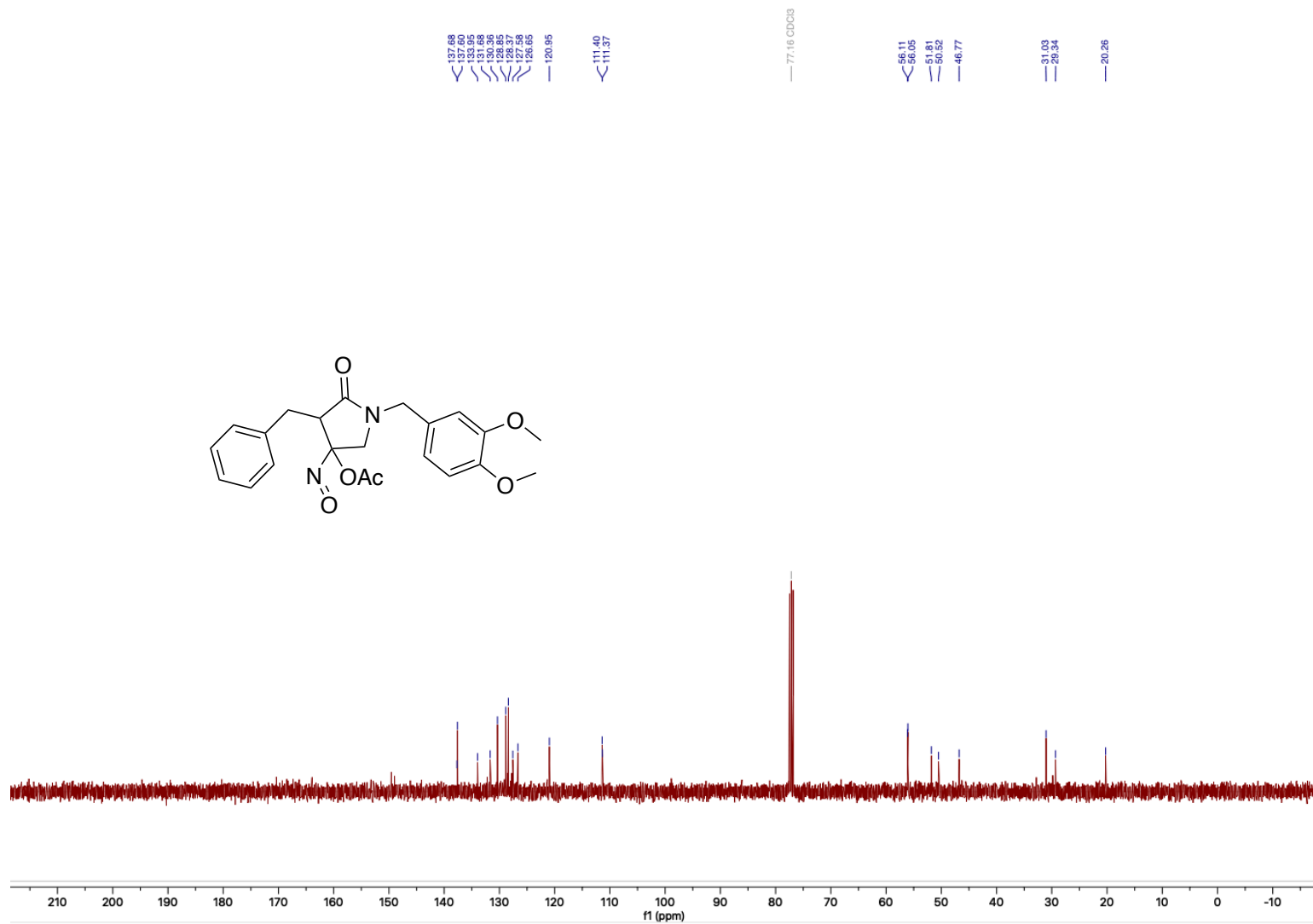


Figure A.31. ^{13}C NMR (101 MHz, CDCl₃) acyloxy nitroso **2.58**

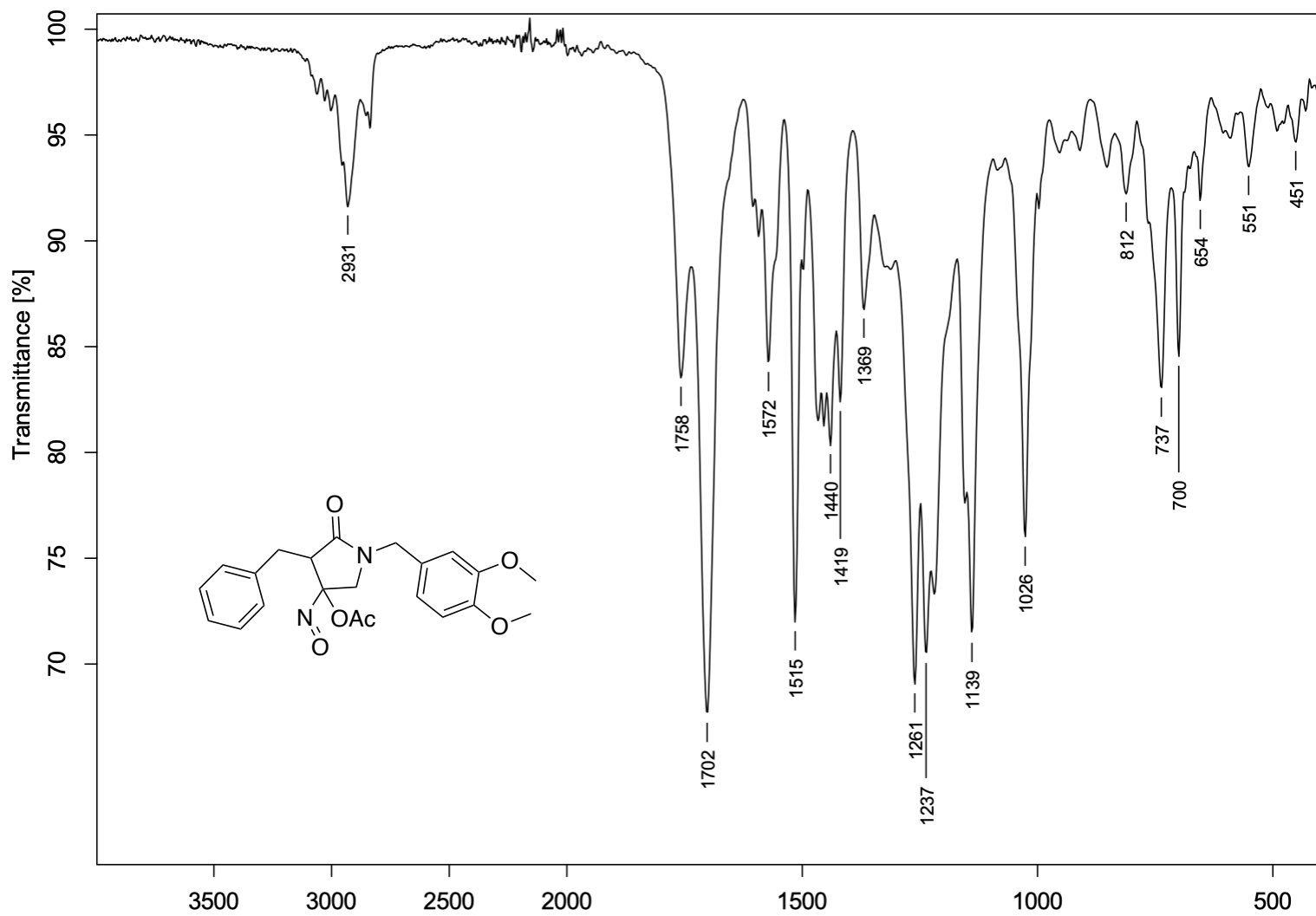


Figure A.32. FTIR (neat) crude acyloxy nitroso **2.58**

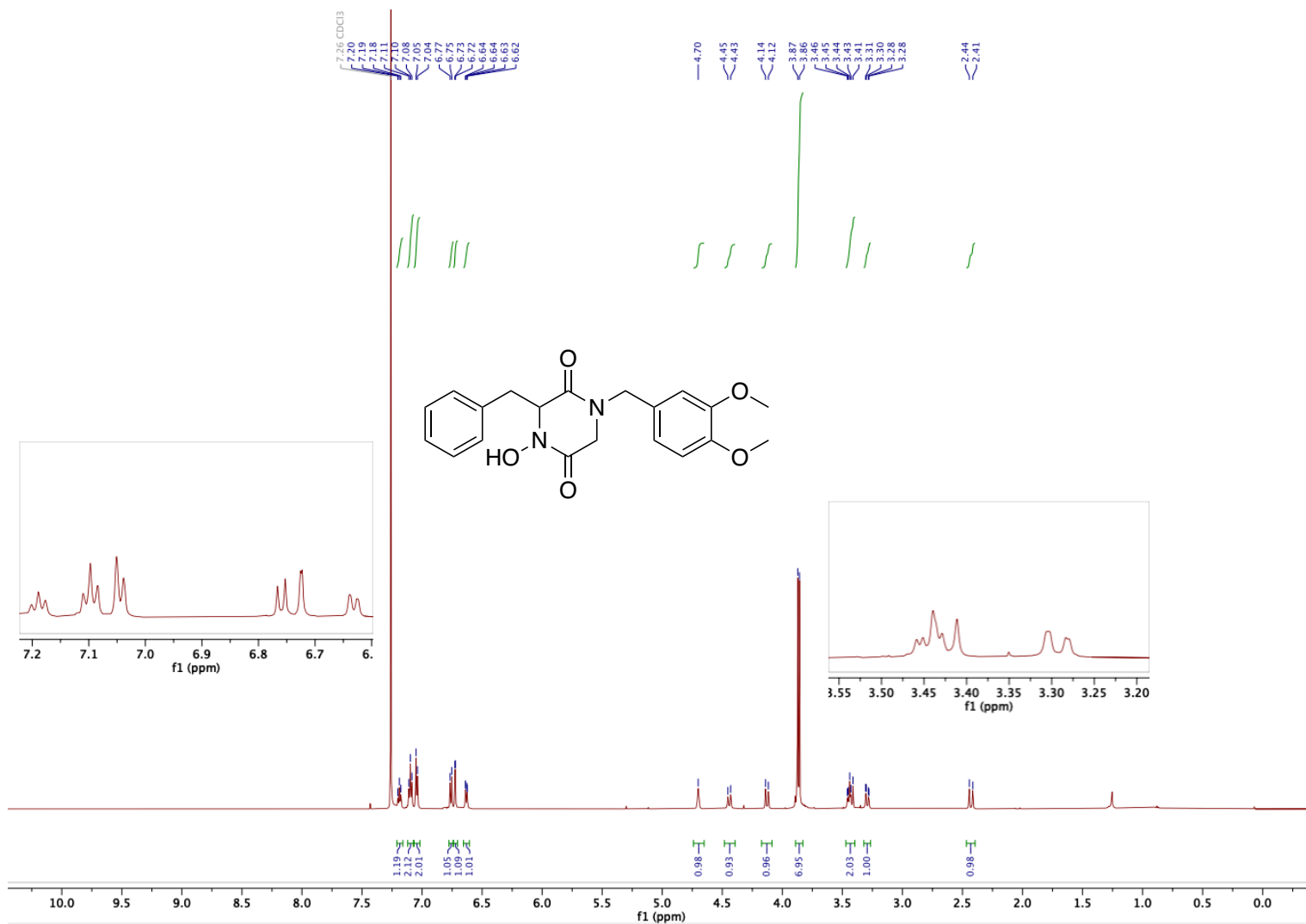


Figure A.33. ^1H NMR (600 MHz, CDCl_3) DKP 2.59

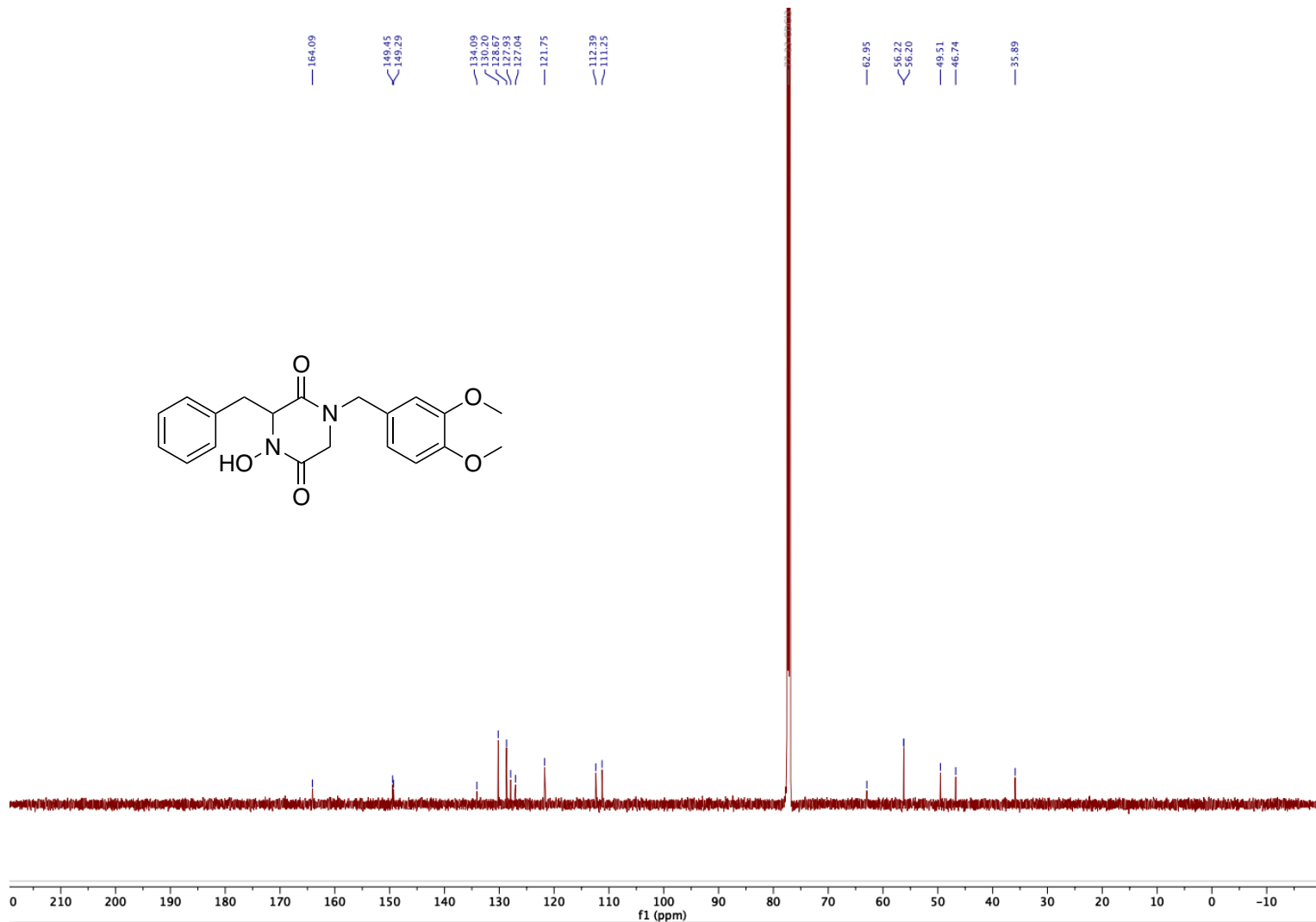


Figure A.34. ^{13}C NMR (151 MHz, CDCl_3) DKP 2.59

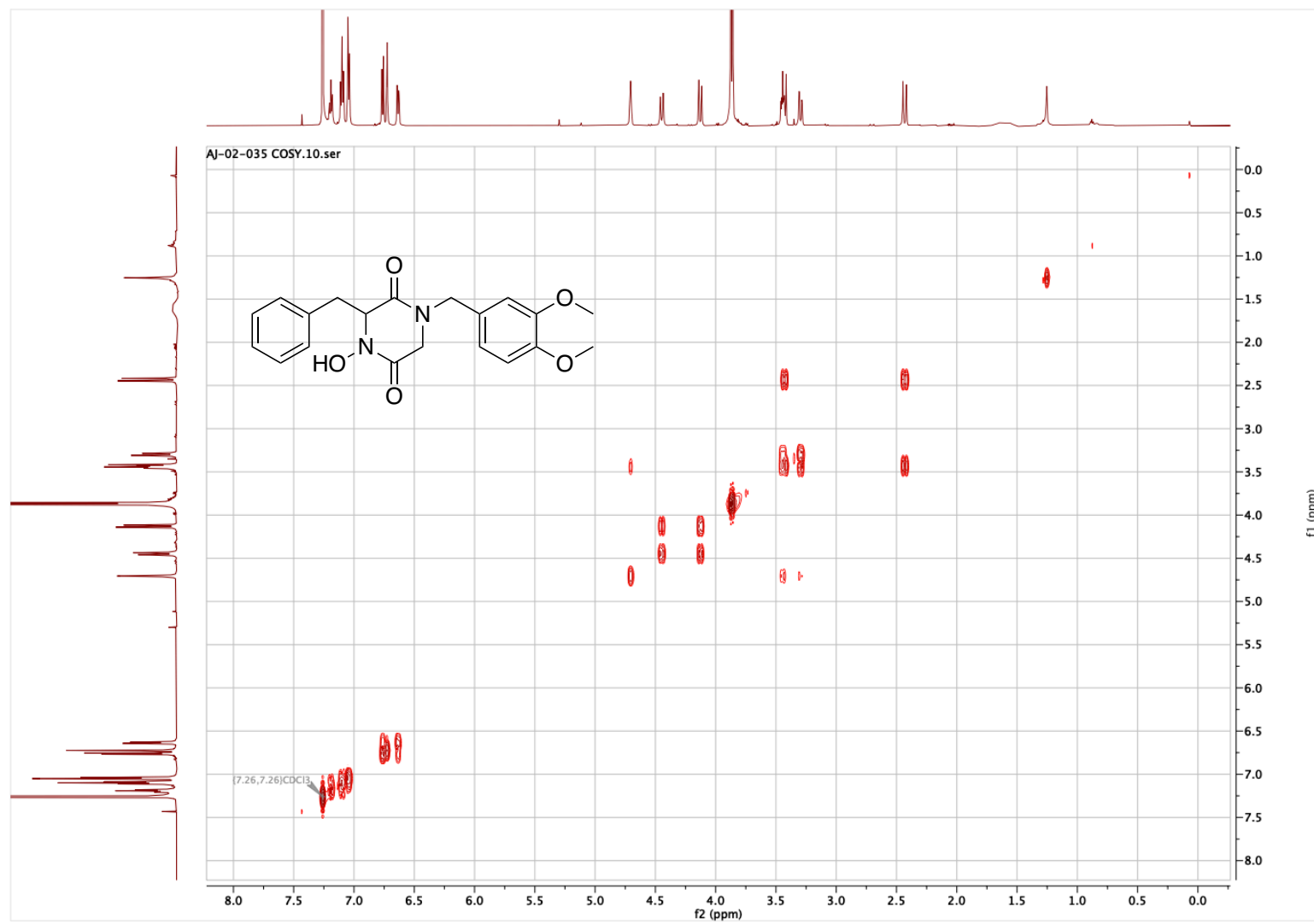


Figure A.35. COSY (600 MHz, CDCl_3) DKP 2.59

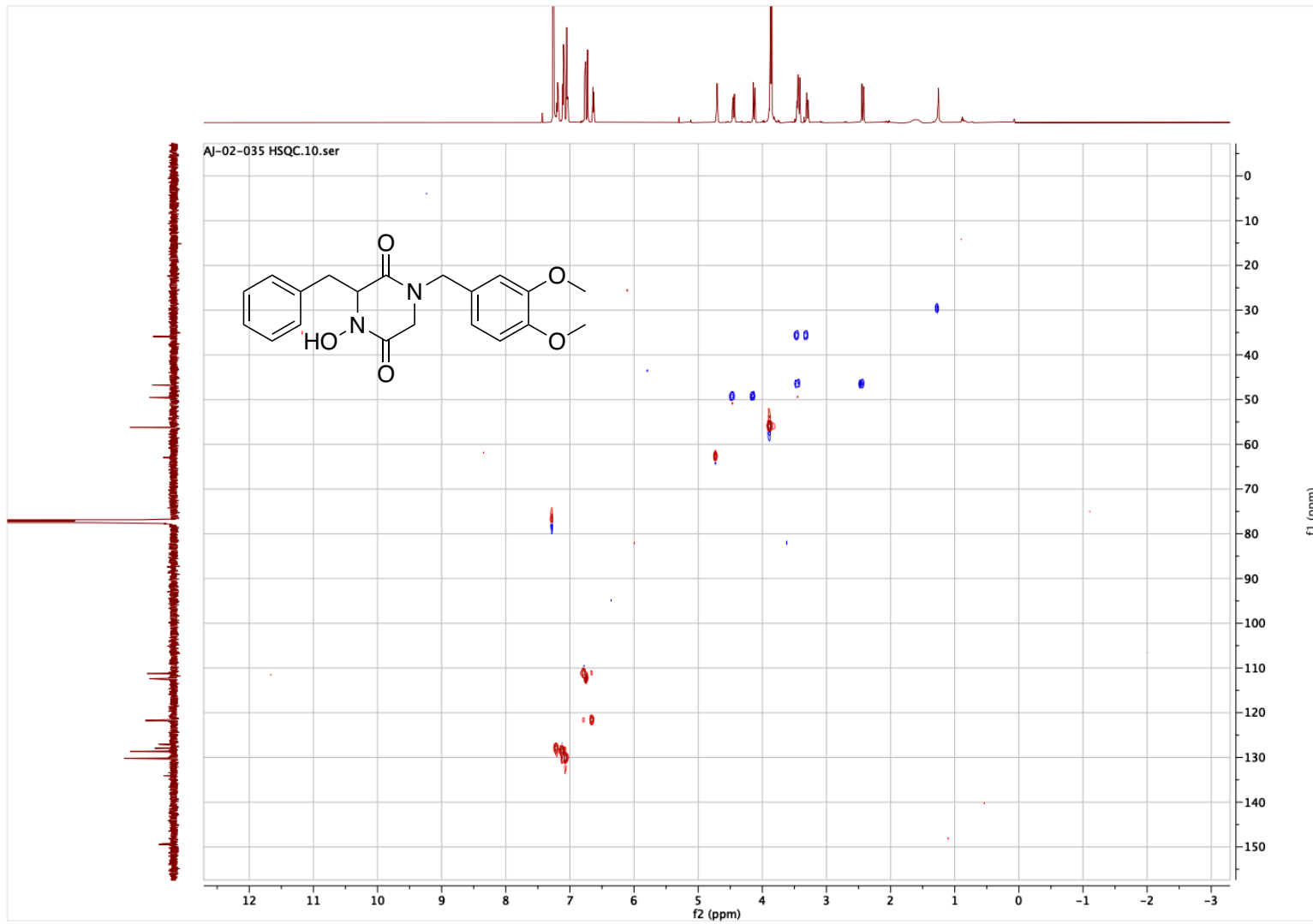


Figure A.36. HSQC (600, 151 MHz, CDCl₃; edited: CH/CH₃ = red, CH₂ = blue) DKP 2.59

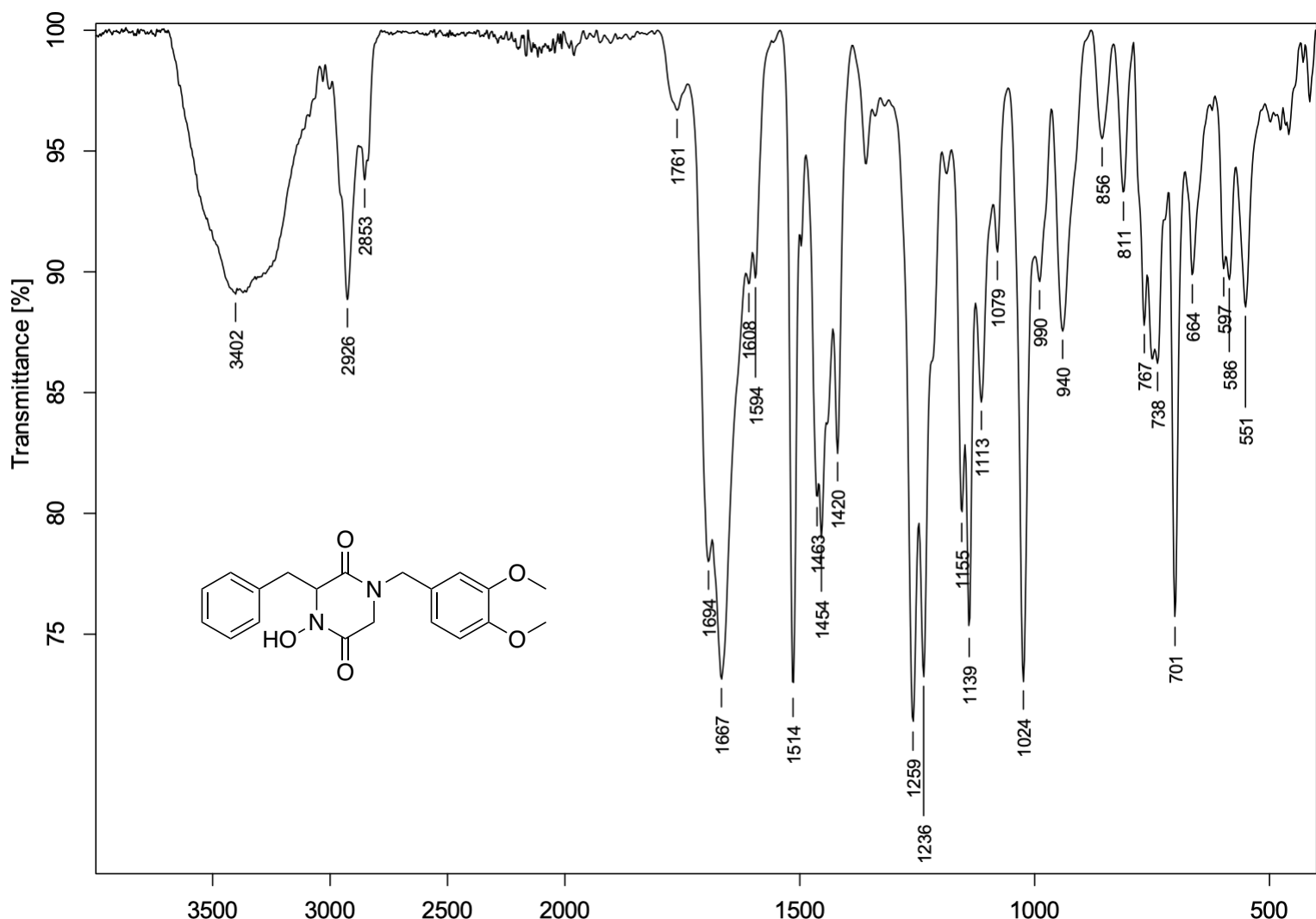


Figure A.37. FTIR (neat) DKP 2.59

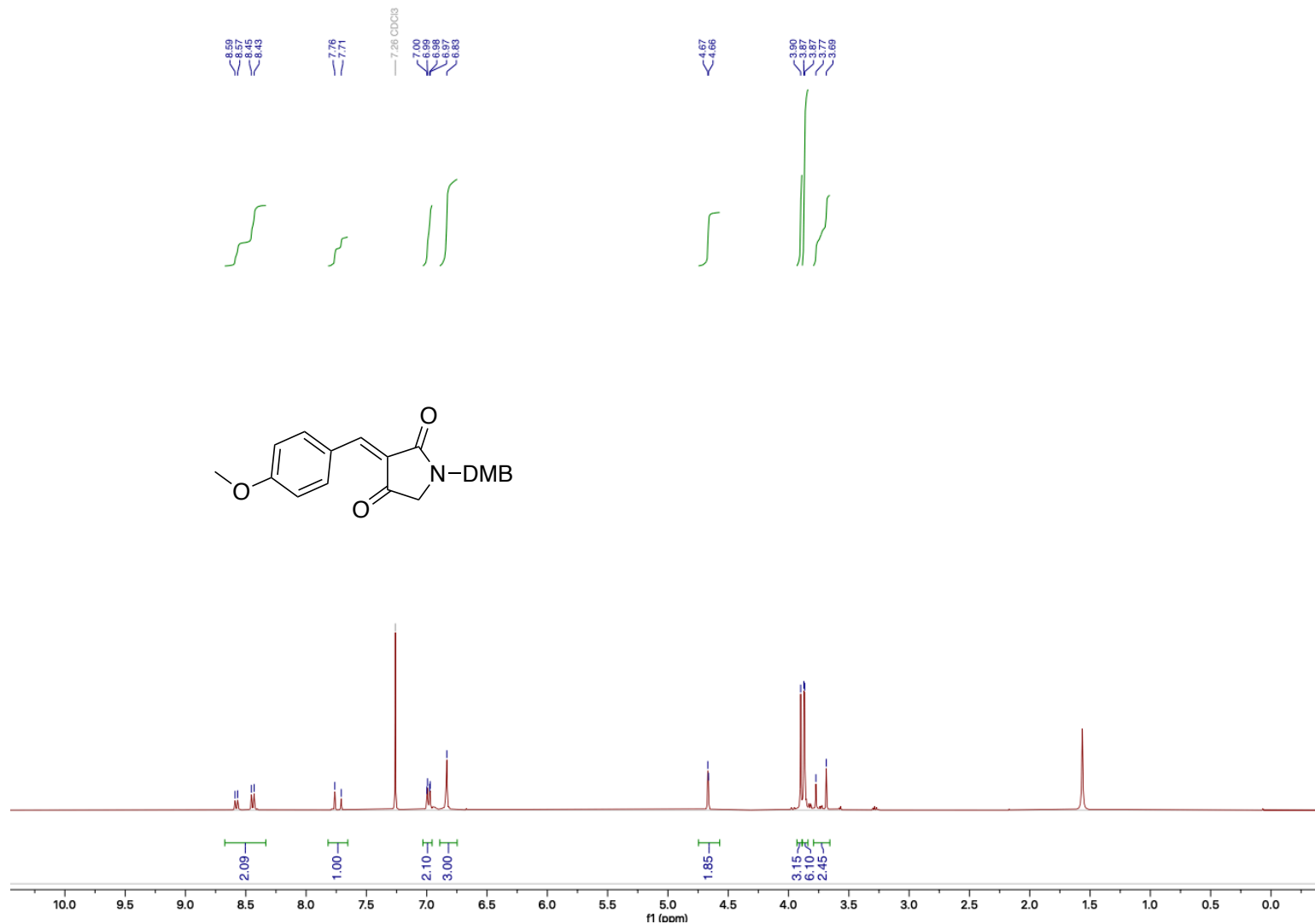


Figure A.38. ^1H NMR (400 MHz, CDCl_3) alkene **2.61**

I-01-I015 13C.1U.n0

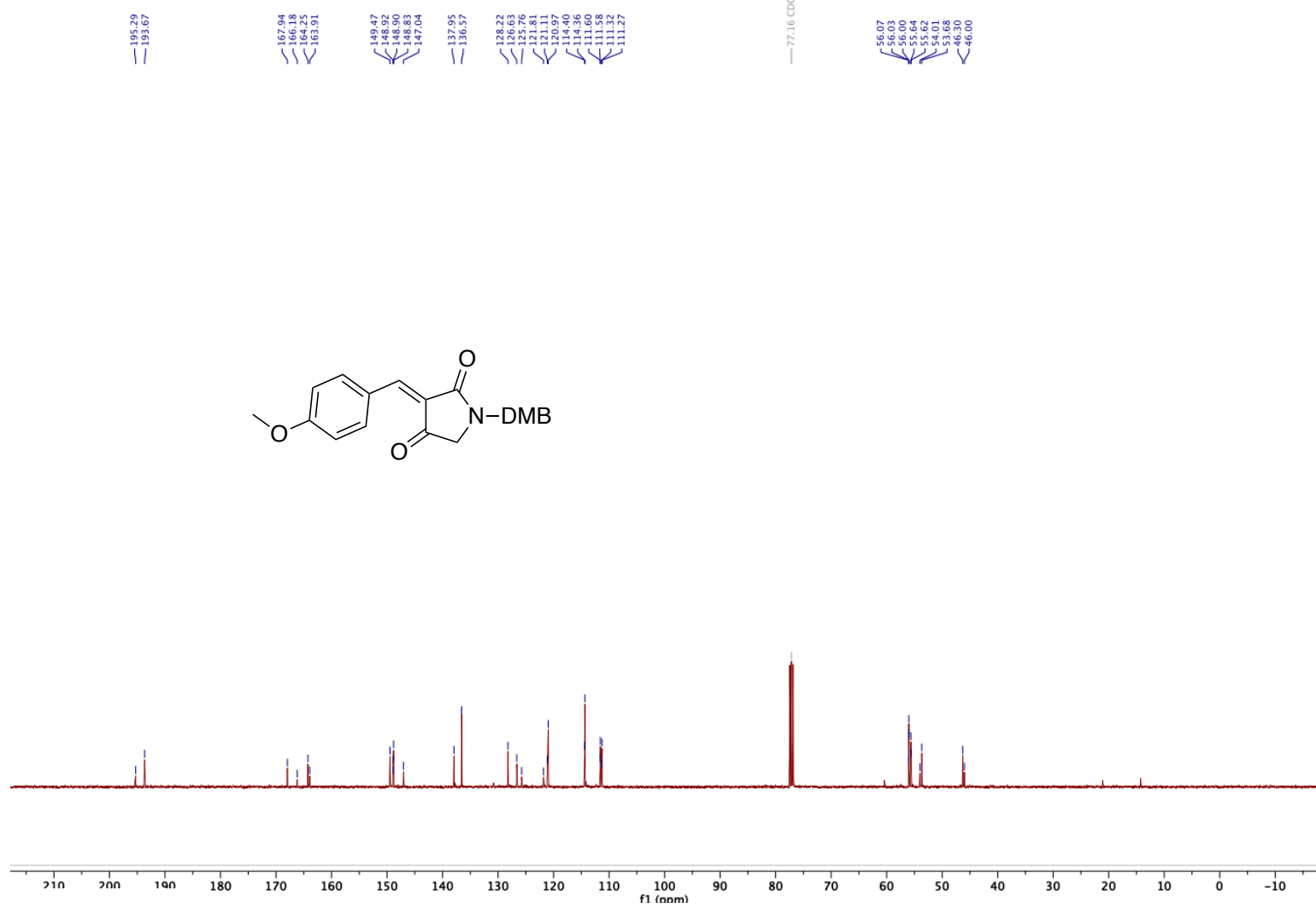


Figure A. 39. ^{13}C NMR (101 MHz, CDCl₃) alkene **2.61**

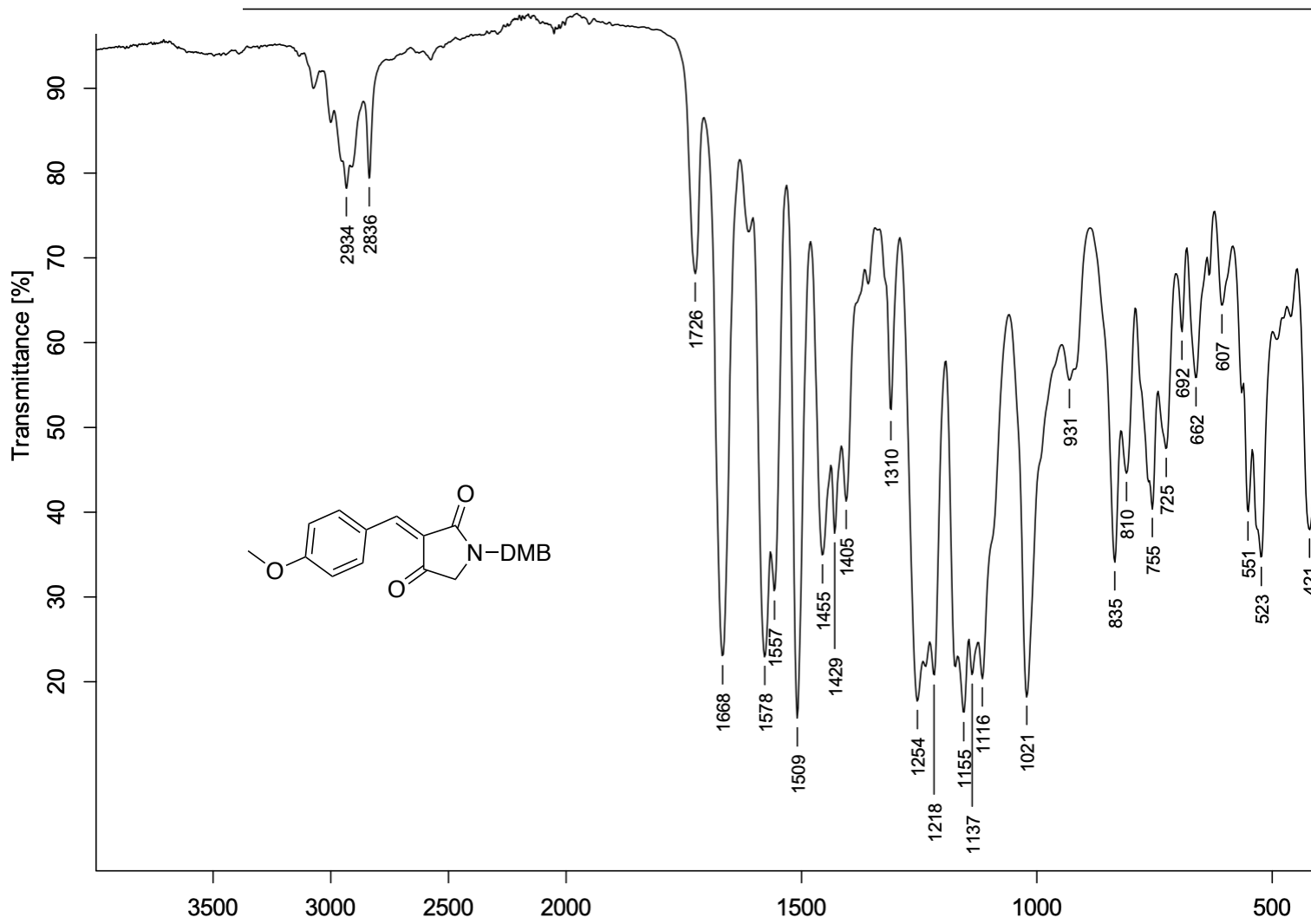


Figure A.40. FTIR (neat) alkene 2.61

V-01-243 1H conc.10.hd

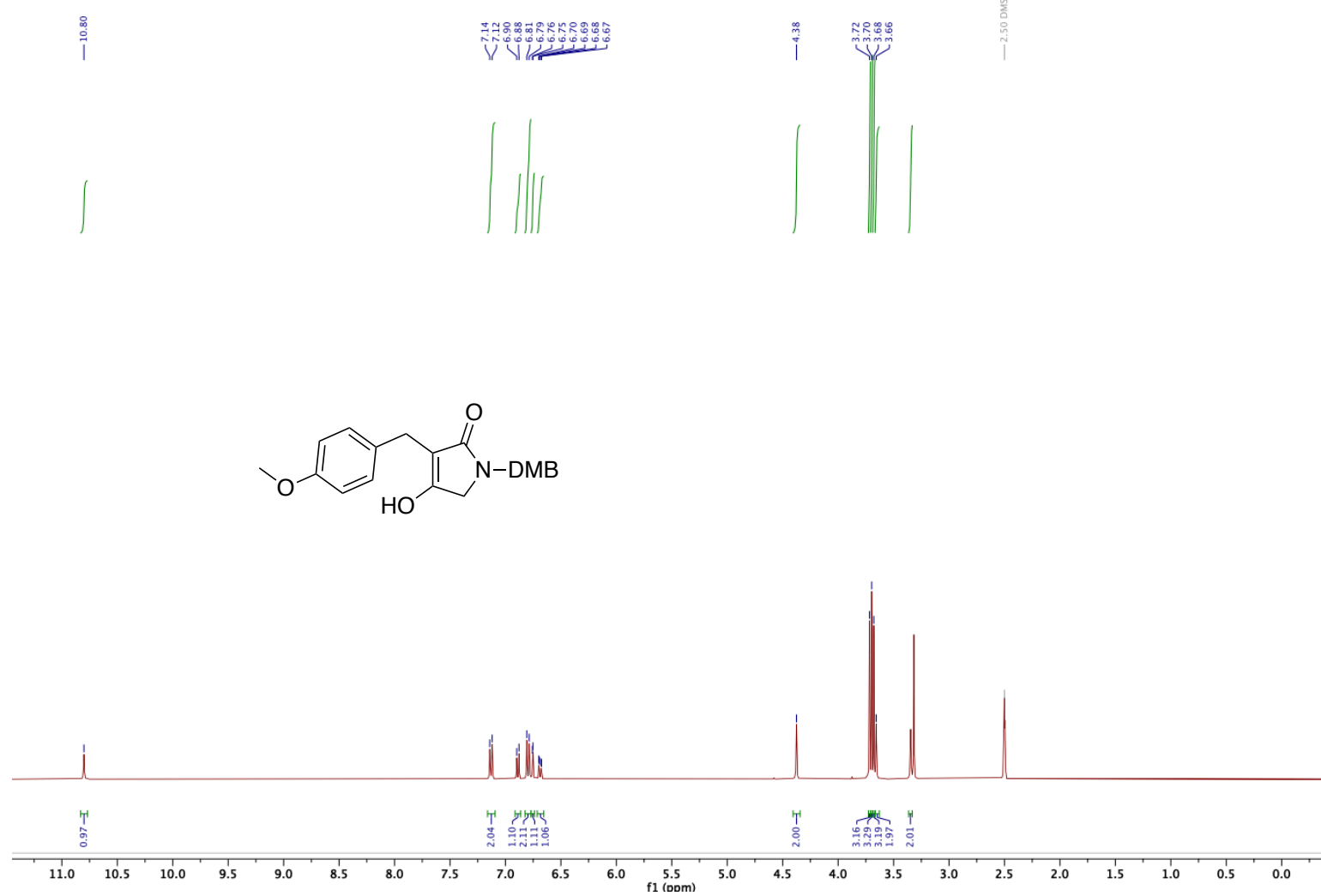


Figure A.41. ¹H NMR (600 MHz, CDCl₃) tetrameric acid **2.62**

J-01-243 ^{13}C conc again.10.n1d

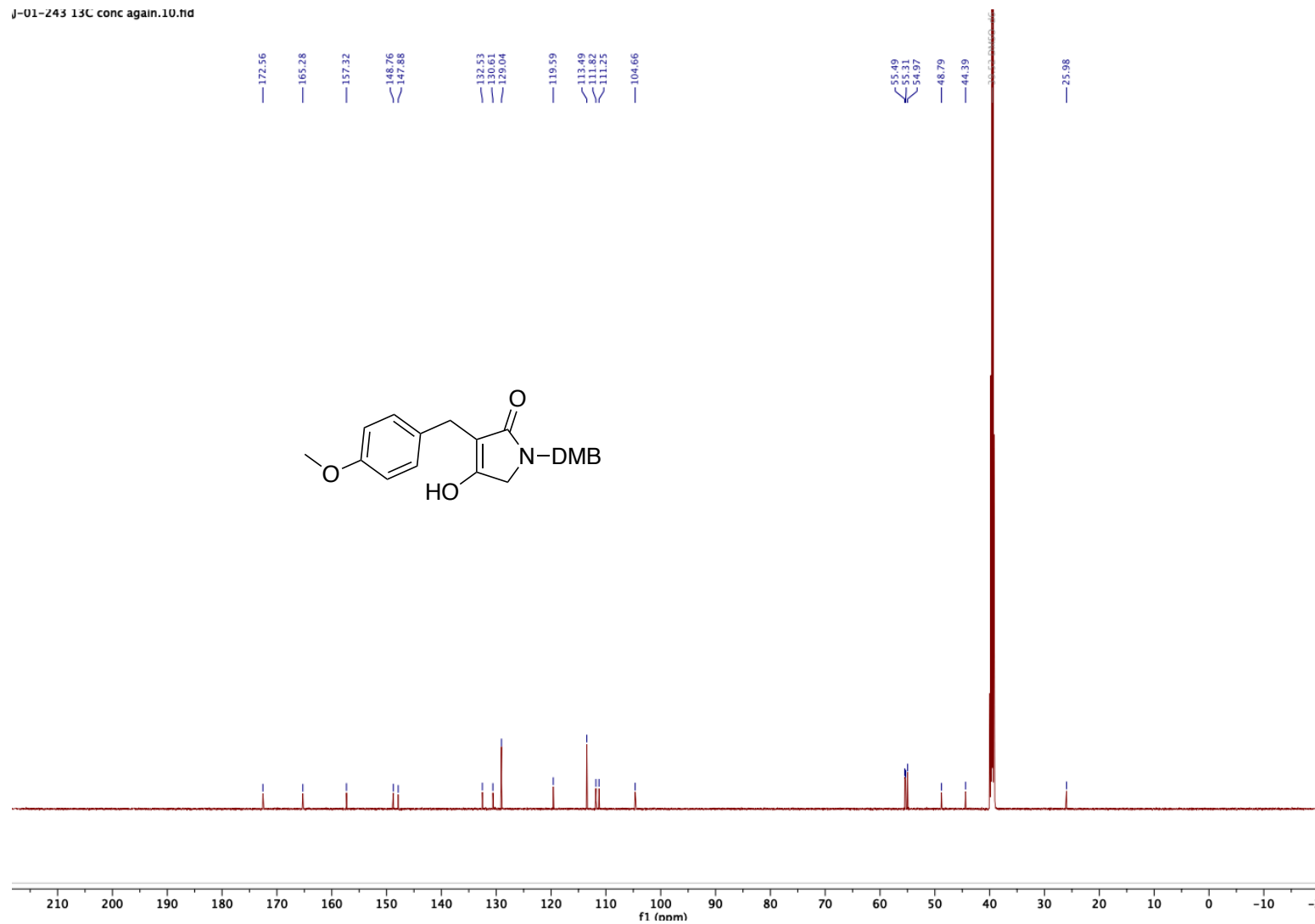


Figure A.42. ^{13}C NMR (151 MHz, CDCl_3) tetrameric acid **2.62**

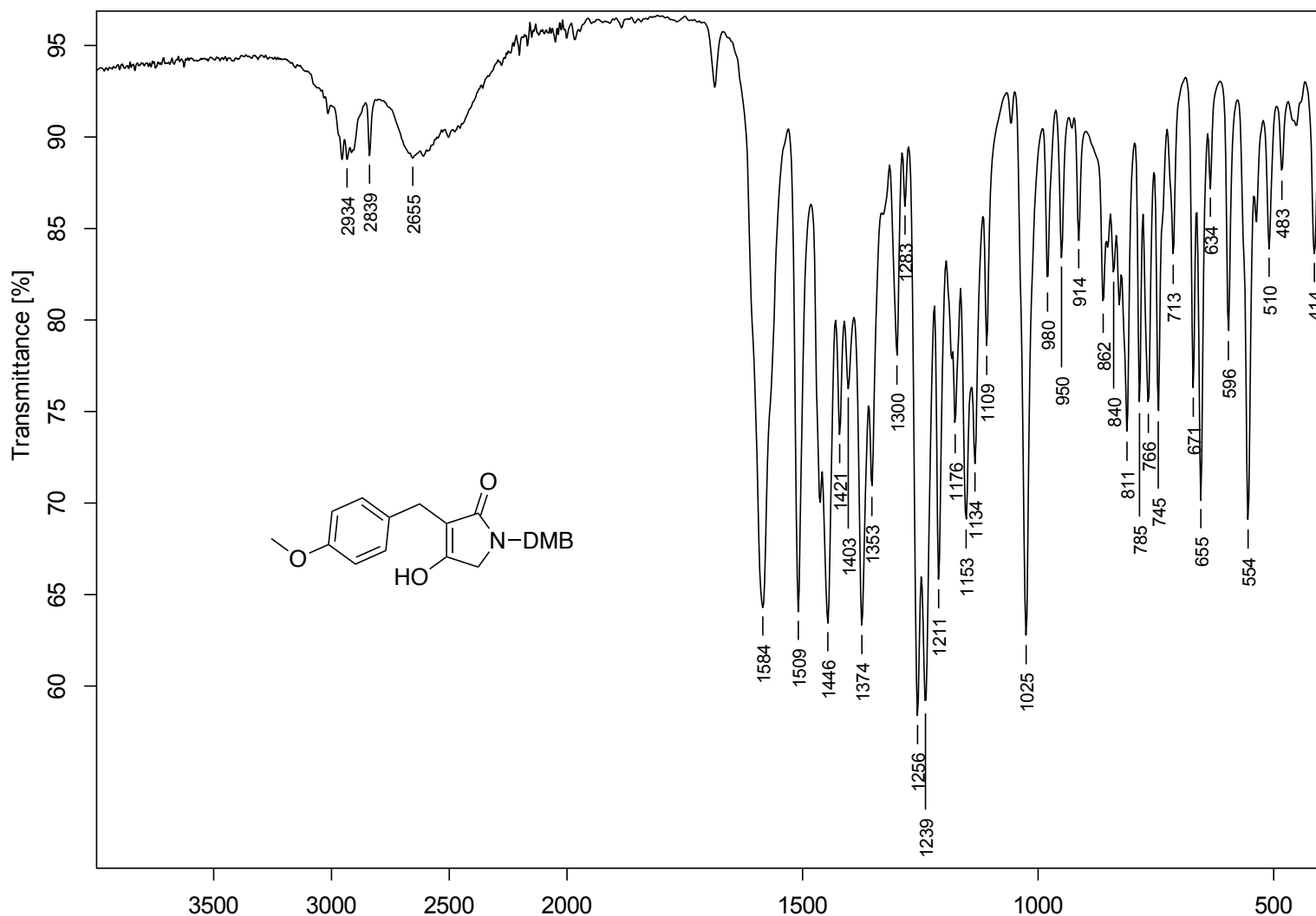


Figure A.43. FTIR (neat) tetrameric acid **2.62**

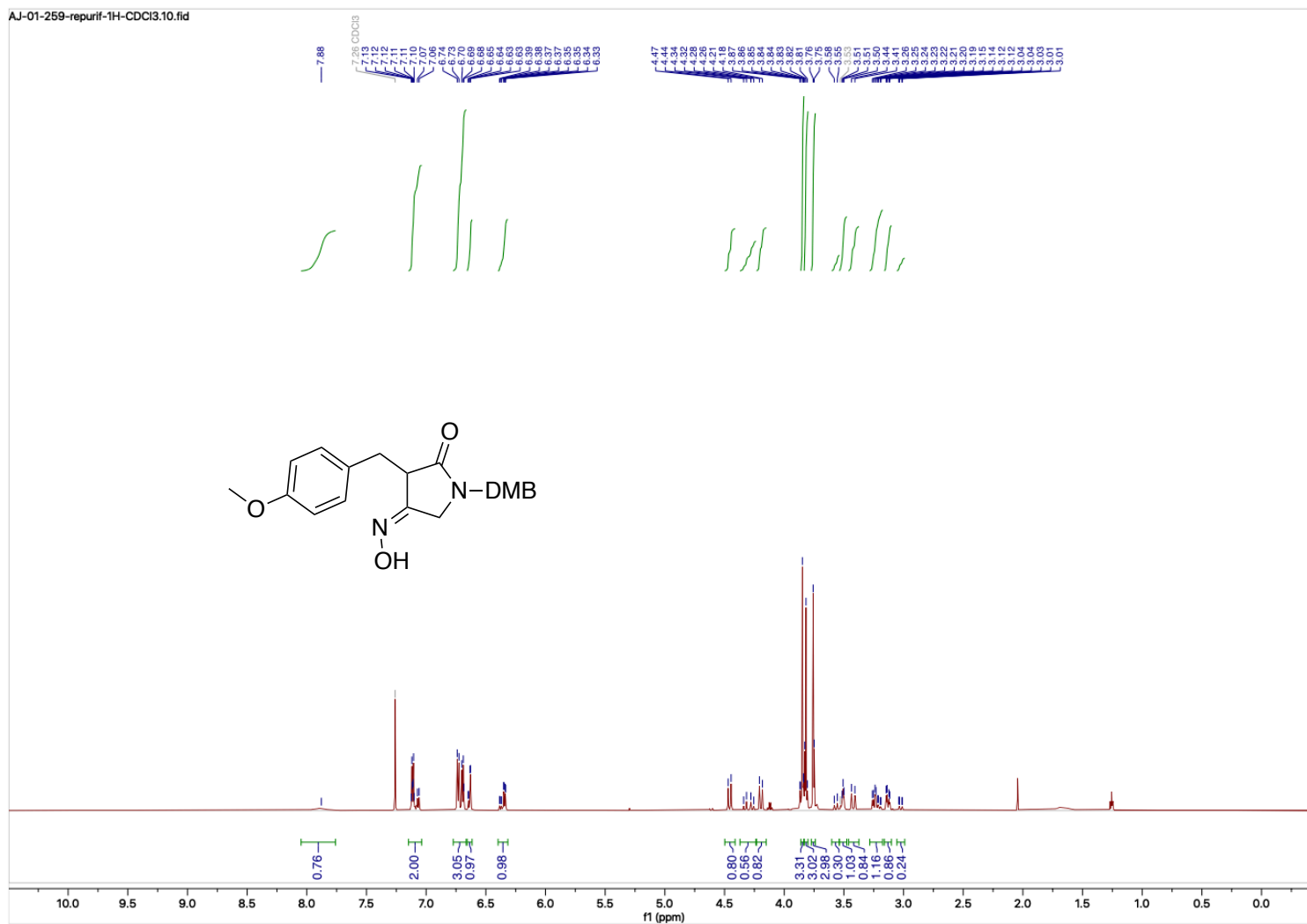


Figure A.44. ¹H NMR (600 MHz, CDCl₃) oxime 2.63

AJ-01-259-repurif-13C-CDCl₃.10.fid

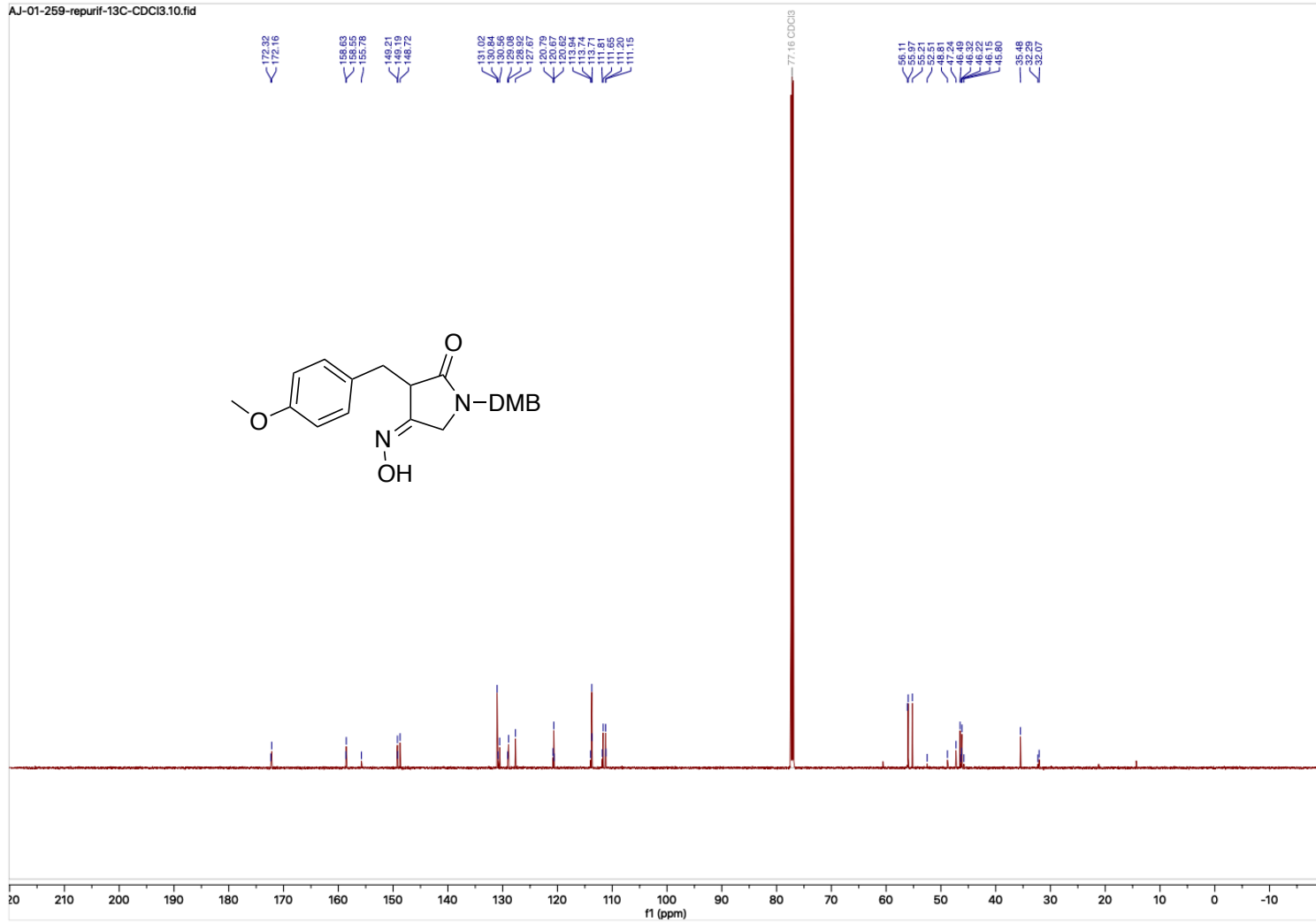


Figure A.45. ¹³C NMR (151 MHz, CDCl₃) oxime **2.63**

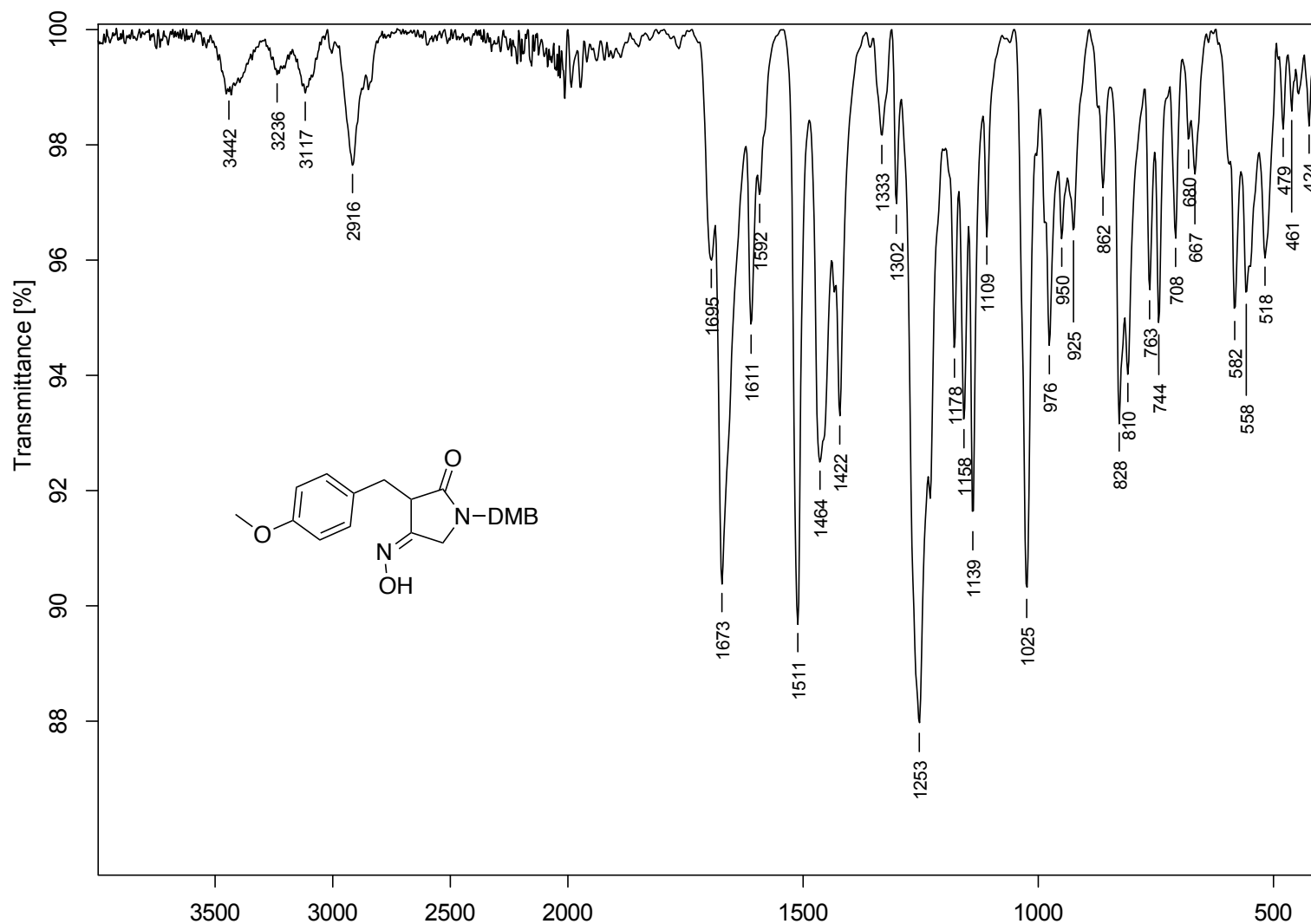


Figure A.46. FTIR (neat) oxime 2.63

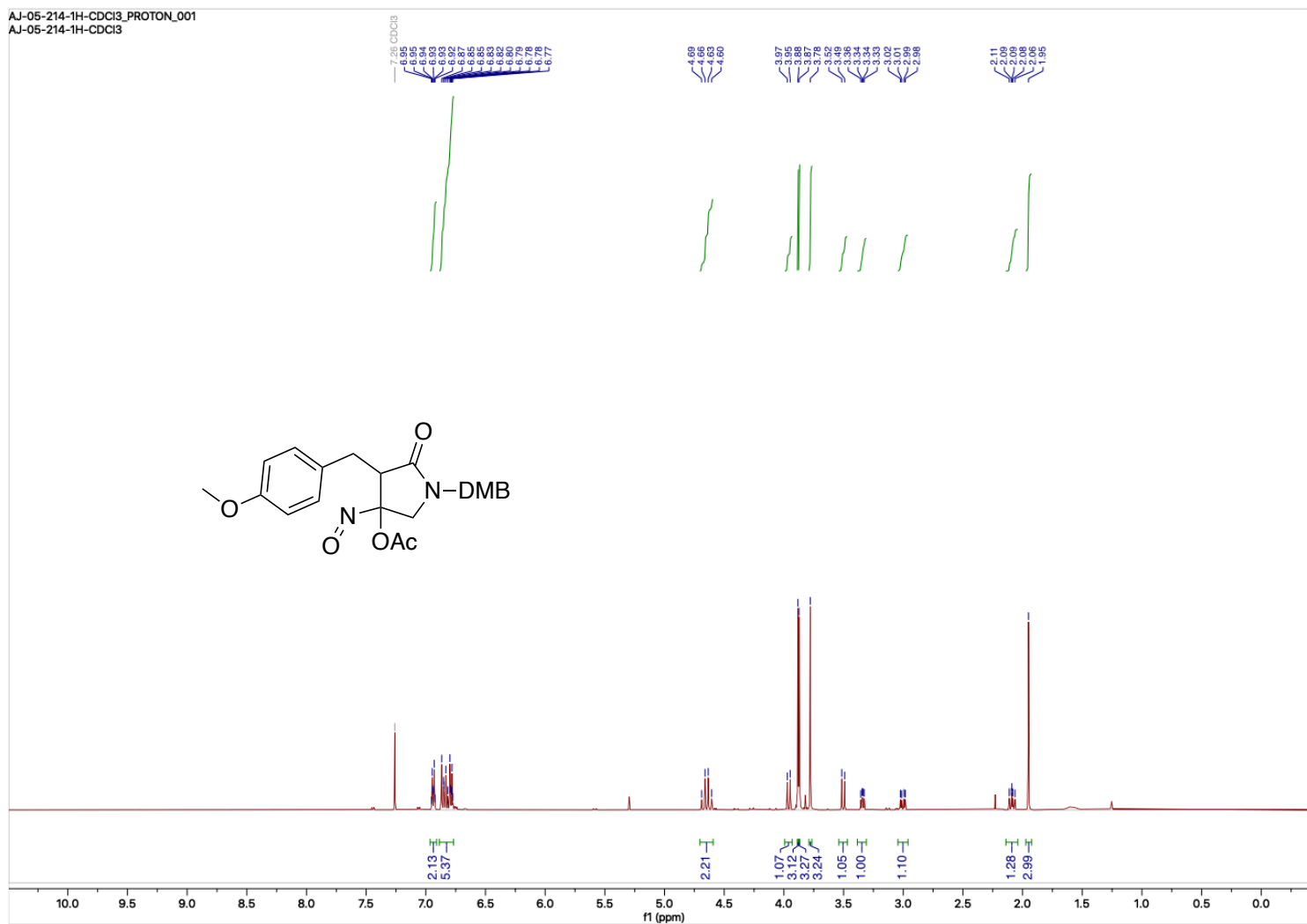


Figure A.47. ¹H NMR (500 MHz, CDCl₃) crude acyloxy nitroso **2.64**

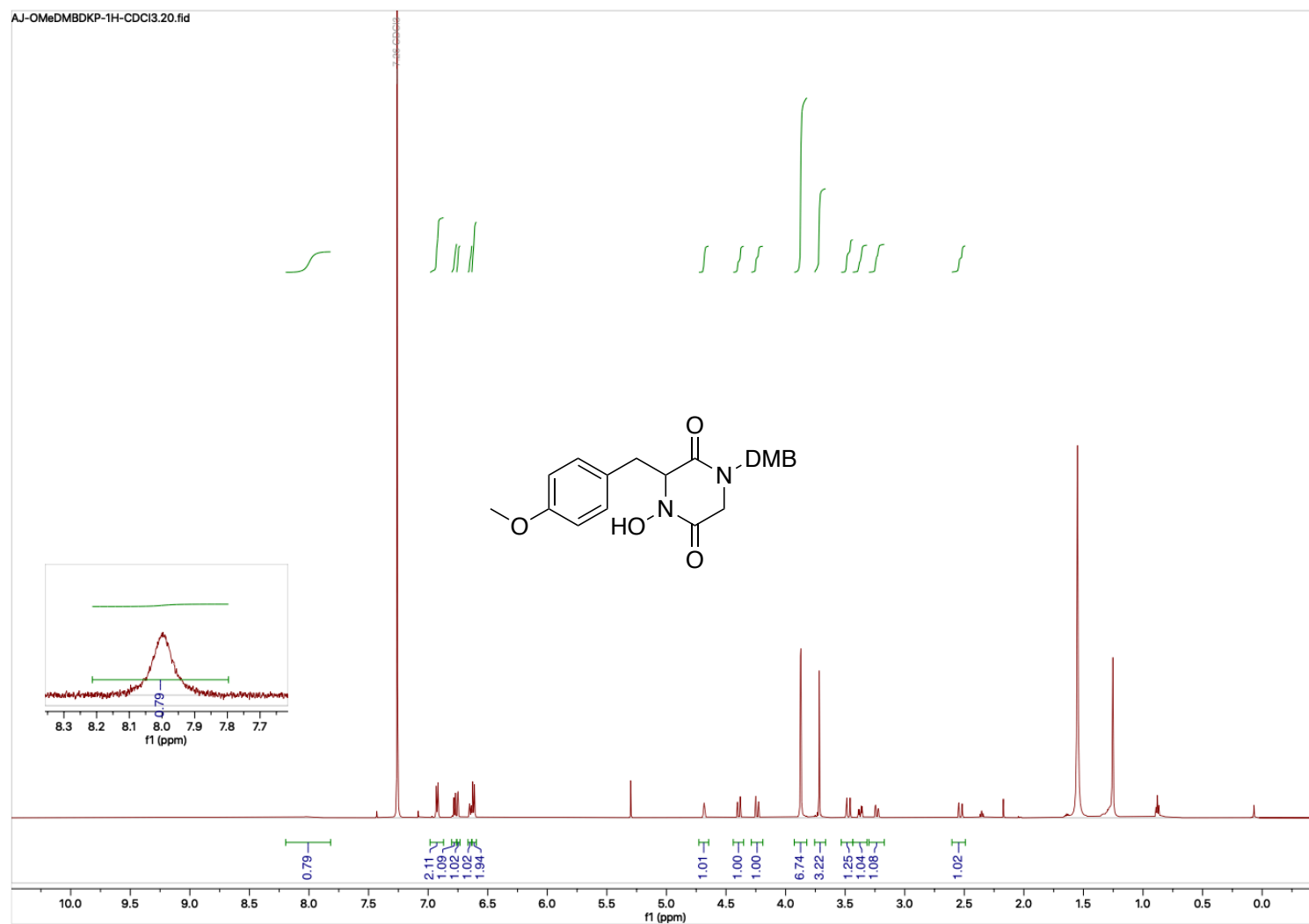


Figure A.48. ¹H NMR (600 MHz, CDCl₃) DKP 2.65

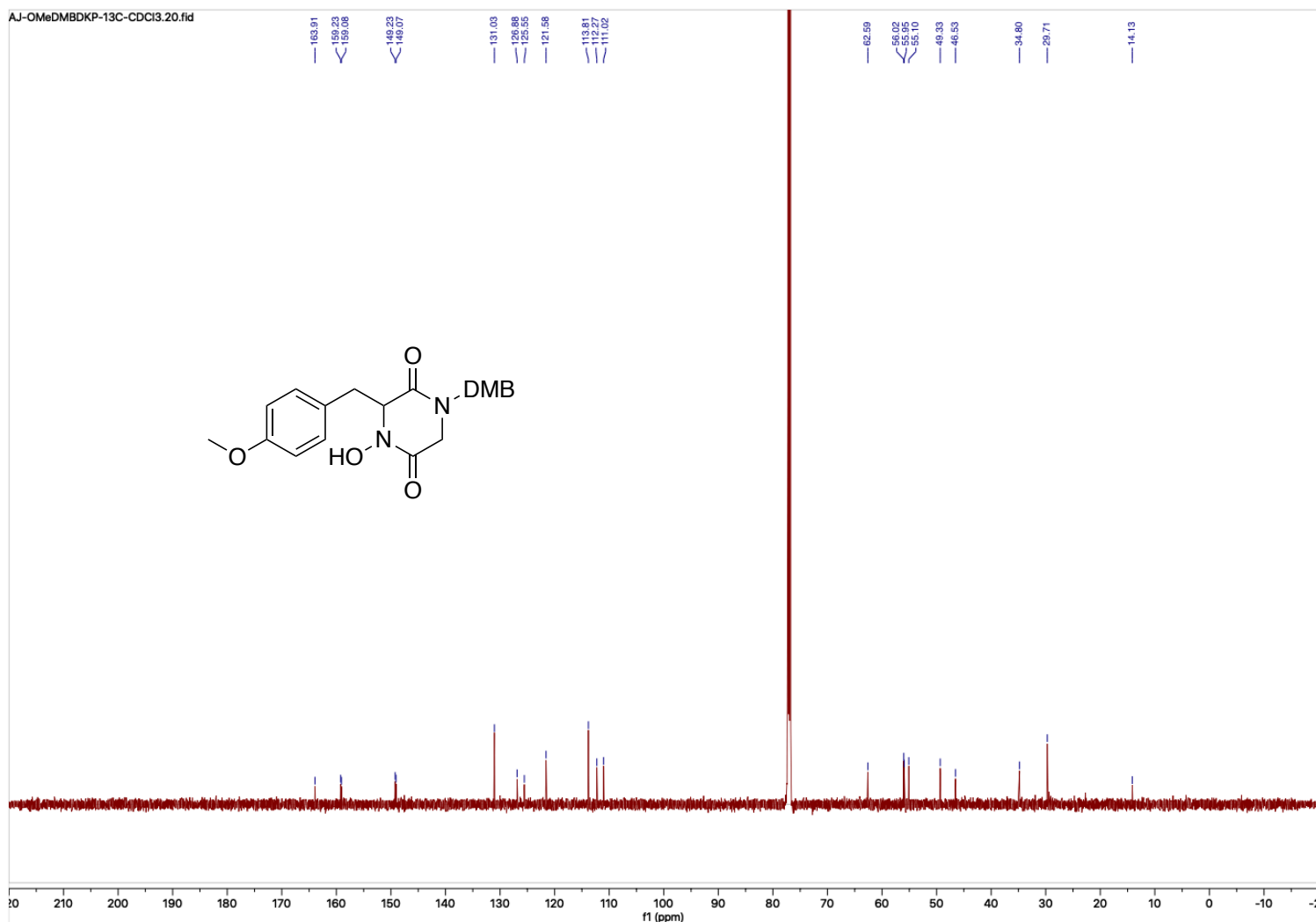


Figure A.49. ¹³C NMR (151 MHz, CDCl₃) DKP 2.65

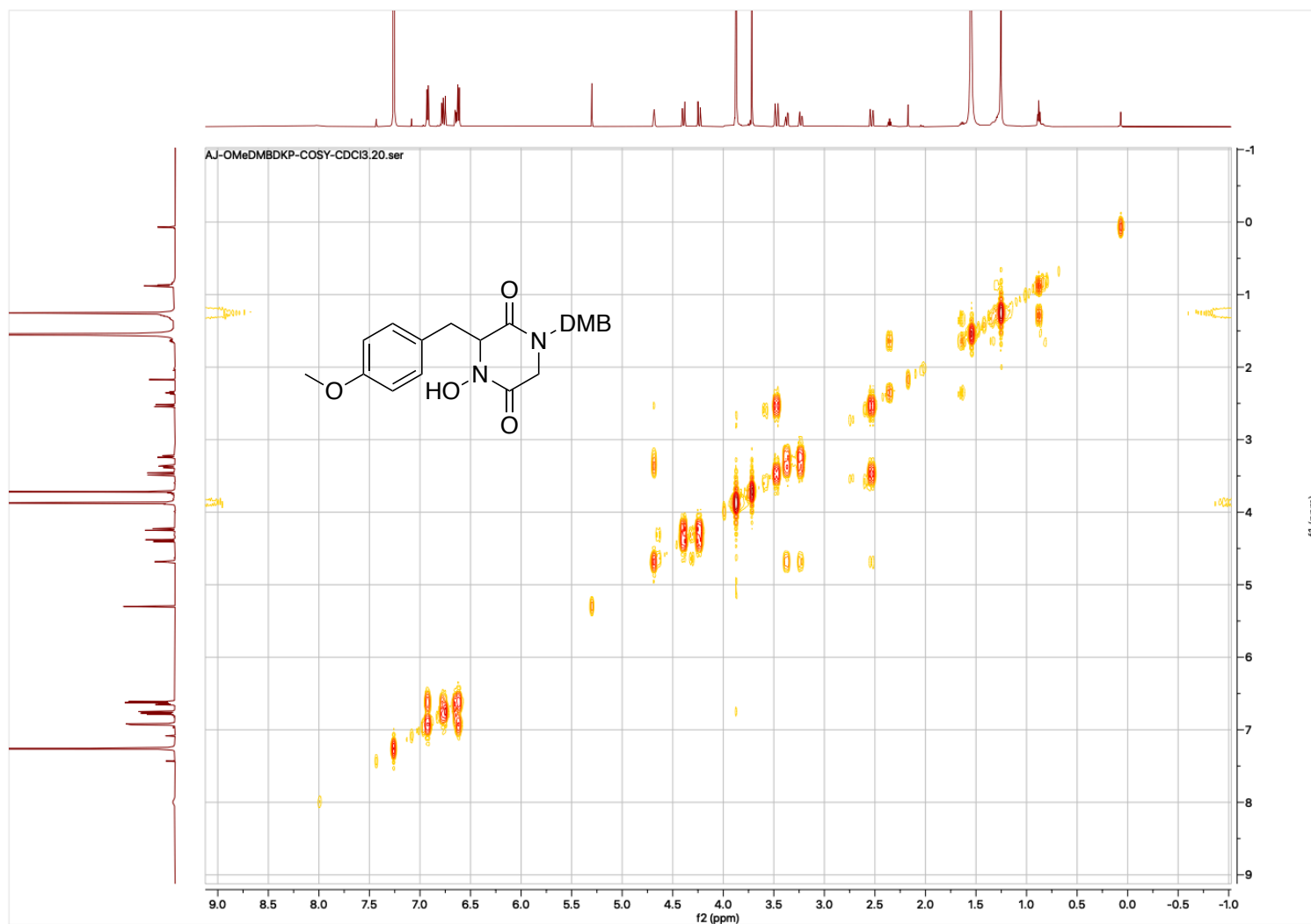


Figure A.50. COSY (600 MHz, CDCl_3) DKP 2.65

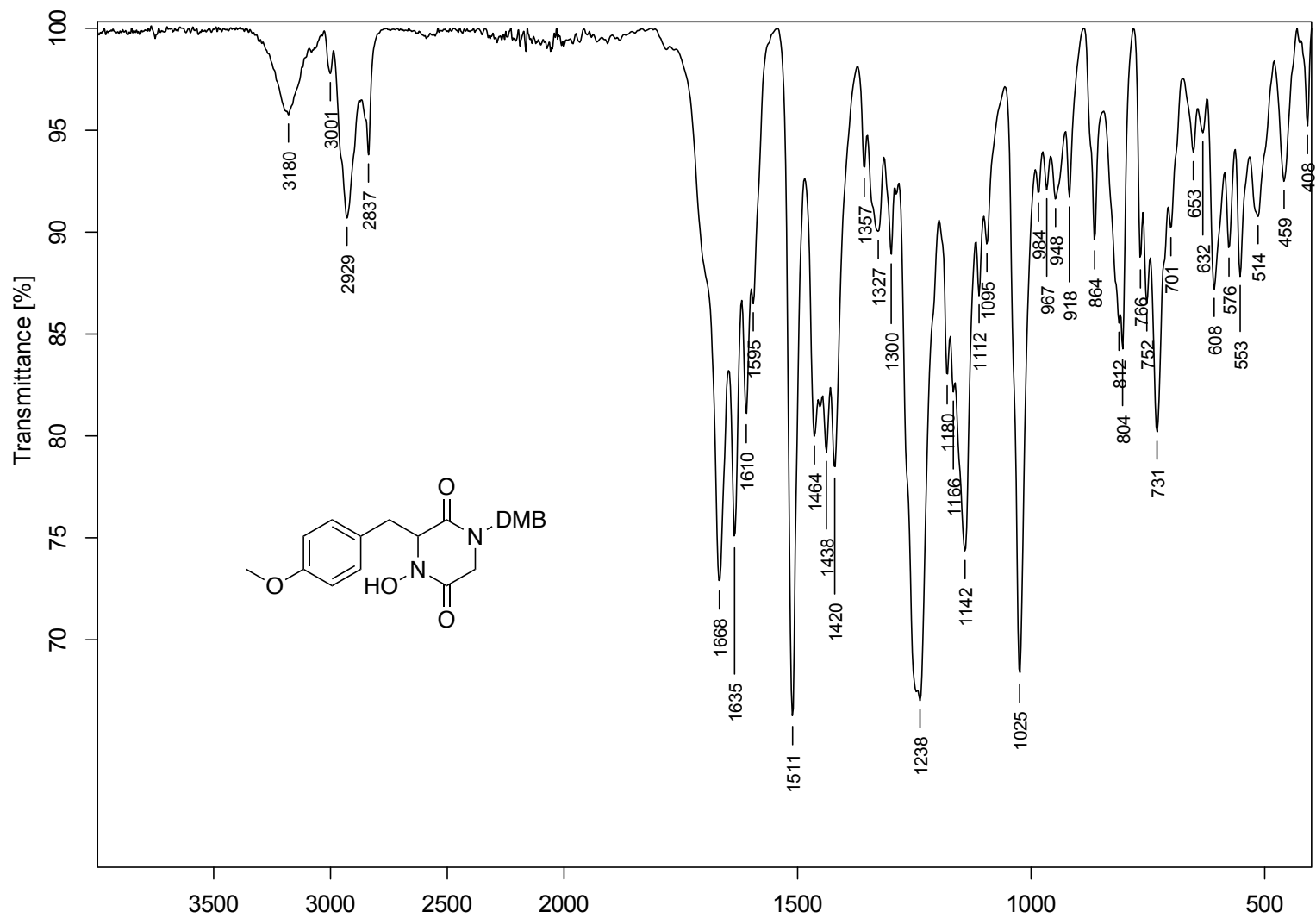


Figure A.51. FTIR (neat) DKP 2.65

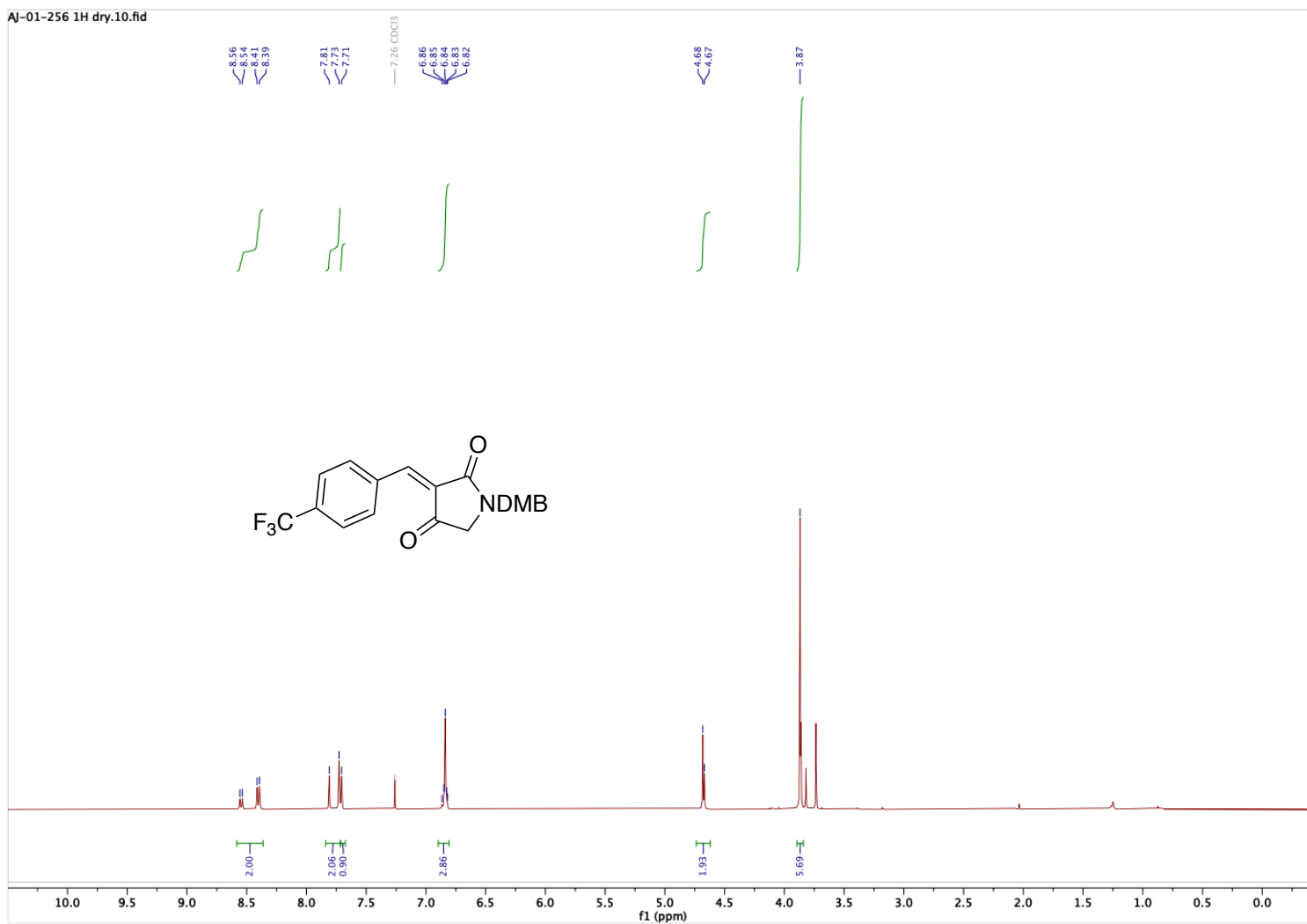


Figure A.52. ^1H NMR (400 MHz, CDCl_3) alkene **2.66**

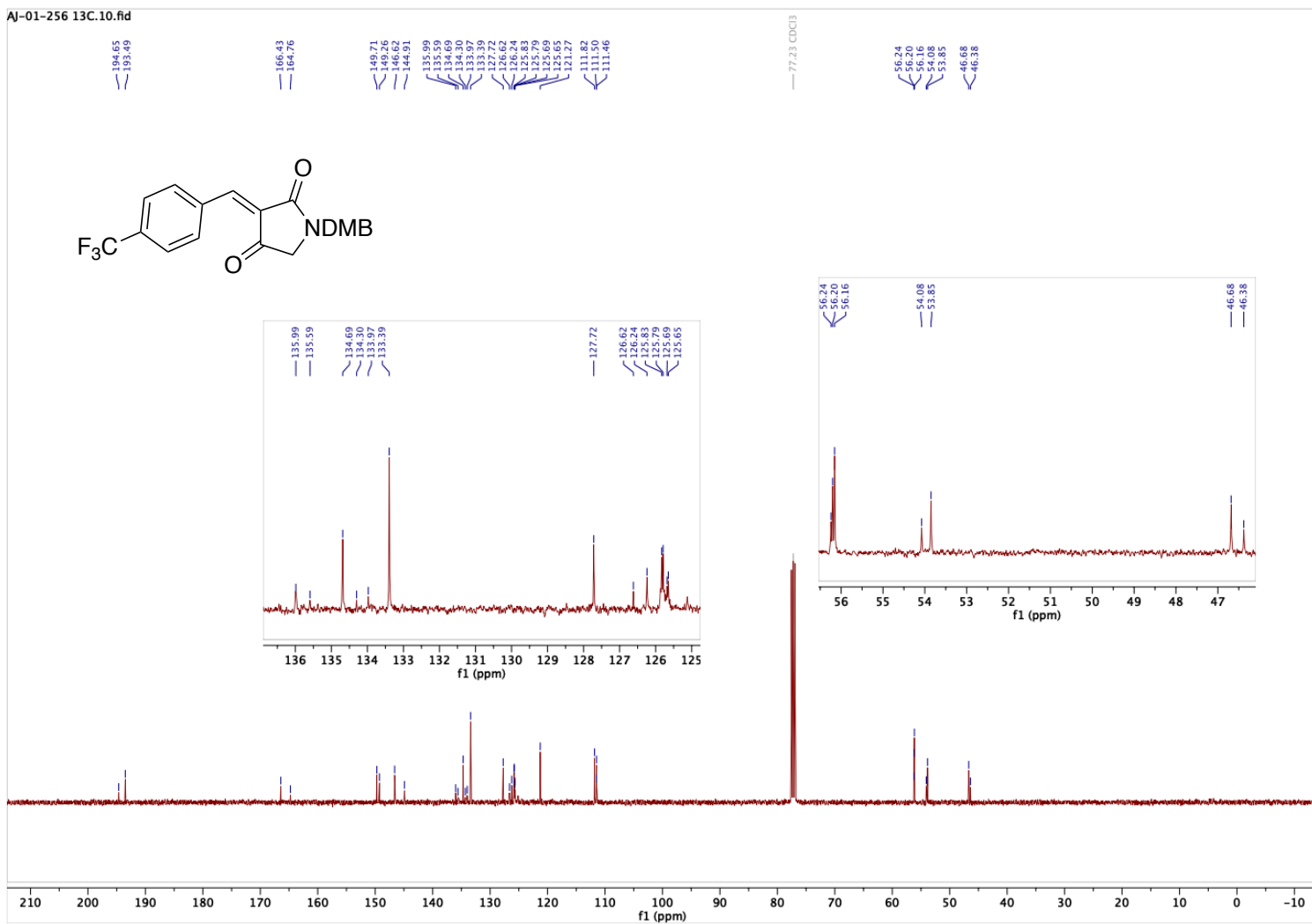


Figure A.53. ^{13}C NMR (101 MHz, CDCl_3) alkene 2.66

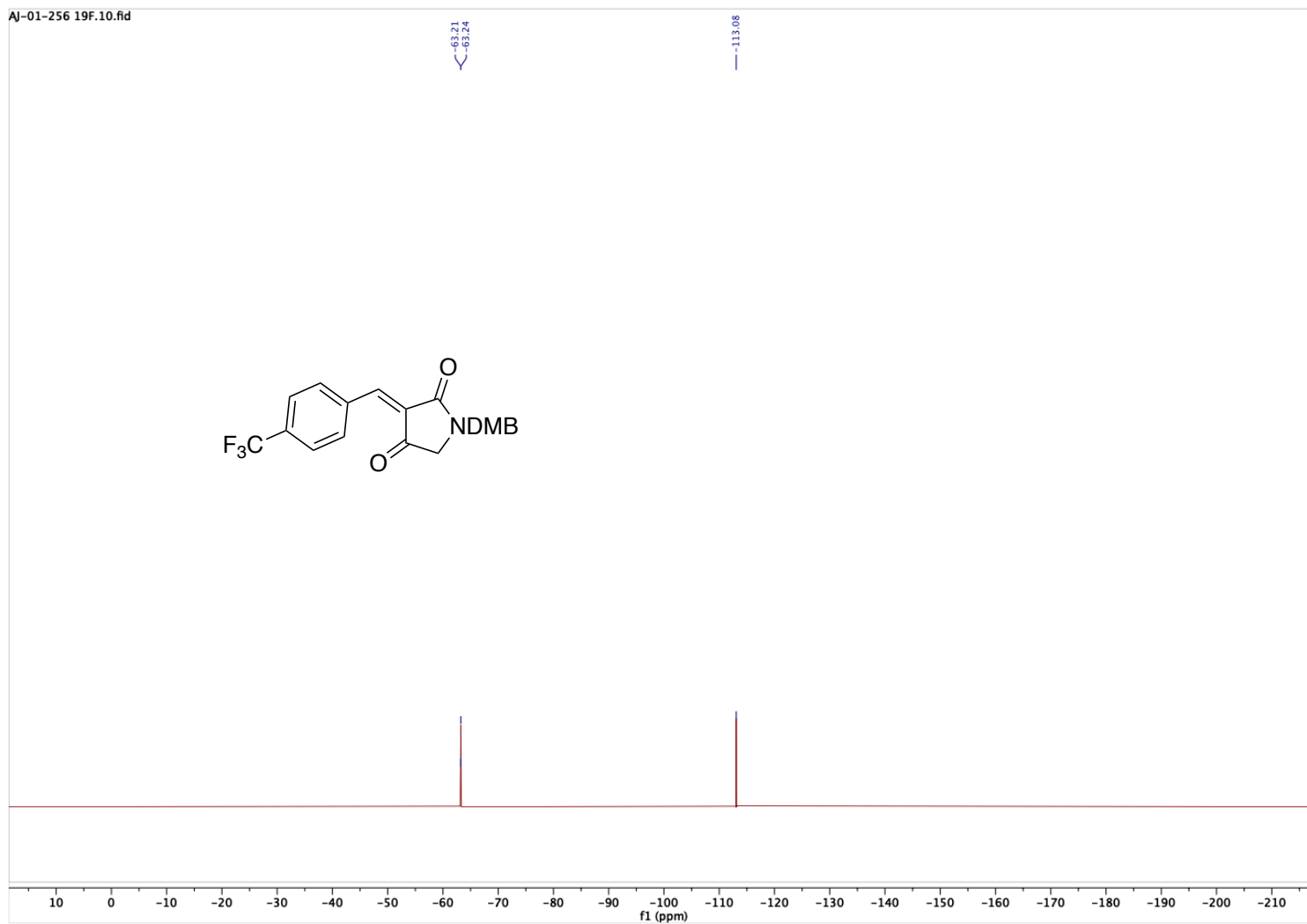


Figure A.54. ^{19}F NMR (400 MHz, CDCl_3) alkene **2.66**

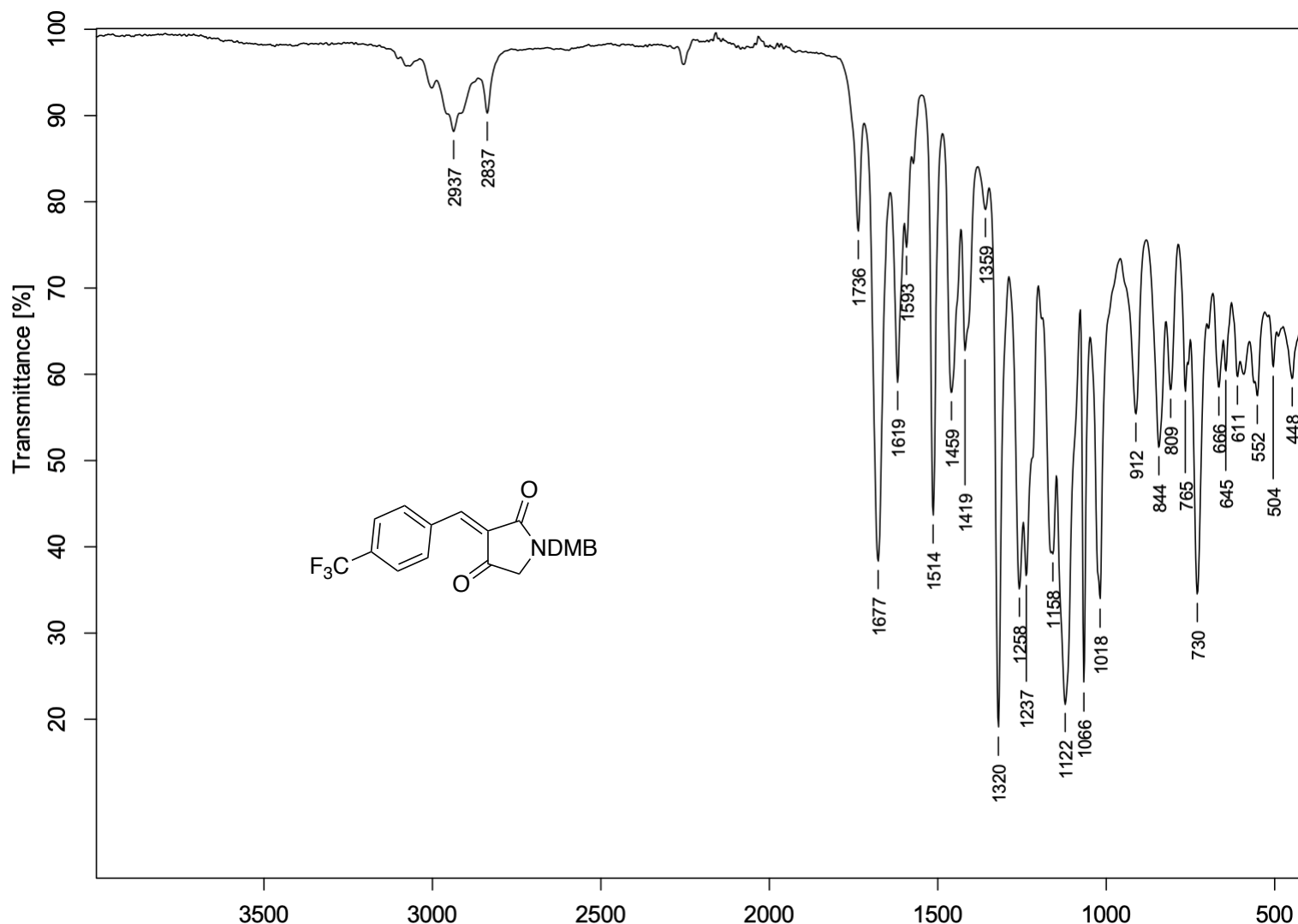


Figure A.55. FTIR (neat) alkene 2.66

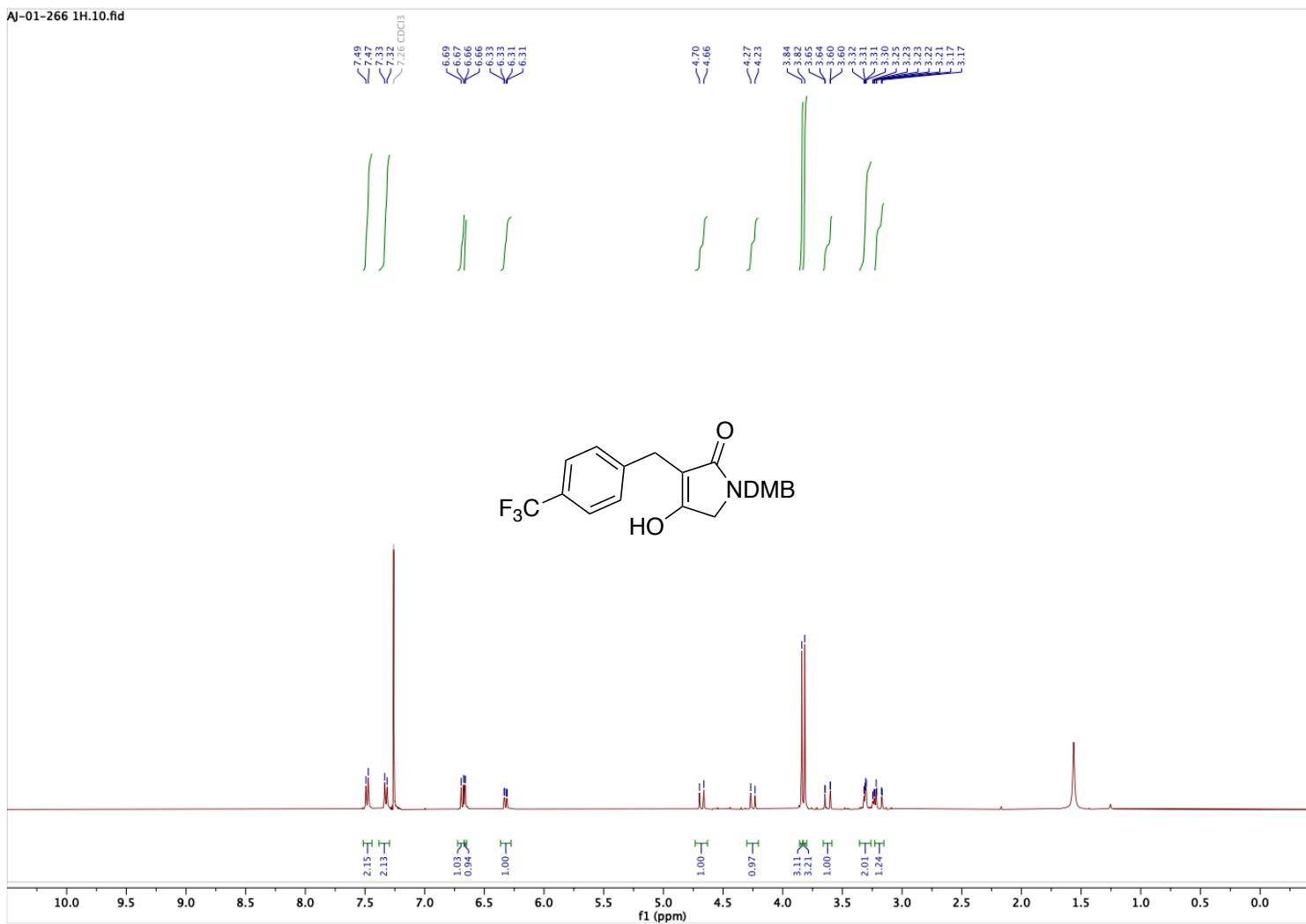


Figure A.56. ¹H NMR (400 MHz, CDCl₃) tetrameric acid **2.67**

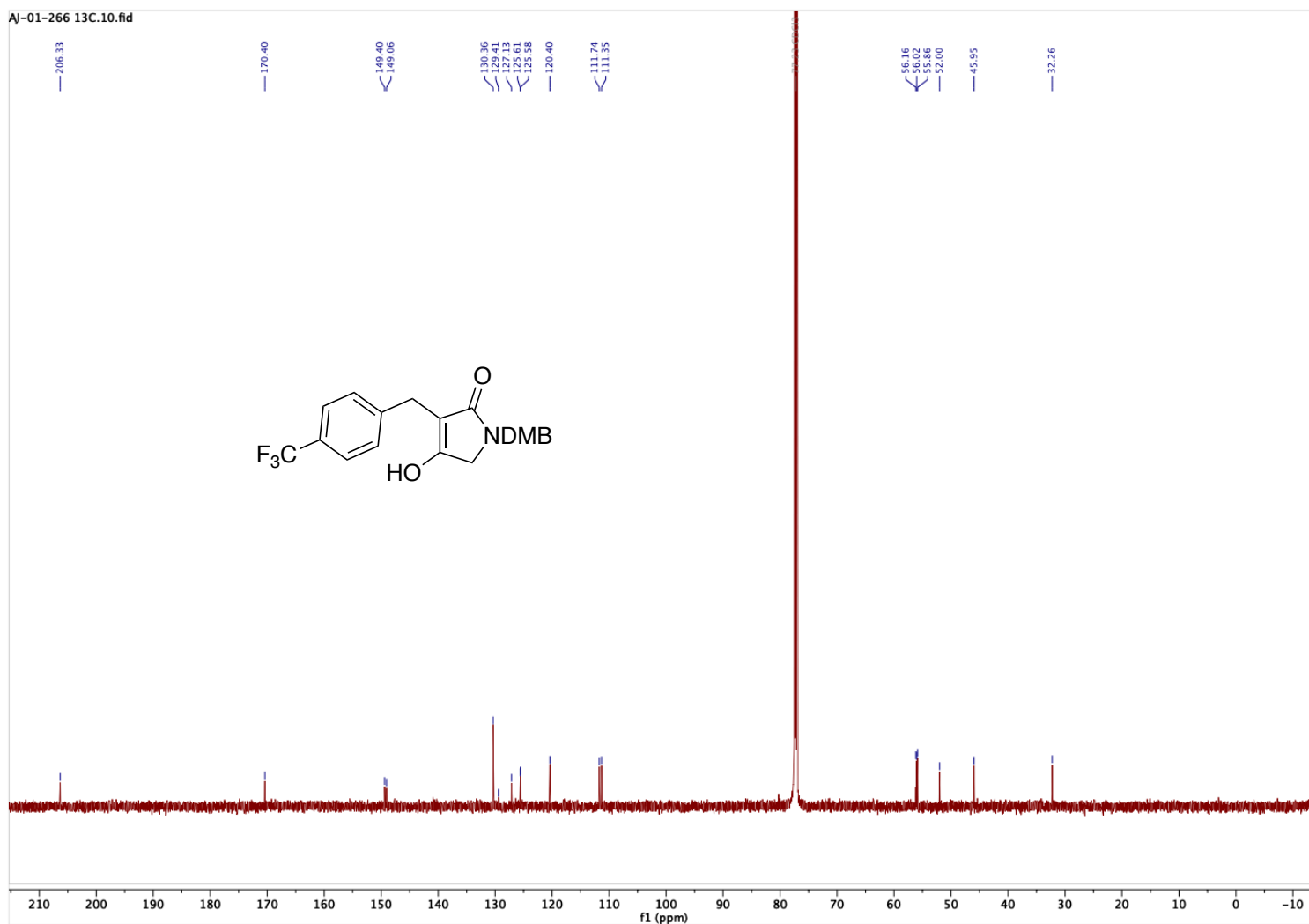


Figure A.57. ¹³C NMR (151 MHz, CDCl₃) tetramic acid **2.67**

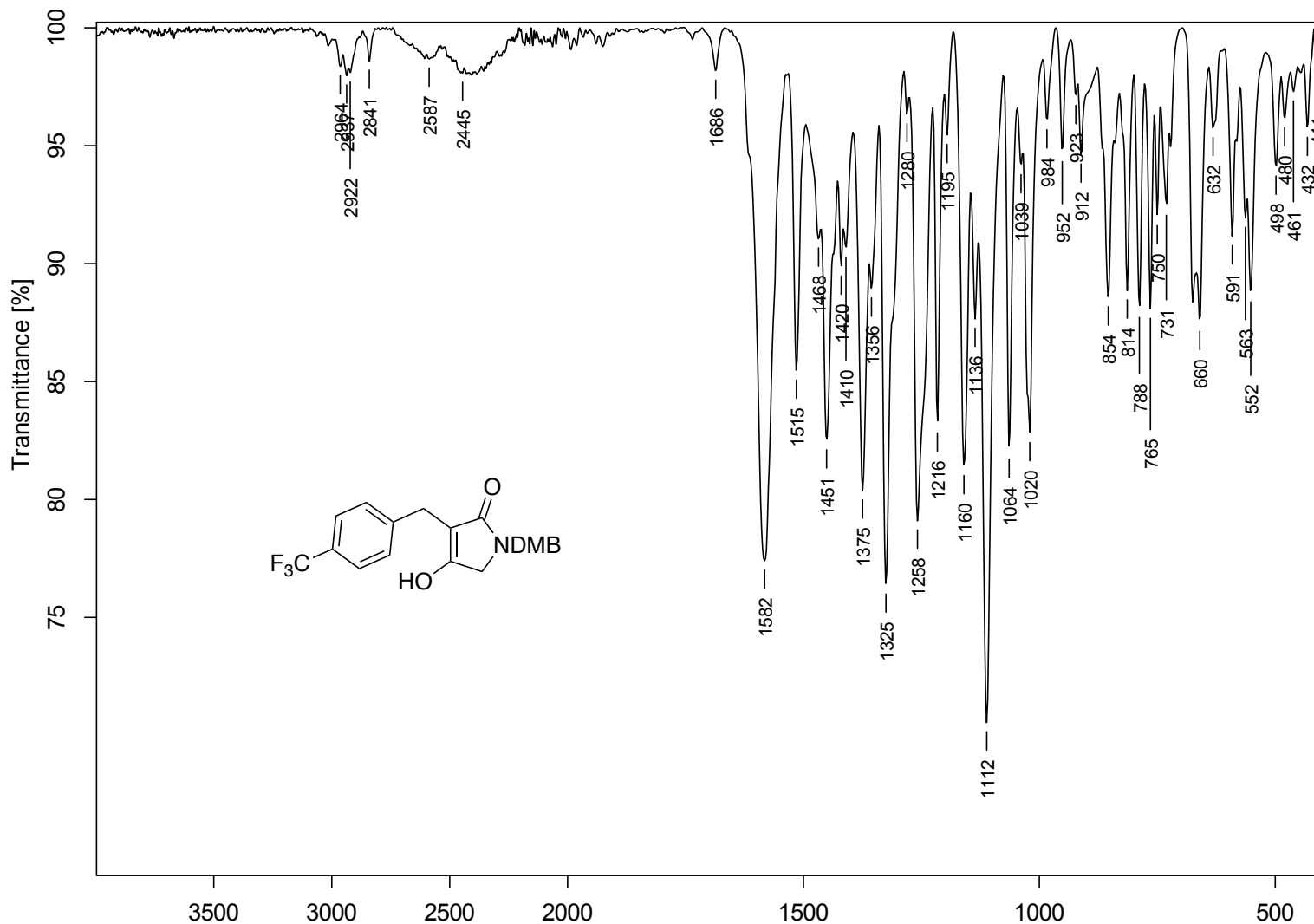


Figure A.58. FTIR (neat) tetramic acid 2.67

AJ-01-050-CF3oxime-repurif-1H-CDCl₃.10.fid

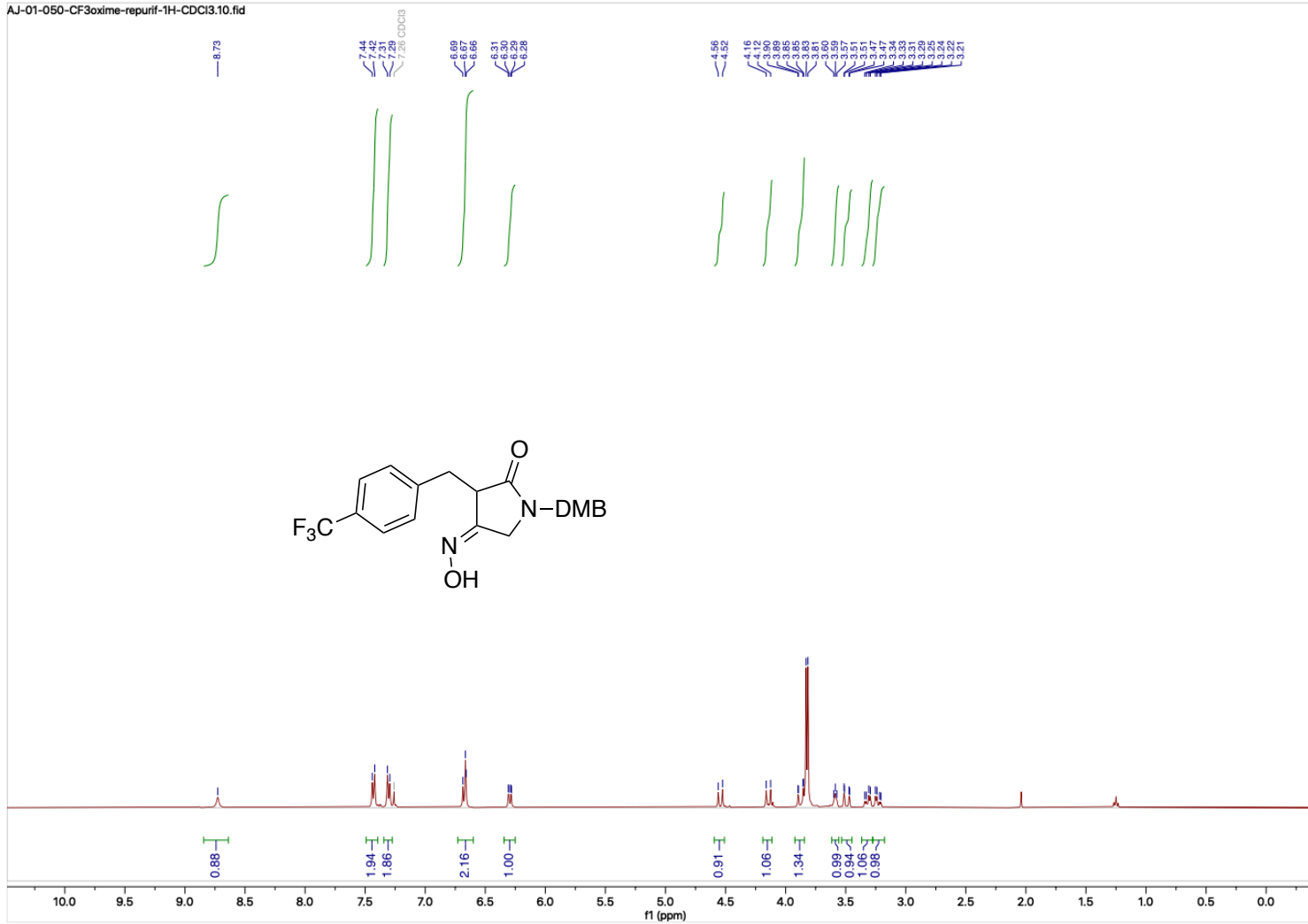


Figure A.59. ¹H NMR (600 MHz, CDCl₃) oxime 2.68

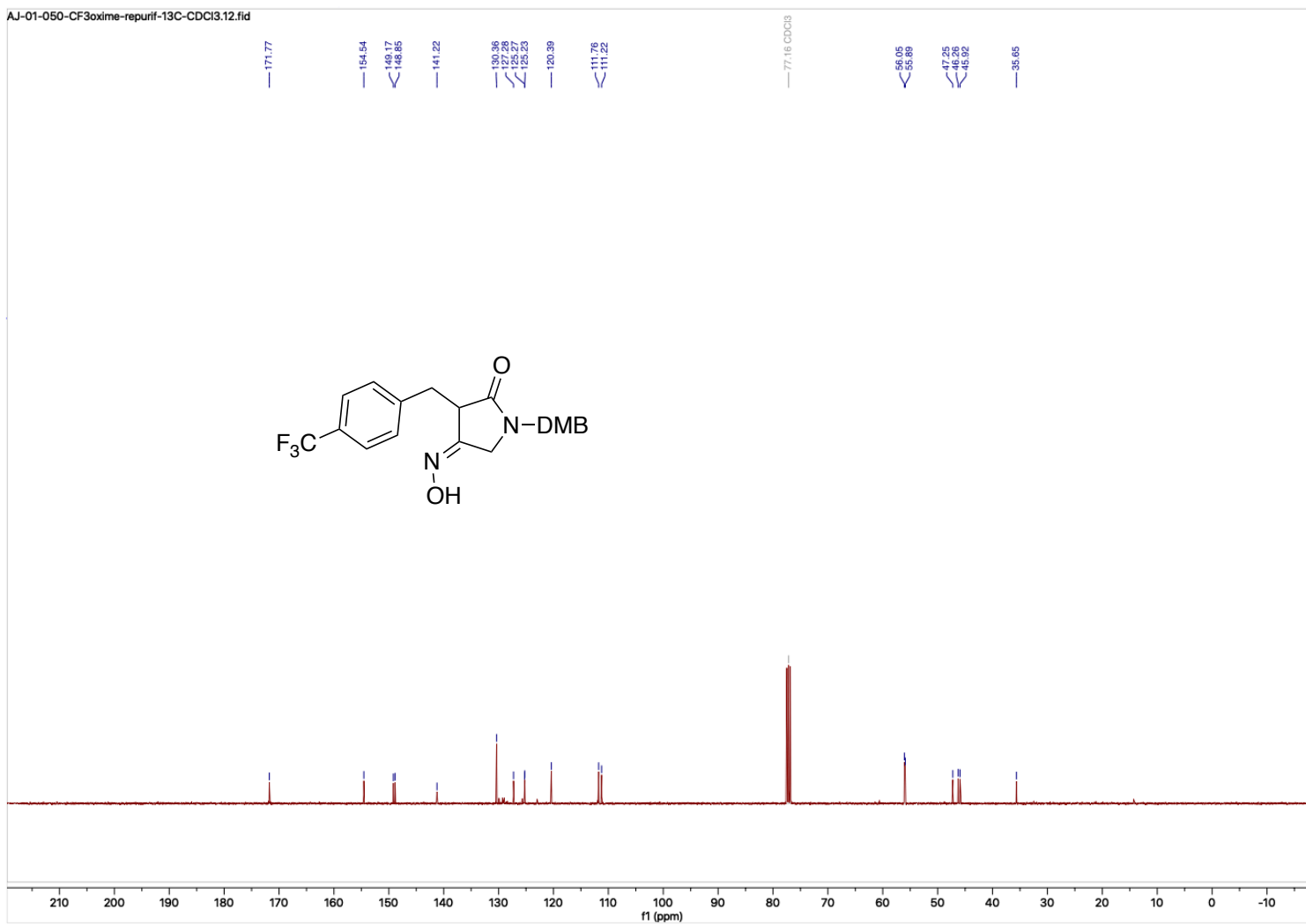


Figure A.60. ¹³C NMR (151 MHz, CDCl₃) oxime **2.68**

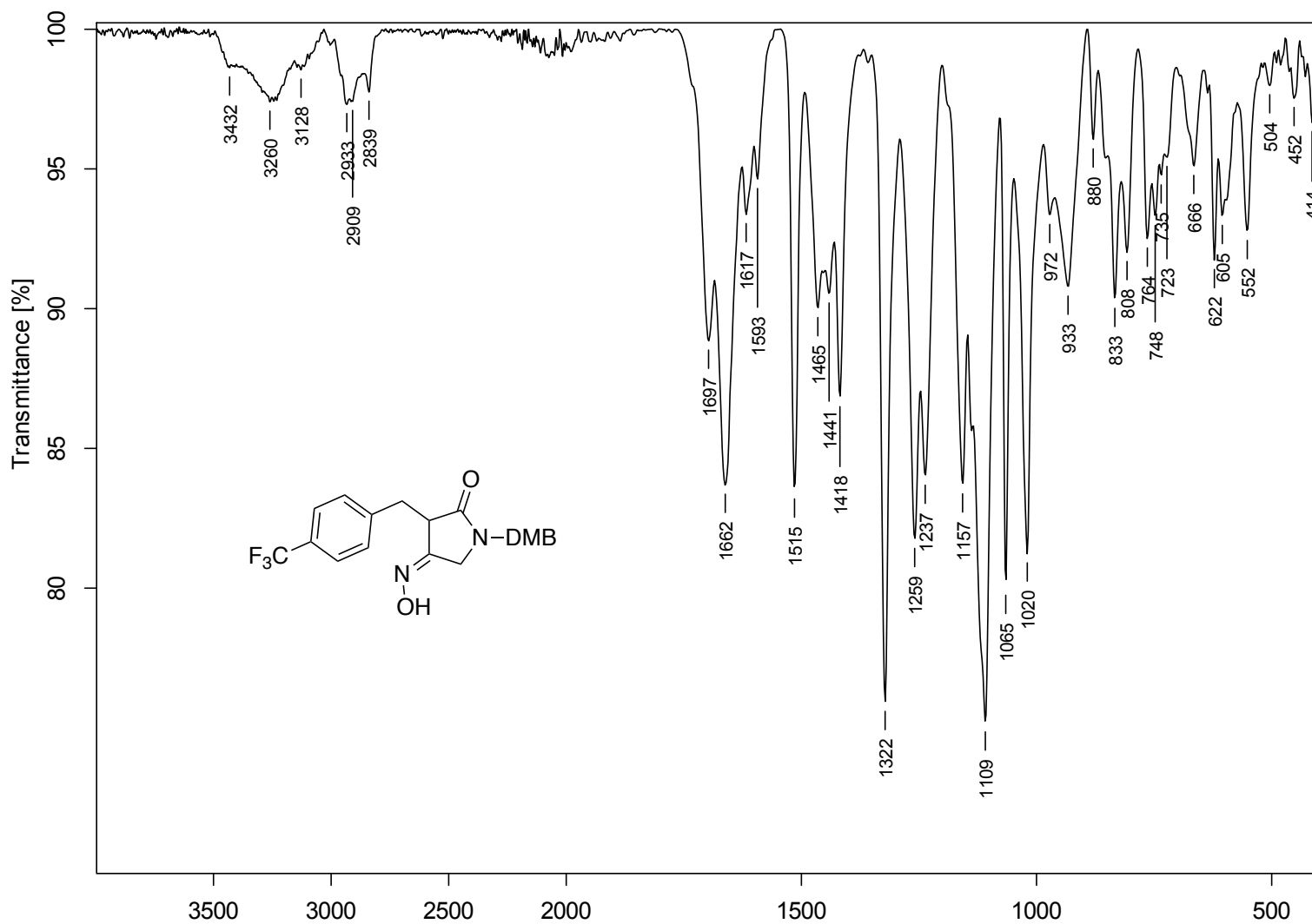


Figure A.61. FTIR (neat) oxime **2.68**

AJ-05-215-1H-CDCl₃_PROTON_001
AJ-05-215-1H-CDCl₃

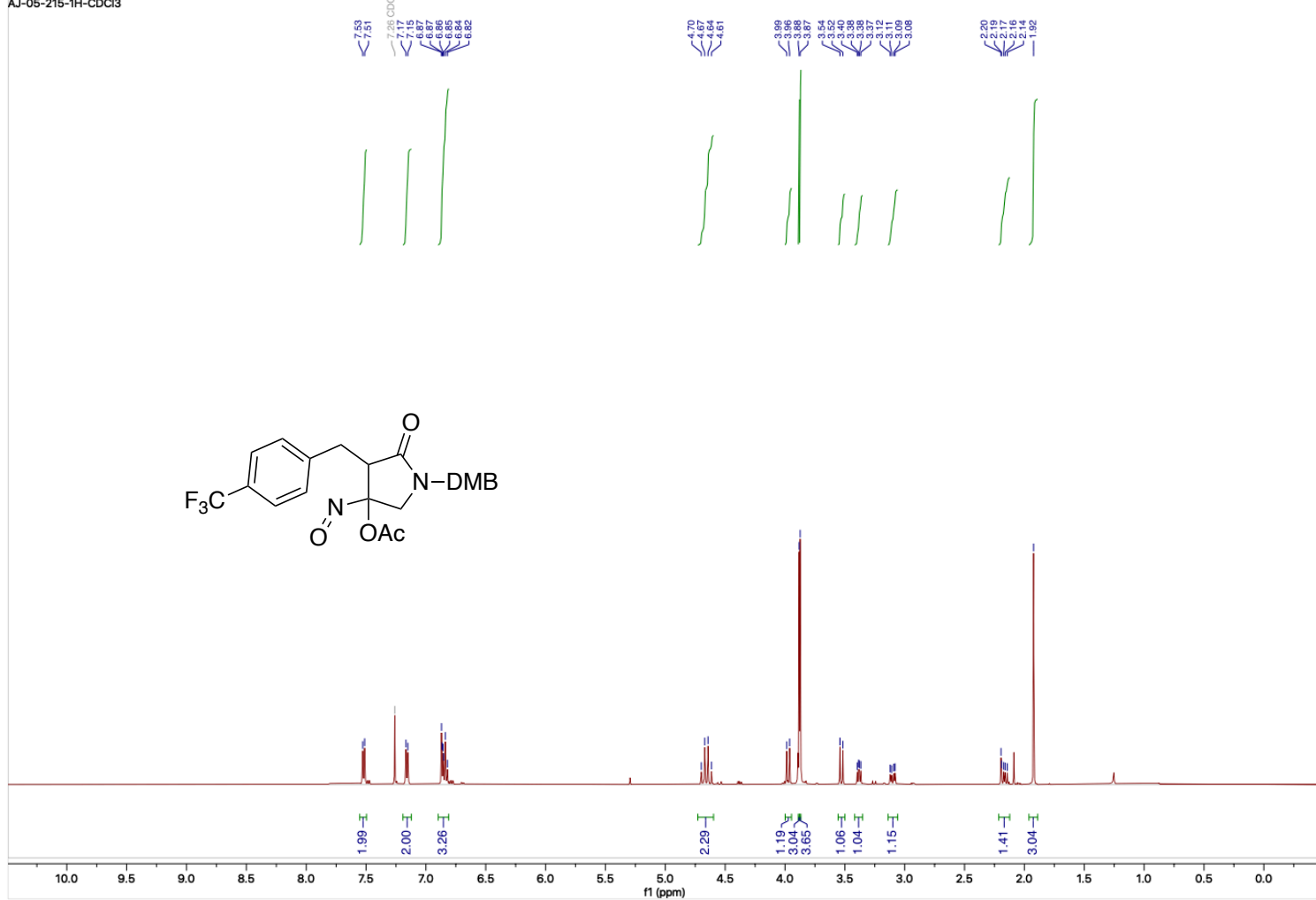


Figure A.62. ¹H NMR (500 MHz, CDCl₃) crude acyloxy nitroso **2.69**

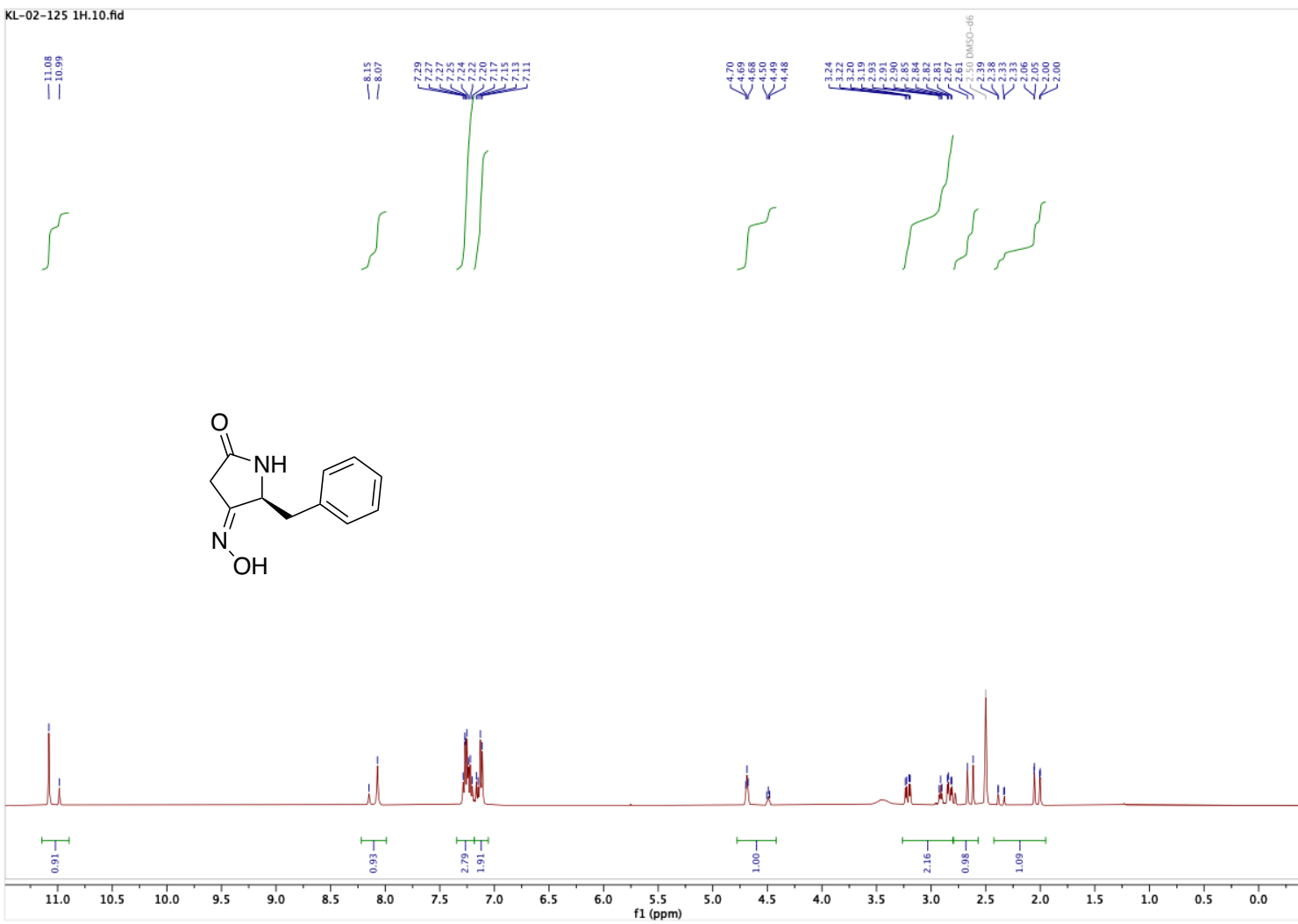


Figure A.63. ^1H NMR (600 MHz, DMSO) oxime **2.71**

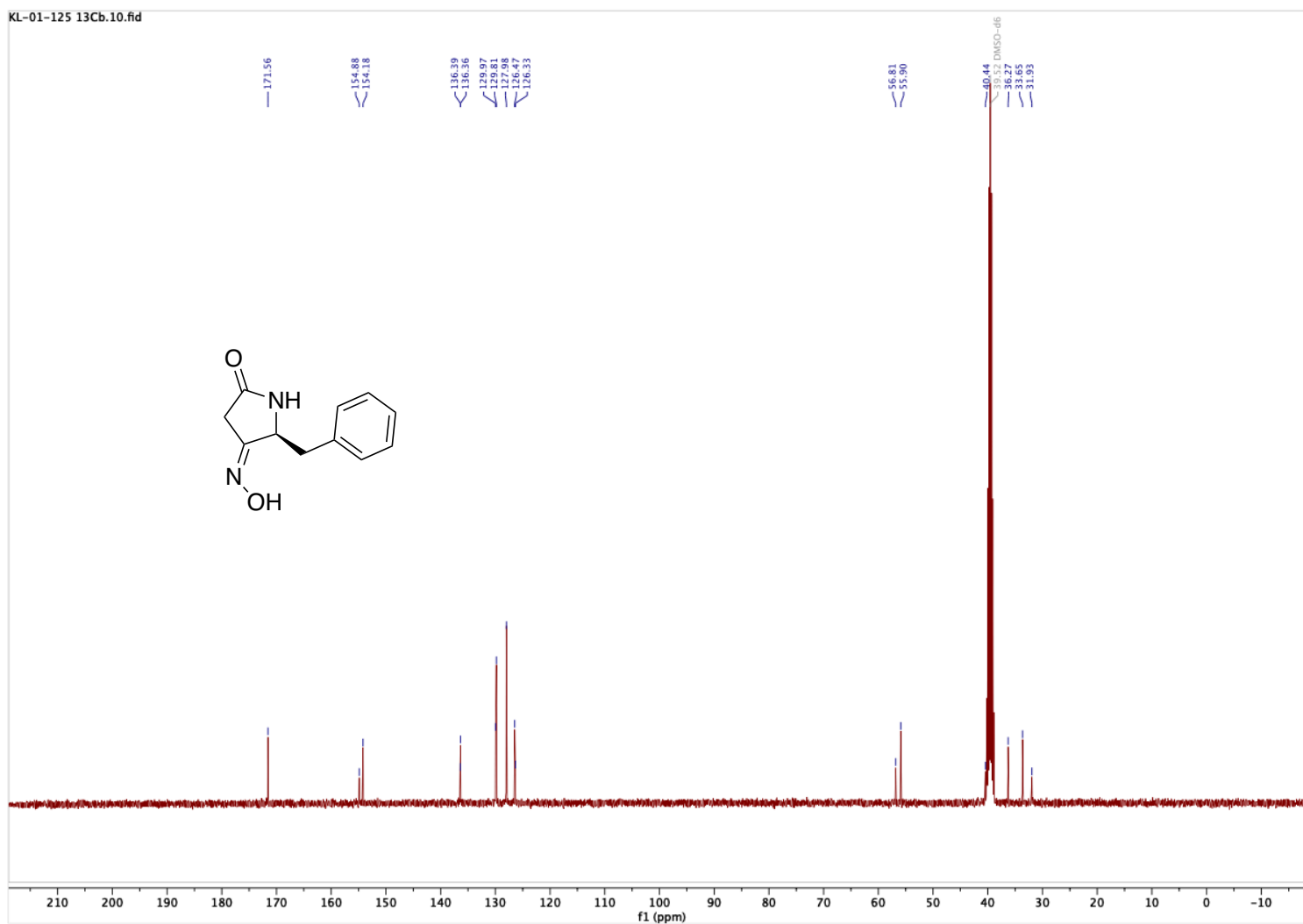


Figure A.64. ^{13}C NMR (600 MHz, DMSO) oxime 2.71

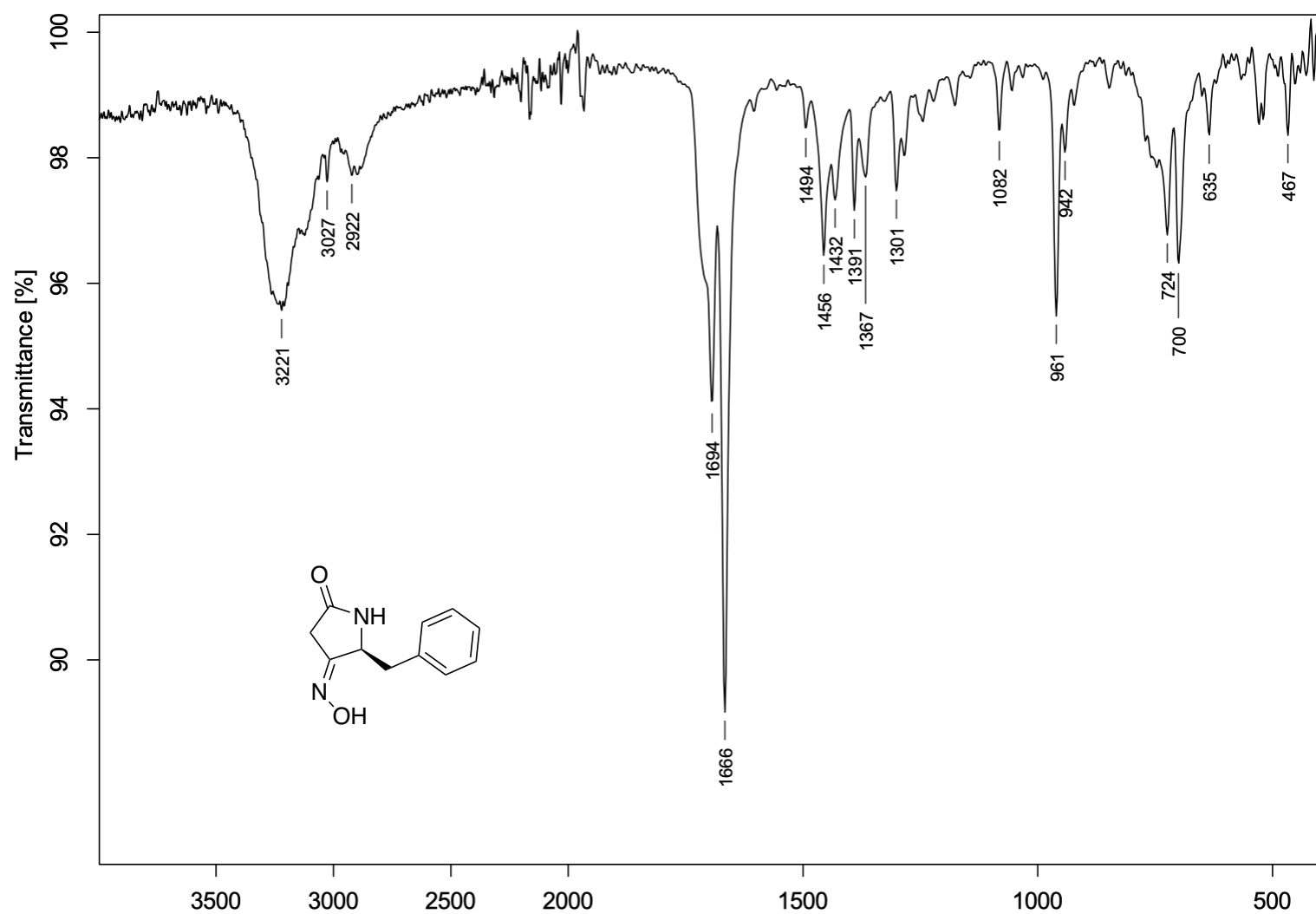


Figure A.65. FTIR (neat) oxime 2.71

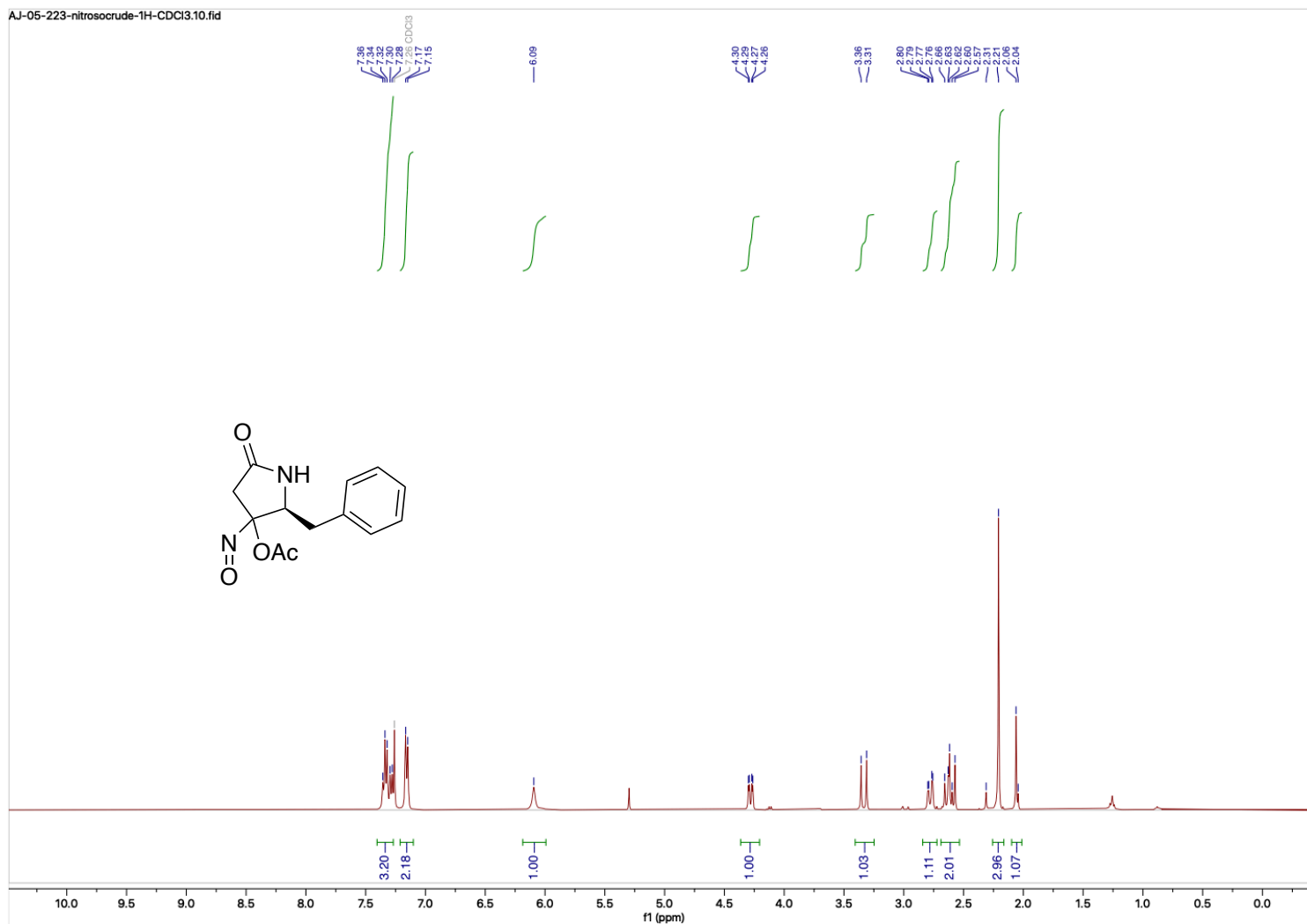


Figure A.66. ¹H NMR (400 MHz, CDCl₃) crude acyloxy nitroso **2.72**

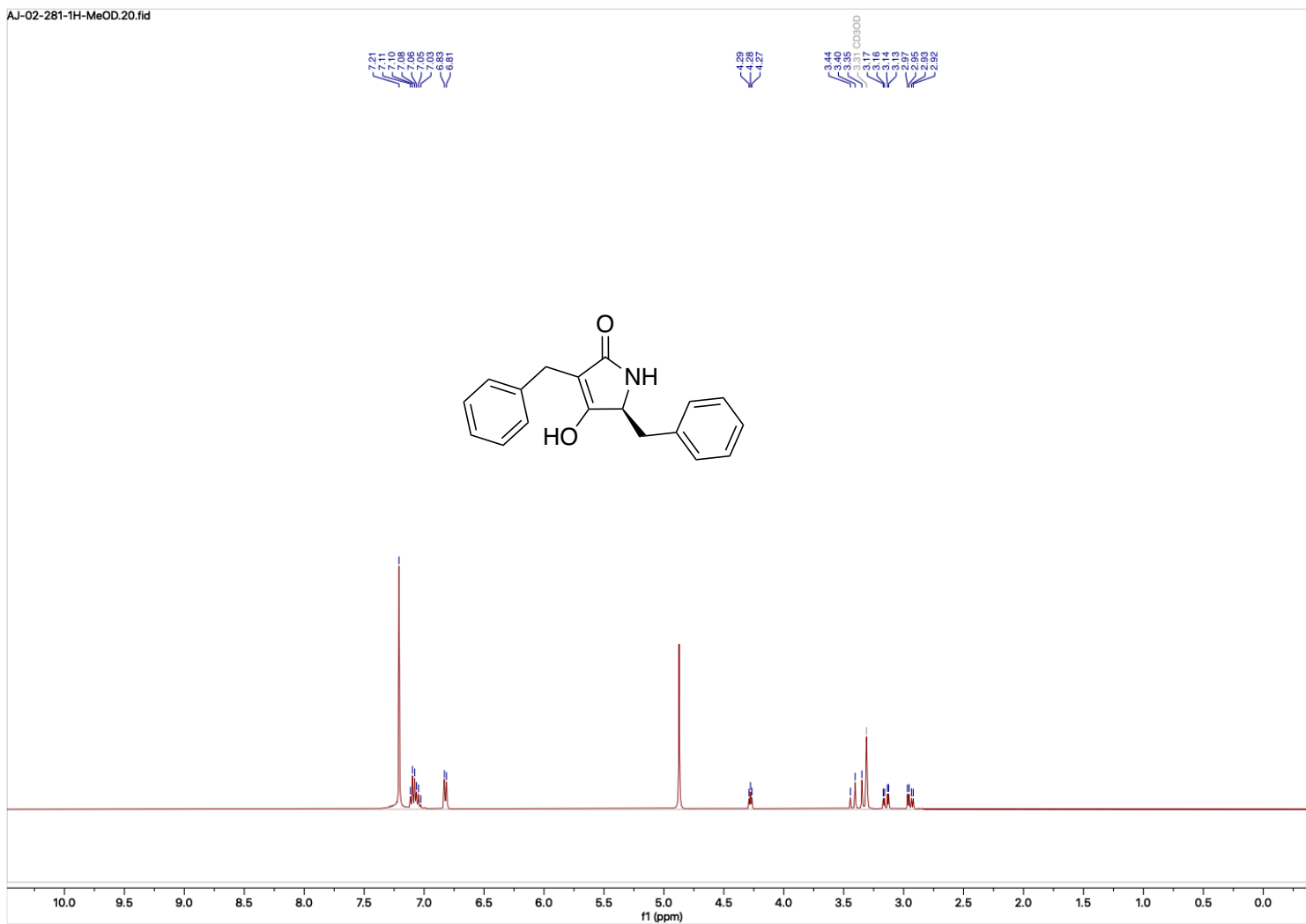


Figure A.67. ^1H NMR (400 MHz, MeOD) known tetrameric acid **2.73**

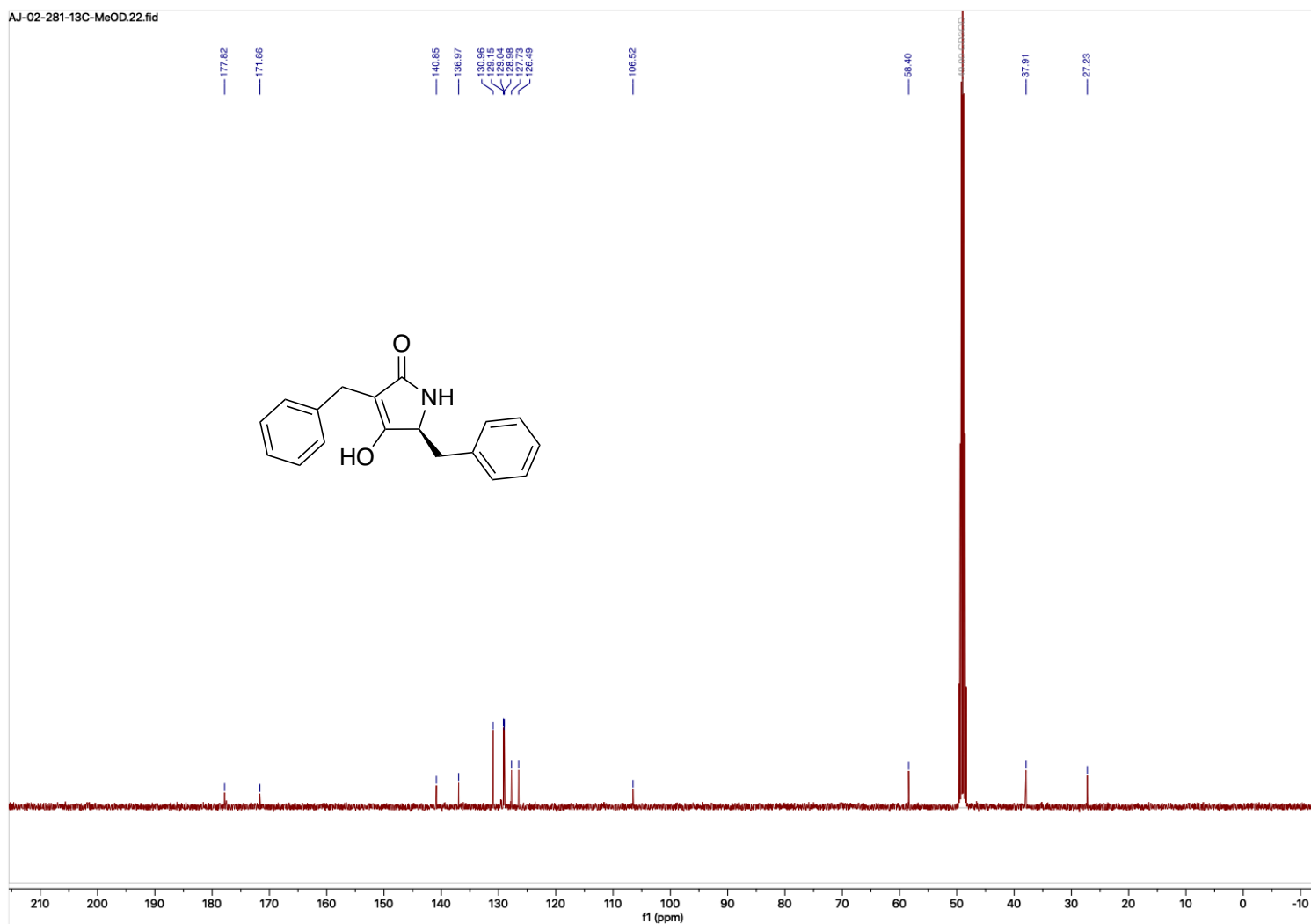


Figure A.68. ^{13}C NMR (101 MHz, MeOD) known tetramic acid **2.73**

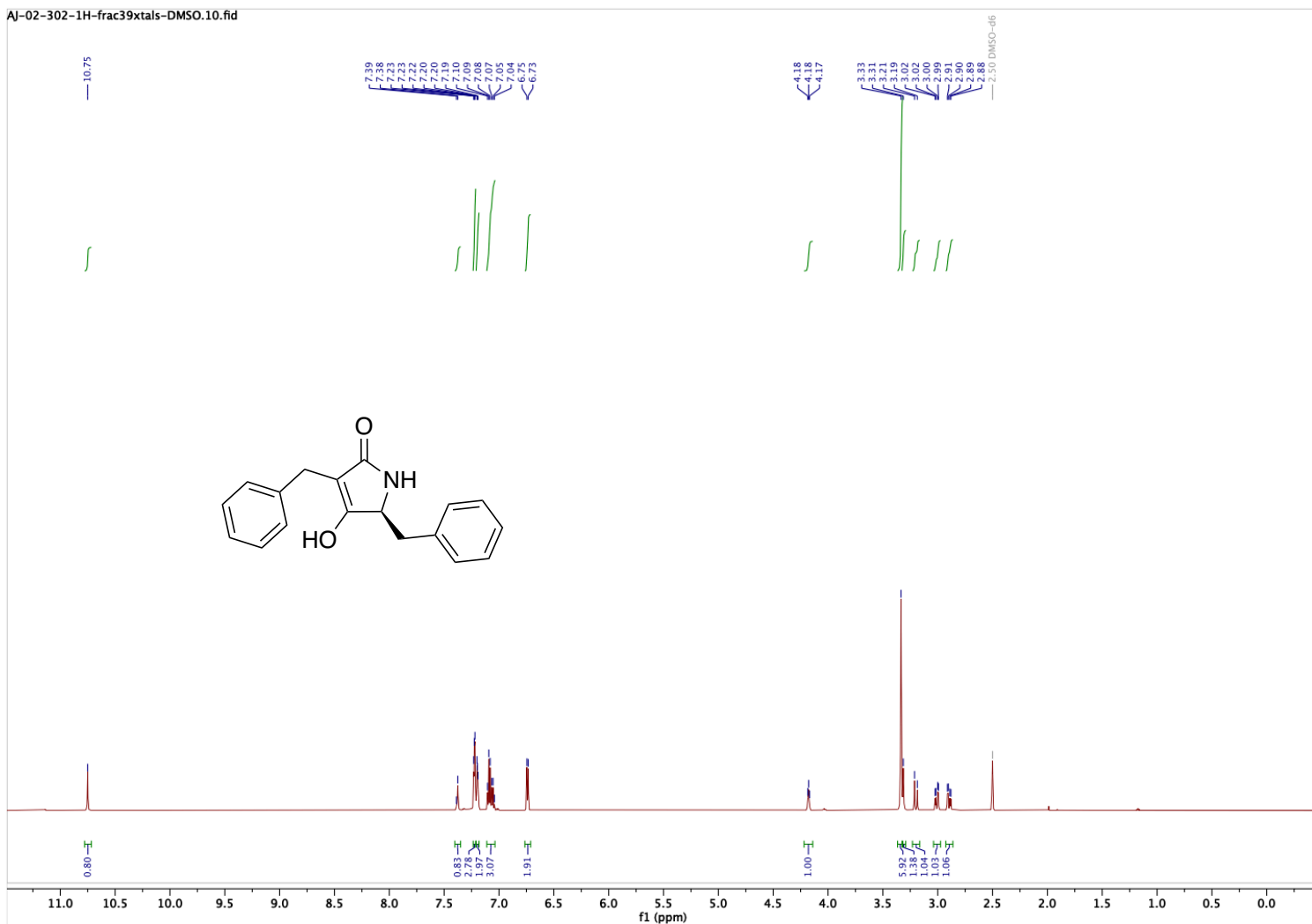


Figure A.69. ^1H NMR (600 MHz, DMSO) known tetrameric acid **2.73**

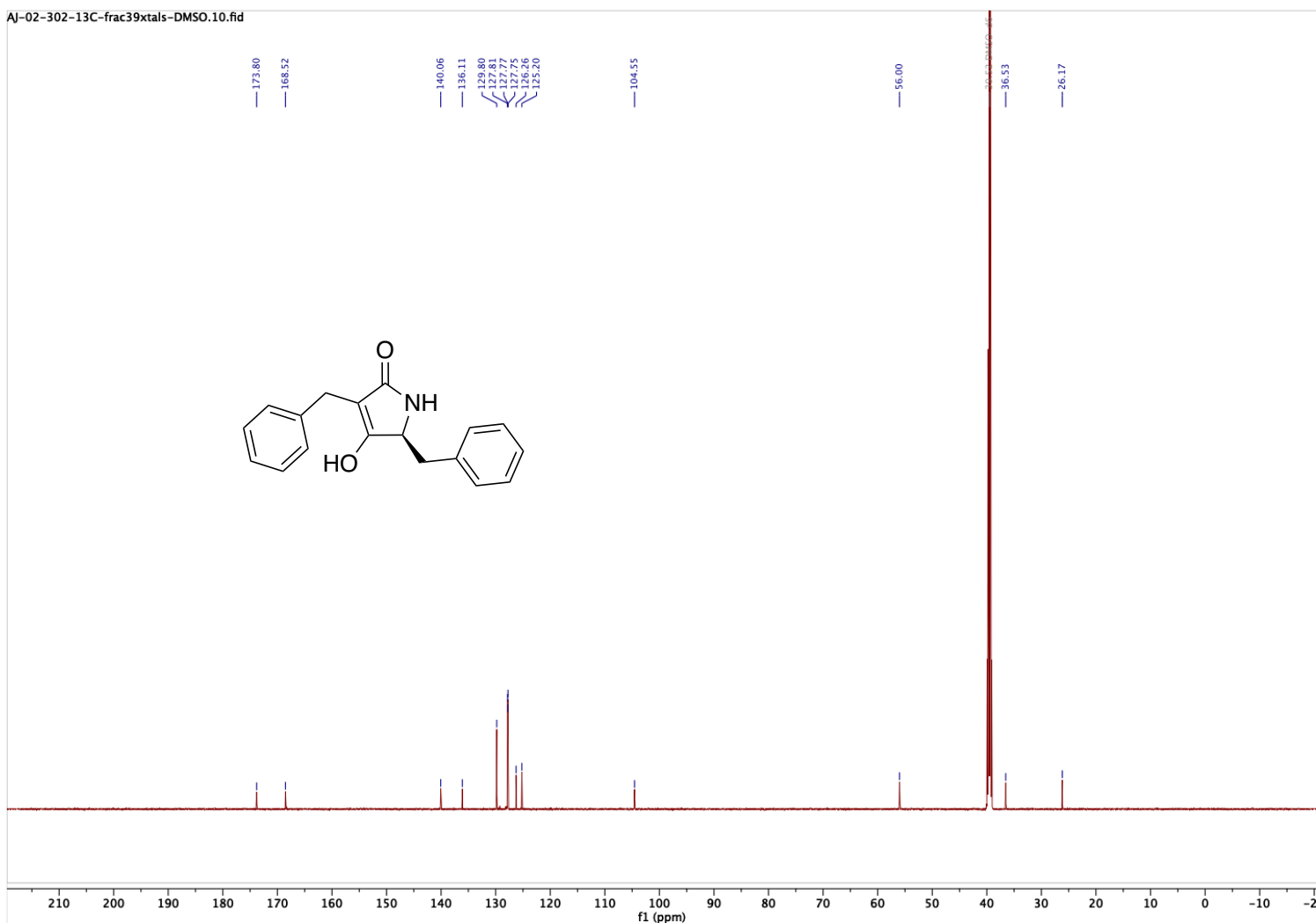


Figure A.70. ¹³C NMR (151 MHz, DMSO) known tetrameric acid **2.73**

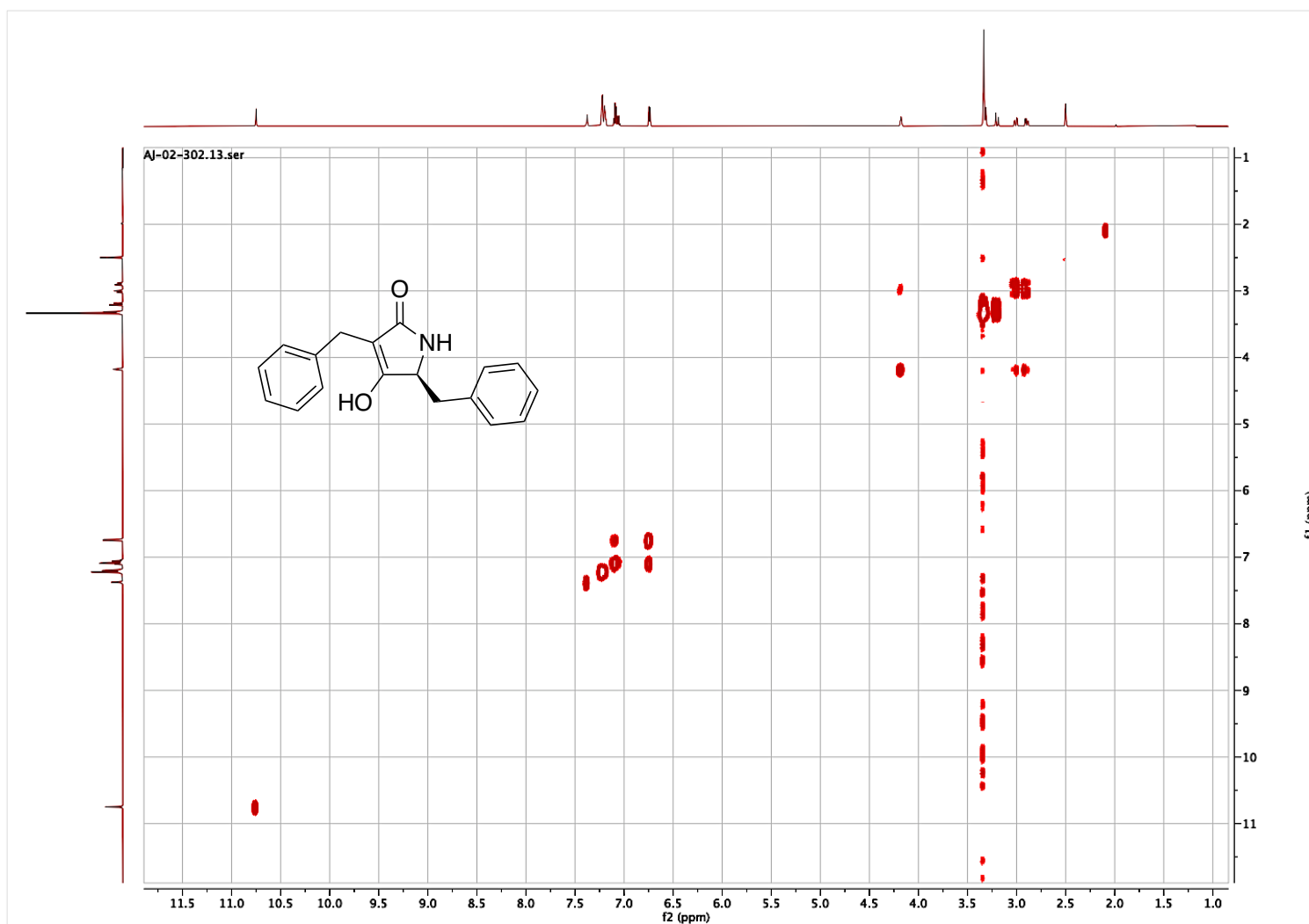


Figure A.71. COSY (600 MHz, DMSO) known tetramic acid **2.73**

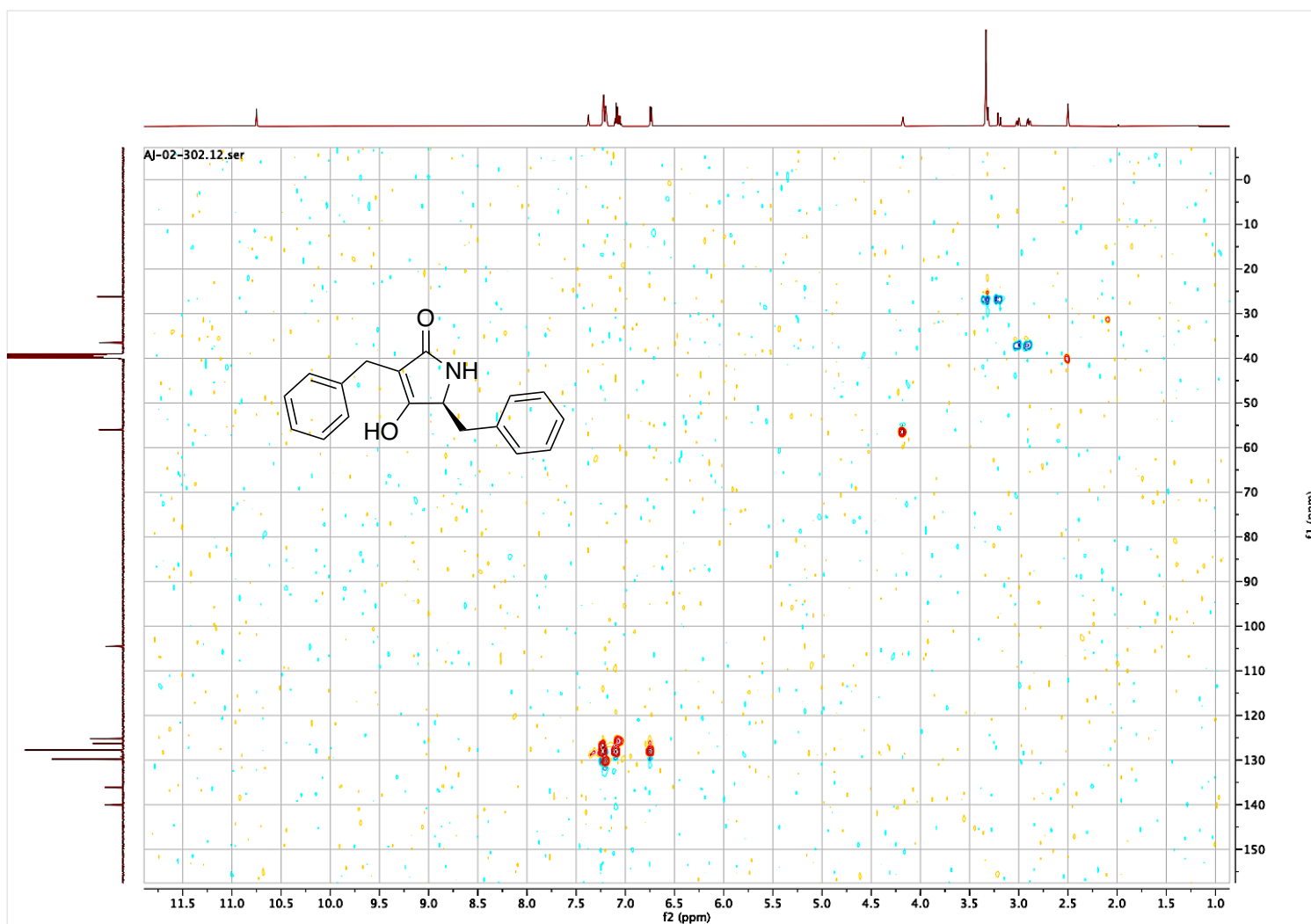


Figure A.72. HSQC (600 MHz, 151 MHz, DMSO; edited: CH/CH₃ = red, CH₂ = blue) known tetrameric acid **2.73**

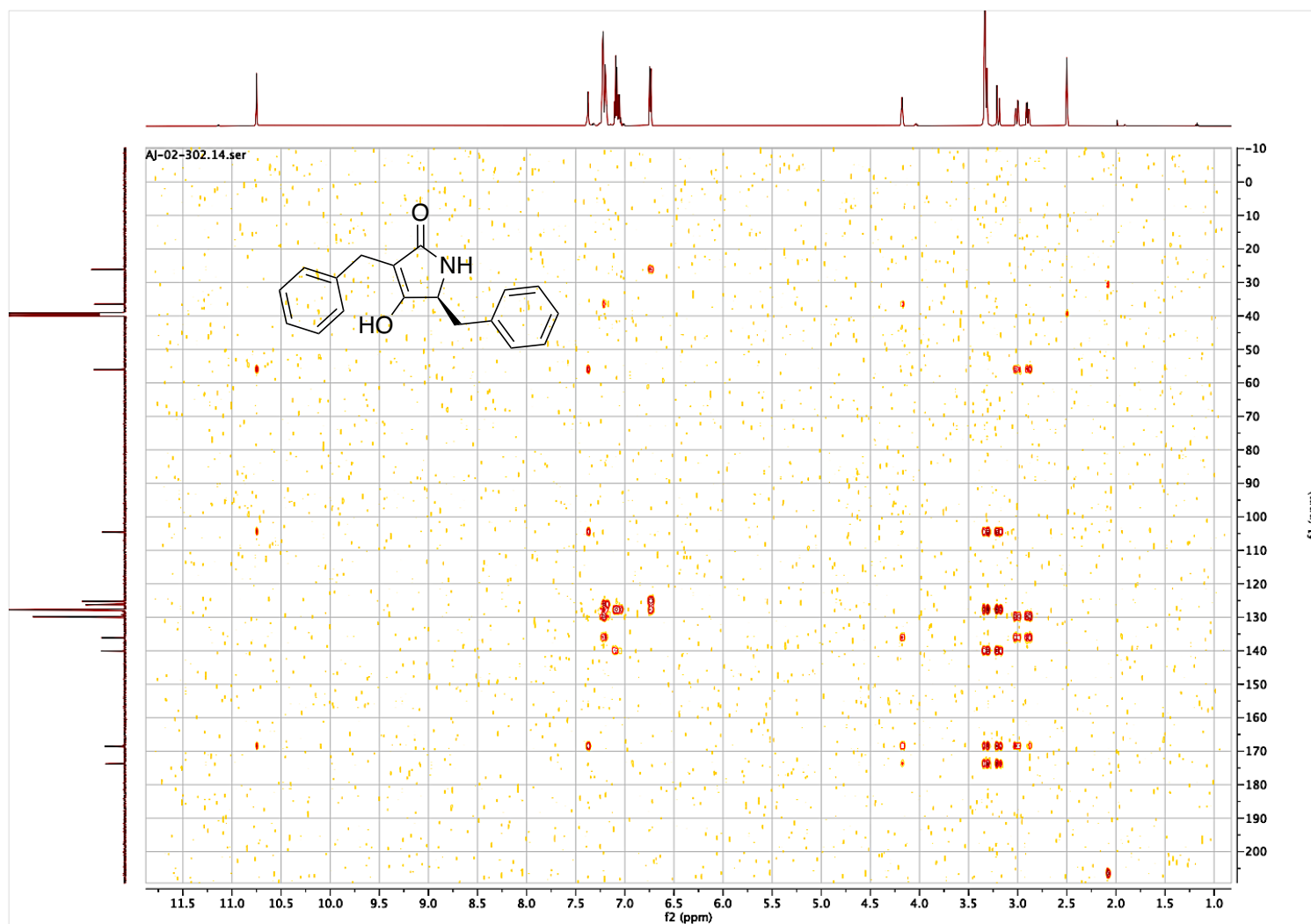


Figure A.73. HMBC (600 MHz, 151 MHz, DMSO) known tetramic acid **2.73**

APPENDIX B
Spectral Data for Chapter Three

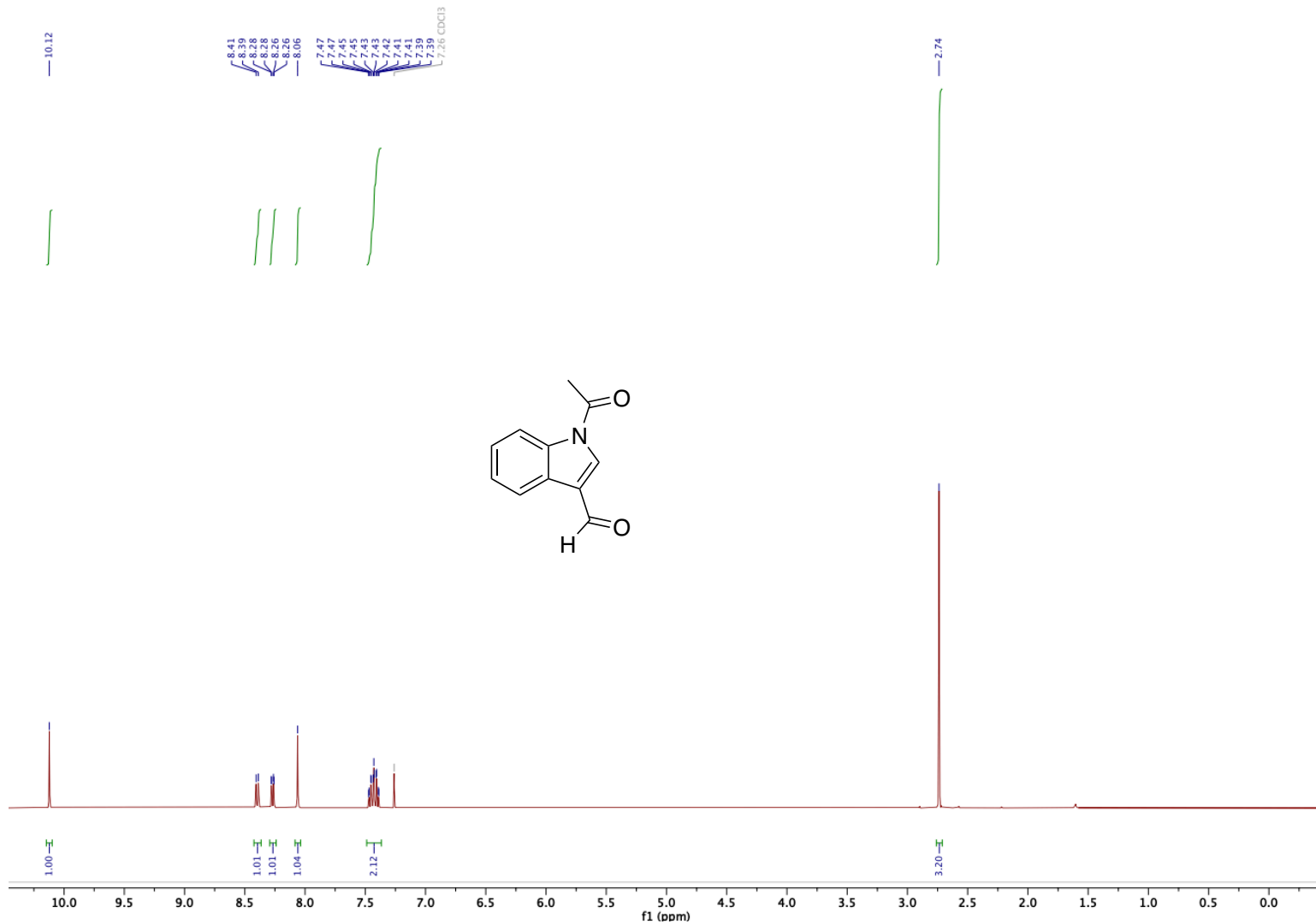


Figure B.01. ^1H NMR (400 MHz, CDCl_3) known indole **3.08**

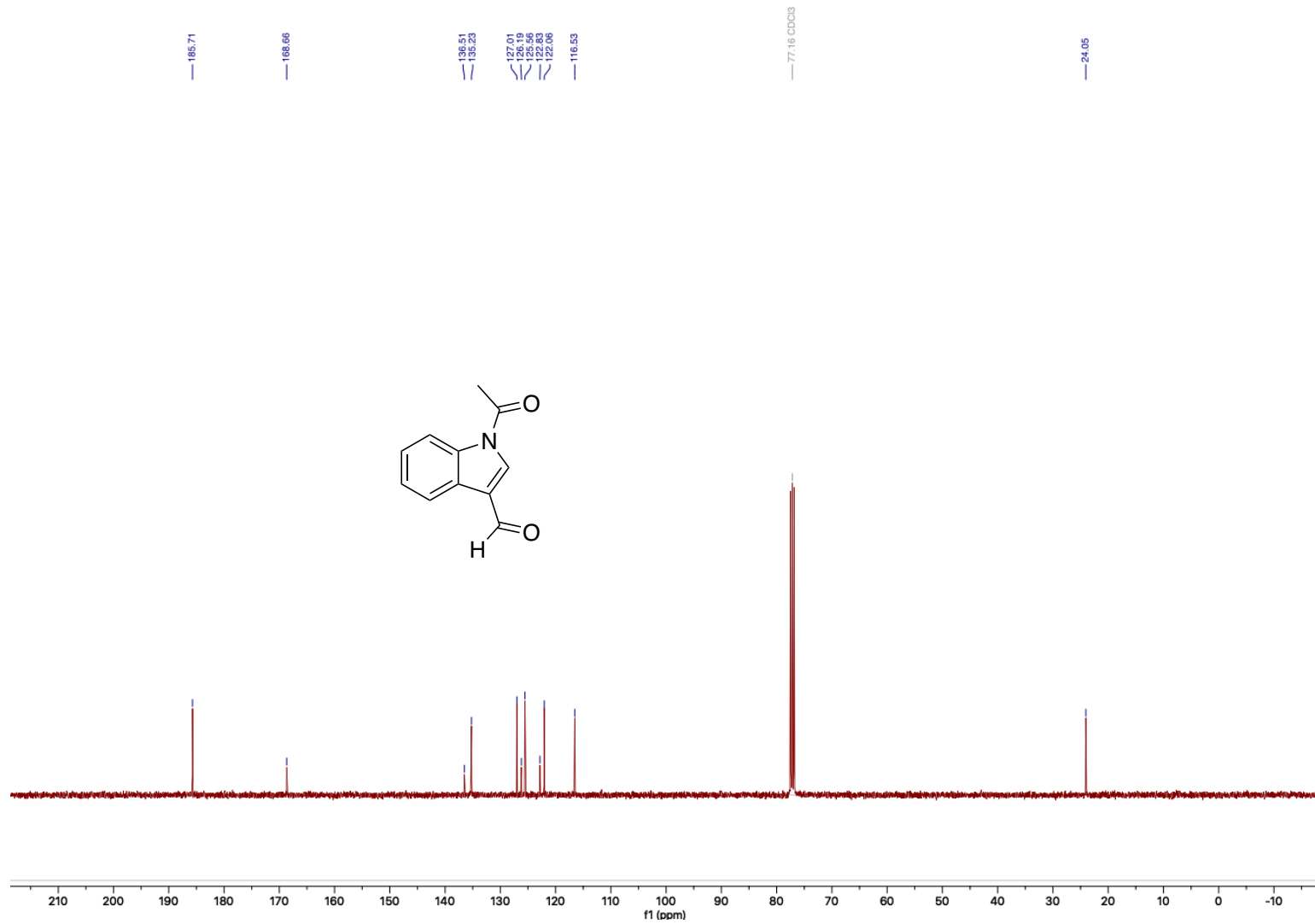


Figure B.02. ^{13}C NMR (101 MHz, CDCl₃) known indole **3.08**

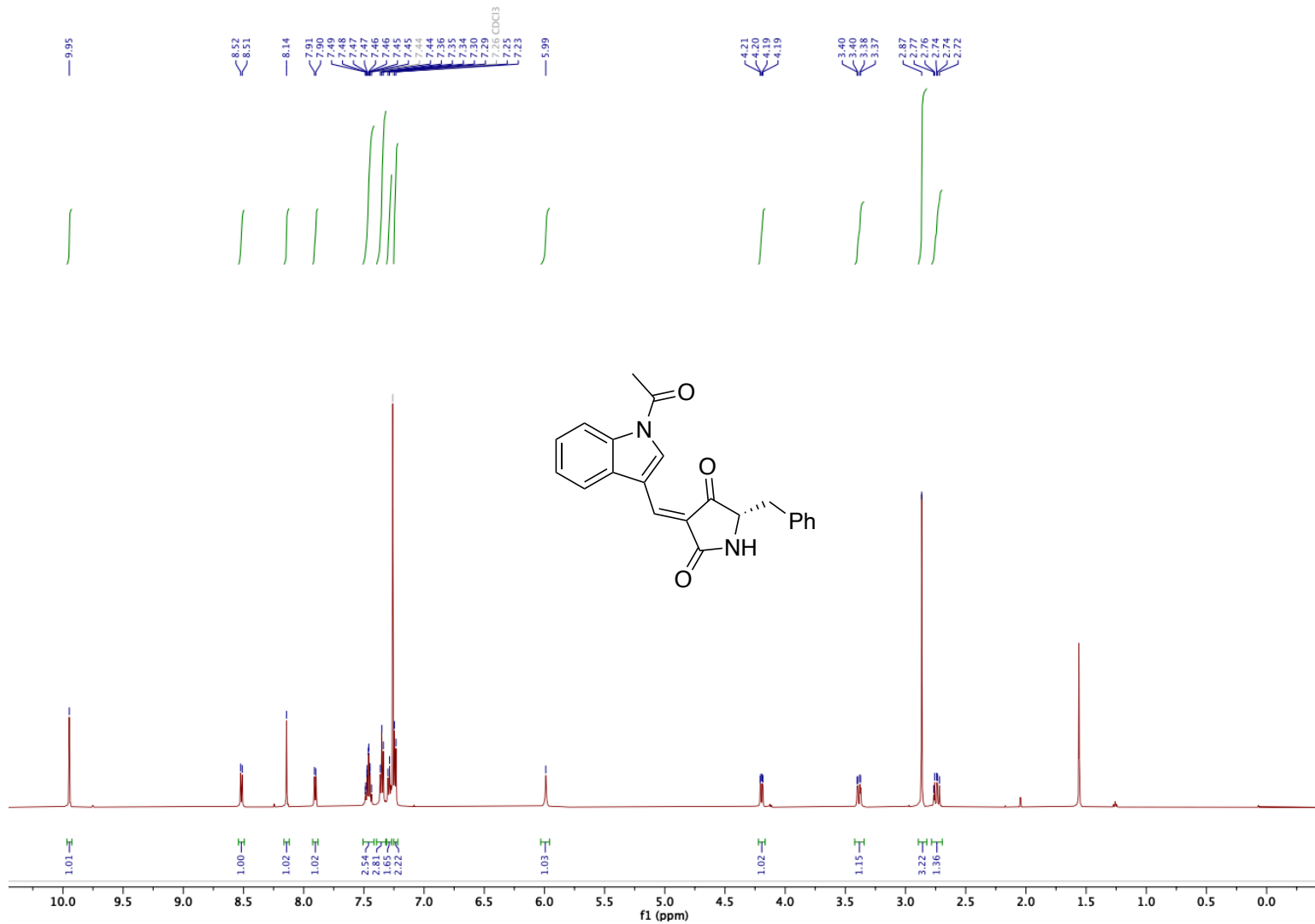


Figure B.03. ^1H NMR (600 MHz, CDCl_3) alkene 3.07

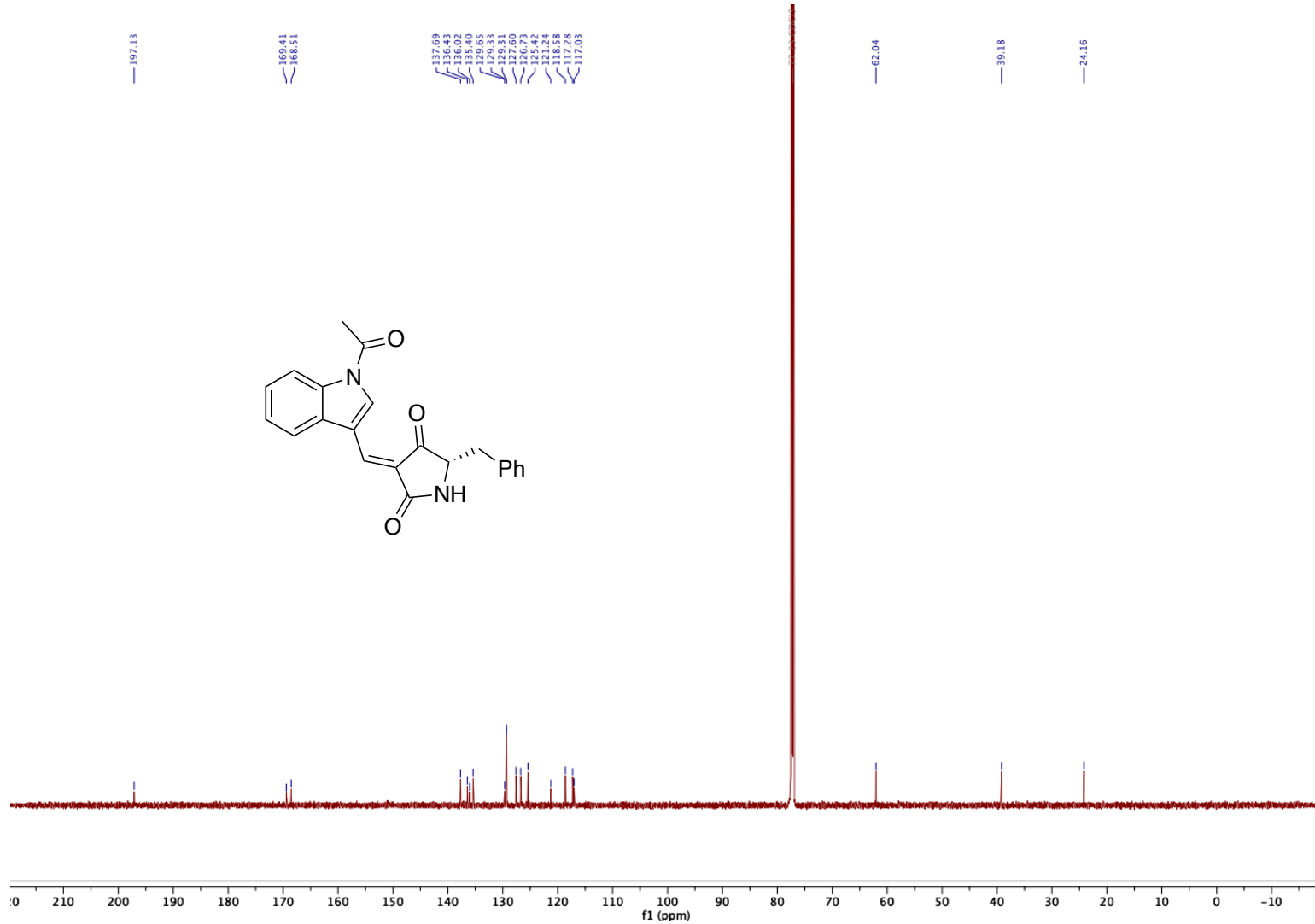


Figure B.04. ^{13}C NMR (151 MHz, CDCl_3) alkene 3.07

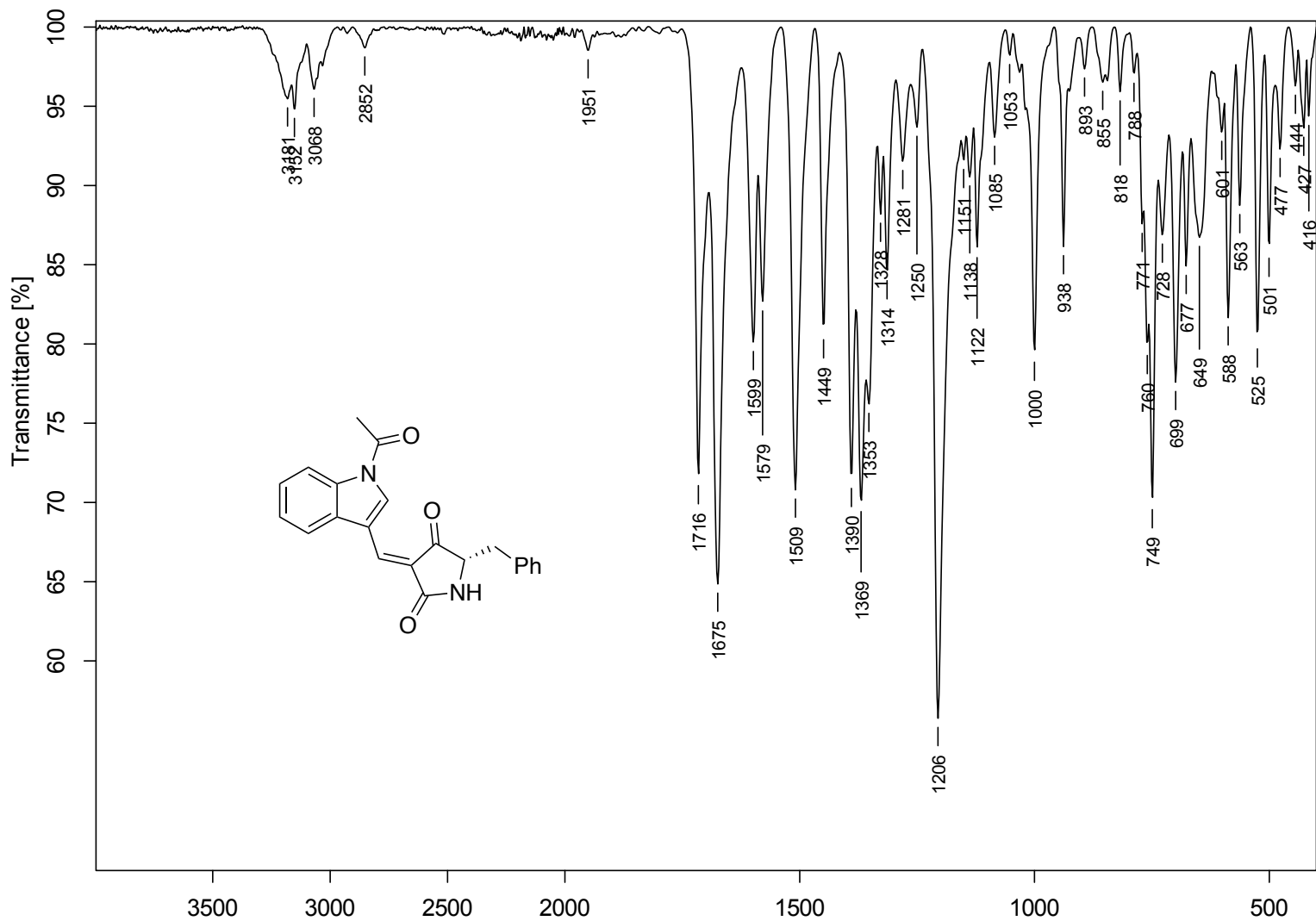


Figure B.05. IR (neat) alkene 3.07

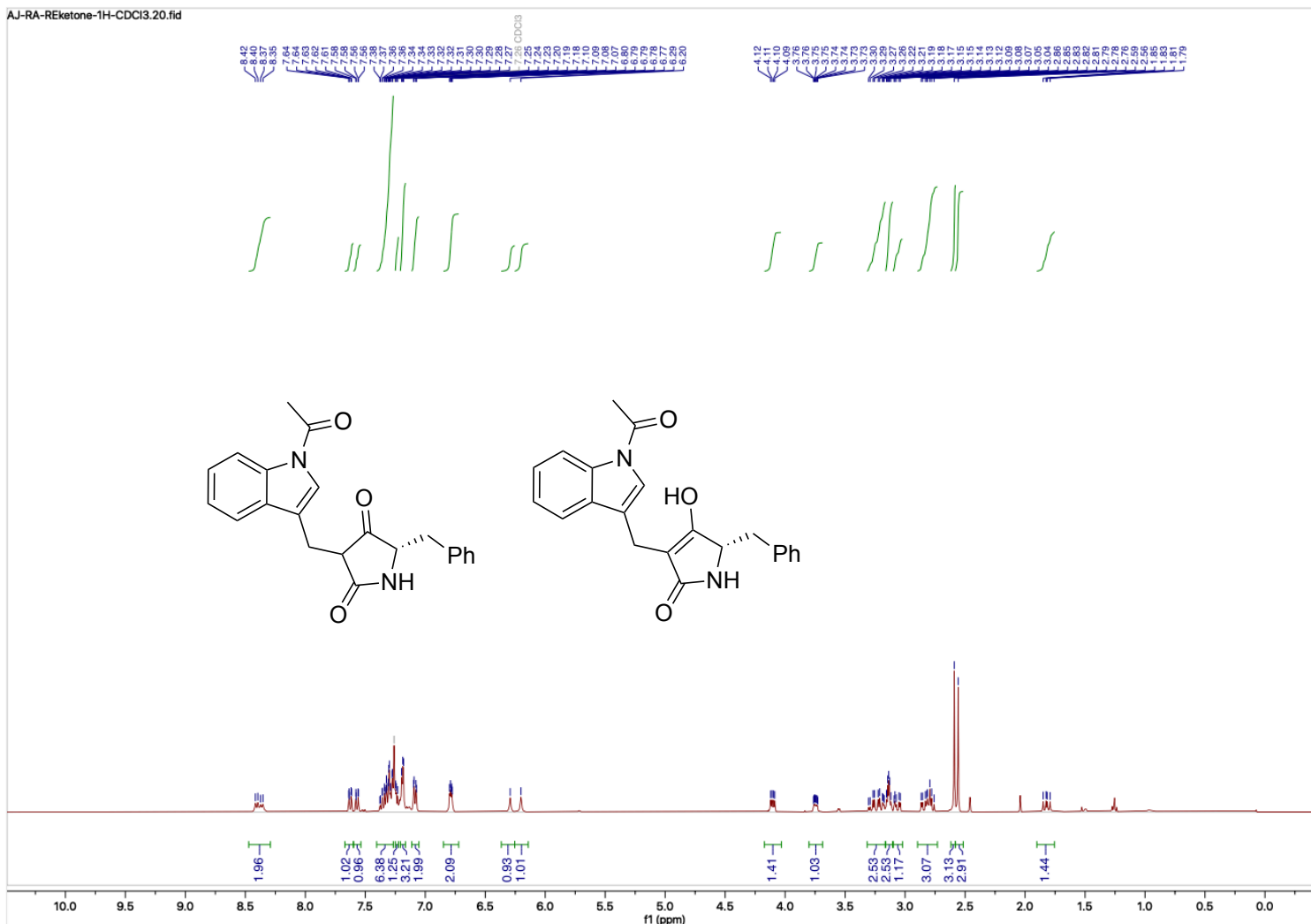


Figure B.06. ¹H NMR (400 MHz, CDCl₃) tetrameric acid **3.06**

AJ-RA-REketone-13C-CDCl₃.22.fid

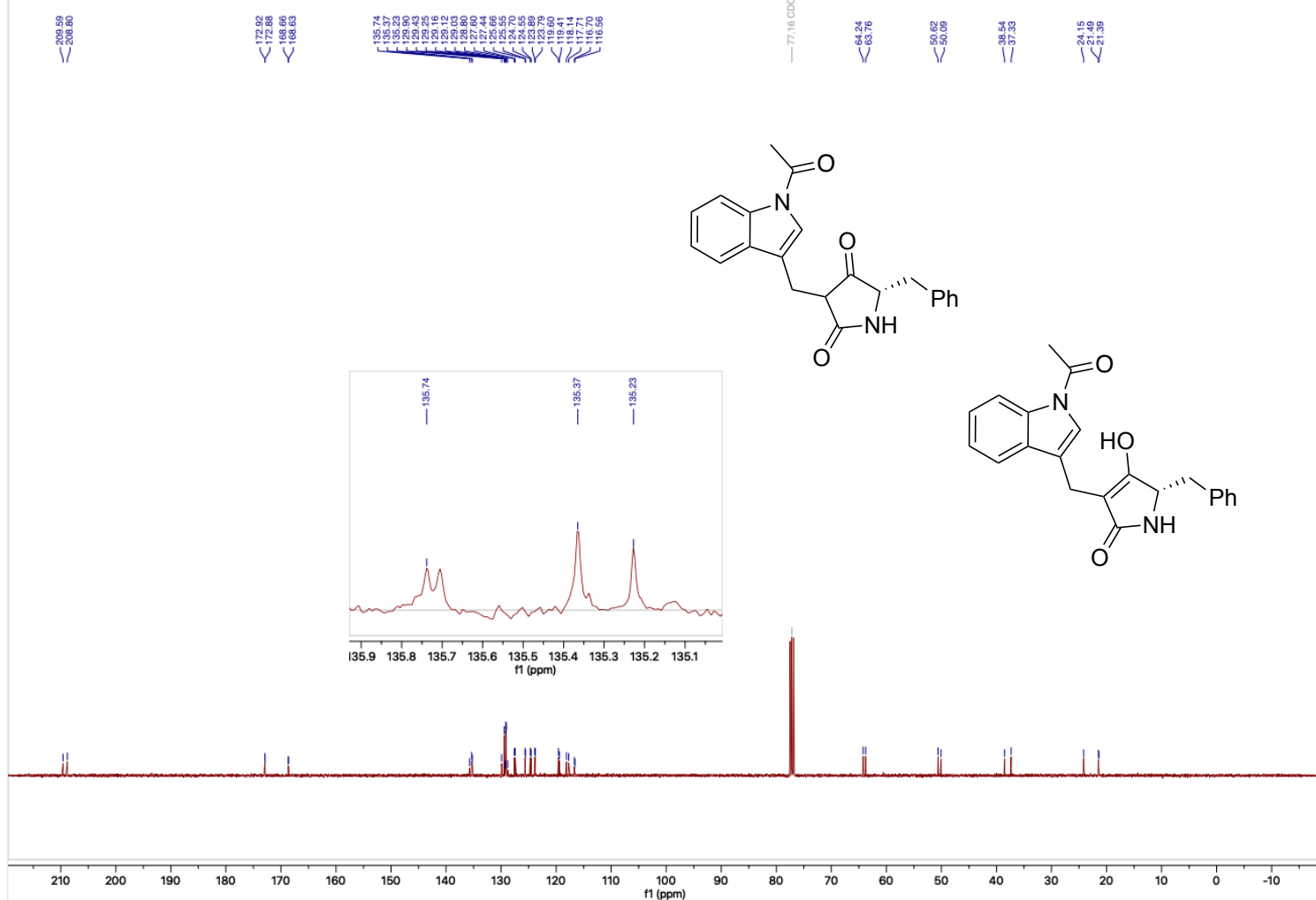


Figure B.07. ¹³C NMR (101 MHz, CDCl₃) tetramic acid **3.06**

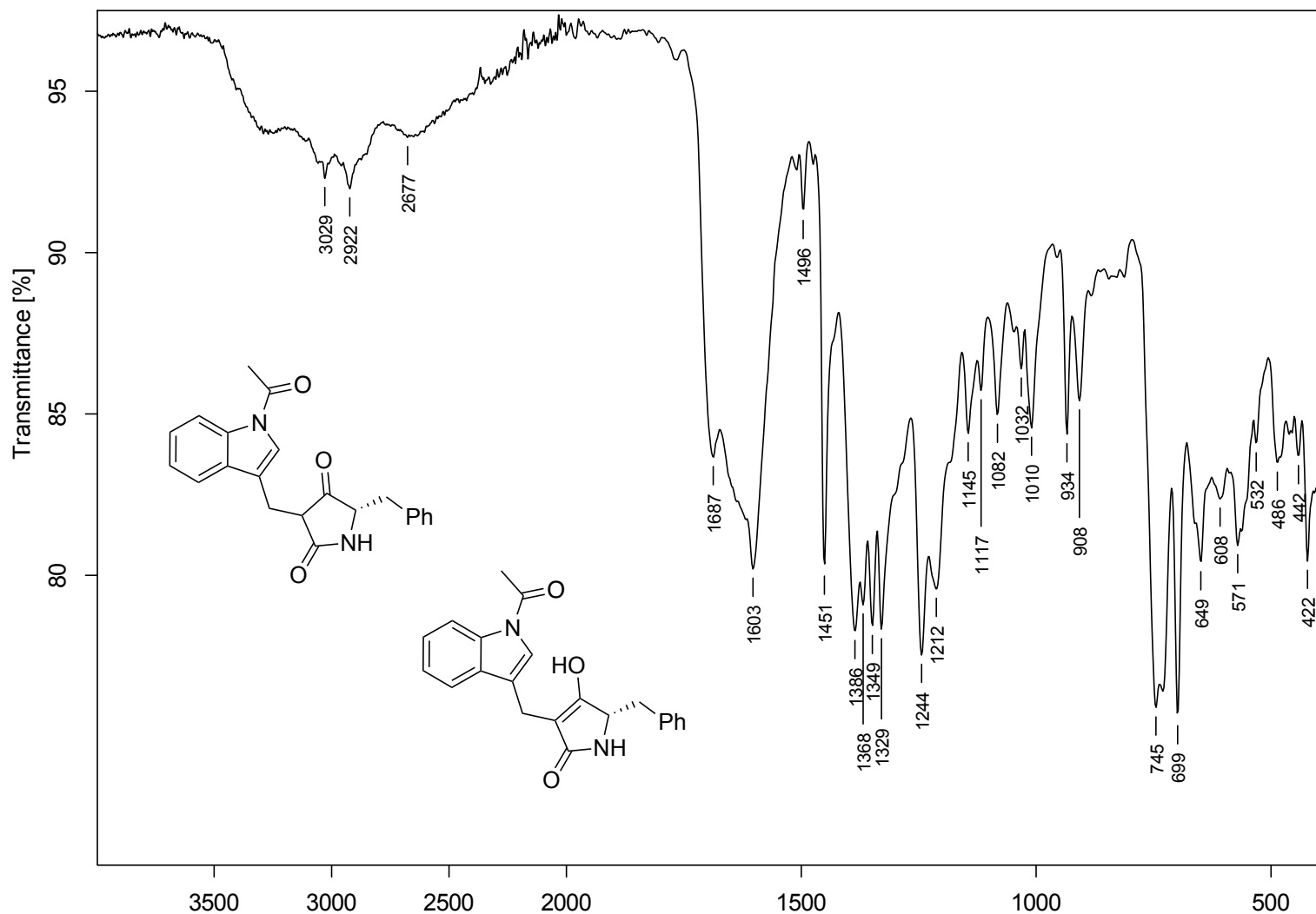


Figure B.08. FTIR (neat) tetramic acid **3.06**

AJ-RA-RE-oxime-major-1H-CDCl₃.10.fid

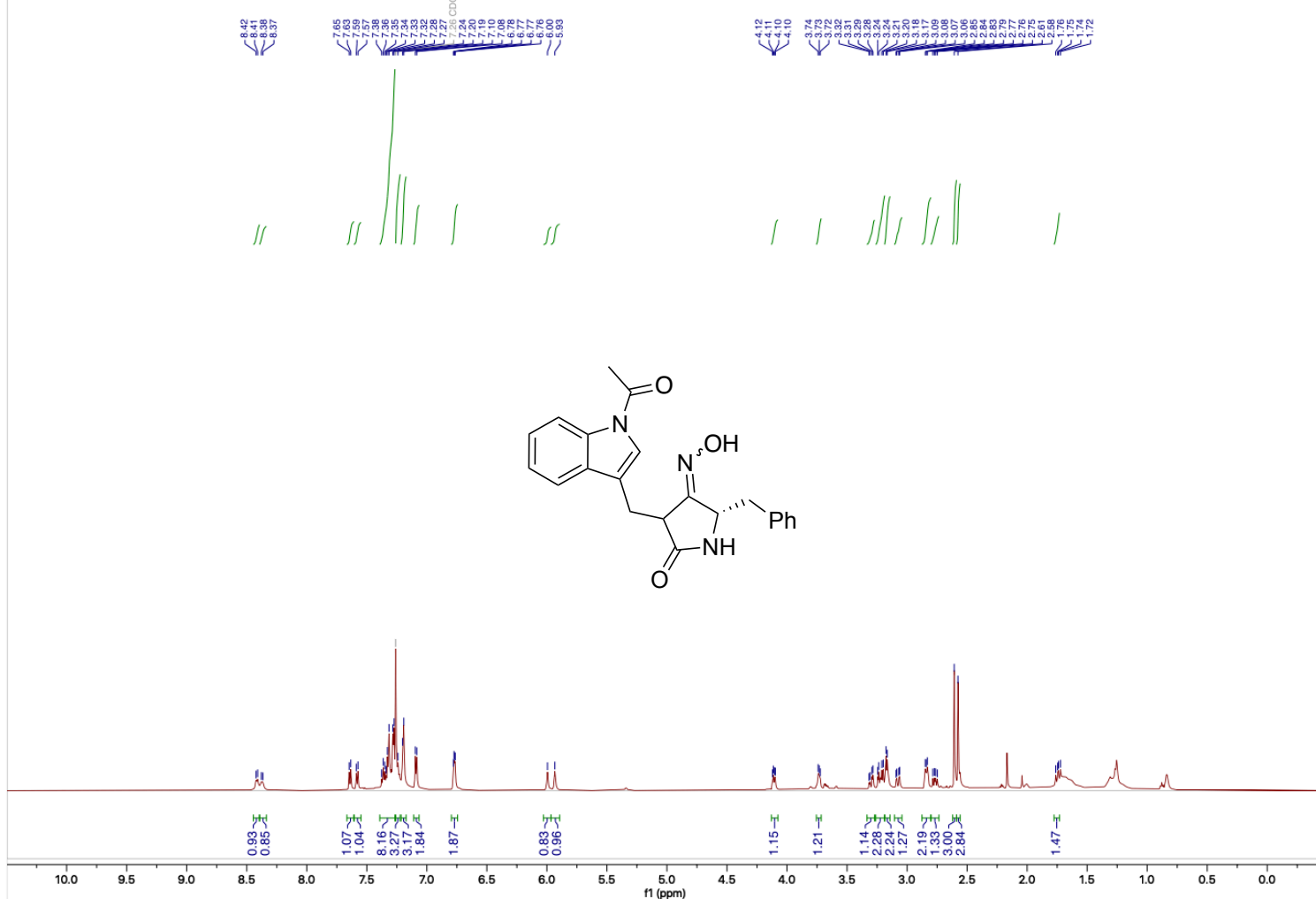


Figure B.09. ¹H NMR (600 MHz, CDCl₃) oxime 3.05

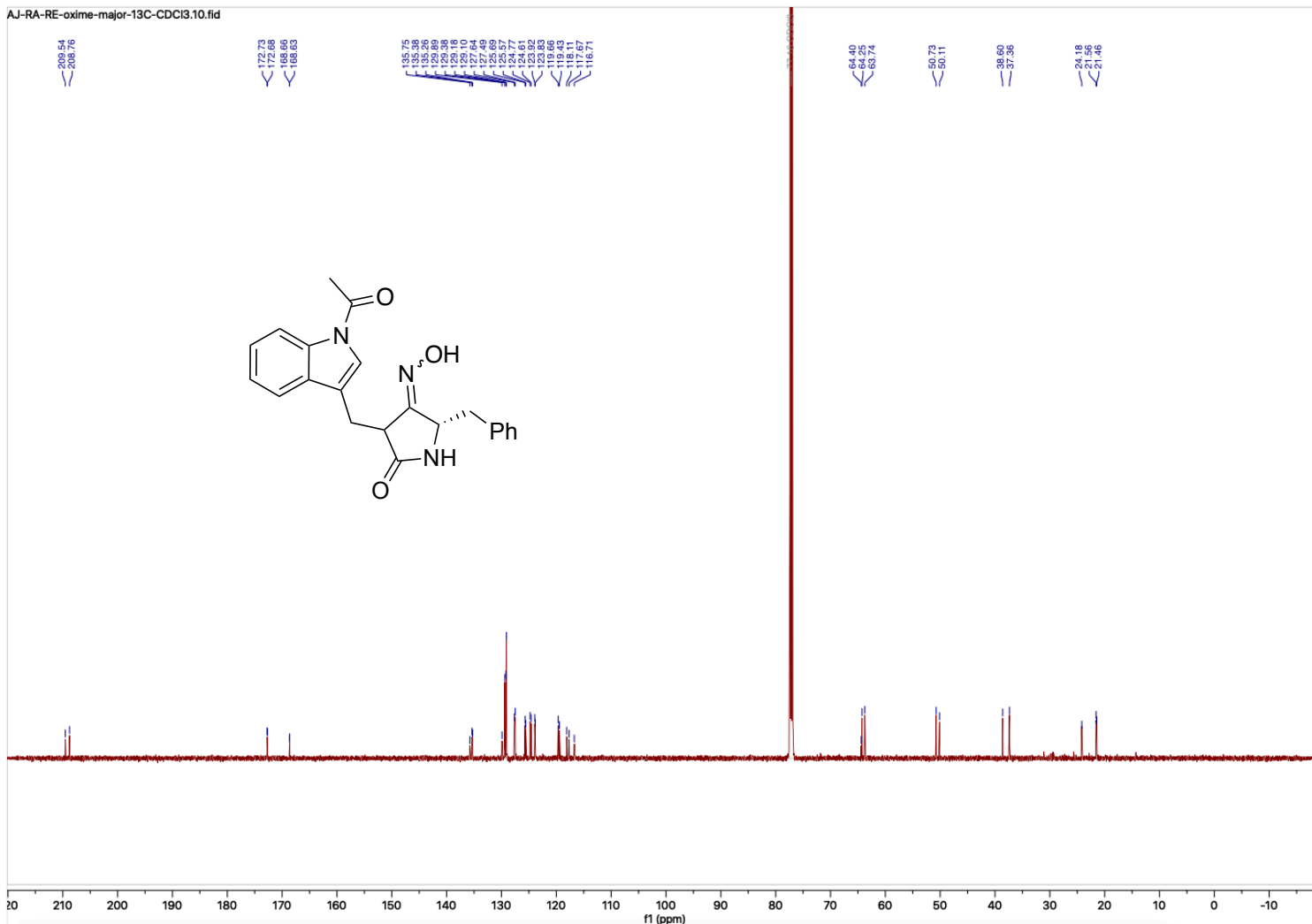


Figure B.10. ^{13}C NMR (151 MHz, CDCl₃) oxime 3.05

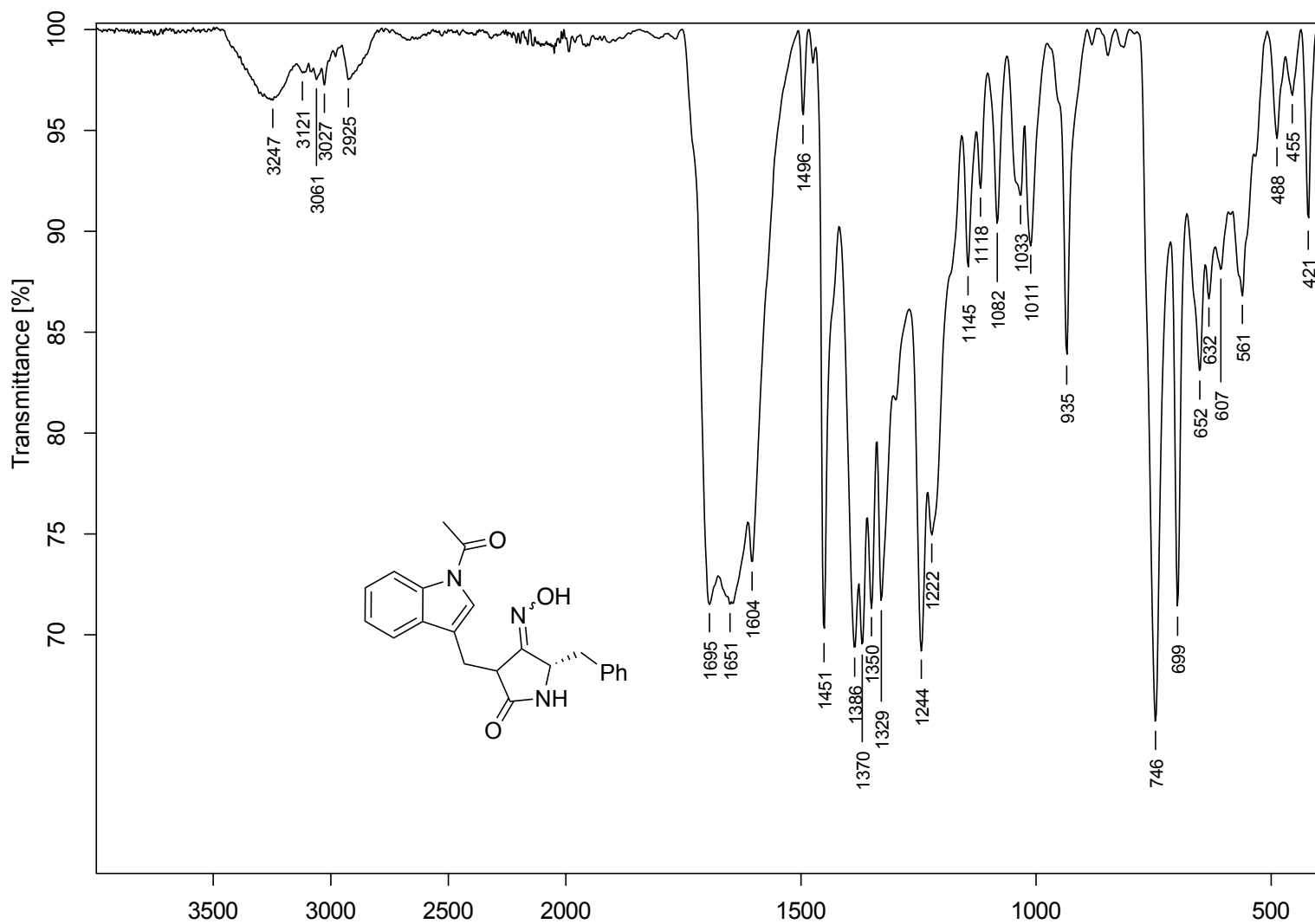


Figure B.11. FTIR (neat) oxime **3.05**

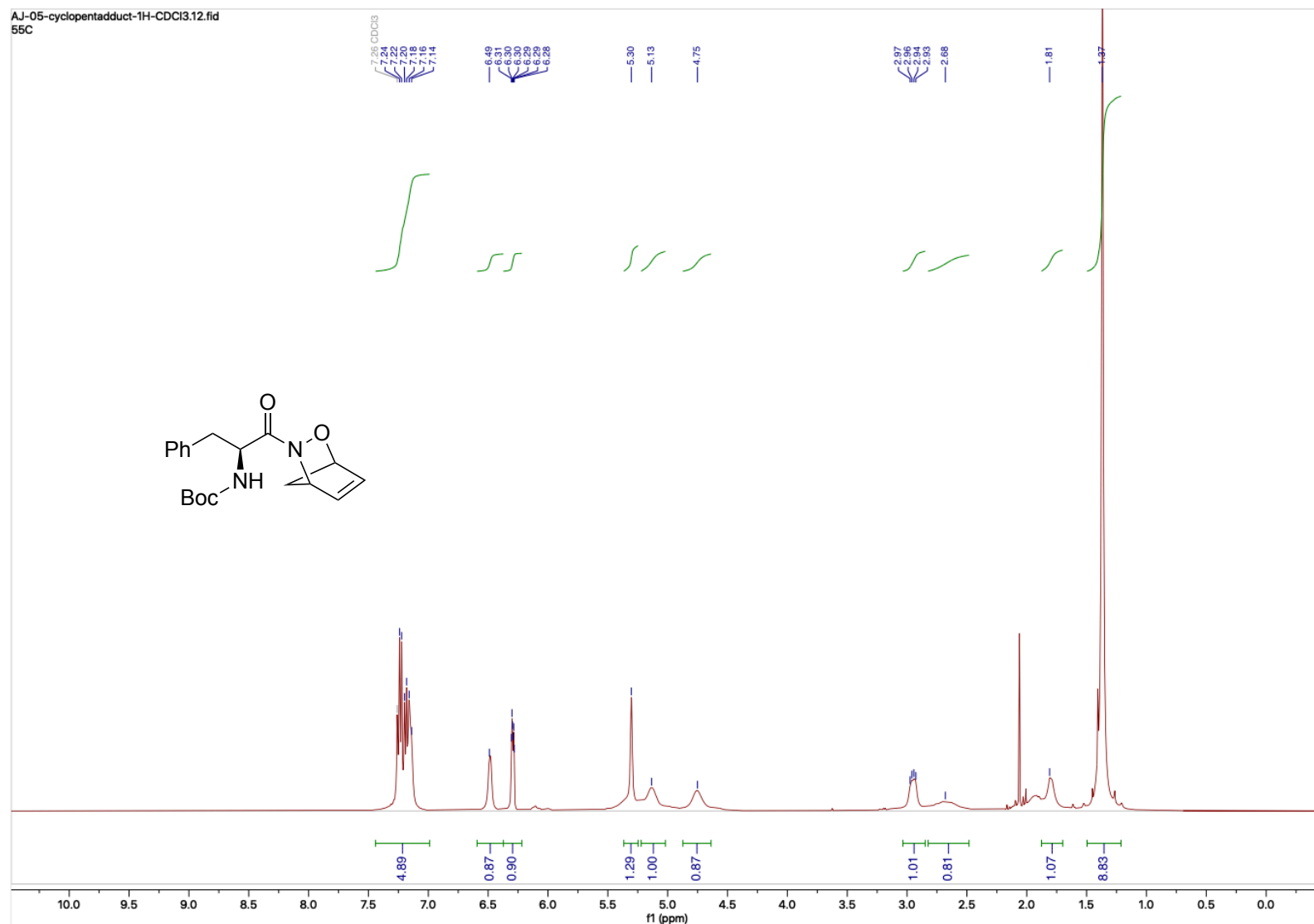


Figure B.12. ^1H NMR (400 MHz, CDCl₃) known cyclopentadiene adduct **3.24**

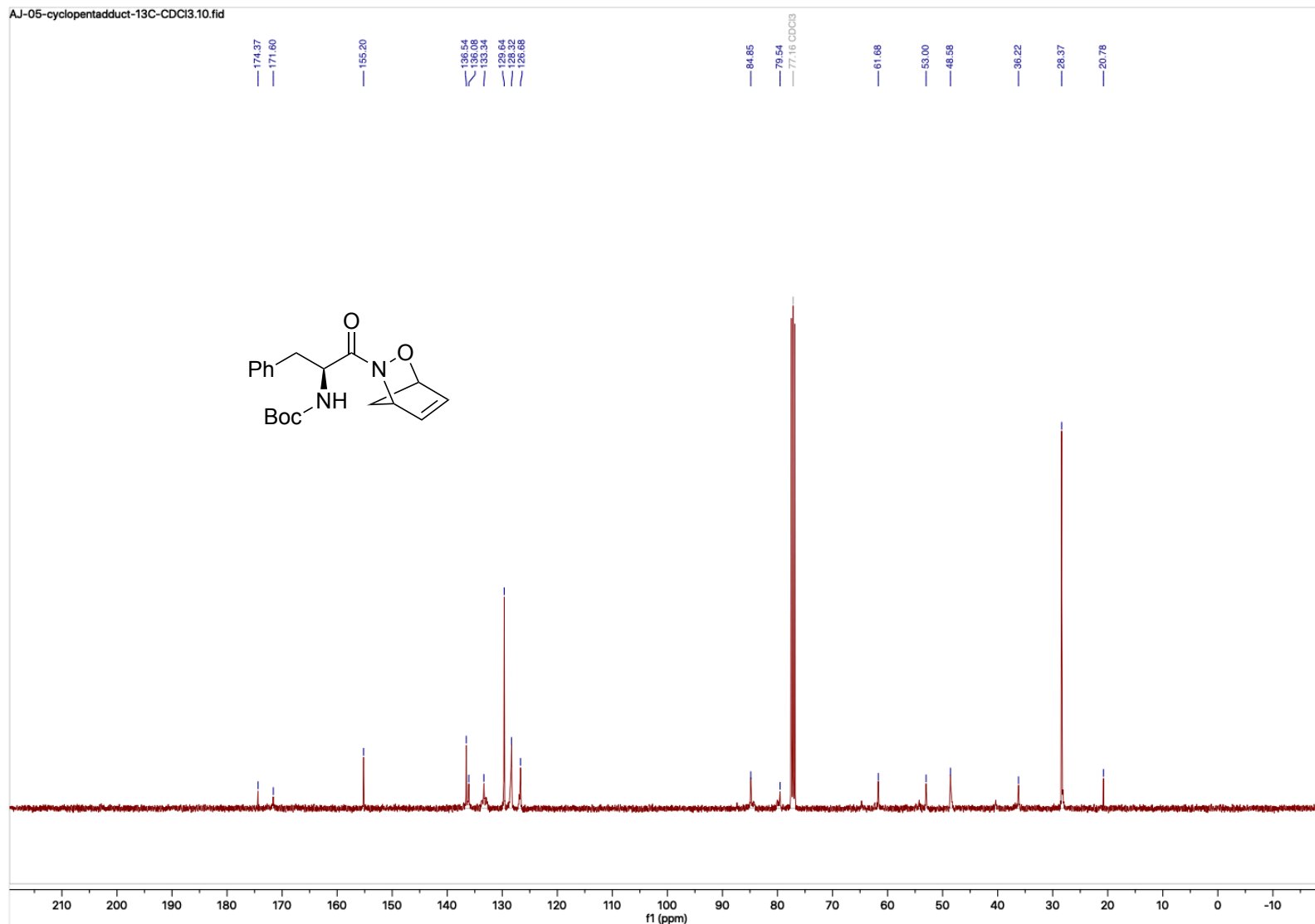


Figure B.13. ¹³C NMR (101 MHz, CDCl₃) known cyclopentadiene adduct **3.24**

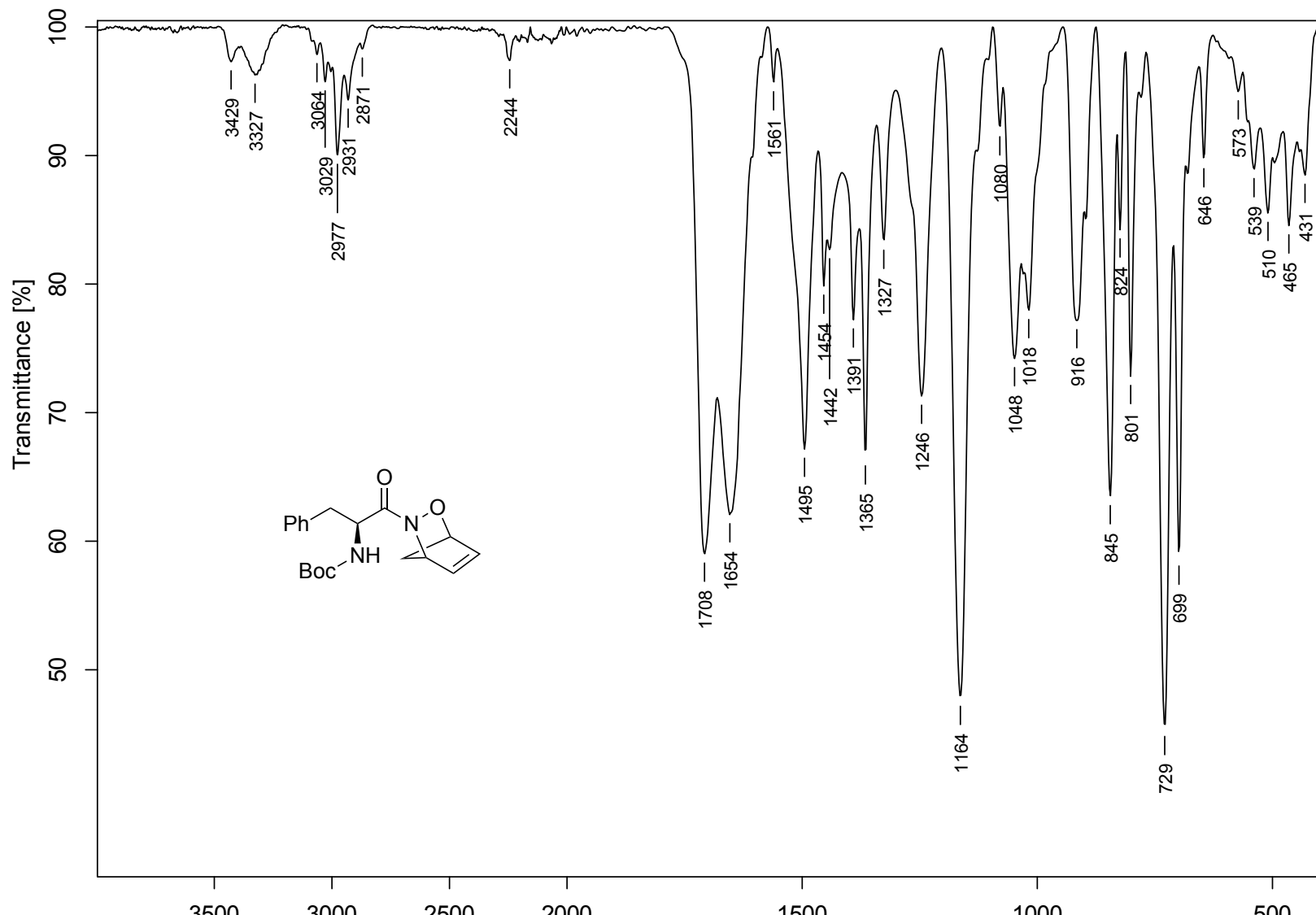


Figure B.14. FTIR (neat) known cyclopentadiene adduct 3.24

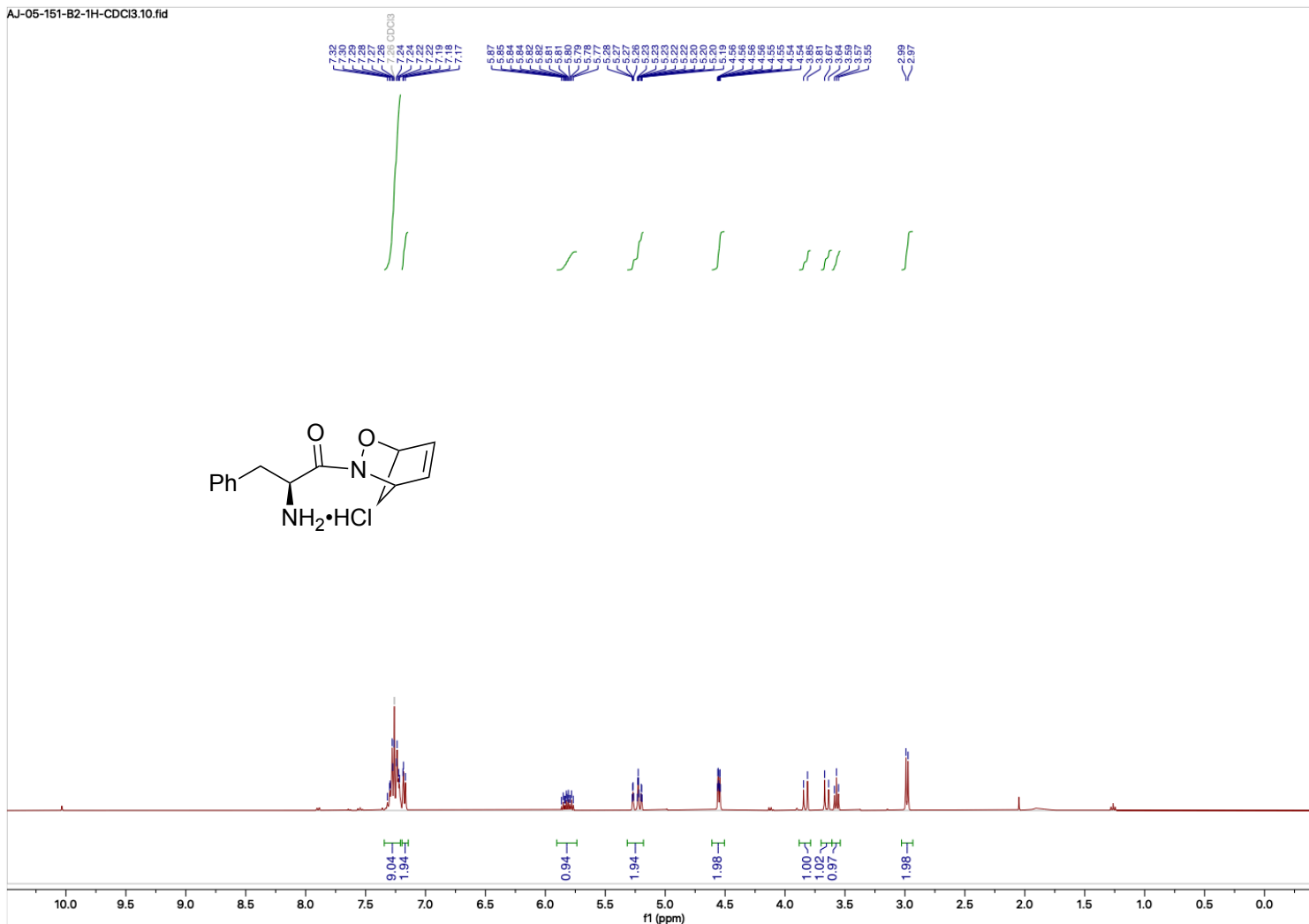


Figure B.15. ¹H NMR (400 MHz, CDCl₃) crude amino salt **3.25**

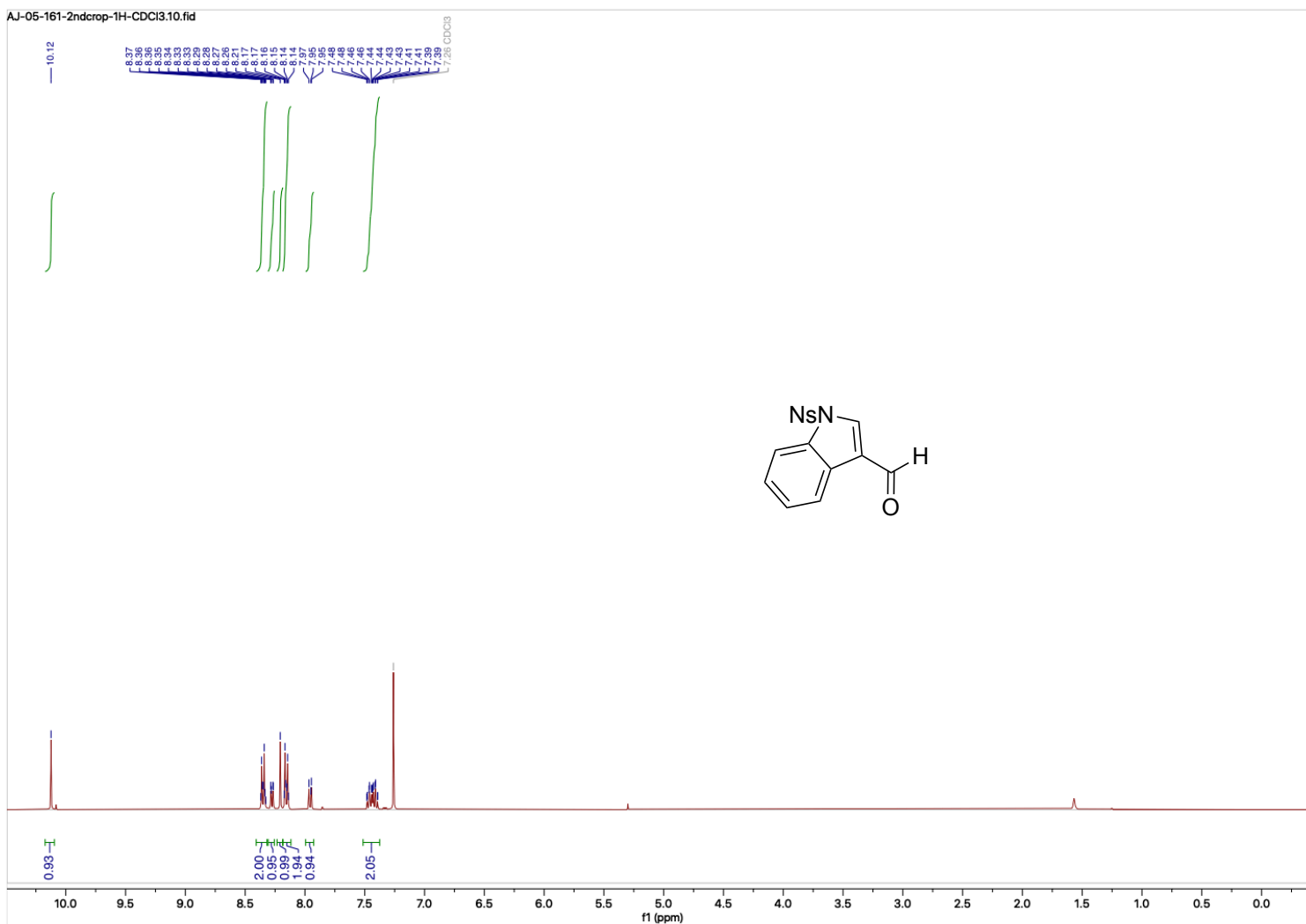


Figure B.16. ¹H NMR (400 MHz, CDCl₃) known Ns-protected indole carbaldehyde 3.27

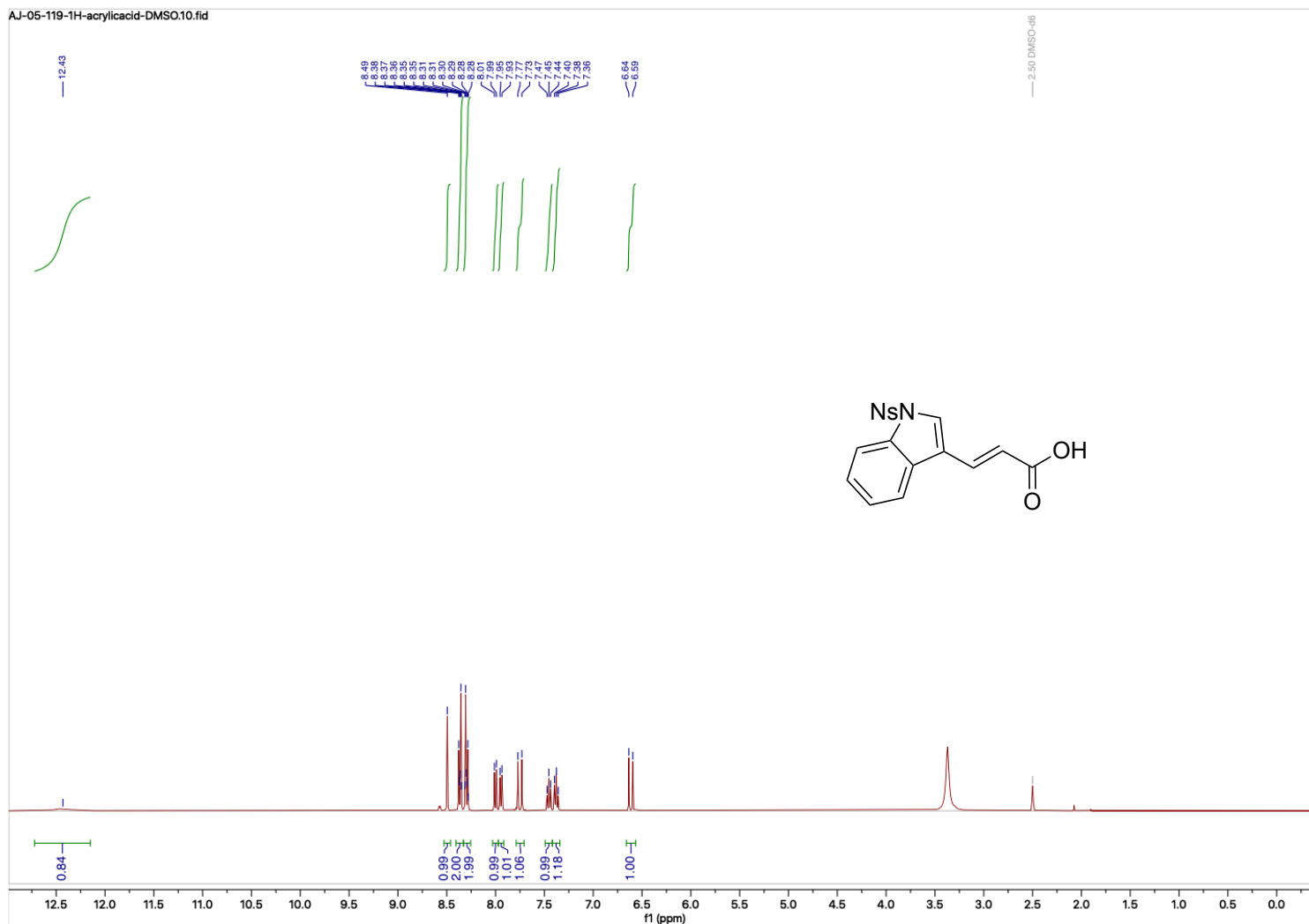


Figure B.17. ^1H NMR (400 MHz, DMSO) indoleacrylic acid **3.28**

AJ-05-119-13C-acrylicacid-DMSO12.fid

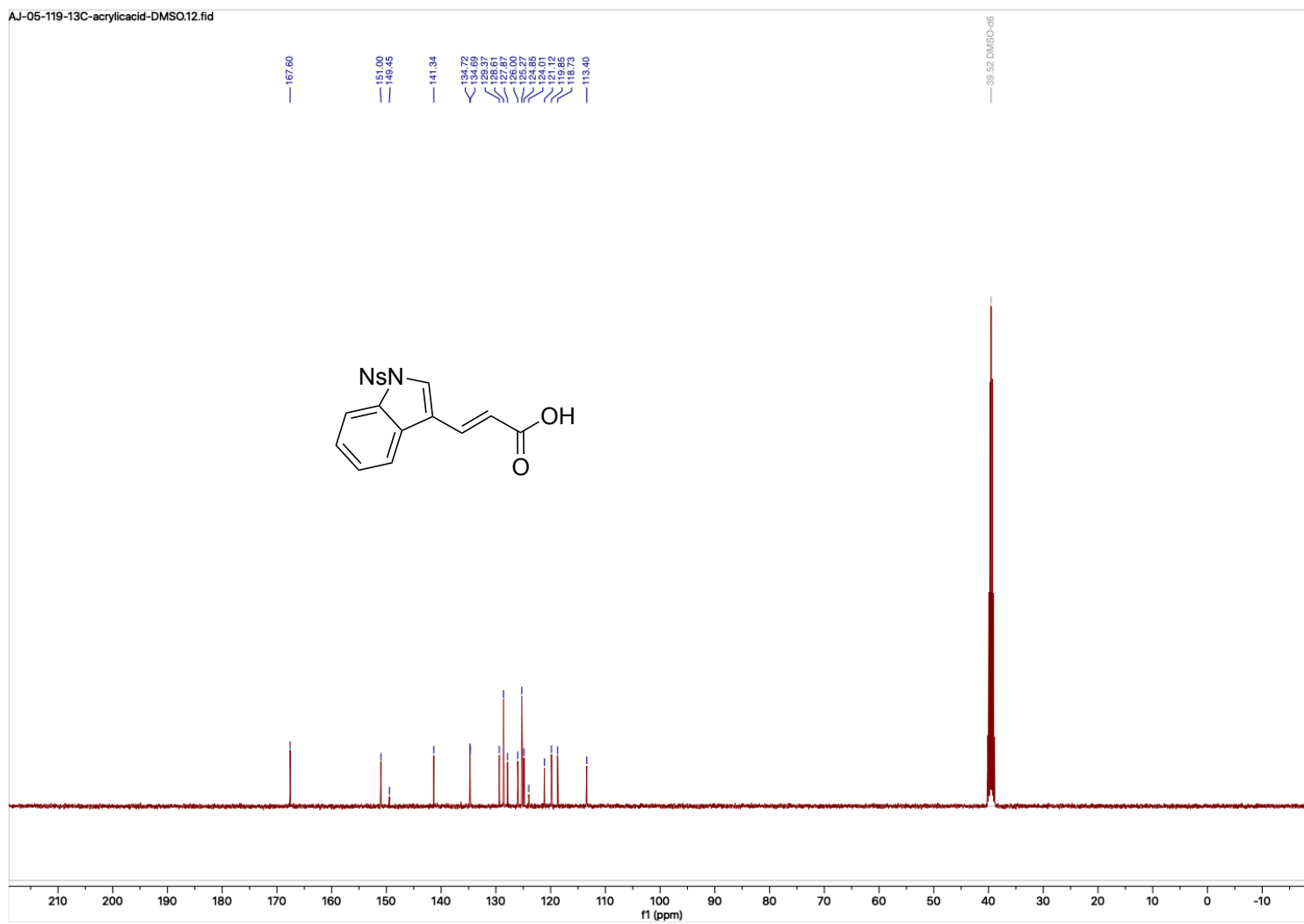


Figure B.18. ¹³C NMR (101 MHz, DMSO) indoleacrylic acid **3.28**

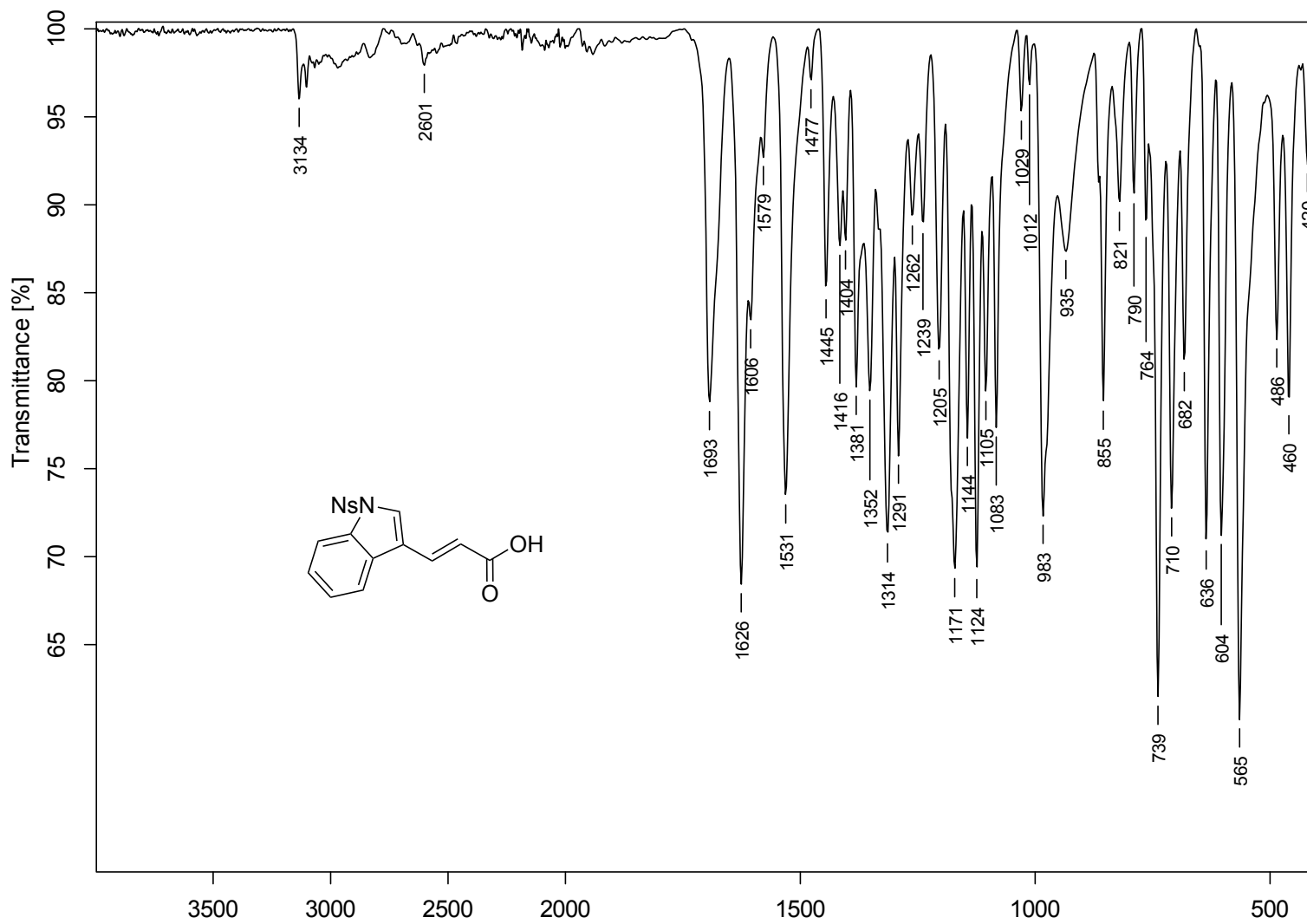


Figure B.19. FTIR (neat) indoleacrylic acid **3.28**

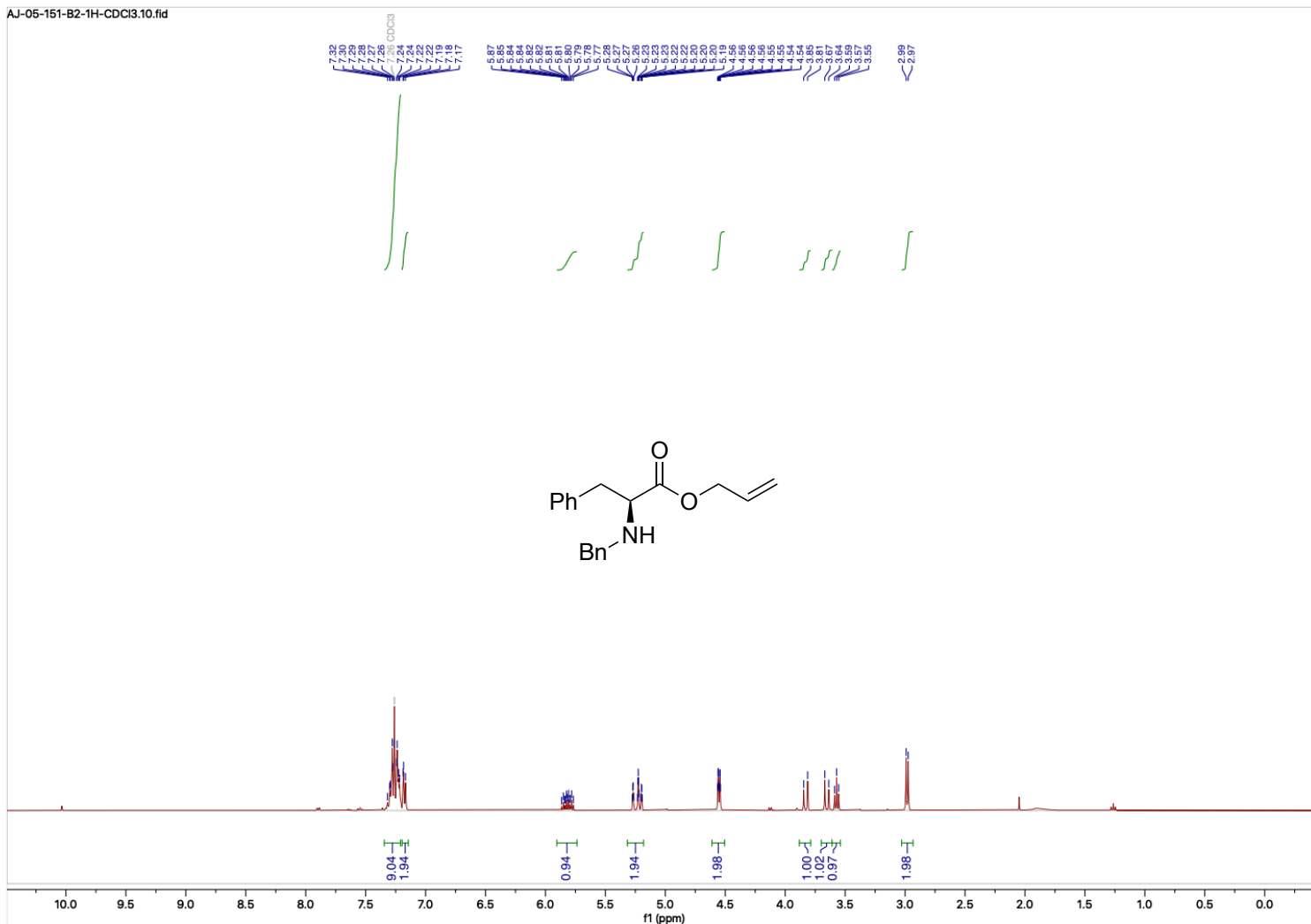


Figure B.20. ¹H NMR (400 MHz, CDCl₃) known Bn-protected allyl ester **3.31**

AJ-05-152-B1.1H-CDCl₃.10.fid

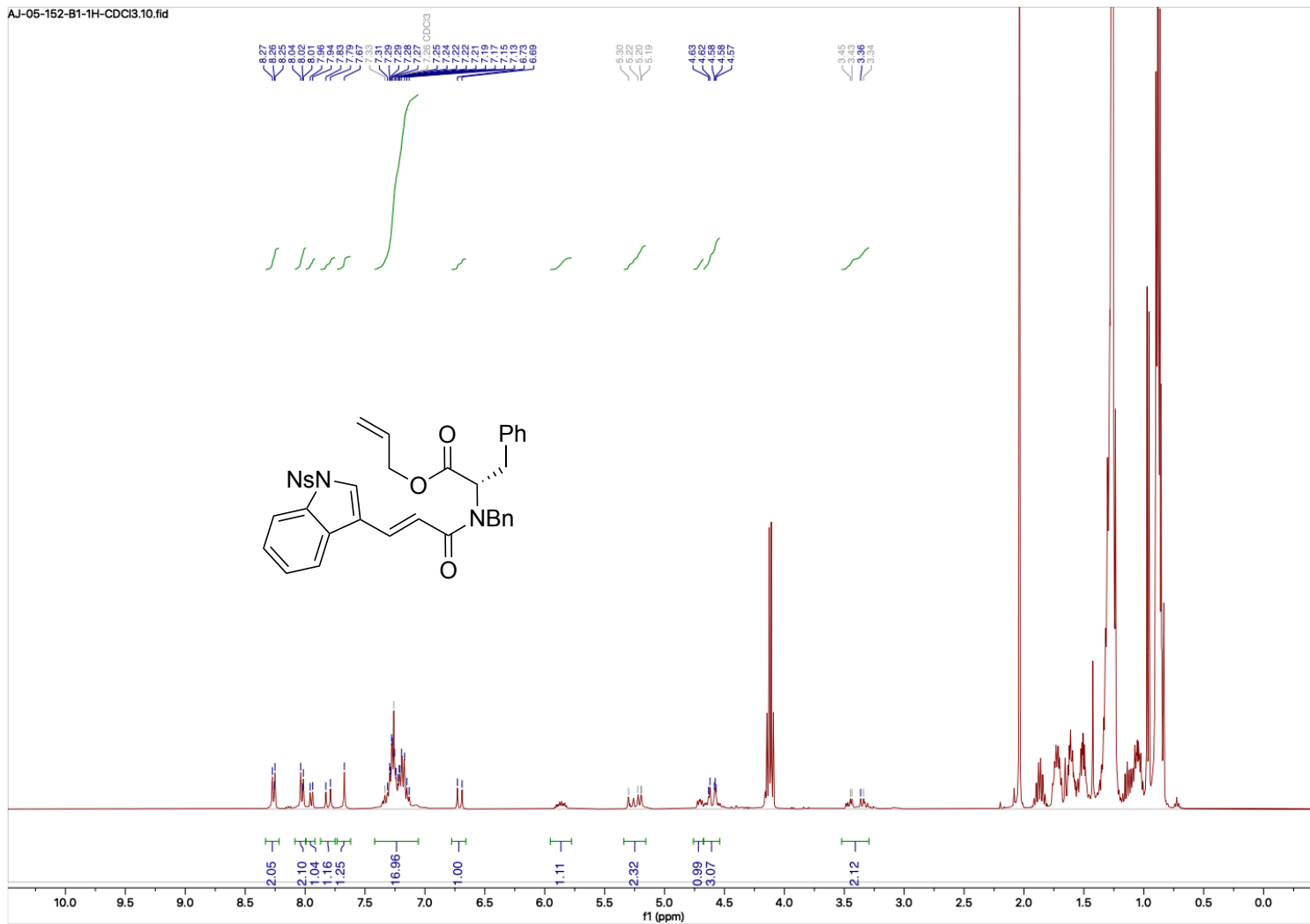


Figure B.21. ¹H NMR (400 MHz, CDCl₃) crude amide 3.32

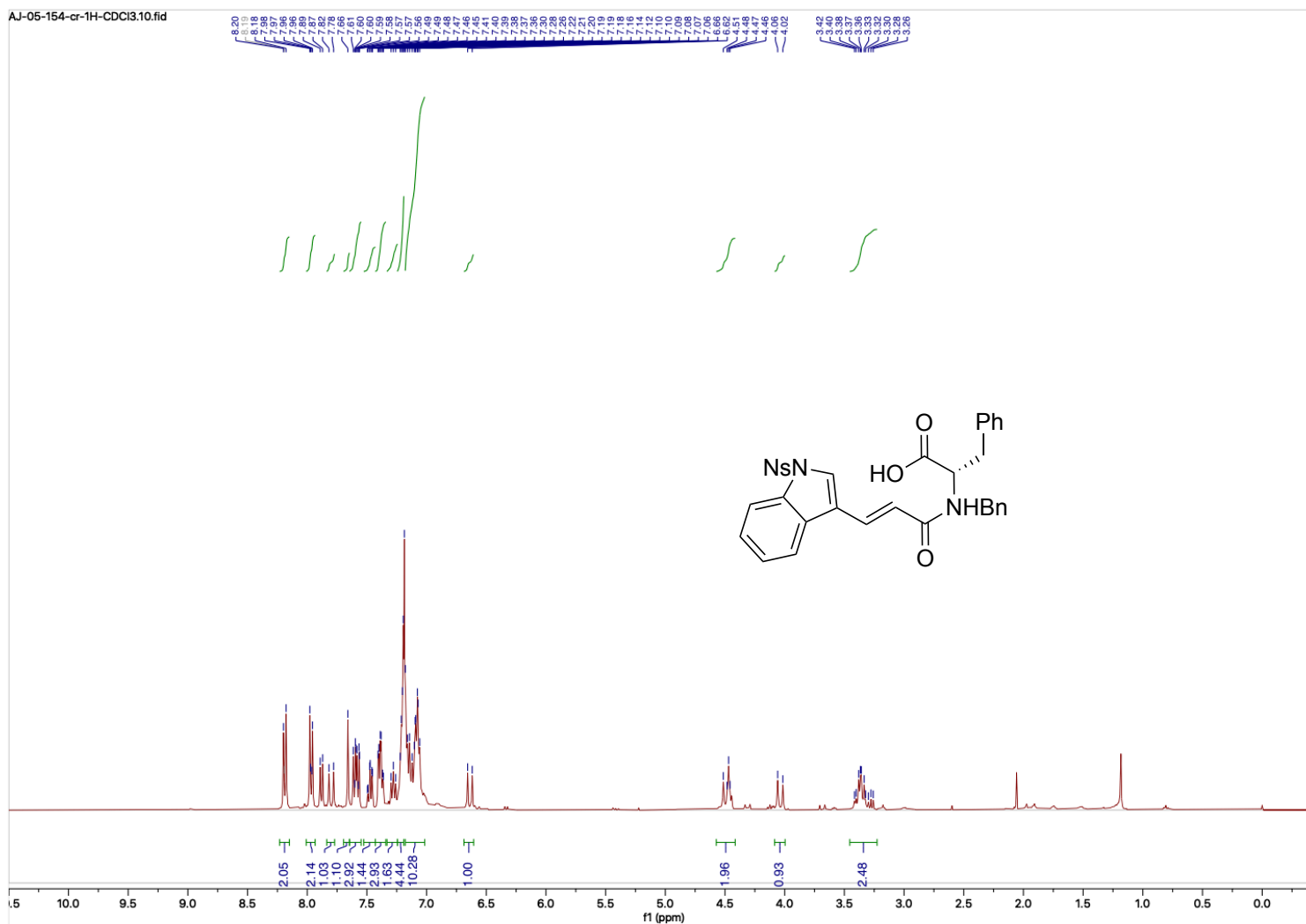


Figure B.22. ^1H NMR (400 MHz, CDCl_3) crude carboxylic acid 3.33

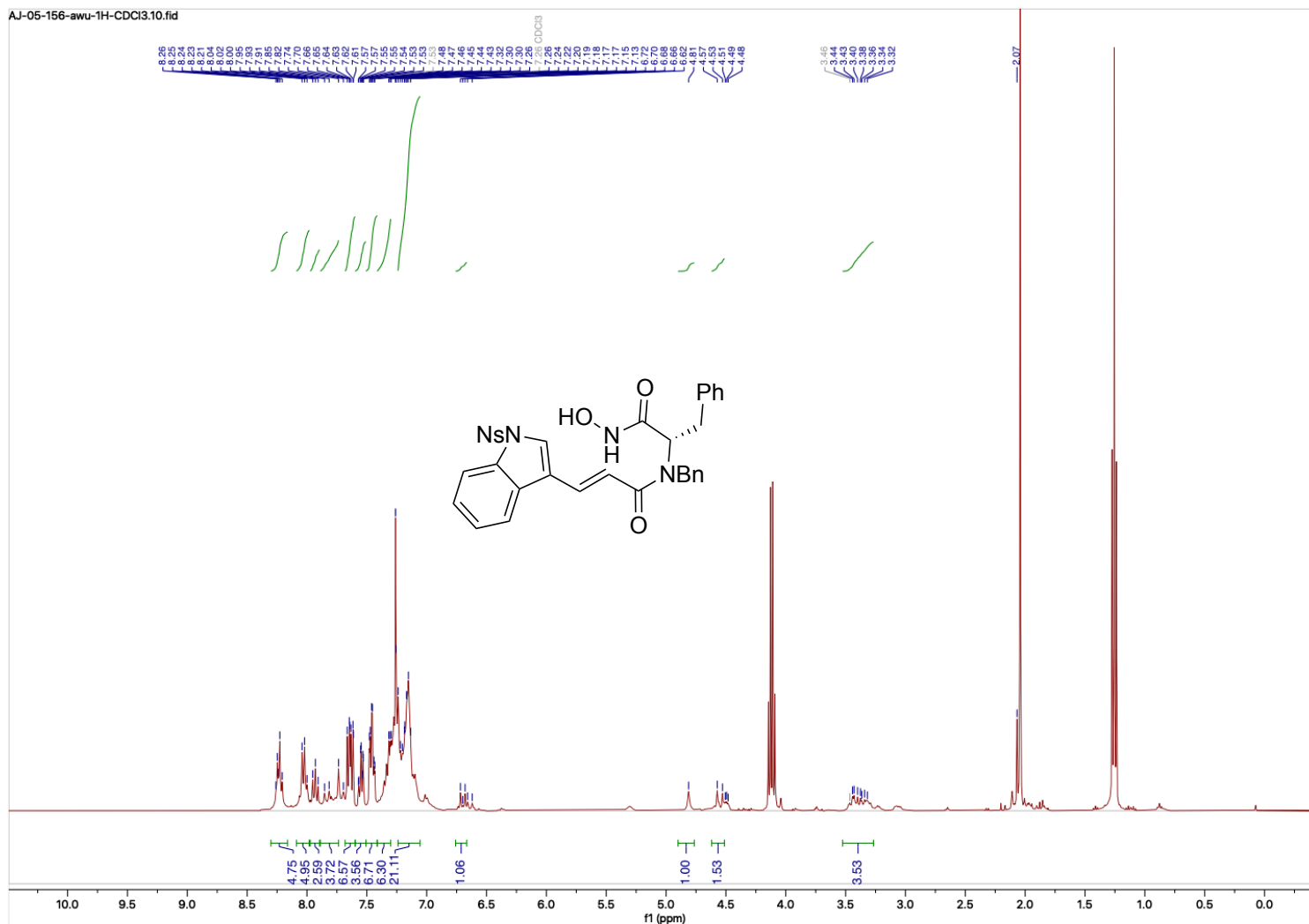


Figure B.23. ^1H NMR (400 MHz, CDCl_3) crude hydroxamic acid 3.34

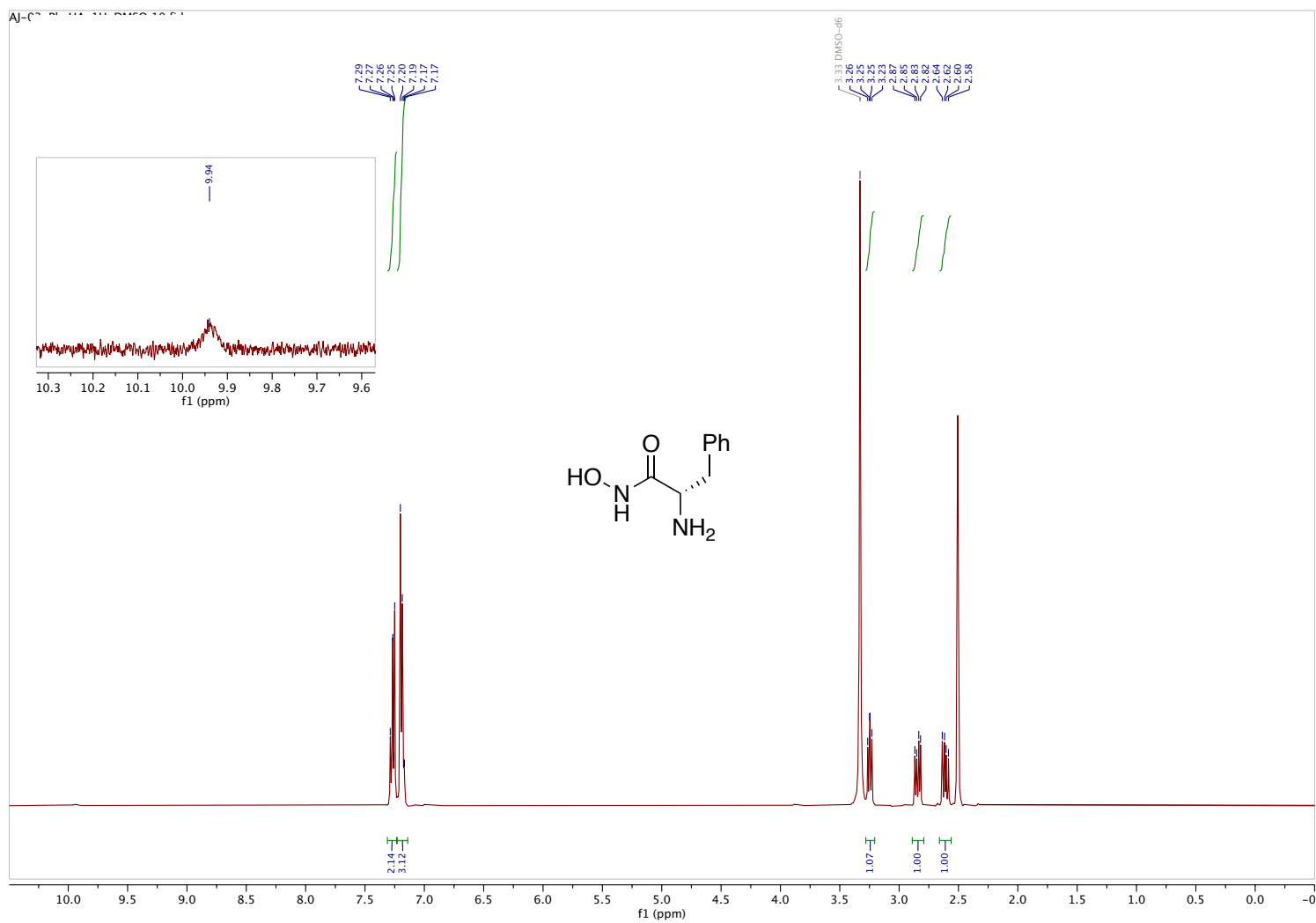


Figure B.24. ^1H NMR (400 MHz, CDCl_3) known hydroxamic acid 3.39

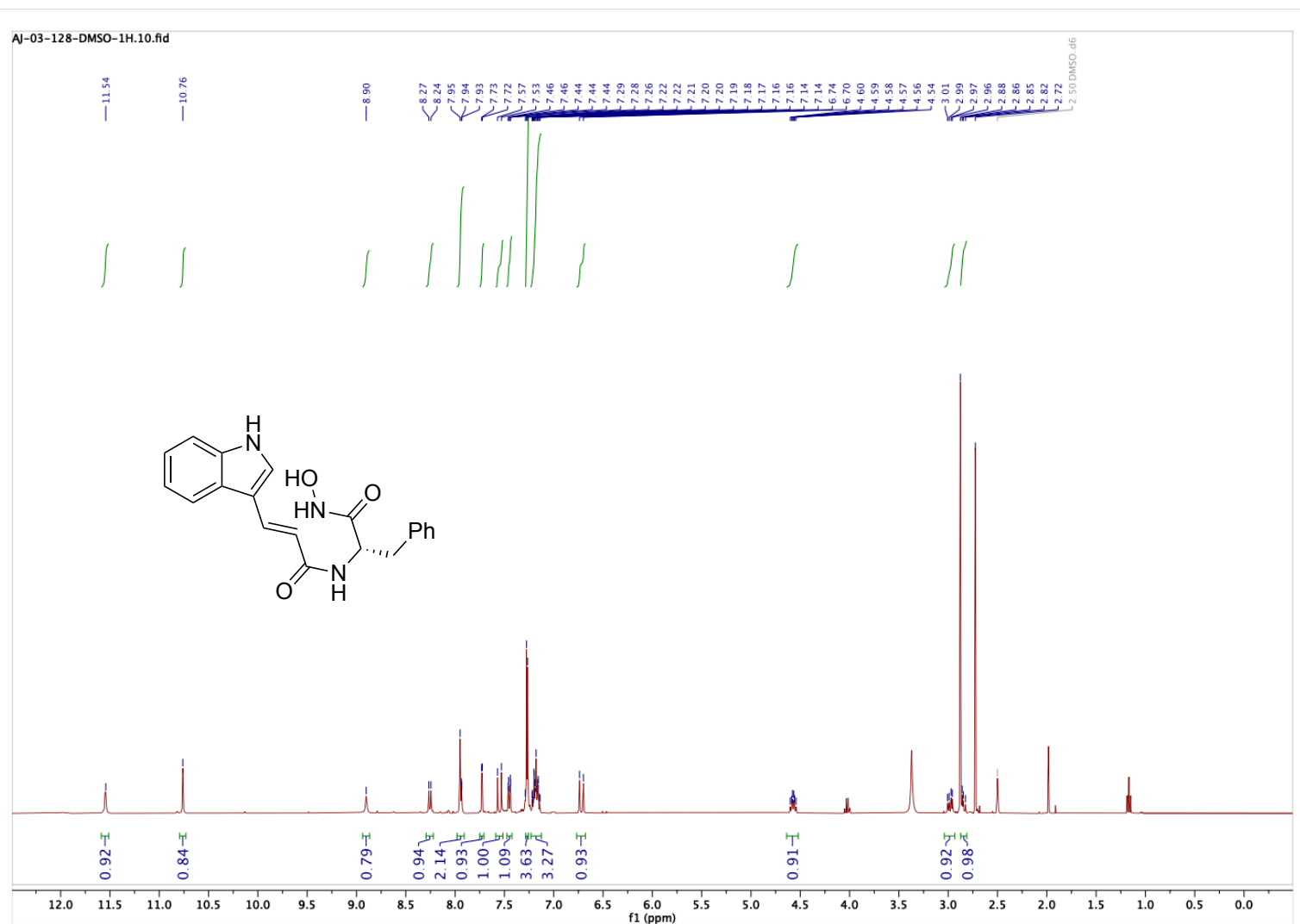


Figure B.25. ^1H NMR (400 MHz, DMSO) hydroxamic acid 3.37

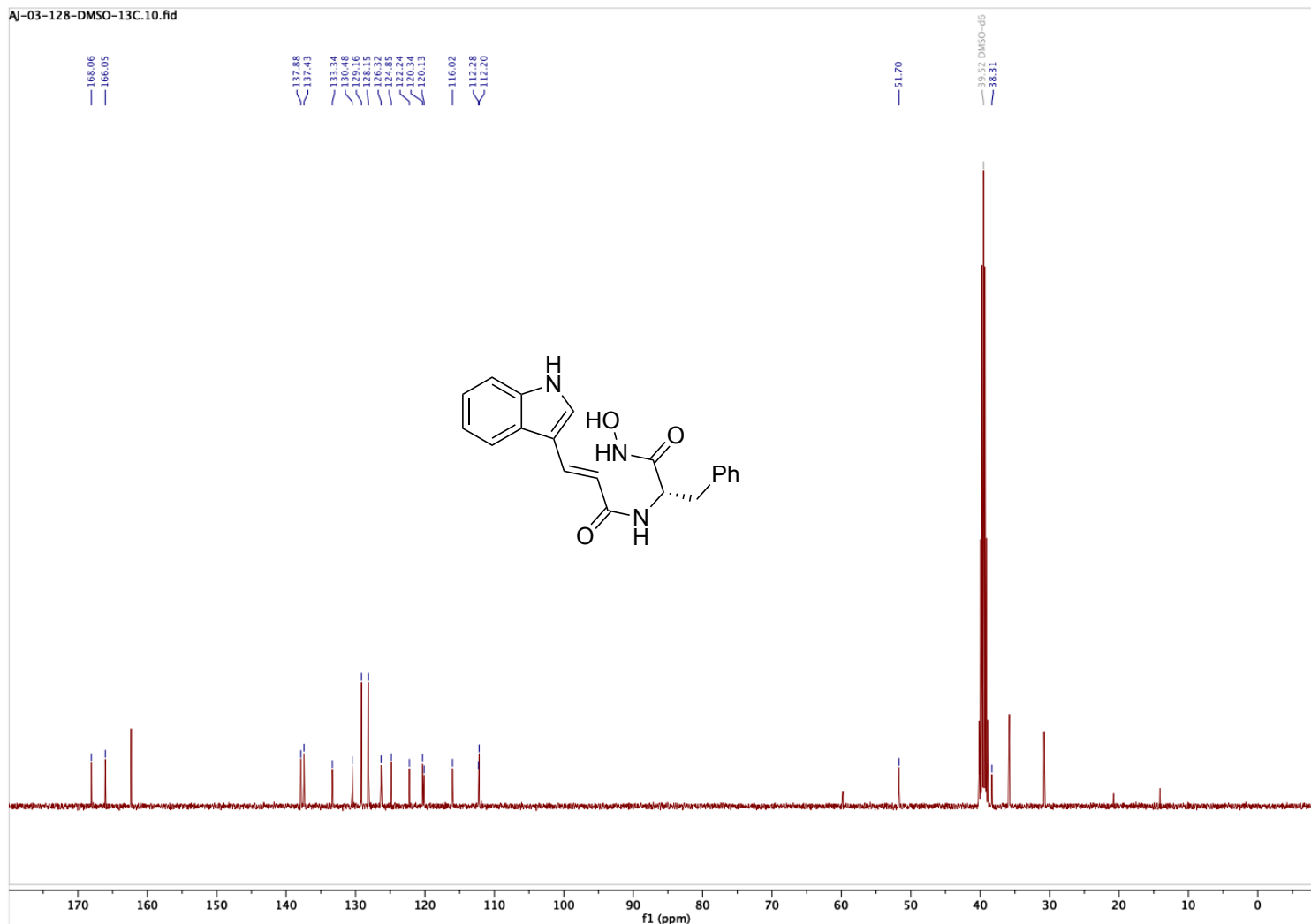


Figure B.26. ^{13}C NMR (101 MHz, DMSO) hydroxamic acid **3.37**

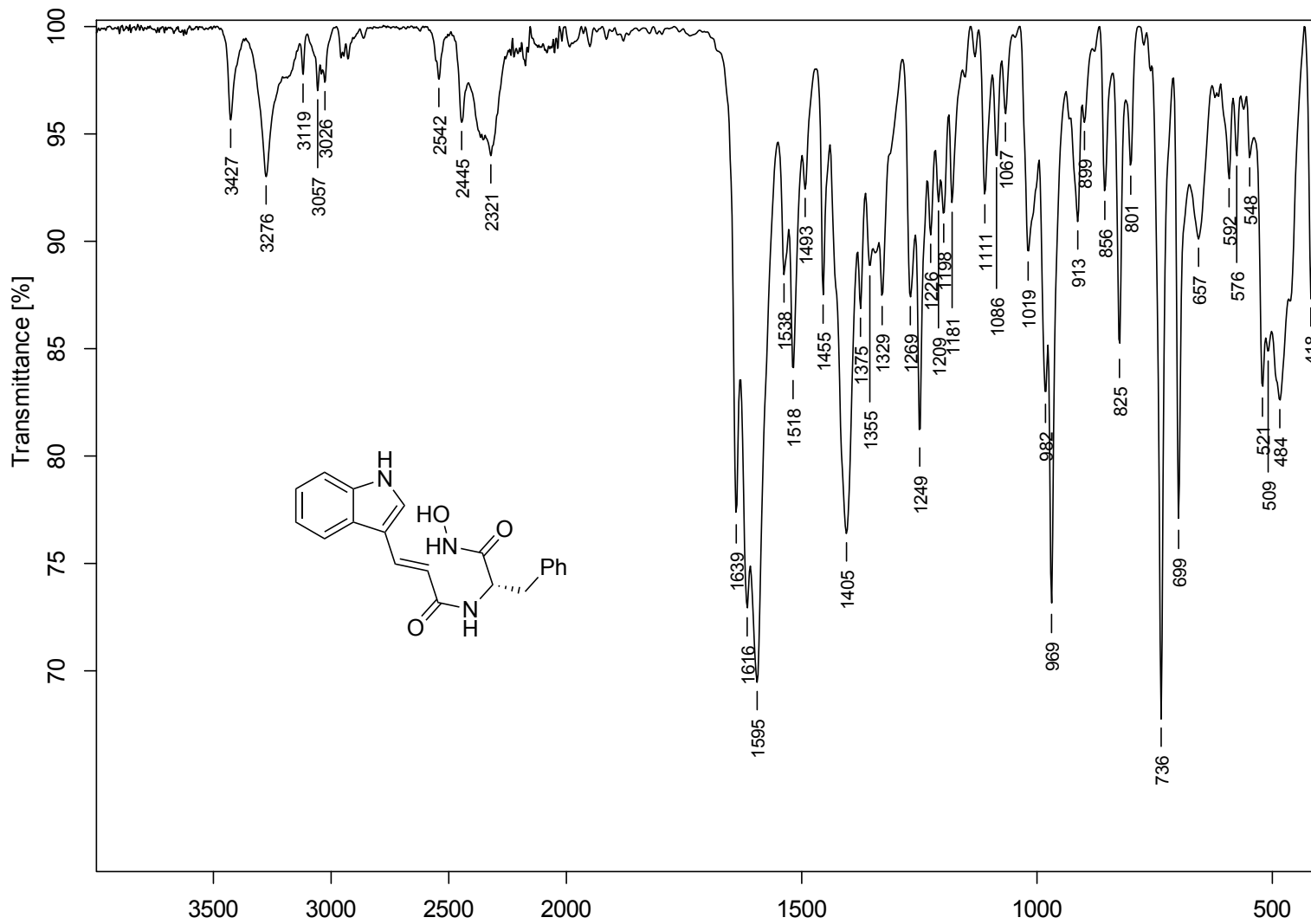


Figure B.27. FTIR (neat) hydroxamic acid **3.37**

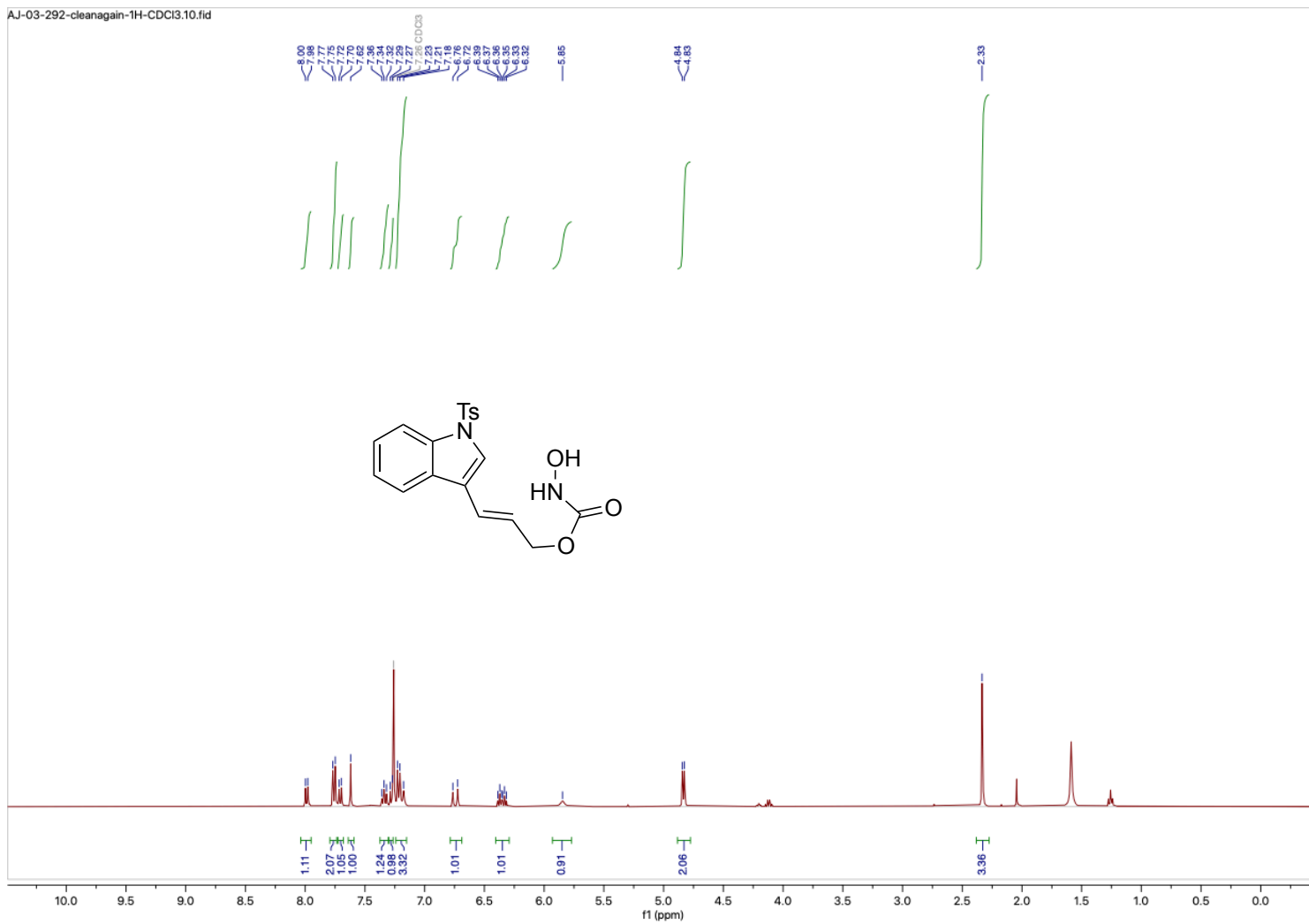


Figure B.28. ^1H NMR (400 MHz, CDCl₃) known hydroxamic acid 3.47

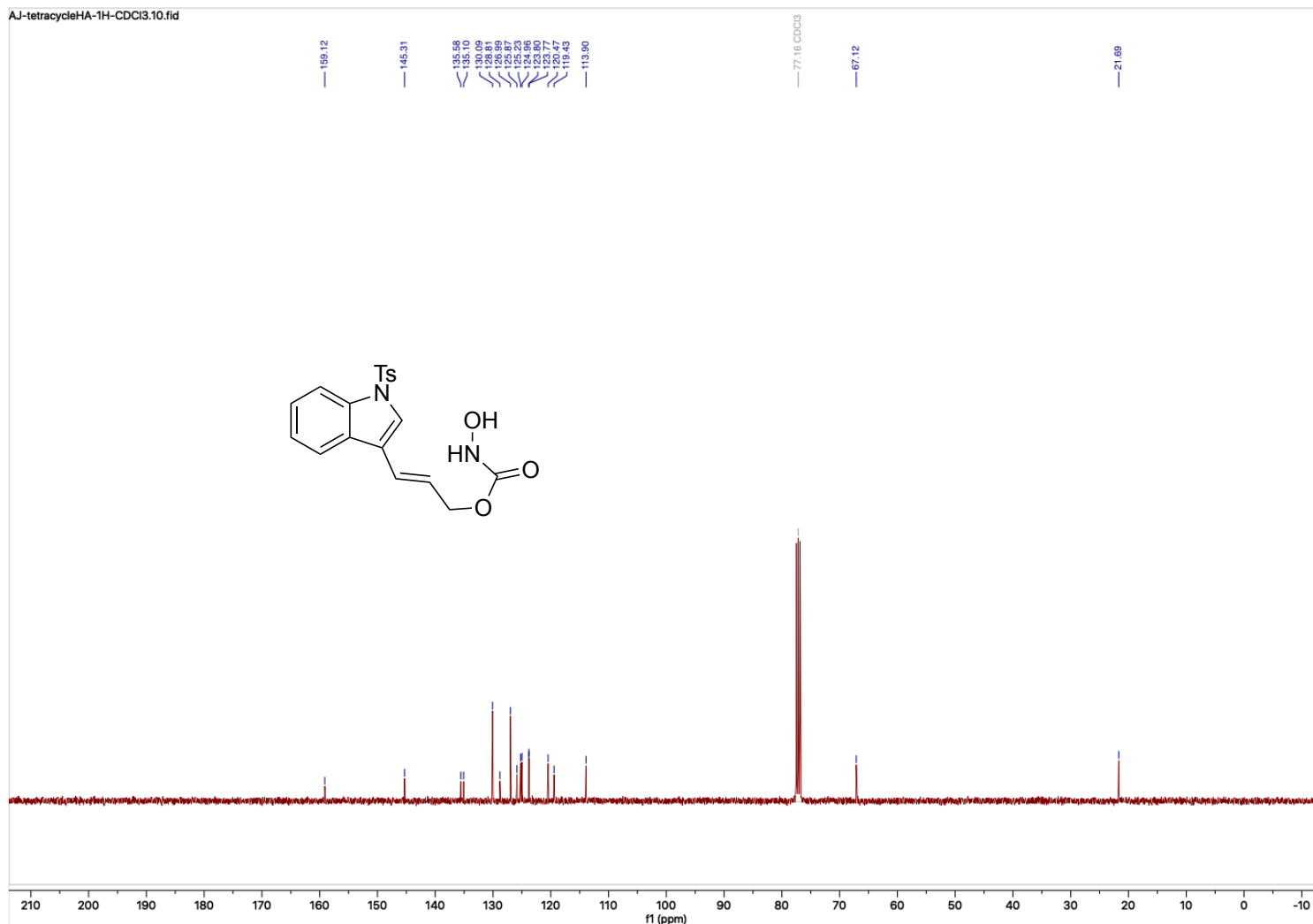


Figure B.29. ¹³C NMR (151 MHz, CDCl₃) known hydroxamic acid 3.47

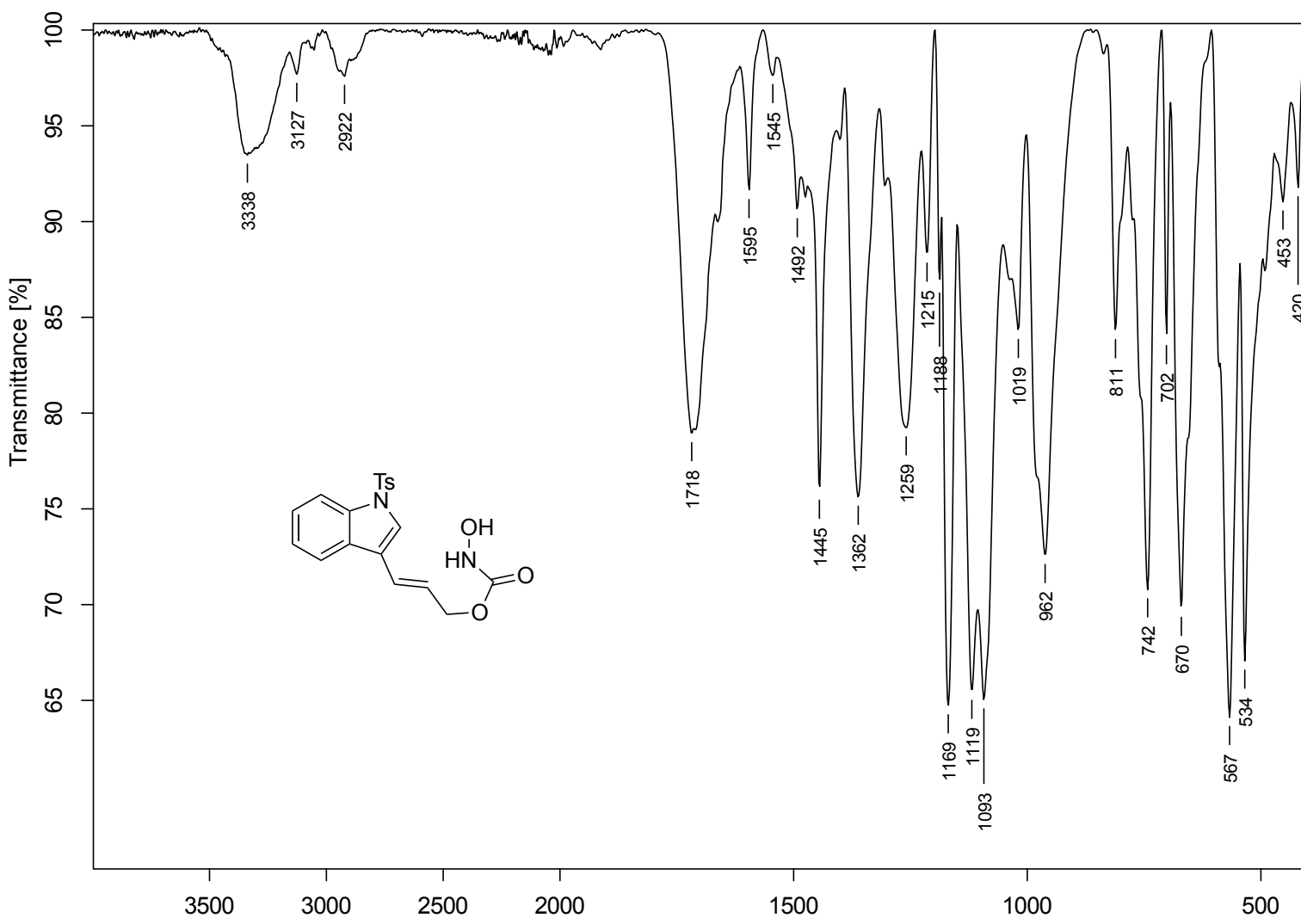


Figure B.30. FTIR (neat) known hydroxamic acid 3.47

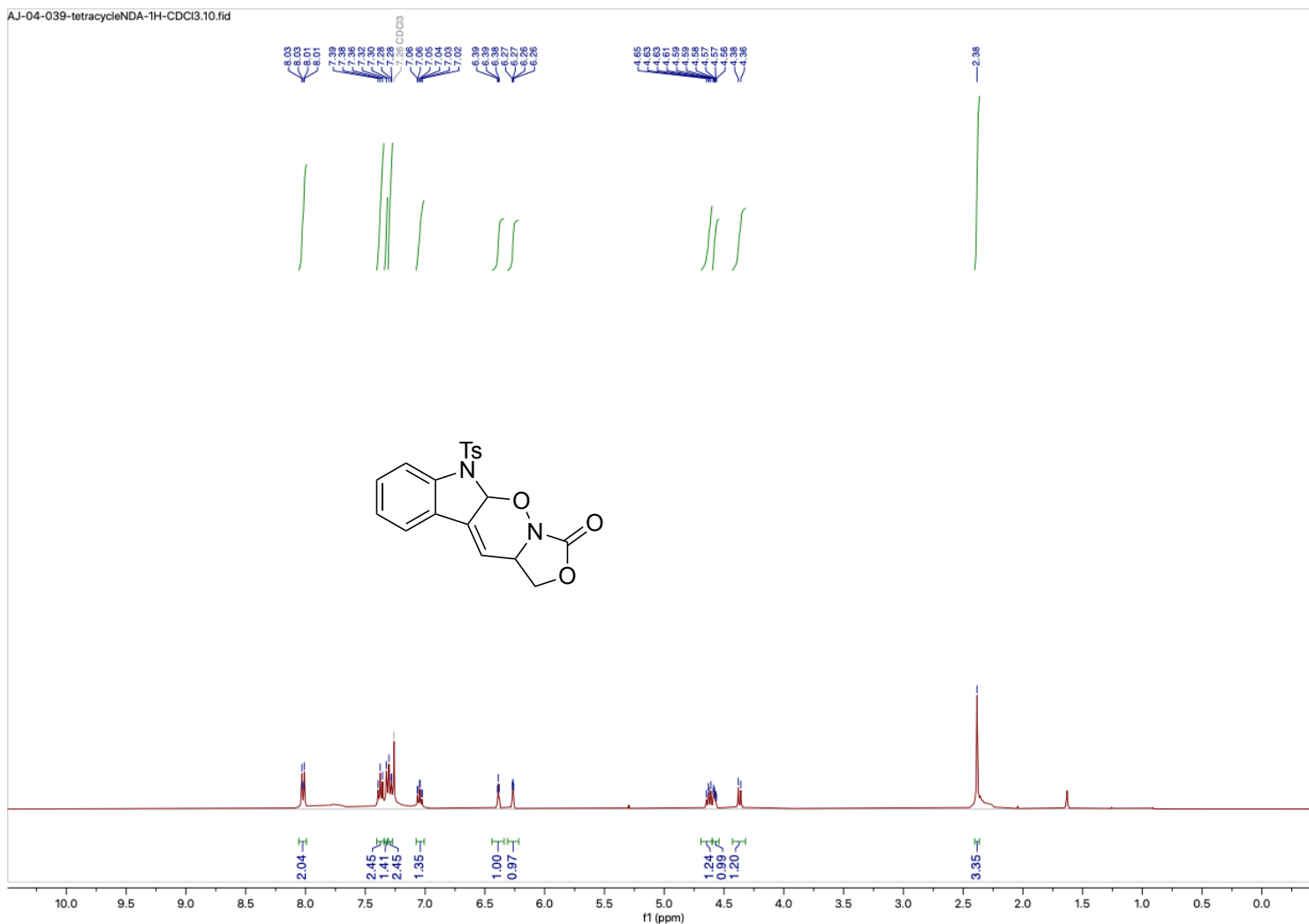


Figure B.31. ^1H NMR (400 MHz, CDCl₃) NDA adduct **3.46**

AJ-04-039-tetracycleNDA-13C-CDCl₃.12.fid

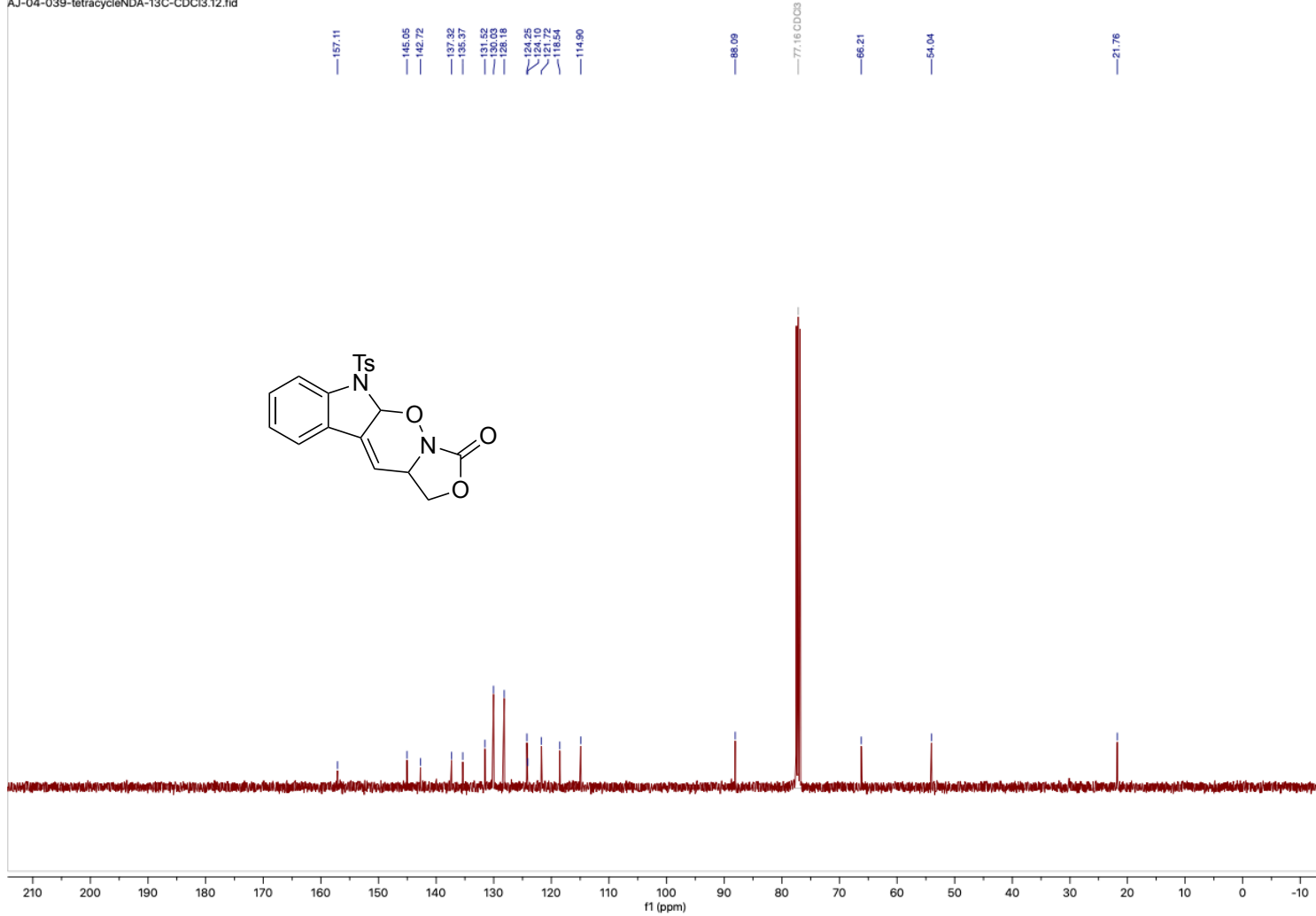


Figure B.32. ¹³C NMR (101 MHz, CDCl₃) NDA adduct **3.46**

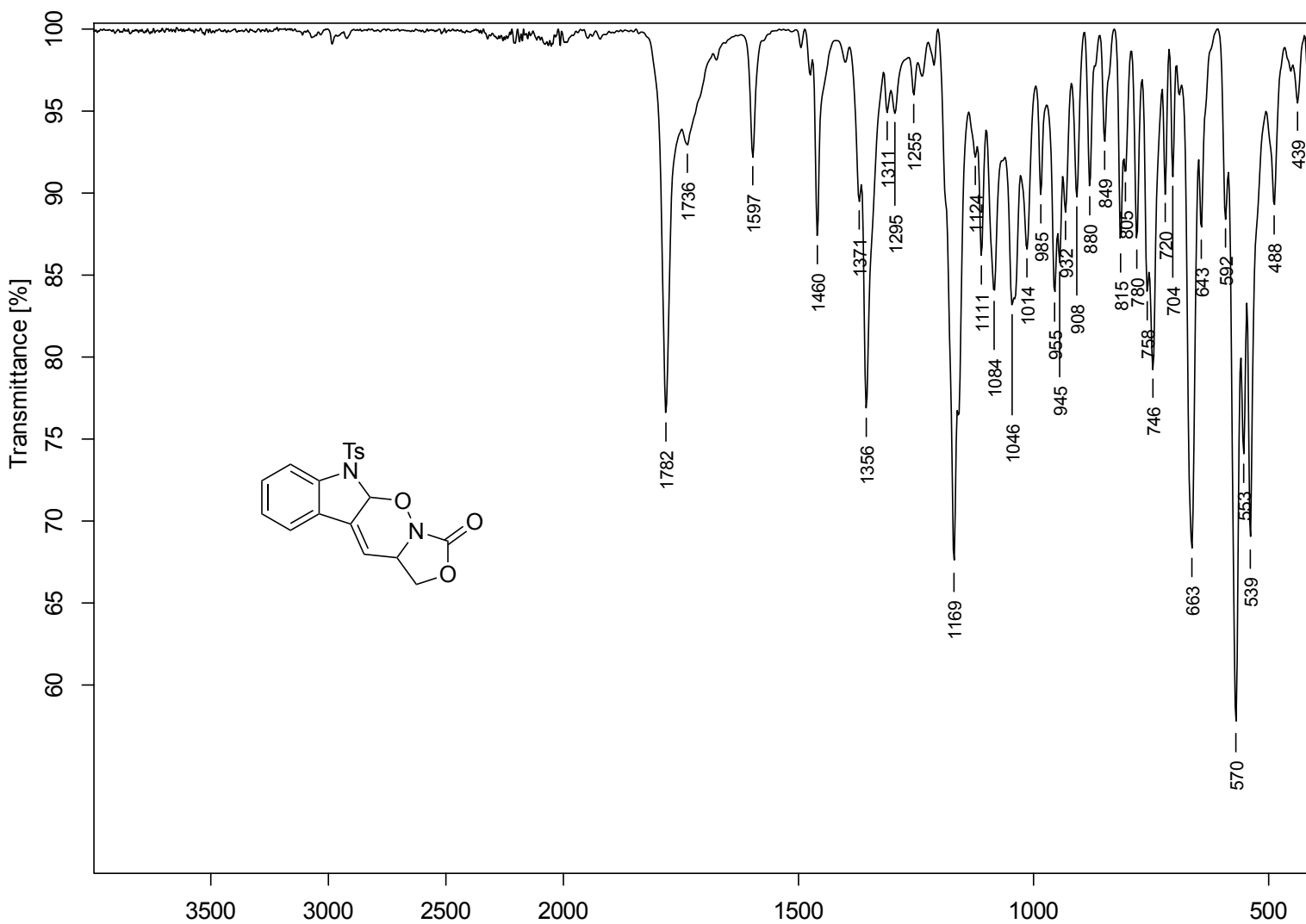


Figure B.33. FTIR (neat) NDA adduct **3.46**

AJ-04-289-singlediast-1H-CDCl₃.10.fid

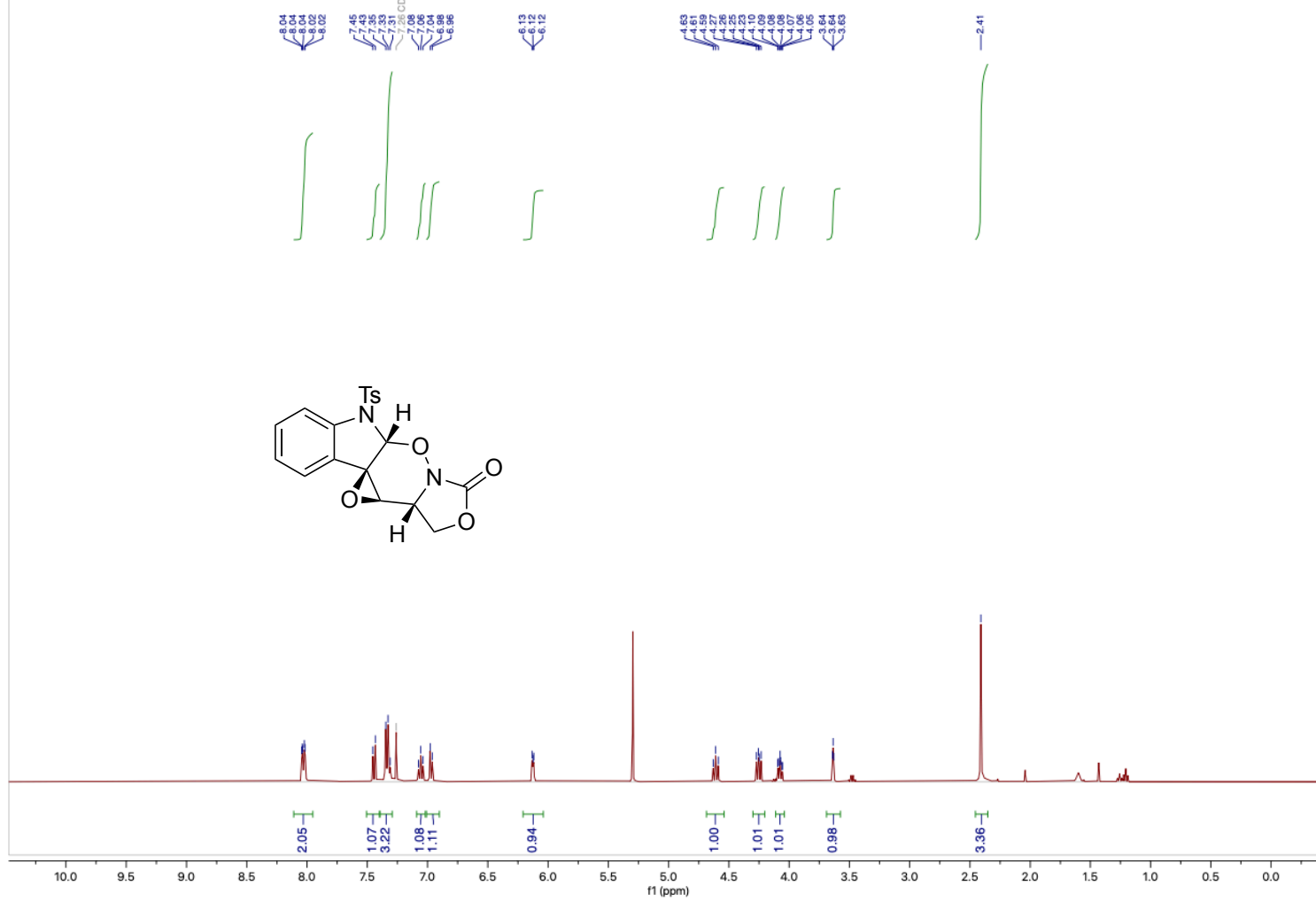


Figure B.34. ¹H NMR (400 MHz, CDCl₃) epoxide 3.52

AJ-04-289-singlediast-13C-CDCl₃.10.fid

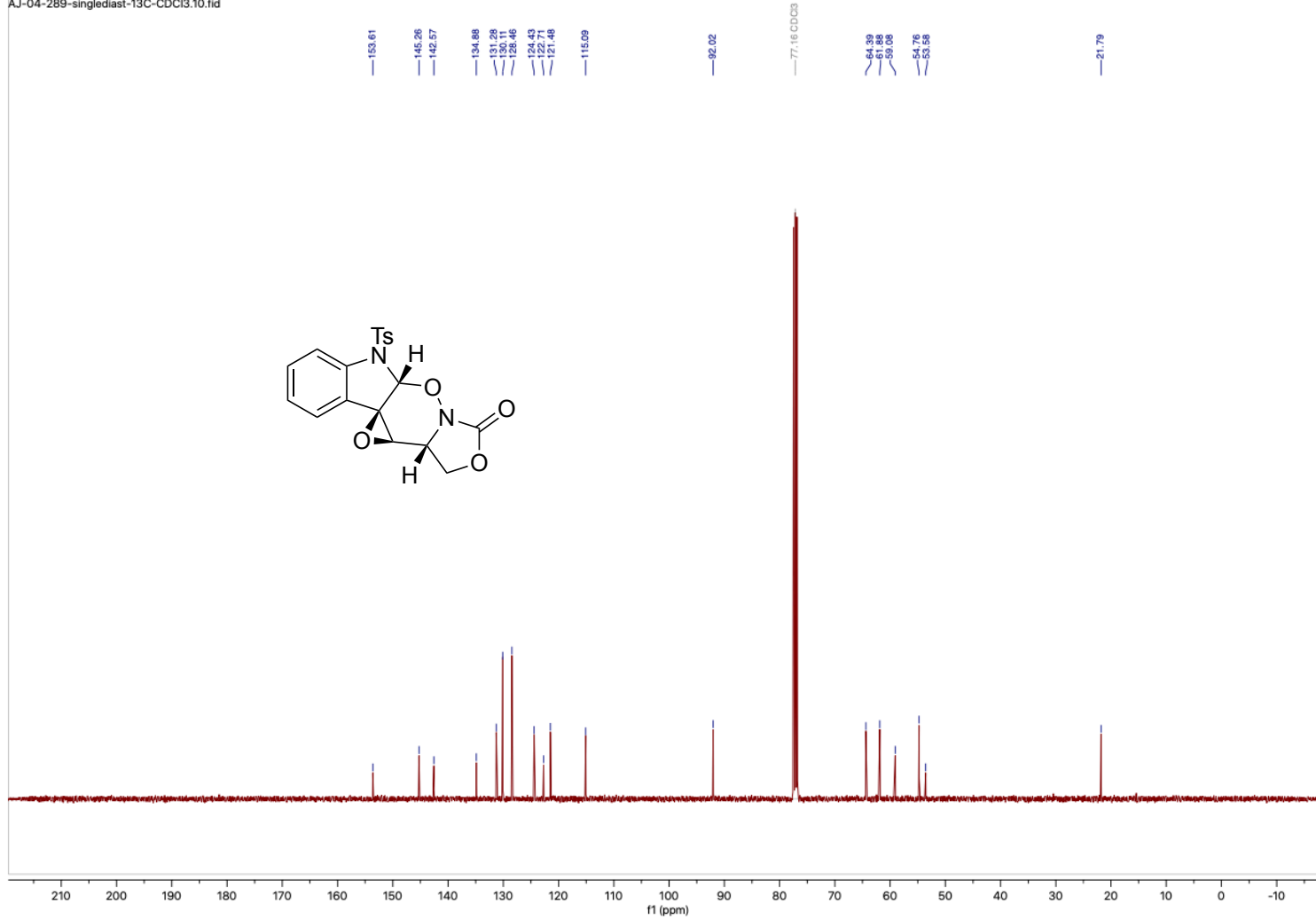


Figure B.35. ¹³C NMR (101 MHz, CDCl₃) epoxide 3.52

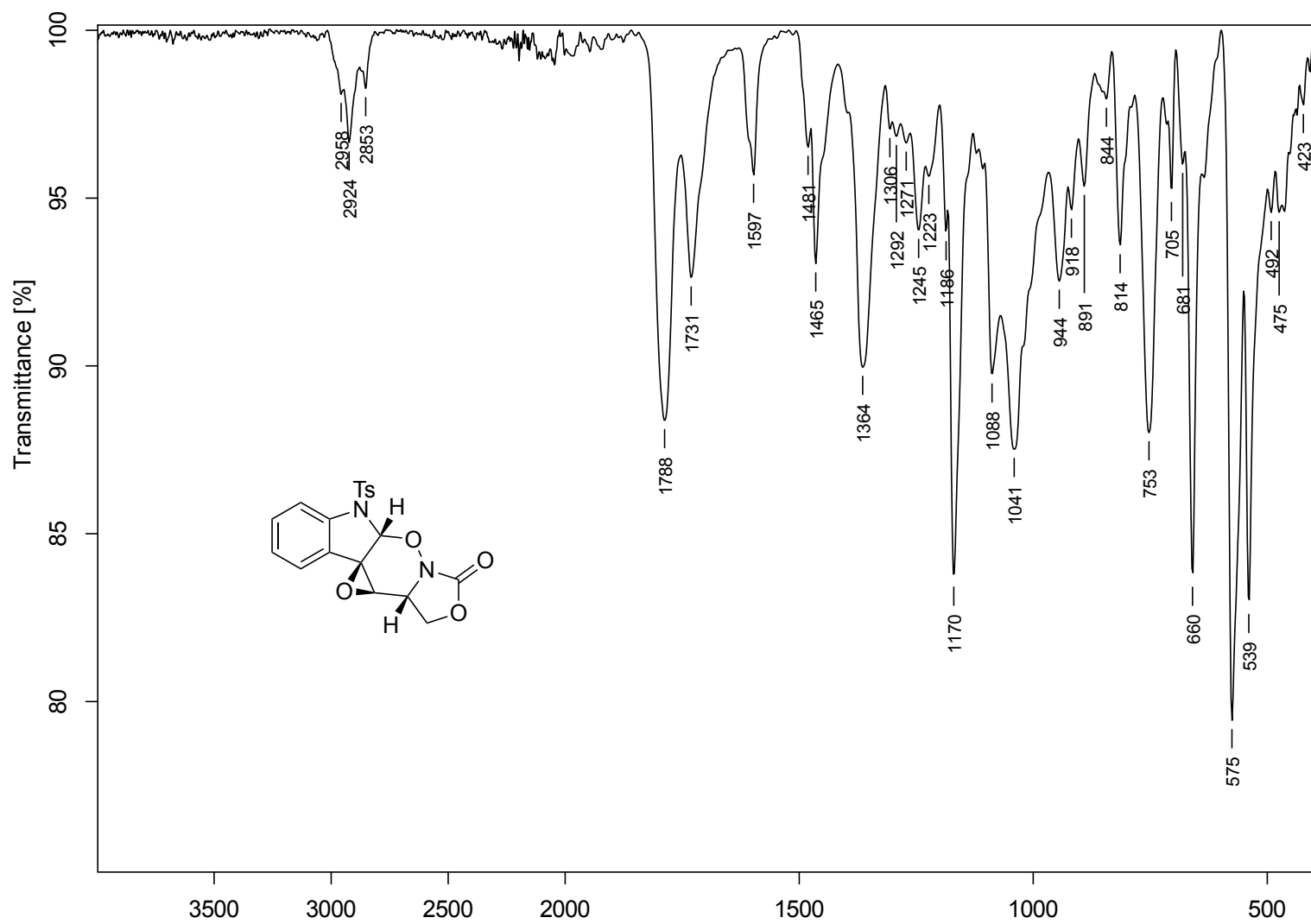


Figure B.36. FTIR (neat) epoxide 3.52

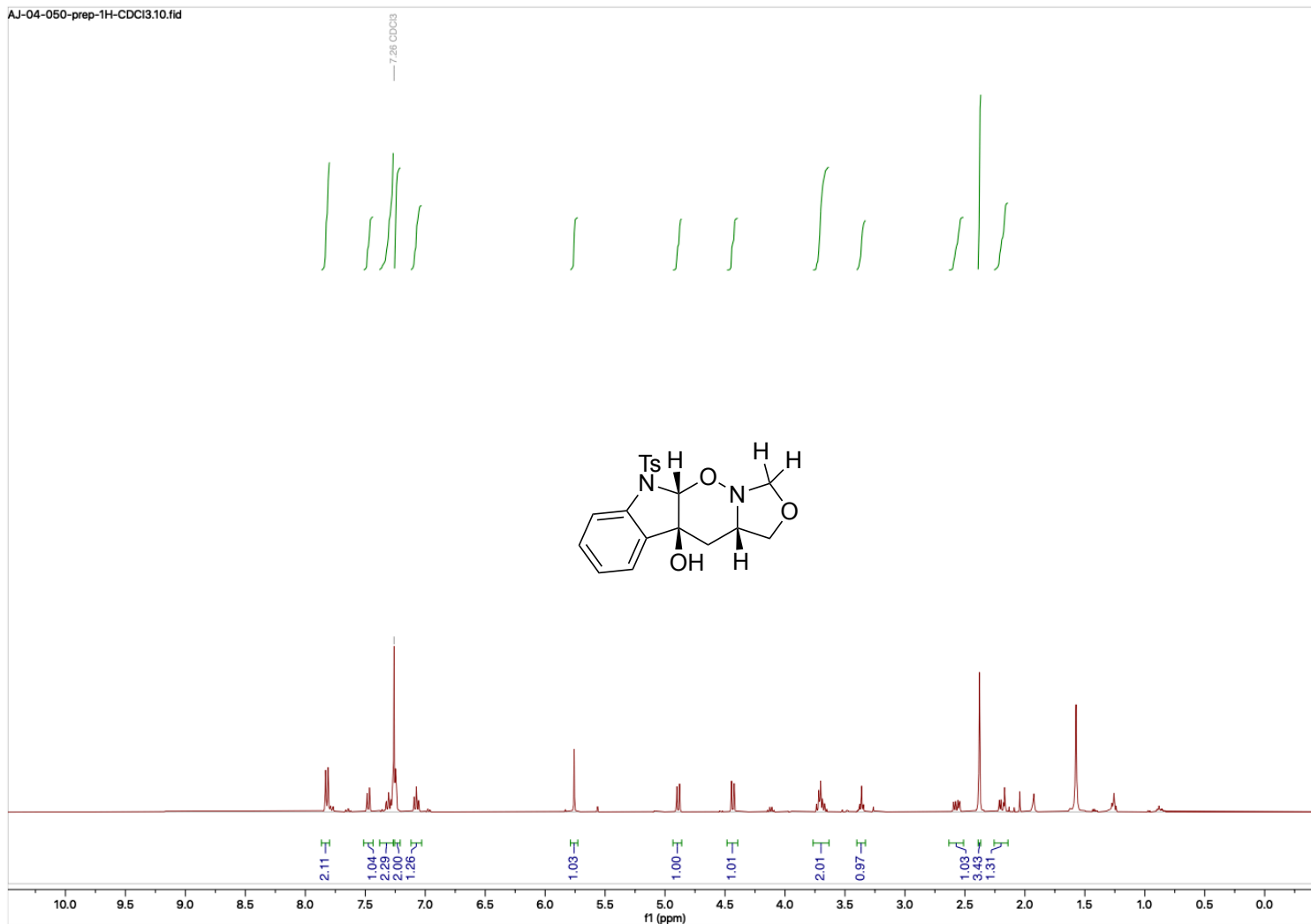


Figure B.37. ¹H NMR (400 MHz, CDCl₃) hemiaminal **3.53**

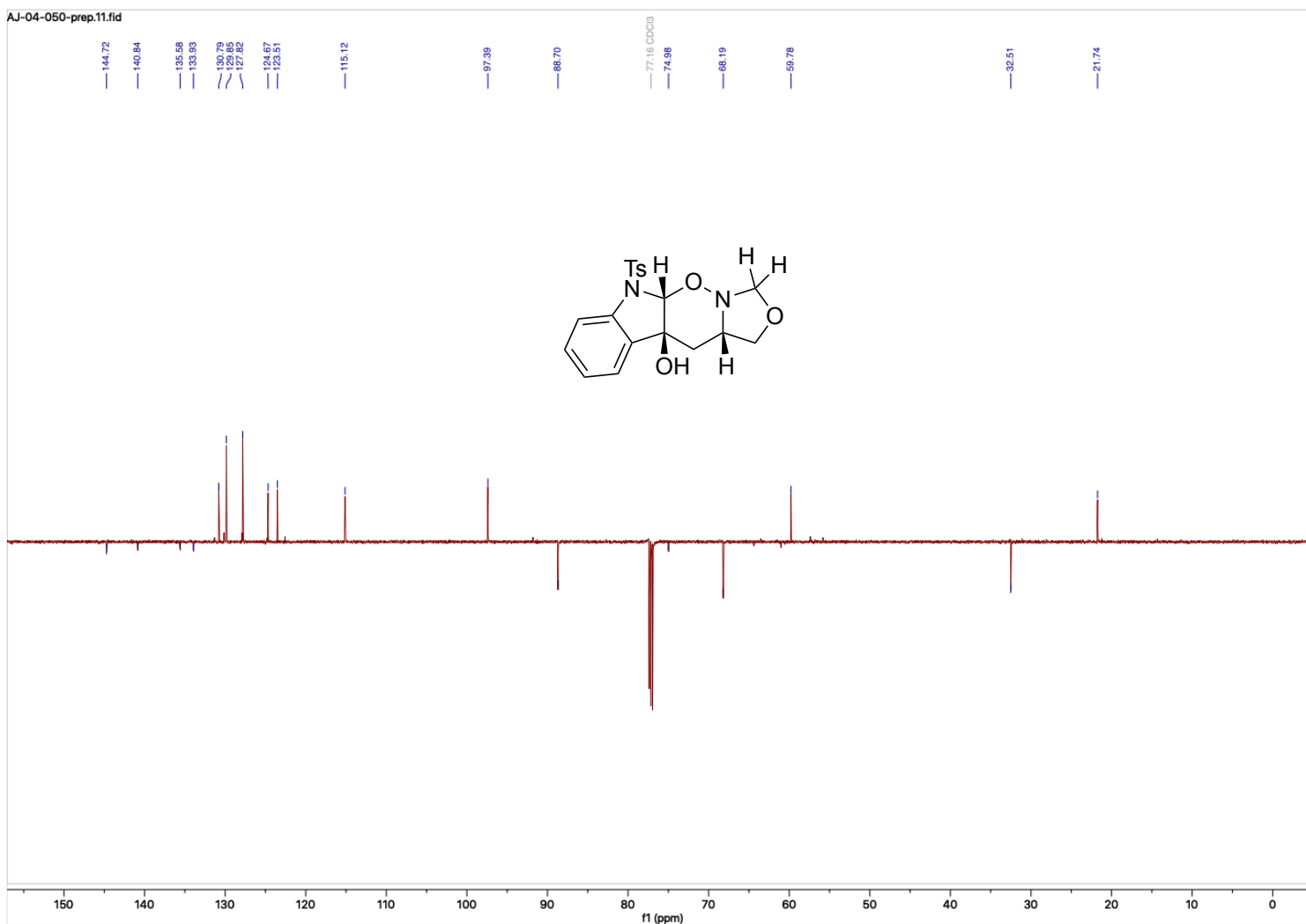


Figure B.38. ¹³C NMR DEPT135 (101 MHz, CDCl₃) hemiaminal 3.53

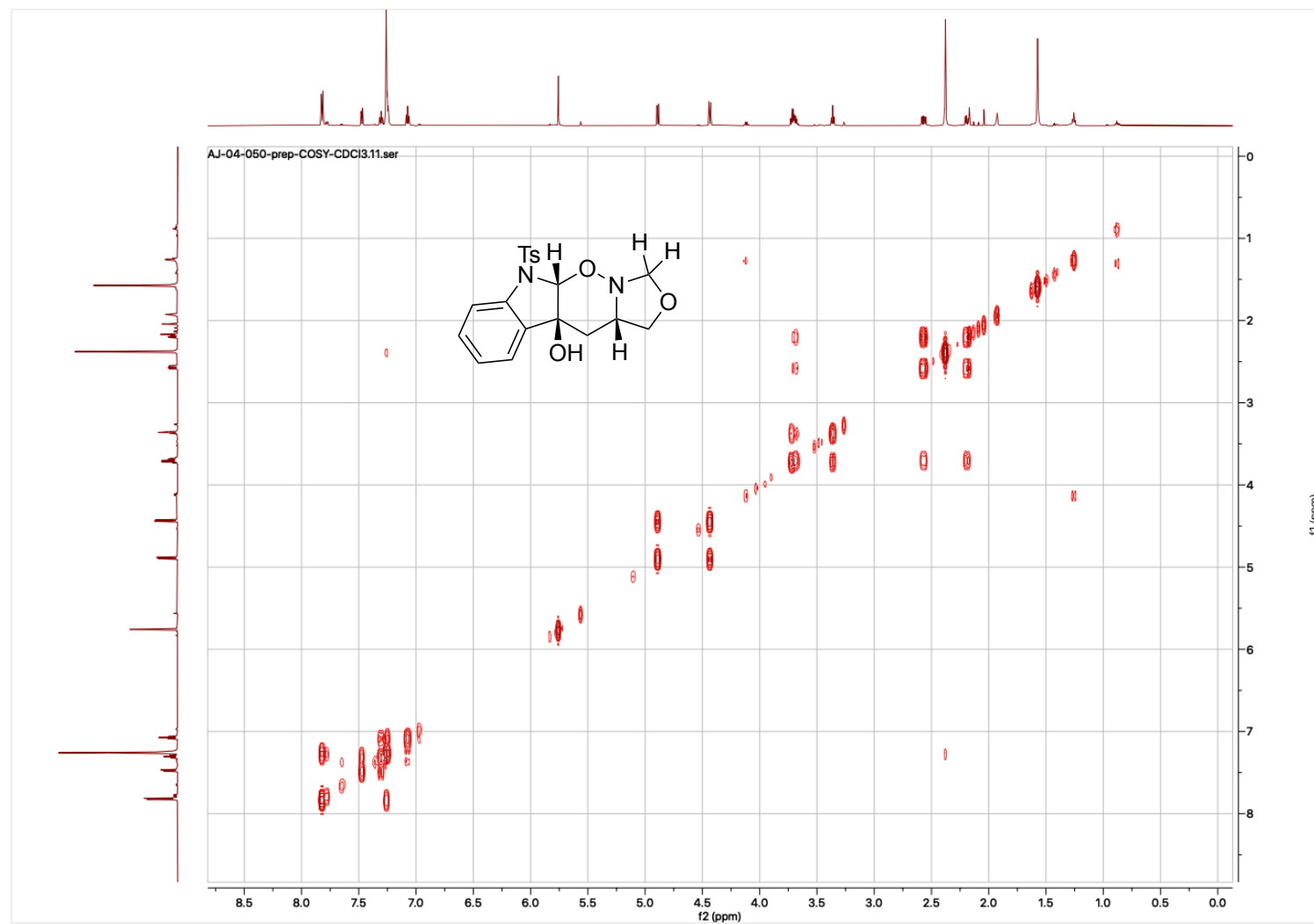


Figure B.39. COSY (400 MHz, CDCl₃) hemiaminal 3.53

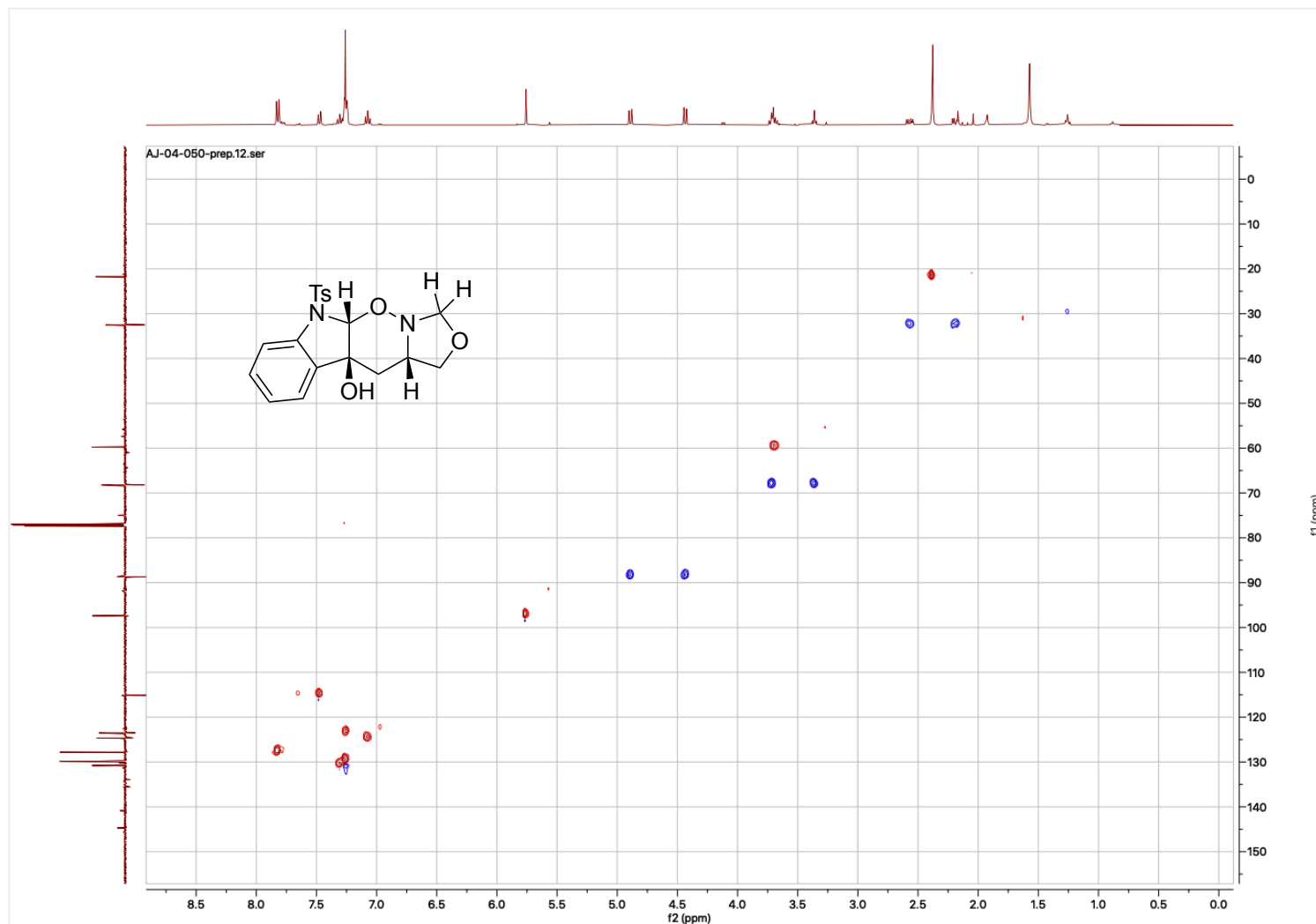


Figure B.40. HSQC (400 MHz, 101 MHz, CDCl_3 ; edited: blue = CH_2 , red = CH_3/CH) hemiaminal 3.53

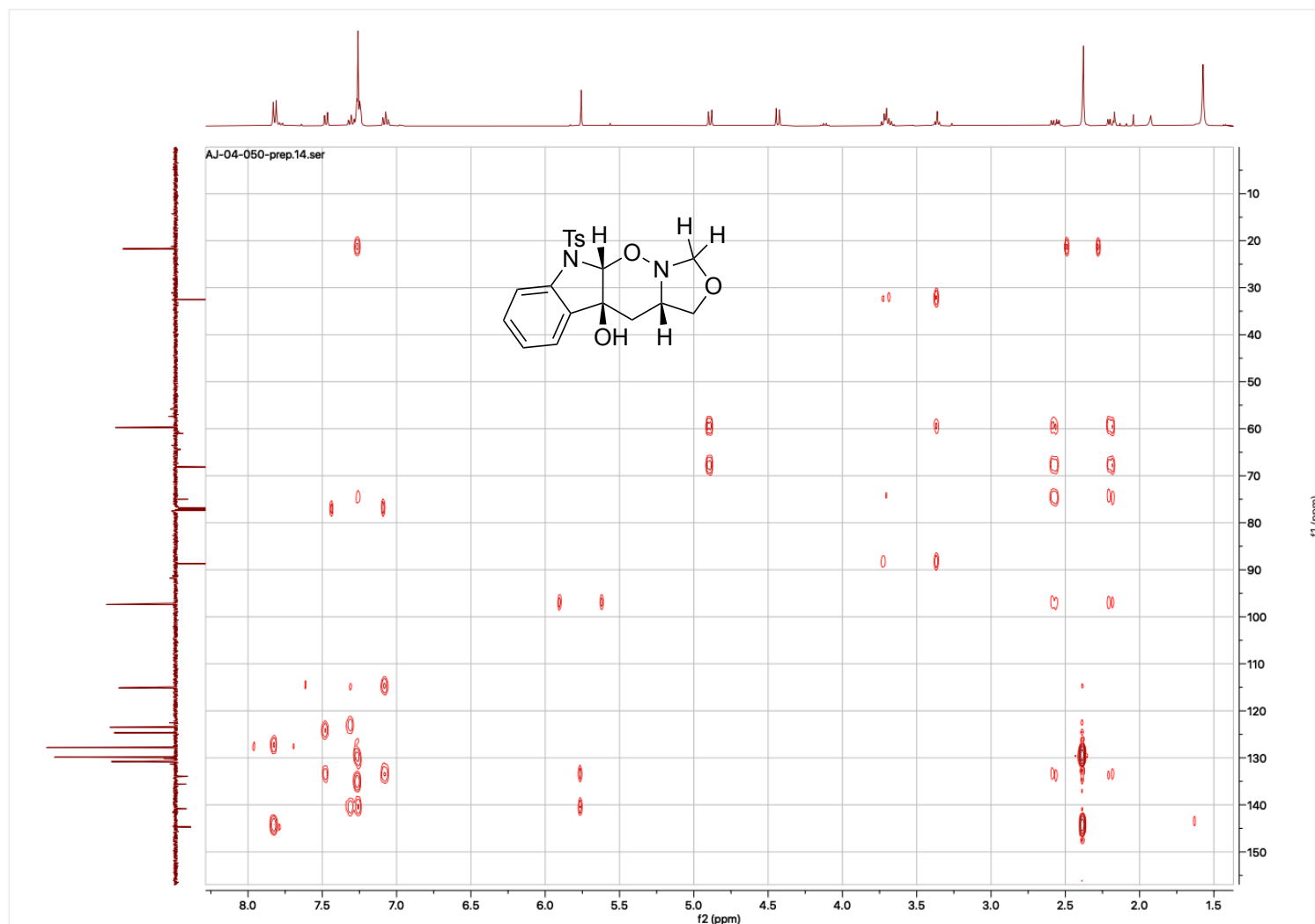


Figure B.41. HMBC (400 MHz, 101 MHz, CDCl₃) hemiaminal **3.53**

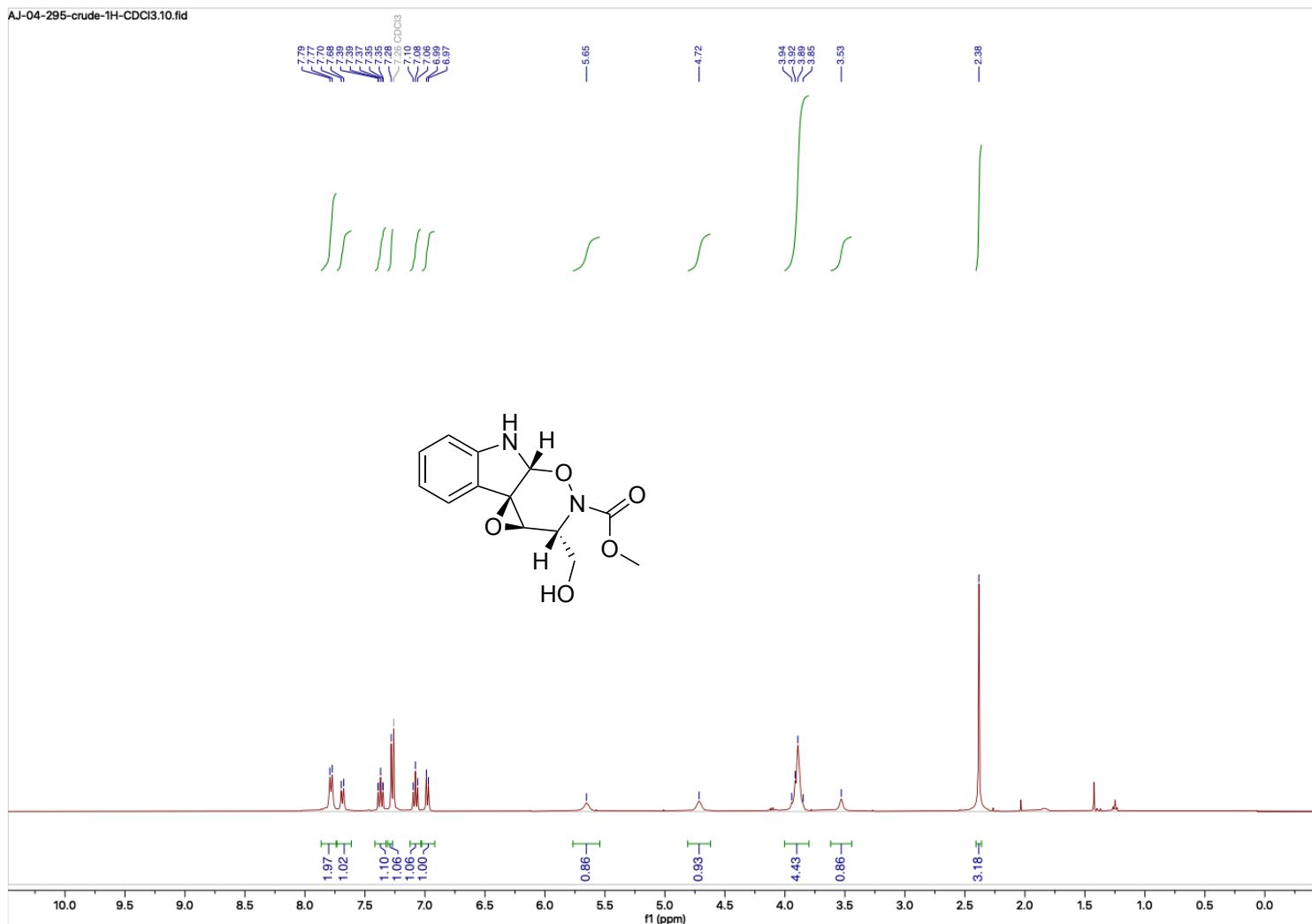


Figure B.42. ¹H NMR (400 MHz, CDCl₃) methyl carbamate **3.54**

AJ-04-297-repurif-13C-CDCl₃.12.fid

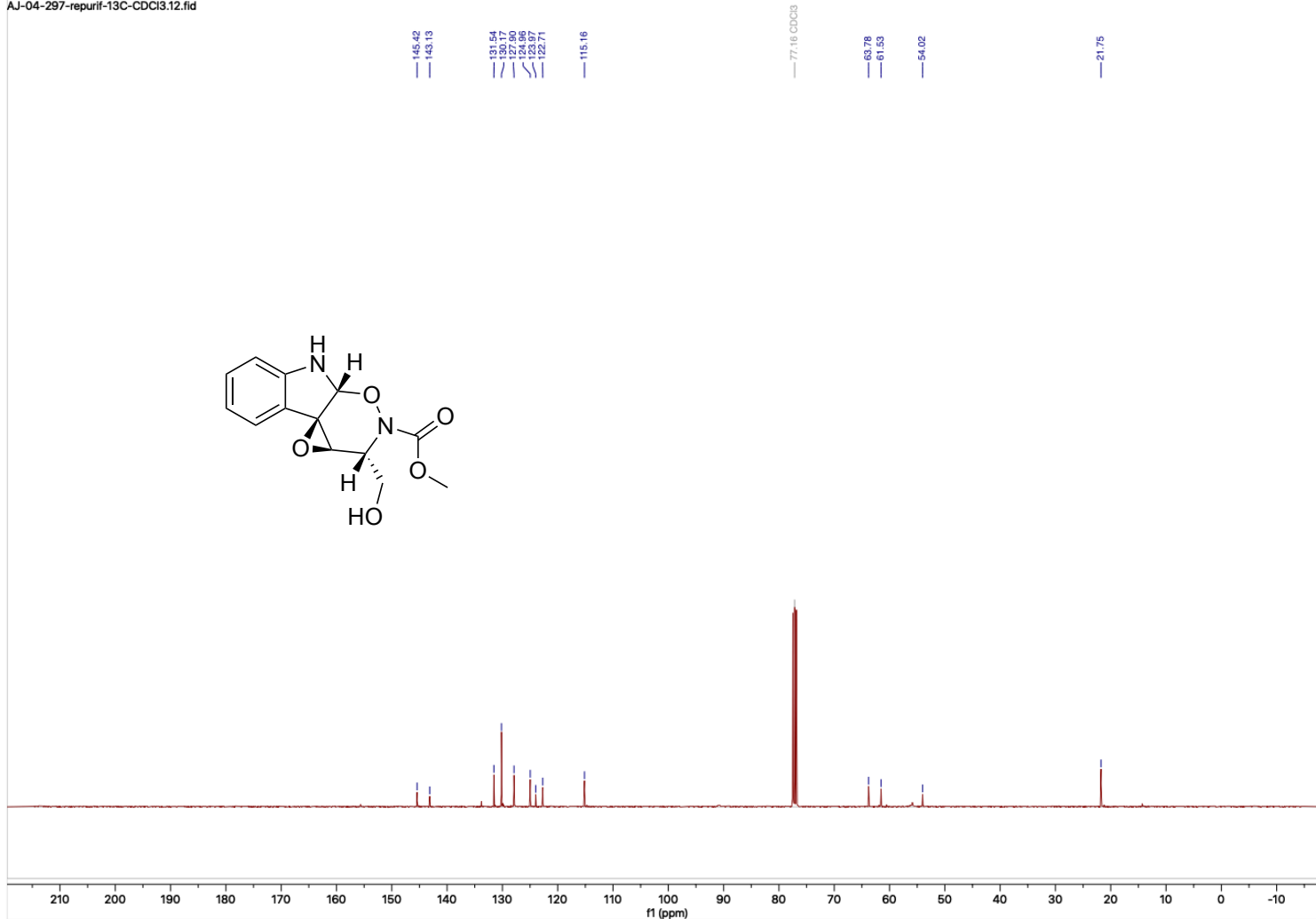


Figure B.43. ¹³C NMR (101 MHz, CDCl₃) methyl carbamate **3.54**

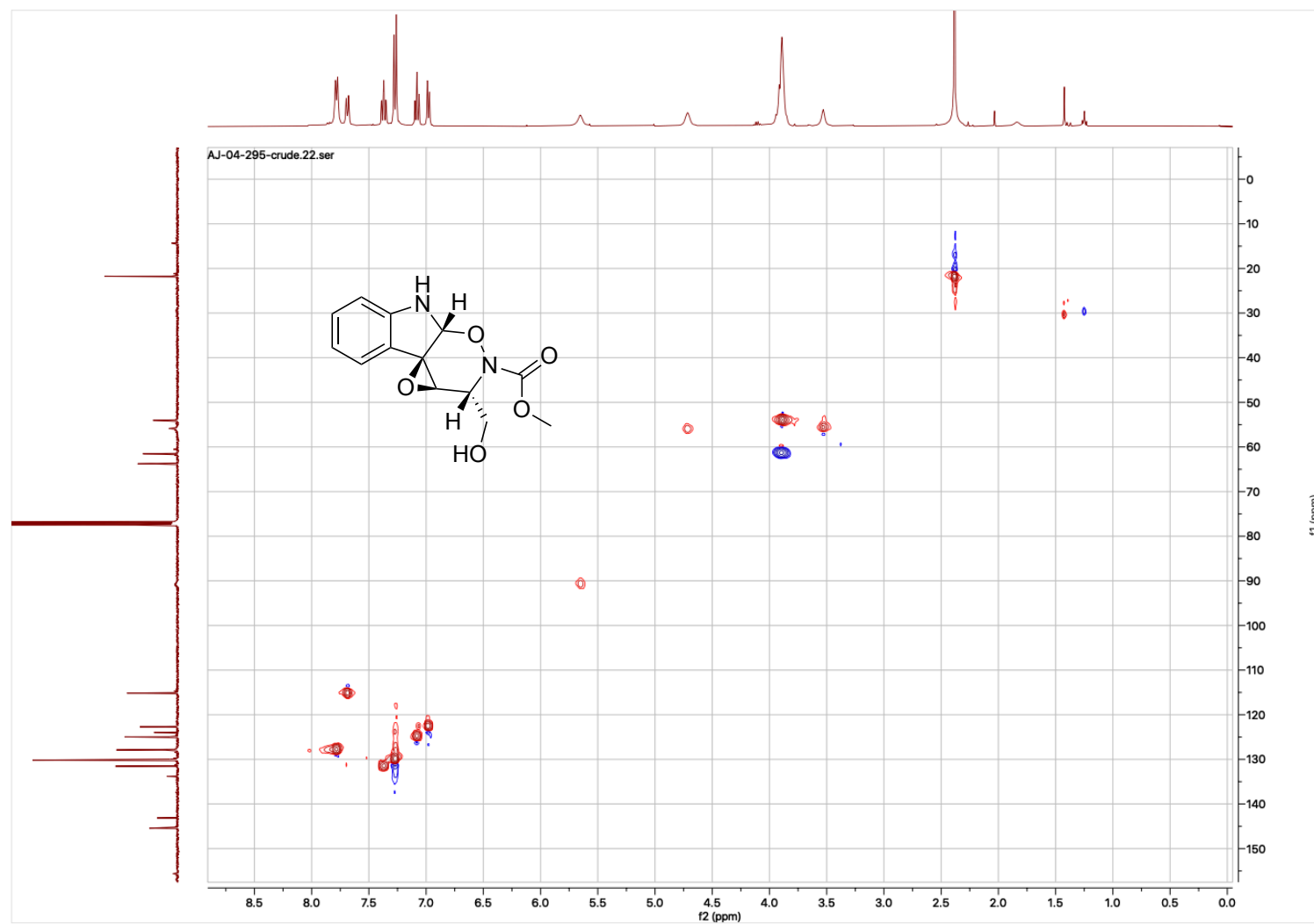


Figure B.44. HSQC (400 MHz, 101 MHz, CDCl₃; edited: blue = CH₂, red = CH₃/CH) methyl carbamate **3.54**

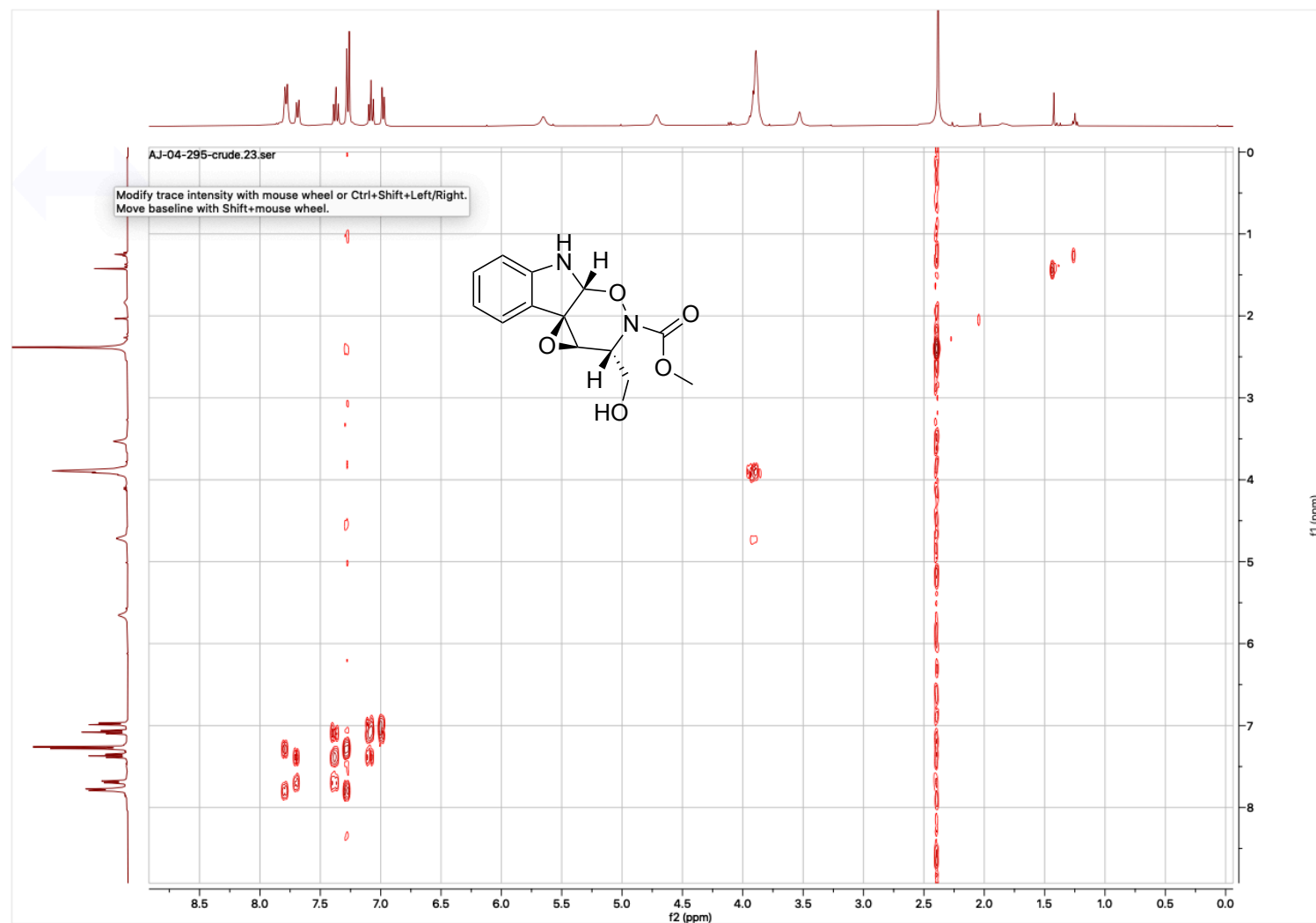


Figure B.45. COSY (400 MHz, CDCl₃) methyl carbamate **3.54**

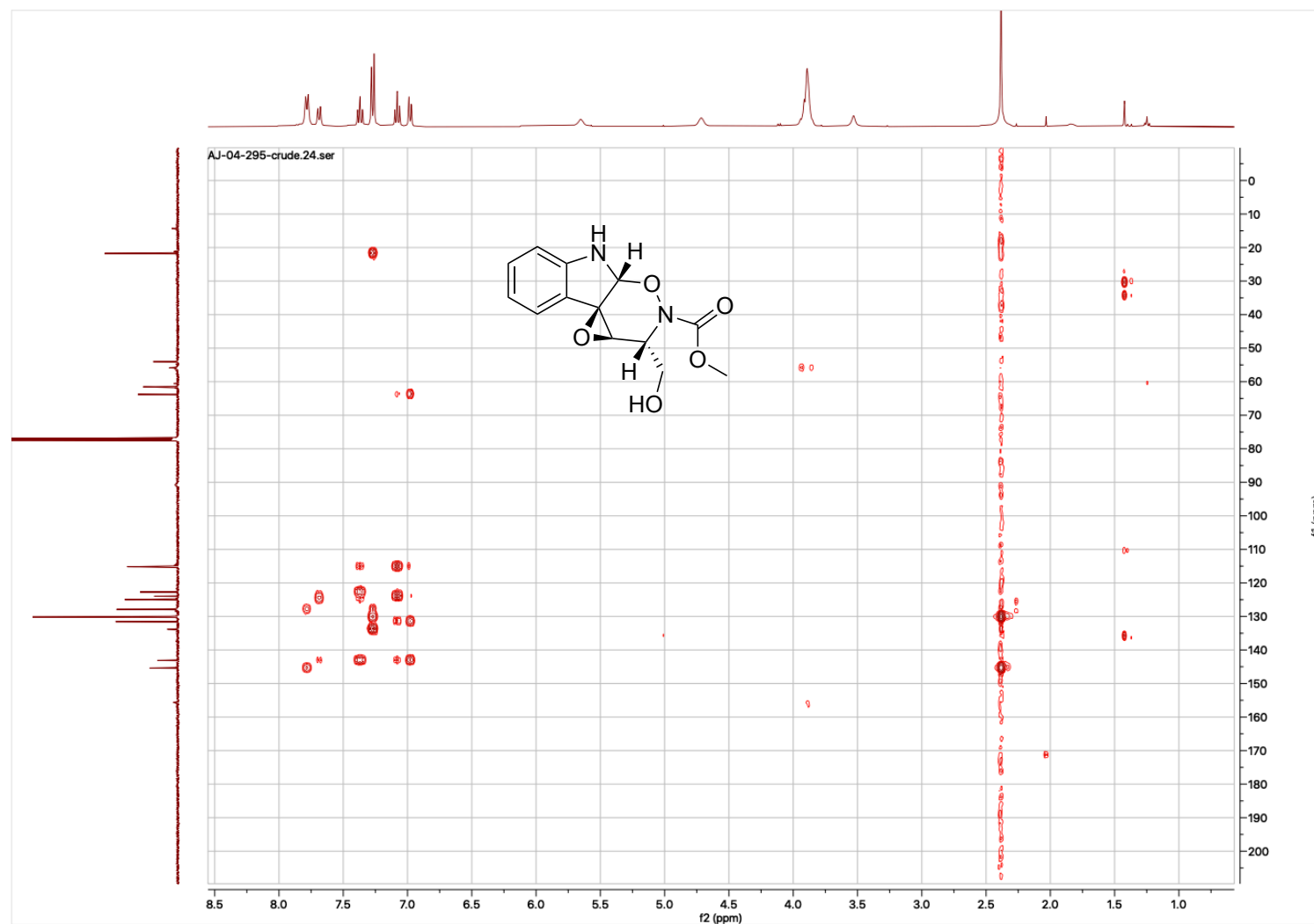


Figure B.46. HMBC (400 MHz, 101 MHz, CDCl₃) methyl carbamate **3.54**

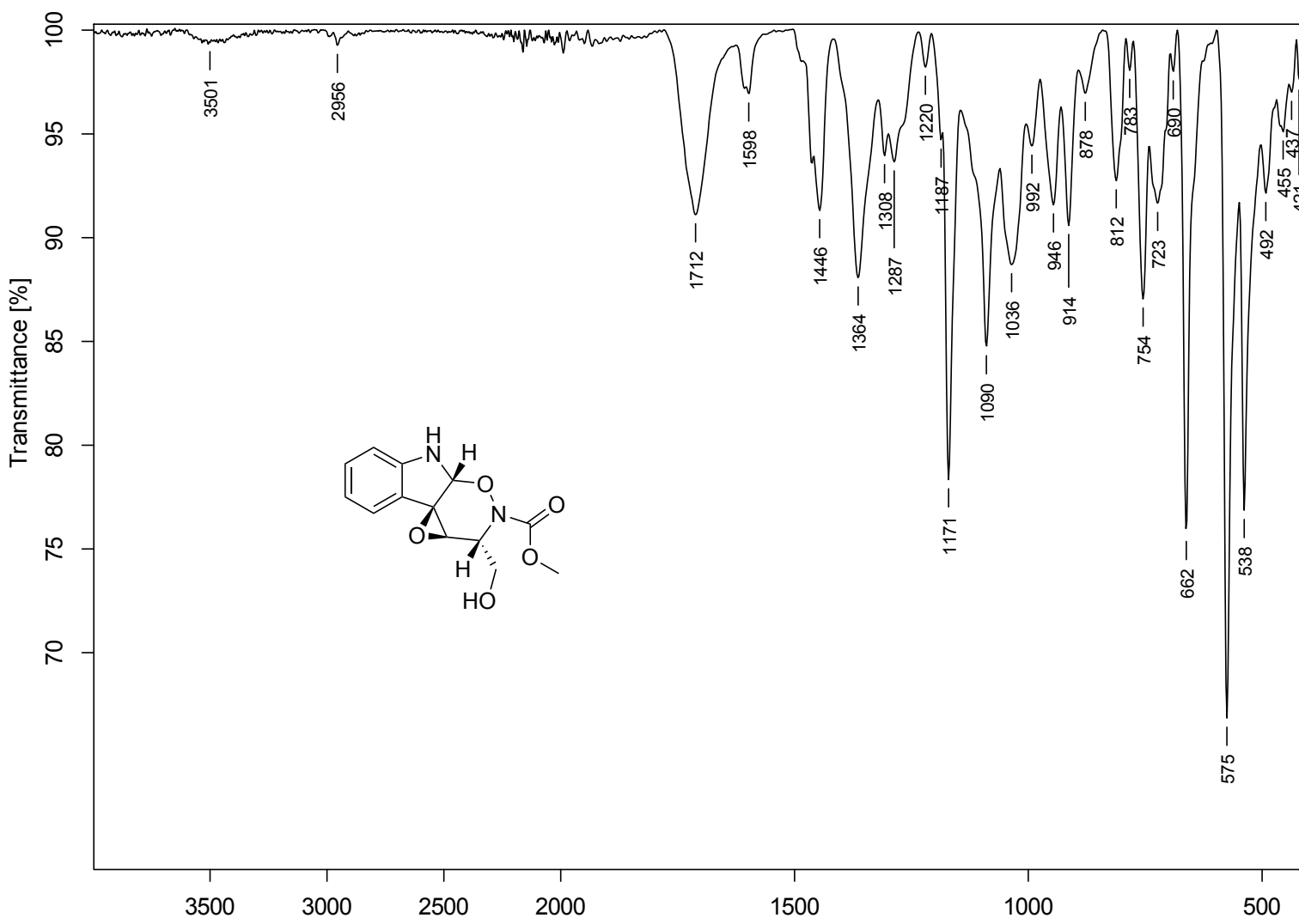


Figure B.47. FTIR (neat) methyl carbamate **3.54**

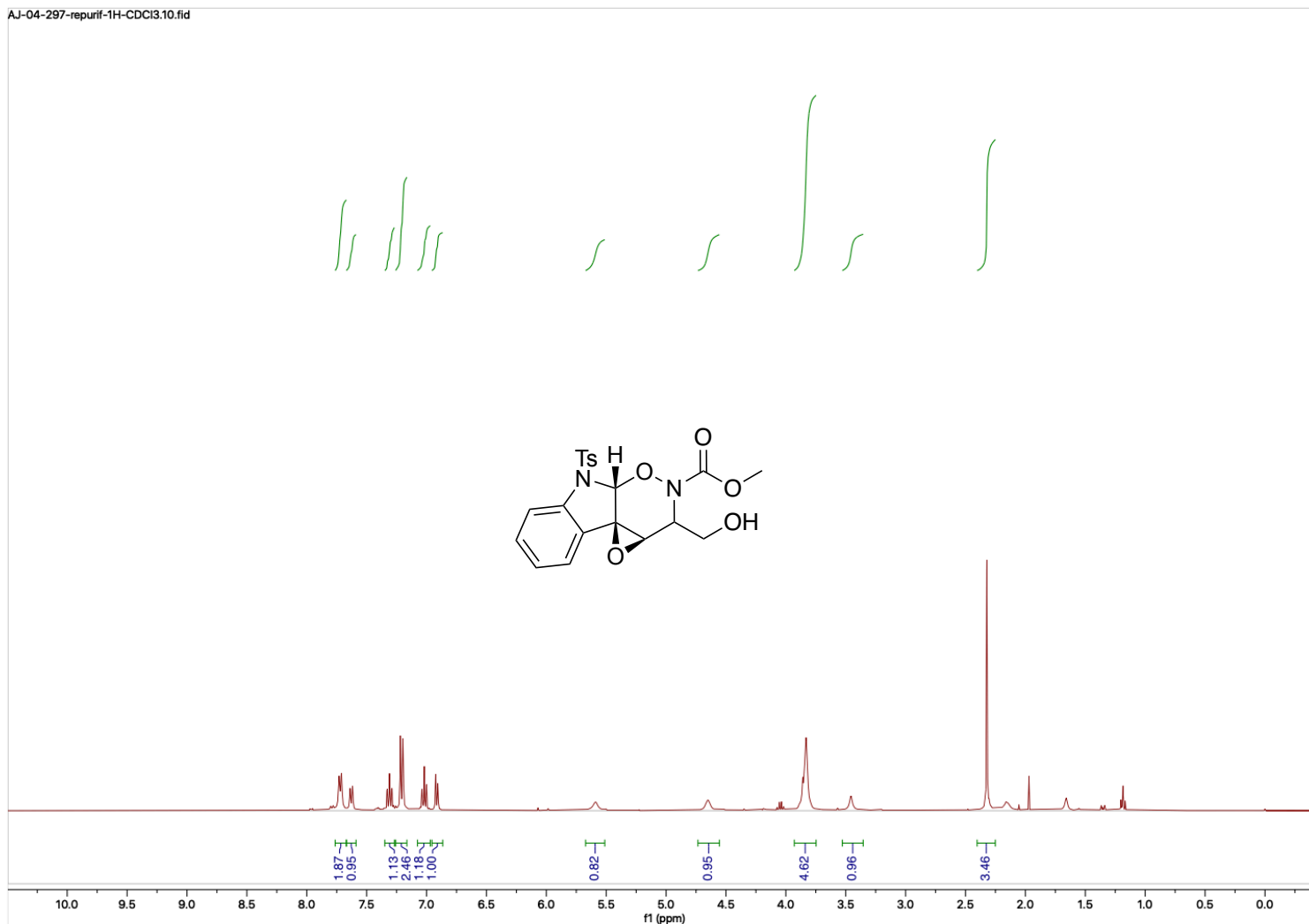


Figure B.48. ¹H NMR (400 MHz, CDCl₃) by-product methyl carbamate **3.56**

AJ-04-297-repurif-13C-CDCl₃.12.fid

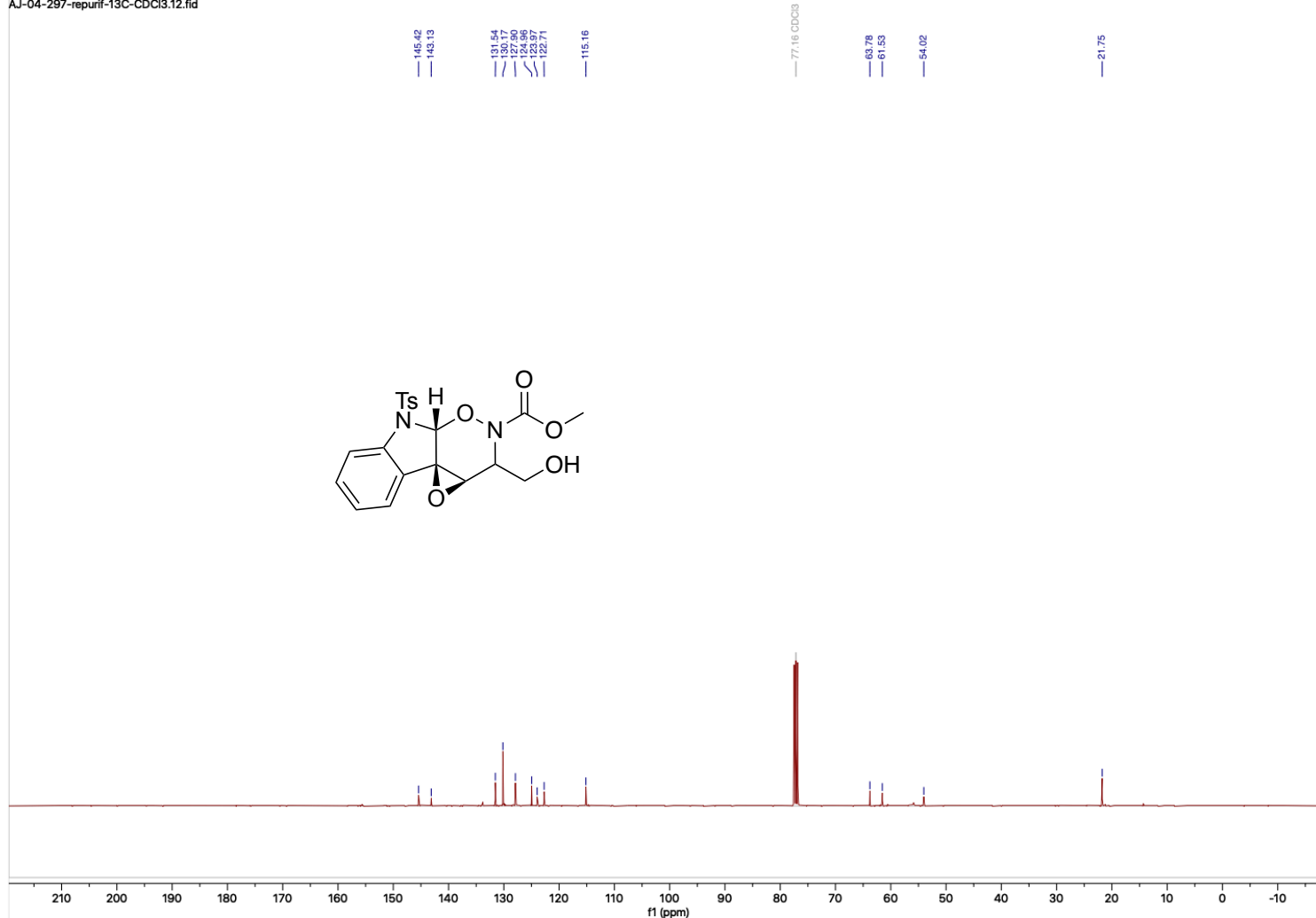


Figure B.49. ¹³C NMR (101 MHz, CDCl₃) by-product methyl carbamate **3.56**

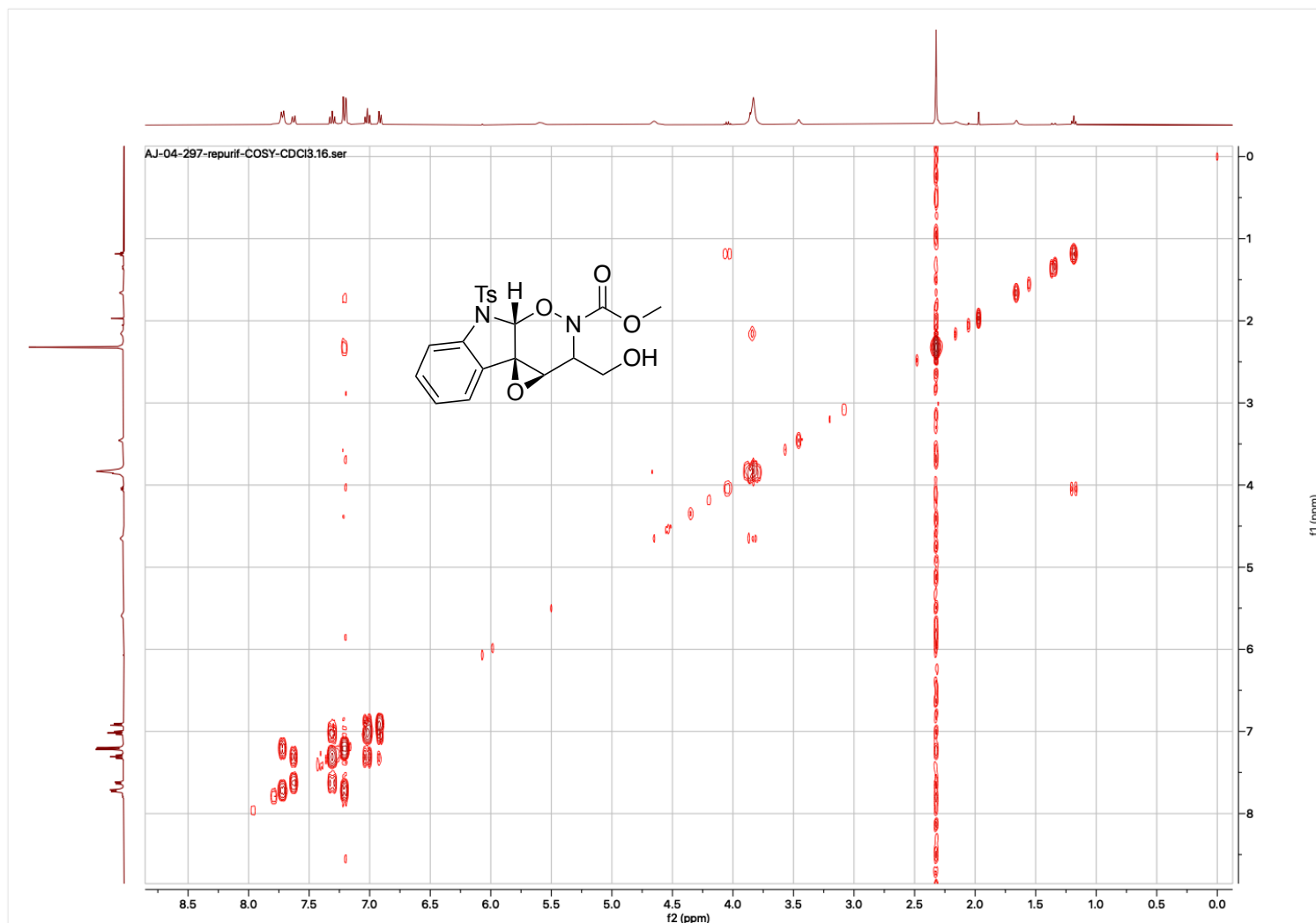


Figure B.50. COSY (400 MHz, CDCl₃) by-product methyl carbamate **3.56**

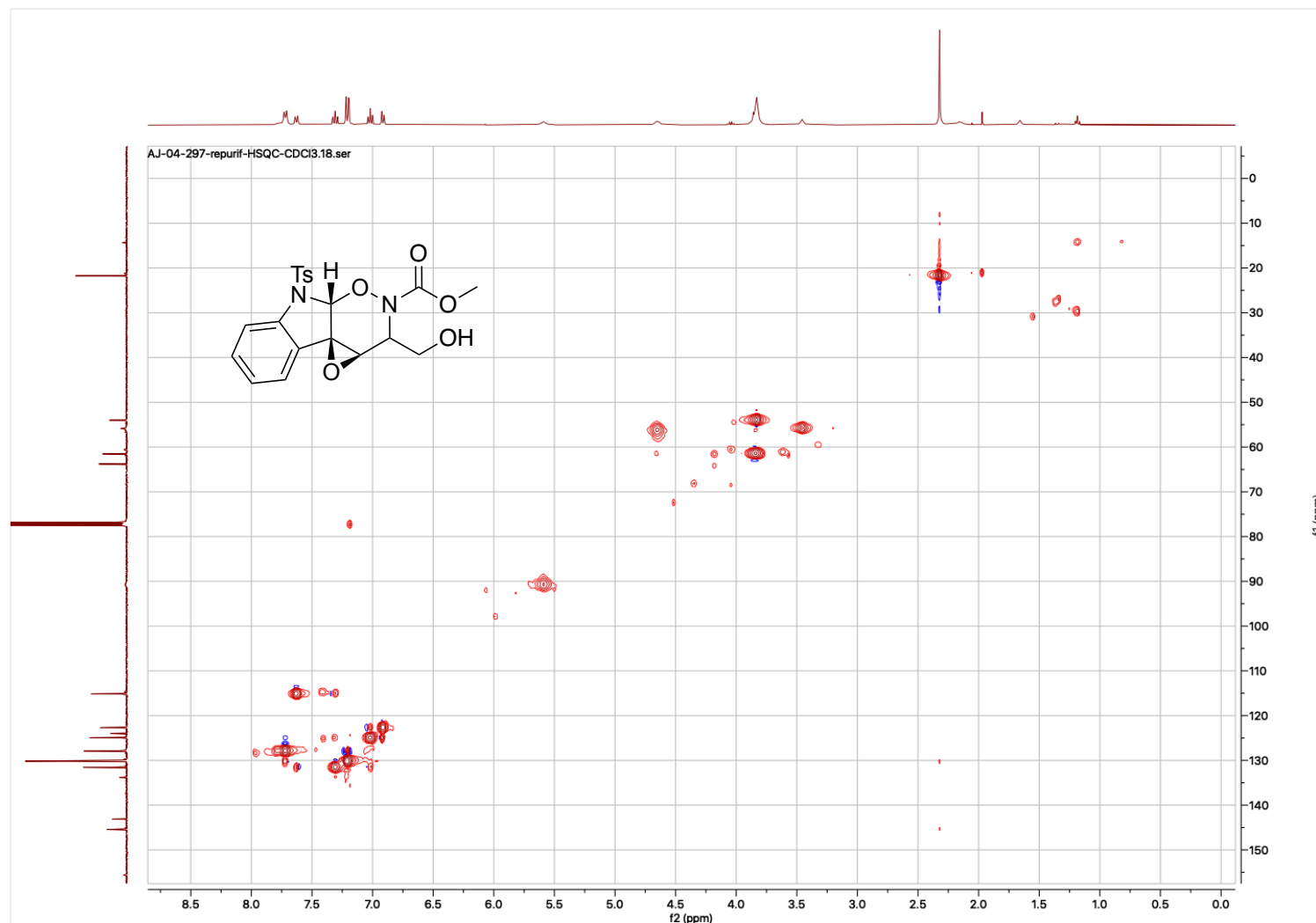


Figure B.51. HSQC (400, 101 MHz, CDCl₃; edited: CH/CH₃ = red, CH₂ = blue) by-product methyl carbamate **3.56**

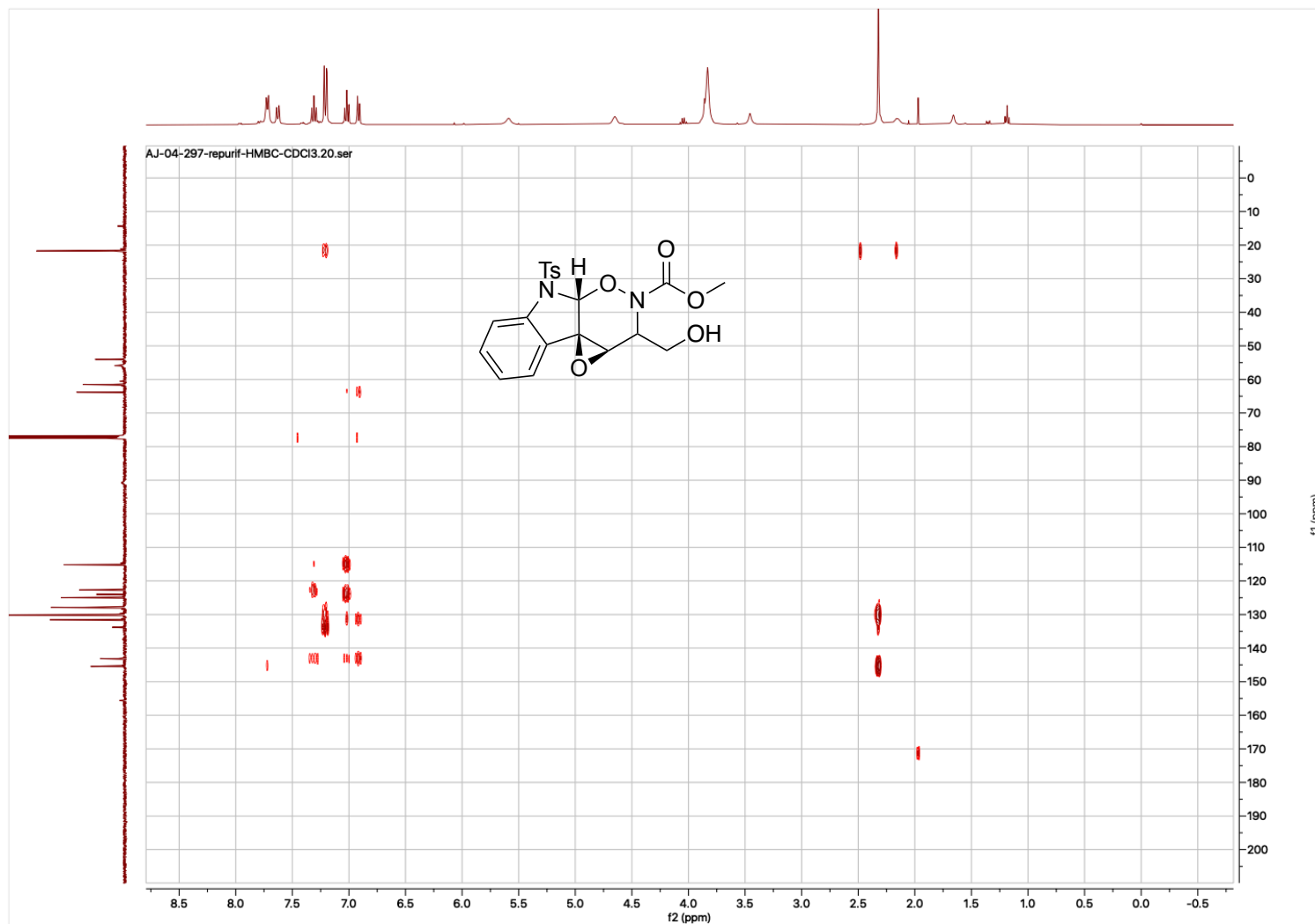


Figure B.52. HMBC (400 MHz, 101 MHz, CDCl₃) by-product methyl carbamate **3.56**

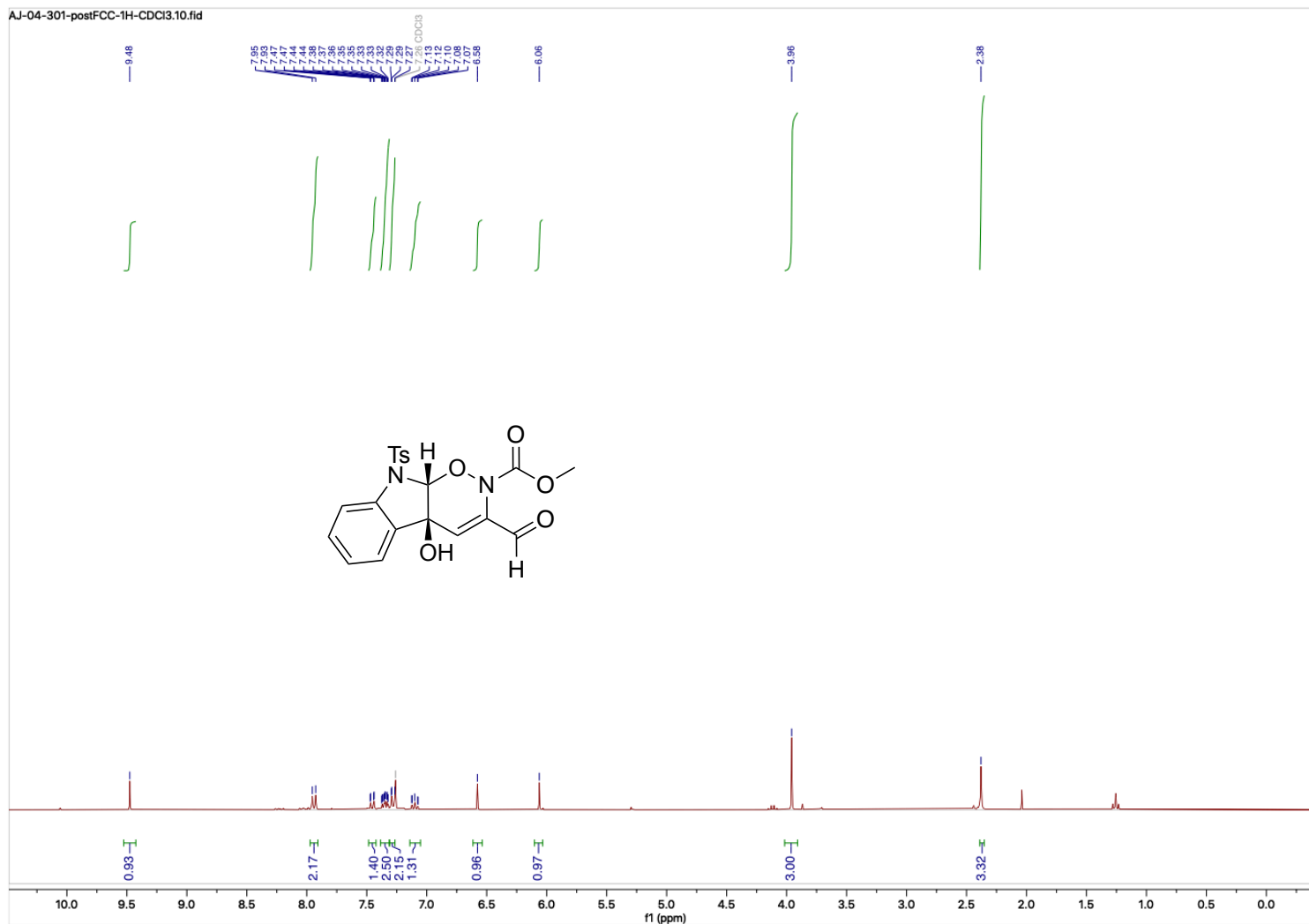


Figure B.53. ¹H NMR (300 MHz, CDCl₃) proposed aldehyde **3.57**

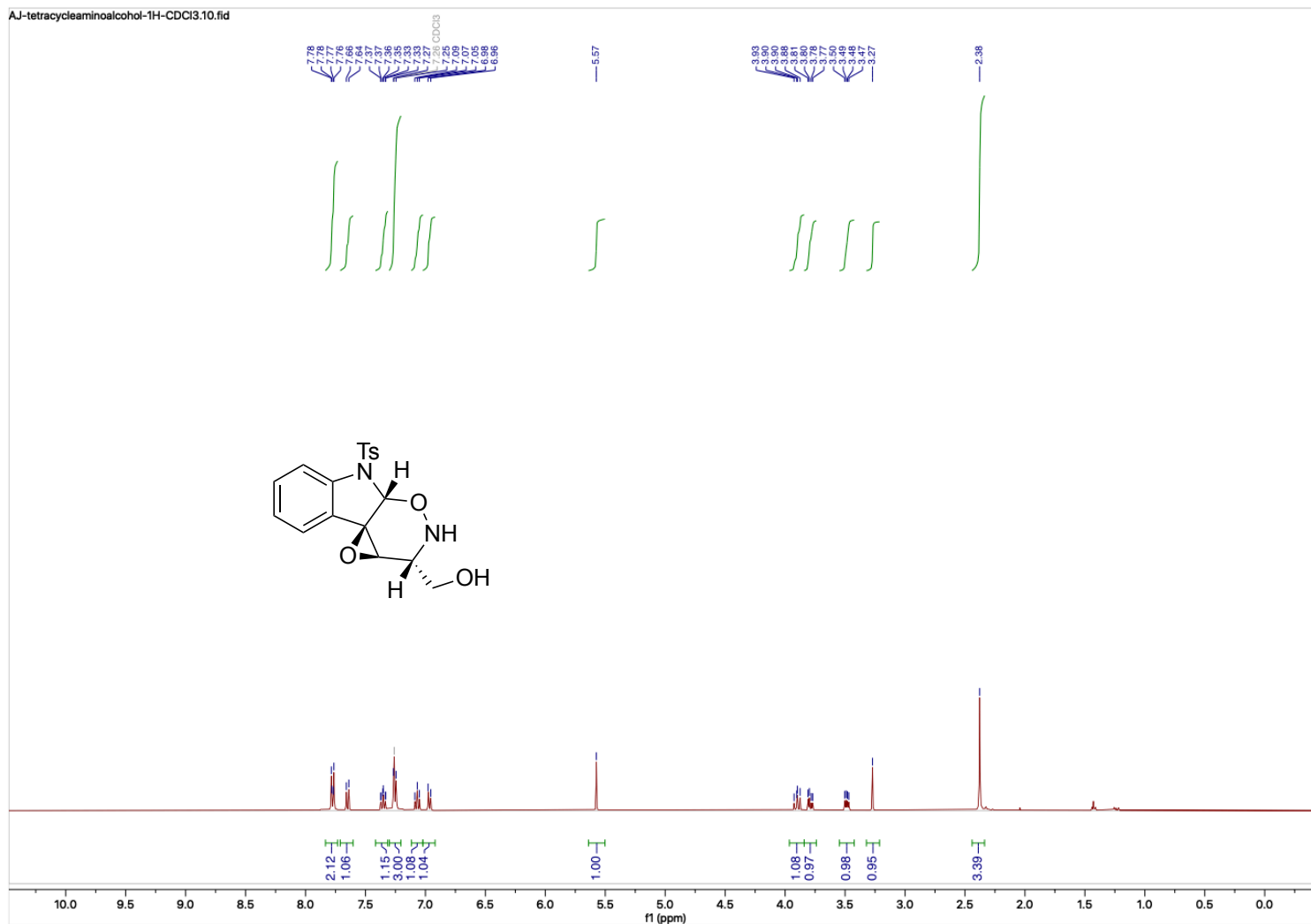


Figure B.54. ¹H NMR (400 MHz, CDCl₃) amino alcohol **3.55**

AJ-tetracyclicaminoalcohol-13C-CDCl₃.12.fid

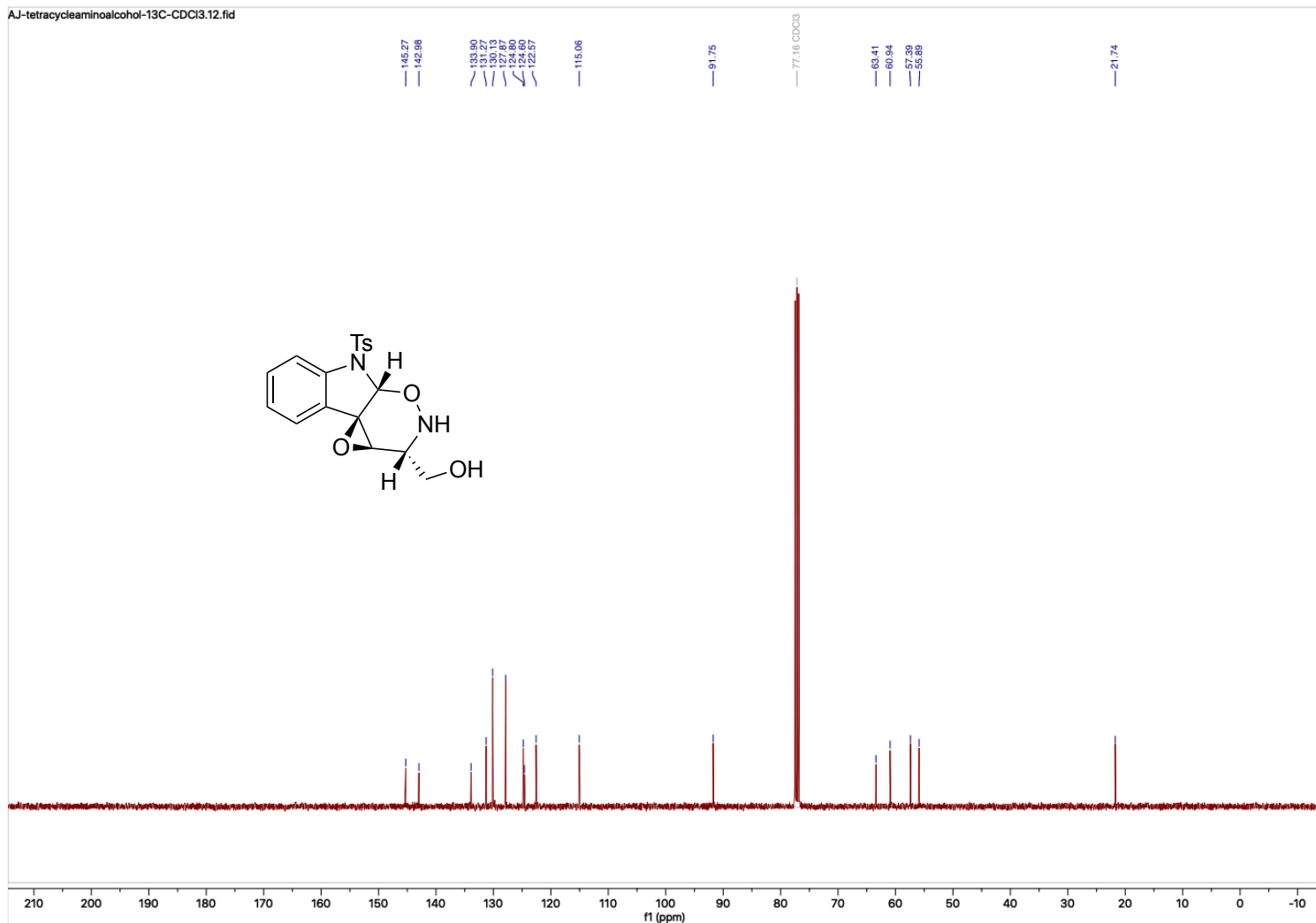


Figure B.55. ¹³C NMR (101 MHz, CDCl₃) amino alcohol **3.55**

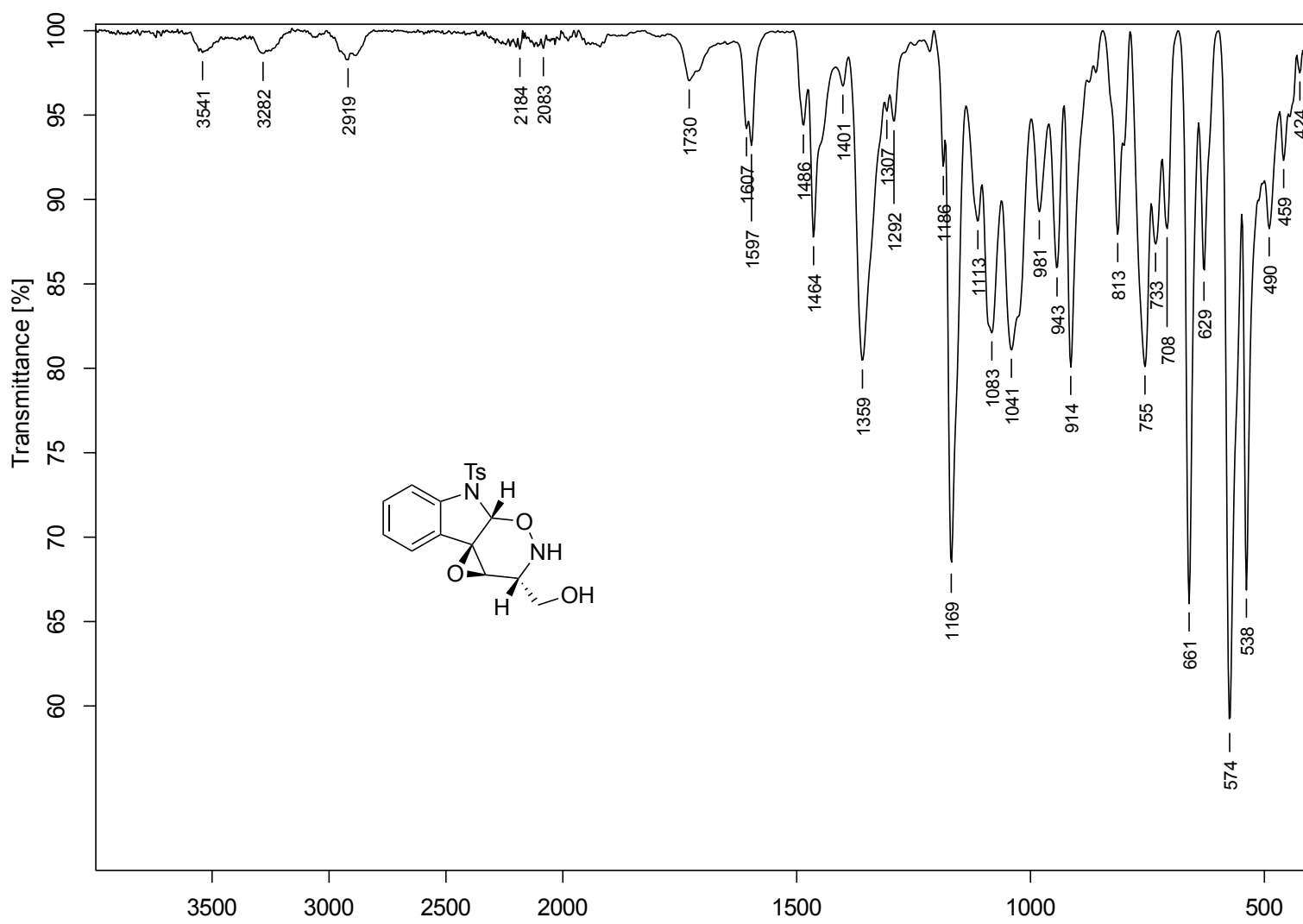


Figure B.56. FTIR (neat) amino alcohol **3.55**

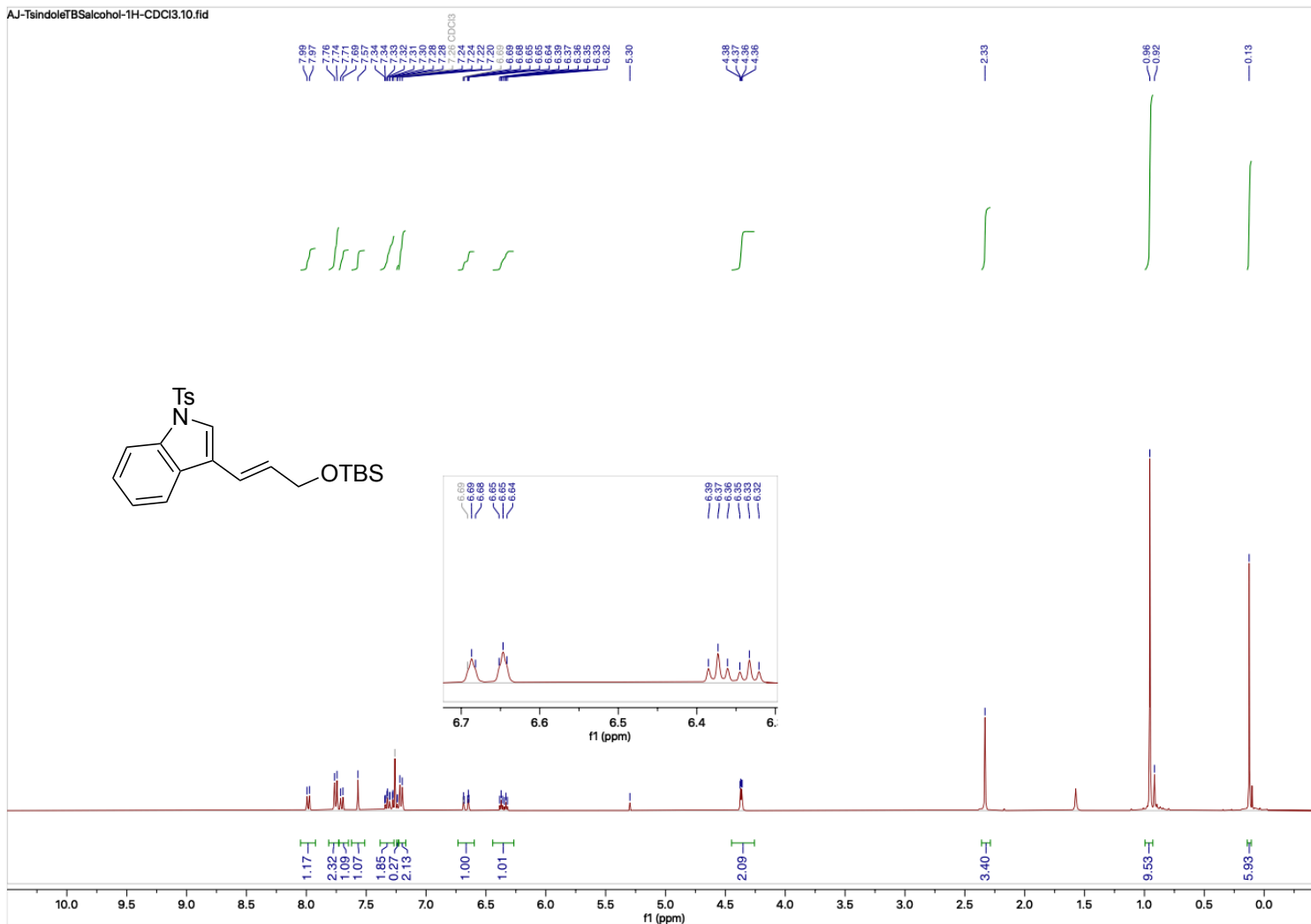


Figure B.57. ^1H NMR (400 MHz, solvent) known TBS alcohol **3.61**

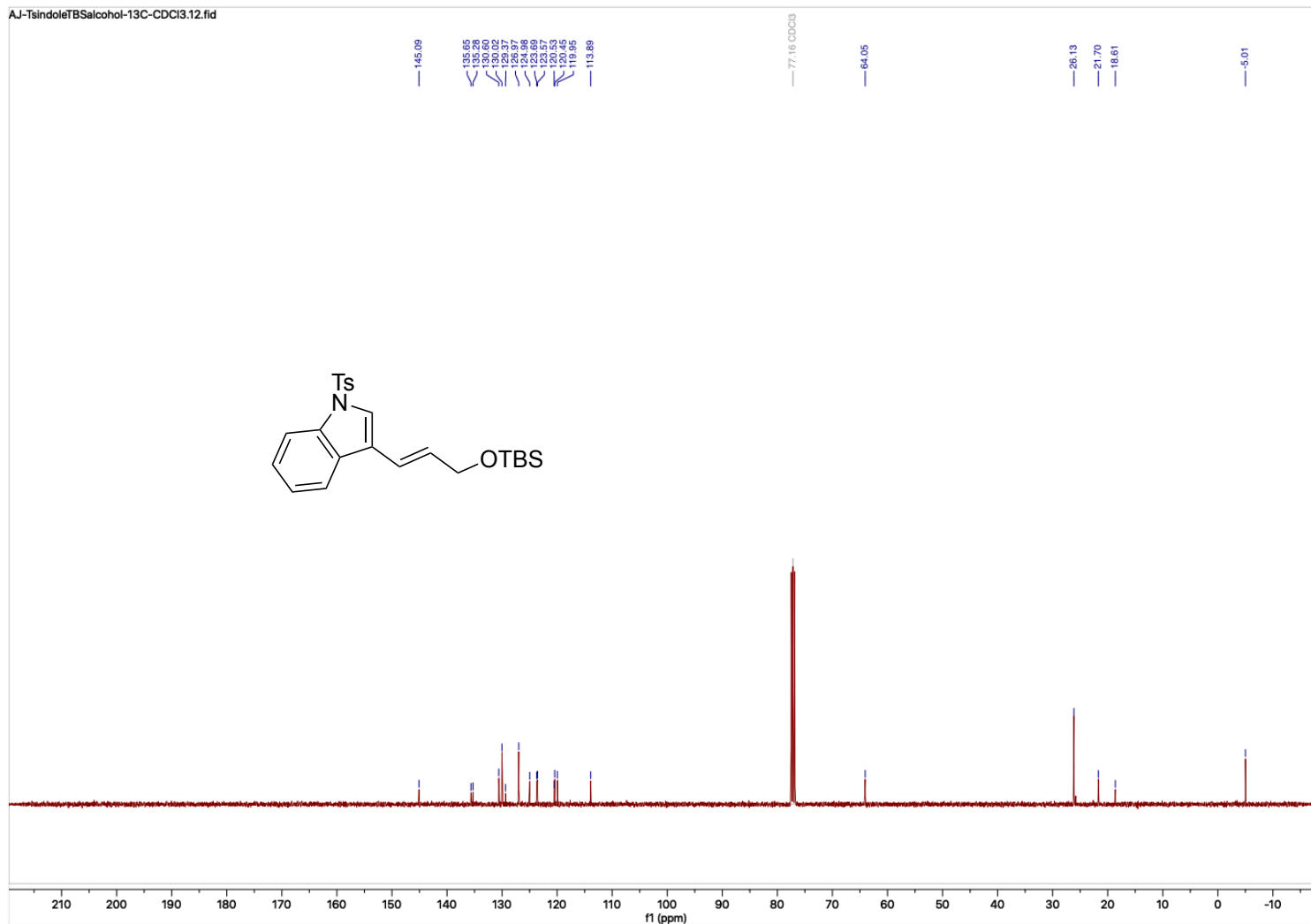


Figure B.58. ¹³C NMR (101 MHz, solvent) known TBS alcohol **3.61**

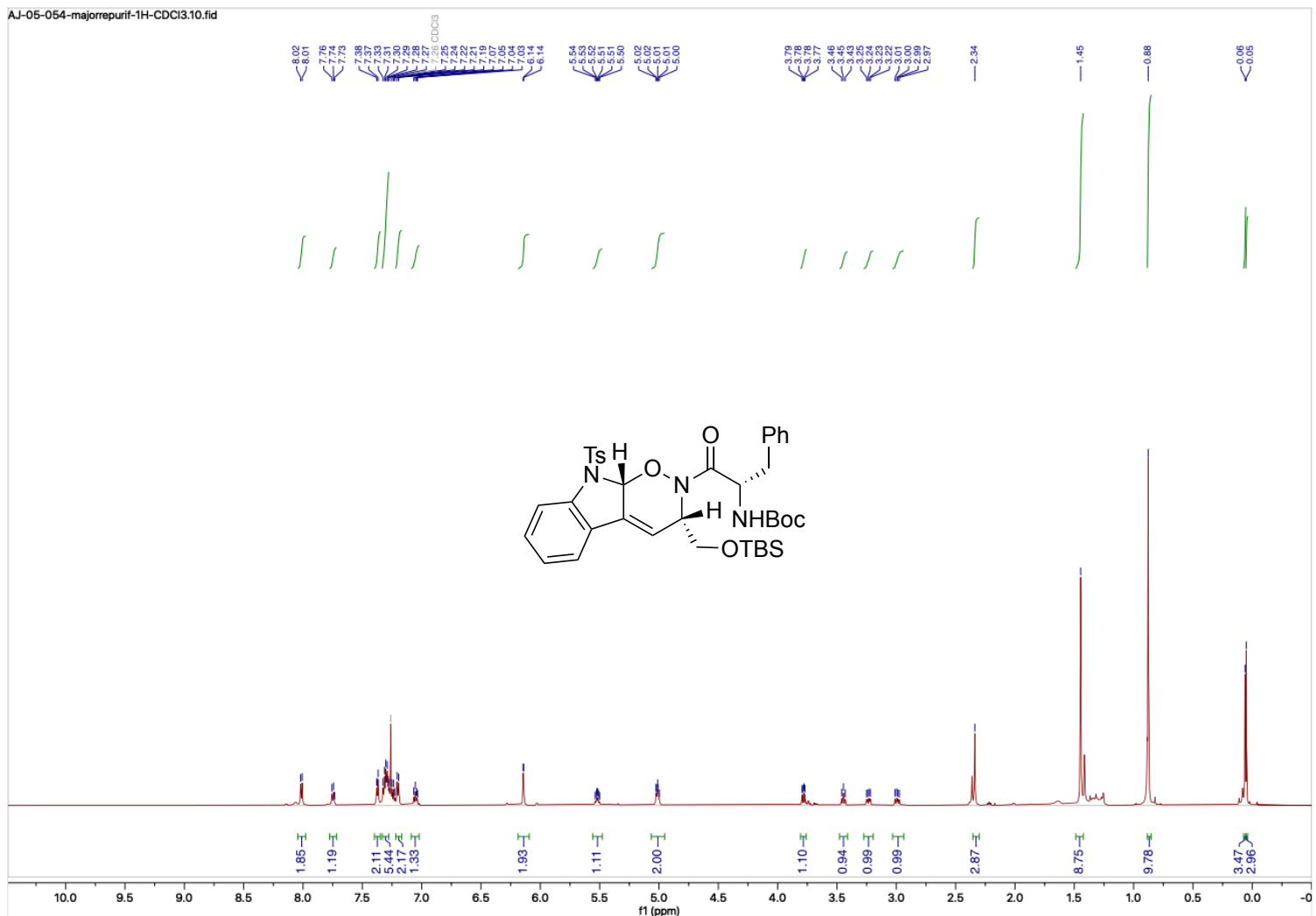


Figure B.59. ^1H NMR (600 MHz, CDCl₃) NDA adduct **3.60**

AJ-05-054-majorrepurif-¹³C-CDCl₃.10.fid

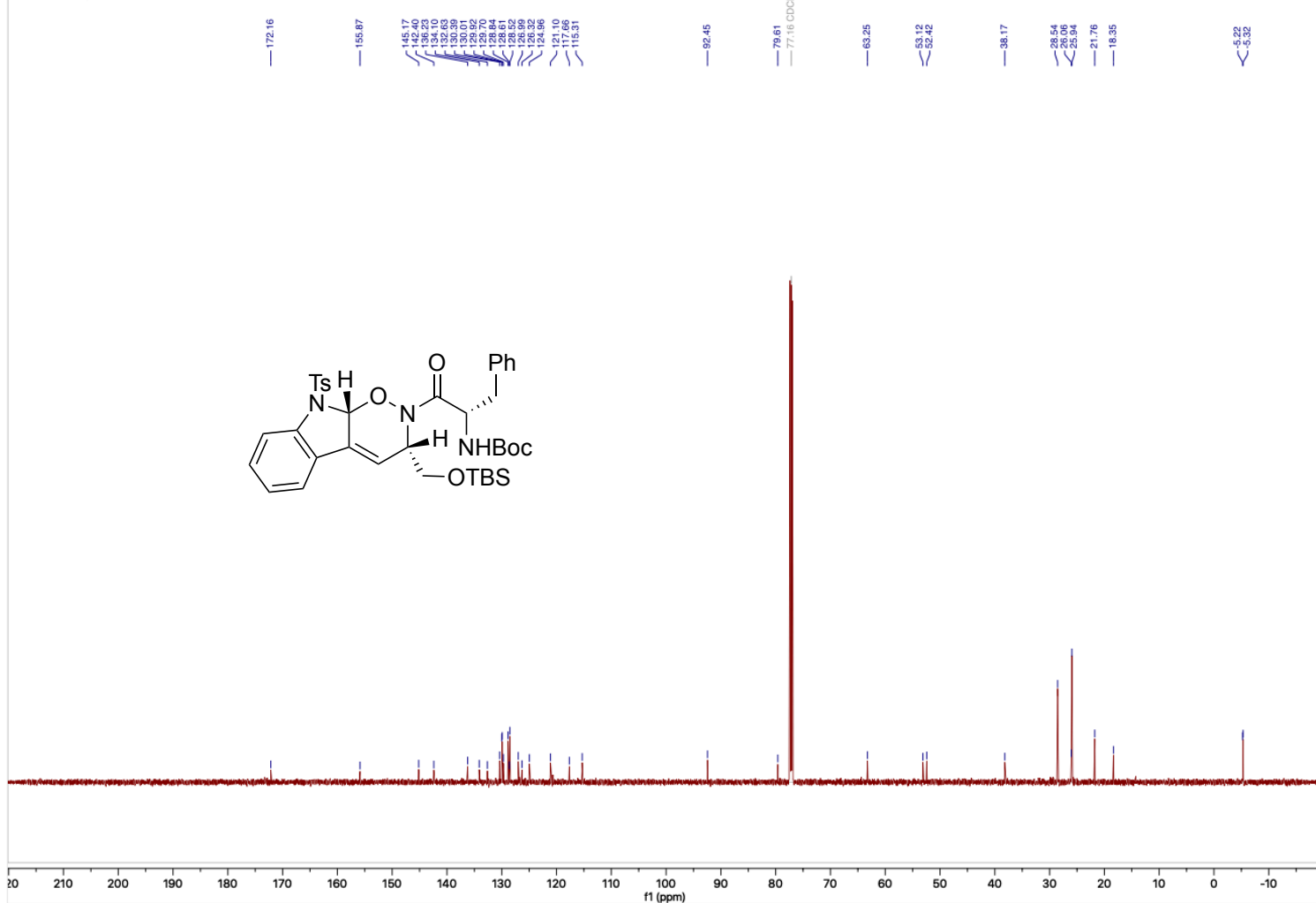


Figure B.60. ¹³C NMR (151 MHz, CDCl₃) NDA adduct **3.60**

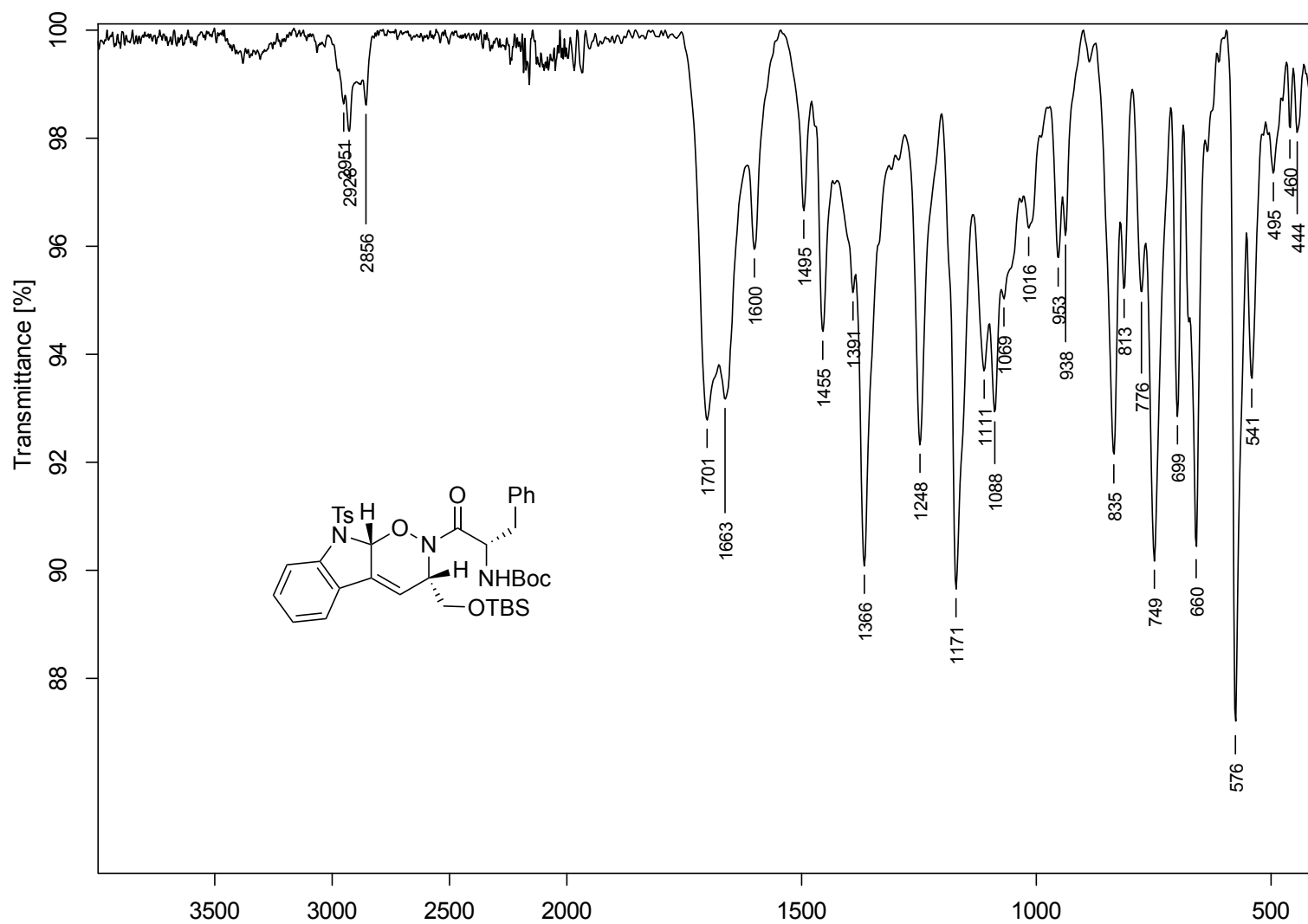


Figure B.61. FTIR (neat) NDA adduct **3.60**

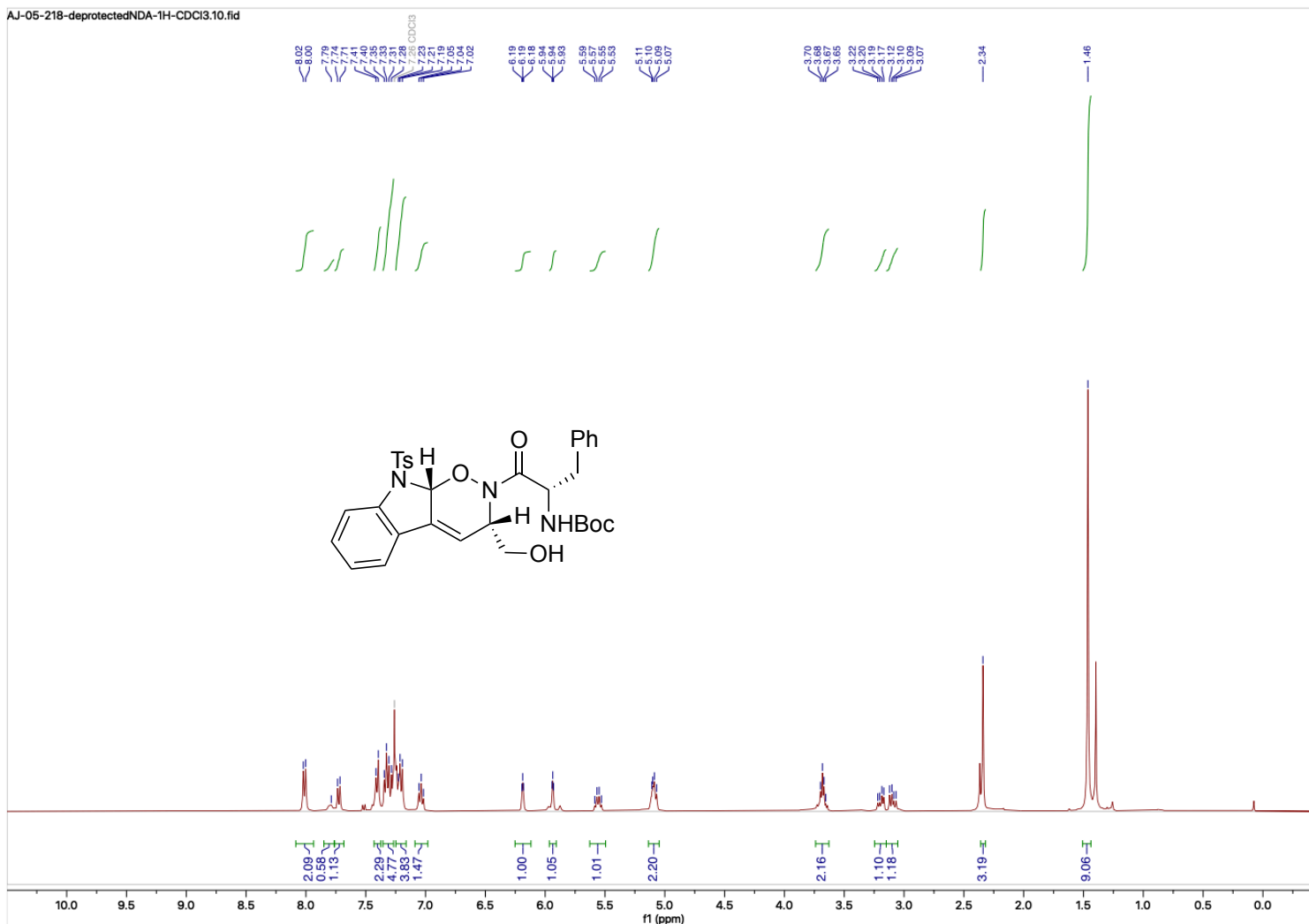


Figure B.62. ^1H NMR (400 MHz, solvent) deprotected NDA adduct 3.63

AJ-05-218-deprotectedNDA-13C-CDCl3.12.fid

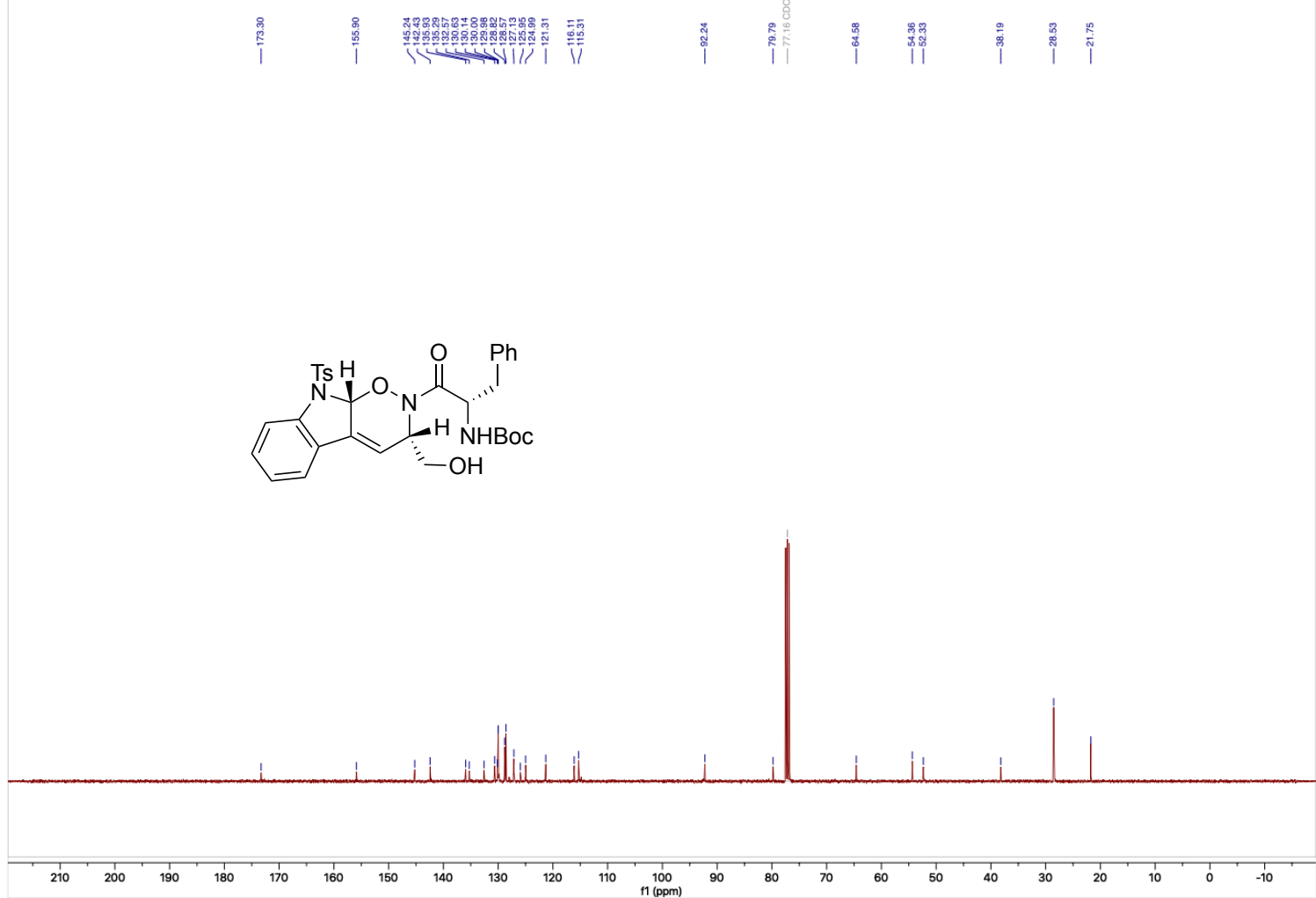


Figure B.63. ^{13}C NMR (101 MHz, solvent) deprotected NDA adduct **3.63**

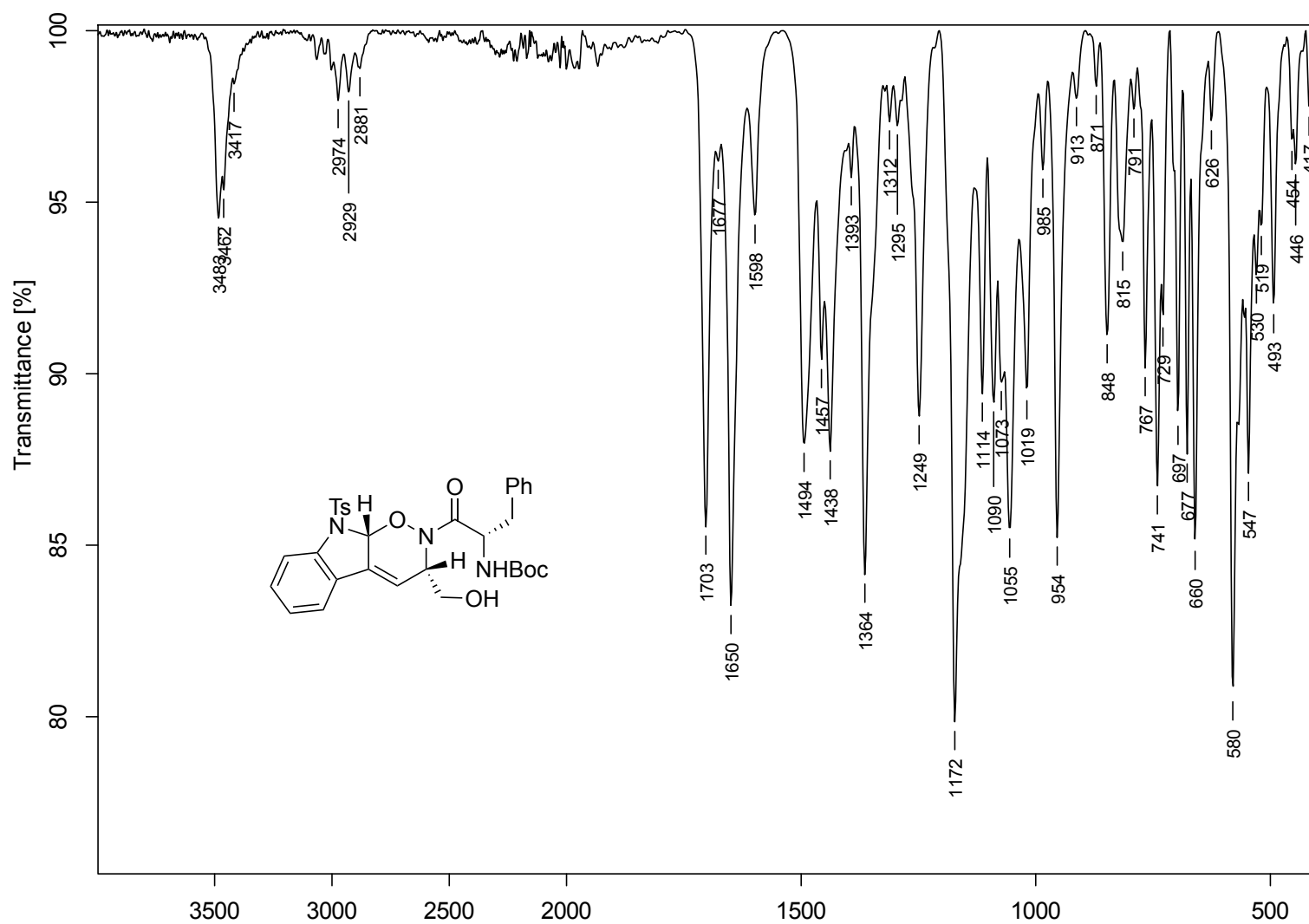


Figure B.64. FTIR (neat) deprotected NDA adduct **3.63**

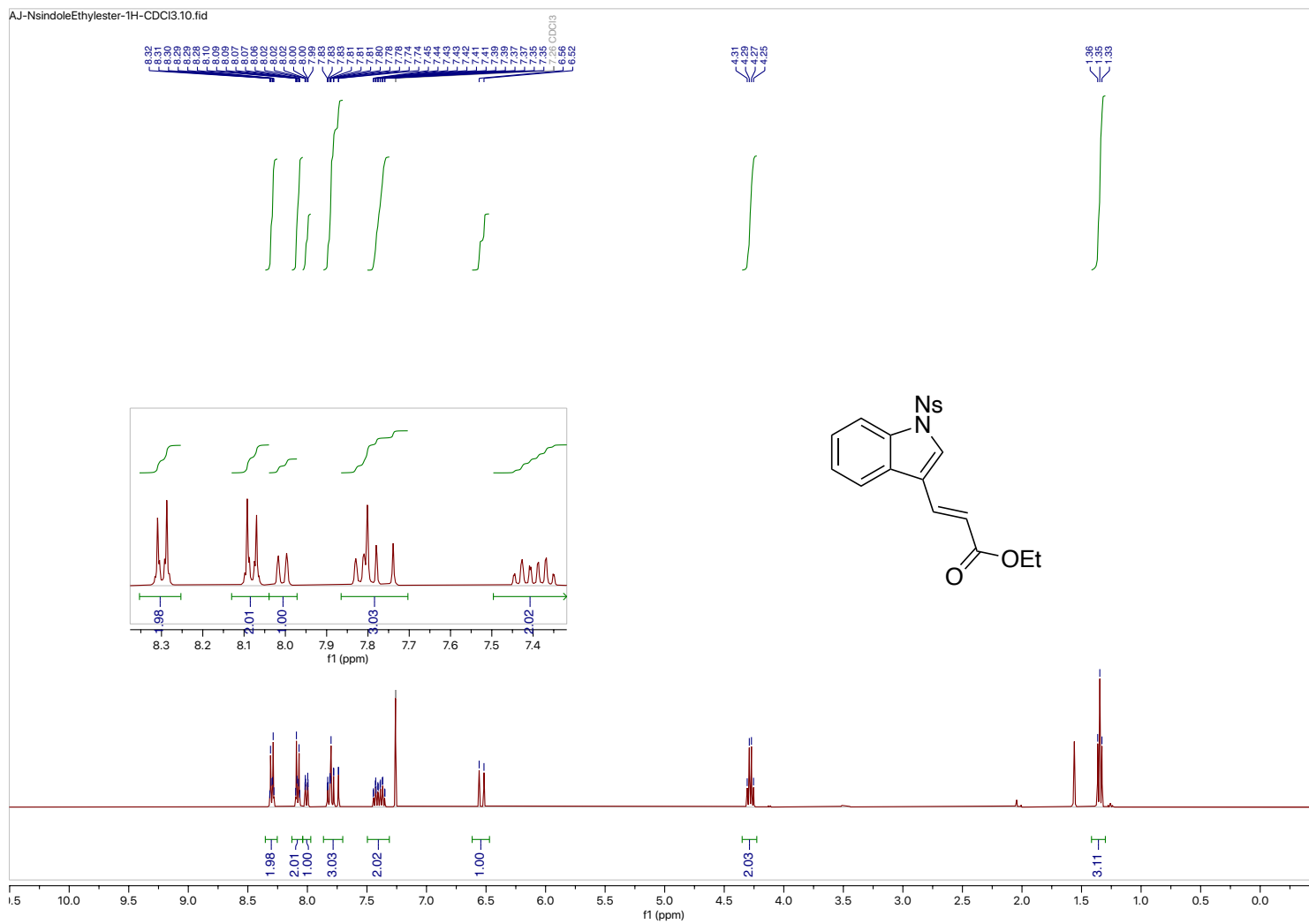


Figure B.65. ¹H NMR (400 MHz, CDCl₃) Ns-protected indole ethyl ester **3.64**

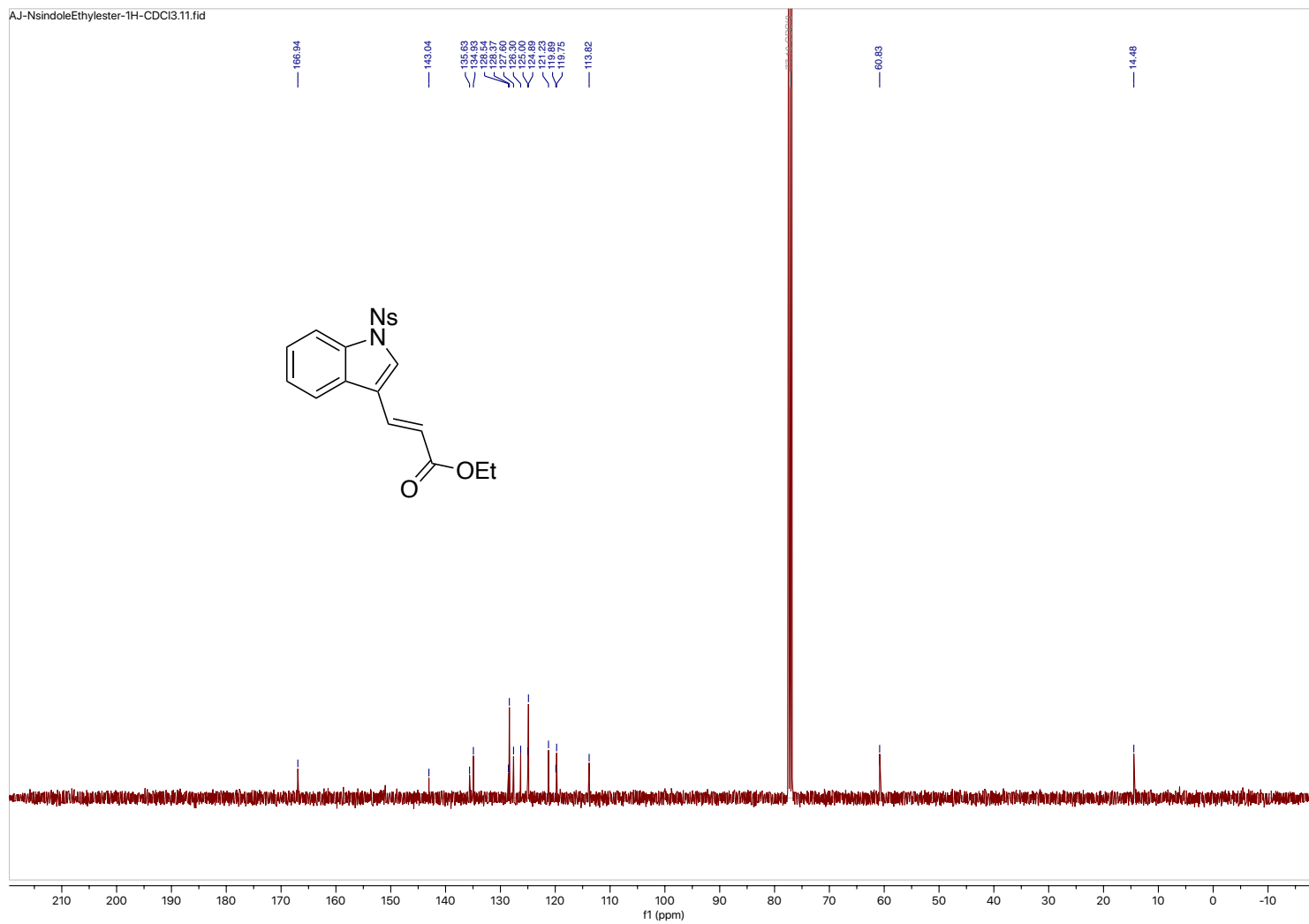


Figure B.66. ^{13}C Spectra (101 MHz, CDCl_3) Ns-protected indole ethyl ester **3.64**

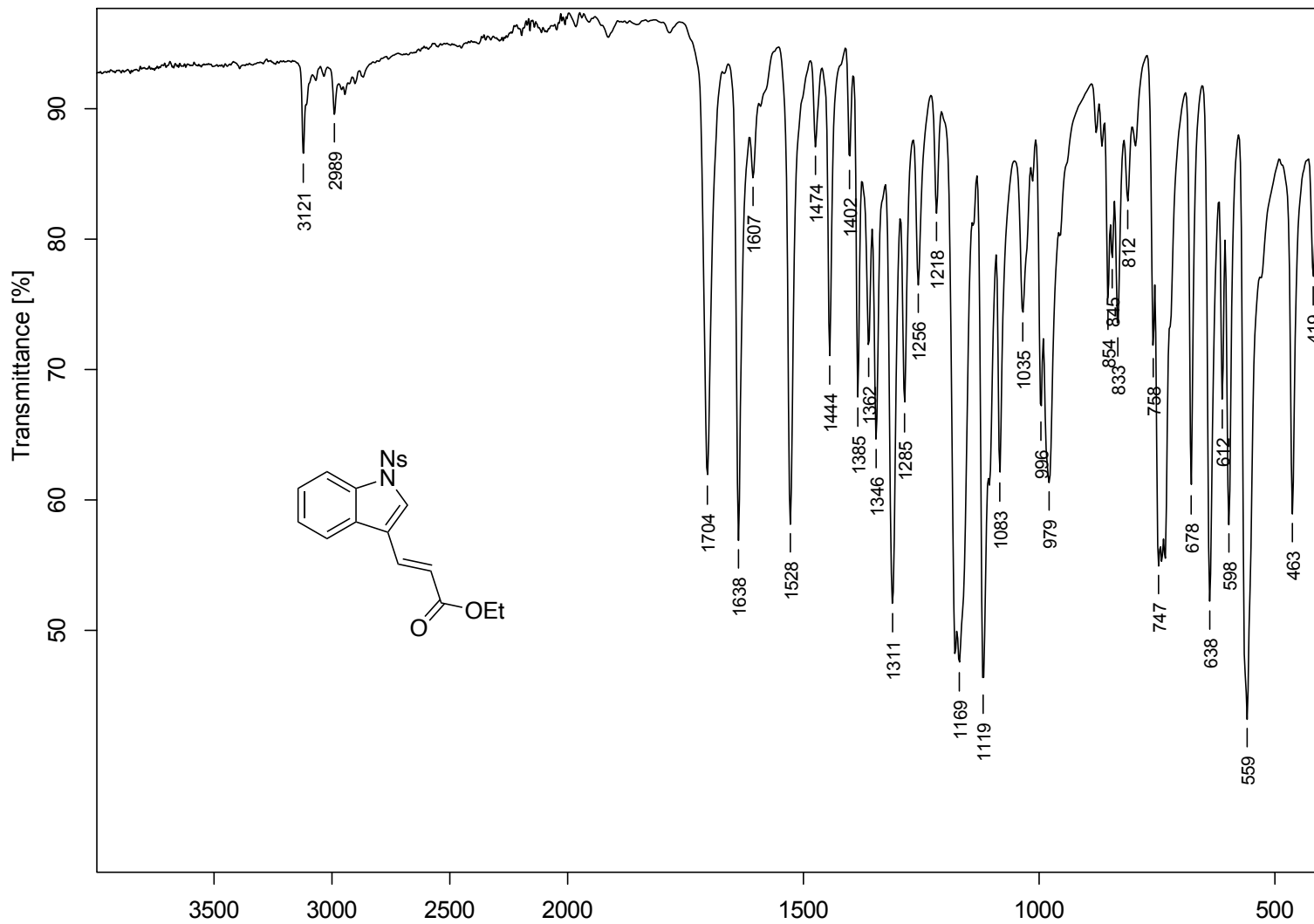


Figure B.67. FTIR Spectrum (neat) Ns-protected indole ethyl ester **3.64**

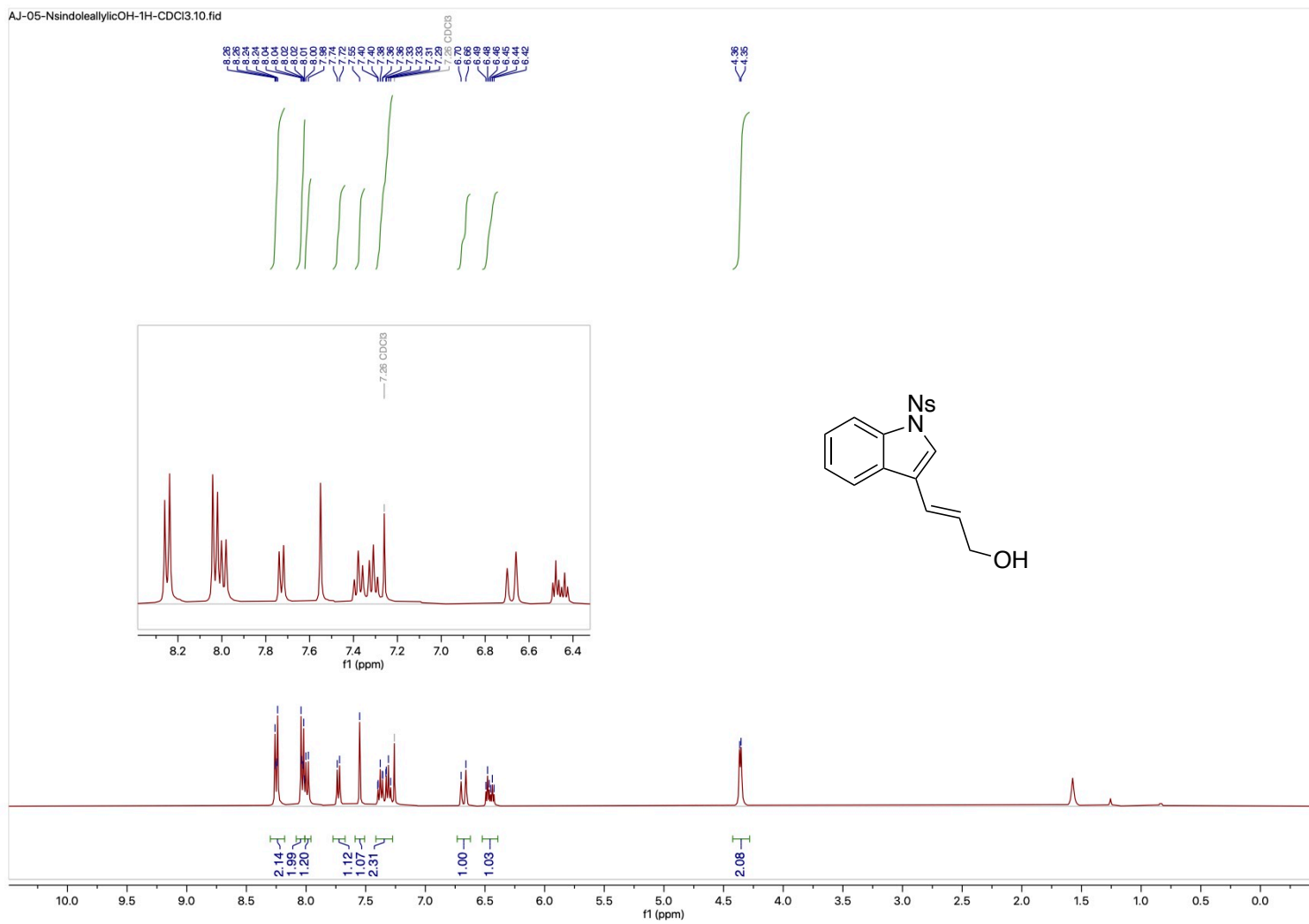


Figure B.68. ¹H Spectra (400 MHz, CDCl₃) Ns-protected indole allylic alcohol **3.65**

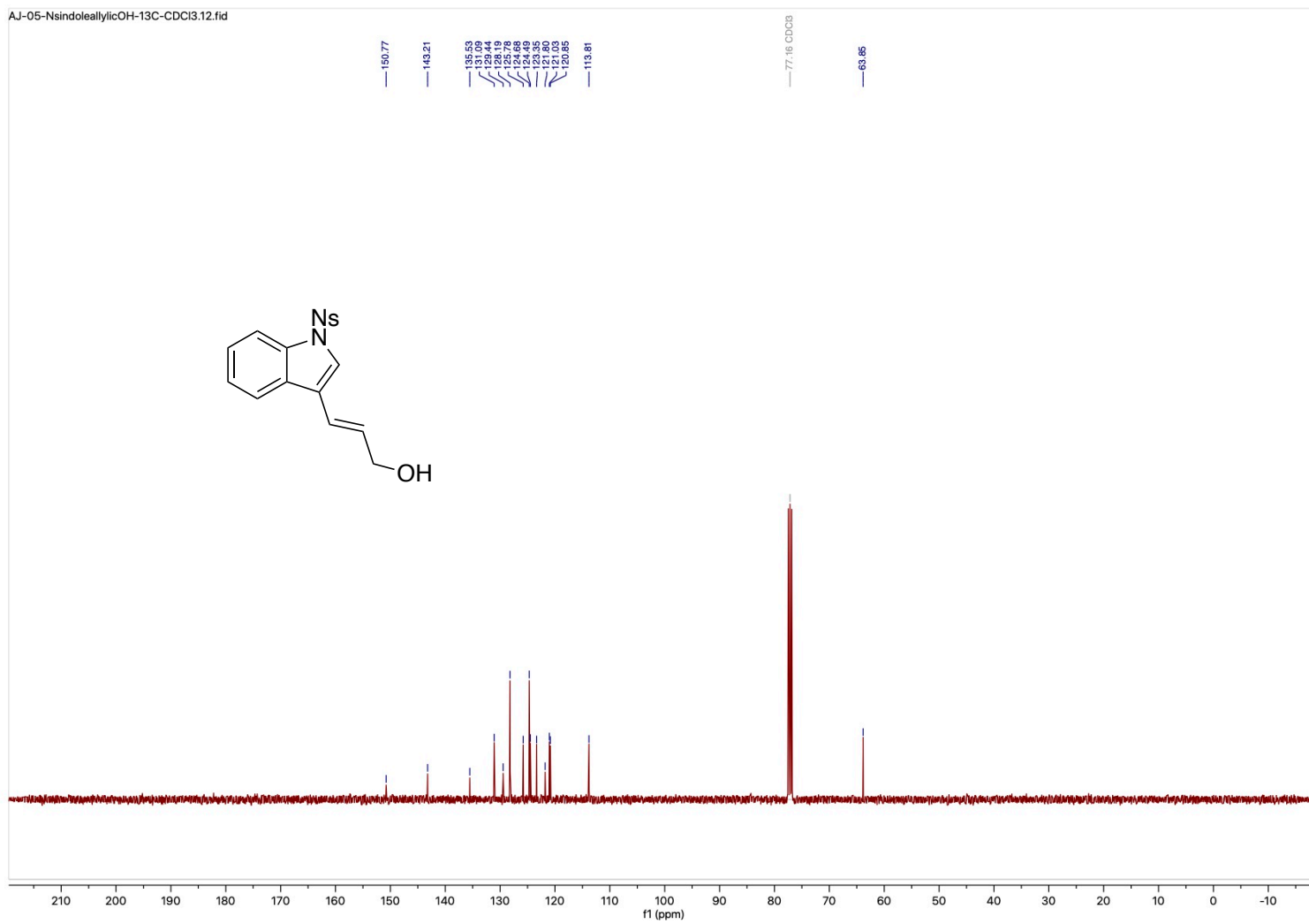


Figure B.69. ¹³C Spectra (101 MHz, CDCl₃) Ns-protected indole allylic alcohol **3.65**

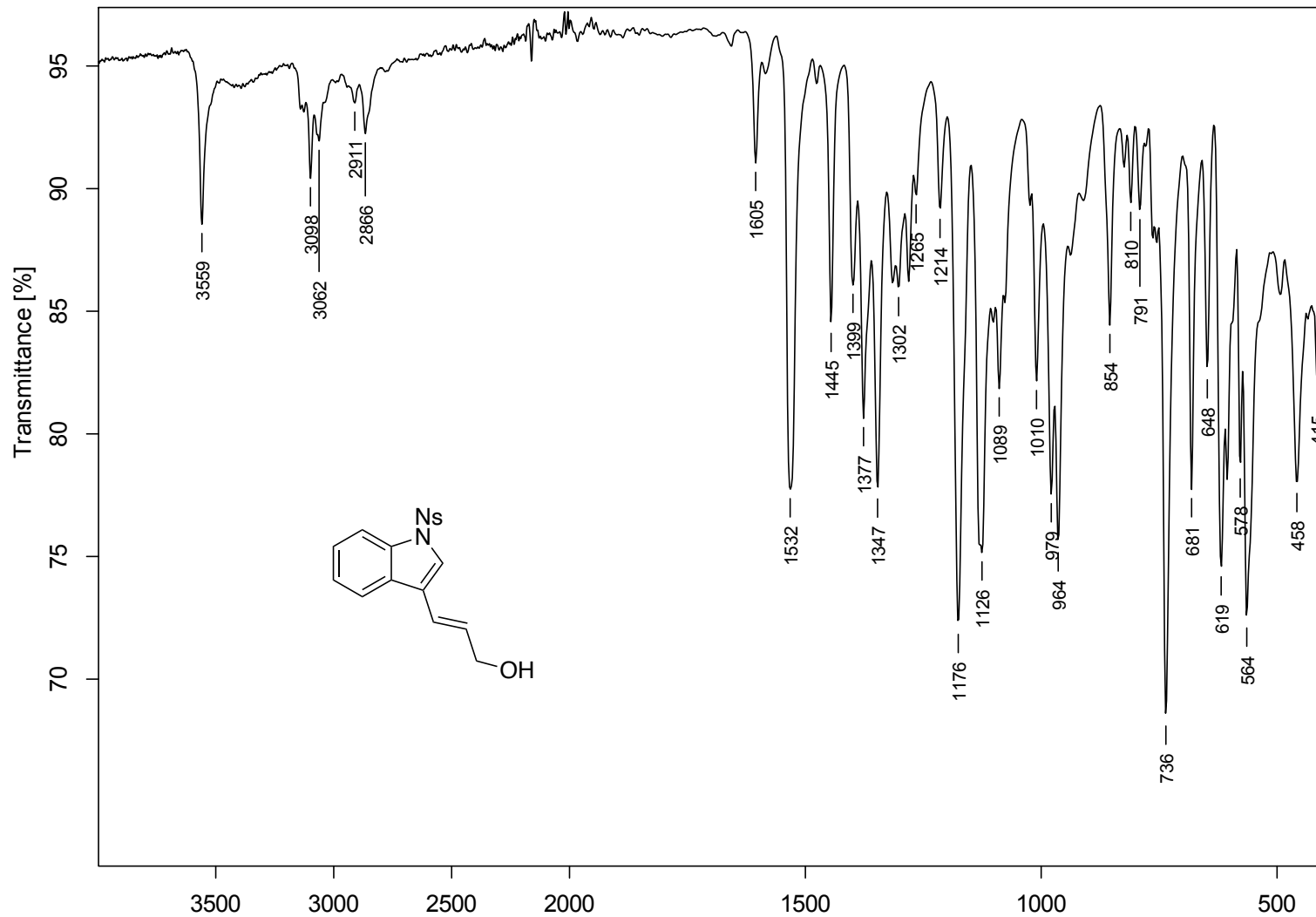


Figure B.70. FTIR Spectrum (neat) Ns-protected indole allylic alcohol **3.65**

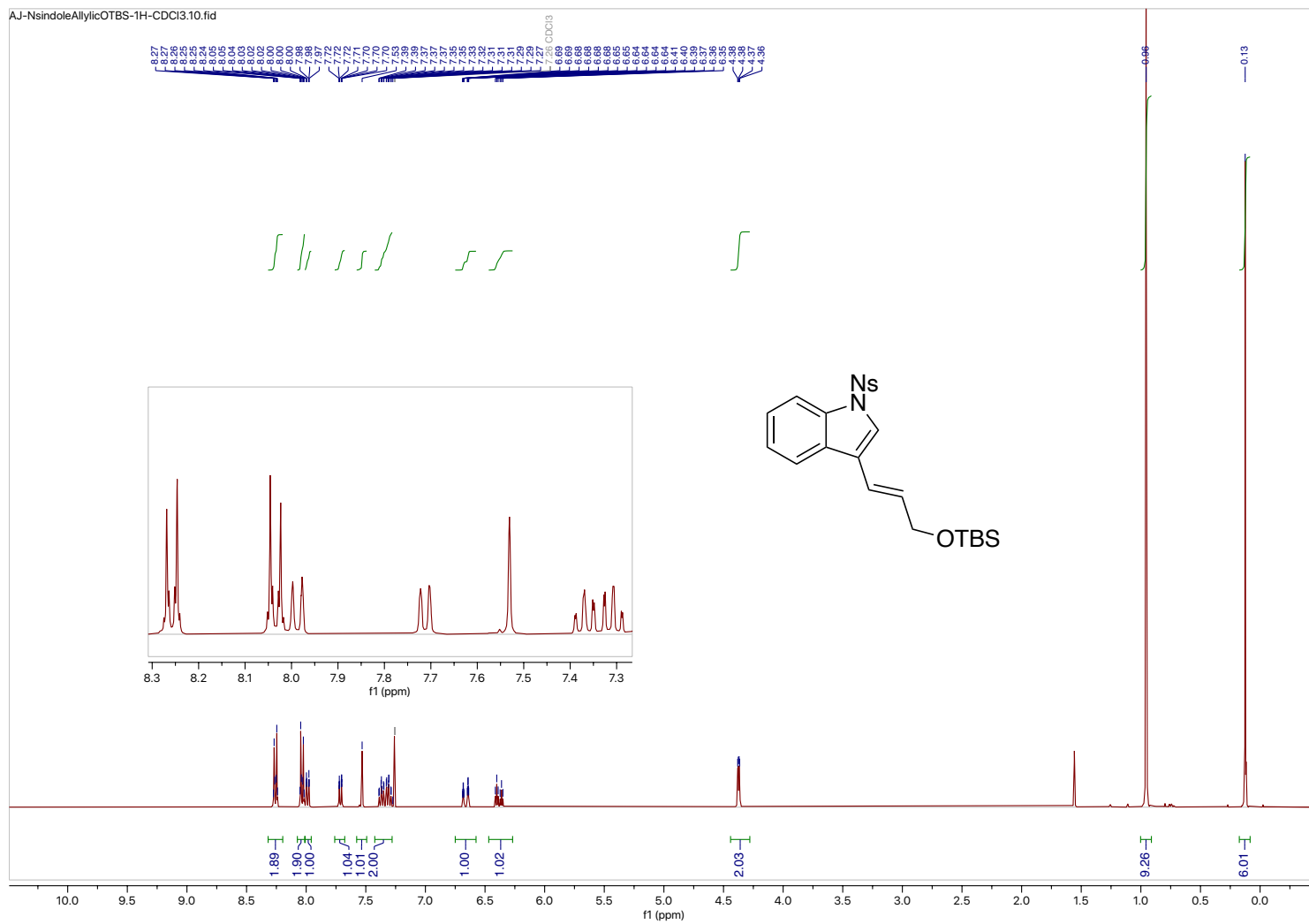


Figure B.71. ¹H Spectra (400 MHz, CDCl₃) Ns-protected indole allylic TBS alcohol **3.66**

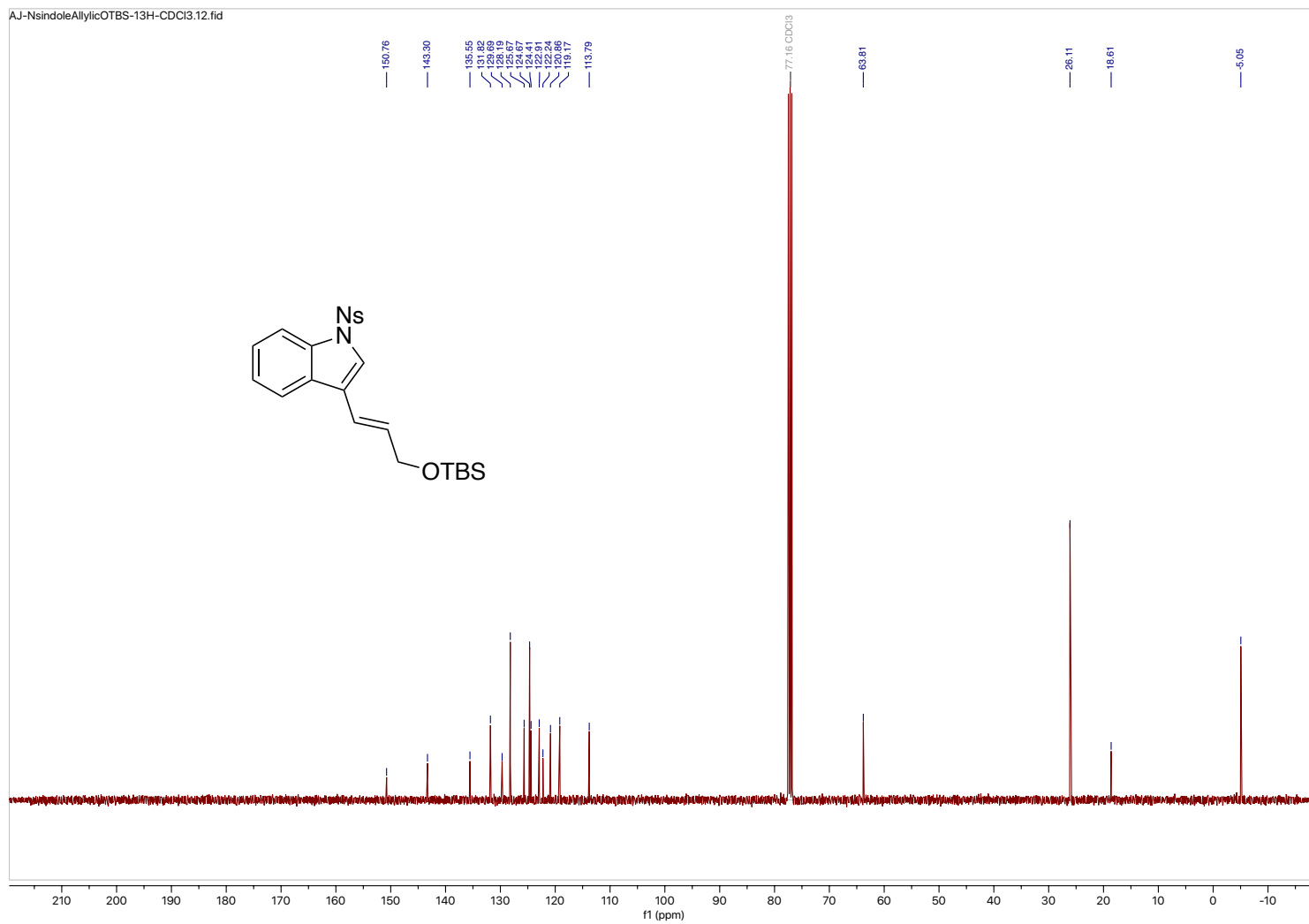


Figure B.72. ¹³C Spectra (101 MHz, CDCl₃) Ns-protected indole allylic TBS alcohol **3.66**

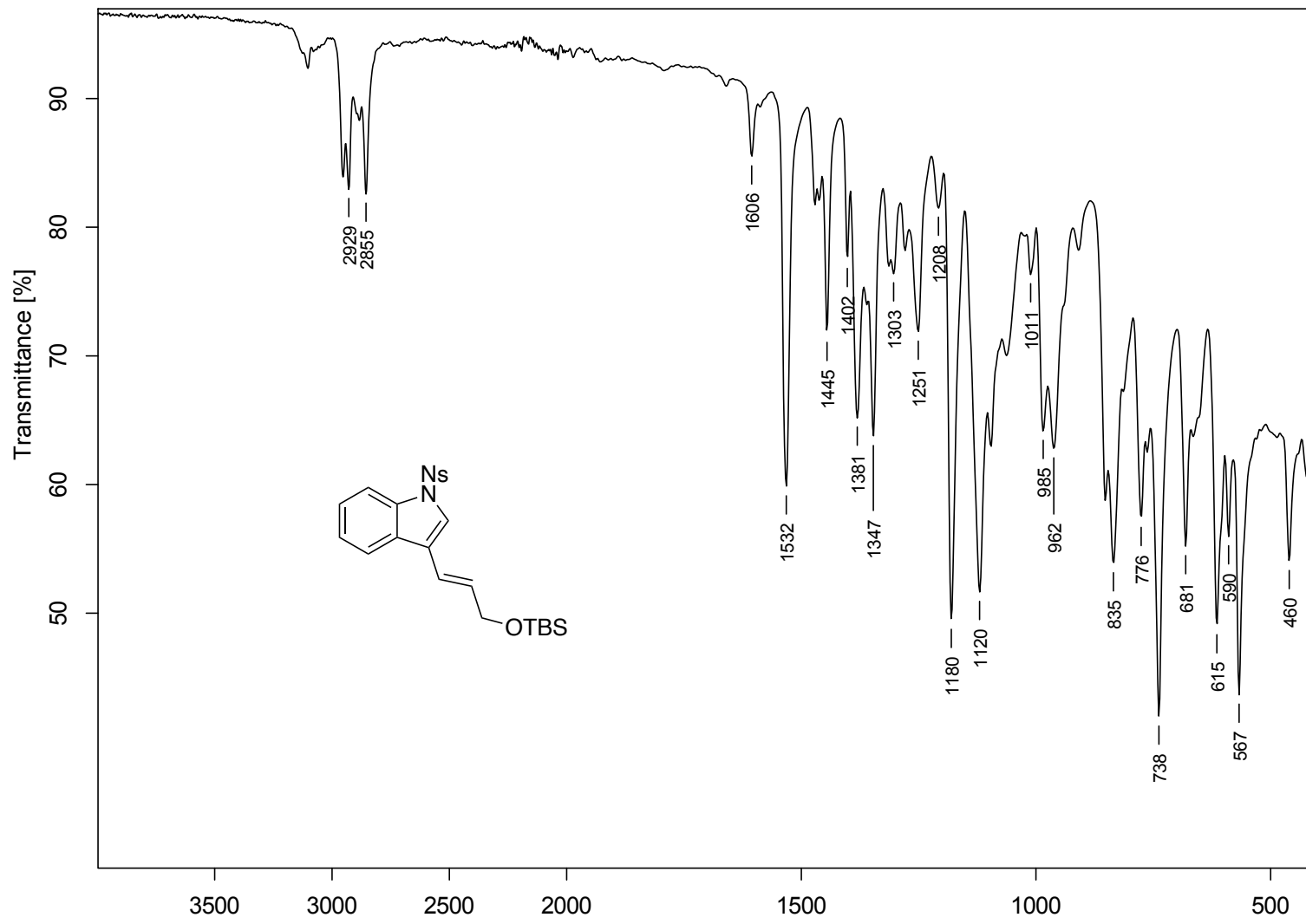


Figure B.73. FTIR Spectrum (neat) Ns-protected indole allylic TBS alcohol **3.66**

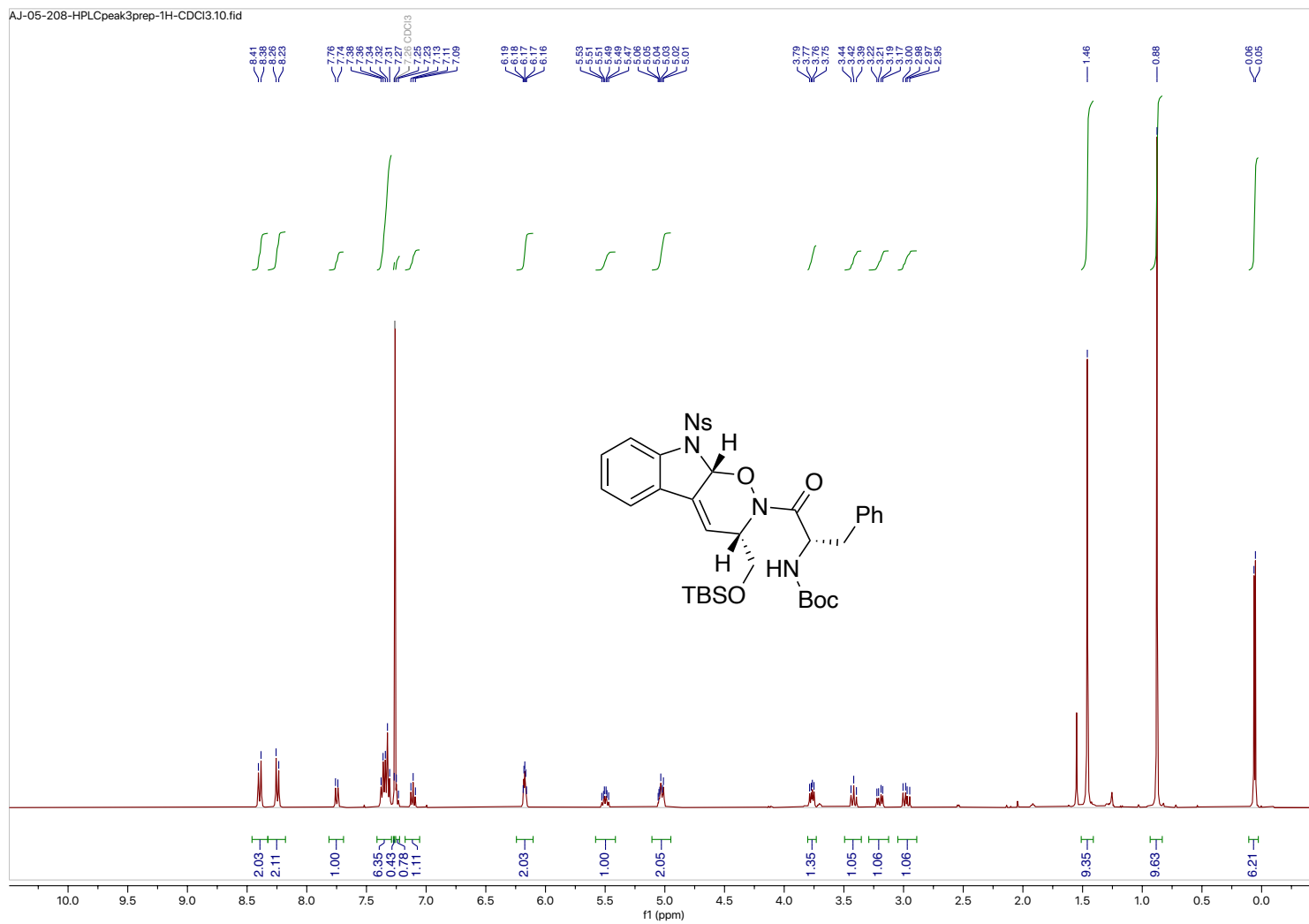


Figure B.74. ¹H Spectra (400 MHz, CDCl₃) Ns-protected indole NDA adduct **3.67**

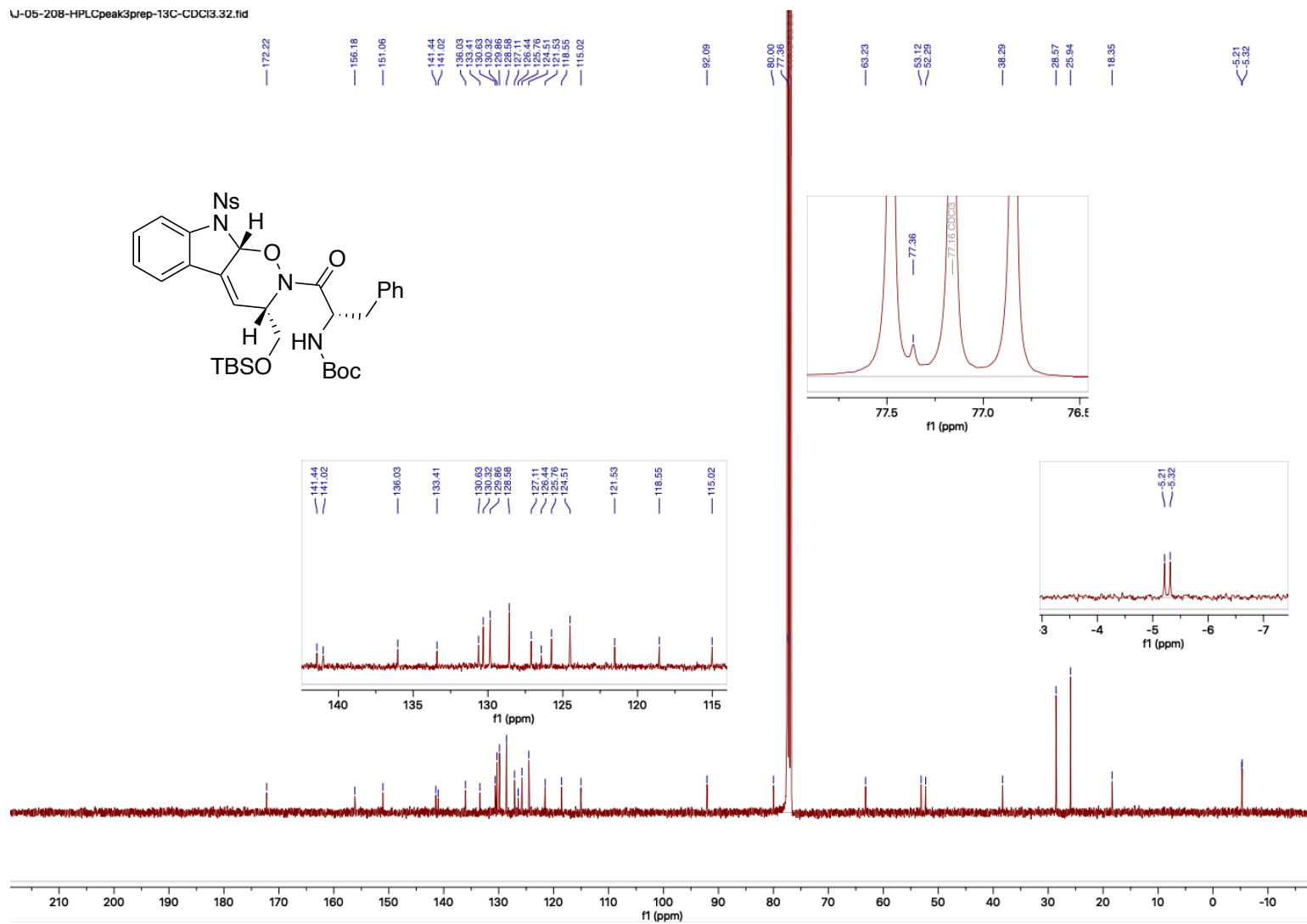


Figure B.75. ^{13}C Spectra (151 MHz, CDCl₃) Ns-protected indole NDA adduct **3.67**

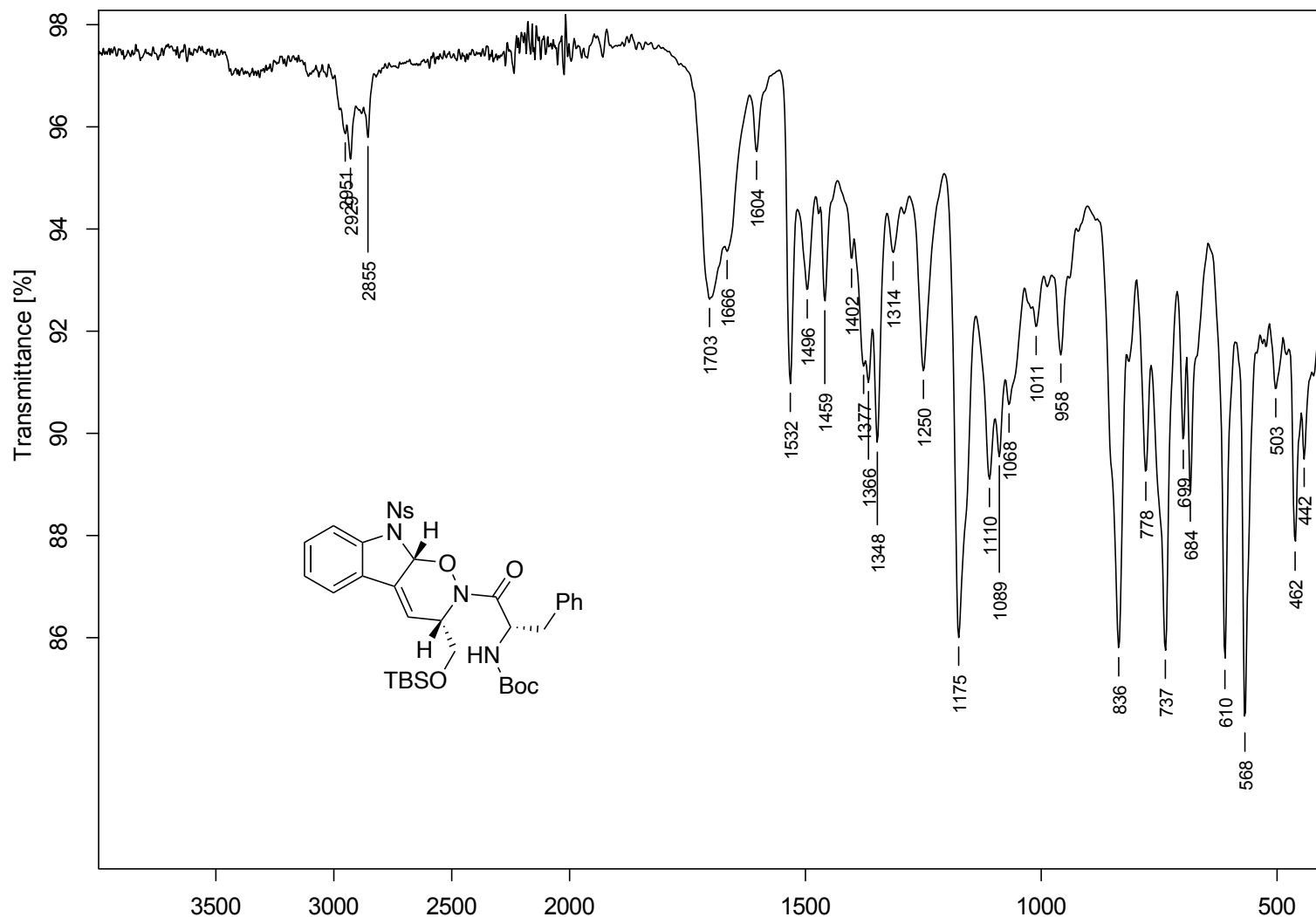
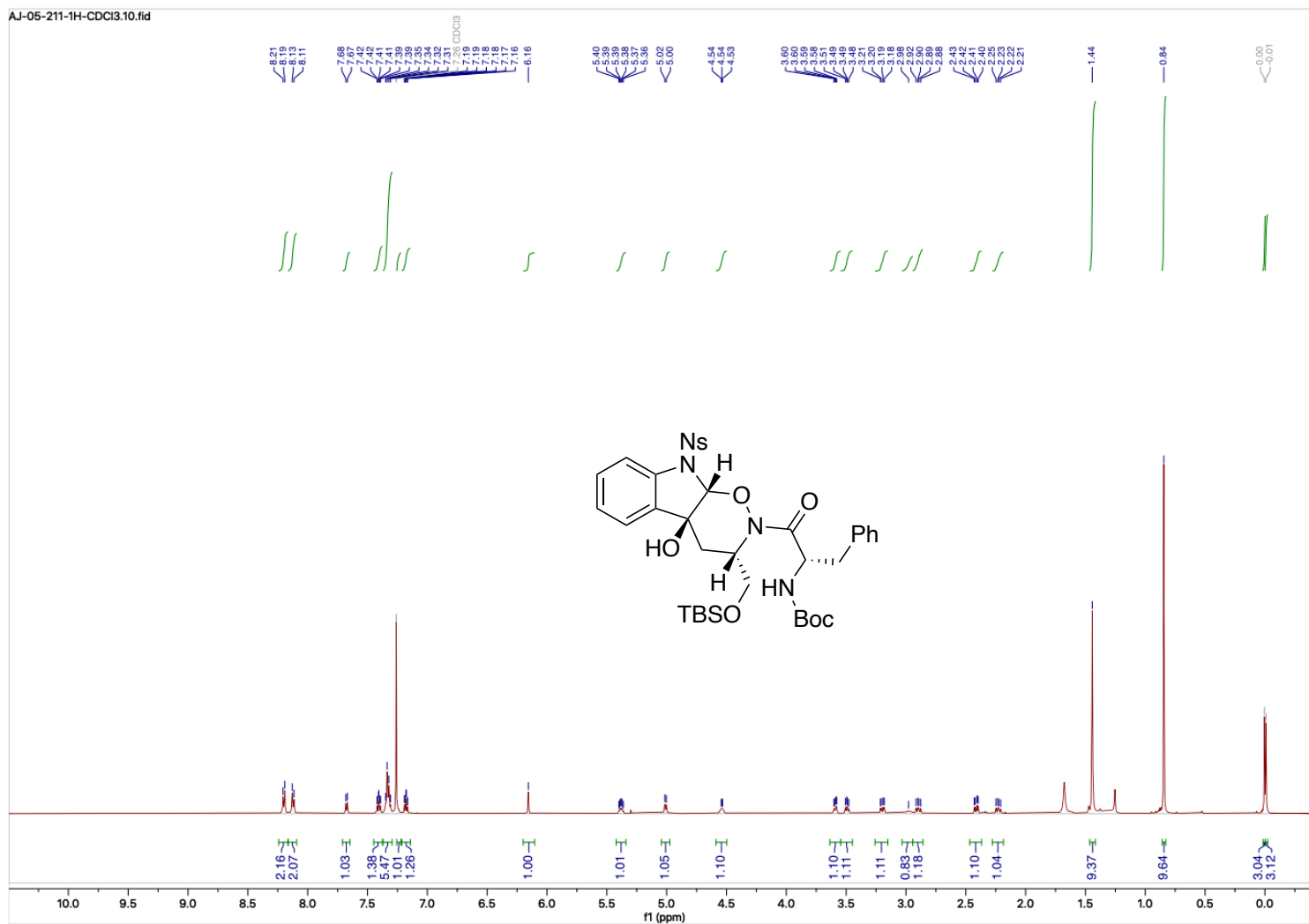


Figure B.76. FTIR Spectrum (neat) Ns-protected indole NDA adduct **3.67**



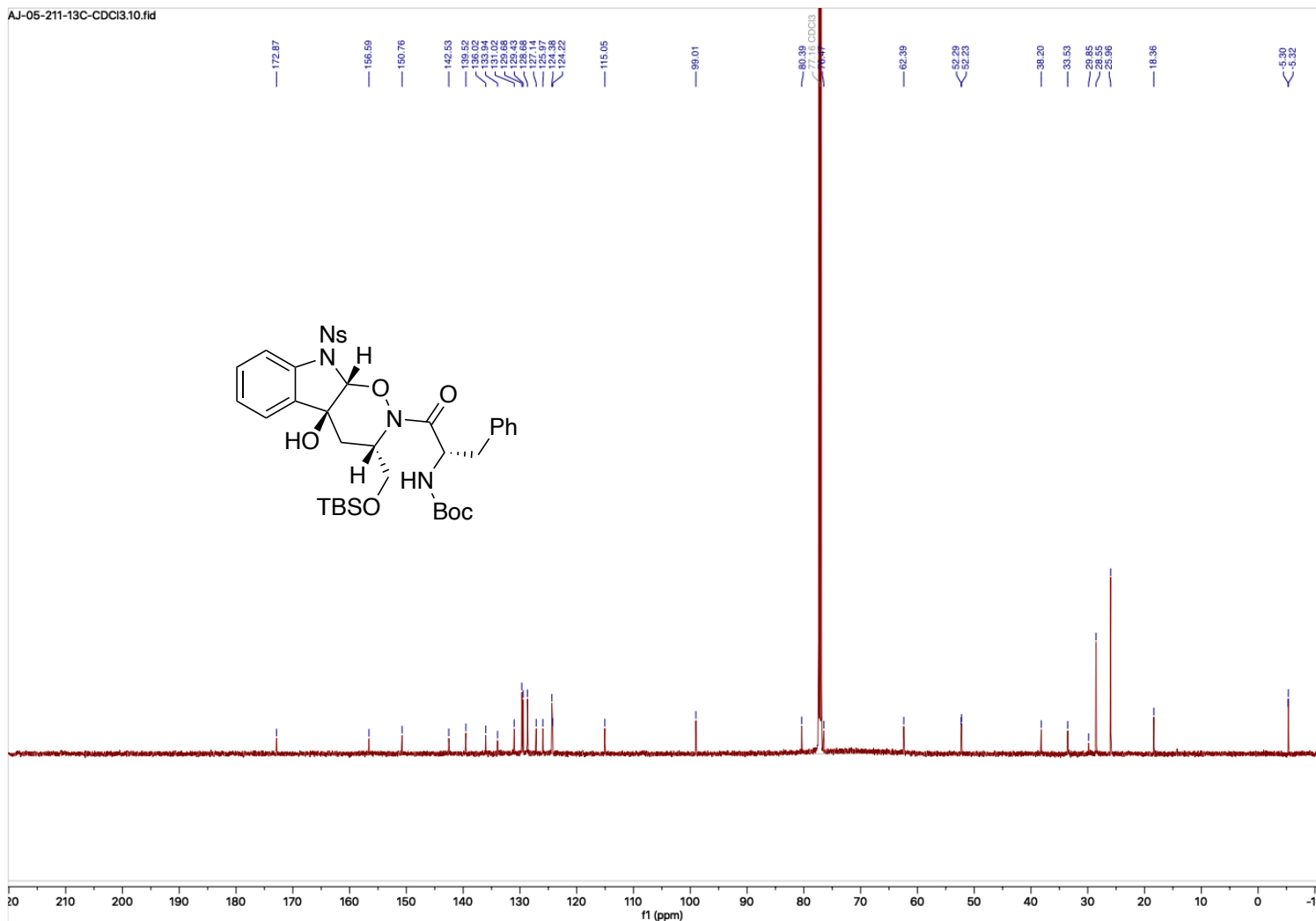


Figure B.78. ¹³C Spectra (151 MHz, CDCl₃) Ns-protected indole Mukaiyama adduct **3.68**

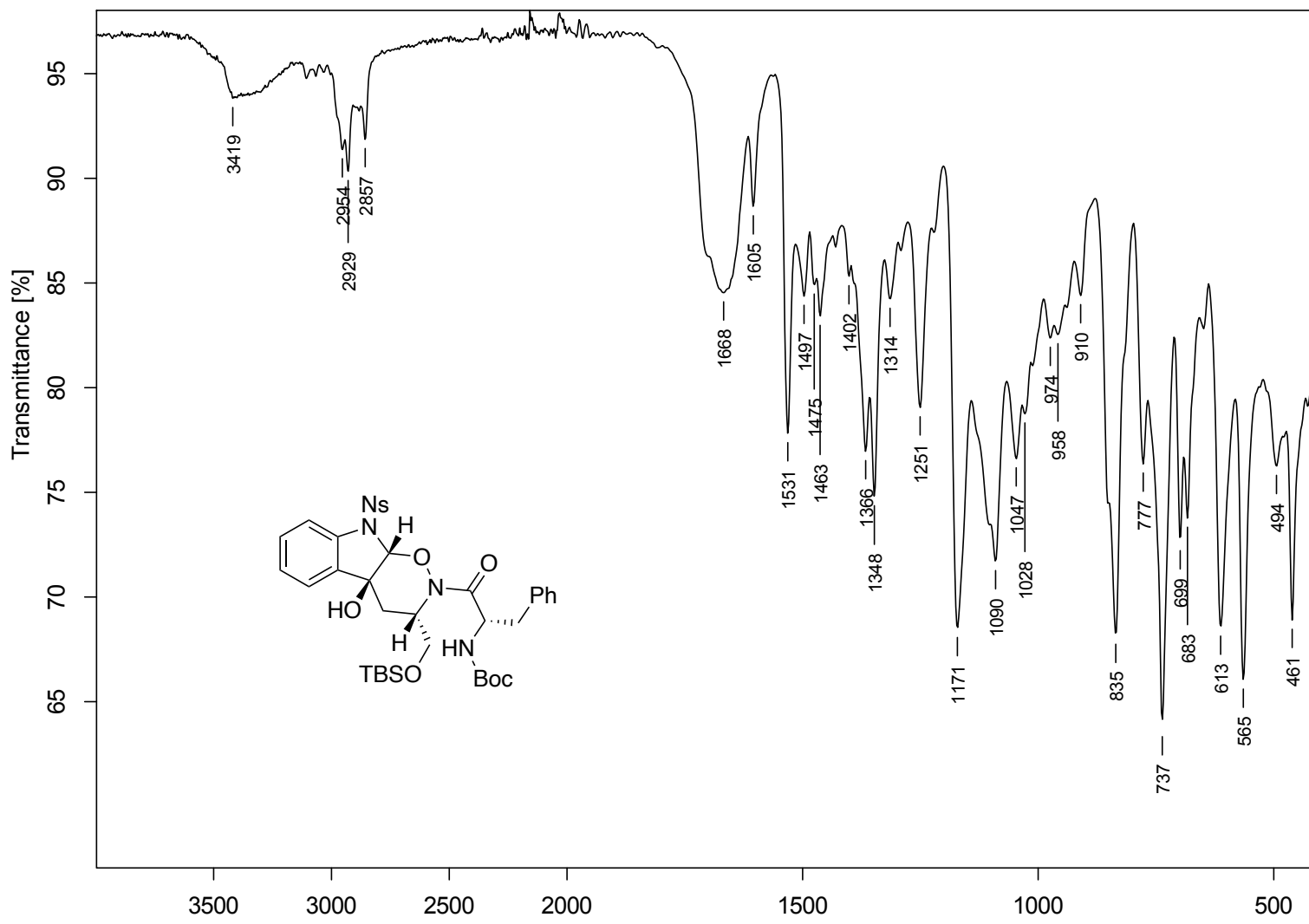


Figure B.79. FTIR Spectrum (neat) Ns-protected indole Mukaiyama adduct **3.68**

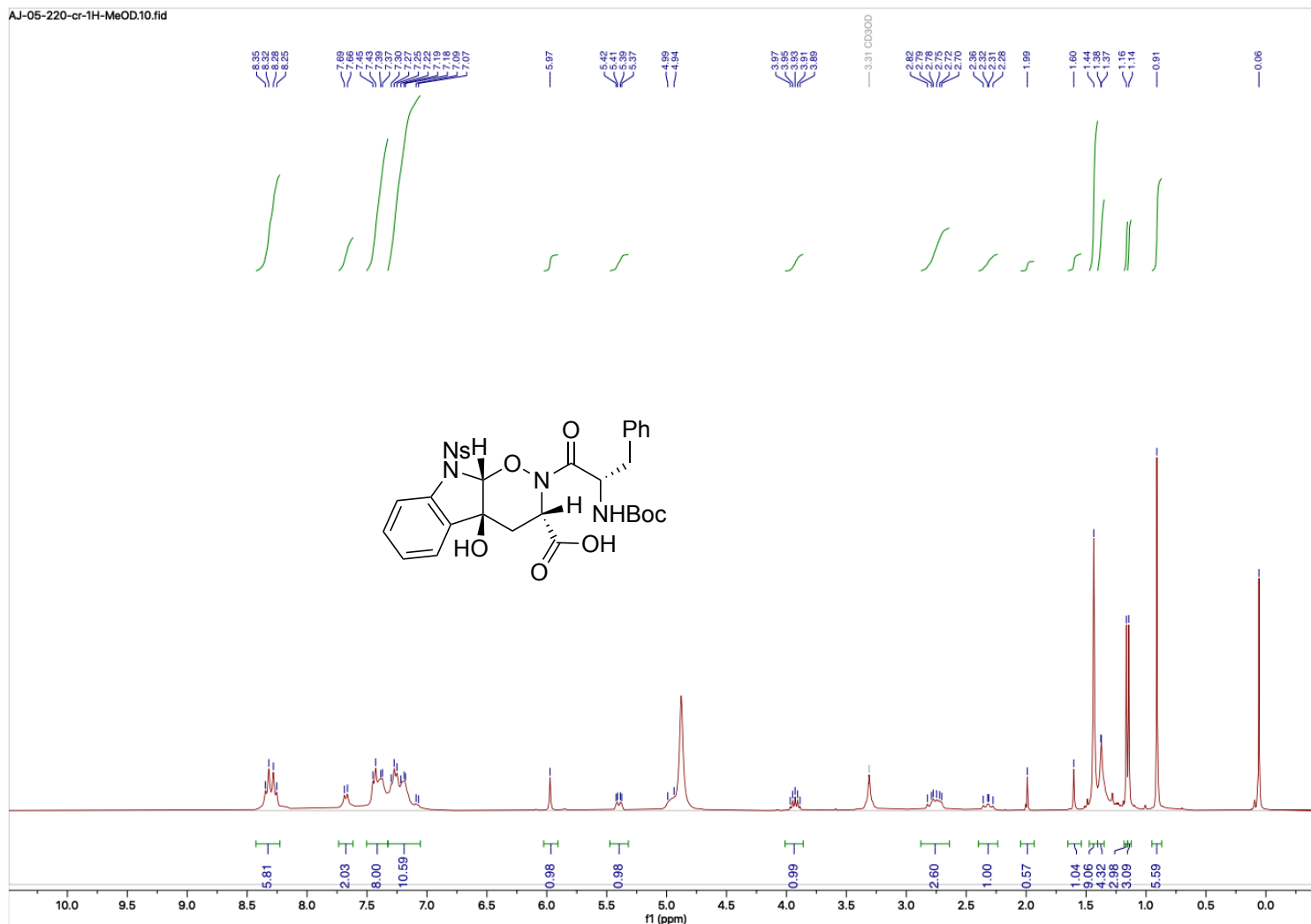


Figure B.80. ^1H Spectra (300 MHz, CDCl_3) crude carboxylic acid **3.69**

AJ-05-221-cr-1H-MeOD.10.fid

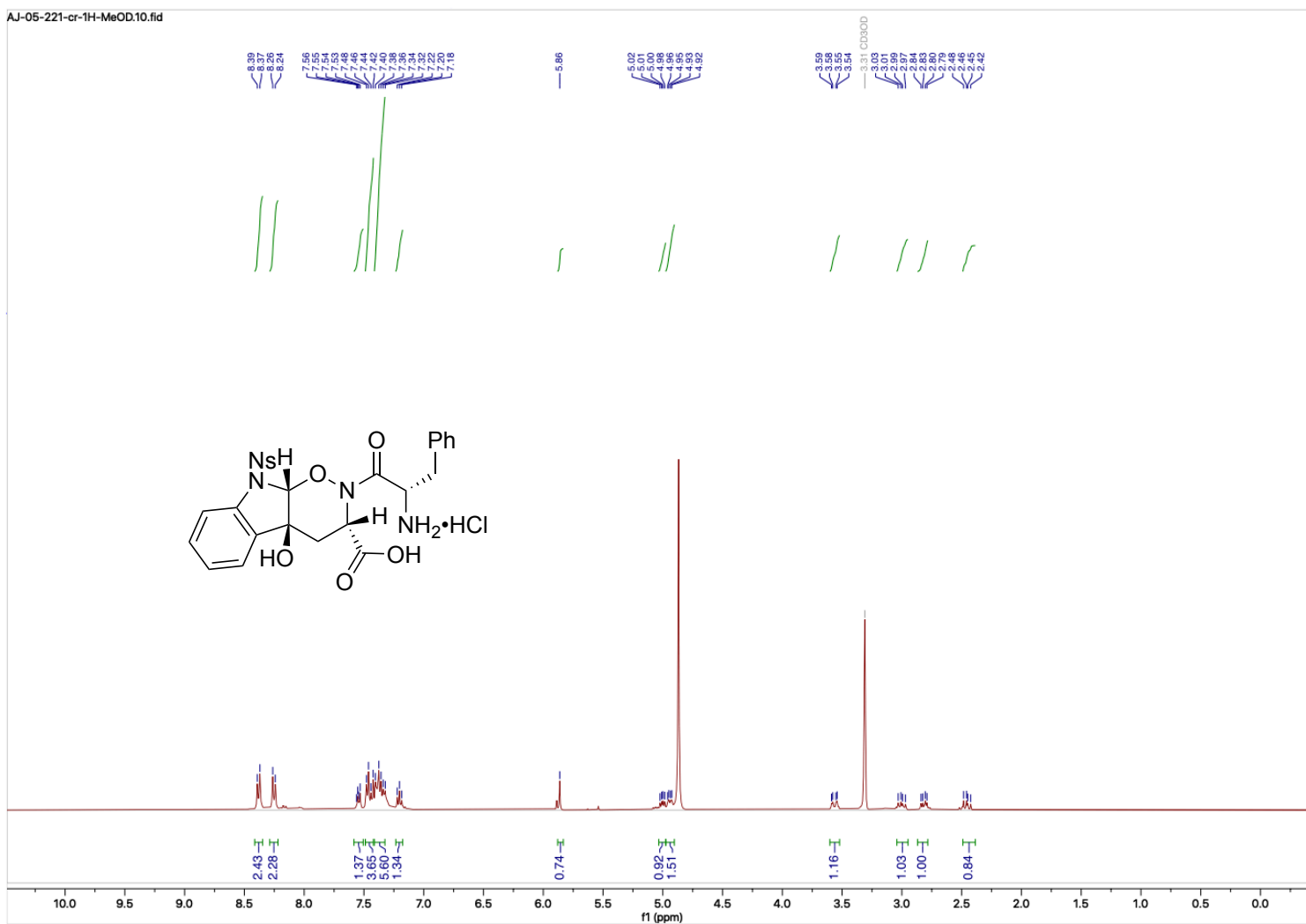


Figure B.81. ¹H Spectra (400 MHz, CDCl₃) Ns-protected indole amino salt **3.70**

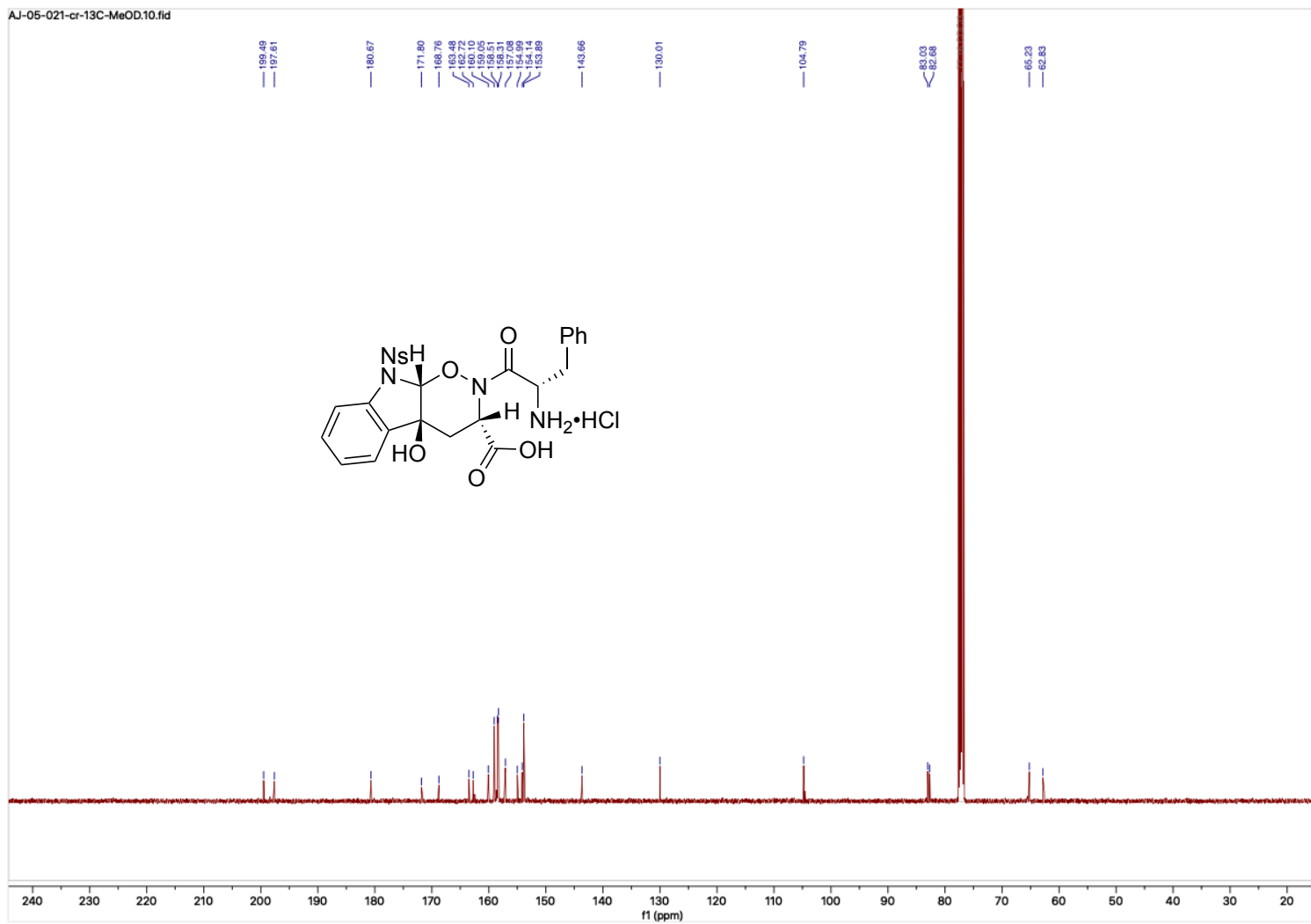


Figure B.82. ^{13}C Spectra (101 MHz, CDCl_3) Ns-protected indole amino salt **3.70**

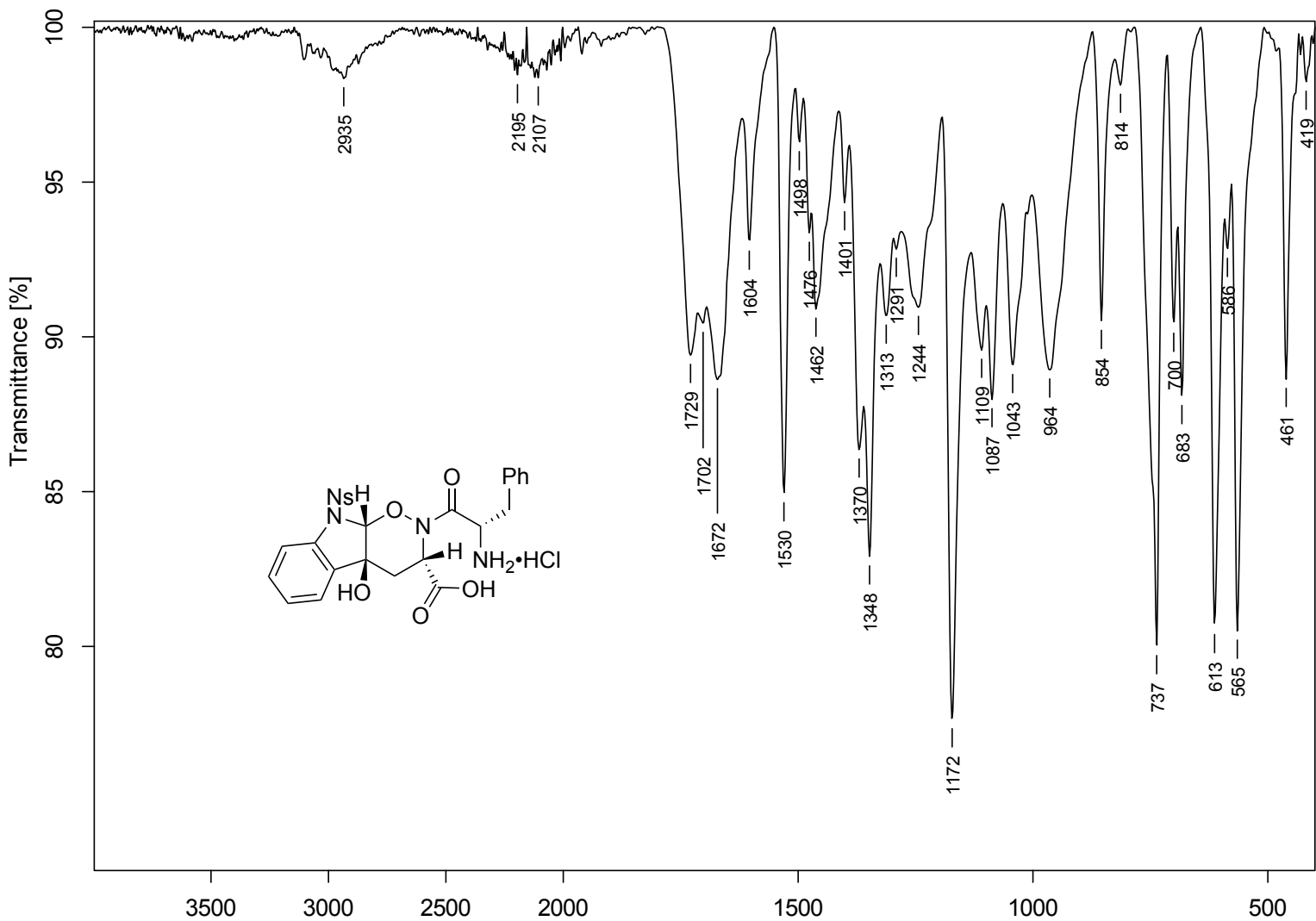


Figure B.83. FTIR Spectrum (neat) Ns-protected indole amino salt **3.70**

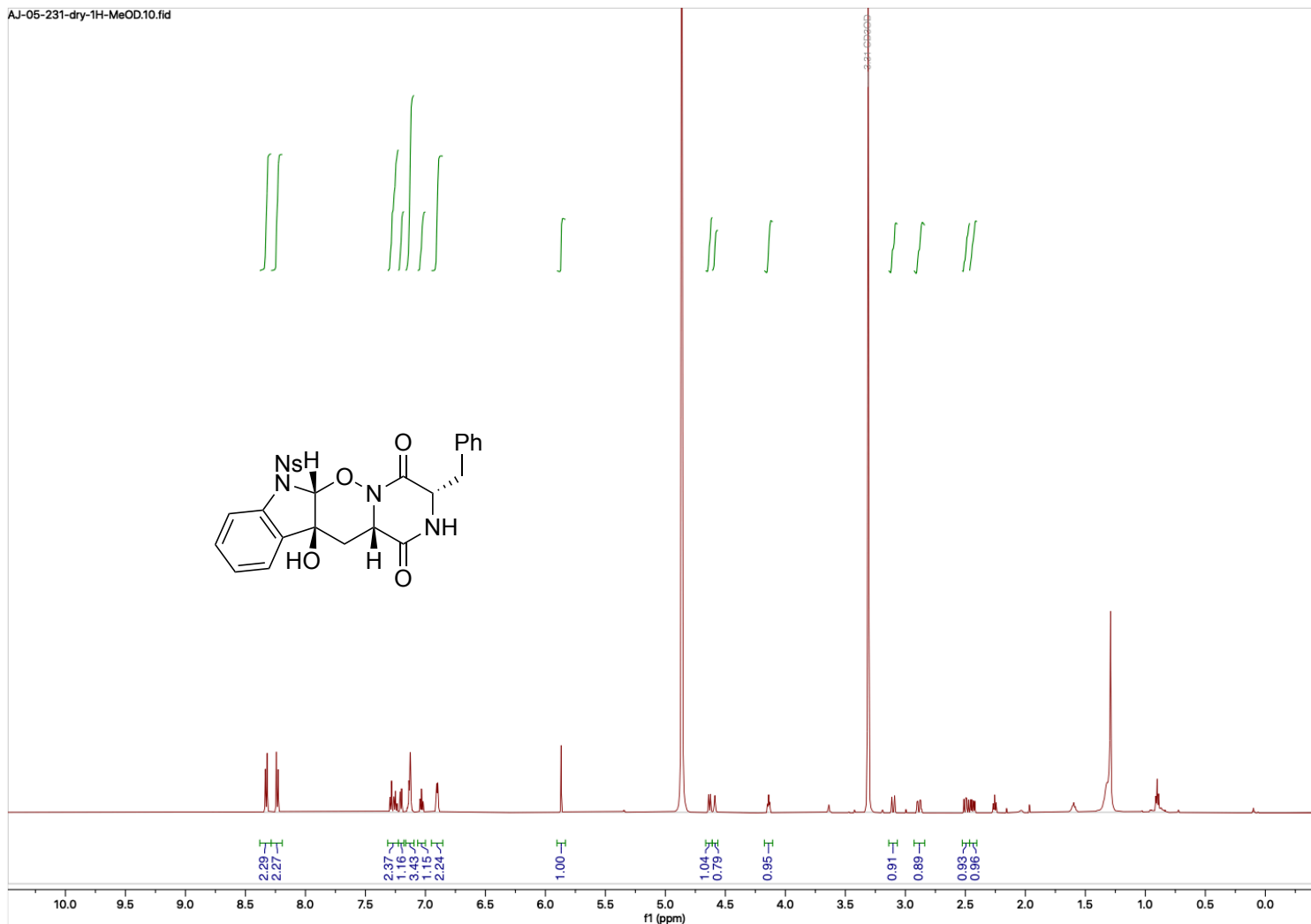


Figure B.84. ^1H Spectra (600 MHz, CDCl_3) Ns-protected indole DKP 3.71

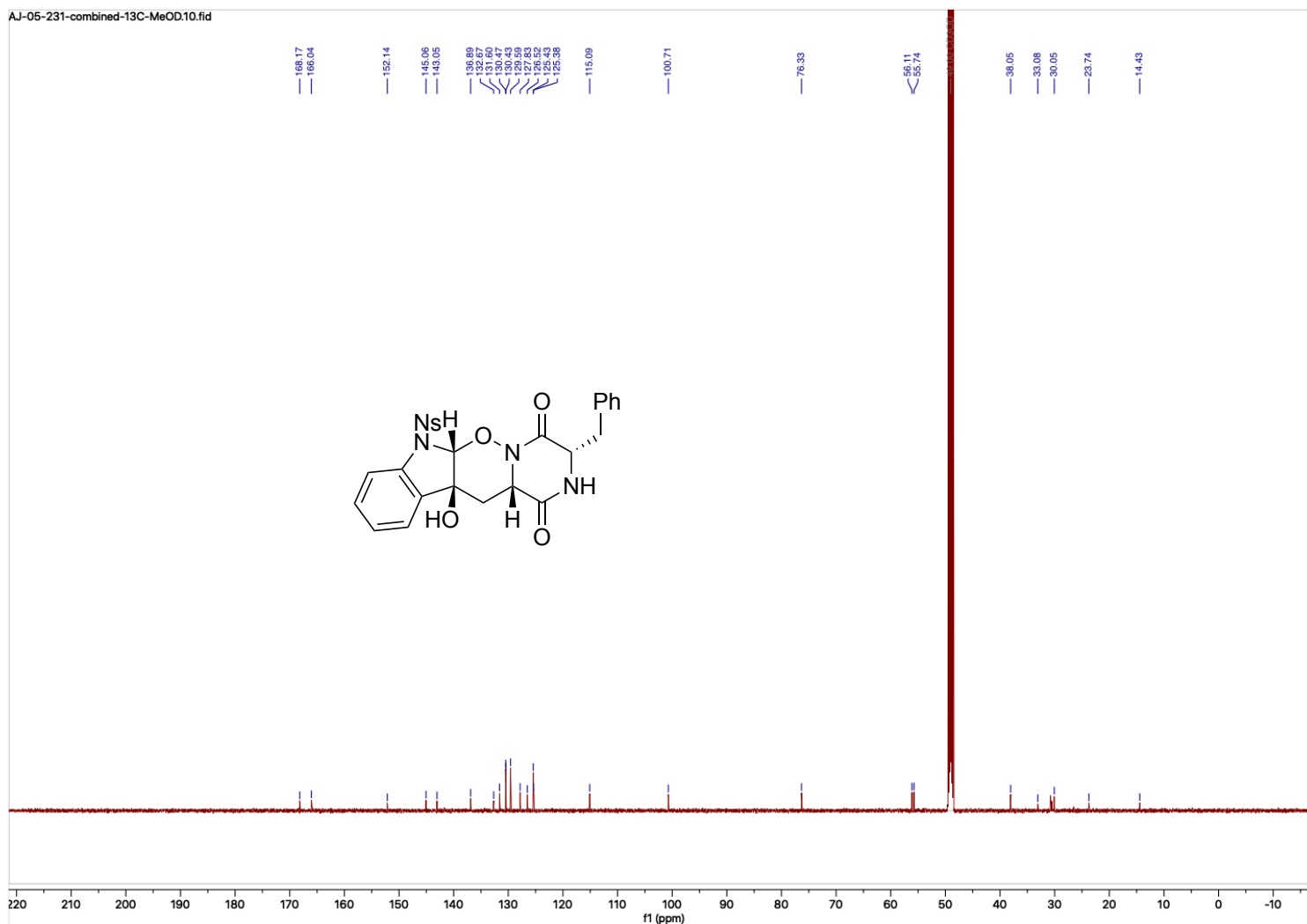


Figure B.85. ¹³C Spectra (151 MHz, CDCl₃) Ns-protected indole DKP **3.71**

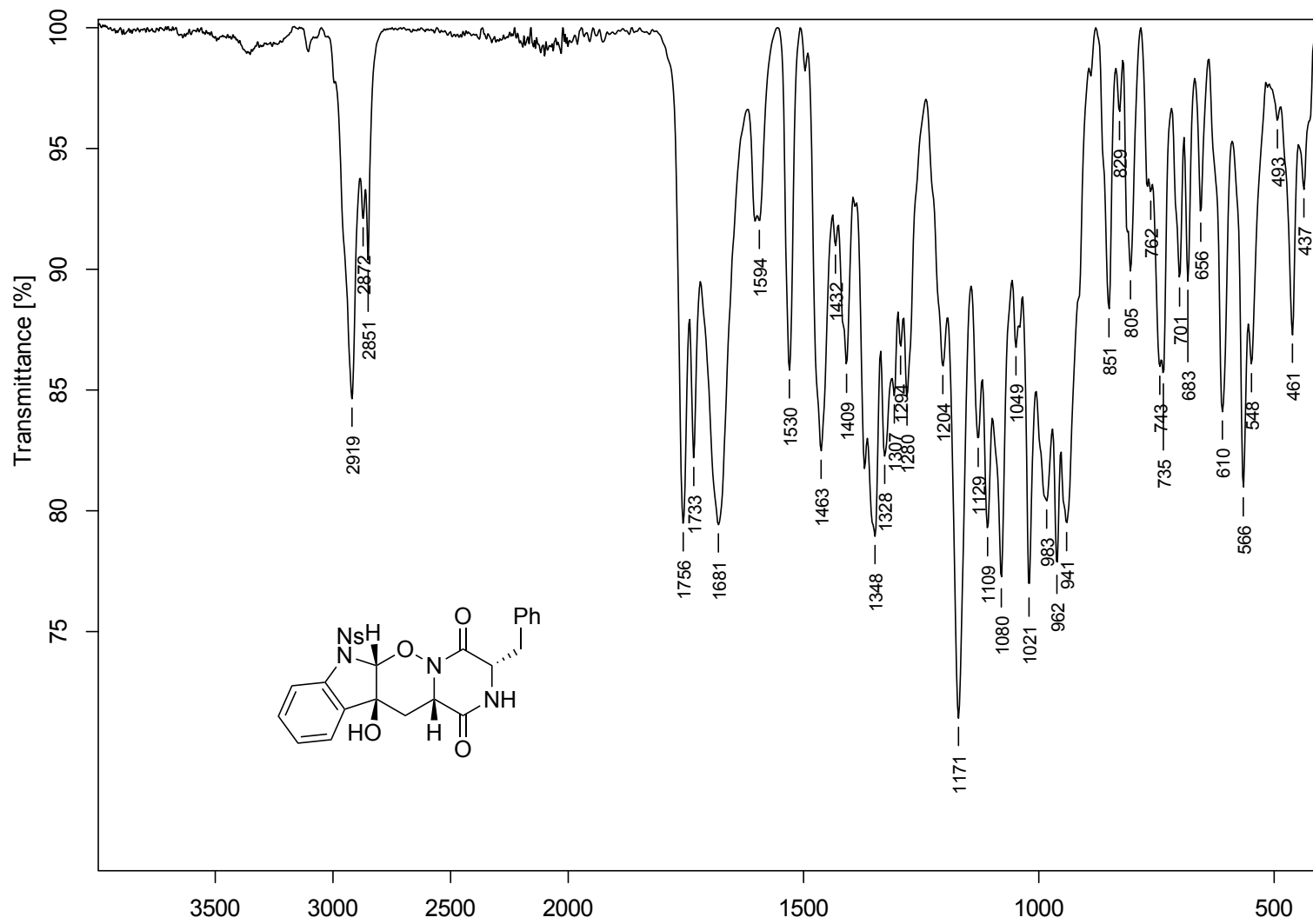


Figure B.86. FTIR Spectrum (neat) Ns-protected indole DKP **3.71**

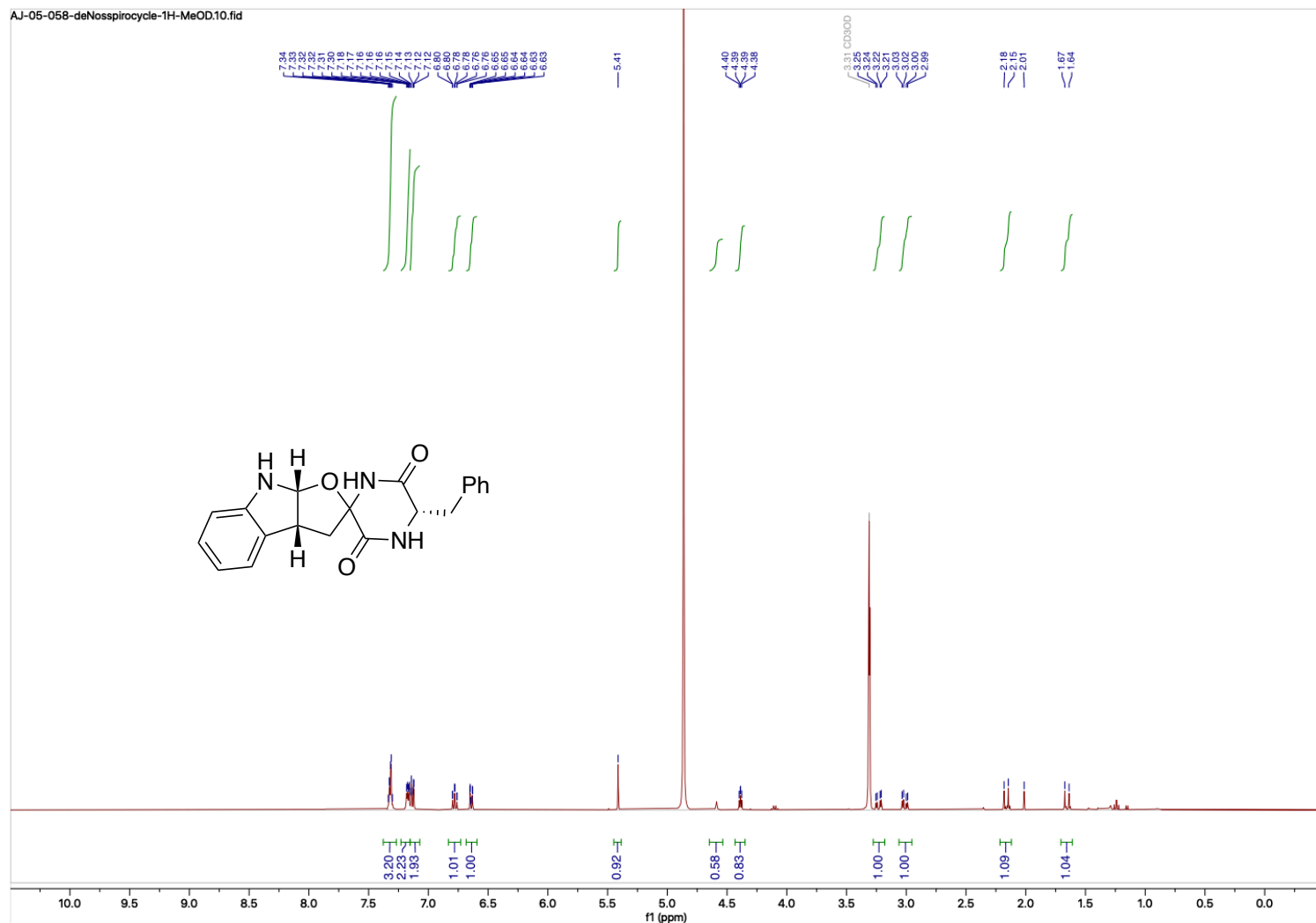


Figure B.87. ^1H Spectra (400 MHz, MeOD) proposed spirocycle by-product 3.72

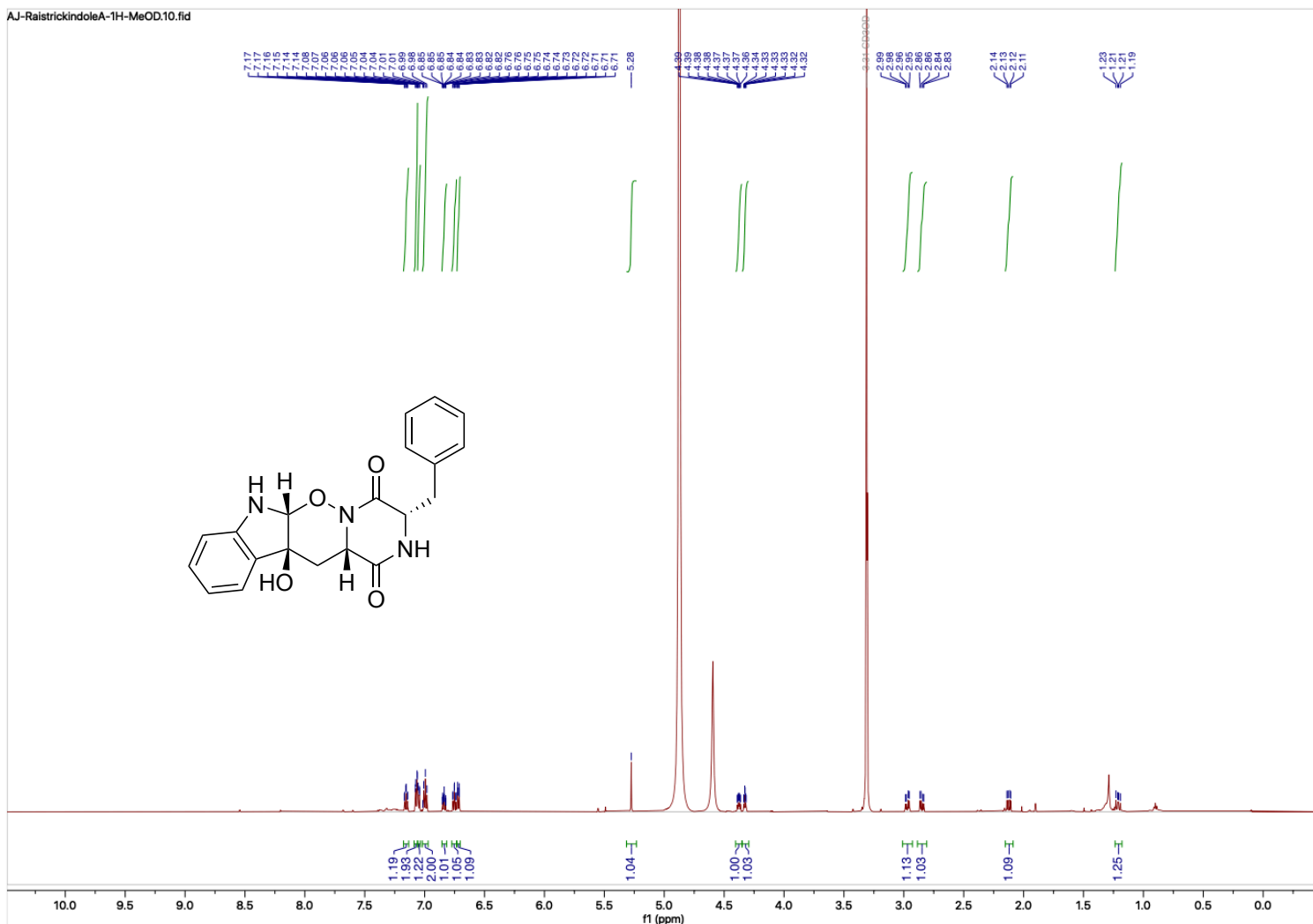


Figure B.88. ^1H Spectra (600 MHz, CDCl_3) (+)-raistrickindole A (3.01)

AJ-RaistrickindoleA-13C-MeOD10.fid

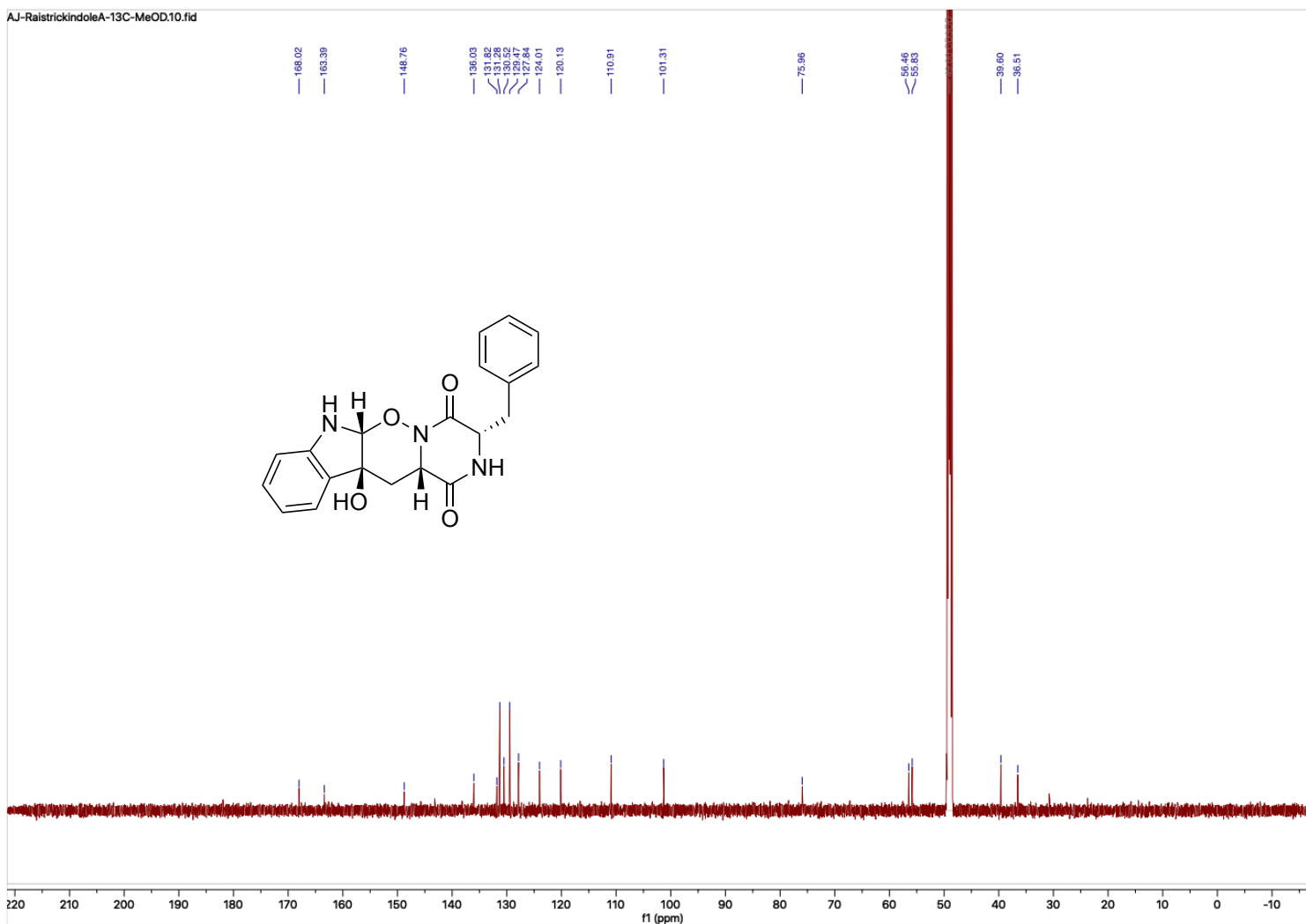


Figure B.89. ^{13}C Spectra (151 MHz, CDCl_3) (+)-raistrickindole A (3.01)

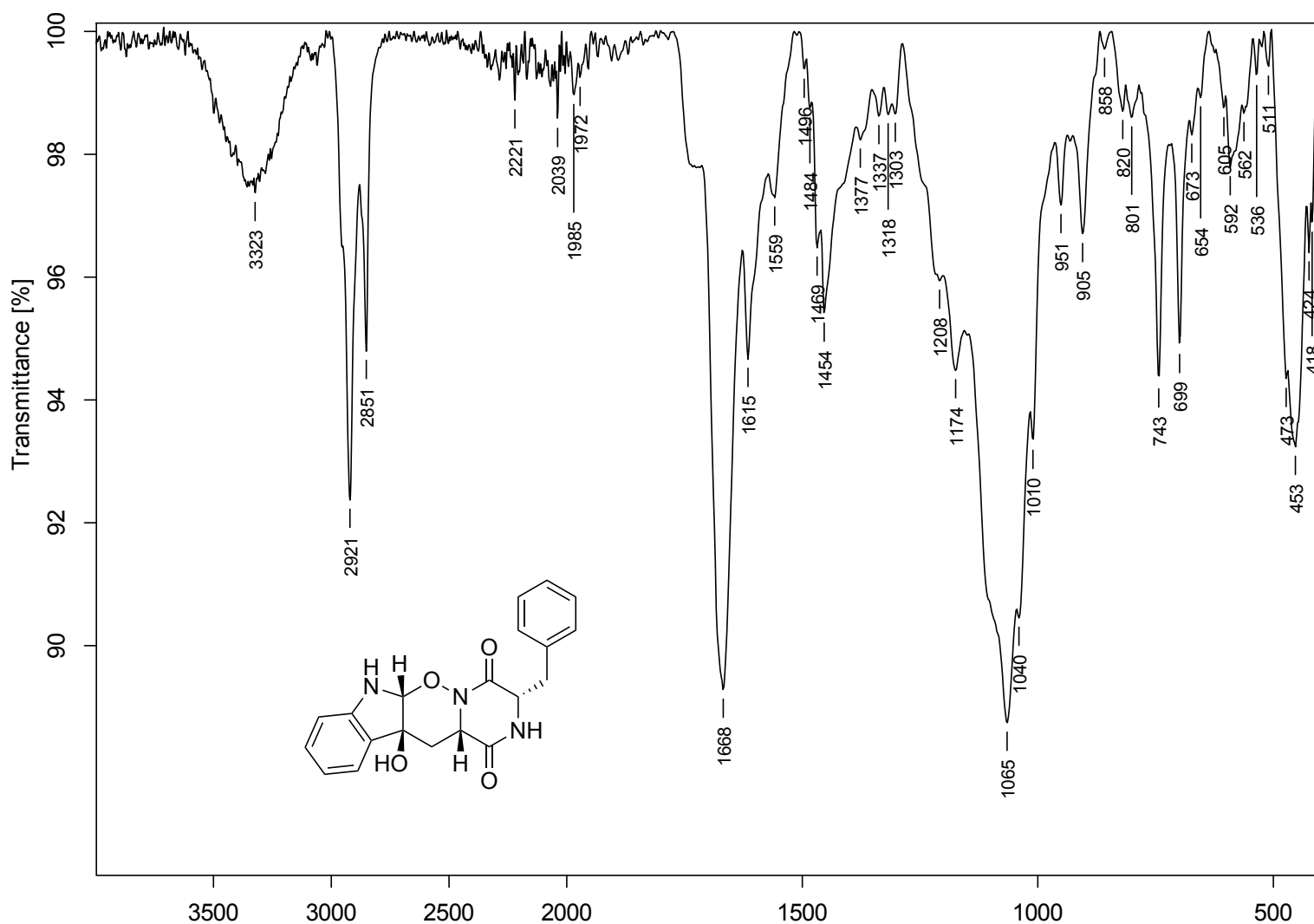
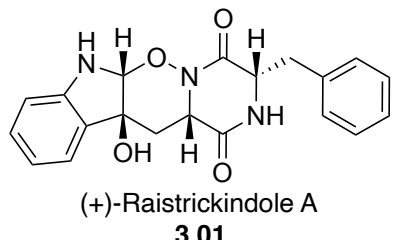


Figure B.90. FTIR Spectrum (neat) (+)-raistrickindole A (**3.01**)



	Natural Raistrickindole A	Synthetic Raistrickindole A	Δ ppm
1			
2			
3			
4	5.27, s	5.28, s	0.01
5			
6			
7	6.71, d	6.72, d	0.01
8	7.15, ddd	7.16, ddd	0.01
9	6.75, ddd	6.74, ddd	0.01
10	7.05, dd	7.06, dd	0.01
11			
12			
13	2.13, dd and 1.22, dd 4.38, ddd	2.13, dd and 1.21, dd 4.38, ddd	0.01
14			-
15			
16			
17	4.32, ddd	4.33, ddd	0.01
18	2.97, dd and 2.84, dd	2.97, dd and 2.85, dd	0.01
19			
20,24	7.07, dd	7.06, dd	0.01
21,23	7.00, t	6.99, t	0.01
22	6.84, tt	6.84, tt	-
OH-12			

Figure B.91. Comparison of ^1H NMR data for natural and synthetic (+)-raistrickindole A (**3.01**).

APPENDIX C
X-ray Crystallographic Data

*C.1. Crystal analysis of tetramic acid **2.51***

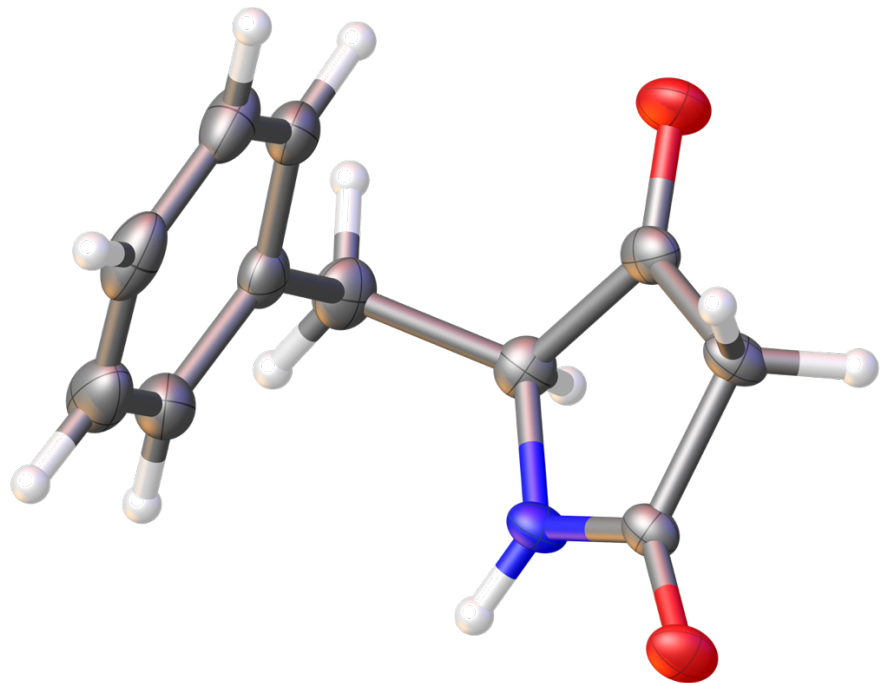


Figure C.01. ORTEP drawing of tetramic acid **2.51**

Table C.10. Crystal data and structure refinement for tetramic acid **2.49** (JLW_100).

Identification code	JLW_100	
Empirical formula	C11 H11 N O2	
Formula weight	189.21	
Temperature	150(2) K	
Wavelength	0.71073 Å	
Crystal system	Orthorhombic	
Space group	P 21 21 21	
Unit cell dimensions	a = 5.7818(3) Å	α= 90°.
	b = 11.1050(6) Å	β= 90°.
	c = 14.7502(9) Å	γ = 90°.
Volume	947.06(9) Å ³	
Z	4	
Density (calculated)	1.327 Mg/m ³	
Absorption coefficient	0.092 mm ⁻¹	
F(000)	400	
Crystal size	0.247 x 0.133 x 0.063 mm ³	
Theta range for data collection	2.296 to 28.288°.	
Index ranges	-7<=h<=7, -14<=k<=14, -17<=l<=19	
Reflections collected	9170	
Independent reflections	2353 [R(int) = 0.0401]	
Completeness to theta = 25.242°	99.9 %	
Absorption correction	Semi-empirical from equivalents	
Max. and min. transmission	0.937 and 0.922	
Refinement method	Full-matrix least-squares on F ²	
Data / restraints / parameters	2353 / 0 / 131	
Goodness-of-fit on F ²	1.368	
Final R indices [I>2sigma(I)]	R1 = 0.0400, wR2 = 0.0837	
R indices (all data)	R1 = 0.0509, wR2 = 0.0869	
Absolute structure parameter	-0.5(6)	
Extinction coefficient	n/a	
Largest diff. peak and hole	0.234 and -0.166 e.Å ⁻³	

Table C.11. Atomic coordinates ($x \times 10^4$) and equivalent isotropic displacement parameters ($\text{\AA}^2 \times 10^3$) for tetramic acid **2.49** (JLW_100). U(eq) is defined as one third of the trace of the orthogonalized U_{ij}^{ij} tensor.

	x	y	z	U(eq)
N(1)	2076(2)	1198(1)	4695(1)	21(1)
O(1)	5675(2)	1328(1)	5338(1)	27(1)
O(2)	923(3)	-1833(1)	4259(1)	35(1)
C(1)	4055(3)	746(1)	5018(1)	19(1)
C(2)	3973(3)	-617(2)	4934(1)	23(1)
C(3)	1678(3)	-864(2)	4493(1)	23(1)
C(4)	396(3)	322(2)	4367(1)	23(1)
C(5)	-410(3)	542(2)	3385(1)	29(1)
C(6)	1569(3)	650(2)	2724(1)	25(1)
C(7)	2580(3)	-365(2)	2337(1)	29(1)
C(8)	4525(4)	-266(2)	1788(1)	34(1)
C(9)	5461(4)	855(2)	1608(1)	37(1)
C(10)	4426(4)	1869(2)	1965(1)	39(1)
C(11)	2513(3)	1773(2)	2525(1)	32(1)

Table C.12. Bond lengths [\AA] and angles [$^\circ$] for tetramic acid **2.49** (JLW_100).

N(1)-C(1)	1.337(2)
N(1)-C(4)	1.458(2)
O(1)-C(1)	1.232(2)
O(2)-C(3)	1.211(2)
C(1)-C(2)	1.520(2)
C(2)-C(3)	1.503(3)
C(3)-C(4)	1.523(2)
C(4)-C(5)	1.540(3)
C(5)-C(6)	1.509(3)
C(6)-C(7)	1.392(3)
C(6)-C(11)	1.393(3)
C(7)-C(8)	1.389(3)
C(8)-C(9)	1.383(3)
C(9)-C(10)	1.379(3)
C(10)-C(11)	1.384(3)
C(1)-N(1)-C(4)	115.97(14)
O(1)-C(1)-N(1)	126.18(16)
O(1)-C(1)-C(2)	125.25(15)
N(1)-C(1)-C(2)	108.57(14)
C(3)-C(2)-C(1)	104.15(13)
O(2)-C(3)-C(2)	127.09(16)
O(2)-C(3)-C(4)	123.96(17)
C(2)-C(3)-C(4)	108.94(13)
N(1)-C(4)-C(3)	102.28(14)
N(1)-C(4)-C(5)	114.08(15)
C(3)-C(4)-C(5)	113.55(15)
C(6)-C(5)-C(4)	113.01(15)
C(7)-C(6)-C(11)	118.32(18)
C(7)-C(6)-C(5)	121.33(17)
C(11)-C(6)-C(5)	120.26(18)
C(8)-C(7)-C(6)	120.94(17)
C(9)-C(8)-C(7)	120.02(19)
C(10)-C(9)-C(8)	119.4(2)

C(9)-C(10)-C(11)	120.8(2)
C(10)-C(11)-C(6)	120.5(2)

Symmetry transformations used to generate equivalent atoms.

Table C.13. Anisotropic displacement parameters ($\text{\AA}^2 \times 10^3$) for tetramic acid **2.49** (JLW_100). The anisotropic displacement factor exponent takes the form: $-2\pi^2 [h^2 a^* U^{11} + \dots + 2 h k a^* b^* U^{12}]$.

	U ¹¹	U ²²	U ³³	U ²³	U ¹³	U ¹²
N(1)	21(1)	15(1)	28(1)	-1(1)	0(1)	2(1)
O(1)	21(1)	22(1)	38(1)	-1(1)	-3(1)	-5(1)
O(2)	43(1)	24(1)	38(1)	-1(1)	-2(1)	-14(1)
C(1)	17(1)	17(1)	24(1)	1(1)	4(1)	-1(1)
C(2)	19(1)	16(1)	33(1)	-1(1)	0(1)	2(1)
C(3)	25(1)	23(1)	22(1)	1(1)	5(1)	-6(1)
C(4)	17(1)	28(1)	25(1)	0(1)	2(1)	-1(1)
C(5)	20(1)	36(1)	30(1)	2(1)	-5(1)	1(1)
C(6)	25(1)	30(1)	21(1)	4(1)	-7(1)	-1(1)
C(7)	35(1)	29(1)	22(1)	3(1)	-6(1)	-2(1)
C(8)	34(1)	46(1)	20(1)	-1(1)	-3(1)	10(1)
C(9)	28(1)	63(1)	21(1)	5(1)	-1(1)	-7(1)
C(10)	47(1)	42(1)	27(1)	5(1)	-2(1)	-16(1)
C(11)	40(1)	29(1)	27(1)	2(1)	-5(1)	-2(1)

Table C.14. Hydrogen bonds for tetramic acid **2.49** (JLW_100) [Å and °].

D-H...A	d(D-H)	d(H...A)	d(D...A)	<(DHA)
N(1)-H(1)...O(1)#1	0.845(19)	2.03(2)	2.8646(18)	171.4(19)

Symmetry transformations used to generate equivalent atoms:

#1 x-1/2,-y+1/2,-z+1

C.2. Crystal analysis of DMB-tetramic acid 2.54

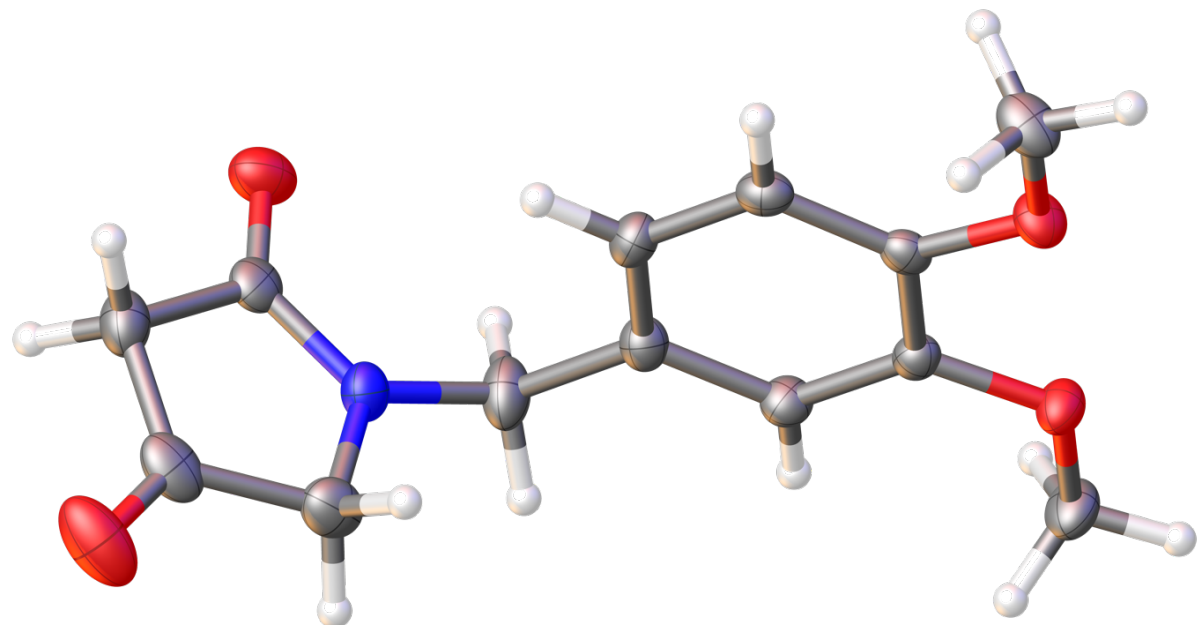


Figure C.02. ORTEP drawing of DMB-tetramic acid **2.54**

Table C.15. Crystal data and structure refinement for DMB-tetramic acid **2.52** (jlw97_acj_0m).

Identification code	jlw97_acj_0m		
Empirical formula	C13 H15 N O4		
Formula weight	249.26		
Temperature	150(2) K		
Wavelength	0.71073 Å		
Crystal system	Orthorhombic		
Space group	P 21 21 21		
Unit cell dimensions	a = 8.6623(5) Å	α= 90°.	
	b = 11.3554(9) Å	β= 90°.	
	c = 12.3256(7) Å	γ = 90°.	
Volume	1212.39(14) Å ³		
Z	4		
Density (calculated)	1.366 Mg/m ³		
Absorption coefficient	0.102 mm ⁻¹		
F(000)	528		
Crystal size	0.287 x 0.247 x 0.231 mm ³		
Theta range for data collection	2.439 to 28.324°.		
Index ranges	-10<=h<=11, -15<=k<=15, -16<=l<=15		
Reflections collected	12195		
Independent reflections	3010 [R(int) = 0.0305]		
Completeness to theta = 25.242°	99.9 %		
Absorption correction	Semi-empirical from equivalents		
Max. and min. transmission	0.928 and 0.922		
Refinement method	Full-matrix least-squares on F ²		
Data / restraints / parameters	3010 / 0 / 165		
Goodness-of-fit on F ²	1.043		
Final R indices [I>2sigma(I)]	R1 = 0.0338, wR2 = 0.0778		
R indices (all data)	R1 = 0.0400, wR2 = 0.0810		
Absolute structure parameter	1.4(3)		
Extinction coefficient	n/a		
Largest diff. peak and hole	0.205 and -0.146 e.Å ⁻³		

Table C.16. Atomic coordinates ($x \times 10^4$) and equivalent isotropic displacement parameters ($\text{\AA}^2 \times 10^3$) for DMB-tetramic acid **2.52** (jlw97_acj_0m). U(eq) is defined as one third of the trace of the orthogonalized U^{ij} tensor.

	x	y	z	U(eq)
O(1)	6094(2)	2515(1)	10088(1)	34(1)
O(2)	10011(2)	2187(2)	12740(1)	50(1)
O(3)	8424(2)	8620(1)	8900(1)	25(1)
O(4)	10399(1)	7561(1)	7663(1)	25(1)
N(1)	7555(2)	3820(1)	11064(1)	26(1)
C(1)	7108(2)	2732(2)	10752(1)	25(1)
C(2)	8068(2)	1837(2)	11363(2)	30(1)
C(3)	9104(2)	2554(2)	12080(2)	32(1)
C(4)	8817(2)	3845(2)	11845(2)	31(1)
C(5)	6854(2)	4897(2)	10662(2)	32(1)
C(6)	7853(2)	5558(2)	9852(1)	23(1)
C(7)	7678(2)	6780(2)	9777(1)	22(1)
C(8)	8523(2)	7424(1)	9033(1)	20(1)
C(9)	9572(2)	6843(2)	8344(1)	20(1)
C(10)	9720(2)	5631(2)	8406(1)	22(1)
C(11)	8869(2)	4991(2)	9167(1)	23(1)
C(12)	7323(2)	9203(2)	9576(2)	31(1)
C(13)	11573(2)	6997(2)	7034(2)	30(1)

Table C.17. Bond lengths [\AA] and angles [$^\circ$] for DMB-tetramic acid **2.52** (jlw97_acj_0m).

O(1)-C(1)	1.225(2)
O(2)-C(3)	1.205(2)
O(3)-C(8)	1.370(2)
O(3)-C(12)	1.430(2)
O(4)-C(9)	1.372(2)
O(4)-C(13)	1.430(2)
N(1)-C(1)	1.351(2)
N(1)-C(5)	1.452(2)
N(1)-C(4)	1.457(2)
C(1)-C(2)	1.514(3)
C(2)-C(3)	1.500(3)
C(2)-H(2A)	0.9900
C(2)-H(2B)	0.9900
C(3)-C(4)	1.516(3)
C(4)-H(4A)	0.9900
C(4)-H(4B)	0.9900
C(5)-C(6)	1.520(2)
C(5)-H(5A)	0.9900
C(5)-H(5B)	0.9900
C(6)-C(11)	1.379(2)
C(6)-C(7)	1.399(2)
C(7)-C(8)	1.382(2)
C(7)-H(7)	0.9500
C(8)-C(9)	1.408(2)
C(9)-C(10)	1.385(2)
C(10)-C(11)	1.397(2)
C(10)-H(10)	0.9500
C(11)-H(11)	0.9500
C(12)-H(12A)	0.9800
C(12)-H(12B)	0.9800
C(12)-H(12C)	0.9800
C(13)-H(13A)	0.9800
C(13)-H(13B)	0.9800

C(13)-H(13C)	0.9800
C(8)-O(3)-C(12)	115.55(13)
C(9)-O(4)-C(13)	115.90(14)
C(1)-N(1)-C(5)	123.59(16)
C(1)-N(1)-C(4)	114.88(16)
C(5)-N(1)-C(4)	121.53(16)
O(1)-C(1)-N(1)	125.38(18)
O(1)-C(1)-C(2)	126.25(18)
N(1)-C(1)-C(2)	108.37(16)
C(3)-C(2)-C(1)	104.94(16)
C(3)-C(2)-H(2A)	110.8
C(1)-C(2)-H(2A)	110.8
C(3)-C(2)-H(2B)	110.8
C(1)-C(2)-H(2B)	110.8
H(2A)-C(2)-H(2B)	108.8
O(2)-C(3)-C(2)	126.9(2)
O(2)-C(3)-C(4)	124.8(2)
C(2)-C(3)-C(4)	108.31(16)
N(1)-C(4)-C(3)	103.34(16)
N(1)-C(4)-H(4A)	111.1
C(3)-C(4)-H(4A)	111.1
N(1)-C(4)-H(4B)	111.1
C(3)-C(4)-H(4B)	111.1
H(4A)-C(4)-H(4B)	109.1
N(1)-C(5)-C(6)	113.68(16)
N(1)-C(5)-H(5A)	108.8
C(6)-C(5)-H(5A)	108.8
N(1)-C(5)-H(5B)	108.8
C(6)-C(5)-H(5B)	108.8
H(5A)-C(5)-H(5B)	107.7
C(11)-C(6)-C(7)	119.46(16)
C(11)-C(6)-C(5)	122.33(15)
C(7)-C(6)-C(5)	118.16(16)
C(8)-C(7)-C(6)	120.74(16)
C(8)-C(7)-H(7)	119.6

C(6)-C(7)-H(7)	119.6
O(3)-C(8)-C(7)	124.77(15)
O(3)-C(8)-C(9)	115.62(14)
C(7)-C(8)-C(9)	119.61(14)
O(4)-C(9)-C(10)	125.16(16)
O(4)-C(9)-C(8)	115.32(14)
C(10)-C(9)-C(8)	119.50(15)
C(9)-C(10)-C(11)	120.33(16)
C(9)-C(10)-H(10)	119.8
C(11)-C(10)-H(10)	119.8
C(6)-C(11)-C(10)	120.33(16)
C(6)-C(11)-H(11)	119.8
C(10)-C(11)-H(11)	119.8
O(3)-C(12)-H(12A)	109.5
O(3)-C(12)-H(12B)	109.5
H(12A)-C(12)-H(12B)	109.5
O(3)-C(12)-H(12C)	109.5
H(12A)-C(12)-H(12C)	109.5
H(12B)-C(12)-H(12C)	109.5
O(4)-C(13)-H(13A)	109.5
O(4)-C(13)-H(13B)	109.5
H(13A)-C(13)-H(13B)	109.5
O(4)-C(13)-H(13C)	109.5
H(13A)-C(13)-H(13C)	109.5
H(13B)-C(13)-H(13C)	109.5

Symmetry transformations used to generate equivalent atoms.

Table C.18. Anisotropic displacement parameters ($\text{\AA}^2 \times 10^3$) for DMB-tetramic acid **2.52** (jlw97_acj_0m). The anisotropic displacement factor exponent takes the form: $-2p^2 [h^2 a^* U^{11} + \dots + 2 h k a^* b^* U^{12}]$.

	U ¹¹	U ²²	U ³³	U ²³	U ¹³	U ¹²
O(1)	33(1)	44(1)	27(1)	-1(1)	-1(1)	-10(1)
O(2)	30(1)	78(1)	42(1)	24(1)	-1(1)	2(1)
O(3)	28(1)	19(1)	27(1)	0(1)	8(1)	0(1)
O(4)	24(1)	28(1)	23(1)	3(1)	7(1)	1(1)
N(1)	26(1)	24(1)	27(1)	4(1)	2(1)	-3(1)
C(1)	25(1)	28(1)	21(1)	2(1)	8(1)	-3(1)
C(2)	32(1)	25(1)	33(1)	6(1)	8(1)	1(1)
C(3)	21(1)	47(1)	28(1)	10(1)	8(1)	-1(1)
C(4)	27(1)	38(1)	30(1)	1(1)	0(1)	-10(1)
C(5)	32(1)	24(1)	40(1)	8(1)	11(1)	1(1)
C(6)	21(1)	22(1)	25(1)	3(1)	1(1)	-1(1)
C(7)	21(1)	23(1)	22(1)	-2(1)	4(1)	0(1)
C(8)	20(1)	19(1)	20(1)	-1(1)	-1(1)	-1(1)
C(9)	18(1)	25(1)	16(1)	0(1)	-2(1)	-2(1)
C(10)	19(1)	26(1)	20(1)	-4(1)	0(1)	2(1)
C(11)	24(1)	19(1)	28(1)	0(1)	0(1)	-1(1)
C(12)	38(1)	21(1)	34(1)	-2(1)	10(1)	3(1)
C(13)	23(1)	41(1)	28(1)	6(1)	7(1)	6(1)

*C.3. Crystal analysis of tetramic acid **2.56***

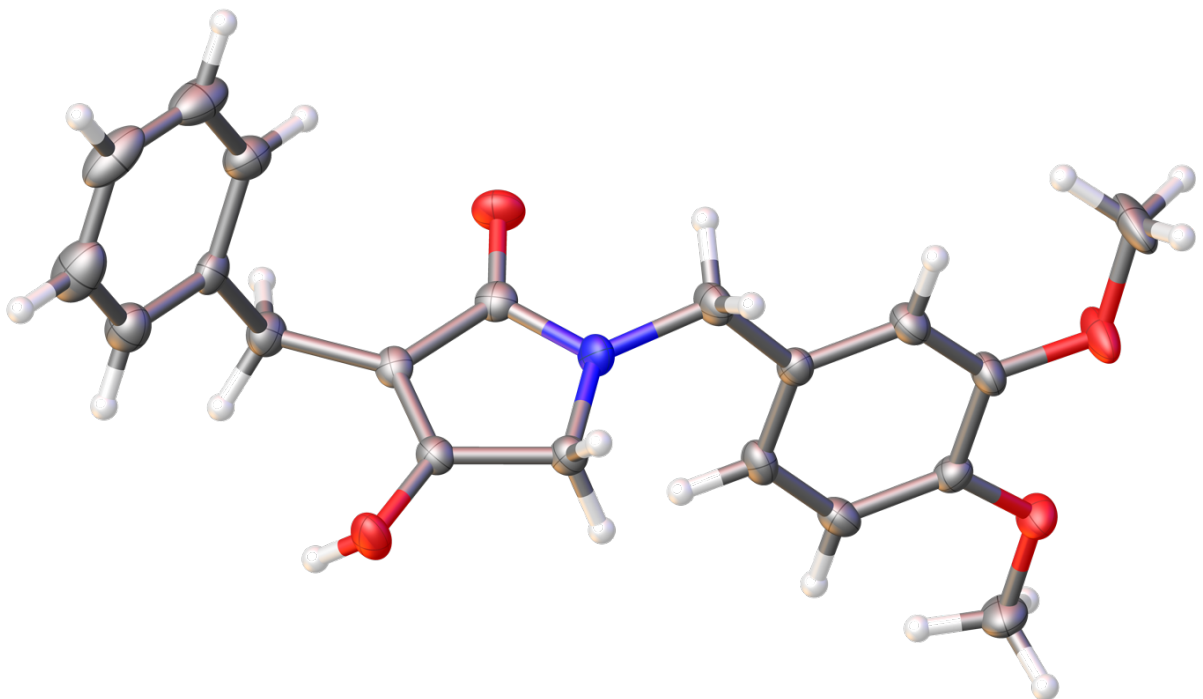


Figure C.03. ORTEP drawing of tetramic acid **2.56**

Table C.19. Crystal data and structure refinement for benzyl tetramic acid **2.54**

(JLW_118).

Identification code	JLW_118		
Empirical formula	C40 H40 N3 O7		
Formula weight	674.75		
Temperature	150(2) K		
Wavelength	0.71073 Å		
Crystal system	Triclinic		
Space group	P-1		
Unit cell dimensions	a = 9.9745(4) Å	α= 109.347(2)°.	
	b = 12.0336(4) Å	β= 99.420(2)°.	
	c = 16.1694(7) Å	γ = 100.0320(10)°.	
Volume	1751.27(12) Å ³		
Z	2		
Density (calculated)	1.280 Mg/m ³		
Absorption coefficient	0.088 mm ⁻¹		
F(000)	714		
Crystal size	0.221 x 0.110 x 0.059 mm ³		
Theta range for data collection	2.135 to 26.362°.		
Index ranges	-12<=h<=11, -15<=k<=13, -20<=l<=20		
Reflections collected	12643		
Independent reflections	6592 [R(int) = 0.0324]		
Completeness to theta = 25.242°	93.1 %		
Absorption correction	None		
Refinement method	Full-matrix least-squares on F ²		
Data / restraints / parameters	6592 / 0 / 455		
Goodness-of-fit on F ²	1.089		
Final R indices [I>2sigma(I)]	R1 = 0.0640, wR2 = 0.1645		
R indices (all data)	R1 = 0.0793, wR2 = 0.1801		
Extinction coefficient	n/a		
Largest diff. peak and hole	0.559 and -0.319 e.Å ⁻³		

Table C.20. Atomic coordinates ($x \times 10^4$) and equivalent isotropic displacement parameters ($\text{\AA}^2 \times 10^3$) for benzyl tetramic acid **2.54** (JLW_118). U(eq) is defined as one third of the trace of the orthogonalized U^{ij} tensor.

	x	y	z	U(eq)
O(1)	1768(2)	6897(2)	4677(1)	30(1)
O(2)	4601(2)	4148(2)	1047(1)	29(1)
O(3)	7572(2)	7942(2)	1532(1)	32(1)
O(4)	777(2)	187(2)	4205(1)	28(1)
O(5)	3027(2)	1151(2)	5462(1)	38(1)
O(6)	6914(2)	-44(2)	2150(1)	30(1)
O(7)	5792(2)	2438(2)	539(1)	28(1)
N(1)	4199(2)	5996(2)	1147(1)	25(1)
N(2)	2936(3)	5134(2)	4077(1)	26(1)
N(3)	5893(2)	1558(2)	2440(1)	23(1)
C(1)	8704(3)	4531(3)	3770(2)	46(1)
C(2)	7957(4)	5397(3)	3764(2)	43(1)
C(3)	7646(3)	5675(3)	2994(2)	33(1)
C(4)	8071(3)	5083(2)	2226(2)	25(1)
C(5)	7744(3)	5370(2)	1376(2)	26(1)
C(6)	6494(3)	5893(2)	1293(2)	22(1)
C(7)	5046(3)	5235(2)	1150(2)	23(1)
C(8)	2724(3)	5712(2)	1162(2)	25(1)
C(9)	2480(3)	6064(2)	2101(2)	24(1)
C(10)	2840(3)	5405(2)	2638(2)	27(1)
C(11)	2612(3)	5711(2)	3499(2)	26(1)
C(12)	1994(3)	6683(2)	3835(2)	25(1)
C(13)	1015(3)	7804(3)	4992(2)	33(1)
C(14)	3539(5)	4129(4)	3761(3)	67(1)
C(15)	5007(3)	7214(2)	1336(2)	24(1)
C(16)	6469(3)	7046(2)	1396(2)	23(1)
C(17)	9145(3)	3954(3)	3010(2)	43(1)
C(18)	8836(3)	4225(3)	2246(2)	34(1)
C(19)	1913(3)	7032(2)	2449(2)	30(1)
C(20)	1664(3)	7341(2)	3312(2)	30(1)

C(21)	11201(3)	2269(3)	459(2)	42(1)
C(22)	10075(4)	2131(3)	-218(2)	43(1)
C(23)	8759(3)	1500(3)	-256(2)	32(1)
C(24)	8544(3)	985(2)	374(2)	22(1)
C(25)	7099(3)	285(2)	337(2)	24(1)
C(26)	6495(2)	967(2)	1087(2)	19(1)
C(27)	6480(2)	746(2)	1916(2)	21(1)
C(28)	5909(3)	1736(3)	3374(2)	26(1)
C(29)	4492(3)	1314(2)	3542(2)	21(1)
C(30)	3289(3)	763(2)	2861(2)	24(1)
C(31)	2011(3)	391(2)	3058(2)	24(1)
C(32)	1945(3)	543(2)	3933(2)	21(1)
C(33)	-498(3)	-386(3)	3521(2)	32(1)
C(34)	4428(3)	1477(2)	4426(2)	24(1)
C(35)	3186(3)	1081(2)	4629(2)	24(1)
C(36)	4273(3)	1502(3)	6161(2)	45(1)
C(37)	5535(3)	2401(2)	2029(2)	21(1)
C(38)	5964(2)	1933(2)	1153(2)	20(1)
C(39)	10995(3)	1773(3)	1098(2)	40(1)
C(40)	9674(3)	1128(3)	1055(2)	31(1)

Table C.21. Bond lengths [\AA] and angles [$^\circ$] for benzyl tetramic acid **2.54** (JLW_118).

O(1)-C(12)	1.363(3)
O(1)-C(13)	1.434(3)
O(2)-C(7)	1.251(3)
O(3)-C(16)	1.331(3)
O(4)-C(32)	1.361(3)
O(4)-C(33)	1.431(3)
O(5)-C(35)	1.359(3)
O(5)-C(36)	1.428(3)
O(6)-C(27)	1.249(3)
O(7)-C(38)	1.328(3)
N(1)-C(7)	1.350(3)
N(1)-C(15)	1.450(3)
N(1)-C(8)	1.457(3)
N(2)-C(11)	1.367(3)
N(2)-C(14)	1.424(4)
N(3)-C(27)	1.352(3)
N(3)-C(37)	1.447(3)
N(3)-C(28)	1.451(3)
C(1)-C(17)	1.380(5)
C(1)-C(2)	1.385(5)
C(1)-H(1)	0.9500
C(2)-C(3)	1.393(4)
C(2)-H(16)	0.9500
C(3)-C(4)	1.386(4)
C(3)-H(13)	0.9500
C(4)-C(18)	1.392(4)
C(4)-C(5)	1.523(3)
C(5)-C(6)	1.498(4)
C(5)-H(17)	0.9900
C(5)-H(12)	0.9900
C(6)-C(16)	1.347(3)
C(6)-C(7)	1.462(4)
C(8)-C(9)	1.509(4)
C(8)-H(9)	0.9900

C(8)-H(8)	0.9900
C(9)-C(19)	1.376(4)
C(9)-C(10)	1.402(3)
C(10)-C(11)	1.385(4)
C(10)-H(7)	0.9500
C(11)-C(12)	1.408(4)
C(12)-C(20)	1.376(4)
C(13)-H(3)	0.9800
C(13)-H(20)	0.9800
C(13)-H(2)	0.9800
C(14)-H(4)	0.9800
C(14)-H(5)	0.9800
C(14)-H(6)	0.9800
C(15)-C(16)	1.499(4)
C(15)-H(11)	0.9900
C(15)-H(10)	0.9900
C(17)-C(18)	1.381(4)
C(17)-H(14)	0.9500
C(18)-H(15)	0.9500
C(19)-C(20)	1.397(4)
C(19)-H(19)	0.9500
C(20)-H(18)	0.9500
C(21)-C(39)	1.381(5)
C(21)-C(22)	1.379(5)
C(21)-H(21)	0.9500
C(22)-C(23)	1.378(4)
C(22)-H(30)	0.9500
C(23)-C(24)	1.382(4)
C(23)-H(29)	0.9500
C(24)-C(40)	1.383(4)
C(24)-C(25)	1.519(3)
C(25)-C(26)	1.503(3)
C(25)-H(28)	0.9900
C(25)-H(33)	0.9900
C(26)-C(38)	1.340(3)
C(26)-C(27)	1.453(3)

C(28)-C(29)	1.515(3)
C(28)-H(36)	0.9900
C(28)-H(37)	0.9900
C(29)-C(30)	1.378(3)
C(29)-C(34)	1.391(3)
C(30)-C(31)	1.399(4)
C(30)-H(38)	0.9500
C(31)-C(32)	1.378(3)
C(31)-H(39)	0.9500
C(32)-C(35)	1.414(3)
C(33)-H(23)	0.9800
C(33)-H(40)	0.9800
C(33)-H(22)	0.9800
C(34)-C(35)	1.378(3)
C(34)-H(27)	0.9500
C(36)-H(25)	0.9800
C(36)-H(26)	0.9800
C(36)-H(24)	0.9800
C(37)-C(38)	1.503(3)
C(37)-H(34)	0.9900
C(37)-H(35)	0.9900
C(39)-C(40)	1.386(4)
C(39)-H(31)	0.9500
C(40)-H(32)	0.9500
C(12)-O(1)-C(13)	116.4(2)
C(32)-O(4)-C(33)	116.84(19)
C(35)-O(5)-C(36)	117.3(2)
C(7)-N(1)-C(15)	110.9(2)
C(7)-N(1)-C(8)	124.3(2)
C(15)-N(1)-C(8)	123.4(2)
C(11)-N(2)-C(14)	117.2(2)
C(27)-N(3)-C(37)	111.49(19)
C(27)-N(3)-C(28)	123.8(2)
C(37)-N(3)-C(28)	123.4(2)
C(17)-C(1)-C(2)	119.3(3)

C(17)-C(1)-H(1)	120.3
C(2)-C(1)-H(1)	120.3
C(1)-C(2)-C(3)	120.2(3)
C(1)-C(2)-H(16)	119.9
C(3)-C(2)-H(16)	119.9
C(4)-C(3)-C(2)	120.5(3)
C(4)-C(3)-H(13)	119.8
C(2)-C(3)-H(13)	119.8
C(3)-C(4)-C(18)	118.7(3)
C(3)-C(4)-C(5)	121.5(2)
C(18)-C(4)-C(5)	119.8(2)
C(6)-C(5)-C(4)	114.2(2)
C(6)-C(5)-H(17)	108.7
C(4)-C(5)-H(17)	108.7
C(6)-C(5)-H(12)	108.7
C(4)-C(5)-H(12)	108.7
H(17)-C(5)-H(12)	107.6
C(16)-C(6)-C(7)	106.7(2)
C(16)-C(6)-C(5)	128.2(2)
C(7)-C(6)-C(5)	124.9(2)
O(2)-C(7)-N(1)	123.0(2)
O(2)-C(7)-C(6)	127.9(2)
N(1)-C(7)-C(6)	109.1(2)
N(1)-C(8)-C(9)	113.6(2)
N(1)-C(8)-H(9)	108.9
C(9)-C(8)-H(9)	108.9
N(1)-C(8)-H(8)	108.9
C(9)-C(8)-H(8)	108.9
H(9)-C(8)-H(8)	107.7
C(19)-C(9)-C(10)	118.8(2)
C(19)-C(9)-C(8)	121.1(2)
C(10)-C(9)-C(8)	120.0(2)
C(11)-C(10)-C(9)	120.7(2)
C(11)-C(10)-H(7)	119.7
C(9)-C(10)-H(7)	119.7
N(2)-C(11)-C(10)	125.2(2)

N(2)-C(11)-C(12)	115.1(2)
C(10)-C(11)-C(12)	119.8(2)
O(1)-C(12)-C(20)	124.8(2)
O(1)-C(12)-C(11)	115.9(2)
C(20)-C(12)-C(11)	119.4(2)
O(1)-C(13)-H(3)	109.5
O(1)-C(13)-H(20)	109.5
H(3)-C(13)-H(20)	109.5
O(1)-C(13)-H(2)	109.5
H(3)-C(13)-H(2)	109.5
H(20)-C(13)-H(2)	109.5
N(2)-C(14)-H(4)	109.5
N(2)-C(14)-H(5)	109.5
H(4)-C(14)-H(5)	109.5
N(2)-C(14)-H(6)	109.5
H(4)-C(14)-H(6)	109.5
H(5)-C(14)-H(6)	109.5
N(1)-C(15)-C(16)	102.0(2)
N(1)-C(15)-H(11)	111.4
C(16)-C(15)-H(11)	111.4
N(1)-C(15)-H(10)	111.4
C(16)-C(15)-H(10)	111.4
H(11)-C(15)-H(10)	109.2
O(3)-C(16)-C(6)	126.0(3)
O(3)-C(16)-C(15)	122.9(2)
C(6)-C(16)-C(15)	111.1(2)
C(1)-C(17)-C(18)	120.7(3)
C(1)-C(17)-H(14)	119.7
C(18)-C(17)-H(14)	119.7
C(17)-C(18)-C(4)	120.6(3)
C(17)-C(18)-H(15)	119.7
C(4)-C(18)-H(15)	119.7
C(9)-C(19)-C(20)	121.0(2)
C(9)-C(19)-H(19)	119.5
C(20)-C(19)-H(19)	119.5
C(12)-C(20)-C(19)	120.3(2)

C(12)-C(20)-H(18)	119.8
C(19)-C(20)-H(18)	119.8
C(39)-C(21)-C(22)	119.3(3)
C(39)-C(21)-H(21)	120.4
C(22)-C(21)-H(21)	120.4
C(23)-C(22)-C(21)	120.2(3)
C(23)-C(22)-H(30)	119.9
C(21)-C(22)-H(30)	119.9
C(22)-C(23)-C(24)	121.0(3)
C(22)-C(23)-H(29)	119.5
C(24)-C(23)-H(29)	119.5
C(23)-C(24)-C(40)	118.8(2)
C(23)-C(24)-C(25)	121.4(2)
C(40)-C(24)-C(25)	119.8(2)
C(26)-C(25)-C(24)	112.09(19)
C(26)-C(25)-H(28)	109.2
C(24)-C(25)-H(28)	109.2
C(26)-C(25)-H(33)	109.2
C(24)-C(25)-H(33)	109.2
H(28)-C(25)-H(33)	107.9
C(38)-C(26)-C(27)	107.1(2)
C(38)-C(26)-C(25)	127.3(2)
C(27)-C(26)-C(25)	125.5(2)
O(6)-C(27)-N(3)	122.7(2)
O(6)-C(27)-C(26)	128.6(2)
N(3)-C(27)-C(26)	108.7(2)
N(3)-C(28)-C(29)	114.6(2)
N(3)-C(28)-H(36)	108.6
C(29)-C(28)-H(36)	108.6
N(3)-C(28)-H(37)	108.6
C(29)-C(28)-H(37)	108.6
H(36)-C(28)-H(37)	107.6
C(30)-C(29)-C(34)	119.4(2)
C(30)-C(29)-C(28)	123.0(2)
C(34)-C(29)-C(28)	117.6(2)
C(29)-C(30)-C(31)	120.3(2)

C(29)-C(30)-H(38)	119.8
C(31)-C(30)-H(38)	119.8
C(32)-C(31)-C(30)	120.5(2)
C(32)-C(31)-H(39)	119.8
C(30)-C(31)-H(39)	119.8
O(4)-C(32)-C(31)	125.9(2)
O(4)-C(32)-C(35)	114.9(2)
C(31)-C(32)-C(35)	119.2(2)
O(4)-C(33)-H(23)	109.5
O(4)-C(33)-H(40)	109.5
H(23)-C(33)-H(40)	109.5
O(4)-C(33)-H(22)	109.5
H(23)-C(33)-H(22)	109.5
H(40)-C(33)-H(22)	109.5
C(35)-C(34)-C(29)	121.0(2)
C(35)-C(34)-H(27)	119.5
C(29)-C(34)-H(27)	119.5
O(5)-C(35)-C(34)	125.5(2)
O(5)-C(35)-C(32)	114.9(2)
C(34)-C(35)-C(32)	119.6(2)
O(5)-C(36)-H(25)	109.5
O(5)-C(36)-H(26)	109.5
H(25)-C(36)-H(26)	109.5
O(5)-C(36)-H(24)	109.5
H(25)-C(36)-H(24)	109.5
H(26)-C(36)-H(24)	109.5
N(3)-C(37)-C(38)	101.28(19)
N(3)-C(37)-H(34)	111.5
C(38)-C(37)-H(34)	111.5
N(3)-C(37)-H(35)	111.5
C(38)-C(37)-H(35)	111.5
H(34)-C(37)-H(35)	109.3
O(7)-C(38)-C(26)	126.6(2)
O(7)-C(38)-C(37)	122.0(2)
C(26)-C(38)-C(37)	111.4(2)
C(21)-C(39)-C(40)	120.5(3)

C(21)-C(39)-H(31)	119.8
C(40)-C(39)-H(31)	119.8
C(24)-C(40)-C(39)	120.3(3)
C(24)-C(40)-H(32)	119.9
C(39)-C(40)-H(32)	119.9

Symmetry transformations used to generate equivalent atoms.

Table C.22. Anisotropic displacement parameters ($\text{\AA}^2 \times 10^3$) for benzyl tetramic acid **2.54** (JLW_118). The anisotropic displacement factor exponent takes the form: $-2p^2[h^2 a^* U^{11} + \dots + 2hk a^* b^* U^{12}]$.

	U ¹¹	U ²²	U ³³	U ²³	U ¹³	U ¹²
O(1)	37(1)	28(1)	26(1)	10(1)	9(1)	12(1)
O(2)	29(1)	22(1)	38(1)	14(1)	9(1)	6(1)
O(3)	31(1)	28(1)	39(1)	17(1)	10(1)	3(1)
O(4)	19(1)	37(1)	26(1)	12(1)	7(1)	2(1)
O(5)	26(1)	63(1)	18(1)	16(1)	6(1)	-4(1)
O(6)	32(1)	27(1)	37(1)	19(1)	6(1)	10(1)
O(7)	41(1)	29(1)	23(1)	15(1)	11(1)	13(1)
N(1)	26(1)	24(1)	28(1)	13(1)	6(1)	7(1)
N(2)	47(1)	27(1)	20(1)	16(1)	14(1)	26(1)
N(3)	25(1)	28(1)	23(1)	15(1)	10(1)	8(1)
C(1)	43(2)	45(2)	41(2)	28(2)	-15(1)	-11(2)
C(2)	49(2)	40(2)	30(2)	13(1)	1(1)	-6(1)
C(3)	36(2)	29(1)	32(2)	12(1)	4(1)	5(1)
C(4)	19(1)	25(1)	31(1)	14(1)	2(1)	-2(1)
C(5)	27(1)	27(1)	30(1)	14(1)	12(1)	8(1)
C(6)	26(1)	25(1)	19(1)	12(1)	7(1)	7(1)
C(7)	30(1)	22(1)	19(1)	10(1)	6(1)	8(1)
C(8)	24(1)	24(1)	26(1)	10(1)	0(1)	5(1)
C(9)	19(1)	23(1)	27(1)	10(1)	3(1)	3(1)
C(10)	30(2)	24(1)	29(1)	11(1)	6(1)	10(1)
C(11)	28(1)	24(1)	29(1)	13(1)	3(1)	8(1)
C(12)	24(1)	22(1)	24(1)	7(1)	4(1)	2(1)
C(13)	37(2)	33(2)	31(1)	9(1)	11(1)	12(1)
C(14)	126(4)	65(2)	49(2)	38(2)	38(2)	72(3)
C(15)	35(2)	20(1)	17(1)	9(1)	6(1)	7(1)
C(16)	30(1)	25(1)	17(1)	10(1)	7(1)	5(1)
C(17)	28(2)	42(2)	61(2)	32(2)	-5(1)	4(1)
C(18)	24(1)	32(2)	48(2)	21(1)	4(1)	4(1)
C(19)	34(2)	28(1)	33(1)	18(1)	6(1)	11(1)
C(20)	33(2)	25(1)	34(1)	11(1)	8(1)	13(1)

C(21)	25(2)	24(1)	75(2)	12(1)	24(2)	2(1)
C(22)	44(2)	39(2)	62(2)	28(2)	29(2)	12(1)
C(23)	33(2)	32(2)	35(2)	16(1)	13(1)	9(1)
C(24)	22(1)	17(1)	23(1)	3(1)	10(1)	5(1)
C(25)	25(1)	21(1)	24(1)	5(1)	6(1)	4(1)
C(26)	15(1)	18(1)	21(1)	6(1)	5(1)	-2(1)
C(27)	16(1)	21(1)	26(1)	10(1)	4(1)	-1(1)
C(28)	24(1)	36(1)	21(1)	15(1)	6(1)	4(1)
C(29)	22(1)	22(1)	22(1)	12(1)	8(1)	6(1)
C(30)	30(1)	25(1)	19(1)	11(1)	8(1)	5(1)
C(31)	25(1)	26(1)	21(1)	11(1)	2(1)	4(1)
C(32)	18(1)	23(1)	26(1)	11(1)	7(1)	5(1)
C(33)	18(1)	41(2)	32(1)	12(1)	5(1)	5(1)
C(34)	23(1)	28(1)	19(1)	9(1)	2(1)	1(1)
C(35)	25(1)	30(1)	16(1)	9(1)	5(1)	3(1)
C(36)	36(2)	73(2)	17(1)	17(1)	1(1)	-6(2)
C(37)	21(1)	21(1)	23(1)	10(1)	7(1)	4(1)
C(38)	18(1)	20(1)	20(1)	8(1)	4(1)	1(1)
C(39)	22(2)	36(2)	50(2)	3(1)	2(1)	6(1)
C(40)	26(1)	32(1)	34(2)	11(1)	7(1)	9(1)

Table C.23. Hydrogen coordinates ($x \times 10^4$) and isotropic displacement parameters ($\text{\AA}^2 \times 10^3$) for benzyl tetramic acid **2.54** (JLW_118).

	x	y	z	U(eq)
H(1)	8910	4336	4293	55
H(16)	7656	5804	4286	51
H(13)	7140	6275	2996	40
H(17)	8572	5952	1369	31
H(12)	7583	4615	843	31
H(9)	2323	4829	835	30
H(8)	2219	6140	835	30
H(7)	3246	4741	2410	33
H(3)	1572	8599	5059	50
H(20)	841	7832	5576	50
H(2)	119	7603	4555	50
H(4)	2888	3502	3221	100
H(5)	3723	3795	4232	100
H(6)	4421	4401	3612	100
H(11)	4919	7796	1912	28
H(10)	4713	7500	843	28
H(14)	9666	3365	3013	52
H(15)	9149	3822	1728	41
H(19)	1689	7498	2096	36
H(18)	1264	8008	3539	36
H(21)	12110	2701	485	50
H(30)	10206	2472	-661	52
H(29)	7988	1418	-721	38
H(28)	6462	124	-250	29
H(33)	7162	-508	379	29
H(36)	6283	2611	3746	31
H(37)	6560	1295	3581	31
H(38)	3328	635	2254	29
H(39)	1182	31	2587	29
H(23)	-739	184	3240	48

H(40)	-1254	-626	3792	48
H(22)	-376	-1107	3061	48
H(27)	5254	1868	4898	29
H(25)	4911	994	5954	68
H(26)	4030	1396	6698	68
H(24)	4731	2356	6309	68
H(34)	6070	3245	2399	25
H(35)	4519	2362	1927	25
H(31)	11763	1874	1572	48
H(32)	9544	784	1495	37

Table C.24. Torsion angles [°] for benzyl tetramic acid **2.54** (JLW_118).

C(17)-C(1)-C(2)-C(3)	0.5(4)
C(1)-C(2)-C(3)-C(4)	0.5(4)
C(2)-C(3)-C(4)-C(18)	-1.3(4)
C(2)-C(3)-C(4)-C(5)	180.0(3)
C(3)-C(4)-C(5)-C(6)	-24.3(3)
C(18)-C(4)-C(5)-C(6)	157.0(2)
C(4)-C(5)-C(6)-C(16)	107.2(3)
C(4)-C(5)-C(6)-C(7)	-67.6(3)
C(15)-N(1)-C(7)-O(2)	176.5(2)
C(8)-N(1)-C(7)-O(2)	9.7(4)
C(15)-N(1)-C(7)-C(6)	-3.3(3)
C(8)-N(1)-C(7)-C(6)	-170.1(2)
C(16)-C(6)-C(7)-O(2)	-178.1(2)
C(5)-C(6)-C(7)-O(2)	-2.4(4)
C(16)-C(6)-C(7)-N(1)	1.6(3)
C(5)-C(6)-C(7)-N(1)	177.4(2)
C(7)-N(1)-C(8)-C(9)	89.1(3)
C(15)-N(1)-C(8)-C(9)	-76.1(3)
N(1)-C(8)-C(9)-C(19)	108.1(3)
N(1)-C(8)-C(9)-C(10)	-71.4(3)
C(19)-C(9)-C(10)-C(11)	1.0(4)
C(8)-C(9)-C(10)-C(11)	-179.5(2)
C(14)-N(2)-C(11)-C(10)	-0.9(5)
C(14)-N(2)-C(11)-C(12)	178.8(3)
C(9)-C(10)-C(11)-N(2)	-179.4(3)
C(9)-C(10)-C(11)-C(12)	0.9(4)
C(13)-O(1)-C(12)-C(20)	6.0(4)
C(13)-O(1)-C(12)-C(11)	-174.1(2)
N(2)-C(11)-C(12)-O(1)	-1.7(3)
C(10)-C(11)-C(12)-O(1)	178.1(2)
N(2)-C(11)-C(12)-C(20)	178.3(3)
C(10)-C(11)-C(12)-C(20)	-2.0(4)
C(7)-N(1)-C(15)-C(16)	3.4(3)
C(8)-N(1)-C(15)-C(16)	170.4(2)

C(7)-C(6)-C(16)-O(3)	-179.3(2)
C(5)-C(6)-C(16)-O(3)	5.1(4)
C(7)-C(6)-C(16)-C(15)	0.6(3)
C(5)-C(6)-C(16)-C(15)	-174.9(2)
N(1)-C(15)-C(16)-O(3)	177.6(2)
N(1)-C(15)-C(16)-C(6)	-2.4(3)
C(2)-C(1)-C(17)-C(18)	-0.6(5)
C(1)-C(17)-C(18)-C(4)	-0.2(4)
C(3)-C(4)-C(18)-C(17)	1.1(4)
C(5)-C(4)-C(18)-C(17)	179.9(3)
C(10)-C(9)-C(19)-C(20)	-1.7(4)
C(8)-C(9)-C(19)-C(20)	178.8(2)
O(1)-C(12)-C(20)-C(19)	-178.8(2)
C(11)-C(12)-C(20)-C(19)	1.3(4)
C(9)-C(19)-C(20)-C(12)	0.6(4)
C(39)-C(21)-C(22)-C(23)	-0.2(5)
C(21)-C(22)-C(23)-C(24)	-0.7(4)
C(22)-C(23)-C(24)-C(40)	1.0(4)
C(22)-C(23)-C(24)-C(25)	-179.9(3)
C(23)-C(24)-C(25)-C(26)	-108.8(3)
C(40)-C(24)-C(25)-C(26)	70.4(3)
C(24)-C(25)-C(26)-C(38)	74.6(3)
C(24)-C(25)-C(26)-C(27)	-100.4(3)
C(37)-N(3)-C(27)-O(6)	177.6(2)
C(28)-N(3)-C(27)-O(6)	10.4(4)
C(37)-N(3)-C(27)-C(26)	-2.5(3)
C(28)-N(3)-C(27)-C(26)	-169.7(2)
C(38)-C(26)-C(27)-O(6)	-177.9(2)
C(25)-C(26)-C(27)-O(6)	-2.0(4)
C(38)-C(26)-C(27)-N(3)	2.2(3)
C(25)-C(26)-C(27)-N(3)	178.0(2)
C(27)-N(3)-C(28)-C(29)	-110.8(3)
C(37)-N(3)-C(28)-C(29)	83.5(3)
N(3)-C(28)-C(29)-C(30)	2.3(4)
N(3)-C(28)-C(29)-C(34)	-178.9(2)
C(34)-C(29)-C(30)-C(31)	1.1(4)

C(28)-C(29)-C(30)-C(31)	179.9(2)
C(29)-C(30)-C(31)-C(32)	-1.6(4)
C(33)-O(4)-C(32)-C(31)	-0.6(4)
C(33)-O(4)-C(32)-C(35)	-178.7(2)
C(30)-C(31)-C(32)-O(4)	-178.0(2)
C(30)-C(31)-C(32)-C(35)	0.1(4)
C(30)-C(29)-C(34)-C(35)	1.0(4)
C(28)-C(29)-C(34)-C(35)	-177.9(2)
C(36)-O(5)-C(35)-C(34)	-9.5(4)
C(36)-O(5)-C(35)-C(32)	170.1(3)
C(29)-C(34)-C(35)-O(5)	177.1(3)
C(29)-C(34)-C(35)-C(32)	-2.5(4)
O(4)-C(32)-C(35)-O(5)	0.6(3)
C(31)-C(32)-C(35)-O(5)	-177.6(2)
O(4)-C(32)-C(35)-C(34)	-179.8(2)
C(31)-C(32)-C(35)-C(34)	2.0(4)
C(27)-N(3)-C(37)-C(38)	1.7(3)
C(28)-N(3)-C(37)-C(38)	169.0(2)
C(27)-C(26)-C(38)-O(7)	180.0(2)
C(25)-C(26)-C(38)-O(7)	4.2(4)
C(27)-C(26)-C(38)-C(37)	-1.1(3)
C(25)-C(26)-C(38)-C(37)	-176.9(2)
N(3)-C(37)-C(38)-O(7)	178.7(2)
N(3)-C(37)-C(38)-C(26)	-0.3(3)
C(22)-C(21)-C(39)-C(40)	0.9(4)
C(23)-C(24)-C(40)-C(39)	-0.3(4)
C(25)-C(24)-C(40)-C(39)	-179.5(2)
C(21)-C(39)-C(40)-C(24)	-0.6(4)

Symmetry transformations used to generate equivalent atoms:

Table C.25. Hydrogen bonds for benzyl tetramic acid **2.54** (JLW_118) [Å and °].

D-H...A	d(D-H)	d(H...A)	d(D...A)	∠(DHA)
C(33)-H(40)...O(5)#1	0.98	2.41	3.387(3)	176.8
C(33)-H(23)...O(6)#2	0.98	2.60	3.293(3)	127.6
C(20)-H(18)...O(4)#3	0.95	2.65	3.577(3)	165.7
C(15)-H(10)...O(7)#4	0.99	2.24	3.189(3)	160.7

Symmetry transformations used to generate equivalent atoms:

#1 -x,-y,-z+1 #2 x-1,y,z #3 x,y+1,z #4 -x+1,-y+1,-z

C.4. Crystal analysis of oxime 2.57

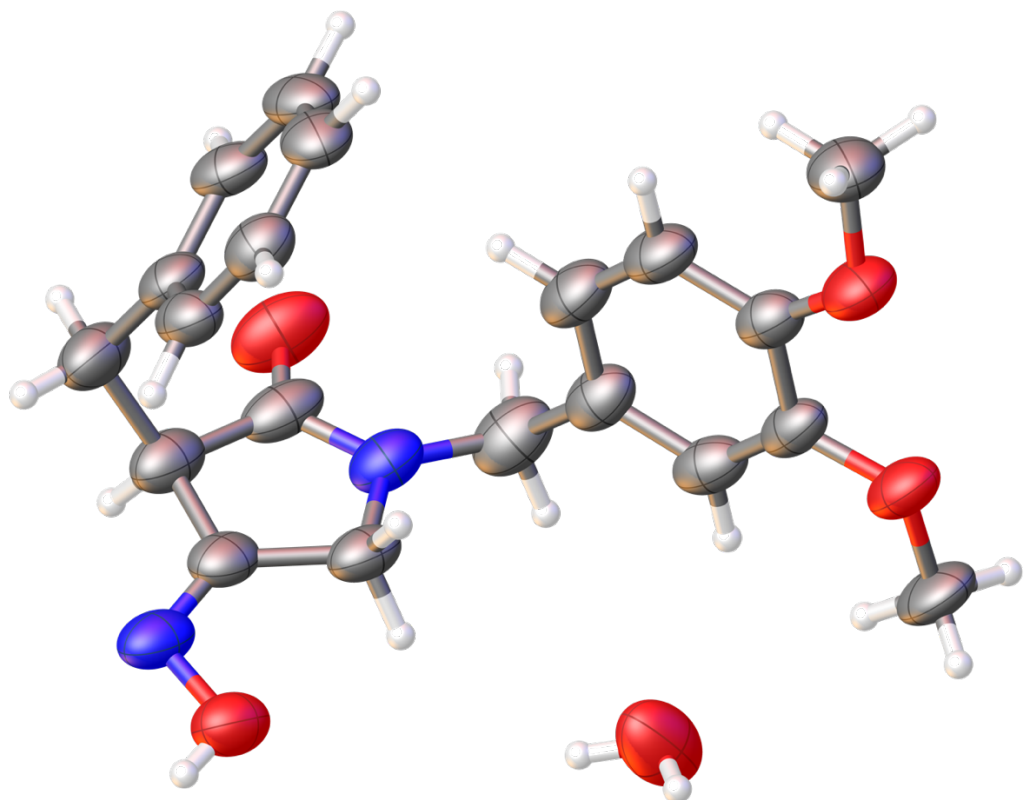


Figure C.04. ORTEP drawing of oxime **2.57**

Table C.26. Crystal data and structure refinement for oxime **2.55** (JLW_114).

Identification code	JLW_114		
Empirical formula	C ₂₀ H ₂₄ N ₂ O ₅		
Formula weight	372.41		
Temperature	150(2) K		
Wavelength	0.71073 Å		
Crystal system	Triclinic		
Space group	P-1		
Unit cell dimensions	a = 7.8846(9) Å	α= 79.976(5)°.	
	b = 8.0923(11) Å	β= 84.100(5)°.	
	c = 15.455(2) Å	γ = 79.637(5)°.	
Volume	952.6(2) Å ³		
Z	2		
Density (calculated)	1.298 Mg/m ³		
Absorption coefficient	0.094 mm ⁻¹		
F(000)	396		
Crystal size	0.187 x 0.092 x 0.053 mm ³		
Theta range for data collection	2.592 to 26.489°.		
Index ranges	-9<=h<=9, -10<=k<=10, -19<=l<=19		
Reflections collected	29067		
Independent reflections	3916 [R(int) = 0.0711]		
Completeness to theta = 25.242°	99.9 %		
Absorption correction	Semi-empirical from equivalents		
Max. and min. transmission	0.861 and 0.851		
Refinement method	Full-matrix least-squares on F ²		
Data / restraints / parameters	3916 / 4 / 255		
Goodness-of-fit on F ²	1.043		
Final R indices [I>2sigma(I)]	R1 = 0.0734, wR2 = 0.1911		
R indices (all data)	R1 = 0.1117, wR2 = 0.2161		
Extinction coefficient	n/a		
Largest diff. peak and hole	0.778 and -0.246 e.Å ⁻³		

Table C.27. Atomic coordinates ($\times 10^4$) and equivalent isotropic displacement parameters ($\text{\AA}^2 \times 10^3$) for oxime **2.55** (JLW_114). U(eq) is defined as one third of the trace of the orthogonalized U^{ij} tensor.

	x	y	z	U(eq)
N(1)	3003(3)	6477(4)	1353(2)	57(1)
N(2)	4480(4)	2447(4)	732(2)	62(1)
O(1)	5423(3)	7647(3)	5001(2)	66(1)
O(2)	7327(3)	8813(3)	3660(2)	62(1)
O(3)	6219(3)	2194(4)	905(2)	69(1)
O(4)	236(3)	7268(4)	942(2)	85(1)
O(5)	7265(4)	9202(5)	392(2)	94(1)
C(1)	599(4)	3284(5)	4162(2)	59(1)
C(2)	-536(4)	4483(5)	3690(2)	62(1)
C(3)	-575(4)	4518(4)	2795(2)	57(1)
C(4)	551(4)	3355(4)	2355(2)	52(1)
C(5)	515(5)	3402(5)	1383(2)	67(1)
C(6)	1809(4)	4429(5)	826(2)	61(1)
C(7)	1568(4)	6221(5)	1030(2)	62(1)
C(8)	3234(5)	8073(5)	1594(3)	72(1)
C(9)	3819(4)	7880(4)	2506(2)	56(1)
C(10)	5340(4)	8427(4)	2634(2)	55(1)
C(11)	5856(4)	8322(4)	3466(2)	52(1)
C(12)	4831(4)	7674(4)	4204(2)	52(1)
C(13)	4290(5)	7227(5)	5758(2)	71(1)
C(14)	8340(5)	9593(5)	2935(3)	73(1)
C(15)	4413(4)	5058(4)	1380(2)	56(1)
C(16)	3680(4)	3810(5)	978(2)	54(1)
C(17)	1707(4)	2111(4)	3747(2)	57(1)
C(18)	1700(4)	2158(4)	2848(2)	54(1)
C(19)	2849(4)	7209(4)	3228(3)	62(1)
C(20)	3342(4)	7111(4)	4073(2)	60(1)

Table C.28. Bond lengths [\AA] and angles [$^\circ$] for oxime **2.55** (JLW_114).

N(1)-C(7)	1.345(4)
N(1)-C(15)	1.446(4)
N(1)-C(8)	1.451(5)
N(2)-C(16)	1.268(5)
N(2)-O(3)	1.396(4)
O(1)-C(12)	1.356(4)
O(1)-C(13)	1.429(4)
O(2)-C(11)	1.368(4)
O(2)-C(14)	1.429(4)
O(3)-H(3A)	0.95(4)
O(4)-C(7)	1.228(4)
O(5)-H(2A)	0.88(2)
O(5)-H(1A)	0.881(19)
C(1)-C(2)	1.360(5)
C(1)-C(17)	1.369(5)
C(1)-H(1)	0.9500
C(2)-C(3)	1.381(5)
C(2)-H(12)	0.9500
C(3)-C(4)	1.391(5)
C(3)-H(15)	0.9500
C(4)-C(18)	1.382(5)
C(4)-C(5)	1.499(5)
C(5)-C(6)	1.532(5)
C(5)-H(16)	0.9900
C(5)-H(11)	0.9900
C(6)-C(16)	1.499(5)
C(6)-C(7)	1.512(6)
C(6)-H(10)	1.0000
C(8)-C(9)	1.502(5)
C(8)-H(18)	0.9900
C(8)-H(17)	0.9900
C(9)-C(19)	1.374(5)
C(9)-C(10)	1.394(4)
C(10)-C(11)	1.372(5)

C(10)-H(21)	0.9500
C(11)-C(12)	1.408(4)
C(12)-C(20)	1.378(5)
C(13)-H(3)	0.9800
C(13)-H(2)	0.9800
C(13)-H(4)	0.9800
C(14)-H(6)	0.9800
C(14)-H(5)	0.9800
C(14)-H(7)	0.9800
C(15)-C(16)	1.498(5)
C(15)-H(9)	0.9900
C(15)-H(8)	0.9900
C(17)-C(18)	1.384(5)
C(17)-H(14)	0.9500
C(18)-H(13)	0.9500
C(19)-C(20)	1.385(5)
C(19)-H(19)	0.9500
C(20)-H(20)	0.9500

C(7)-N(1)-C(15)	114.7(3)
C(7)-N(1)-C(8)	124.6(3)
C(15)-N(1)-C(8)	120.5(3)
C(16)-N(2)-O(3)	110.5(3)
C(12)-O(1)-C(13)	116.8(3)
C(11)-O(2)-C(14)	116.6(3)
N(2)-O(3)-H(3A)	103(3)
H(2A)-O(5)-H(1A)	123(5)
C(2)-C(1)-C(17)	119.7(3)
C(2)-C(1)-H(1)	120.1
C(17)-C(1)-H(1)	120.1
C(1)-C(2)-C(3)	120.3(3)
C(1)-C(2)-H(12)	119.9
C(3)-C(2)-H(12)	119.9
C(2)-C(3)-C(4)	121.2(3)
C(2)-C(3)-H(15)	119.4
C(4)-C(3)-H(15)	119.4

C(18)-C(4)-C(3)	117.5(3)
C(18)-C(4)-C(5)	121.4(3)
C(3)-C(4)-C(5)	121.1(3)
C(4)-C(5)-C(6)	113.6(3)
C(4)-C(5)-H(16)	108.8
C(6)-C(5)-H(16)	108.8
C(4)-C(5)-H(11)	108.8
C(6)-C(5)-H(11)	108.8
H(16)-C(5)-H(11)	107.7
C(16)-C(6)-C(7)	101.6(3)
C(16)-C(6)-C(5)	116.3(3)
C(7)-C(6)-C(5)	111.7(3)
C(16)-C(6)-H(10)	109.0
C(7)-C(6)-H(10)	109.0
C(5)-C(6)-H(10)	109.0
O(4)-C(7)-N(1)	125.0(4)
O(4)-C(7)-C(6)	124.9(3)
N(1)-C(7)-C(6)	110.0(3)
N(1)-C(8)-C(9)	113.2(3)
N(1)-C(8)-H(18)	108.9
C(9)-C(8)-H(18)	108.9
N(1)-C(8)-H(17)	108.9
C(9)-C(8)-H(17)	108.9
H(18)-C(8)-H(17)	107.7
C(19)-C(9)-C(10)	118.8(3)
C(19)-C(9)-C(8)	120.9(3)
C(10)-C(9)-C(8)	120.2(3)
C(11)-C(10)-C(9)	120.9(3)
C(11)-C(10)-H(21)	119.5
C(9)-C(10)-H(21)	119.5
O(2)-C(11)-C(10)	125.3(3)
O(2)-C(11)-C(12)	114.8(3)
C(10)-C(11)-C(12)	119.9(3)
O(1)-C(12)-C(20)	125.2(3)
O(1)-C(12)-C(11)	115.8(3)
C(20)-C(12)-C(11)	119.0(3)

O(1)-C(13)-H(3)	109.5
O(1)-C(13)-H(2)	109.5
H(3)-C(13)-H(2)	109.5
O(1)-C(13)-H(4)	109.5
H(3)-C(13)-H(4)	109.5
H(2)-C(13)-H(4)	109.5
O(2)-C(14)-H(6)	109.5
O(2)-C(14)-H(5)	109.5
H(6)-C(14)-H(5)	109.5
O(2)-C(14)-H(7)	109.5
H(6)-C(14)-H(7)	109.5
H(5)-C(14)-H(7)	109.5
N(1)-C(15)-C(16)	102.0(3)
N(1)-C(15)-H(9)	111.4
C(16)-C(15)-H(9)	111.4
N(1)-C(15)-H(8)	111.4
C(16)-C(15)-H(8)	111.4
H(9)-C(15)-H(8)	109.2
N(2)-C(16)-C(15)	127.5(3)
N(2)-C(16)-C(6)	121.4(3)
C(15)-C(16)-C(6)	111.0(3)
C(1)-C(17)-C(18)	120.4(3)
C(1)-C(17)-H(14)	119.8
C(18)-C(17)-H(14)	119.8
C(4)-C(18)-C(17)	120.9(3)
C(4)-C(18)-H(13)	119.5
C(17)-C(18)-H(13)	119.5
C(9)-C(19)-C(20)	121.0(3)
C(9)-C(19)-H(19)	119.5
C(20)-C(19)-H(19)	119.5
C(12)-C(20)-C(19)	120.4(3)
C(12)-C(20)-H(20)	119.8
C(19)-C(20)-H(20)	119.8

Symmetry transformations used to generate equivalent atoms.

Table C.29. Anisotropic displacement parameters ($\text{\AA}^2 \times 10^3$) for oxime **2.55** (JLW_114). The anisotropic displacement factor exponent takes the form: $-2p^2[h^2 a^*{}^2 U^{11} + \dots + 2h k a^* b^* U^{12}]$.

	U ¹¹	U ²²	U ³³	U ²³	U ¹³	U ¹²
N(1)	46(2)	62(2)	58(2)	6(1)	0(1)	-16(1)
N(2)	48(2)	91(2)	45(2)	-4(1)	5(1)	-18(2)
O(1)	55(1)	73(2)	70(2)	-7(1)	12(1)	-26(1)
O(2)	45(1)	61(1)	78(2)	-6(1)	9(1)	-20(1)
O(3)	52(1)	91(2)	64(2)	-16(1)	3(1)	-13(1)
O(4)	55(2)	92(2)	94(2)	21(2)	-13(1)	-6(1)
O(5)	78(2)	116(3)	90(2)	-41(2)	-28(2)	13(2)
C(1)	59(2)	66(2)	53(2)	-6(2)	16(2)	-25(2)
C(2)	54(2)	57(2)	71(2)	-10(2)	26(2)	-18(2)
C(3)	40(2)	58(2)	68(2)	2(2)	12(2)	-14(2)
C(4)	39(2)	58(2)	60(2)	-4(2)	6(1)	-19(1)
C(5)	50(2)	92(3)	62(2)	-8(2)	-1(2)	-27(2)
C(6)	49(2)	86(3)	48(2)	-1(2)	-2(1)	-20(2)
C(7)	43(2)	85(3)	51(2)	15(2)	0(1)	-19(2)
C(8)	63(2)	63(2)	83(3)	13(2)	-7(2)	-20(2)
C(9)	48(2)	44(2)	73(2)	1(2)	0(2)	-13(1)
C(10)	45(2)	43(2)	70(2)	2(2)	10(2)	-8(1)
C(11)	38(2)	39(2)	76(2)	-5(2)	6(2)	-10(1)
C(12)	44(2)	45(2)	63(2)	-4(1)	6(2)	-9(1)
C(13)	70(2)	79(3)	65(2)	-10(2)	18(2)	-28(2)
C(14)	51(2)	79(3)	91(3)	-7(2)	20(2)	-34(2)
C(15)	42(2)	75(2)	50(2)	-2(2)	6(1)	-16(2)
C(16)	48(2)	72(2)	40(2)	-4(2)	9(1)	-17(2)
C(17)	51(2)	54(2)	65(2)	1(2)	-2(2)	-16(2)
C(18)	45(2)	51(2)	64(2)	-11(2)	11(2)	-13(1)
C(19)	50(2)	57(2)	80(3)	-1(2)	3(2)	-21(2)
C(20)	48(2)	58(2)	72(2)	-4(2)	13(2)	-19(2)

C.5. Crystal analysis of oxime 2.63

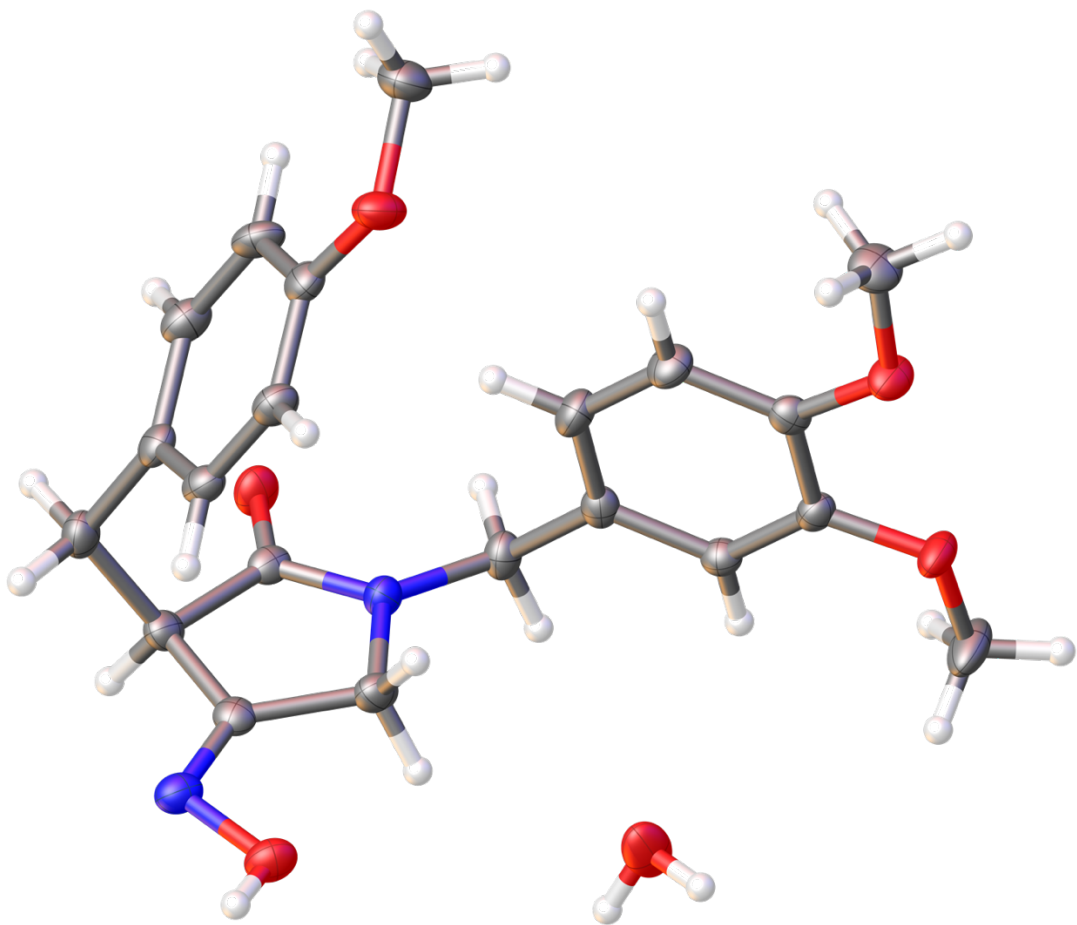


Figure C.05. ORTEP drawing of oxime 2.63

Table C.30. Crystal data and structure refinement for oxime **2.60** (JLW_110).

Identification code	JLW_110_a		
Empirical formula	C21 H24 N2 O5		
Formula weight	384.42		
Temperature	293(2) K		
Wavelength	0.71073 Å		
Crystal system	Monoclinic		
Space group	Pc		
Unit cell dimensions	a = 7.818(10) Å	α= 90°.	
	b = 16.517(17) Å	β= 102.11(4)°.	
	c = 8.041(8) Å	γ = 90°.	
Volume	1015.3(19) Å ³		
Z	2		
Density (calculated)	1.257 Mg/m ³		
Absorption coefficient	0.090 mm ⁻¹		
F(000)	408		
Crystal size	0.259 x 0.067 x 0.032 mm ³		
Theta range for data collection	2.466 to 25.681°.		
Index ranges	-9<=h<=8, -20<=k<=20, -9<=l<=9		
Reflections collected	18855		
Independent reflections	3675 [R(int) = 0.0598]		
Completeness to theta = 25.242°	99.7 %		
Refinement method	Full-matrix least-squares on F ²		
Data / restraints / parameters	3675 / 2 / 277		
Goodness-of-fit on F ²	1.634		
Final R indices [I>2sigma(I)]	R1 = 0.0395, wR2 = 0.0467		
R indices (all data)	R1 = 0.0558, wR2 = 0.0483		
Absolute structure parameter	0.2(5)		
Extinction coefficient	n/a		
Largest diff. peak and hole	0.177 and -0.157 e.Å ⁻³		

Table C.31. Atomic coordinates ($x \times 10^4$) and equivalent isotropic displacement parameters ($\text{\AA}^2 \times 10^3$) for oxime **2.60** (JLW_110). U(eq) is defined as one third of the trace of the orthogonalized U^{ij} tensor.

	x	y	z	U(eq)
O(6)	746(4)	485(2)	7510(4)	38(1)
O(1)	6284(3)	4560(1)	2788(3)	29(1)
O(2)	7539(3)	960(1)	6636(3)	26(1)
O(3)	1895(3)	821(1)	799(3)	27(1)
O(4)	-89(3)	3387(1)	8422(3)	27(1)
O(5)	1142(3)	4633(1)	7181(3)	25(1)
N(1)	4781(3)	1324(1)	5595(3)	19(1)
N(2)	3669(3)	616(1)	1209(3)	24(1)
C(1)	7451(4)	5085(2)	3902(4)	34(1)
C(2)	6654(4)	3749(2)	2816(4)	21(1)
C(3)	8036(4)	3396(2)	3923(4)	25(1)
C(4)	8269(4)	2568(2)	3864(4)	26(1)
C(5)	7159(4)	2076(2)	2701(4)	21(1)
C(6)	5795(4)	2454(2)	1601(4)	20(1)
C(7)	5548(4)	3274(2)	1645(4)	22(1)
C(8)	7396(4)	1169(2)	2683(4)	24(1)
C(9)	6153(4)	701(2)	3585(4)	20(1)
C(10)	4308(4)	827(2)	2762(4)	18(1)
C(11)	3426(4)	1242(2)	4035(4)	23(1)
C(12)	6275(4)	993(2)	5426(4)	19(1)
C(13)	4455(4)	1604(2)	7243(4)	22(1)
C(14)	3602(3)	2423(2)	7124(4)	19(1)
C(15)	2132(4)	2503(2)	7789(4)	18(1)
C(16)	1345(4)	3249(2)	7791(4)	18(1)
C(17)	2033(4)	3923(2)	7123(4)	18(1)
C(18)	3474(4)	3843(2)	6447(4)	24(1)
C(19)	4251(4)	3087(2)	6446(4)	23(1)
C(20)	-763(4)	2716(2)	9227(5)	42(1)
C(21)	1898(4)	5365(2)	6719(4)	33(1)

Table C.32. Bond lengths [\AA] and angles [$^\circ$] for oxime **2.60** (JLW_110).

O(6)-H(7A)	0.72(3)
O(6)-H(6B)	0.84(7)
O(1)-C(2)	1.370(4)
O(1)-C(1)	1.429(3)
O(2)-C(12)	1.234(4)
O(3)-N(2)	1.399(3)
O(3)-H(3A)	0.96(3)
O(4)-C(16)	1.343(4)
O(4)-C(20)	1.438(3)
O(5)-C(17)	1.368(3)
O(5)-C(21)	1.429(3)
N(1)-C(12)	1.323(4)
N(1)-C(11)	1.469(4)
N(1)-C(13)	1.475(4)
N(2)-C(10)	1.292(4)
C(1)-H(1A)	0.9600
C(1)-H(1B)	0.9600
C(1)-H(1C)	0.9600
C(2)-C(3)	1.377(4)
C(2)-C(7)	1.382(4)
C(3)-C(4)	1.383(4)
C(3)-H(3)	0.9300
C(4)-C(5)	1.395(4)
C(4)-H(4)	0.9300
C(5)-C(6)	1.384(4)
C(5)-C(8)	1.509(4)
C(6)-C(7)	1.369(4)
C(6)-H(6)	0.9300
C(7)-H(7)	0.9300
C(8)-C(9)	1.537(4)
C(8)-H(8A)	0.9700
C(8)-H(8B)	0.9700
C(9)-C(10)	1.470(4)
C(9)-C(12)	1.540(4)

C(9)-H(9)	0.9800
C(10)-C(11)	1.513(4)
C(11)-H(11A)	0.9700
C(11)-H(11B)	0.9700
C(13)-C(14)	1.503(4)
C(13)-H(13A)	0.9700
C(13)-H(13B)	0.9700
C(14)-C(19)	1.369(4)
C(14)-C(15)	1.371(4)
C(15)-C(16)	1.378(4)
C(15)-H(15)	0.9300
C(16)-C(17)	1.393(4)
C(17)-C(18)	1.356(4)
C(18)-C(19)	1.390(4)
C(18)-H(18)	0.9300
C(19)-H(19)	0.9300
C(20)-H(20A)	0.9600
C(20)-H(20B)	0.9600
C(20)-H(20C)	0.9600
C(21)-H(21A)	0.9600
C(21)-H(21B)	0.9600
C(21)-H(21C)	0.9600
H(7A)-O(6)-H(6B)	116(5)
C(2)-O(1)-C(1)	118.6(2)
N(2)-O(3)-H(3A)	108.0(19)
C(16)-O(4)-C(20)	117.0(2)
C(17)-O(5)-C(21)	118.3(2)
C(12)-N(1)-C(11)	111.6(3)
C(12)-N(1)-C(13)	123.0(2)
C(11)-N(1)-C(13)	124.5(2)
C(10)-N(2)-O(3)	109.0(2)
O(1)-C(1)-H(1A)	109.5
O(1)-C(1)-H(1B)	109.5
H(1A)-C(1)-H(1B)	109.5
O(1)-C(1)-H(1C)	109.5

H(1A)-C(1)-H(1C)	109.5
H(1B)-C(1)-H(1C)	109.5
O(1)-C(2)-C(3)	124.0(3)
O(1)-C(2)-C(7)	116.4(3)
C(3)-C(2)-C(7)	119.6(3)
C(2)-C(3)-C(4)	119.2(3)
C(2)-C(3)-H(3)	120.4
C(4)-C(3)-H(3)	120.4
C(3)-C(4)-C(5)	122.1(3)
C(3)-C(4)-H(4)	118.9
C(5)-C(4)-H(4)	118.9
C(6)-C(5)-C(4)	116.9(3)
C(6)-C(5)-C(8)	121.4(3)
C(4)-C(5)-C(8)	121.6(3)
C(7)-C(6)-C(5)	121.6(3)
C(7)-C(6)-H(6)	119.2
C(5)-C(6)-H(6)	119.2
C(6)-C(7)-C(2)	120.5(3)
C(6)-C(7)-H(7)	119.7
C(2)-C(7)-H(7)	119.7
C(5)-C(8)-C(9)	113.8(2)
C(5)-C(8)-H(8A)	108.8
C(9)-C(8)-H(8A)	108.8
C(5)-C(8)-H(8B)	108.8
C(9)-C(8)-H(8B)	108.8
H(8A)-C(8)-H(8B)	107.7
C(10)-C(9)-C(8)	111.9(3)
C(10)-C(9)-C(12)	104.2(3)
C(8)-C(9)-C(12)	112.2(2)
C(10)-C(9)-H(9)	109.4
C(8)-C(9)-H(9)	109.4
C(12)-C(9)-H(9)	109.4
N(2)-C(10)-C(9)	122.7(3)
N(2)-C(10)-C(11)	129.6(3)
C(9)-C(10)-C(11)	107.6(3)
N(1)-C(11)-C(10)	105.7(2)

N(1)-C(11)-H(11A)	110.6
C(10)-C(11)-H(11A)	110.6
N(1)-C(11)-H(11B)	110.6
C(10)-C(11)-H(11B)	110.6
H(11A)-C(11)-H(11B)	108.7
O(2)-C(12)-N(1)	121.0(3)
O(2)-C(12)-C(9)	128.5(3)
N(1)-C(12)-C(9)	110.5(3)
N(1)-C(13)-C(14)	112.5(3)
N(1)-C(13)-H(13A)	109.1
C(14)-C(13)-H(13A)	109.1
N(1)-C(13)-H(13B)	109.1
C(14)-C(13)-H(13B)	109.1
H(13A)-C(13)-H(13B)	107.8
C(19)-C(14)-C(15)	119.3(3)
C(19)-C(14)-C(13)	123.3(3)
C(15)-C(14)-C(13)	117.3(3)
C(16)-C(15)-C(14)	119.8(3)
C(16)-C(15)-H(15)	120.1
C(14)-C(15)-H(15)	120.1
O(4)-C(16)-C(15)	124.1(3)
O(4)-C(16)-C(17)	115.5(3)
C(15)-C(16)-C(17)	120.4(3)
C(18)-C(17)-O(5)	124.7(3)
C(18)-C(17)-C(16)	119.8(3)
O(5)-C(17)-C(16)	115.5(3)
C(17)-C(18)-C(19)	119.2(3)
C(17)-C(18)-H(18)	120.4
C(19)-C(18)-H(18)	120.4
C(14)-C(19)-C(18)	121.4(3)
C(14)-C(19)-H(19)	119.3
C(18)-C(19)-H(19)	119.3
O(4)-C(20)-H(20A)	109.5
O(4)-C(20)-H(20B)	109.5
H(20A)-C(20)-H(20B)	109.5
O(4)-C(20)-H(20C)	109.5

H(20A)-C(20)-H(20C)	109.5
H(20B)-C(20)-H(20C)	109.5
O(5)-C(21)-H(21A)	109.5
O(5)-C(21)-H(21B)	109.5
H(21A)-C(21)-H(21B)	109.5
O(5)-C(21)-H(21C)	109.5
H(21A)-C(21)-H(21C)	109.5
H(21B)-C(21)-H(21C)	109.5

Symmetry transformations used to generate equivalent atoms.

Table C.33. Anisotropic displacement parameters ($\text{\AA}^2 \times 10^3$) for oxime **2.60** (JLW_110). The anisotropic displacement factor exponent takes the form: $-2p^2[h^2 a^*{}^2 U^{11} + \dots + 2h k a^* b^* U^{12}]$.

	U ¹¹	U ²²	U ³³	U ²³	U ¹³	U ¹²
O(6)	23(2)	45(2)	41(2)	-18(2)	-5(1)	9(1)
O(1)	22(1)	22(1)	41(2)	-5(1)	1(1)	-5(1)
O(2)	17(1)	31(1)	28(1)	-1(1)	0(1)	7(1)
O(3)	19(1)	31(1)	28(2)	2(1)	-1(1)	-2(1)
O(4)	21(1)	20(1)	44(2)	4(1)	17(1)	0(1)
O(5)	24(1)	15(1)	39(2)	4(1)	10(1)	0(1)
N(1)	16(1)	22(2)	20(2)	-1(1)	4(1)	1(1)
N(2)	17(2)	22(2)	32(2)	2(1)	2(1)	-1(1)
C(1)	31(2)	26(2)	46(3)	-10(2)	6(2)	-7(2)
C(2)	18(2)	23(2)	24(2)	0(2)	8(2)	-3(2)
C(3)	19(2)	30(2)	25(2)	0(2)	-1(2)	-8(2)
C(4)	18(2)	29(2)	31(2)	6(2)	4(2)	-1(2)
C(5)	19(2)	23(2)	22(2)	2(2)	9(2)	0(2)
C(6)	16(2)	27(2)	18(2)	0(2)	4(2)	-3(2)
C(7)	16(2)	26(2)	23(2)	1(2)	2(2)	-2(2)
C(8)	18(2)	27(2)	29(2)	-2(2)	7(2)	4(2)
C(9)	19(2)	15(2)	26(2)	-2(2)	5(2)	2(1)
C(10)	22(2)	13(2)	21(2)	0(2)	5(2)	-2(2)
C(11)	16(2)	22(2)	29(2)	-2(2)	2(2)	-3(1)
C(12)	17(2)	13(2)	26(2)	4(2)	4(2)	2(1)
C(13)	18(2)	27(2)	22(2)	-2(2)	6(2)	4(2)
C(14)	17(2)	23(2)	16(2)	-3(2)	1(2)	3(1)
C(15)	17(2)	18(2)	20(2)	2(2)	3(1)	-1(1)
C(16)	16(2)	21(2)	19(2)	1(2)	5(2)	0(1)
C(17)	17(2)	18(2)	19(2)	-1(2)	1(2)	1(2)
C(18)	24(2)	23(2)	27(2)	5(2)	10(2)	-4(2)
C(19)	17(2)	28(2)	28(2)	3(2)	11(2)	1(2)
C(20)	34(2)	30(2)	73(3)	6(2)	36(2)	1(2)
C(21)	37(2)	17(2)	45(3)	6(2)	10(2)	1(2)

Table C.34. Hydrogen coordinates ($x \times 10^4$) and isotropic displacement parameters ($\text{\AA}^2 \times 10^3$) for oxime **2.60** (JLW_110).

	x	y	z	U(eq)
H(1A)	7539	4913	5057	51
H(1B)	7011	5629	3773	51
H(1C)	8585	5066	3623	51
H(3)	8803	3712	4701	30
H(4)	9196	2331	4623	32
H(6)	5028	2144	813	24
H(7)	4628	3512	881	26
H(8A)	8593	1040	3226	29
H(8B)	7210	988	1511	29
H(9)	6428	122	3589	24
H(11A)	2986	1769	3618	27
H(11B)	2457	918	4245	27
H(13A)	5557	1626	8064	27
H(13B)	3709	1215	7652	27
H(15)	1668	2054	8236	22
H(18)	3936	4289	5988	28
H(19)	5234	3030	5974	28
H(20A)	-1138	2297	8405	63
H(20B)	-1739	2894	9686	63
H(20C)	136	2510	10129	63
H(21A)	3062	5423	7390	49
H(21B)	1198	5817	6920	49
H(21C)	1943	5346	5535	49
H(3A)	1460(40)	698(18)	-380(50)	40(11)
H(7A)	950(50)	150(20)	7030(50)	31(13)
H(6B)	-310(90)	640(40)	7280(90)	210(40)

C.6. Crystal analysis of NDA adduct 3.46

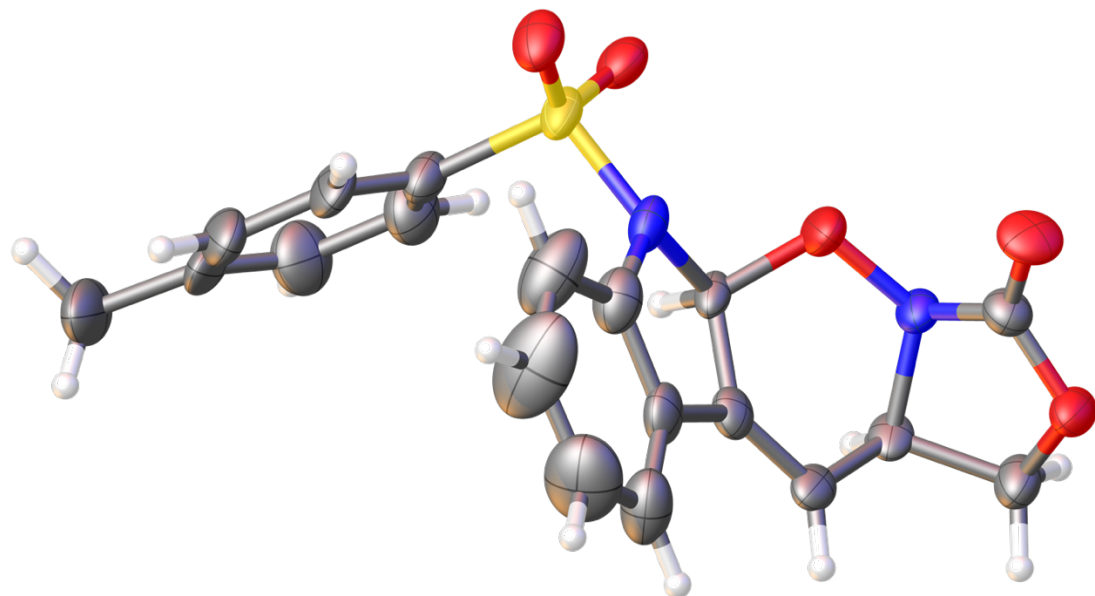


Figure C.06. ORTEP drawing of NDA adduct **3.46**

Table C.35. Crystal data and structure refinement for NDA adduct **3.46** (JLW_143).

Identification code	JLW_143		
Empirical formula	C42 H40 N7 O12 S2		
Formula weight	898.93		
Temperature	150(2) K		
Wavelength	0.71073 Å		
Crystal system	Monoclinic		
Space group	C2/c		
Unit cell dimensions	a = 23.903(5) Å	α= 90°.	
	b = 18.530(3) Å	β= 113.312(7)°.	
	c = 10.7498(15) Å	γ = 90°.	
Volume	4372.5(13) Å ³		
Z	4		
Density (calculated)	1.366 Mg/m ³		
Absorption coefficient	0.192 mm ⁻¹		
F(000)	1876		
Crystal size	0.160 x 0.146 x 0.070 mm ³		
Theta range for data collection	2.193 to 26.371°.		
Index ranges	-29<=h<=29, -23<=k<=23, -13<=l<=13		
Reflections collected	42836		
Independent reflections	4469 [R(int) = 0.1127]		
Completeness to theta = 25.242°	99.8 %		
Absorption correction	None		
Refinement method	Full-matrix least-squares on F ²		
Data / restraints / parameters	4469 / 0 / 245		
Goodness-of-fit on F ²	10.754		
Final R indices [I>2sigma(I)]	R1 = 0.2995, wR2 = 0.5515		
R indices (all data)	R1 = 0.3222, wR2 = 0.5546		
Extinction coefficient	n/a		
Largest diff. peak and hole	5.750 and -1.293 e.Å ⁻³		

Table C.36. Atomic coordinates ($\times 10^4$) and equivalent isotropic displacement parameters ($\text{\AA}^2 \times 10^3$) for NDA adduct **3.46** (JLW_143). U(eq) is defined as one third of the trace of the orthogonalized U_{ij}^{ij} tensor.

	x	y	z	U(eq)
S(1)	3565(2)	3137(2)	2047(4)	29(1)
O(1)	4267(6)	4724(6)	3088(13)	37(3)
O(2)	4378(6)	6578(6)	3388(11)	35(3)
O(3)	4254(6)	5868(6)	1531(11)	35(3)
O(4)	4224(6)	3118(6)	2650(11)	35(3)
O(5)	3221(6)	2910(7)	657(11)	41(4)
N(1)	3354(6)	3996(6)	2097(12)	20(3)
N(2)	4471(6)	5382(7)	3692(12)	18(3)
C(1)	2597(13)	1315(12)	5390(30)	83(10)
C(2)	2843(10)	1770(9)	4580(20)	39(5)
C(3)	2515(11)	1899(11)	3340(20)	53(7)
C(4)	2719(10)	2294(10)	2500(20)	46(6)
C(5)	3269(8)	2615(9)	3039(18)	28(4)
C(6)	3761(8)	4425(8)	3292(15)	22(4)
C(7)	4301(8)	5623(9)	4808(15)	27(4)
C(8)	4525(9)	6389(10)	4865(16)	39(5)
C(9)	4363(9)	5912(10)	2719(17)	32(5)
C(10)	3310(9)	4997(9)	3359(17)	30(5)
C(11)	3561(9)	5550(9)	4173(16)	30(5)
C(12)	2725(8)	4784(9)	2448(16)	23(4)
C(13)	2747(8)	4213(11)	1693(16)	32(5)
C(14)	3378(11)	2048(11)	5100(20)	53(6)
C(15)	3600(11)	2479(11)	4360(20)	56(7)
C(16)	2297(11)	3900(15)	780(30)	89(9)
C(17)	1790(20)	4170(20)	540(30)	149(17)
C(18)	1721(13)	4759(17)	1240(30)	79(8)
C(19)	2176(12)	5098(14)	2130(20)	62(7)

Table C.37. Bond lengths [\AA] and angles [$^\circ$] for NDA adduct **3.46** (JLW_143).

S(1)-O(5)	1.454(12)
S(1)-O(4)	1.446(14)
S(1)-N(1)	1.678(13)
S(1)-C(5)	1.780(16)
O(1)-N(2)	1.377(16)
O(1)-C(6)	1.424(18)
O(2)-C(9)	1.42(2)
O(2)-C(8)	1.526(18)
O(3)-C(9)	1.201(18)
N(1)-C(13)	1.40(2)
N(1)-C(6)	1.50(2)
N(2)-C(9)	1.38(2)
N(2)-C(7)	1.480(17)
C(1)-C(2)	1.49(2)
C(1)-H(7)	0.9800
C(1)-H(8)	0.9800
C(1)-H(1)	0.9800
C(2)-C(3)	1.28(3)
C(2)-C(14)	1.28(3)
C(3)-C(4)	1.39(3)
C(3)-H(9)	0.9500
C(4)-C(5)	1.35(3)
C(4)-H(10)	0.9500
C(5)-C(15)	1.35(3)
C(6)-C(10)	1.53(2)
C(6)-H(15)	1.0000
C(7)-C(8)	1.51(2)
C(7)-C(11)	1.63(2)
C(7)-H(16)	1.0000
C(8)-H(2)	0.9900
C(8)-H(3)	0.9900
C(10)-C(11)	1.33(2)
C(10)-C(12)	1.41(2)
C(11)-H(4)	0.9500

C(12)-C(13)	1.35(2)
C(12)-C(19)	1.35(3)
C(13)-C(16)	1.27(3)
C(14)-C(15)	1.37(2)
C(14)-H(5)	0.9500
C(15)-H(6)	0.9500
C(16)-C(17)	1.24(5)
C(16)-H(14)	0.9500
C(17)-C(18)	1.36(4)
C(17)-H(13)	0.9500
C(18)-C(19)	1.29(3)
C(18)-H(11)	0.9500
C(19)-H(12)	0.9500
O(5)-S(1)-O(4)	121.8(7)
O(5)-S(1)-N(1)	104.6(7)
O(4)-S(1)-N(1)	107.2(7)
O(5)-S(1)-C(5)	105.1(8)
O(4)-S(1)-C(5)	109.9(8)
N(1)-S(1)-C(5)	107.5(7)
N(2)-O(1)-C(6)	115.9(10)
C(9)-O(2)-C(8)	106.0(12)
C(13)-N(1)-C(6)	110.8(13)
C(13)-N(1)-S(1)	123.5(12)
C(6)-N(1)-S(1)	115.5(11)
C(9)-N(2)-O(1)	110.3(12)
C(9)-N(2)-C(7)	111.7(13)
O(1)-N(2)-C(7)	119.3(11)
C(2)-C(1)-H(7)	109.6
C(2)-C(1)-H(8)	109.5
H(7)-C(1)-H(8)	109.5
C(2)-C(1)-H(1)	109.4
H(7)-C(1)-H(1)	109.5
H(8)-C(1)-H(1)	109.5
C(3)-C(2)-C(14)	118.1(18)
C(3)-C(2)-C(1)	120(2)

C(14)-C(2)-C(1)	122(2)
C(2)-C(3)-C(4)	123(2)
C(2)-C(3)-H(9)	118.4
C(4)-C(3)-H(9)	118.3
C(5)-C(4)-C(3)	119(2)
C(5)-C(4)-H(10)	120.5
C(3)-C(4)-H(10)	120.4
C(15)-C(5)-C(4)	116.0(18)
C(15)-C(5)-S(1)	121.7(16)
C(4)-C(5)-S(1)	122.2(16)
O(1)-C(6)-N(1)	112.1(11)
O(1)-C(6)-C(10)	113.2(12)
N(1)-C(6)-C(10)	100.2(14)
O(1)-C(6)-H(15)	110.4
N(1)-C(6)-H(15)	110.1
C(10)-C(6)-H(15)	110.3
N(2)-C(7)-C(8)	96.3(11)
N(2)-C(7)-C(11)	103.7(12)
C(8)-C(7)-C(11)	113.8(15)
N(2)-C(7)-H(16)	113.8
C(8)-C(7)-H(16)	113.7
C(11)-C(7)-H(16)	113.8
O(2)-C(8)-C(7)	104.0(12)
O(2)-C(8)-H(2)	110.9
C(7)-C(8)-H(2)	111.0
O(2)-C(8)-H(3)	111.0
C(7)-C(8)-H(3)	110.9
H(2)-C(8)-H(3)	109.0
O(3)-C(9)-O(2)	123.2(15)
O(3)-C(9)-N(2)	130.8(17)
O(2)-C(9)-N(2)	106.0(12)
C(11)-C(10)-C(12)	137.7(18)
C(11)-C(10)-C(6)	114.9(18)
C(12)-C(10)-C(6)	107.2(15)
C(10)-C(11)-C(7)	118.2(16)
C(10)-C(11)-H(4)	121.0

C(7)-C(11)-H(4)	120.7
C(13)-C(12)-C(19)	116.8(18)
C(13)-C(12)-C(10)	112.0(16)
C(19)-C(12)-C(10)	130.8(19)
C(12)-C(13)-C(16)	127(2)
C(12)-C(13)-N(1)	108.8(15)
C(16)-C(13)-N(1)	124.4(19)
C(2)-C(14)-C(15)	122(2)
C(2)-C(14)-H(5)	119.0
C(15)-C(14)-H(5)	118.9
C(5)-C(15)-C(14)	121(2)
C(5)-C(15)-H(6)	119.3
C(14)-C(15)-H(6)	119.5
C(13)-C(16)-C(17)	116(3)
C(13)-C(16)-H(14)	122.8
C(17)-C(16)-H(14)	121.5
C(18)-C(17)-C(16)	122(3)
C(18)-C(17)-H(13)	117.5
C(16)-C(17)-H(13)	120.5
C(19)-C(18)-C(17)	123(3)
C(19)-C(18)-H(11)	117.0
C(17)-C(18)-H(11)	120.0
C(18)-C(19)-C(12)	115(3)
C(18)-C(19)-H(12)	122.9
C(12)-C(19)-H(12)	121.9

Symmetry transformations used to generate equivalent atoms.

Table C.38. Anisotropic displacement parameters ($\text{\AA}^2 \times 10^3$) for NDA adduct **3.46** (JLW_143). The anisotropic displacement factor exponent takes the form: $-2p^2 [h^2 a^* U^{11} + \dots + 2 h k a^* b^* U^{12}]$.

	U ¹¹	U ²²	U ³³	U ²³	U ¹³	U ¹²
S(1)	51(4)	21(2)	17(2)	-8(2)	18(2)	-16(2)
O(1)	55(9)	17(7)	57(9)	-22(6)	43(7)	-16(6)
O(2)	72(10)	18(6)	33(7)	-10(5)	40(7)	-20(6)
O(3)	69(10)	30(7)	18(7)	-6(5)	29(6)	-12(7)
O(4)	68(10)	26(7)	18(6)	-10(5)	25(6)	-14(7)
O(5)	65(11)	41(8)	18(6)	-21(6)	18(6)	-37(7)
N(1)	38(10)	13(7)	4(6)	0(5)	3(6)	-9(7)
N(2)	28(9)	12(7)	18(7)	-4(5)	14(6)	-4(6)
C(1)	130(30)	36(13)	140(20)	20(14)	120(20)	-8(14)
C(2)	64(16)	6(9)	60(15)	2(9)	38(13)	-6(10)
C(3)	76(17)	44(13)	53(15)	-42(12)	42(13)	-56(13)
C(4)	56(15)	29(11)	64(15)	-34(10)	38(12)	-31(11)
C(5)	30(12)	28(10)	37(11)	-14(8)	25(9)	-15(9)
C(6)	49(13)	13(8)	17(9)	-11(7)	25(8)	-17(8)
C(7)	48(13)	24(9)	17(9)	-4(7)	22(9)	0(9)
C(8)	59(15)	52(13)	17(9)	-18(9)	27(10)	-23(11)
C(9)	43(13)	36(11)	23(10)	-1(8)	19(9)	-23(9)
C(10)	56(14)	19(10)	29(11)	12(8)	30(10)	0(9)
C(11)	49(14)	16(9)	40(11)	-2(8)	33(10)	-13(9)
C(12)	19(11)	19(9)	23(10)	8(8)	-1(8)	-6(8)
C(13)	15(11)	55(14)	9(9)	4(9)	-12(7)	7(10)
C(14)	76(19)	53(14)	34(13)	20(10)	25(13)	5(14)
C(15)	90(20)	51(14)	30(12)	32(10)	29(12)	13(13)
C(16)	17(14)	100(20)	130(20)	-74(17)	16(15)	-6(15)
C(17)	220(40)	140(40)	41(19)	-40(20)	0(20)	-110(30)
C(18)	46(19)	100(20)	100(20)	-12(19)	34(17)	6(17)
C(19)	70(20)	62(17)	63(16)	1(13)	31(14)	-14(15)

Table C.39. Hydrogen coordinates ($x \times 10^4$) and isotropic displacement parameters ($\text{\AA}^2 \times 10^3$) for NDA adduct **3.46** (JLW_143).

	x	y	z	U(eq)
H(7)	2242	1045	4778	124
H(8)	2476	1624	5980	124
H(1)	2911	975	5945	124
H(9)	2110	1716	2967	63
H(10)	2474	2337	1558	55
H(15)	3905	4120	4128	27
H(16)	4508	5348	5670	32
H(2)	4310	6716	5257	47
H(3)	4968	6420	5413	47
H(4)	3316	5895	4380	36
H(5)	3628	1953	6018	64
H(6)	3995	2684	4783	67
H(14)	2346	3485	317	107
H(13)	1440	3969	-145	179
H(11)	1321	4925	1058	95
H(12)	2127	5537	2532	74

C.7. Crystal analysis of epoxide **3.52**

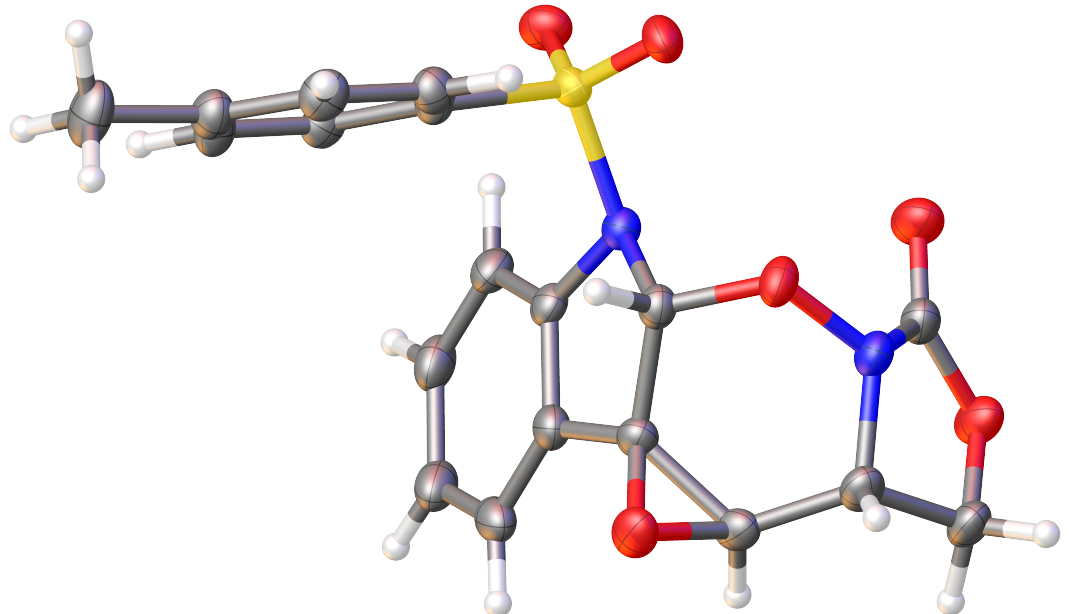


Figure C.07. ORTEP drawing of epoxide **3.52**

Table C.40. Crystal data and structure refinement for epoxide **3.52** (JLW_144).

Identification code	JLW_144		
Empirical formula	C38 H32 N4 O12 S2		
Formula weight	800.79		
Temperature	150(2) K		
Wavelength	0.71073 Å		
Crystal system	Triclinic		
Space group	P-1		
Unit cell dimensions	a = 10.3917(5) Å	α= 112.346(2)°.	
	b = 12.4405(5) Å	β= 93.256(2)°.	
	c = 14.7067(7) Å	γ = 90.228(2)°.	
Volume	1754.96(14) Å ³		
Z	2		
Density (calculated)	1.515 Mg/m ³		
Absorption coefficient	0.227 mm ⁻¹		
F(000)	832		
Crystal size	0.274 x 0.175 x 0.108 mm ³		
Theta range for data collection	1.964 to 26.344°.		
Index ranges	-12<=h<=12, -15<=k<=15, -14<=l<=18		
Reflections collected	8361		
Independent reflections	5780 [R(int) = 0.0311]		
Completeness to theta = 25.242°	81.8 %		
Absorption correction	None		
Refinement method	Full-matrix least-squares on F ²		
Data / restraints / parameters	5780 / 0 / 507		
Goodness-of-fit on F ²	1.032		
Final R indices [I>2sigma(I)]	R1 = 0.0476, wR2 = 0.1200		
R indices (all data)	R1 = 0.0616, wR2 = 0.1327		
Extinction coefficient	n/a		
Largest diff. peak and hole	0.303 and -0.315 e.Å ⁻³		

Table C.41. Atomic coordinates ($x \times 10^4$) and equivalent isotropic displacement parameters ($\text{\AA}^2 \times 10^3$) for epoxide **3.52** (JLW_144). U(eq) is defined as one third of the trace of the orthogonalized U^{ij} tensor.

	x	y	z	U(eq)
S(1)	1140(1)	7635(1)	2292(1)	24(1)
S(2)	5073(1)	4138(1)	2789(1)	30(1)
O(1)	1919(2)	6792(2)	1616(2)	32(1)
O(2)	-172(2)	7376(2)	2388(2)	32(1)
O(3)	-1066(2)	9557(2)	2266(2)	29(1)
O(4)	-1497(2)	10043(2)	79(2)	36(1)
O(5)	-1203(2)	8306(2)	194(2)	39(1)
O(6)	544(2)	11902(2)	3090(2)	34(1)
O(7)	5683(2)	3949(2)	3612(2)	41(1)
O(8)	5003(2)	3235(2)	1835(2)	40(1)
O(9)	8935(2)	4941(2)	619(2)	31(1)
O(10)	5644(2)	4755(2)	914(1)	29(1)
O(11)	7992(2)	3758(2)	1236(2)	41(1)
O(12)	5768(2)	7479(2)	1652(2)	29(1)
N(1)	1091(2)	8761(2)	1936(2)	23(1)
N(2)	-1535(2)	9992(2)	1559(2)	28(1)
N(3)	5888(2)	5229(2)	2687(2)	26(1)
N(4)	6812(2)	4844(2)	510(2)	25(1)
C(1)	-1737(3)	11224(3)	762(2)	34(1)
C(2)	-1303(3)	11231(2)	1773(2)	29(1)
C(3)	112(3)	11552(2)	2058(2)	28(1)
C(4)	901(3)	10784(2)	2401(2)	25(1)
C(5)	301(2)	9734(2)	2519(2)	24(1)
C(6)	1929(2)	8125(2)	3473(2)	23(1)
C(7)	1216(3)	8372(2)	4299(2)	27(1)
C(8)	1846(3)	8676(3)	5214(2)	31(1)
C(9)	3188(3)	8756(3)	5338(2)	30(1)
C(10)	3889(3)	9035(3)	6329(2)	41(1)
C(11)	3276(3)	8209(2)	3575(2)	26(1)
C(12)	3882(3)	8526(3)	4498(2)	30(1)

C(13)	2283(2)	9253(2)	1770(2)	24(1)
C(14)	2214(3)	10461(2)	2103(2)	26(1)
C(15)	3209(3)	11123(3)	1967(2)	32(1)
C(16)	4276(3)	10555(3)	1503(3)	36(1)
C(17)	4333(3)	9352(3)	1167(2)	34(1)
C(18)	3334(3)	8675(3)	1291(2)	30(1)
C(19)	-1372(3)	9334(3)	579(2)	29(1)
C(20)	-409(3)	5516(4)	3755(4)	64(1)
C(21)	962(3)	5220(3)	3515(3)	42(1)
C(22)	1979(3)	5611(3)	4239(3)	41(1)
C(23)	3243(3)	5319(3)	4018(2)	35(1)
C(24)	3492(3)	4608(3)	3068(2)	30(1)
C(25)	5484(2)	5601(2)	1867(2)	24(1)
C(26)	6246(2)	6739(2)	2136(2)	22(1)
C(27)	7012(2)	6947(2)	1406(2)	22(1)
C(28)	7107(2)	5953(2)	428(2)	23(1)
C(29)	8489(3)	5711(3)	137(2)	28(1)
C(30)	1254(3)	4534(3)	2559(3)	41(1)
C(31)	2507(3)	4225(3)	2329(2)	37(1)
C(32)	7913(3)	4445(2)	845(2)	30(1)
C(33)	6591(2)	7150(2)	3199(2)	24(1)
C(34)	7161(3)	8199(2)	3832(2)	30(1)
C(35)	7427(3)	8350(3)	4814(2)	36(1)
C(36)	7136(3)	7470(3)	5131(2)	37(1)
C(37)	6604(3)	6408(3)	4495(2)	33(1)
C(38)	6349(2)	6251(2)	3518(2)	25(1)

Table C.42. Bond lengths [\AA] and angles [$^\circ$] for epoxide **3.52** (JLW_144).

S(1)-O(2)	1.4267(19)
S(1)-O(1)	1.431(2)
S(1)-N(1)	1.673(2)
S(1)-C(6)	1.757(3)
S(2)-O(8)	1.423(2)
S(2)-O(7)	1.433(2)
S(2)-N(3)	1.655(2)
S(2)-C(24)	1.764(3)
O(3)-N(2)	1.408(3)
O(3)-C(5)	1.441(3)
O(4)-C(19)	1.349(3)
O(4)-C(1)	1.463(4)
O(5)-C(19)	1.204(4)
O(6)-C(4)	1.441(3)
O(6)-C(3)	1.454(3)
O(9)-C(32)	1.345(3)
O(9)-C(29)	1.455(3)
O(10)-N(4)	1.404(3)
O(10)-C(25)	1.416(3)
O(11)-C(32)	1.199(4)
O(12)-C(26)	1.436(3)
O(12)-C(27)	1.455(3)
N(1)-C(13)	1.453(3)
N(1)-C(5)	1.474(4)
N(2)-C(19)	1.381(4)
N(2)-C(2)	1.467(4)
N(3)-C(38)	1.444(4)
N(3)-C(25)	1.489(3)
N(4)-C(32)	1.387(4)
N(4)-C(28)	1.463(3)
C(1)-C(2)	1.526(4)
C(1)-H(3)	0.9900
C(1)-H(1)	0.9900
C(2)-C(3)	1.515(4)

C(2)-H(16)	1.0000
C(3)-C(4)	1.471(4)
C(3)-H(15)	1.0000
C(4)-C(14)	1.467(4)
C(4)-C(5)	1.519(3)
C(5)-H(14)	1.0000
C(6)-C(7)	1.393(4)
C(6)-C(11)	1.398(4)
C(7)-C(8)	1.376(4)
C(7)-H(6)	0.9500
C(8)-C(9)	1.394(4)
C(8)-H(7)	0.9500
C(9)-C(12)	1.401(4)
C(9)-C(10)	1.506(4)
C(10)-H(9)	0.9800
C(10)-H(8)	0.9800
C(10)-H(2)	0.9800
C(11)-C(12)	1.375(4)
C(11)-H(4)	0.9500
C(12)-H(5)	0.9500
C(13)-C(18)	1.383(4)
C(13)-C(14)	1.396(4)
C(14)-C(15)	1.389(4)
C(15)-C(16)	1.386(5)
C(15)-H(13)	0.9500
C(16)-C(17)	1.390(5)
C(16)-H(10)	0.9500
C(17)-C(18)	1.396(4)
C(17)-H(12)	0.9500
C(18)-H(11)	0.9500
C(20)-C(21)	1.501(5)
C(20)-H(19)	0.9800
C(20)-H(32)	0.9800
C(20)-H(17)	0.9800
C(21)-C(30)	1.392(5)
C(21)-C(22)	1.401(5)

C(22)-C(23)	1.388(5)
C(22)-H(20)	0.9500
C(23)-C(24)	1.380(4)
C(23)-H(21)	0.9500
C(24)-C(31)	1.390(4)
C(25)-C(26)	1.523(3)
C(25)-H(29)	1.0000
C(26)-C(27)	1.470(4)
C(26)-C(33)	1.471(4)
C(27)-C(28)	1.507(4)
C(27)-H(24)	1.0000
C(28)-C(29)	1.521(4)
C(28)-H(23)	1.0000
C(29)-H(22)	0.9900
C(29)-H(18)	0.9900
C(30)-C(31)	1.382(5)
C(30)-H(31)	0.9500
C(31)-H(30)	0.9500
C(33)-C(34)	1.388(4)
C(33)-C(38)	1.394(4)
C(34)-C(35)	1.393(4)
C(34)-H(28)	0.9500
C(35)-C(36)	1.383(5)
C(35)-H(27)	0.9500
C(36)-C(37)	1.386(4)
C(36)-H(26)	0.9500
C(37)-C(38)	1.384(4)
C(37)-H(25)	0.9500
O(2)-S(1)-O(1)	121.29(12)
O(2)-S(1)-N(1)	105.27(11)
O(1)-S(1)-N(1)	105.76(12)
O(2)-S(1)-C(6)	107.58(12)
O(1)-S(1)-C(6)	108.85(13)
N(1)-S(1)-C(6)	107.31(12)
O(8)-S(2)-O(7)	120.31(15)

O(8)-S(2)-N(3)	105.93(12)
O(7)-S(2)-N(3)	106.04(12)
O(8)-S(2)-C(24)	107.70(14)
O(7)-S(2)-C(24)	108.94(14)
N(3)-S(2)-C(24)	107.24(13)
N(2)-O(3)-C(5)	115.07(18)
C(19)-O(4)-C(1)	109.6(2)
C(4)-O(6)-C(3)	61.08(18)
C(32)-O(9)-C(29)	109.5(2)
N(4)-O(10)-C(25)	115.18(18)
C(26)-O(12)-C(27)	61.14(16)
C(13)-N(1)-C(5)	107.7(2)
C(13)-N(1)-S(1)	119.72(18)
C(5)-N(1)-S(1)	115.32(17)
C(19)-N(2)-O(3)	118.0(2)
C(19)-N(2)-C(2)	110.7(2)
O(3)-N(2)-C(2)	117.7(2)
C(38)-N(3)-C(25)	107.8(2)
C(38)-N(3)-S(2)	123.75(19)
C(25)-N(3)-S(2)	117.96(16)
C(32)-N(4)-O(10)	118.0(2)
C(32)-N(4)-C(28)	109.6(2)
O(10)-N(4)-C(28)	116.8(2)
O(4)-C(1)-C(2)	104.3(2)
O(4)-C(1)-H(3)	110.9
C(2)-C(1)-H(3)	110.9
O(4)-C(1)-H(1)	110.9
C(2)-C(1)-H(1)	110.9
H(3)-C(1)-H(1)	108.9
N(2)-C(2)-C(3)	110.2(2)
N(2)-C(2)-C(1)	98.1(2)
C(3)-C(2)-C(1)	113.6(2)
N(2)-C(2)-H(16)	111.4
C(3)-C(2)-H(16)	111.4
C(1)-C(2)-H(16)	111.4
O(6)-C(3)-C(4)	59.03(17)

O(6)-C(3)-C(2)	117.9(2)
C(4)-C(3)-C(2)	118.2(2)
O(6)-C(3)-H(15)	116.5
C(4)-C(3)-H(15)	116.5
C(2)-C(3)-H(15)	116.5
O(6)-C(4)-C(14)	125.2(2)
O(6)-C(4)-C(3)	59.89(17)
C(14)-C(4)-C(3)	123.4(2)
O(6)-C(4)-C(5)	115.9(2)
C(14)-C(4)-C(5)	106.1(2)
C(3)-C(4)-C(5)	120.9(2)
O(3)-C(5)-N(1)	114.5(2)
O(3)-C(5)-C(4)	115.1(2)
N(1)-C(5)-C(4)	103.8(2)
O(3)-C(5)-H(14)	107.6
N(1)-C(5)-H(14)	107.6
C(4)-C(5)-H(14)	107.6
C(7)-C(6)-C(11)	120.2(2)
C(7)-C(6)-S(1)	119.9(2)
C(11)-C(6)-S(1)	119.8(2)
C(8)-C(7)-C(6)	119.6(2)
C(8)-C(7)-H(6)	120.2
C(6)-C(7)-H(6)	120.2
C(7)-C(8)-C(9)	121.5(3)
C(7)-C(8)-H(7)	119.2
C(9)-C(8)-H(7)	119.2
C(8)-C(9)-C(12)	117.8(3)
C(8)-C(9)-C(10)	122.0(3)
C(12)-C(9)-C(10)	120.2(3)
C(9)-C(10)-H(9)	109.5
C(9)-C(10)-H(8)	109.5
H(9)-C(10)-H(8)	109.5
C(9)-C(10)-H(2)	109.5
H(9)-C(10)-H(2)	109.5
H(8)-C(10)-H(2)	109.5
C(12)-C(11)-C(6)	119.1(2)

C(12)-C(11)-H(4)	120.5
C(6)-C(11)-H(4)	120.5
C(11)-C(12)-C(9)	121.8(3)
C(11)-C(12)-H(5)	119.1
C(9)-C(12)-H(5)	119.1
C(18)-C(13)-C(14)	121.5(2)
C(18)-C(13)-N(1)	128.4(2)
C(14)-C(13)-N(1)	110.0(2)
C(15)-C(14)-C(13)	120.7(3)
C(15)-C(14)-C(4)	130.0(3)
C(13)-C(14)-C(4)	108.2(2)
C(16)-C(15)-C(14)	118.3(3)
C(16)-C(15)-H(13)	120.9
C(14)-C(15)-H(13)	120.9
C(15)-C(16)-C(17)	120.6(3)
C(15)-C(16)-H(10)	119.7
C(17)-C(16)-H(10)	119.7
C(16)-C(17)-C(18)	121.7(3)
C(16)-C(17)-H(12)	119.2
C(18)-C(17)-H(12)	119.2
C(13)-C(18)-C(17)	117.2(3)
C(13)-C(18)-H(11)	121.4
C(17)-C(18)-H(11)	121.4
O(5)-C(19)-O(4)	123.7(3)
O(5)-C(19)-N(2)	128.6(3)
O(4)-C(19)-N(2)	107.7(3)
C(21)-C(20)-H(19)	109.5
C(21)-C(20)-H(32)	109.5
H(19)-C(20)-H(32)	109.5
C(21)-C(20)-H(17)	109.5
H(19)-C(20)-H(17)	109.5
H(32)-C(20)-H(17)	109.5
C(30)-C(21)-C(22)	118.1(3)
C(30)-C(21)-C(20)	120.4(3)
C(22)-C(21)-C(20)	121.5(4)
C(23)-C(22)-C(21)	121.4(3)

C(23)-C(22)-H(20)	119.3
C(21)-C(22)-H(20)	119.3
C(24)-C(23)-C(22)	118.9(3)
C(24)-C(23)-H(21)	120.5
C(22)-C(23)-H(21)	120.5
C(23)-C(24)-C(31)	121.0(3)
C(23)-C(24)-S(2)	119.8(2)
C(31)-C(24)-S(2)	119.2(3)
O(10)-C(25)-N(3)	114.5(2)
O(10)-C(25)-C(26)	115.8(2)
N(3)-C(25)-C(26)	102.5(2)
O(10)-C(25)-H(29)	107.9
N(3)-C(25)-H(29)	107.9
C(26)-C(25)-H(29)	107.9
O(12)-C(26)-C(27)	60.06(16)
O(12)-C(26)-C(33)	123.7(2)
C(27)-C(26)-C(33)	125.6(2)
O(12)-C(26)-C(25)	114.8(2)
C(27)-C(26)-C(25)	120.5(2)
C(33)-C(26)-C(25)	106.2(2)
O(12)-C(27)-C(26)	58.81(16)
O(12)-C(27)-C(28)	118.6(2)
C(26)-C(27)-C(28)	117.3(2)
O(12)-C(27)-H(24)	116.6
C(26)-C(27)-H(24)	116.6
C(28)-C(27)-H(24)	116.6
N(4)-C(28)-C(27)	110.7(2)
N(4)-C(28)-C(29)	97.6(2)
C(27)-C(28)-C(29)	112.9(2)
N(4)-C(28)-H(23)	111.6
C(27)-C(28)-H(23)	111.6
C(29)-C(28)-H(23)	111.6
O(9)-C(29)-C(28)	104.0(2)
O(9)-C(29)-H(22)	111.0
C(28)-C(29)-H(22)	111.0
O(9)-C(29)-H(18)	111.0

C(28)-C(29)-H(18)	111.0
H(22)-C(29)-H(18)	109.0
C(31)-C(30)-C(21)	121.3(3)
C(31)-C(30)-H(31)	119.4
C(21)-C(30)-H(31)	119.4
C(30)-C(31)-C(24)	119.3(3)
C(30)-C(31)-H(30)	120.4
C(24)-C(31)-H(30)	120.4
O(11)-C(32)-O(9)	124.1(3)
O(11)-C(32)-N(4)	128.4(3)
O(9)-C(32)-N(4)	107.4(2)
C(34)-C(33)-C(38)	121.4(3)
C(34)-C(33)-C(26)	129.7(2)
C(38)-C(33)-C(26)	108.8(2)
C(33)-C(34)-C(35)	117.9(3)
C(33)-C(34)-H(28)	121.1
C(35)-C(34)-H(28)	121.1
C(36)-C(35)-C(34)	120.2(3)
C(36)-C(35)-H(27)	119.9
C(34)-C(35)-H(27)	119.9
C(37)-C(36)-C(35)	122.0(3)
C(37)-C(36)-H(26)	119.0
C(35)-C(36)-H(26)	119.0
C(36)-C(37)-C(38)	117.9(3)
C(36)-C(37)-H(25)	121.1
C(38)-C(37)-H(25)	121.1
C(37)-C(38)-C(33)	120.4(3)
C(37)-C(38)-N(3)	130.1(3)
C(33)-C(38)-N(3)	109.4(2)

Symmetry transformations used to generate equivalent atoms.

Table C.43. Anisotropic displacement parameters ($\text{\AA}^2 \times 10^3$) for epoxide **3.52** (JLW_144). The anisotropic displacement factor exponent takes the form: $-2p^2 [h^2 a^* U^{11} + \dots + 2 h k a^* b^* U^{12}]$.

	U ¹¹	U ²²	U ³³	U ²³	U ¹³	U ¹²
S(1)	26(1)	21(1)	22(1)	7(1)	-4(1)	-3(1)
S(2)	31(1)	26(1)	37(1)	16(1)	0(1)	-2(1)
O(1)	42(1)	23(1)	26(1)	4(1)	0(1)	2(1)
O(2)	28(1)	33(1)	35(1)	16(1)	-9(1)	-9(1)
O(3)	24(1)	37(1)	30(1)	19(1)	-2(1)	2(1)
O(4)	50(1)	29(1)	28(1)	11(1)	-10(1)	2(1)
O(5)	51(1)	25(1)	36(1)	7(1)	-9(1)	1(1)
O(6)	41(1)	27(1)	27(1)	3(1)	-8(1)	2(1)
O(7)	41(1)	40(1)	51(2)	30(1)	-3(1)	2(1)
O(8)	45(1)	27(1)	45(1)	10(1)	6(1)	-8(1)
O(9)	24(1)	32(1)	35(1)	11(1)	3(1)	4(1)
O(10)	24(1)	31(1)	27(1)	6(1)	-1(1)	-10(1)
O(11)	46(1)	29(1)	50(2)	18(1)	7(1)	10(1)
O(12)	24(1)	32(1)	37(1)	19(1)	2(1)	7(1)
N(1)	24(1)	24(1)	23(1)	10(1)	-2(1)	1(1)
N(2)	28(1)	29(1)	29(1)	14(1)	-6(1)	2(1)
N(3)	27(1)	24(1)	25(1)	9(1)	-3(1)	-5(1)
N(4)	23(1)	21(1)	28(1)	5(1)	1(1)	-2(1)
C(1)	39(2)	27(2)	37(2)	13(1)	-9(1)	6(1)
C(2)	31(1)	23(2)	30(2)	7(1)	-3(1)	7(1)
C(3)	36(2)	21(1)	22(2)	5(1)	-3(1)	0(1)
C(4)	29(1)	19(1)	24(1)	6(1)	-3(1)	0(1)
C(5)	24(1)	26(2)	22(1)	9(1)	-2(1)	1(1)
C(6)	26(1)	22(1)	20(1)	8(1)	-4(1)	-1(1)
C(7)	23(1)	27(2)	29(2)	9(1)	2(1)	3(1)
C(8)	33(1)	33(2)	25(2)	10(1)	6(1)	6(1)
C(9)	33(1)	29(2)	25(2)	9(1)	-4(1)	3(1)
C(10)	42(2)	53(2)	27(2)	13(2)	-4(1)	12(2)
C(11)	26(1)	28(2)	25(2)	9(1)	4(1)	6(1)
C(12)	22(1)	36(2)	30(2)	12(1)	-1(1)	6(1)

C(13)	25(1)	26(1)	22(1)	12(1)	-4(1)	1(1)
C(14)	25(1)	27(2)	27(2)	12(1)	-6(1)	-1(1)
C(15)	34(2)	31(2)	31(2)	15(1)	-11(1)	-8(1)
C(16)	26(1)	43(2)	46(2)	28(2)	-6(1)	-3(1)
C(17)	24(1)	46(2)	40(2)	24(2)	-1(1)	4(1)
C(18)	28(1)	32(2)	36(2)	20(1)	-3(1)	2(1)
C(19)	29(1)	26(2)	29(2)	9(1)	-7(1)	1(1)
C(20)	41(2)	73(3)	101(4)	59(3)	13(2)	7(2)
C(21)	35(2)	41(2)	65(2)	36(2)	6(2)	3(2)
C(22)	48(2)	37(2)	47(2)	23(2)	14(2)	2(2)
C(23)	38(2)	37(2)	38(2)	22(1)	1(1)	-5(2)
C(24)	30(1)	32(2)	38(2)	22(1)	1(1)	-4(1)
C(25)	21(1)	24(1)	28(2)	10(1)	-1(1)	1(1)
C(26)	19(1)	21(1)	26(1)	8(1)	-1(1)	4(1)
C(27)	18(1)	21(1)	28(2)	9(1)	-2(1)	1(1)
C(28)	23(1)	22(1)	23(1)	6(1)	-2(1)	-2(1)
C(29)	27(1)	29(2)	25(2)	8(1)	0(1)	-2(1)
C(30)	33(2)	44(2)	58(2)	33(2)	-6(2)	-6(2)
C(31)	39(2)	39(2)	38(2)	23(2)	-3(1)	-5(2)
C(32)	32(1)	22(2)	28(2)	3(1)	2(1)	2(1)
C(33)	18(1)	26(2)	25(2)	7(1)	2(1)	1(1)
C(34)	25(1)	25(2)	31(2)	2(1)	4(1)	0(1)
C(35)	27(1)	36(2)	31(2)	-2(1)	-3(1)	-4(1)
C(36)	29(1)	51(2)	25(2)	10(1)	-5(1)	-1(2)
C(37)	30(1)	40(2)	31(2)	15(1)	-4(1)	0(1)
C(38)	20(1)	28(2)	25(2)	9(1)	-3(1)	0(1)

Table C.44. Hydrogen coordinates ($x \times 10^4$) and isotropic displacement parameters ($\text{\AA}^2 \times 10^3$) for epoxide **3.52** (JLW_144).

	x	y	z	U(eq)
H(3)	-2664	11398	732	41
H(1)	-1232	11803	609	41
H(16)	-1862	11728	2294	35
H(15)	554	11944	1676	33
H(14)	446	9839	3226	29
H(6)	300	8331	4231	32
H(7)	1355	8835	5774	37
H(9)	3322	9465	6850	62
H(8)	4664	9511	6380	62
H(2)	4136	8312	6402	62
H(4)	3765	8050	3014	32
H(5)	4797	8590	4569	36
H(13)	3158	11945	2185	38
H(10)	4976	10993	1415	43
H(12)	5069	8979	844	41
H(11)	3375	7852	1056	36
H(19)	-698	6089	3485	95
H(32)	-465	5841	4471	95
H(17)	-958	4812	3465	95
H(20)	1800	6087	4895	50
H(21)	3927	5603	4513	42
H(29)	4548	5784	1916	29
H(24)	7792	7471	1667	27
H(23)	6548	6067	-103	28
H(22)	8521	5329	-587	33
H(18)	9020	6439	373	33
H(31)	580	4273	2054	50
H(30)	2692	3756	1673	44
H(28)	7363	8794	3604	36
H(27)	7809	9061	5266	43

H(26)	7307	7597	5806	44
H(25)	6421	5808	4723	40

Table C.45. Torsion angles [°] for epoxide **3.52** (JLW_144).

O(2)-S(1)-N(1)-C(13)	179.87(19)
O(1)-S(1)-N(1)-C(13)	-50.6(2)
C(6)-S(1)-N(1)-C(13)	65.5(2)
O(2)-S(1)-N(1)-C(5)	48.8(2)
O(1)-S(1)-N(1)-C(5)	178.36(17)
C(6)-S(1)-N(1)-C(5)	-65.6(2)
C(5)-O(3)-N(2)-C(19)	80.1(3)
C(5)-O(3)-N(2)-C(2)	-56.8(3)
O(8)-S(2)-N(3)-C(38)	-170.1(2)
O(7)-S(2)-N(3)-C(38)	-41.1(3)
C(24)-S(2)-N(3)-C(38)	75.1(3)
O(8)-S(2)-N(3)-C(25)	49.6(2)
O(7)-S(2)-N(3)-C(25)	178.5(2)
C(24)-S(2)-N(3)-C(25)	-65.2(2)
C(25)-O(10)-N(4)-C(32)	77.2(3)
C(25)-O(10)-N(4)-C(28)	-56.8(3)
C(19)-O(4)-C(1)-C(2)	18.3(3)
C(19)-N(2)-C(2)-C(3)	-88.7(3)
O(3)-N(2)-C(2)-C(3)	51.2(3)
C(19)-N(2)-C(2)-C(1)	30.3(3)
O(3)-N(2)-C(2)-C(1)	170.1(2)
O(4)-C(1)-C(2)-N(2)	-27.8(3)
O(4)-C(1)-C(2)-C(3)	88.5(3)
C(4)-O(6)-C(3)-C(2)	107.9(3)
N(2)-C(2)-C(3)-O(6)	-88.1(3)
C(1)-C(2)-C(3)-O(6)	163.0(2)
N(2)-C(2)-C(3)-C(4)	-20.2(4)
C(1)-C(2)-C(3)-C(4)	-129.1(3)
C(3)-O(6)-C(4)-C(14)	111.7(3)
C(3)-O(6)-C(4)-C(5)	-112.3(3)
C(2)-C(3)-C(4)-O(6)	-107.3(3)
O(6)-C(3)-C(4)-C(14)	-114.6(3)
C(2)-C(3)-C(4)-C(14)	138.1(3)
O(6)-C(3)-C(4)-C(5)	104.0(3)

C(2)-C(3)-C(4)-C(5)	-3.3(4)
N(2)-O(3)-C(5)-N(1)	-92.7(3)
N(2)-O(3)-C(5)-C(4)	27.6(3)
C(13)-N(1)-C(5)-O(3)	143.6(2)
S(1)-N(1)-C(5)-O(3)	-79.9(2)
C(13)-N(1)-C(5)-C(4)	17.2(3)
S(1)-N(1)-C(5)-C(4)	153.75(17)
O(6)-C(4)-C(5)-O(3)	69.5(3)
C(14)-C(4)-C(5)-O(3)	-146.7(2)
C(3)-C(4)-C(5)-O(3)	0.5(4)
O(6)-C(4)-C(5)-N(1)	-164.5(2)
C(14)-C(4)-C(5)-N(1)	-20.7(3)
C(3)-C(4)-C(5)-N(1)	126.5(3)
O(2)-S(1)-C(6)-C(7)	-10.2(3)
O(1)-S(1)-C(6)-C(7)	-143.3(2)
N(1)-S(1)-C(6)-C(7)	102.7(2)
O(2)-S(1)-C(6)-C(11)	166.6(2)
O(1)-S(1)-C(6)-C(11)	33.4(3)
N(1)-S(1)-C(6)-C(11)	-80.6(3)
C(11)-C(6)-C(7)-C(8)	-1.4(4)
S(1)-C(6)-C(7)-C(8)	175.4(2)
C(6)-C(7)-C(8)-C(9)	0.7(4)
C(7)-C(8)-C(9)-C(12)	0.5(5)
C(7)-C(8)-C(9)-C(10)	-177.2(3)
C(7)-C(6)-C(11)-C(12)	0.7(4)
S(1)-C(6)-C(11)-C(12)	-176.0(2)
C(6)-C(11)-C(12)-C(9)	0.6(4)
C(8)-C(9)-C(12)-C(11)	-1.2(5)
C(10)-C(9)-C(12)-C(11)	176.6(3)
C(5)-N(1)-C(13)-C(18)	177.4(3)
S(1)-N(1)-C(13)-C(18)	43.1(3)
C(5)-N(1)-C(13)-C(14)	-7.4(3)
S(1)-N(1)-C(13)-C(14)	-141.7(2)
C(18)-C(13)-C(14)-C(15)	-0.3(4)
N(1)-C(13)-C(14)-C(15)	-175.9(2)
C(18)-C(13)-C(14)-C(4)	169.3(2)

N(1)-C(13)-C(14)-C(4)	-6.3(3)
O(6)-C(4)-C(14)-C(15)	-35.3(4)
C(3)-C(4)-C(14)-C(15)	39.1(4)
C(5)-C(4)-C(14)-C(15)	-174.7(3)
O(6)-C(4)-C(14)-C(13)	156.4(2)
C(3)-C(4)-C(14)-C(13)	-129.2(3)
C(5)-C(4)-C(14)-C(13)	17.0(3)
C(13)-C(14)-C(15)-C(16)	-0.8(4)
C(4)-C(14)-C(15)-C(16)	-167.9(3)
C(14)-C(15)-C(16)-C(17)	1.3(4)
C(15)-C(16)-C(17)-C(18)	-0.7(5)
C(14)-C(13)-C(18)-C(17)	0.9(4)
N(1)-C(13)-C(18)-C(17)	175.6(2)
C(16)-C(17)-C(18)-C(13)	-0.4(4)
C(1)-O(4)-C(19)-O(5)	177.9(3)
C(1)-O(4)-C(19)-N(2)	0.7(3)
O(3)-N(2)-C(19)-O(5)	22.3(4)
C(2)-N(2)-C(19)-O(5)	162.0(3)
O(3)-N(2)-C(19)-O(4)	-160.7(2)
C(2)-N(2)-C(19)-O(4)	-21.0(3)
C(30)-C(21)-C(22)-C(23)	-0.6(5)
C(20)-C(21)-C(22)-C(23)	178.9(3)
C(21)-C(22)-C(23)-C(24)	-1.3(4)
C(22)-C(23)-C(24)-C(31)	2.6(4)
C(22)-C(23)-C(24)-S(2)	-175.4(2)
O(8)-S(2)-C(24)-C(23)	167.5(2)
O(7)-S(2)-C(24)-C(23)	35.5(3)
N(3)-S(2)-C(24)-C(23)	-78.9(2)
O(8)-S(2)-C(24)-C(31)	-10.5(3)
O(7)-S(2)-C(24)-C(31)	-142.5(2)
N(3)-S(2)-C(24)-C(31)	103.1(2)
N(4)-O(10)-C(25)-N(3)	-93.7(2)
N(4)-O(10)-C(25)-C(26)	25.2(3)
C(38)-N(3)-C(25)-O(10)	148.9(2)
S(2)-N(3)-C(25)-O(10)	-64.9(3)
C(38)-N(3)-C(25)-C(26)	22.7(3)

S(2)-N(3)-C(25)-C(26)	168.84(18)
C(27)-O(12)-C(26)-C(33)	115.0(3)
C(27)-O(12)-C(26)-C(25)	-112.2(3)
O(10)-C(25)-C(26)-O(12)	72.9(3)
N(3)-C(25)-C(26)-O(12)	-161.7(2)
O(10)-C(25)-C(26)-C(27)	4.4(4)
N(3)-C(25)-C(26)-C(27)	129.7(2)
O(10)-C(25)-C(26)-C(33)	-146.6(2)
N(3)-C(25)-C(26)-C(33)	-21.2(3)
C(26)-O(12)-C(27)-C(28)	106.3(2)
C(33)-C(26)-C(27)-O(12)	-112.1(3)
C(25)-C(26)-C(27)-O(12)	102.9(3)
O(12)-C(26)-C(27)-C(28)	-108.5(3)
C(33)-C(26)-C(27)-C(28)	139.4(3)
C(25)-C(26)-C(27)-C(28)	-5.6(4)
C(32)-N(4)-C(28)-C(27)	-84.6(3)
O(10)-N(4)-C(28)-C(27)	53.0(3)
C(32)-N(4)-C(28)-C(29)	33.4(3)
O(10)-N(4)-C(28)-C(29)	171.0(2)
O(12)-C(27)-C(28)-N(4)	-88.2(3)
C(26)-C(27)-C(28)-N(4)	-20.7(3)
O(12)-C(27)-C(28)-C(29)	163.5(2)
C(26)-C(27)-C(28)-C(29)	-129.0(2)
C(32)-O(9)-C(29)-C(28)	19.9(3)
N(4)-C(28)-C(29)-O(9)	-30.7(2)
C(27)-C(28)-C(29)-O(9)	85.6(3)
C(22)-C(21)-C(30)-C(31)	1.3(5)
C(20)-C(21)-C(30)-C(31)	-178.2(3)
C(21)-C(30)-C(31)-C(24)	0.0(5)
C(23)-C(24)-C(31)-C(30)	-1.9(4)
S(2)-C(24)-C(31)-C(30)	176.0(2)
C(29)-O(9)-C(32)-O(11)	178.9(3)
C(29)-O(9)-C(32)-N(4)	1.2(3)
O(10)-N(4)-C(32)-O(11)	22.0(4)
C(28)-N(4)-C(32)-O(11)	159.0(3)
O(10)-N(4)-C(32)-O(9)	-160.4(2)

C(28)-N(4)-C(32)-O(9)	-23.4(3)
O(12)-C(26)-C(33)-C(34)	-36.2(4)
C(27)-C(26)-C(33)-C(34)	38.7(5)
C(25)-C(26)-C(33)-C(34)	-172.3(3)
O(12)-C(26)-C(33)-C(38)	148.6(2)
C(27)-C(26)-C(33)-C(38)	-136.5(3)
C(25)-C(26)-C(33)-C(38)	12.6(3)
C(38)-C(33)-C(34)-C(35)	-3.1(4)
C(26)-C(33)-C(34)-C(35)	-177.8(3)
C(33)-C(34)-C(35)-C(36)	0.6(4)
C(34)-C(35)-C(36)-C(37)	1.4(5)
C(35)-C(36)-C(37)-C(38)	-0.9(5)
C(36)-C(37)-C(38)-C(33)	-1.7(4)
C(36)-C(37)-C(38)-N(3)	175.2(3)
C(34)-C(33)-C(38)-C(37)	3.8(4)
C(26)-C(33)-C(38)-C(37)	179.4(2)
C(34)-C(33)-C(38)-N(3)	-173.7(2)
C(26)-C(33)-C(38)-N(3)	2.0(3)
C(25)-N(3)-C(38)-C(37)	166.7(3)
S(2)-N(3)-C(38)-C(37)	23.0(4)
C(25)-N(3)-C(38)-C(33)	-16.2(3)
S(2)-N(3)-C(38)-C(33)	-159.9(2)

Symmetry transformations used to generate equivalent atoms:

Table C.46. Hydrogen bonds for epoxide **3.52** (JLW_144) [Å and °].

D-H...A	d(D-H)	d(H...A)	d(D...A)	∠(DHA)
C(37)-H(25)...O(7)	0.95	2.36	2.963(4)	120.8
C(28)-H(23)...O(10)#1	1.00	2.53	3.295(3)	133.1
C(23)-H(21)...O(7)#2	0.95	2.60	3.370(4)	138.0
C(18)-H(11)...O(1)	0.95	2.38	2.964(3)	119.5

Symmetry transformations used to generate equivalent atoms:

#1 -x+1,-y+1,-z #2 -x+1,-y+1,-z+1

C.8. Crystal analysis of alcohol 3.63

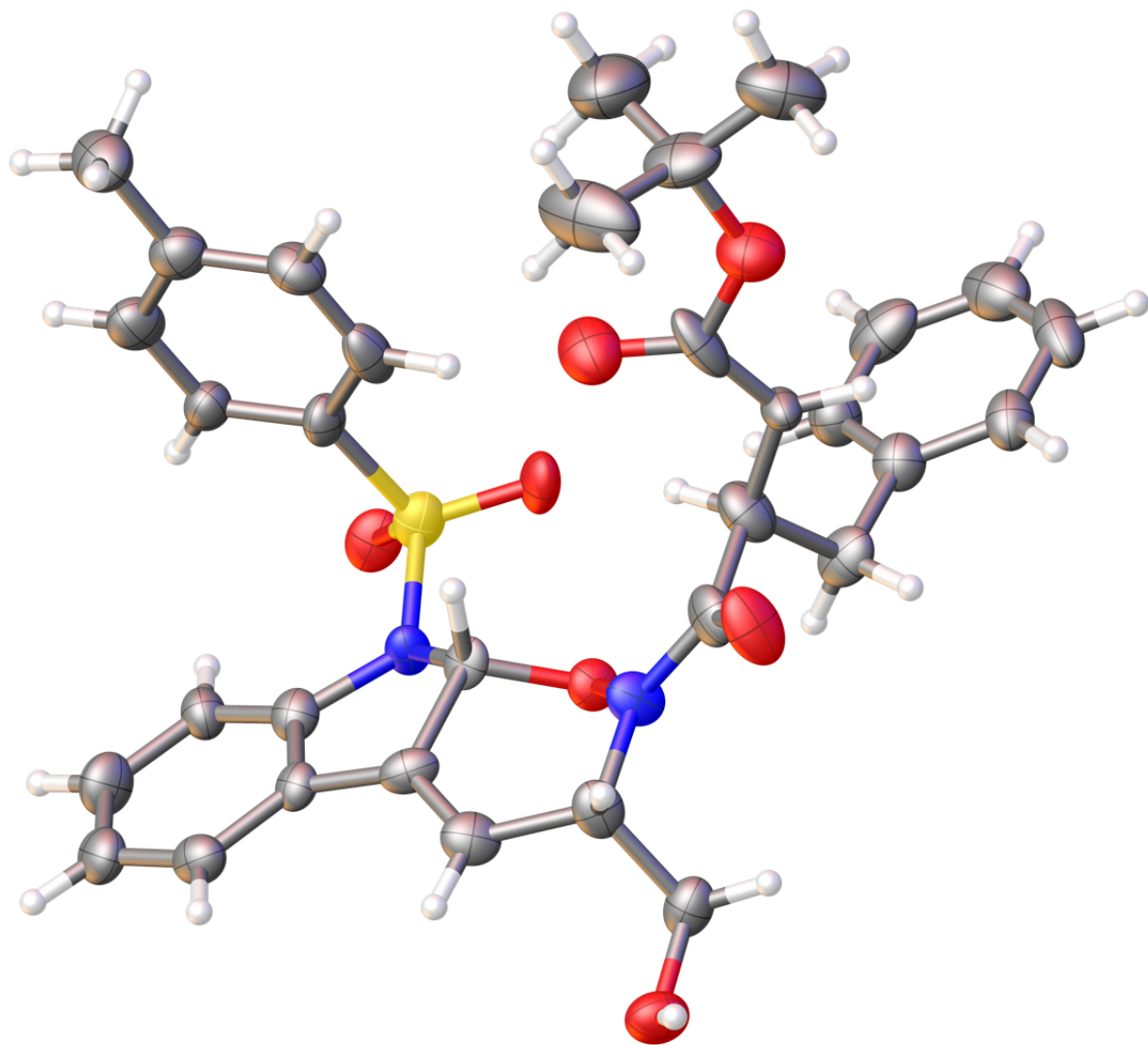


Figure C.08. ORTEP drawing of alcohol **3.63**

Table C.47. Crystal data and structure refinement for **3.63** (JLW_162_a).

Identification code	JLW_162_a		
Empirical formula	C33 H35 N2 O7 S		
Formula weight	603.69		
Temperature	150(2) K		
Wavelength	0.71073 Å		
Crystal system	Triclinic		
Space group	P-1		
Unit cell dimensions	a = 11.316(4) Å	α= 72.68(2)°.	
	b = 11.385(4) Å	β= 80.161(12)°.	
	c = 14.038(5) Å	γ = 62.810(11)°.	
Volume	1534.5(9) Å ³		
Z	2		
Density (calculated)	1.307 Mg/m ³		
Absorption coefficient	0.156 mm ⁻¹		
F(000)	638		
Crystal size	0.303 x 0.093 x 0.042 mm ³		
Theta range for data collection	2.077 to 25.027°.		
Index ranges	-12<=h<=13, -11<=k<=11, -16<=l<=16		
Reflections collected	7808		
Independent reflections	4392 [R(int) = 0.1399]		
Completeness to theta = 25.027°	81.0 %		
Refinement method	Full-matrix least-squares on F ²		
Data / restraints / parameters	4392 / 0 / 393		
Goodness-of-fit on F ²	1.120		
Final R indices [I>2sigma(I)]	R1 = 0.1003, wR2 = 0.2319		
R indices (all data)	R1 = 0.2316, wR2 = 0.2989		
Extinction coefficient	n/a		
Largest diff. peak and hole	0.572 and -0.537	e.Å ⁻³	

Table C.48. Atomic coordinates ($\times 10^4$) and equivalent isotropic displacement parameters ($\text{\AA}^2 \times 10^3$) for **3.63** (JLW_162_a). U(eq) is defined as one third of the trace of the orthogonalized U^{ij} tensor.

	x	y	z	U(eq)
S(1)	7281(2)	5431(3)	6092(2)	37(1)
O(1)	2023(6)	6788(8)	9465(4)	51(2)
O(2)	4243(5)	6842(6)	5295(4)	31(2)
O(3)	1308(6)	9752(7)	3023(4)	48(2)
O(4)	3534(7)	7268(8)	8307(5)	54(2)
O(5)	1086(6)	8288(7)	6439(5)	53(2)
O(6)	8536(5)	4613(6)	5668(4)	39(2)
O(7)	6391(5)	4840(7)	6602(4)	40(2)
N(1)	2918(6)	7809(8)	5442(5)	35(2)
N(2)	6456(6)	6669(7)	5143(5)	28(2)
C(1)	1993(15)	8839(13)	9775(8)	97(5)
C(2)	2235(11)	7312(13)	10208(7)	60(3)
C(3)	2733(9)	6777(11)	8558(7)	41(3)
N(3)	2427(8)	6147(9)	8039(5)	49(2)
C(5)	2973(9)	6096(10)	7042(6)	43(3)
C(6)	2243(9)	7497(10)	6295(6)	38(3)
C(7)	5043(7)	7533(8)	5318(6)	25(2)
C(8)	7586(8)	6181(10)	6890(6)	32(2)
C(9)	6631(8)	6613(10)	7656(6)	42(3)
C(10)	6867(9)	7157(10)	8333(6)	39(3)
C(11)	8029(9)	7338(11)	8226(6)	41(3)
C(12)	8310(10)	7889(12)	8959(7)	53(3)
C(13)	8742(8)	6348(10)	6774(6)	34(2)
C(14)	8958(9)	6919(10)	7436(6)	42(3)
C(15)	6994(8)	7582(10)	4471(6)	32(2)
C(16)	8328(8)	7251(10)	4214(6)	34(2)
C(17)	8594(8)	8284(11)	3548(7)	42(3)
C(18)	7603(9)	9549(10)	3128(6)	38(2)
C(19)	6277(9)	9802(10)	3366(6)	35(2)
C(20)	5962(7)	8823(9)	4064(6)	26(2)

C(21)	4701(8)	8788(9)	4454(6)	32(2)
C(22)	2389(8)	9023(10)	4594(6)	35(2)
C(23)	1790(8)	8660(10)	3885(6)	38(2)
C(24)	3479(8)	9463(10)	4122(6)	36(2)
C(25)	2834(9)	5028(10)	6691(7)	41(3)
C(26)	3391(8)	3600(10)	7394(6)	38(3)
C(27)	2552(9)	3073(11)	7928(6)	39(3)
C(28)	3066(12)	1769(13)	8575(7)	54(3)
C(29)	4390(13)	1017(13)	8668(7)	58(3)
C(30)	5249(11)	1538(12)	8141(8)	54(3)
C(31)	4729(9)	2845(10)	7511(6)	41(3)
C(32)	3672(13)	6525(16)	10551(8)	89(5)
C(4)	1218(11)	7111(13)	11022(7)	73(4)

Table C.49. Bond lengths [\AA] and angles [$^\circ$] for **3.63** (JLW_162_a).

S(1)-O(7)	1.437(6)
S(1)-O(6)	1.438(6)
S(1)-N(2)	1.655(6)
S(1)-C(8)	1.755(10)
O(1)-C(3)	1.385(10)
O(1)-C(2)	1.445(13)
O(2)-N(1)	1.423(8)
O(2)-C(7)	1.455(10)
O(3)-C(23)	1.420(10)
O(3)-H(3)	0.8400
O(4)-C(3)	1.224(11)
O(5)-C(6)	1.227(10)
N(1)-C(6)	1.351(10)
N(1)-C(22)	1.481(11)
N(2)-C(15)	1.463(11)
N(2)-C(7)	1.468(9)
C(1)-C(2)	1.569(17)
C(1)-H(21)	0.9800
C(1)-H(22)	0.9800
C(1)-H(1)	0.9800
C(2)-C(4)	1.522(14)
C(2)-C(32)	1.536(15)
C(3)-N(3)	1.338(13)
N(3)-C(5)	1.436(10)
N(3)-H(20)	0.8800
C(5)-C(25)	1.517(14)
C(5)-C(6)	1.557(13)
C(5)-H(29)	1.0000
C(7)-C(21)	1.512(11)
C(7)-H(30)	1.0000
C(8)-C(13)	1.382(11)
C(8)-C(9)	1.413(11)
C(9)-C(10)	1.396(14)
C(9)-H(35)	0.9500

C(10)-C(11)	1.399(13)
C(10)-H(5)	0.9500
C(11)-C(14)	1.422(12)
C(11)-C(12)	1.493(14)
C(12)-H(3)	0.9800
C(12)-H(4)	0.9800
C(12)-H(2)	0.9800
C(13)-C(14)	1.389(13)
C(13)-H(6)	0.9500
C(14)-H(7)	0.9500
C(15)-C(20)	1.388(11)
C(15)-C(16)	1.388(11)
C(16)-C(17)	1.385(13)
C(16)-H(34)	0.9500
C(17)-C(18)	1.387(12)
C(17)-H(33)	0.9500
C(18)-C(19)	1.392(11)
C(18)-H(8)	0.9500
C(19)-C(20)	1.387(12)
C(19)-H(32)	0.9500
C(20)-C(21)	1.452(11)
C(21)-C(24)	1.325(10)
C(21)-H(31)	1.0000
C(22)-C(24)	1.516(12)
C(22)-C(23)	1.533(13)
C(22)-H(12)	1.0000
C(23)-H(10)	0.9900
C(23)-H(9)	0.9900
C(24)-H(11)	0.9500
C(25)-C(26)	1.528(13)
C(25)-H(19)	0.9900
C(25)-H(13)	0.9900
C(26)-C(27)	1.354(12)
C(26)-C(31)	1.368(11)
C(27)-C(28)	1.399(14)
C(27)-H(18)	0.9500

C(28)-C(29)	1.350(14)
C(28)-H(17)	0.9500
C(29)-C(30)	1.365(14)
C(29)-H(14)	0.9500
C(30)-C(31)	1.392(14)
C(30)-H(16)	0.9500
C(31)-H(15)	0.9500
C(32)-H(23)	0.9800
C(32)-H(24)	0.9800
C(32)-H(25)	0.9800
C(4)-H(28)	0.9800
C(4)-H(27)	0.9800
C(4)-H(26)	0.9800
O(7)-S(1)-O(6)	120.3(4)
O(7)-S(1)-N(2)	105.6(3)
O(6)-S(1)-N(2)	105.7(3)
O(7)-S(1)-C(8)	108.8(4)
O(6)-S(1)-C(8)	108.2(4)
N(2)-S(1)-C(8)	107.6(4)
C(3)-O(1)-C(2)	122.1(9)
N(1)-O(2)-C(7)	103.6(6)
C(23)-O(3)-H(3)	109.5
C(6)-N(1)-O(2)	117.8(7)
C(6)-N(1)-C(22)	126.6(7)
O(2)-N(1)-C(22)	115.4(6)
C(15)-N(2)-C(7)	105.8(6)
C(15)-N(2)-S(1)	122.7(5)
C(7)-N(2)-S(1)	118.0(5)
C(2)-C(1)-H(21)	109.5
C(2)-C(1)-H(22)	109.5
H(21)-C(1)-H(22)	109.5
C(2)-C(1)-H(1)	109.5
H(21)-C(1)-H(1)	109.5
H(22)-C(1)-H(1)	109.5
O(1)-C(2)-C(4)	100.9(10)

O(1)-C(2)-C(32)	111.7(9)
C(4)-C(2)-C(32)	113.5(9)
O(1)-C(2)-C(1)	111.0(9)
C(4)-C(2)-C(1)	113.8(10)
C(32)-C(2)-C(1)	106.2(11)
O(4)-C(3)-N(3)	126.8(9)
O(4)-C(3)-O(1)	122.7(11)
N(3)-C(3)-O(1)	110.4(9)
C(3)-N(3)-C(5)	120.4(9)
C(3)-N(3)-H(20)	119.8
C(5)-N(3)-H(20)	119.8
N(3)-C(5)-C(25)	112.3(8)
N(3)-C(5)-C(6)	110.4(8)
C(25)-C(5)-C(6)	107.4(8)
N(3)-C(5)-H(29)	108.9
C(25)-C(5)-H(29)	108.9
C(6)-C(5)-H(29)	108.9
O(5)-C(6)-N(1)	119.9(8)
O(5)-C(6)-C(5)	122.7(8)
N(1)-C(6)-C(5)	117.4(8)
O(2)-C(7)-N(2)	110.2(7)
O(2)-C(7)-C(21)	109.3(6)
N(2)-C(7)-C(21)	105.0(6)
O(2)-C(7)-H(30)	110.7
N(2)-C(7)-H(30)	110.7
C(21)-C(7)-H(30)	110.7
C(13)-C(8)-C(9)	120.4(9)
C(13)-C(8)-S(1)	120.6(7)
C(9)-C(8)-S(1)	119.0(7)
C(10)-C(9)-C(8)	120.6(8)
C(10)-C(9)-H(35)	119.7
C(8)-C(9)-H(35)	119.7
C(9)-C(10)-C(11)	119.8(8)
C(9)-C(10)-H(5)	120.1
C(11)-C(10)-H(5)	120.1
C(10)-C(11)-C(14)	118.2(9)

C(10)-C(11)-C(12)	120.4(9)
C(14)-C(11)-C(12)	121.3(9)
C(11)-C(12)-H(3)	109.5
C(11)-C(12)-H(4)	109.5
H(3)-C(12)-H(4)	109.5
C(11)-C(12)-H(2)	109.5
H(3)-C(12)-H(2)	109.5
H(4)-C(12)-H(2)	109.5
C(8)-C(13)-C(14)	118.8(8)
C(8)-C(13)-H(6)	120.6
C(14)-C(13)-H(6)	120.6
C(13)-C(14)-C(11)	122.2(9)
C(13)-C(14)-H(7)	118.9
C(11)-C(14)-H(7)	118.9
C(20)-C(15)-C(16)	124.0(8)
C(20)-C(15)-N(2)	109.9(7)
C(16)-C(15)-N(2)	126.0(8)
C(17)-C(16)-C(15)	115.4(8)
C(17)-C(16)-H(34)	122.3
C(15)-C(16)-H(34)	122.3
C(16)-C(17)-C(18)	123.0(8)
C(16)-C(17)-H(33)	118.5
C(18)-C(17)-H(33)	118.5
C(17)-C(18)-C(19)	119.3(9)
C(17)-C(18)-H(8)	120.4
C(19)-C(18)-H(8)	120.4
C(20)-C(19)-C(18)	119.8(8)
C(20)-C(19)-H(32)	120.1
C(18)-C(19)-H(32)	120.1
C(15)-C(20)-C(19)	118.3(7)
C(15)-C(20)-C(21)	109.2(7)
C(19)-C(20)-C(21)	132.4(7)
C(24)-C(21)-C(20)	133.6(8)
C(24)-C(21)-C(7)	120.0(8)
C(20)-C(21)-C(7)	105.5(6)
C(24)-C(21)-H(31)	93.2

C(20)-C(21)-H(31)	93.2
C(7)-C(21)-H(31)	93.2
N(1)-C(22)-C(24)	109.6(7)
N(1)-C(22)-C(23)	107.5(8)
C(24)-C(22)-C(23)	114.7(7)
N(1)-C(22)-H(12)	108.3
C(24)-C(22)-H(12)	108.3
C(23)-C(22)-H(12)	108.3
O(3)-C(23)-C(22)	111.4(8)
O(3)-C(23)-H(10)	109.4
C(22)-C(23)-H(10)	109.4
O(3)-C(23)-H(9)	109.4
C(22)-C(23)-H(9)	109.4
H(10)-C(23)-H(9)	108.0
C(21)-C(24)-C(22)	121.8(8)
C(21)-C(24)-H(11)	119.1
C(22)-C(24)-H(11)	119.1
C(5)-C(25)-C(26)	114.5(8)
C(5)-C(25)-H(19)	108.6
C(26)-C(25)-H(19)	108.6
C(5)-C(25)-H(13)	108.6
C(26)-C(25)-H(13)	108.6
H(19)-C(25)-H(13)	107.6
C(27)-C(26)-C(31)	118.9(9)
C(27)-C(26)-C(25)	119.9(8)
C(31)-C(26)-C(25)	121.2(8)
C(26)-C(27)-C(28)	119.7(9)
C(26)-C(27)-H(18)	120.2
C(28)-C(27)-H(18)	120.2
C(29)-C(28)-C(27)	121.0(10)
C(29)-C(28)-H(17)	119.5
C(27)-C(28)-H(17)	119.5
C(28)-C(29)-C(30)	120.0(11)
C(28)-C(29)-H(14)	120.0
C(30)-C(29)-H(14)	120.0
C(29)-C(30)-C(31)	118.7(10)

C(29)-C(30)-H(16)	120.7
C(31)-C(30)-H(16)	120.7
C(26)-C(31)-C(30)	121.7(10)
C(26)-C(31)-H(15)	119.2
C(30)-C(31)-H(15)	119.2
C(2)-C(32)-H(23)	109.5
C(2)-C(32)-H(24)	109.5
H(23)-C(32)-H(24)	109.5
C(2)-C(32)-H(25)	109.5
H(23)-C(32)-H(25)	109.5
H(24)-C(32)-H(25)	109.5
C(2)-C(4)-H(28)	109.5
C(2)-C(4)-H(27)	109.5
H(28)-C(4)-H(27)	109.5
C(2)-C(4)-H(26)	109.5
H(28)-C(4)-H(26)	109.5
H(27)-C(4)-H(26)	109.5

Symmetry transformations used to generate equivalent atoms.

Table C.50. Anisotropic displacement parameters ($\text{\AA}^2 \times 10^3$) for **3.63** (JLW_162_a). The anisotropic displacement factor exponent takes the form: $-2\pi^2 [h^2 a^*{}^2 U^{11} + \dots + 2 h k a^* b^* U^{12}]$.

	U ¹¹	U ²²	U ³³	U ²³	U ¹³	U ¹²
S(1)	30(1)	25(2)	49(1)	-6(1)	-9(1)	-6(1)
O(1)	56(4)	53(6)	43(4)	-20(3)	4(3)	-19(4)
O(2)	22(3)	29(4)	36(3)	-12(3)	3(2)	-5(3)
O(3)	36(4)	49(5)	46(4)	-13(3)	-7(3)	-8(3)
O(4)	60(5)	53(6)	57(4)	-25(4)	10(3)	-29(4)
O(5)	30(4)	35(5)	74(5)	-14(4)	19(3)	-5(3)
O(6)	28(3)	21(4)	59(4)	-13(3)	-7(3)	1(3)
O(7)	39(4)	28(4)	58(4)	-2(3)	-12(3)	-21(3)
N(1)	22(4)	30(5)	38(4)	-12(3)	4(3)	0(3)
N(2)	19(4)	21(5)	37(4)	-1(3)	-5(3)	-4(3)
C(1)	175(15)	42(10)	63(8)	-13(7)	-7(8)	-39(9)
C(2)	84(8)	54(9)	46(6)	-25(6)	-12(6)	-23(6)
C(3)	40(6)	30(7)	48(6)	-10(5)	17(5)	-16(5)
N(3)	58(6)	50(7)	43(5)	-13(4)	2(4)	-28(4)
C(5)	44(6)	41(7)	36(5)	-11(5)	17(4)	-18(5)
C(6)	49(6)	27(7)	47(6)	-15(5)	9(5)	-23(5)
C(7)	23(4)	10(5)	40(5)	-13(4)	-2(3)	-2(3)
C(8)	22(5)	35(7)	39(5)	-7(4)	-2(4)	-13(4)
C(9)	24(5)	38(7)	50(6)	4(5)	1(4)	-12(4)
C(10)	42(6)	40(7)	33(5)	-13(4)	7(4)	-15(5)
C(11)	42(6)	38(8)	40(5)	-6(5)	-7(4)	-14(5)
C(12)	71(7)	51(9)	48(6)	-21(5)	5(5)	-34(6)
C(13)	32(5)	34(7)	38(5)	-5(4)	-6(4)	-16(4)
C(14)	35(5)	40(7)	41(6)	-3(5)	-8(4)	-12(5)
C(15)	31(5)	30(7)	38(5)	-17(4)	3(4)	-13(4)
C(16)	34(5)	34(7)	36(5)	-10(4)	3(4)	-18(4)
C(17)	27(5)	42(7)	55(6)	-18(5)	0(4)	-11(5)
C(18)	45(6)	36(7)	45(6)	-14(5)	-3(4)	-23(5)
C(19)	43(6)	24(7)	37(5)	-7(4)	-8(4)	-12(4)
C(20)	26(5)	24(6)	33(5)	-14(4)	0(4)	-11(4)

C(21)	32(5)	23(6)	31(5)	-11(4)	-8(4)	0(4)
C(22)	23(5)	24(6)	46(5)	-8(4)	1(4)	-2(4)
C(23)	31(5)	27(7)	52(6)	-10(5)	-9(4)	-8(4)
C(24)	32(5)	29(6)	37(5)	-14(4)	4(4)	-4(4)
C(25)	46(6)	23(7)	54(6)	-16(5)	-9(4)	-10(4)
C(26)	37(6)	34(7)	45(6)	-16(5)	2(4)	-14(5)
C(27)	41(6)	42(8)	45(6)	-24(5)	12(4)	-25(5)
C(28)	82(9)	61(9)	47(6)	-32(6)	29(6)	-54(7)
C(29)	92(9)	48(9)	45(6)	-16(5)	-4(6)	-36(7)
C(30)	58(7)	39(9)	71(7)	-27(6)	-24(6)	-9(6)
C(31)	39(6)	37(7)	47(6)	-11(5)	0(4)	-17(5)
C(32)	104(11)	124(15)	56(8)	-25(7)	-9(7)	-61(9)
C(4)	76(8)	72(10)	47(6)	-9(6)	-2(6)	-16(7)

Table C.51. Hydrogen coordinates ($\times 10^4$) and isotropic displacement parameters ($\text{\AA}^2 \times 10^3$) for **3.63** (JLW_162_a).

	x	y	z	U(eq)
H(3)	679	10428	3192	71
H(21)	2712	8888	9289	145
H(22)	1974	9223	10320	145
H(1)	1141	9360	9446	145
H(20)	1889	5761	8310	58
H(29)	3937	5880	7023	51
H(30)	4895	7782	5967	30
H(35)	5822	6532	7711	50
H(5)	6241	7404	8866	47
H(3)	9241	7350	9142	79
H(4)	7729	7835	9558	79
H(2)	8145	8842	8658	79
H(6)	9377	6077	6251	41
H(7)	9753	7034	7358	50
H(34)	9013	6376	4476	40
H(33)	9495	8118	3372	50
H(8)	7827	10236	2683	46
H(32)	5589	10644	3051	42
H(31)	4525	9402	4895	38
H(12)	1660	9782	4858	42
H(10)	2476	7839	3680	45
H(9)	1051	8445	4240	45
H(11)	3280	10243	3573	43
H(19)	3296	4982	6028	49
H(13)	1880	5324	6607	49
H(18)	1618	3587	7863	46
H(17)	2474	1406	8955	65
H(14)	4724	125	9100	70
H(16)	6182	1019	8203	65
H(15)	5320	3223	7153	49
H(23)	3931	5543	10712	133

H(24)	3736	6774	11145	133
H(25)	4267	6757	10015	133
H(28)	328	7614	10752	109
H(27)	1242	7453	11579	109
H(26)	1430	6138	11260	109

Table C.52. Torsion angles [°] for **3.63** (JLW_162_a).

C(7)-O(2)-N(1)-C(6)	-113.8(8)
C(7)-O(2)-N(1)-C(22)	70.6(8)
O(7)-S(1)-N(2)-C(15)	176.1(7)
O(6)-S(1)-N(2)-C(15)	-55.5(8)
C(8)-S(1)-N(2)-C(15)	60.0(8)
O(7)-S(1)-N(2)-C(7)	41.0(8)
O(6)-S(1)-N(2)-C(7)	169.5(6)
C(8)-S(1)-N(2)-C(7)	-75.0(7)
C(3)-O(1)-C(2)-C(4)	179.1(8)
C(3)-O(1)-C(2)-C(32)	-60.1(13)
C(3)-O(1)-C(2)-C(1)	58.2(12)
C(2)-O(1)-C(3)-O(4)	-3.7(15)
C(2)-O(1)-C(3)-N(3)	175.2(9)
O(4)-C(3)-N(3)-C(5)	-5.6(16)
O(1)-C(3)-N(3)-C(5)	175.6(7)
C(3)-N(3)-C(5)-C(25)	164.0(9)
C(3)-N(3)-C(5)-C(6)	-76.3(11)
O(2)-N(1)-C(6)-O(5)	-178.1(9)
C(22)-N(1)-C(6)-O(5)	-3.1(15)
O(2)-N(1)-C(6)-C(5)	-0.4(12)
C(22)-N(1)-C(6)-C(5)	174.6(9)
N(3)-C(5)-C(6)-O(5)	-27.7(14)
C(25)-C(5)-C(6)-O(5)	94.9(11)
N(3)-C(5)-C(6)-N(1)	154.6(8)
C(25)-C(5)-C(6)-N(1)	-82.8(10)
N(1)-O(2)-C(7)-N(2)	-178.3(6)
N(1)-O(2)-C(7)-C(21)	-63.4(7)
C(15)-N(2)-C(7)-O(2)	138.3(6)
S(1)-N(2)-C(7)-O(2)	-79.9(7)
C(15)-N(2)-C(7)-C(21)	20.7(9)
S(1)-N(2)-C(7)-C(21)	162.5(6)
O(7)-S(1)-C(8)-C(13)	154.8(7)
O(6)-S(1)-C(8)-C(13)	22.6(9)
N(2)-S(1)-C(8)-C(13)	-91.2(8)

O(7)-S(1)-C(8)-C(9)	-25.1(8)
O(6)-S(1)-C(8)-C(9)	-157.3(7)
N(2)-S(1)-C(8)-C(9)	88.9(7)
C(13)-C(8)-C(9)-C(10)	-2.9(14)
S(1)-C(8)-C(9)-C(10)	177.1(8)
C(8)-C(9)-C(10)-C(11)	3.1(15)
C(9)-C(10)-C(11)-C(14)	-1.8(14)
C(9)-C(10)-C(11)-C(12)	-178.5(10)
C(9)-C(8)-C(13)-C(14)	1.4(14)
S(1)-C(8)-C(13)-C(14)	-178.6(7)
C(8)-C(13)-C(14)-C(11)	-0.1(14)
C(10)-C(11)-C(14)-C(13)	0.3(14)
C(12)-C(11)-C(14)-C(13)	177.0(10)
C(7)-N(2)-C(15)-C(20)	-13.7(10)
S(1)-N(2)-C(15)-C(20)	-153.3(6)
C(7)-N(2)-C(15)-C(16)	170.4(8)
S(1)-N(2)-C(15)-C(16)	30.8(13)
C(20)-C(15)-C(16)-C(17)	3.6(14)
N(2)-C(15)-C(16)-C(17)	178.9(9)
C(15)-C(16)-C(17)-C(18)	-2.6(15)
C(16)-C(17)-C(18)-C(19)	-1.0(15)
C(17)-C(18)-C(19)-C(20)	4.0(14)
C(16)-C(15)-C(20)-C(19)	-0.8(14)
N(2)-C(15)-C(20)-C(19)	-176.8(8)
C(16)-C(15)-C(20)-C(21)	176.4(8)
N(2)-C(15)-C(20)-C(21)	0.4(10)
C(18)-C(19)-C(20)-C(15)	-3.1(14)
C(18)-C(19)-C(20)-C(21)	-179.5(8)
C(15)-C(20)-C(21)-C(24)	-155.8(10)
C(19)-C(20)-C(21)-C(24)	20.8(18)
C(15)-C(20)-C(21)-C(7)	12.6(9)
C(19)-C(20)-C(21)-C(7)	-170.7(10)
O(2)-C(7)-C(21)-C(24)	31.6(11)
N(2)-C(7)-C(21)-C(24)	149.8(8)
O(2)-C(7)-C(21)-C(20)	-138.8(7)
N(2)-C(7)-C(21)-C(20)	-20.6(9)

C(6)-N(1)-C(22)-C(24)	146.5(9)
O(2)-N(1)-C(22)-C(24)	-38.4(10)
C(6)-N(1)-C(22)-C(23)	-88.3(10)
O(2)-N(1)-C(22)-C(23)	86.8(8)
N(1)-C(22)-C(23)-O(3)	-177.4(6)
C(24)-C(22)-C(23)-O(3)	-55.3(10)
C(20)-C(21)-C(24)-C(22)	167.9(10)
C(7)-C(21)-C(24)-C(22)	0.8(13)
N(1)-C(22)-C(24)-C(21)	1.2(12)
C(23)-C(22)-C(24)-C(21)	-119.8(9)
N(3)-C(5)-C(25)-C(26)	-53.4(10)
C(6)-C(5)-C(25)-C(26)	-174.8(7)
C(5)-C(25)-C(26)-C(27)	109.1(10)
C(5)-C(25)-C(26)-C(31)	-69.6(11)
C(31)-C(26)-C(27)-C(28)	-0.8(15)
C(25)-C(26)-C(27)-C(28)	-179.6(9)
C(26)-C(27)-C(28)-C(29)	-0.8(16)
C(27)-C(28)-C(29)-C(30)	1.3(17)
C(28)-C(29)-C(30)-C(31)	-0.2(17)
C(27)-C(26)-C(31)-C(30)	1.9(15)
C(25)-C(26)-C(31)-C(30)	-179.3(10)
C(29)-C(30)-C(31)-C(26)	-1.4(17)

Symmetry transformations used to generate equivalent atoms.

C.9. Crystal analysis of intermolecular NDA adduct **3.67**

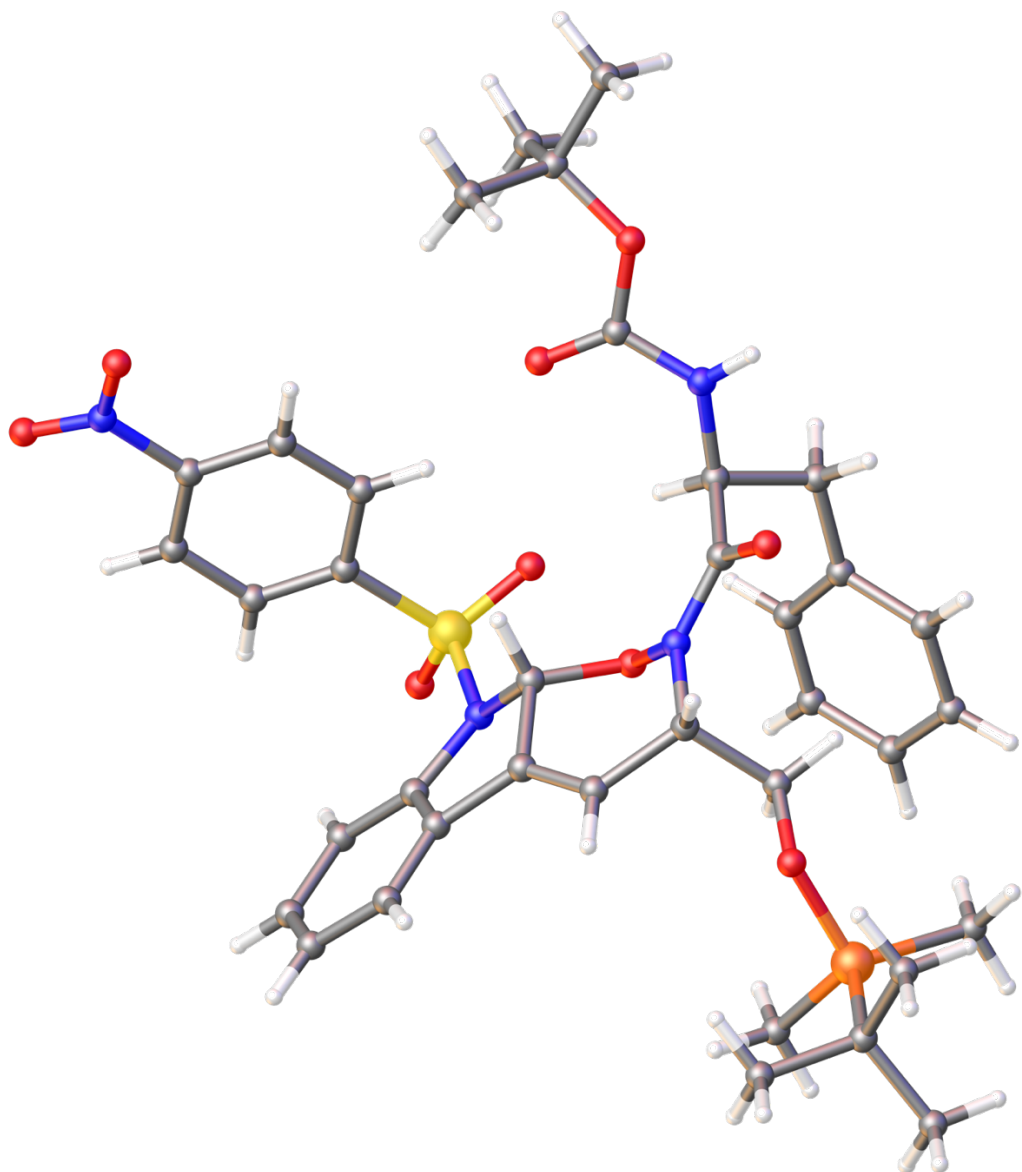


Figure C.09. ORTEP drawing of intermolecular NDA adduct **3.67**

X-ray data for this compound was poor, resolving only up to $\sim 1\text{\AA}$. However, the data was sufficient enough to allow for elucidation of connectivity and relative stereochemistry.

APPENDIX D
Compound Notebook Cross Reference

COMPOUND NOTEBOOK CROSS REFERENCE

<u>Compound</u>	<u>Notebook</u>
2.49.....	AJ-01-141, AJ-01-145, AJ-01-148
2.50.....	AJ-01-142, AJ-01-146, AJ-01-149
2.51.....	AJ-01-143, AJ-01-147, AJ-01-150
2.52.....	AJ-01-069, AJ-01-081
2.53.....	AJ-02-032, AJ-02-206
2.54.....	AJ-01-098, AJ-03-029
2.55.....	AJ-01-013, AJ-02-058, AJ-02-192
2.56.....	AJ-01-131, AJ-02-049, AJ-02-071
2.57.....	AJ-01-157, AJ-03-037
2.58.....	AJ-01-172, AJ-02-100
2.59.....	AJ-01-176, AJ-02-124
2.61.....	AJ-01-015, AJ-01-045
2.62.....	AJ-01-243, AJ-01-250
2.63.....	AJ-01-047, AJ-01-259
2.64.....	AJ-01-281, AJ-02-229
2.65.....	AJ-01-282, AJ-02-230
2.66.....	AJ-01-238, AJ-01-244
2.67.....	AJ-01-048, AJ-01-252
2.68.....	AJ-01-050, AJ-01-273
2.69.....	AJ-02-231
2.70.....	AJ-02-232
2.71.....	AJ-05-213
2.72.....	AJ-02-307
2.74.....	AJ-02-302, AJ-02-303
3.01.....	AJ-05-062, AJ-05-082
3.05.....	AJ-01-181, AJ-02-156
3.06.....	AJ-02-151, AJ-02-173
3.07.....	AJ-03-088, AJ-03-097
3.24.....	AJ-05-099, AJ-05-123
3.25.....	AJ-05-102
3.28.....	AJ-05-091, AJ-05-141
3.32.....	AJ-05-152
3.33.....	AJ-05-154
3.34.....	AJ-05-156
3.37.....	AJ-03-148, AJ-03-162
3.46.....	AJ-03-298, AJ-03-300
3.52.....	AJ-04-063, AJ-04-289
3.53.....	AJ-04-050, AJ-04-056/7
3.54.....	AJ-04-295, AJ-04-297
3.55.....	AJ-05-001, AJ-05-015

3.56	AJ-04-297
3.57	AJ-04-301
3.60	AJ-05-033, AJ-05-054
3.63	AJ-05-056
3.64	AJ-05-168, AJ-05-174
3.65	AJ-05-166, AJ-05-173
3.66	AJ-05-165, AJ-05-183
3.67	AJ-05-071, AJ-05-083
3.68	AJ-05-067, AJ-05-211
3.69	AJ-05-079, AJ-05-206
3.70	AJ-05-080, AJ-05-207
3.71	AJ-05-060, AJ-05-081

BIBLIOGRAPHY

- Anand, A.; Bhargava, G.; Singh, P.; Mehra, S.; Kumar, V.; Mahajan, M. P.; Singh, P.; Bisetty, K. *Lett. Org. Chem.* **2012**, *9*, 411-421.
- Andersch, J.; Hennig, L.; Wilde, H. *Carbohydr. Res.* **2000**, *329*(3), 693-697.
- Athanassellis, G.; Iglessi-Markopoulou, O.; Markopoulos, J. *Bioinorg. Chem. Appl.* **2010**, *1*-11.
- Avenoza, A.; Bustos, J. H.; Cativiela, C.; Peregrina, J. M.; Rodriguez, F. *Tetrahedron Lett.* **2002**, *43*(8), 1429-1432.
- Bai, W. -J.; Jackson, S. K.; Pettus, T. R. R. *Org. Lett.* **2012**, *14*, 3862-3865.
- Bai, W. -J.; Pettus, T. R. R. *Org. Lett.* **2018**, *20*, 901-904.
- Banerjee, R.; King, S. B. *Org. Lett.* **2009**, *11*(20), 4580-4583.
- Bapat, J. B.; Black, D. C.; Brown, R. F. C. *Adv. Heterocycl. Chem.* **1969**, *10*, 199-240.
- Berg, D. H.; Massing, R. P.; Hoehn, M. M.; Boeck, L. D.; Hamill, R. L. *J. Antibiot.*, **1976**, *29*, 394-397.
- Bobbitt, J. M.; Eddy, N. A.; Richardson, J. J.; Murray, S. A.; Tilley, L. J. *Org. Synth.* **2013**, *90*, 215-228.
- Boeckman, R. K.; Starrett, J. E.; Nickell, D.G.; Sum, P.-E. *J. Am. Chem. Soc.* **1986**, *108*, 5549-5559.
- Boger, D. L.; Patel, M.; Takusagawa, F. *J. Org. Chem.* **1985**, *50*, 1911-1916.
- Bollans, L.; Bacsa, J.; Iggo, J. A.; Morris, G. A.; Stachulski, A. V. *Org. Biomol. Chem.* **2009**, *7*, 4531-4538.
- Borthwick, A. D. *Chem. Rev.* **2012**, *112*, 3641-3716.
- Brown, R.; Meehan, G. *Aust. J. Chem.* **1968**, *21*(6), 1581-1599.
- Brulíková, L.; Harrison, A.; Miller, M. J.; Hlaváč, J. *Beilstein J. Org. Chem.* **2016**, *12*, 1949-1980, and references therein.
- Carlsen, P. N.; Mann, T. J.; Hoveyda, A. H.; Frontier, A. J. *Angew. Chem. Int. Ed.* **2014**, *53*, 9334-9338.

- Carson, C. A.; Kerr, M. A. *Angew. Chem. Int. Ed.* **2006**, *45*(39), 6560-6563.
- Chen, F. M. F.; Sleboda, M.; Benoiton, N. L. *Int. J. Pept. Protein Res.* **1988**, *31*(3), 339-344.
- Chen, J-H.; Levine, S. R.; Buergler, J. F.; McMahon, T. C.; Medeiros, M. R.; Wood, J. L. *Org. Lett.* **2012**, *14*, 4531-4533.
- Chirkin, E.; Atkatlian, W.; Poreé, F. -H. *The Alkaloids. Chemistry and Biology* (Ed.: H.-J. Knölker), Academic Press, London, **2015**, 1-120, and references therein.
- Coffen, D. L.; Katonak, D. A. *Helv. Chim. Acta.* **1981**, *64*, 1645.
- Cox, J. B. (2019) "Total Synthesis of (-)-Herquiline B and (+)-Herquiline C, Total Synthesis of (\pm)-Phyllantidine, and Synthetic Studies Toward Longeracemine" [Doctoral dissertation, Baylor University], and references therein.
- Cramer, N.; Laschat, S.; Baro, A.; Schwalbe, H.; Richter, C. *Angew. Chem. Int. Ed.* **2005**, *44*, 820-822.
- David, J. G.; Bai, W. -J.; Weaver, M. G.; Pettus, T. R. R. *Org. Lett.* **2014**, *16*, 4384-4387.
- Deshong, P.; Ramesh, S.; Elango, V.; Perez, J. J. *J. Am. Chem. Soc.* **1985**, *107*, 5219-5224.
- Dhanjee, H. H.; Kobayashi, Y.; Buergler, J. F.; McMahon, T. C.; Haley, M. W.; Howell, J. M.; Fujiwara, K.; Wood, J. L. *J. Am. Chem. Soc.* **2017**, *139*, 14901-14904.
- Erlenmeyer, F. "Ueber die Condensation der Hippursäure mit Phtalsäureanhydrid und mit Benzaldehyd" [On the condensation of hippuric acid with phthalic acid anhydride and with benzaldehyde] *Annalen der Chemie* **1893**, *275*, 1-8. doi:10.1002/jlac.18932750102; see especially pp. 3-8.
- Fujita, M.; Nakao, Y.; Matsunaga, S.; Seiki, M.; Itoh, Y.; van Soest, R. W. M.; Fusetani, N. *Tetrahedron* **2001**, *57*, 1229-1234.
- Gayler, K. M. (2020) "Synthetic Studies towards Penicisulfuranol B; C-H Activation Borylation of Staurosporine; Design, Synthesis, and Biological Evaluation of Rapamycin and Tak-242 Bioconjugates; Design, Synthesis, and Evaluation of Gemfibrozil Analogs." [Doctoral dissertation, Baylor University].
- Gayler, K. M.; Lambert, K. M.; Wood, J. L. *Tetrahedron*, **2019**, *75*(24), 3154-3159.
- Ghisalberti, E. L. *Studies in natural products chemistry*, **2003**, *28*, 109-163.
- Gil, C.; Bräse, S. *Chem. Eur. J.* **2005**, *11*(9), 2680-2688.

Gossauer, A. *Fortschritte der Chemie organischer Naturstoffe/Progress in the Chemistry of Organic Natural Products*, Springer, **2003**, 1-188.

Gritsch, P. J.; Stempel, E.; Gaich, J. *Org. Lett.* **2013**, *15*(21), 5472-5475.

Gruver, J. M.; Liou, L. R.; McNeil, A. J.; Ramirez, A.; Collum, D. B. *J. Org. Chem.* **2008**, *73*, 7743-7747.

Hadimani, M. B.; Mukherjee, R.; Banerjee, R.; Shoman, M. E.; Aly, O. M.; King, S. B. *Tetrahedron Lett.* **2015**, *56*(43), 5870-5873.

Hart, A. C.; Philips, A. *J. Am. Chem. Soc.* **2006**, *128*, 1094-1095.

Henderson, J. A.; Philips, A. *J. Angew. Chem. Int. Ed.* **2008**, *47*, 8499-8501.

Henning, H-G.; Gelbin, A. *Adv. Heterocycl. Chem.* **1993**, *57*, 139-185.

Herscheid, J. D. M.; Colstee, J.; Ottenheijm, H.; *J. Org. Chem.* **1981**, *46*, 3346-3348.
Ottenheijm, H.; Herscheid, J. D. M. *J. Chem. Rev.* **1986**, *86*, 697-707.

Herscheid, J. D. M.; Nivard, R.; Tijhuis, M.; Ottenheijm, H. *J. Org. Chem.* **1980**, *45*, 1885-1888.

Herscheid, J. D. M.; Nivard, R.; Tijhuis, M.; Scholten, H.; Ottenheijm, H. *J. Org. Chem.* **1980**, *45*, 1880-1885.

Hirsch, S.; Miroz, A.; McCarthy, JP.; Kashman, Y. *Tetrahedron Lett.* **1989**, *30*(32), 4291-4294.

Horii, Z.; Hanaoka, M.; Yamawaki, Y.; Tamura, Y.; Saito, S.; Shigematsu, N.; Kotera, K.; Yoshikawa, H.; Sato, Y.; Nakai, H.; Sugimoto. N. *Tetrahedron* **1967**, *23*, 1165-1174.

Horii, Z.; Imanishi, T.; Yamauchi, M.; Hanaoka, M.; Parello, J.; Munavalli, S. *Tetrahedron Lett.* **1972**, *13*, 1877-1880.

Houk, K. N.; Leach, A. *J. Org. Chem.* **2001**, *66*, 5192.

Hruska, A. *J. CAB Reviews*, **2019**, *14*, 043.

Huang, R.; Zhou, X.; Xu, T.; Yang, X.; Liu, Y. *Chem. Biodivers.* **2010**, *7*, 2809-2829.

Hwang, I. H.; Che, Y.; Swenson, D. C.; Gloer, J. B.; Wicklow, D. T.; Peterson, S. W.; Dowd, P. F. *J. Antibiot.* **2016**, *69*, 631-636.

- Iwata, Y.; Maekawara, N.; Tanino, K.; Miyashita, M. *Angew. Chem. Int. Ed.* **2005**, *44*, 1532-1536.
- Jackson, A. C.; Olsen, J. T.; Sundstrom, S. S.; Lambert, K. M. *Tetrahedron Lett.* **2022**, *99*(153851), 1-5.
- Jankolovits, J.; Lim, C-S.; Mezei, G.; Kampf, J. W.; Pecoraro, V. L. *Inorg. Chem.* **2012**, *51*, 4527-4538.
- Jenkins, N. E.; Ware, R. W.; Atkinson, R. N.; King, S. B. *Synth. Comm.* **2000**, *30*(5), 947-953.
- Jeon, S.; Han, S. *J. Am. Chem. Soc.* **2017**, *139*, 6302-6305, and references therein.
- Jida, M.; Ballet, S. *Chemistry Select*, **2018**, *3*, 1027-1031.
- Jouin, P.; Castro, B.; Nisato, D. *J. Chem. Soc. Perkin Trans. I* **1987**, 1177-1182.
- Karaiskos, C. S. *Molecules*, **2011**, *16*, 6116-6128. Xie, Z. China, CN107056672 A 2017-08-18.
- Katoh, T.; Watanabe, T.; Nishitani, M.; Ozeki, M.; Kajimoto, T.; Node, M. *Tetrahedron Lett.* **2008**, *49*(4), 598-600.
- Kaufmann, G. F.; Sartorio, R.; Lee, S. H.; Rogers, C. J.; Meijler, M. M.; Moss, J. A.; Clapham, B.; Brogan, A. P.; Dickerson, T. J.; Janda, K. D. *Proc. Natl. Acad. Sci. U.S.A.* **2005**, *102*, 309-314.
- Keck, G. E. *Tetrahedron Lett.* **1978**, *19*, 4767.
- Kim, J. W.; Ko, S.; Son, S.; Shin, K.; Ryoo, I.; Hong, Y.; Oh, H.; Hwang, B. Y.; Hirota, H.; Takahashi, S.; Kim, B. Y.; Osada, H.; Jang, J.; Ahn, J. *Bioorg. Med. Chem. Lett.* **2015**, *25*, 5398-5401.
- Known extended hydroxamic acid: Tan, Y.; Han, F.; Hemming, M.; Wang, J.; Harms, K.; Xie, X.; Meggers, E. *Org. Lett.* **2020**, *22*(16), 6653-6656.
- Kouchaksaraee, R. M.; Li, F.; Nazemi, M.; Farimani, M. M.; Tasdemir, D. *Mar. Drugs* **2021**, *19*, 439.
- Lacey, R. N. *J. Chem. Soc.* **1954**, 850-854.
- Lajis, N. H.; Guan, O. B.; Sargent, M. V.; Skelton, B. W.; White, A. H. *Aust. J. Chem.* **1992**, *45*, 1893-1897.

- Lambert, K. M.; Cox, J. B.; Liu, L.; Jackson, A. C.; Yruegas, S.; Wiberg, K. B.; Wood, J. L. *Angew. Chem. Int. Ed.* **2020**, *59*, 9757-9766, and references therein.
- Lambert, K. M.; Medley, A. W.; Jackson, A. C.; Markham, L. E.; Wood, J. L. *Org. Synth.* **2019**, *96*, 528-585.
- Laurence, C.; Gal, J.-F. in *Lewis Basicity and Affinity Scales: Data and Measurement*, Wiley, Chichester, **2010**, 1-447, and references therein.
- Leach, A. G.; Houk, K. N. *Chem. Commun.* **2002**, 1243-1255.
- Lebrun, M. H.; Duvert, P.; Gaudemer, F.; Gaudemer, A.; Deballon, C.; Boucly, P. *Inorg. Biochem.* **1985**, *24*, 167-181.
- Lebrun, M. H.; Nicolas, L.; Boutar, M.; Gaudemer, F.; Ranomenjanahary, S.; Gaudemer, A. *Phytochemistry* **1988**, *27*, 77-84.
- Levandowski, B. J.; Houk, K. N. *J. Org. Chem.* **2015**, *80*, 3530-3537.
- Ley, S.; Smith, S. C.; Woodward, P. R. *Tetrahedron* **1992**, *48*, 1145-1174.
- Li, J.; Hu, Y.; Hao, X.; Tan, J.; Li, F.; Qiao, X.; Chen, S.; Xiao, C.; Chen, M.; Peng, Z.; Gan, M. *J. Nat. Prod.* **2019**, *82*, 1391-1395.
- Lin, D. W.; Masuda, T.; Biskup, M. B.; Nelson, J. D.; Baran, P. S. *J. Org. Chem.* **2011**, *76*(4), 1013-1030.
- Liu, S.; Mu, Y.; Han, J.; Zhen, X.; Yang, Y.; Tian, X.; Whiting, A. *Org. Biomol. Chem.* **2011**, *9*, 7476-7481.
- Marcus, A. P.; Sarpong, R. *Org. Lett.* **2010**, *12*, 4560-4563. (For a correction see: Marcus, A. P.; Sarpong, R. *Org. Lett.* **2014**, *16*, 3420.)
- Medeiros, M. R.; Wood, J. L. *Tetrahedron* **2010**, *66*, 4701-4709.
- Merbouh, N.; Bobbitt, J. M.; Brückner, C. *The New Journal for Organic Synthesis*, **2004**, *36*(1), 1-31.
- Miknis, G. F.; Williams, R. M. *J. Am. Chem. Soc.* **1993**, *115*, 536-547.
- Miller, M. J.; Carosso, S. *Org. Biomol. Chem.* **2014**, *12*(38), 7445-7468, and references therein.
- Mo, X.; Li, Q.; Ju, J. *RSC Adv.* **2014**, *4*, 50566-50593, and references within.

- Moraes, L. S.; Donza, M. R.; Rodrigues, A. P.; Silva, B. J.; Brasil, D. S.; Zoghbi, M.; Andrade, E. H.; Guilhon, G. M.; Silva, E. O. *Molecules* **2015**, *20*, 22157.
- Moulay, S. *Chem. Educ. Res. Pract. Eur.* **2002**, *3*, 33-64, and references therein.
- Mulholland, T. P. C.; Foster, R.; Haydock, D. B. *J. Chem. Soc., Perkin Trans. I.* **1972**, 2121-2128.
- Nakhla, M. C.; Wood, J. L. *J. Am. Chem. Soc.* **2017**, *139*, 18504-18507.
- Neukom, C.; Richardson, D. P.; Myerson, J. H.; Bartlett, P. A. *J. Am. Chem. Soc.* **1986**, *108*, 5559-5568.
- O'Brien, P.; Poumellec, P. *J. Chem. Soc. Perkin. Trans. I.* **1998**, *15*, 2435-2441.
- Ottenheim, H.; Herscheid, J. D. M.; Nivard, R. *J. Org. Chem.* **1977**, *42*(5), 925-926.
- Parello, J.; Munavalli, S.; Hebd. C. R. *Seances Acad. Sci.* **1965**, *260*, 337-340.
- Park, J.; Jeon, S.; Kang, G.; Lee, J.; Baik, M. -H.; Han, S. *J. Org. Chem.* **2019**, *84*, 1398-1406, and references therein.
- Parry, R. *J. Bioorg. Chem.* **1978**, *7*, 277.
- Parry, R. *J. Tetrahedron Lett.* **1974**, *15*, 307.
- Pau, B.; Felix, B; Marta, F. *Targets in Heterocyclic Systems* **2005**, *9*, 281, and references therein.
- Pedras, M.; Soledade, C.; Okinyo-Owiti, D. P.; Thoms, K.; Adio, A. M. *Phytochemistry* **2009**, *70*(9), 1129-1138.
- Petsch, D. T. (1999) "The Design and Synthesis of Selective Kinase Inhibitors Based on the Indolocarbazole Natural Product K252a." [Doctoral Dissertation, Yale University].
- Pettersson, B.; Hasimbegovic, V.; Bergman, J. *J. Org. Chem.* **2011**, *76*(6), 1554-1561.
- Pirrung, M. C.; Chau, J. H-L. *J. Org. Chem.* **1995**, *60*(24), 8084-8085.
- Plöchl, J. "Über einige Derivate der Benzoylimidozimtsäure" [On some derivatives of benzoyl-imido-cinnaminic acid] *Berichte der deutschen chemischen Gesellschaft* **1884**, *17*(2), 1616-1624.
- Poncet, J.; Jouin, P.; Castro, B.; Louisette, N.; Boutar, M.; Gaudemer, A. *J. Chem. Soc. Perkin, Trans. I* **1990**, 611-616.

- R. J. Parry, *J. Chem. Soc. Chem. Commun.* **1975**, 144-145.
- Raj, D.; Luczkiewicz, M. *Fitoterapia* **2008**, 79, 419, and references therein.
- Reich, H. *J. Org. Chem.* **2012**, 77, 5471-5491, and references therein.
- Renz, M.; Meunier, B. *Eur. J. Org. Chem.* **1999**, 737-750, and references therein.
- Royles, B. J. L. *Chem. Rev.* **1995**, 95, 1981-2001.
- Sakata, K.; Kuwatsuka, T.; Sakurai, A.; Takahashi, N.; Tamura, G. *Agric. Biol. Chem.* **1983**, 47(11), 2673-2674.
- Sakata, K.; Maruyama, M.; Uzawa, J.; Sakurai, A.; Lu, H. S. M.; Clardy, J. *Tetrahedron Lett.* **1987**, 28(46), 5607-5610.
- Sakata, K.; Masago, H.; Sakurai, A.; Takahashi, N. *Tetrahedron Lett.* **1982**, 28, 5607-5610.
- Schlessinger, R. H.; Bebernitz, G. R.; Lin, P. *J. Am. Chem. Soc.* **1985**, 107, 1777- 1778.
- Schobert, R.; Schlenk, A. *Bioorg. Med. Chem.* **2008**, 16, 4203-4221.
- Schotten, C. *Ber. Dtsch. Chem. Ger.* **1884**, 17, 2544-2547. Baumann, E. *Ber. Dtsch. Chem. Ger.* **1886**, 19, 2982-2992.
- Sheradsky, T.; Silcoff, E. R. *Molecules* **1998**, 3, 80-87.
- Shimizu, H.; Yoshimura, A.; Noguchi, K.; Nemykin, V. N.; Zhdankin, V. V.; Saito, A. *Beilstein J. Org. Chem.* **2018**, 14, 531-536.
- Shinmon, N.; Cava, M. P. *J. C. S. Chem. Comm.* **1980**, 21, 1020-1021.
- Sparks, S. M.; Chow, C. P.; Zhu, L.; Shea, K. J. *J. Org. Chem.* **2004**, 69, 3025-3035.
- Steyn, P. S.; Rabie, C. J. *Phytochemistry* **1976**, 15, 1977-1979.
- Taber, D. F.; DeMatteo, P. W.; Hassan, R. A. *Org. Synth.* **2013**, 90, 350-357 (*checked by Wood, J. L.; Enquist, J. A., Jr.*).
- Tan, Y.; Han, F.; Hemming, M.; Wang, J.; Harms, K.; Xie, X.; Meggers, E. *Org. Lett.* **2020**, 22(16), 6653-6656.
- Tani, K.; Stoltz, B. M. *Nature*, **2006**, 441, 731.
- The chemistry of hydroxylamines, oximes and hydroxamic acids* (Eds.: Z. Rappoport, J. F. Lieberman), Wiley, Chichester, 2009.

Tian, X.; Feng, J.; Fan, S.; Zhen, X.; Han, J.; Liu, S. *Bioorg. Med. Chem.* **2016**, *24*(21), 5197-5205.

Trapencieris, P.; Strazdina, J.; Bertrand, P. *Chem. Heterocycl. Compd.* **2012**, *48*, 833-835.

UN News, <https://news.un.org/en/story/2019/03/1035071>, “‘Growing alarm’ over Fall Armyworm advance, with cash crops ‘under attack’ across Asia” (see Food and Agriculture Organization of the United Nations).

Usachova, N.; Leitis, G.; Jirgensons, A.; Kalvinsh, I. *Synth. Commun.* **2010**, *40*(6), 927-935.

Usui, I.; Lin, D. W.; Masuda, T.; Baran, P. S. *Org. Lett.* **2013**, *15*(9), 2080-2083.

Visagie, C. M., Hirooka, Y., Tanney, J. B., Whitfield, E., Mwange, K., Meijer, M., Amend, A. S., Seifert, K. A., Samson, R. A. *Studies in Mycology*, **2014**, *78*, 63-139.

Vogt, P. F.; Miller, M. J. *Tetrahedron*, **1998**, *54*, 1317-1348.

Wang, X.; Porco, J. A. *Angew. Chem. Int. Ed.* **2005**, *44*, 3067-3071.

Watson, K. D.; Carosso, S.; Miller, M. J. *Org. Lett.* **2013**, *15*(2), 358.

Wehlauch, R.; Gademann, K. *Asian J. Org. Chem.* **2017**, *6*, 1146-1159.

Weinreb, S. M. *Nat. Prod. Rep.* **2009**, *26*, 758-775, and references therein.

Wichterle, O. *Collect. Czech. Chem. Commun.* **1947**, *12*, 292-304.

Wipf, P.; Li, W. Sekhar, V. *Bioorg. Med. Chem. Lett.* **1991**, *1*(12), 745-750.

Wood, J. L.; Stoltz, B. M.; Dietrich, H. J. *J. Am. Chem. Soc.* **1995**, *117*, 10413-10414.

Wood, J. L.; Stoltz, B. M.; Dietrich, H. J.; Pfleum, D. A.; Petsch, D. T. *J. Am. Chem. Soc.* **1997**, *119*, 9641-9651.

Wood, J. L.; Stoltz, B. M.; Goodman, S. N. *J. Am. Chem. Soc.* **1996**, *118*, 10656-10657.

Wood, J. L.; Stoltz, B. M.; Goodman, S. N.; Onwueme, K. *J. Am. Chem. Soc.* **1997**, *119*, 9652-9661.

Xu, X-B.; Liu, Y-N.; Rao, G-W. *Russ. J. Org. Chem.* **2019**, *55*(4), 559-568, and references therein.

Yamamoto, H.; Kawasaki, M. *Bull. Chem. Soc. Jpn.* **2007**, *80*(4), 595-607.

Yoshinari, T.; Ohmori, K.; Schrems, M. G.; Pfaltz, A.; Suzuki, K. *Angew. Chem. Int. Ed.* **2010**, *49*, 881-885.

Zhangtao, Z.; Weiping, Y.; Anjie, F.; Yang, W.; Zhongwen, Q.; Xingbao, Z. CN109651178, 2019, A.

Zheng, C.; You, S-L. *Chem. Soc. Rev.* **2012**, *41*, 2498-2518.

Zhu, M.; Zhang, X.; Feng, H.; Dai, J.; Li, J.; Che, Q.; Gu, Q.; Zhu, T.; Li, D. *J. Nat. Prod.* **2017**, *80*(1), 71-75.

ABOUT THE AUTHOR



Amy Catherine Joan Jackson was born on November 8th, 1995 in Escondido, California to Charles E. Jackson Jr. and Siem T. Jackson. One of her earliest memories is of walking the grounds of Eagle's Point with her mom, and seeing a friendly old man every day who would toss her down a box of Barnum's animal crackers. On her second birthday, after picking the ballerina figurines off of her cake, she stood up on the dinner table and sang her ABCs aloud to everyone in the room.

She and her younger brother, Daniel, had a perfect childhood growing up by the ocean in beautiful Carmel Valley. Spending most of their time with mom and relatives while dad worked full-time, they both learned how to speak Hakka, Chinese. The family frequented Torrey Pines State Reserve, visiting the "stay-still" animal lodge, hiking, fishing, and building sand castles.

Amy's first passion was art, and one could find an extensive archive of stick figure drawings with pig noses wearing top hats, with smiling suns decorating the pages. She realized her talent for sketching when her dad sat her down one day to sketch a still-life of an egg and a spoon. She became known as the "artist" among her classmates and she continues to express herself with pencil and chalk.

She developed a love and respect for nature at an early age, studying backyard plants and animals and making her own hand-drawn field guides. Little did she know, this would eventually bloom into a well-appointed career in STEM.

She was part of the first graduating class from Sage Canyon Elementary School where she met her first mentor, her Kindergarten teacher Mrs. Maurer, who taught her the true meaning of friendship, trust, and how to find the joys in everyday life. In elementary school, she grew close to all of her teachers, learned to stand up to bullying, and struggled indefinitely with mathematics. By her own initiative, she began studying piano at age 8, and still plays occasionally while also having picked up the violin and the guitar. She enjoys singing while playing, and will someday drop her whole career and run away to the hill country to start a bluegrass band. Just kidding...

She had always been a shy and self-conscious child growing up, but at Carmel Valley Middle School she remembers a pivotal moment in drama class when she embraced the role of Juliet in the “balcony soliloquy,” and many of her inhibitions fell away. She attended Torrey Pines High School where she ran varsity track and cross country and played violin in the school orchestra. She got her driver’s license at age 17, passing her driving test on the first try, and got her first car that she named “Paige” (later known as Turbo-Deez when the car was inherited by her younger brother). Paige was there to witness many core memories: blasting the “Mr. Blue Sky mixtape” on the way to school with Daniel every morning, driving 90 mph to surf at Marine Street with all the neighborhood kids, and her first breakup.

She began her undergraduate studies at Mira Costa College where she adopted the attitude of “it’s better to ask for forgiveness than for permission,” and became a spirited,

independent and resilient young woman. College was a very difficult period for her, but while having to fight hard to transfer from community college to a 4-year institution, she honed her public speaking and negotiation skills, and landed acceptance to San Diego State University. At SDSU, her family's legacy institution, she joined Dr. Jeff Gustafson's organic chemistry research lab, accepted a prestigious IMSD scholarship, and earned authorship on her first publication with her graduate student mentor Dr. Andrew Dinh. She graduated from SDSU in 2018, and was urged by her mentors and peers to pursue a PhD in Organic Chemistry. Walking across the stage at Viejas Arena, smiling ear to ear, and giving Dr. Gustafson a big hug after accepting her diploma still remains one of the happiest moments of her life.

Amy joined Dr. John L. Wood's prestigious total synthesis group at Baylor University in the summer of 2018, and has since worked hard to establish herself as a peer-reviewed member of the chemistry community, and a loyal representative of the W6. In graduate school, she worked on the total synthesis of natural products and methods development, and pursued independent study in X-ray crystallography. She made some lasting friendships with her mentor and co-workers, and the long, strenuous hours at the bench ingrained in her patience, resilience, and the strength to tackle unique and complex problems. She also learned to trust her gut and to trust the process. At Baylor, she also finally went through the rigorous process of getting Confirmed with the Catholic Church and, although she regrets not having completed this earlier in her life when she wasn't overwhelmed with lab work, the decision was all her own out of a desire to grow closer to God and the Church. She chose to be named after Saint Joan of Arc: a martyr who suffered for her purity, country, and faith.

Amy recalls a moment when, in a time of crisis, her brother asked her “when do you feel closest to God?” She answered “when I’m at the ranch with Alex.” She later relayed this to Alex and her family, and they replied “Why, because your life is always at risk when you’re with her?” Texas called to her for many years, and during her time there she had never felt more like her true self. Someday she’ll plant her roots in the place where life and death walk side-by-side.

Amy recently accepted a position as a Science Advisor at Goodwin Procter, LLP in Boston, on track to become a patent attorney. Although this decision seems unconventional to some, she believes that, looking back, it is all quite fitting.

Sometime in the distant future, when she’s old and in the way, she hopes to become a volunteer museum curator in San Diego and to foster a catch-and-release program for stray animals.

Some of Amy’s Favorite Quotes:

“History will be kind to me for I intend to write it.” -Winston Churchill

“Whatever you are, be a good one.” -Abraham Lincoln

“I have never in my life envied a human being who led an easy life.” -Teddy Roosevelt

“Eighty percent of success is showing up.” -Woody Allen

“There is no genius without a touch of madness.” -Seneca

“A sign of intelligence is an awareness of one’s own ignorance.” -Machiavelli

“Better to remain silent and be thought a fool than to speak out and remove all doubt.”

-Abraham Lincoln

“Brevity is the soul of wit.” -William Shakespeare

“It is dangerous to be right in matters where established men are wrong.” -Voltaire

“You have enemies? Good. That means you’ve stood up for something, sometime in your life.” -Winston Churchill

“Diplomacy is the art of telling people to go to hell in such a way that they ask for directions.” -Winston Churchill

“God is a comedian, playing to an audience too afraid to laugh.” -Voltaire

“Men judge us by the success of our efforts. God looks at the efforts themselves.”
-Charlotte Brontë

“Gratitude is not only the greatest of virtues, but the parent of all others.” -Cicero

“We are never so defenseless against suffering as when we love.” -Sigmund Freud

“Courage is not the lack of fear, it is acting in spite of it.” -Mark Twain

“Sometimes even to live is an act of courage.” -Seneca

“How lucky I am to have something that makes saying goodbye so hard.” -A. A. Milne